

CYSTIC FIBROSIS ORGANOIDS FOR PERSONALIZED MEDICINE AND THERAPY DEVELOPMENT

Eyleen de Poel

CYSTIC FIBROSIS ORGANOIDS FOR PERSONALIZED MEDICINE AND THERAPY DEVELOPMENT

Eyleen de Poel

Cystic fibrosis organoids for personalized medicine and therapy development
PhD thesis, Utrecht University, The Netherlands

©Eyleen de Poel, 2022, Hoef en Haag, the Netherlands

ISBN: 978-94-6458-111-9

Cover design & lay-out: Publiss

Printed by: Ridderprint

Printing of this thesis was financially supported by Chiesi pharmaceuticals B.V., Cresco Pharma B.V. en Westfalen Medical B.V.

CYSTIC FIBROSIS ORGANOIDS FOR PERSONALIZED MEDICINE AND THERAPY DEVELOPMENT

**Cystic fibrose organoiden voor gepersonaliseerde behandeling en
therapie ontwikkeling**

(met een samenvatting in het Nederlands)

Proefschrift

ter verkrijging van de graad van doctor aan de Universiteit Utrecht

op gezag van de rector magnificus, prof.dr. H.R.B.M. Kummeling,

ingevolge het besluit van het college voor promoties
in het openbaar te verdedigen op

donderdag 14 april 2022 des middags te 4.15 uur

door

Eyleen de Poel

geboren op 23 februari 1992
te Groningen

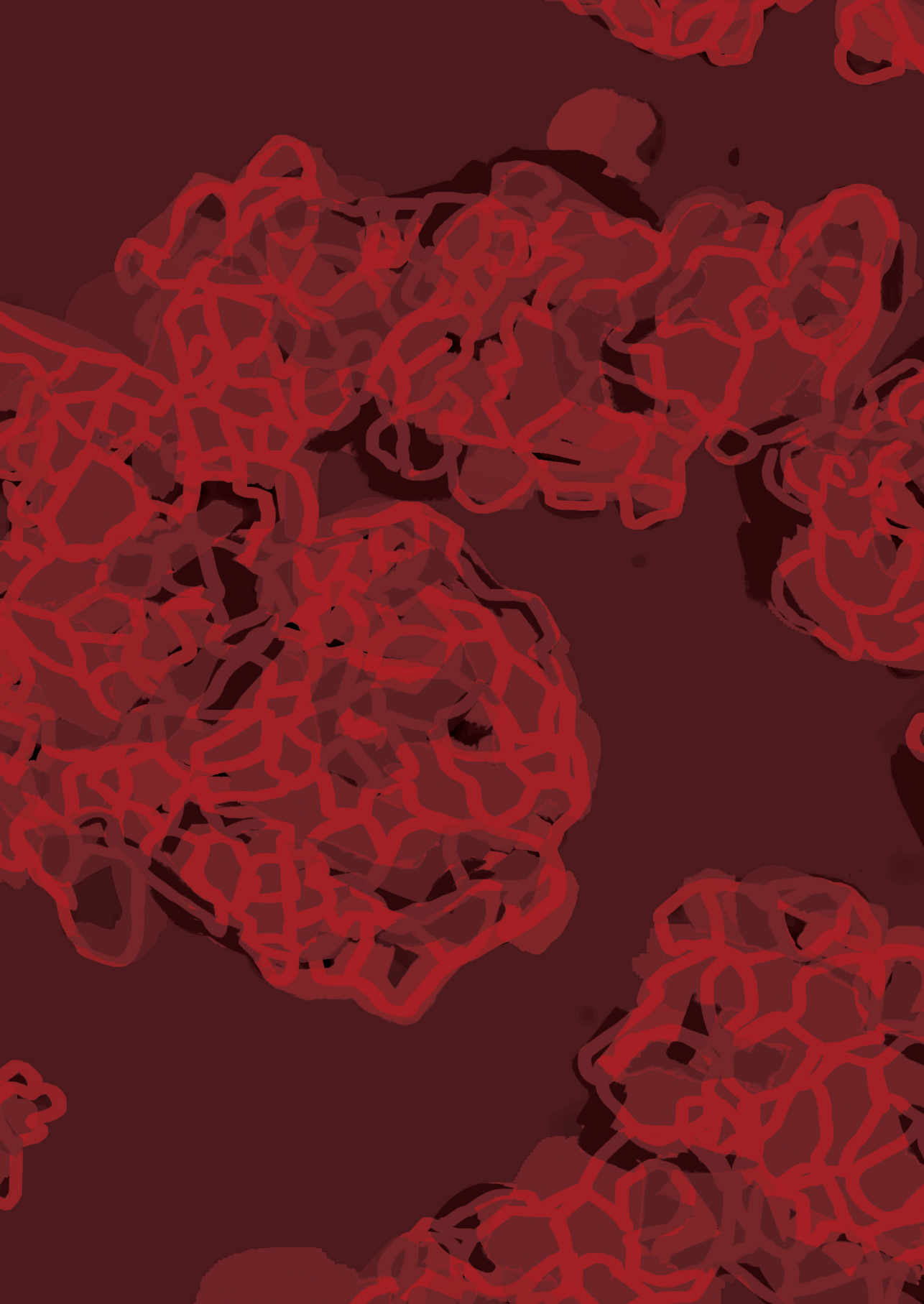
Promotoren:

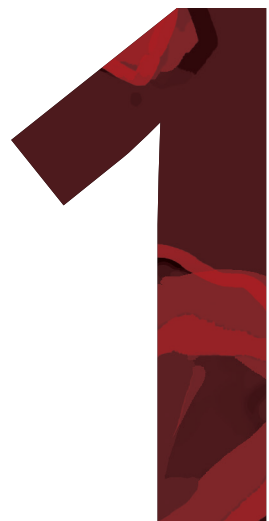
Prof. dr. C.K. van der Ent

Prof. dr. J.M. Beekman

CONTENTS

Chapter 1	General introduction	7
Part I - Predicting long-term cystic fibrosis disease progression		
Chapter 2	Forskolin-induced organoid swelling is associated with long-term CF disease progression	21
Part II - Preclinical testing of CFTR modulators and other FDA approved drugs		
Chapter 3	CFTR rescue in intestinal organoids with GLPG/ABBV-2737, ABBV/GLPG-2222 and ABBV/GLPG-2451 triple therapy	75
Chapter 4	Pre-clinical efficacy testing of FDA-approved drugs for nonhomozygous F508del-CFTR genotypes	85
Chapter 5	Functional restoration of CFTR nonsense mutations in intestinal organoids.	139
Part III - Gene editing technologies for the rescue of CF		
Chapter 6	CRISPR-based adenine editors correct nonsense mutations in a cystic fibrosis organoid biobank	161
Chapter 7	Evaluating CRISPR-based Prime Editing for cancer modeling and CFTR repair in organoids	273
Chapter 8	General discussion	303
Chapter 9	Summary in Dutch – Nederlandse samenvatting	323
Addenda	Abbreviations	334
	Contributing authors	337
	Acknowledgements – Dankwoord	342
	List of publications	346
	About the author	348





GENERAL INTRODUCTION

Partially published as review:

E. de Poel, J.W. Lefferts and J.M. Beekman

Organoids for Cystic Fibrosis research. Journal of Cystic Fibrosis 19: S60-S64 (2020)

CYSTIC FIBROSIS AND MUTATIONS IN THE CFTR GENE

Cystic fibrosis (CF) remains the most common life-shortening hereditary disease in white populations. While high morbidity and mortality is predominantly caused by chronic airway mucus obstruction, inflammation, infection, and progressive lung damage^{1,2}, people with CF (pwCF) also exhibit malfunctioning of other organs throughout the body, including the pancreas, the liver, gastro-intestinal tract, the male reproductive system and sweat glands³⁻⁵.

These clinical symptoms are caused by mutations in the cystic fibrosis transmembrane conductance regulator (CFTR) gene, which encodes for an ion channel and is expressed in the epithelial lining of these organs. Under healthy conditions CFTR transports chloride and bicarbonate and subsequently water across these epithelial linings. It is currently estimated that >1700 mutations reduce ion and water transport to such extent that it causes CF^{6,7}. These mutations are clustered into six distinct classes based on their molecular impact in the CFTR protein (**table 1**)⁸, and association with functional abnormality⁹ and clinical disease severity⁸.

CLASS I	CLASS II	CLASS III	CLASS IV	CLASS V	CLASS VI
No functional CFTR protein	No trafficking of CFTR to cell membrane	Loss of channel gating	Decreased channel conductance	less CFTR protein at cell membrane	Less stable protein at cell membrane
Decreased number of CFTR protein	Decreased number of CFTR protein	Decreased function of CFTR protein	Decreased function of CFTR protein	Decreased number of CFTR protein	Decreased number of CFTR protein
More severe CF disease	More severe CF disease	More severe CF disease	Less severe CF disease	Less severe CF disease	Less severe CF disease

Table 1: CFTR mutations classified in six classes based on functional CFTR defect.
mRNA; messenger ribonucleic acid

A PARADIGM SHIFT IN CYSTIC FIBROSIS THERAPIES

Before 2012 therapy of pwCF relied on treating the symptoms downstream of the functional CFTR defect. But with the discovery of the so-called CFTR modulators, oral drugs acting at CFTR function at the cellular level, it became possible to tackle the root cause of CF. However, 15% of pwCF have mutations that are poorly responsive to CFTR modulator therapy, including the class I and class VII mutations that do not lead to full length protein (e.g. by non-sense mutations, frameshifts, consensus splice mutations, or larger rearrangements). A considerable number of severe missense mutations (e.g. N1303K or R560S) also do not respond to these modulators. This adds to the desire to optimize current CFTR modulator therapies, to repurpose therapies for rare mutations and to develop new (genetic-modifying) therapies that increase the synthesis of CFTR or permanently repair the CFTR defect independent of the CFTR mutation.

First generation CFTR modulators

Patients carrying gating mutations have problems with opening and closing of the CFTR channel, resulting in impaired chloride transport across the epithelium. Yet, with the development of the first so-called potentiator VX-770 (Kalydeco®), a CFTR modulator that enhances channel opening probability, it became possible to successfully target and restore the impaired CFTR function in individuals carrying class III and IV mutations¹⁰. VX-770 (Kalydeco®) was first approved in 2012 for pwCF carrying the gating mutation G551D on at least one allele¹¹. Clinical studies including more rare CFTR gating mutations facilitated the extension of the indication to 9 additional VX-770-responsive mutations¹². The feasibility of restoring the CFTR functional defect with a small molecule showing such a huge clinical benefit was an exciting step forward in the treatment of cystic fibrosis and paved the way for the development of other modulator therapies.

For the treatment of pwCF carrying a deletion of phenylalanine at position 508 (F508del) on both alleles additional CFTR modulating therapies have been developed. In the case of F508del, the CFTR protein is improperly folded which strongly reduces trafficking of CFTR protein to the plasma membrane. CFTR correctors help the protein to form the conformation needed to traffic the protein to the plasma membrane and increases the protein retention time in the plasma membrane¹³. However, the proteins that reach the cell membrane upon corrector therapy still do not gate sufficiently. Therefore, the two first generation correctors are only registered in combination with the potentiator VX-770. The first approved combination therapy consisted of VX-770 + VX-809 (Orkambi®), which later was complemented with VX-770 + VX-661 (Symdeko®)¹⁴. Orkambi and Symdeko currently are only approved for pwCF carrying F508del/F508del-CFTR, but the Dutch health institute advocates for approving Symdeko for pwCF who have one copy of the F508del and at least one copy of an additional¹⁴ specified mutations¹². These modulators are associated with considerable clinical benefit, but did not reach efficacies as observed with ivacaftor in people with gating mutations.

The search to more efficacious small molecule treatments of F508del is ongoing. Since the start of the studies in this thesis, so called next generation modulators that consists of three small molecules are being investigated for repair of F508del. The first next generation triple therapy is currently approved for treatment of people with a single F508del allele, and several other potentiators and correctors are in phase I or II clinical trials¹⁵. The potential of some of these next generation modulators and other types of modulators currently in the drug development pipeline (e.g. co-potentiators or amplifiers¹⁵) will be evaluated and discussed in following chapters of this thesis.

Other pharmacotherapies for CF that target CFTR function

Class I mutations can result in premature termination codons (PTC) leading to the production of truncated CFTR protein. Approximately 10% of the worldwide CF population carry mutations that result in PTCs. Early work demonstrates that aminoglycoside antibiotics including gentamicin and G418 enable rescue of PTC's in cell lines¹⁶. These compounds reduce the fidelity of translation by affecting the pairing of cognate and near-cognate

tRNAs with the mRNA, resulting in incorporation of non-cognate amino acids at the PTC site. This readthrough (RT) process facilitates continuation of translation, albeit at low efficacy¹⁶. Subsequent efforts identified the PTC124 (Ataluren) as selective inducer of PTC-readthrough¹⁷. However, efficacy in many preclinical models was not reproduced^{18,19} and clinical trials with Ataluren failed to reach their primary endpoints²⁰. A recently chemically-engineered aminoglycosides derivative termed ELX-02 (NB124; Eloxx Pharmaceuticals) is currently in early clinical development²¹ and showed to be effective as single treatment in intestinal organoids²², albeit with moderate efficacy.

Whilst readthrough agents hold potential for increasing full length protein production, their efficacy is inhibited by a control system called nonsense-mediated mRNA decay (NMD) that leads to degradation of PTC-containing mRNA molecules^{23,24}. By pharmacological inhibition of critical effectors of NMD such as SMG1 kinase (through SMG1i) or SMG7 (through NMDI-14), increased efficacy of readthrough agents has been observed in various preclinical models and laboratories²⁴⁻²⁸, yet no NMD-inhibitors have entered clinical trials for treatment of CF.

Therapeutic approaches for CF caused by PTC mutations have mainly focused on promoting read-through to generate full-length CFTR protein and have raised hope that pharmacological restoration of PTCs seems feasible. Yet limited efficiency of read-through and ambiguity about the mechanism of action regarding the incorporation of non-native amino acids at the PTC site raise concerns about clinical efficacy. Future research should consider the potential effects of other commercially-available compounds with different modes-of-action on increasing ELX-02ds-induced CFTR function rescue. In addition, the potential of the truncated protein product to be efficiently processed and gated using combinations of the newest developed CFTR modulators in the absence of read-through might prove an important area for future research.

GENETIC RESTORATION OF THE CFTR DEFECT

Despite the huge benefits of CFTR modulators for responsive patients, these pharmacotherapies require lifelong administration, and are not effective in individuals with non-responsive missense mutations, frameshifts, consensus splice mutations, or larger CFTR gene rearrangements. An alternative solution to pharmacotherapy is the restoration of the CFTR defect using gene therapy, which remains a longstanding goal of therapeutic development in CF.

Introducing normal copies of the CFTR gene

The classic gene therapy approach introduces a normal copy of the CFTR gene with a gene transfer agent, either a viral or non-viral vector²⁹ into a desired organ. The monogenic and recessive nature of CF makes this disease an optimal target for gene complementation strategies²⁹. Although several studies have exploited viral and non-viral approaches to restore CFTR function^{21,30}, multiple challenges are being faced with gene complementation which hamper their clinical potential. First of all, expression of CFTR is driven by a non-endogenous promotor²⁹. Second, the use of non-viral, AAV or adenovirus vectors or turnover of the airway epithelium results in loss of the CFTR transgene, suggesting repeated rounds of CFTR

gene therapy are required. However, a clinical trial using nebulizing a non-viral vector on a monthly basis did not improve lung function to such extend the patients' quality of life was detectably improved. This has led to the development of more potent gene transfer agents: retroviral-based vectors fused with Fuson protein/Hemagglutinin/Neuraminidase protein (F/HN/-pseudotyped viral vectors) to enable targeting of the vector to specifically the lungs³¹. In contrast to adenoviral or non-viral vectors, lentiviral vectors hold substantial promise for the development of gene therapy due to their high efficacy, their potential to integrate their cargo into the host genome, ensuring persistent expression for the life of the cell and the fact that pre-existing and the acquired immune responses do not interfere with vector efficacy on repeated administration³¹. In addition, lentiviral vectors have a sufficient packaging capacity for a CFTR expression cassette and can transduce non-dividing cells. This is particularly important for CF gene therapy because most airway epithelial cells are mitotically quiescent³¹. The lead F/HN/-pseudotyped viral vector candidate expressed functional CFTR and retained 90–100% transduction efficiency in clinically relevant delivery devices, yet number of clinical trials using lentiviral vectors for rescue of CF disease are limited due the unpredictable results, namely transgene silencing and/or acquisition of tumorigenic phenotypes through insertional mutagenesis, occasionally reported in gene therapy clinical trials²⁹.

To address these shortcomings integration into the human AAVS1 (also known as PPP1R12C) locus could be an interesting strategy, as insertion has been shown to be safe with no phenotypic effects reported³², yet require a targeted-gene editing approach.

Targeted gene-editing approaches to restore the genetic CFTR defect

Besides the integration approaches that non-specifically introduce a normal copy of the CFTR gene, CFTR function can be restored by partially correcting or fully replacing the mutated CFTR gene with targeted gene-editing techniques. For example, inserting genes into. In addition, several classes of sequence-specific nucleases are available, including zinc finger nucleases (ZFNs), transcription activator-like effector nucleases (TALENs), meganucleases and clustered regularly interspaced short palindromic repeats (CRISPR)/CRISPR-associated 9 (Cas9) that enable targeted gene insertion or editing³³. These sequence-specific nucleases create a double stranded break (DSB) at the target site which recruits components of cellular DNA repair machinery to repair the lesion using two different DNA repair mechanisms: non-homologous end joining (NHEJ) or homology-directed repair (HDR). While NHEJ is mainly used to knockout or knock-in at preferred genomic sites, HDR allows introducing desired editing in the target sequence using HDR-dependent donor templates²⁹. HDR-based gene editing of the F508del mutation was achieved with ZFNs, TALENs and CRISPR-Cas9 in patient-derived cells^{29,34,35}. CRISPR-CAS is the preferred gene-editing technique, as it is the most versatile, efficient and inexpensive compared to other methods and is the easiest to customize. However, the repair of DSBs is often error-prone and can result in unwanted DNA damage at the target site as well as at off-target sites that closely resemble the guide RNA^{36–39}. Recently developed Cas9-fusion proteins, so-called base editors and prime-editors, circumvent these issues and the promising pre-clinical results has led to entering CRISPR-Cas9 genome editing into the clinic for the treatment of cancer and hematologic diseases by ex-vivo delivery of CRISPR-Cas-9 edited cells²⁹. The fast developments of CRISPR technology

and the early encouraging pre-clinical and clinical⁴⁰⁻⁴³ results suggest an upcoming larger use of CRISPR-Cas9 technology for the treatment of numerous monogenic diseases, including CF. As such, the feasibility and safety of the newest CRISPR-Cas-9-mediated gene editing techniques for the treatment of CF are being explored in this thesis.

A SECOND PARADIGM SHIFT: CULTURING 3D ORGANOIDS AS PATIENT AVATARS IN THE LAB

In parallel with the development of CFTR modulators, a complementary paradigm shift in stem cell culture technology allowed for the long-term culture of individual patient stem cells that self-organize in complex 3D multicellular structures. These 3D-cultured structures, termed organoids, can be expanded, cultured and stored for prolonged periods while remaining genetically stable and maintaining the CF phenotype. This facilitates the generation of a living biobank with (almost) infinite material. Compared to the traditional 2D culturing methods, organoids have the advantage of retaining the original patient's characteristics enabling the generation of paired laboratory and clinical datasets which will help in understanding variability in disease and drug efficacy among patients.

Historical perspective on the organoid technology

The term 'organoid' was first adopted in 1933 to describe a tumorous mass that was extracted from a two-month-old patient⁴⁴. At that time, 'organoids' referred to organ fragments generated by mechanical or enzymatic-dissociation, cultured *in vitro* on top of coverslips⁴⁵. Later, organoids were generated from established cell lines^{46,47} or by fully dissociating organ fragments into single cells⁴⁸ that re-aggregated into tissue-like 3D-structures. The discovery and characterization of extracellular matrix proteins (reviewed by Simian et al.⁴⁹), together with the finding that interactions between the extracellular matrix and cells regulated tissue-specific function and morphogenesis⁵⁰, further stimulated organoid research in the 70s and 80s of the 20th century.

Recent progress in stem cell biology led to a strong revival of the organoid field (**figure 2**), which are now defined as a three-dimensional collection of organ-specific cell types that self-organizes through cell sorting and spatially restricted lineage commitment comparable with the *in vivo* situation⁵¹. Adult stem cells, progenitor cells that reside in multiple types of tissues with high regenerative capacity⁵², are widely used for the generation of organoids. The behavior and function of adult stem cells depend on their localization in the human body, to which they remain lineage-committed *in vitro*. The primary role of adult stem cells is to maintain tissue homeostasis, in the context of normal cell turn-over, or tissue repair after damage. The first example of an *ex vivo* long-term adults stem cell culture showed the use of LGR5+ intestinal crypt-based stem cells⁵³.

LGR5+ intestinal epithelial stem cells self-organize into 3D crypt-like structures containing all differentiated cell types when cultured in matrigel and when the stem cell niche environment is mimicked with growth factors to favor tissue self-renewal⁵⁴. This exploratory work using mouse cells was shortly thereafter followed up by human stem cell culture protocols³⁴.

Adult stem cell-derived organoids can typically be generated within days-to-weeks and can be expanded for over a year. Moreover, these organoids can be stored in living biobanks and retain patient-specific functional characteristics^{52,55}.

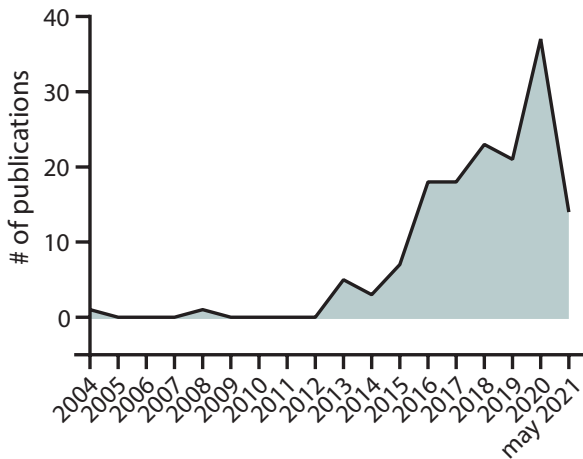


Figure 1: Number of publications per year using organoid technology for cystic fibrosis research according to pubmed. The following pubmed searches: 'cystic fibrosis[TW] AND organoid[TW]'; 'cystic fibrosis[TW] AND organoids[TW]'; 'CFTR[TW] AND organoid[TW]'; 'CFTR[TW] AND organoids[TW]' were conducted to find all publications related to cystic fibrosis research and the organoid technology.

A perfect example where adult stem cell-based organoid technology has generated impact is in the field of CF research. Here, patient-derived intestinal organoids have been used for disease modeling and drug screening in a personalized setting⁵⁵. Liu et al. reported the first use of intestinal organoids in the CF field, showing that mouse organoids exhibit CFTR expression and activity comparable to that of crypt epithelium *in vivo*⁵⁶. Independent parallel work with human CF intestinal organoids described the first functional readout in human adult stem cell-based organoids⁵⁵. The functional readout enabled measurement of CFTR function, and relied on forskolin-induced swelling (FIS) of whole organoids⁵⁵. Because the CFTR protein is located at the inner (apical) side of the organoids, cyclic adenosine monophosphate (cAMP)-inducing stimuli (e.g. forskolin) lead to ion and fluid transport into the organoid lumen and subsequently into rapid swelling of the organoids⁵⁵. Remarkably, the FIS was completely CFTR dependent, whereas raising intracellular calcium has little to no effect on whole organoid swelling⁵⁷. FIS is highly useful to quantitate and compare CFTR function between CF organoids but later studies found that CFTR function is underestimated in healthy control organoids, as their FIS response is lower due to fluid-filled lumens prior to forskolin stimulation⁵⁸. To compare healthy control and CF organoids, the steady state lumen area (SLA) assay was developed in which the lumen surface area is measured as a percentage of the total organoid surface area, which can also be used to measure drug response⁵⁸. This pioneering work led to today's revival of organoid research in the field of CF (**figure 1**).

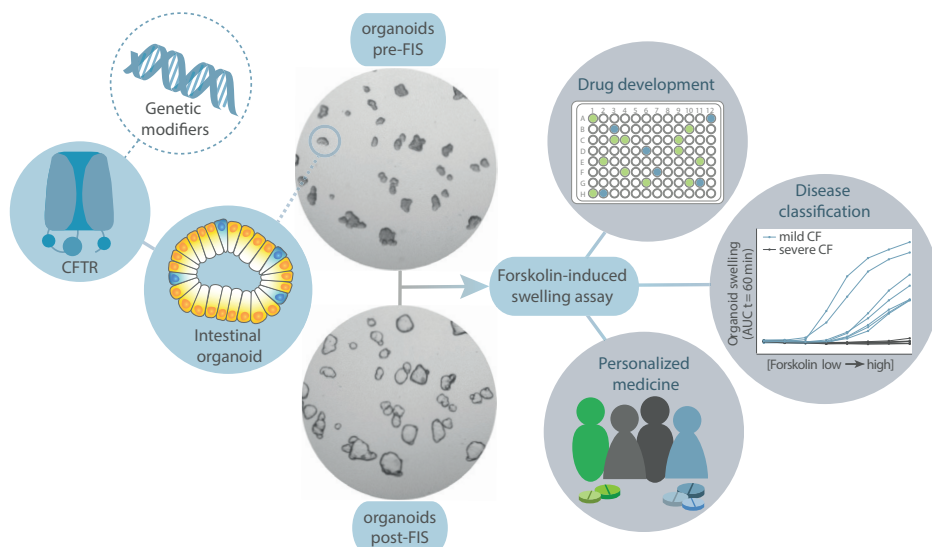


Figure 2: Besides the CFTR mutation, environmental factors and genetic modifiers (genotype) can affect CFTR function. These patient-specific characteristics are nicely recapitulated in intestinal organoids and the FIS-assay. This in vitro model therefore better predicts in vivo residual CFTR function and allows for better classifying CF disease. The FIS-assay also accurately estimates in vivo drug efficacy and will help in developing clinically effective drugs as well as defining the most optimal individual therapy (personalized medicine).

Patient-derived intestinal organoids for drug development and personalized medicine

CF remains incurable up until today, but the development of CFTR modulators has increased the prospects that CF disease manifestation might be stalled or even prevented, in the near future⁵⁹. Two phase 2 clinical trials have shown that the efficacy of the newest triple combination therapy exceeds the efficacy of the previous developed combinations, but is still only accessible for patients with particular CFTR mutations^{60,61}. PwCF with other mutational defects or rare CFTR genotypes, encompassing roughly 10% of the CF population, are therefore left behind. Additionally, heterogeneity in in vivo modulator response has been reported among individuals carrying identical CFTR mutations, adding to the desire for an optimal prediction of response-to-therapy on an individual level.

Many health care systems are reluctant to approve reimbursement for these therapies due to limited cost-efficacy. Not only stratifying responders from non-responders will enhance the cost-effectiveness of therapies, also the development of new therapeutic strategies such as repurposing current modulators for rare mutations as well as the development of new CFTR-directed therapies will help in lowering the drug prices⁶².

However, before clinical benefit of new therapeutic agents can be properly predicted, suitable pre-clinical models need to be established, since as much as 80% of all newly developed

compounds currently fail in clinical trials⁶³. For CF, it is clear that the disease shows a huge variability between patients, for which several reasons can be found (**figure 2**). First in the CFTR gene itself, as the existence of an estimated 1,700 different CF-causing contribute to CF disease heterogeneity³. Although these mutations have been identified, many of the rare CF mutations have not been characterized in detail, making it difficult to interpret and translate the molecular genotype(s) into a clinical trajectory^{4,64}. Second, other individual variables include genetic modifiers that regulate CFTR or other functions (epithelial or non-epithelial), and interactions with the environment^{65,66}. However, it is very challenging to identify and integrate all such disease variables at the individual patient level. Patient-derived intestinal organoids (PDOs) may therefore enable a more precise measurement of individual CFTR function and modulation thereof by therapy. PDOs provide an alternative to current pre-clinical models by combining high validity together with high-throughput potential. PDOs recapitulate human epithelial biology and patient-specific characteristics, like the expression of intronic and intergenic enhancers that regulate CFTR gene expression. Also (epi)genetic signatures contributing to disease severity are recapitulated in organoids and are retained during prolonged organoid culturing^{52,65-67}. This is especially relevant for capturing patient variation within identical mutation groups or for (ultra)rare mutations because of the low incidence, lack of mechanistic insight and difficulty of clinical trial design⁵⁷.

In conclusion, small proof of concept studies show the potential of the organoid model for drug development and treatment optimization in a personalized manner, also taking into account both rare mutations and additional clinical heterogeneity among individuals with CF.

AIMS AND THESIS OUTLINE

In this thesis we aim to validate in vitro patient-derived organoid-based FIS as tool to:

- I. predict long-term cystic fibrosis disease progression**
- II. preclinically test CFTR modulators and other FDA approved drugs**
- III. explore gene editing technologies for rescue of CF**

In **part I** of this thesis we assess the potential of the PDO-based FIS assay as predictive biomarker for disease progression. Clinical disease expression in people with CF (pwCF) is variable and is difficult to predict. To better understand how CFTR function contributes to disease expression we quantitated the in vitro CFTR function in intestinal organoids of 176 individuals with diverse CFTR mutations. In **chapter 2** we evaluate the predictive value of these FIS measurements on individual long-term disease progression defined by rate of FEV1pp decline and development of co-morbidities such as pancreatic insufficiency, CF-related liver disease and CF-related diabetes.

In **part II** of this thesis we implemented the FIS-assay for pre-clinical testing of multiple CFTR modulators and other FDA-approved drugs. In **chapter 3** we assess the efficacy of the CFTR modulators ABBV/GLPG-2222, GLPG/ABBV-2737 and ABBV/GLPG-2541 in organoids mainly

CHAPTER 1

compound heterozygous for the F508del allele and a class I mutation. **Chapter 4** evaluates CFTR function rescue of rare CFTR mutations by the CFTR modulators VX-770 , VX-809 and VX-809 + VX-770 as well as by 1400 other FDA-approved drugs. **Chapter 4** also describes validation and implementation of the high-throughput FIS-assay, a miniaturized version of the conventional FIS-assay. In **chapter 5** we set out to determine the functional restoration of CFTR nonsense mutations by molecules that a) amplify CFTR transcription (PTI-428), b) enhance PTC-read through (ELX-02ds), c) inhibit nonsense mediated decay (SMG1i, NMDi-14 and Vidaza), d) stimulate correct CFTR protein trafficking (VX-661 and VX-445) and e) enhance gating activity of CFTR at the cell membrane (VX-770 and ASP-11).

In **part III** we implement the PDO-based FIS-organoid model for exploring the feasibility and safety of permanently rescuing the functional defect in CFTR with the newest CRISPR-CAS9 gene editing technologies. Whereas **chapter 6** describes the rescue of specific point mutations with CRISPR-Cas9 base editing, **chapter 7** explores the potential of CRISPR-Cas9 prime editing for the repair of larger mutational defects (e.g. F508del). Finally, **chapter 8** discusses the strengths and limitations of the PDO-based FIS assay as living biomarker and as preclinical platform for therapy development. This chapter also compares the organoid model to other in vitro model systems and evaluates the (potential) impact of the organoid model on CF care in general.

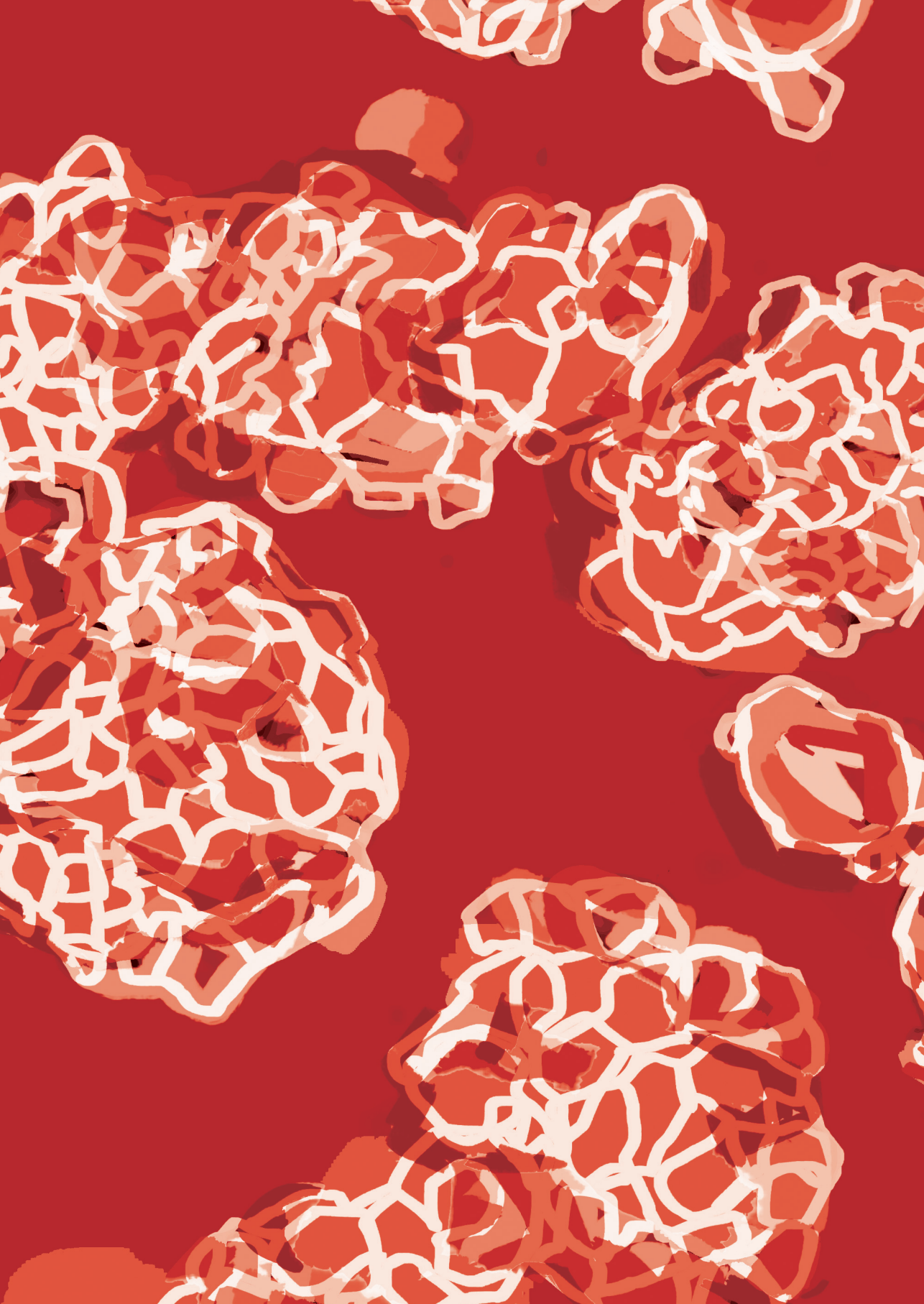
REFERENCES

1. Mall, M. A., Mayer-Hamblett, N. & Rowe, S. M. Cystic fibrosis: Emergence of highly effective targeted therapeutics and potential clinical implications. *Am. J. Respir. Crit. Care Med.* 201, 1193–1208 (2020).
2. Cystic Fibrosis Foundation Patient Registry. 2019 Annual Data Report. *Lung* (2019).
3. Cutting, G. R. Cystic fibrosis genetics: From molecular understanding to clinical application. *Nat. Rev. Genet.* 16, 45–56 (2015).
4. Sosnay, P. R. et al. Defining the disease liability of variants in the cystic fibrosis transmembrane conductance regulator gene. *Nat. Genet.* 45, 1160–1167 (2013).
5. De Boeck, K. & Amaral, M. D. Progress in therapies for cystic fibrosis. *Lancet Respir. Med.* 4, 662–674 (2016).
6. CFTR2 database. <https://cftr2.org/>.
7. CFTR1 database. <http://www.genet.sickkids.on.ca/>.
8. Marson, F. A. L., Bertuzzo, C. S. & Ribeiro, J. D. Classification of CFTR mutation classes. *Lancet Respir. Med.* 4, e37–e38 (2016).
9. Ratjen, F. et al. Cystic Fibrosis. *Nat. Rev. Dis. Prim.* 1, 1–44 (2015).
10. Yu, H. et al. Ivacaftor potentiation of multiple CFTR channels with gating mutations. *J. Cyst. Fibros.* 11, 237–245 (2012).
11. Accurso, F. J. et al. Effect of VX-770 in Persons with Cystic Fibrosis and the G551D-CFTR Mutation. *N. Engl. J. Med.* 363, 1991–2003 (2010).
12. Dutch cystic fibrosis society - approved mutations for CFTR modulator usage in the Netherlands - 2021. <https://ncfs.nl/over-taaislijmziekte/behandeling/status-cftr-modulatoren/>.
13. Wainwright, C. E. et al. Lumacaftor-Ivacaftor in Patients with Cystic Fibrosis Homozygous for Phe508del CFTR. *N. Engl. J. Med.* 373, 220–231 (2015).
14. Taylor-Cousar, J. L. et al. Tezacaftor-Ivacaftor in Patients with Cystic Fibrosis Homozygous for Phe508del. *N. Engl. J. Med.* 377, 2013–2023 (2017).
15. drug development pipeline CFF - 2021. <https://www.cff.org/trials/pipeline>.
16. Howard, M., Frizzell, R. A. & Bedwell, D. M. Aminoglycoside antibiotics restore CFTR function by overcoming premature stop mutations. *Nat. Med.* 2, 467–469 (1996).
17. Welch, E. M. et al. PTC124 targets genetic disorders caused by nonsense mutations. *Nature* 447, 87–91 (2007).
18. Zomer-van Ommen, D. D. et al. Limited premature termination codon suppression by read-through agents in cystic fibrosis intestinal organoids. *J. Cyst. Fibros.* 15, 158–162 (2016).
19. McElroy, S. P. et al. A Lack of Premature Termination Codon Read-Through Efficacy of PTC124 (Ataluren) in a Diverse Array of Reporter Assays. *PLoS Biol.* 11, (2013).
20. Kerem, E. et al. Ataluren for the treatment of nonsense-mutation cystic fibrosis: A randomised, double-blind, placebo-controlled phase 3 trial. *Lancet Respir. Med.* 2, 539–547 (2014).
21. Leubitz, A. et al. A Randomized, Double-Blind, Placebo-Controlled, Multiple Dose Escalation Study to Evaluate the Safety and Pharmacokinetics of ELX-02 in Healthy Subjects. *Clin. Pharmacol. Drug Dev.* 02451, (2021).
22. Crawford, D. K. et al. Targeting G542X CFTR nonsense alleles with ELX-02 restores CFTR function in human-derived intestinal organoids. *J. Cyst. Fibros.* 1–7 (2021) doi:10.1016/j.jcf.2021.01.009.
23. Sharma, N. et al. Capitalizing on the heterogeneous effects of CFTR nonsense and frameshift variants to inform therapeutic strategy for cystic fibrosis. *PLoS Genetics.* 14 (2018).
24. Laselva, O. et al. Functional rescue of c.3846G>A (W1282X) in patient-derived nasal cultures achieved by inhibition of nonsense mediated decay and protein modulators with complementary mechanisms of action. *J. Cyst. Fibros.* 19, 717–727 (2020).

CHAPTER 1

25. Keenan, M. M. et al. Nonsense-mediated RNA decay pathway inhibition restores expression and function of W1282X CFTR. *Am. J. Respir. Cell Mol. Biol.* 61, 290–300 (2019).
26. Yeh, J. T. & Hwang, T. C. Positional effects of premature termination codons on the biochemical and biophysical properties of CFTR. *J. Physiol.* 598, 517–541 (2020).
27. Aksit, M. A. et al. Decreased mRNA and protein stability of W1282X limits response to modulator therapy. *J. Cyst. Fibros.* 18, 606–613 (2019).
28. Valley, H. C. et al. Isogenic cell models of cystic fibrosis-causing variants in natively expressing pulmonary epithelial cells. *J. Cyst. Fibros.* 18, 476–483 (2019).
29. Maule, G., Arosio, D. & Cereseto, A. Gene therapy for cystic fibrosis: Progress and challenges of genome editing. *Int. J. Mol. Sci.* 21, 1–13 (2020).
30. Alton, E. W. et al. A randomised, double-blind, placebo-controlled trial of repeated nebulisation of non-viral cystic fibrosis transmembrane conductance regulator (CFTR) gene therapy in patients with cystic fibrosis. *Effic. Mech. Eval.* 3, 1–210 (2016).
31. Alton, E. W. F. W. et al. Preparation for a first-in-man lentivirus trial in patients with cystic fibrosis. *Thorax* 72, 137–147 (2017).
32. Biosciences, S. User Manual AAVS1 Safe Harbor Targeting System.
33. Hirakawa, M. P., Krishnakumar, R., Timlin, J. A., Carney, J. P. & Butler, K. S. Gene editing and CRISPR in the clinic: Current and future perspectives. *Biosci. Rep.* 40, (2020).
34. Sato, T. et al. Long-term Expansion of Epithelial Organoids From Human Colon, Adenoma, Adenocarcinoma, and Barrett's Epithelium. *Gastroenterology* 141, 1762–1772 (2011).
35. Schwank, G. et al. Functional repair of CFTR by CRISPR/Cas9 in intestinal stem cell organoids of cystic fibrosis patients. *Cell Stem Cell* 13, 653–658 (2013).
36. Cho, S. W. et al. Analysis of off-target effects of CRISPR/Cas-derived RNA-guided endonucleases and nickases. *Genome Res.* 24, 132–141 (2014).
37. Fu, Y. et al. High-frequency off-target mutagenesis induced by CRISPR-Cas nucleases in human cells. *Nat. Biotechnol.* 31, 822–826 (2013).
38. Kosicki, M., Tomberg, K. & Bradley, A. Repair of double-strand breaks induced by CRISPR-Cas9 leads to large deletions and complex rearrangements. *Nat. Biotechnol.* 36, (2018).
39. Pattanayak, V. et al. High-throughput profiling of off-target DNA cleavage reveals RNA-programmed Cas9 nuclease specificity. *Nat. Biotechnol.* 31, 839–843 (2013).
40. Frangoul, H. et al. CRISPR-Cas9 Gene Editing for Sickle Cell Disease and β -Thalassemia. *N. Engl. J. Med.* 384, 252–260 (2021).
41. Stadtmauer, E. A. et al. CRISPR-engineered T cells in patients with refractory cancer. *Science*. 367, (2020).
42. Lu, Y. et al. Safety and feasibility of CRISPR-edited T cells in patients with refractory non-small-cell lung cancer. *Nat. Med.* 26, 732–740 (2020).
43. Lacey, S. F. & Fraietta, J. A. First Trial of CRISPR-Edited T cells in Lung Cancer. *Trends Mol. Med.* 26, 713–715 (2020).
44. Smith, E. & Cochrane, W. J. CYSTIC ORGANOID TERATOMA: (Report of a Case). *Can. Med. Assoc. J.* 55, 151–2 (1946).
45. Lasfargues, E. Y. Cultivation and behavior in vitro of the normal mammary epithelium of the adult mouse. *Anat. Rec.* 127, 117–129 (1957).
46. Whitehead, R. H., Jones, J. K., Gabriel, A. & Lukies, R. E. A New Colon Carcinoma Cell Line (LIM1863) That Grows as Organoids with Spontaneous Differentiation into Crypt-like Structures in Vitro. *Cancer Res.* 47, 2683–2689 (1987).

- 1
47. Sambuy, Y. & De Angelis, I. Formation of organoid structures and extracellular matrix production in an intestinal epithelial cell line during long-term in vitro culture. *Cell Differ.* 19, 139–147 (1986).
 48. Halbert, S. P. in *IV* Organization of Dissociated Rat Cardiac Cells Into Beating Three-Dimensional Structures. *J. Exp. Med.* 133, 677–695 (1971).
 49. Simian, M. & Bissell, M. J. Organoids: A historical perspective of thinking in three dimensions. *J. Cell Biol.* 216, 31–40 (2017).
 50. Bissell, M. J., Hall, H. G. & Parry, G. How does the extracellular matrix direct gene expression? *J. Theor. Biol.* 99, 31–68 (1982).
 51. Lancaster, M. A. & Knoblich, J. A. Organogenesis in a dish: Modeling development and disease using organoid technologies. *Science* (80-.), 345, (2014).
 52. Clevers, H. Modeling Development and Disease with Organoids. *Cell* 165, 1586–1597 (2016).
 53. Barker, N. et al. Identification of stem cells in small intestine and colon by marker gene Lgr5. *Nature* 449, 1003–1007 (2007).
 54. Sato, T. et al. Single Lgr5 stem cells build crypt-villus structures in vitro without a mesenchymal niche. *Nature* 459, 262–265 (2009).
 55. Dekkers, J. F. et al. A functional CFTR assay using primary cystic fibrosis intestinal organoids. *Nat. Med.* 19, 939–945 (2013).
 56. Liu, J., Walker, N. M., Cook, M. T., Ootani, A. & Clarke, L. L. Functional Cftr in crypt epithelium of organotypic enteroid cultures from murine small intestine. *Am. J. Physiol. Physiol.* 302, C1492–C1503 (2012).
 57. Boj, S. F. et al. Forskolin-induced Swelling in Intestinal Organoids: An In Vitro Assay for Assessing Drug Response in Cystic Fibrosis Patients. *J. Vis. Exp.* 1–12 (2017) doi:10.3791/55159.
 58. Dekkers, J. F. et al. Characterizing responses to CFTR-modulating drugs using rectal organoids derived from subjects with cystic fibrosis. *Sci. Transl. Med* 8, 344–84 (2016).
 59. Chaudary, N. Triplet CFTR modulators: Future prospects for treatment of cystic fibrosis. *Ther. Clin. Risk Manag.* 14, 2375–2383 (2018).
 60. Keating, D. et al. VX-445–Tezacaftor–Ivacaftor in Patients with Cystic Fibrosis and One or Two Phe508del Alleles. *N. Engl. J. Med.* 379, 1612–1620 (2018).
 61. Davies, J. C. et al. VX-659–Tezacaftor–Ivacaftor in Patients with Cystic Fibrosis and One or Two Phe508del Alleles. *N. Engl. J. Med.* 379, 1599–1611 (2018).
 62. Mall, M. A., Hwang, T. C. & Braakman, I. Cystic fibrosis research topics featured at the 14th ECFS Basic Science Conference: Chairman's summary. *J. Cyst. Fibros.* 17, S1–S4 (2018).
 63. Kondo, J. & Inoue, M. Application of Cancer Organoid Model for Drug Screening and Personalized Therapy. *Cells* 8, 470 (2019).
 64. Castellani, C. et al. Consensus on the use and interpretation of cystic fibrosis mutation analysis in clinical practice. *J. Cyst. Fibros.* 7, 179–196 (2008).
 65. Strug, L. J., Stephenson, A. L., Panjwani, N. & Harris, A. Recent advances in developing therapeutics for cystic fibrosis. *Hum. Mol. Genet.* 27, R173–R186 (2018).
 66. Kraiczy, J. et al. DNA methylation defines regional identity of human intestinal epithelial organoids and undergoes dynamic changes during development. *Gut* 68, 49–61 (2019).
 67. Yin, Y. B., de Jonge, H. R., Wu, X. & Yin, Y. L. Mini-gut: a promising model for drug development. *Drug Discov. Today* 00, 1–11 (2019).





FORSKOLIN-INDUCED ORGANOID SWELLING IS ASSOCIATED WITH LONG-TERM CF DISEASE PROGRESSION

D. Muilwijk*, E. de Poel*, P. van Mourik, S.W.F. Suen, A.M. Vonk, J.E. Brunsveld, E. Kruisselbrink, H. Oppelaar, M.C. Hagemeijer, G. Berkers, K.M. de Winter-de Groot, S. Heida-Michel, S.R. Jans, H. van Panhuis, M.M. van der Eerden, R. van der Meer, J. Roukema, E. Dompeling, E.J.M. Weersink, G.H. Koppelman, R. Vries, D.D. Zomer-van Ommen, M.J.C. Eijkemans, C.K. van der Ent and J.M. Beekman

European Respiratory Journal (2022), in press

* These authors contributed equally

ABSTRACT

Background: Cystic fibrosis (CF) is a monogenic life-shortening disease associated with highly variable individual disease progression which is difficult to predict. Here we assessed the association of forskolin-induced swelling (FIS) of patient-derived organoids (PDO) with long-term CF disease progression in multiple organs and compared FIS with the golden standard biomarker sweat chloride concentration (SCC).

Methods: We retrieved 9-year longitudinal clinical data from the Dutch CF Registry of 173 people with mutations in the cystic fibrosis transmembrane conductance regulator (CFTR) gene. Individual CFTR function was defined by FIS, measured as the relative size increase of intestinal organoids after stimulation with 0.8 µM forskolin, quantified as area under the curve (AUC). We used linear mixed effect models and multivariable logistic regression to estimate the association of FIS with long-term FEV1pp decline and development of pancreatic insufficiency, CF-related liver disease and diabetes. Within these models, FIS was compared with SCC.

Results: FIS was strongly associated with longitudinal changes of lung function, with an estimated difference in annual FEV1pp decline of 0.32% (95%CI: 0.11%–0.54%; p=0.004) per 1000-points change in AUC. Moreover, increasing FIS levels were associated with lower odds of developing pancreatic insufficiency (adjusted OR: 0.18, 95%CI: 0.07–0.46, p<0.001), CF-related liver disease (adjusted OR: 0.18, 95%CI: 0.06–0.54, p=0.002) and diabetes (adjusted OR: 0.34, 95%CI: 0.12–0.97, p=0.044). These associations were absent for SCC.

Conclusion: This study exemplifies the prognostic value of a PDO-based biomarker within a clinical setting, which is especially important for people carrying rare CFTR mutations with unclear clinical consequences.

TAKE HOME MESSAGE

Forskolin-induced swelling of patient-derived intestinal organoids is associated with long-term cystic fibrosis disease progression, expressed as FEV1pp decline and development of pancreatic insufficiency, CF-related liver disease and CF-related diabetes.

INTRODUCTION

Clinical disease expression in people with CF (pwCF) is variable and results from a combination of genetic, environmental and stochastic factors which are unique for each individual. CF is a recessive, monogenic disease caused by mutations in the cystic fibrosis transmembrane conductance regulator (CFTR) gene [1]. Over 2000 CFTR variants which differentially affect CFTR function and clinical phenotype have been identified until now (<http://cftr2.org>). The more common mutations have been categorized into distinct classes according to the mechanism by which CFTR function is disrupted [2]. To better understand how CFTR function contributes to disease expression, biomarkers such as sweat chloride concentration (SCC), intestinal current measurements (ICM) and nasal potential difference (NPD) are used to estimate individual CFTR function. These biomarkers have mostly been validated in the context of CF diagnosis, but their ability to accurately discriminate between pwCF with differential disease progression is limited despite clear relations at population level [3–9]. Forskolin-induced swelling (FIS) of patient-derived intestinal organoids is an *in vitro* biomarker that quantifies CFTR-dependent fluid transport into the organoid lumen [10, 11] and may provide a more precise and accurate estimation of CFTR function compared to other biomarkers. Small proof of concept studies showed that FIS correlates with SCC and ICM and that clinical disease phenotypes could be stratified based on FIS level [12, 13]. We hypothesized that individual CFTR function measured by FIS is associated with long-term disease progression defined by rate of FEV₁pp decline and development of co-morbidities such as pancreatic insufficiency (PI), CF-related liver disease (CFRLD) and CF-related diabetes (CFRD). Such an association supports a potential role for FIS as biomarker for long-term disease progression, which is especially relevant to people with rare, uncharacterized CFTR genotypes or CFTR genotypes with varying clinical consequences.

MATERIALS AND METHODS

Study design and population

A longitudinal cohort study was conducted in Dutch people carrying mutations in the CFTR gene who are included in the Dutch Cystic Fibrosis Foundation Patient Registry (DCFFPR). Of all participants, intestinal organoids were generated before January 2020 and written informed consent was obtained to use their intestinal organoids and clinical data for the present study. This study was approved by the institutional review board of the University Medical Center Utrecht, The Netherlands.

Study parameters

The primary outcome variable was defined as long-term lung function decline, expressed as FEV1 percent predicted (FEV1pp), calculated according to global lung function initiative (GLI) guidelines [14]. Secondary outcome variables were occurrence of pancreatic insufficiency (PI), defined by fecal elastase < 200 µg/g, CF-related liver disease (CFRLD), defined by hepatic steatosis or cirrhosis confirmed by imaging, and occurrence of insulin-dependent CF-related diabetes (CFRD) defined by daily insulin treatment.

The primary explanatory variable of interest was forskolin induced swelling (FIS), defined by the relative size increase of intestinal organoids after 1h stimulation with 0.8 µM forskolin, quantified as area under the curve (AUC). Previous studies showed that discrimination between individual FIS responses was most optimal and correlated best with other *in vitro* and *in vivo* CFTR biomarkers when FIS was performed with 0.8 µM forskolin [11, 12]. Other included explanatory variables were: age in years at time of each lung function measurement; treatment status at time of each lung function measurement categorized as no CFTR modulator treatment, treatment with ivacaftor or with lumacaftor/ivacaftor; sex; sweat chloride concentration (SCC) in mmol/L; and genotype, categorized as class I-V or unclassified, defined by genotype class of the mildest of both mutations according to available literature (**supplementary table 1 and 2**). Additionally, genotypes were categorized in groups according to the combination of the following mutation types: insertion/deletion, nonsense, missense, splice and unknown.

Study procedures

Organoid measurements:

The generation of intestinal organoids from biopsies and subsequent fluid secretion assays (FIS-assays) were performed according to a previously described protocol [15]. Rectal biopsies were collected at one timepoint during the 9-year study period. The specific time-point of rectal biopsy collection varied per study participant, but was always prior to the start of modulator therapy. FIS-assays were performed between 2014 and 2020 by analysts who were blinded for genotype and clinical data. All FIS-assay experiments were conducted in duplicate and for the majority of the donors at multiple culturing time points with a maximum of 7 consecutive culture time points (n=7).

Clinical data collection:

Data on clinical study parameters were retrieved from the DCFFPR, independent of FIS-assay results. Annual best FEV1pp values between 2010 and 2018 were used to estimate lung function decline. Treatment status at the time of each lung function measurement was calculated based on start and stop dates of CFTR modulators as registered in the DCFFPR. For SCC, PI, CFRLD and CFRD, we only collected the most recent value registered before 2019 (or before CFTR modulator treatment initiation, if applicable), as repeated measurements were unavailable or inconsistently collected. For SCC, PI, CFRLD and CFRD, data was missing in 59 (34.1%), 63 (36.4%), 5 (2.9%) and 3 (1.7%) participants, respectively. SCC values were mostly missing for older participants, which may have been performed years before start of the registry in 2010 and were not archived within the local CF centers.

Statistical analysis

The association between age and long-term lung function decline was analyzed using a linear mixed effects model. FEV1pp was specified as outcome variable in the model, with FIS, SCC, genotype class (reference category: unclassified), sex (reference category: male), age, CFTR modulator treatment (reference category: none) and FIS*age as fixed effects, where the interaction term FIS*age reflected the difference in annual FEV1pp decline by FIS level. The model included a random intercept and random slope for age per subject, assuming a first order auto-regressive (cAR1) correlation structure. Conditional R² was calculated to assess complete model performance and marginal R² to estimate the relative contribution of the fixed effects.

To account for selection bias towards a milder phenotype in participants surviving to an older age, a subgroup analysis was conducted including measurements between 4-25 years, in which the relationship between age and FEV1pp decline can reasonably be assumed to be linear in this dataset (**figure 2a**). Sensitivity analyses were performed using genotype group, defined by the combination of mutation types, e.g. insertion/deletion, nonsense, missense, splice, unknown. Genotype group was used instead of genotype class, to assess whether the association of FIS with FEV1pp decline was influenced by categorization of genotype. To obtain reliable effect estimates and standard errors for genotype group, groups with less than 5 participants were excluded from this part of the analysis.

To compare the association of long-term FEV1pp decline with FIS versus SCC, four models were built which all included FIS, SCC, genotype class, sex, age and treatment as fixed effects. A baseline model was built without any interaction term, and the other three models were built with the addition of either the interaction term FIS*age, SCC*age or both FIS*age and SCC*age in the model. Performance of these models was compared using the Likelihood Ratio test.

Multilevel multiple imputation based on the method of chained equations [16] was used to handle missing SCC data in the linear mixed effects models. All analyses were performed on 20 imputed datasets (m=20, iterations=20) with pooling of the results.

CHAPTER 2

Secondary outcomes were analyzed using multivariable logistic regression, with FIS, SCC, sex, and age at the last study measurement as explanatory variables. Given the low proportion of outcome events within some of the genotype classes as well as within genotype groups (defined by the combination of the mutation types on both alleles), genotype could not be included in these analyses. In addition, CFTR modulator usage was not included as we only collected most recent values of PI, CFRLD and CFRD before modulator initiation. Nagelkerke's R² was calculated to assess model performance.

Single level multiple imputation [16] was used to handle missing data of SCC, PI and CFRD in the logistic regression models. The analyses were performed on 20 imputed datasets (m=20, iterations=20) with pooling of the results.

Significance levels were set at 0.05. All statistical analyses were performed with R version 4.1.1 using packages mice, micemd, nlme and lme4 in combination with the performance package.

RESULTS

Participant characteristics

In total, 173 participants carrying different CFTR genotypes provided written informed consent to collect intestinal organoid data and retrieve their clinical data from the DCFFPR. Participant characteristics are summarized in **table 1**. Three participants were excluded from the analysis because clinical data was not available. No data was excluded based on organoid measurements. Classification per mutation, individual genotypes with corresponding mutation classification and mutation group are listed in **supplementary table 1 and 2**, respectively.

N=173	
Age, median (IQR)	19.5 (9.5 – 30.5)
Sex, n (%)	
Male	87 (50.3)
Female	86 (49.7)
Mutation class, n (%)	
Class I	15 (8.7)
Class II	91 (52.5)
Class III	11 (6.4)
Class IV	10 (5.8)
Class V	23 (13.3)
Unclassified	23 (13.3)
CFTR modulator usage, n (%)	
Ivacaftor	16 (9.2)
Lumacaftor/ivacaftor	8 (4.6)
FIS, median (IQR)	141.3 (30.3 – 1176.3)
SCC, mean (SD)	92.6 (25.9)
Missing values, n (%)	59 (34.1)
FEV1pp, mean (SD)	75.9 (23.2)
Pancreatic function, n (%)	
Insufficient (fecal elastase <200 µg/g)	75 (43.4)
Sufficient (fecal elastase ≥ 200 µg/g)	35 (20.2)
Missing values	63 (36.4)
CF-related liver disease, n (%)	44 (25.4)
Missing values	5 (2.9)
CF-related diabetes, n (%)	25 (14.5)
Missing values	3 (1.7)

Table 1. Participant characteristics.

Age in years. Genotype: genotype class of the mildest of both mutations. FIS: Forskolin induced swelling, defined as the relative size increase of intestinal organoids (AUC) after 1h stimulation with 0.8 µmol/L forskolin. SCC: Sweat chloride concentration in mmol/L. FEV1pp: Forced expiratory volume in 1 second, percent predicted.

N=149, obs=1054	Coefficient (95% CI)	P-value
Age	-1.16 (-1.43 – -0.88)	<0.001*
FIS	-2.47 (-8.92 – 3.99)	0.454
FIS*age	0.32 (0.11 – 0.54)	0.004*
Treatment		
- none	Reference category	
- ivacaftor	7.99 (4.58 – 11.40)	<0.001*
- lumacaftor/ivacaftor	-3.83 (-8.28 – -0.62)	0.092
Sex		
- male	Reference category	
- female	-0.96 (-7.00 – 5.08)	0.754
Genotype class		
- unclassified	Reference category	
- class I	0.18 (-13.92 – 14.27)	0.980
- class II	5.13 (-5.76 – 16.01)	0.356
- class III	10.25 (-3.79 – 24.28)	0.152
- class IV	11.01 (-5.36 – 27.38)	0.187
- class V	-2.31 (-16.95 – 12.33)	0.757
SCC	-0.09 (-0.25 – 0.06)	0.239

Table 2: association of FIS with FEV1pp decline.

Regression coefficients of linear mixed effects model for FEV1pp. FEV1pp: Forced expiratory volume in 1 second, percent predicted. Age in years. FIS: Forskolin-induced swelling, defined as the relative size increase of intestinal organoids (AUC) after 1h stimulation with 0.8 µM/L forskolin, coefficient scaled 1:1000 AUC. SCC: Sweat chloride concentration in mmol/L. FIS*age indicates the difference in annual FEV1pp decline per 1000 AUC change in FIS level. Genotype class: CFTR protein function class of the mildest of both CFTR mutations. Pooled conditional R² = 0.979, marginal R² = 0.179. *Significance level P < 0.05.

Individual FIS responses

Individual FIS responses after 1 hour of stimulation with different forskolin concentrations are shown for all participants in **figure 1a**. Between-subject variability was most apparent at 0.8 µM and 5.0 µM forskolin, but no evident clustering was observed. Consistent with prior studies investigating relations between FIS and CF disease or biomarkers [11, 12, 17], our analyses were performed with FIS levels upon 0.8 µM forskolin stimulation. FIS data at 0.8 µM forskolin was skewed and highly variable among participants (median AUC 141.3, IQR: 30.3 – 1176.3 AUC, range: -268.0 – 4508.8 AUC; **figure 1a** and supplementary **figure 1a**) as well as within genotype classes (**figure 1b-c**) and between genotype groups, defined by the combination of the two mutation types (supplementary **figure 1b**). As expected, most organoid cultures that showed residual CFTR function (AUC>750) expressed genotypes belonging to class III-V (**figure 1c**). Surprisingly however, seven organoid cultures expressing genotypes categorized as class II mutation, a class for which no residual organoid swelling upon stimulation with 0.8 µM for one hour has been previously reported [11–13], exhibited moderate to high organoid swelling (**figure 1b**).

Association of Forskolin-induced Organoid Swelling with Long-term CF Disease Progression

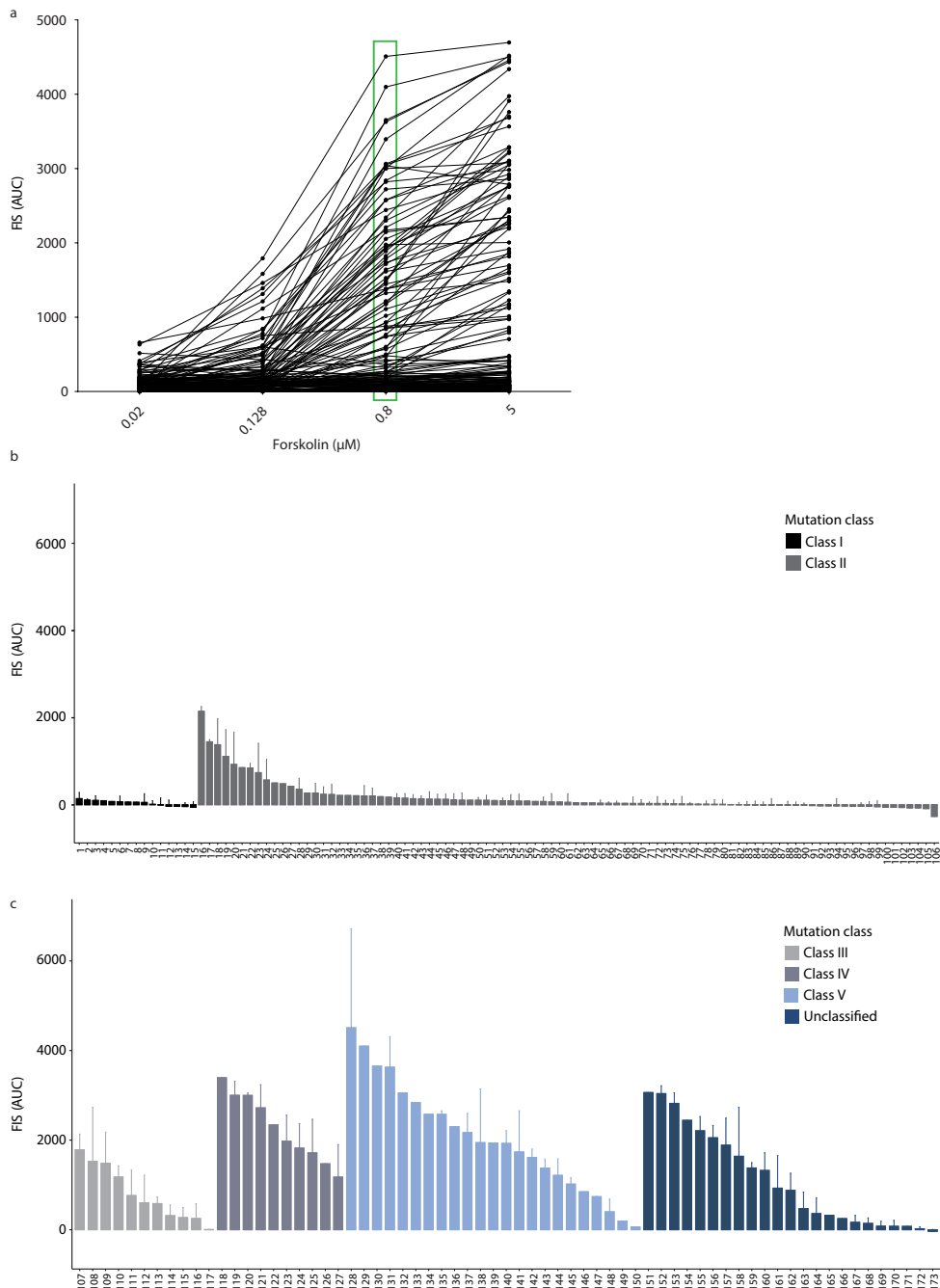


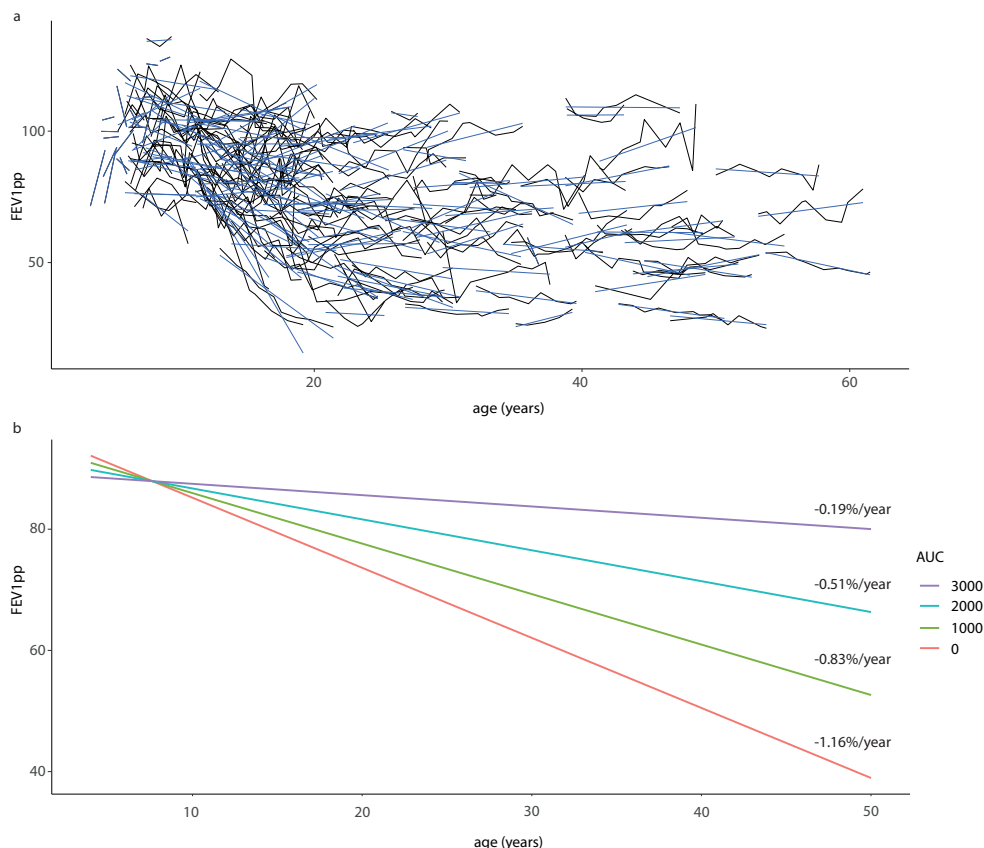
Figure 1. Forskolin-induced swelling (FIS) levels of organoids derived from the 173 study participants.

a) FIS levels, defined by relative size increase of intestinal organoids after 1h stimulation with four ascending forskolin concentrations, quantified as area under the curve (AUC). Each line represents swelling of organoids of individual study participants. Each data point (black dot) represents mean AUC of both technical ($n=2$) and biological replicates (ranging from $n=1$ to $n=7$). **b)** Waterfall plots of FIS responses at 0.8 μ M forskolin (highlighted by the green box) of all study participants grouped based on mutation class I or II or **c)** mutation class III-V or unclassified. Genotypes are categorized into one mutation class based on the mildest mutation class of the two alleles. Bars represent mean+SD of all replicates. The numbers on the x-axes represent participant number, whereas corresponding genotypes are specified in **supplementary table 2**.

Association of long-term FEV1pp decline and FIS

In total, 1054 observations of 149 participants with available FEV1pp measurements (**figure 2a**) were included in the analysis to assess the association of FIS with long-term FEV1pp decline. Linear mixed model analysis showed that average FEV1pp decline per year of age varied with FIS level, adjusted for sex, genotype class, CFTR modulator usage and SCC (**table 2**). To illustrate this association of FEV1pp decline by age with FIS, **figure 2b** shows that average annual FEV1pp – decline was -1.16% (95% CI: -1.43% – -0.88%; $p<0.001$) per year of age for participants with a FIS level of 0. Per 1000-points increase in AUC, FEV1pp decline was 0.32% (95% CI: 0.11% – 0.54%; $p=0.004$) per year of age lower, leading to a very mild estimated FEV1pp decline of only -0.19% per year for participants with an AUC of 3000. Model performance was excellent based on a pooled conditional R^2 of 0.979 (pooled marginal $R^2 = 0.179$).

The validity of these results was verified by assessing the potential impact of selection bias and confounding with separate subgroup and sensitivity analyses. A subgroup analysis in participants between 4-25 years showed a slightly higher average annual FEV1pp decline compared to the complete population (-1.57% per year (95% CI: -2.03% – -1.10%, $p<0.001$). Similar to the analysis in the complete cohort, FEV1pp decline varied by FIS level with 0.49% (95% CI: 0.03-0.96, $p=0.039$; **supplementary table 3 and supplementary figure 2**) per 1000-points change in AUC, suggesting a negligible impact of selection bias due to inclusion of people with CFTR mutations who have a milder phenotype and survive to an older age. Since at least one CFTR mutation was unclassified in 13.3% of participants (**figure 1c, table 1 and supplementary table 1 and 2**), a sensitivity analysis was performed in which we refitted both models with genotype group instead of genotype class, to assess whether the association of FIS with FEV1pp decline was influenced by categorization of genotype. The association of FIS with FEV1pp decline in these models was still statistically significant, comparable to the models categorizing genotype by mutation class (**supplementary table 4**).

**Figure 2. Association of FIS with long-term FEV1pp decline.**

- a)** Individual FEV1pp trajectories of study participants over time in years. Black lines represent individual observed FEV1pp trajectories, whereas the blue lines represent estimated average annual FEV1pp slope per individual.
- b)** Predicted FEV1pp decline based on linear mixed effects model coefficients in **table 2**, illustrating the association between different levels of residual CFTR function and long-term FEV1pp decline. Analysis was performed with FIS as continuous variable, yet for illustrative purposes predicted FEV1pp decline is plotted by steps of 1000 AUC. Average predicted annual FEV1pp decline per 1000 AUC is specified on the right. The lower limit of the x-axis was set at 4 years, because the feasibility and generalizability of ppFEV1 measurements is limited for younger children. Pooled conditional $R^2 = 0.977$, marginal $R^2 = 0.179$.

In addition, we compared the association of FIS with FEV1pp decline versus SCC with FEV1pp decline in similar linear mixed models. SCC alone was not significantly associated with FEV1pp decline ($p=0.121$; **supplementary table 5**). An association with SCC was also absent ($p=0.995$, **supplementary table 6**) when combined with FIS in the model, suggesting a stronger association of FIS with FEV1pp decline compared to SCC. These results, however, should be interpreted with caution due to the proportion of missing SCC data and the use of multiple imputation.

Association of CF-related co-morbidities and FIS

To investigate the association of FIS with the occurrence of other CF-related co-morbidities, we performed multivariable logistic regression with PI, CFRLD and CFRD, adjusted for age, sex and SCC. We found a significant association of FIS with the occurrence of PI (adjusted OR: 0.18, 95% CI: 0.07 – 0.46, p<0.001, Nagelkerke's R² = 0.496), CFRLD (adjusted OR: 0.18, 95% CI: 0.06 – 0.54, p=0.002, Nagelkerke's R² = 0.222) and CFRD (adjusted OR: 0.34, 95% CI: 0.12 – 0.97, p=0.044, Nagelkerke's R² = 0.195; **table 3 and figure 3a-d**). This indicates that the odds was on average 5-fold lower for developing PI and CFRLD and 3-fold lower for developing CFRD per 1000 point increase in FIS level. As illustrated in **table 3 and figure 3d**, age was also significantly associated with the odds of developing CFRD (adjusted OR 1.05, 95% CI: 1.02 – 1.08, p=0.004).

In combination with FIS, SCC was not associated with any of the CF-related co-morbidities, given the non-significant odds ratios of 1 (**table 3**). Even though multiple imputation of SCC may have influenced the strength of the associations, these results suggest that FIS is stronger associated with CF-related co-morbidities than SCC when comparing both biomarkers within the same model.

N=170	Pancreatic insufficiency		CF-related liver disease		CF-related diabetes	
	Odds ratio (95% CI)	P-value	Odds ratio (95% CI)	P-value	Odds ratio (95% CI)	P-value
FIS	0.18 (0.07 – 0.46)	<0.001*	0.18 (0.06 – 0.54)	0.002*	0.34 (0.12 – 0.97)	0.044*
Age	0.98 (0.93 – 1.02)	0.300	1.02 (0.99 – 1.05)	0.229	1.05 (1.02 – 1.08)	0.004*
Sex						
male	Reference category		Reference category		Reference category	
female	0.46 (0.14 – 1.46)	0.181	0.68 (0.32 – 1.44)	0.313	2.08 (0.81 – 5.37)	0.127
SCC	1.00 (0.97 – 1.04)	0.944	1.00 (0.98 – 1.02)	0.913	1.00 (0.97 – 1.04)	0.838

Table 3. Association of FIS with CF-related co-morbidities.

Adjusted odds ratios of multivariable logistic regression for pancreatic insufficiency, CF-related diabetes and CF-related liver disease. FIS: Forskolin-induced swelling, defined as the relative size increase of intestinal organoids (AUC) after 1h stimulation with 0.8 µM forskolin, coefficients scaled 1:1000 AUC. Age in years. SCC: sweat chloride concentration in mmol/L. Nagelkerke's R² pancreatic insufficiency = 0.496, CF-related liver disease = 0.223, CF-related diabetes = 0.195.

* Significance level P < 0.05.

Association of Forskolin-induced Organoid Swelling with Long-term CF Disease Progression

2
2

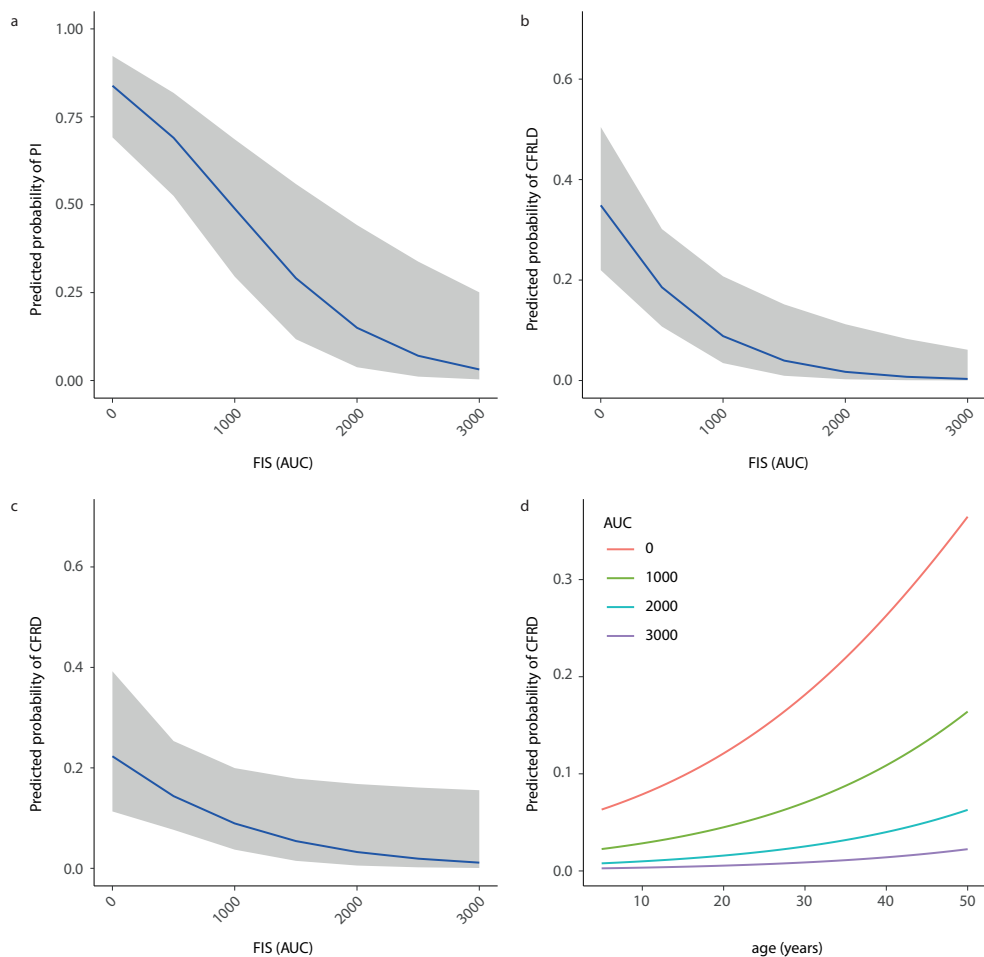


Figure 3. Association of FIS with CF-related comorbidities.

Association between residual CFTR function (illustrated by steps of 1000 AUC) and probability of developing pancreatic insufficiency (PI) (a), CF-related liver disease (CFRLD) (b) and CF-related diabetes (CFRD) (c). In addition to FIS, age is also associated with probability of developing CFRD (d). Nagelkerke's R²: PI = 0.496, CFRLD = 0.223, CFRD = 0.195.

DISCUSSION

This study shows that residual CFTR function quantified by FIS of patient-derived cystic fibrosis organoids is associated with long-term annual FEV1pp decline and odds of developing CF-related co-morbidities PI, CFRLD and CFRD, using 9-year longitudinal data of Dutch people with many distinct CFTR mutations and ages ranging from 0 to 61 years old.

Despite the influence of genetic modifiers and other non-CFTR dependent environmental factors on CF disease severity [1, 18–20], it was remarkable to observe that in vitro FIS on intestinal cells has such a broad association with many non-intestinal organ systems. It illustrates that fluid secretion properties of CFTR in intestinal organoids are reflective of or related to CFTR function across many tissues. As this study aimed to characterize in vitro CFTR function of many different common and rare CFTR mutations with FIS, the distribution of genotypes in our dataset does not correspond to the distribution of genotypes typical for the Dutch population, in which F508del/F508del is the most common genotype. Yet it improves generalizability of our results to the population with rare CFTR mutations for which this study is especially relevant. In addition, rectal biopsies of the participants that have received modulator therapy were collected prior to the start of modulator therapy, so intestinal organoid measurements were not influenced by treatment. Direct comparison of FIS with SCC revealed that FIS was stronger associated with long-term multi-organ disease expression compared to SCC, which has been the most important and well-validated biomarker of CF disease until now and is a commonly used endpoint to measure efficacy of CFTR modulating drugs [5, 6]. Although the association with SCC could have been influenced by missing values and type of imputation method, the difference between FIS and SCC might also be explained by a more precise and accurate estimation of CFTR function by FIS. FIS facilitates repeated measures and is completely CFTR dependent, which reduces the impact of technological and non-CFTR biological variability in the in vitro assay [10, 11], whereas a substantial part of variability in SCC is caused by technical and other non-CFTR dependent biological factors [5]. Additional studies with complete datasets including repeated measurements for more precise typing of SCC are required to confirm these findings. Alternatively, it would be interesting to explore if novel sweat-based readouts that may show a higher dependency on CFTR function might also lead to better correlations with clinical observations.

In addition, FIS could be compared with other biomarkers that are being used for CF diagnosis, such as NPD and ICM. Although NPD has been used to discriminate between non-CF and CF [3, 4, 6–9] its ability to accurately discriminate between pwCF with differential disease progression is limited. While ICM measurements are more sensitive and have a larger dynamic range than NPD, generation of a large dataset with repeated measures is hampered by the need for fresh rectal biopsies.

The data also suggested that FIS has additional value in the context of disease severity association beyond the current CFTR mutation classification system. For our statistical models, we needed to prioritize one particular mutational subclass for each CFTR mutation, which is difficult due to lack of detailed experimental data for many rare (missense) mutations and the impact of potential multiple mechanistic defects for single mutations [21]. This complicates

studies between mutation classification and relation with disease severity. CFTR function by FIS demonstrated a large variability in CFTR function between participants with different genotypes but also within genotype classes. FIS may thus have the potential to help to further refine patient-based classification systems beyond current genotype classification models. This might lead to more precise individual typing and prediction of disease, compared to the current classification of 'mild' and 'severe' CF phenotypes [22–24] or the CFTR2 based classification of mutations (CF-causing, varying clinical consequences, non-CF causing).

Rates of annual FEV₁pp decline in this study were within the same range as reported by other recent European studies, which also showed that annual FEV₁pp decline was lower for pwCF with a 'milder' disease severity as classified by genotype [25] or pancreatic status [26] and was highest in the age group between 18 and 28 years [26]. Moreover, our results are consistent with a previous study showing a more severe CF disease phenotype in terms of pulmonary and gastro-intestinal outcome parameters in infants with low FIS compared to infants with high FIS [12]. In line with our observations, Davis et al. also demonstrated that SCC by itself does not predict lung disease in pwCF [27].

In addition to the relation of FIS with disease severity, several studies already showed that average FIS response to CFTR modulators was also correlated with short-term clinical drug response across groups with different genotypes [11, 17] and in individuals with a variety of CFTR mutations [28]. On the other hand, different exploratory studies did not detect an association of FIS with short-term clinical response to lumacaftor/ivacaftor in pwCF homozygous for F508del [29] or heterozygous for the A455E mutation [30] or to ivacaftor in people with residual CFTR-function mutations [31]. These studies also did not demonstrate associations between FIS and biomarkers of CFTR function (NPD, SCC and ICM) [29] or FIS and SCC [30, 31], and no relations between any biomarker of CFTR function and clinical response. Also, treatment magnitude at group level was absent [29, 30] or limited [31], suggesting that the relative impact of CFTR-dependent factors over non-CFTR dependent factors to between-patient variations was lower as compared to the study of Berkers et al [28]. This generally lowers the ability of FIS or any individual outcome to correlate after a CFTR modulator treatment. Further research in larger study populations is therefore warranted to study the association of changes in FIS or other biomarkers of CFTR function with long-term clinical effects upon CFTR modulator therapy in homogeneous and heterogeneous populations with CF.

An important limitation of this research is the retrospective observational study design. We adjusted for several confounders, but were unable to account for other prognostic factors such as pulmonary exacerbations and sputum cultures. As 34% of SCC values was missing, we used multiple imputation methods to prevent bias due to selective missing data, but this may still have influenced the associations with SCC and its comparison with FIS. Potential impact of survival bias was minimized by our subgroup and sensitivity analyses, but could not completely be excluded. Additional prospective studies should be performed to confirm the predictive value of FIS in comparison with other biomarkers such as SCC, NPD and ICM, yet our findings are in line with previous work that already demonstrated the potential of FIS as biomarker of CF disease.

CHAPTER 2

In summary, this study showed that FIS of cystic fibrosis intestinal organoids is strongly associated with long-term FEV1pp decline and odds of developing different CF-related co-morbidities, suggesting that estimation of CFTR function by FIS could have important prognostic value for individual disease expression of multiple, critical organs that are affected by CF.

ACKNOWLEDGEMENTS

We would like to thank all participants who gave informed consent for generating and testing their individual organoids and the use of their data; all members of the research teams of the Dutch CF clinics that contributed to this work; and all colleagues of the HUB Organoid Technology for their help with generating intestinal organoids and performing FIS experiments.

FUNDING

This work was funded by grants of the Dutch Cystic Fibrosis Foundation (NCFS) as part of the HIT-CF Program and by ZonMW.

AUTHOR CONTRIBUTIONS

D.M. and E.d.P. contributed substantially to the design of the study, the acquisition, verification, analysis and interpretation of the data and have drafted the manuscript. S.W.F.S., A.M.V., J.E.B., E.K., H.O., M.C.H., P.v.M. G.B., K.M.d.W-d.G., S.H.-M., S.R.J., H.v.P., M.M.v.d.E., R.v.d.M., J.R., E.D., E.J.M.W., G.H.K., R.V. and D.D.Z.-v.O. contributed to the acquisition of study data and revised the manuscript. M.J.C.E. contributed to the design of the study, analysis and interpretation of data and revised the manuscript. C.K.v.d.E and J.M.B. have made substantial contributions to the conception and design of the study, interpretation of data and revised the manuscript.

DECLARATION OF INTERESTS

J.M.B. reports personal fees from Vertex Pharmaceuticals, Proteostasis Therapeutics, Eloxx Pharmaceuticals, Teva Pharmaceutical Industries and Galapagos, outside the submitted work; In addition, J.M.B. has a patent patent(s) related to the FIS-assay with royalties paid. C.K.v.d.E. reports grants from GSK, Nutricia, TEVA, Gilead, Vertex, ProQR, Proteostasis, Galapagos NV and Eloxx, outside the submitted work; In addition, C.K.v.d.E. has a patent 10006904 with royalties paid. G.H.K. reports grants from Lung Foundation of the Netherlands, Vertex Pharmaceuticals, UBBO EMMIUS foundation, GSK, TEVA the Netherlands, TETRI Foundation, European Union (H2020), outside the submitted work; and he has participated in advisory boards meetings to GSK and PURE-IMS outside the submitted work (Money to institution). P.v.M. reports financial compensation (money to institution) from Vertex for participation in a webinar, outside the submitted work. All other authors have nothing to disclose.

REFERENCES

- Cutting GR. Cystic fibrosis genetics: From molecular understanding to clinical application. *Nat. Rev. Genet.* 2015; 16: 45–56.
- Elborn JS. Cystic fibrosis. *Lancet (London, England)* England; 2016; 388: 2519–2531.
- Beekman JM, Sermet-Gaudelus I, de Boeck K, Gonska T, Derichs N, Mall MA, Mehta A, Martin U, Drumm M, Amaral MD. CFTR functional measurements in human models for diagnosis, prognosis and personalized therapy: Report on the pre-conference meeting to the 11th ECFS Basic Science Conference, Malta, 26-29 March 2014. *J. Cyst. Fibros. Off. J. Eur. Cyst. Fibros. Soc. Netherlands*; 2014; 13: 363–372.
- Bronsveld I, Mekus F, Bijman J, Ballmann M, Greipel J, Hundrieser J, Halley DJ, Laabs U, Busche R, De Jonge HR, Tümmeler B, Veeze HJ. Residual chloride secretion in intestinal tissue of deltaF508 homozygous twins and siblings with cystic fibrosis. The European CF Twin and Sibling Study Consortium. *Gastroenterology United States*; 2000; 119: 32–40.
- Collaco JM, Blackman SM, Raraigh KS, Corvol H, Rommens JM, Pace RG, Boelle P-Y, McGready J, Sosnay PR, Strug LJ, Knowles MR, Cutting GR. Sources of Variation in Sweat Chloride Measurements in Cystic Fibrosis. *Am. J. Respir. Crit. Care Med.* 2016; 194: 1375–1382.
- De Boeck K, Kent L, Davies J, Derichs N, Amaral M, Rowe SM, Middleton P, de Jonge H, Bronsveld I, Wilschanski M, Melotti P, Danner-Boucher I, Boerner S, Fajac I, Southern K, de Nooijer RA, Bot A, de Rijke Y, de Wachter E, Leal T, Vermeulen F, Hug MJ, Rault G, Nguyen-Khoa T, Barreto C, Proesmans M, Sermet-Gaudelus I. CFTR biomarkers: time for promotion to surrogate end-point. *Eur. Respir. J. England*; 2013; 41: 203–216.
- Kyrilli S, Henry T, Wilschanski M, Fajac I, Davies JC, Jais J-P, Sermet-Gaudelus I. Insights into the variability of nasal potential difference, a biomarker of CFTR activity. *J. Cyst. Fibros. Off. J. Eur. Cyst. Fibros. Soc. Netherlands*; 2020; 19: 620–626.
- Mall M, Kreda SM, Mengos A, Jensen TJ, Hirtz S, Seydewitz HH, Yankaskas J, Kunzelmann K, Riordan JR, Boucher RC. The DeltaF508 mutation results in loss of CFTR function and mature protein in native human colon. *Gastroenterology United States*; 2004; 126: 32–41.
- Minso R, Schulz A, Dopfer C, Alfeis N, Barneveld A van, Makartian-Gyulumyan L, Hansen G, Junge S, Müller C, Ringshausen FCC, Sauer-Heilborn A, Stanke F, Stolpe C, Tamm S, Welte T, Dittrich A-M, Tümmeler B. Intestinal current measurement and nasal potential difference to make a diagnosis of cases with inconclusive CFTR genetics and sweat test. *BMJ open Respir. Res.* 2020; 7.
- Dekkers JF, Wiegerinck CL, de Jonge HR, Bronsveld I, Janssens HM, de Winter-de Groot KM, Brandsma AM, de Jong NWM, Bijvelds MJC, Scholte BJ, Nieuwenhuis EES, van den Brink S, Clevers H, van der Ent CK, Middendorp S, Beekman JM. A functional CFTR assay using primary cystic fibrosis intestinal organoids. *Nat. Med. United States*; 2013; 19: 939–945.
- Dekkers JF, Berkers G, Kruisselbrink E, Vonk A, de Jonge HR, Janssens HM, Bronsveld I, van de Graaf EA, Nieuwenhuis EES, Houwen RHJ, Vleggaar FP, Escher JC, de Rijke YB, Majoor CJ, Heijerman HGM, de Winter-de Groot KM, Clevers H, van der Ent CK, Beekman JM. Characterizing responses to CFTR-modulating drugs using rectal organoids derived from subjects with cystic fibrosis. *Sci. Transl. Med. United States*; 2016; 8: 344ra84.
- de Winter-de Groot KM, Janssens HM, van Uum RT, Dekkers JF, Berkers G, Vonk A, Kruisselbrink E, Oppelaar H, Vries R, Clevers H, Houwen RHJ, Escher JC, Elias SG, de Jonge HR, de Rijke YB, Tiddens HAWM, van der Ent CK, Beekman JM. Stratifying infants with cystic fibrosis for disease severity using intestinal organoid swelling as a biomarker of CFTR function. *Eur. Respir. J. England*; 2018; 52.
- de Winter-de Groot KM, Berkers G, Marck-van der Wilt REP, van der Meer R, Vonk A, Dekkers JF, Geerdink M, Michel S, Kruisselbrink E, Vries R, Clevers H, Vleggaar FP, Elias SG, Heijerman HGM, van der Ent CK, Beekman JM. Forskolin-induced swelling of intestinal organoids correlates with disease severity in adults with cystic fibrosis and homozygous F508del mutations. *J. Cyst. Fibros. Off. J. Eur. Cyst. Fibros. Soc. Netherlands*; 2020; 19: 614–619.

CHAPTER 2

14. Quanjer PH, Stanojevic S, Cole TJ, Baur X, Hall GL, Culver BH, Enright PL, Hankinson JL, Ip MSM, Zheng J, Stocks J. Multi-ethnic reference values for spirometry for the 3-95-yr age range: the global lung function 2012 equations. *Eur. Respir. J.* 2012; 40: 1324–1343.
15. Vonk AM, van Mourik P, Ramalho AS, Silva IAL, Statia M, Kruisselbrink E, Suen SWF, Dekkers JF, Vleggaar FP, Houwen RHJ, Mullenders J, Boj SF, Vries R, Amaral MD, de Boeck K, van der Ent CK, Beekman JM. Protocol for Application, Standardization and Validation of the Forskolin-Induced Swelling Assay in Cystic Fibrosis Human Colon Organoids. *STAR Protoc.* 2020; 1: 100019.
16. van Buuren S. Flexible Imputation of Missing Data [Internet]. 2nd editio. Chapman & Hall/CRC; 2018. Available from: <https://stefvanbuuren.name/fimd/>.
17. Ramalho AS, Fürstová E, Vonk AM, Ferrante M, Verfaillie C, Dupont L, Boon M, Proesmans M, Beekman JM, Sarouk I, Vazquez Cordero C, Vermeulen F, De Boeck K. Correction of CFTR function in intestinal organoids to guide treatment of cystic fibrosis. *Eur. Respir. J.* England; 2021; 57.
18. Collaco JM, Blackman SM, McGready J, Naughton KM, Cutting GR. Quantification of the relative contribution of environmental and genetic factors to variation in cystic fibrosis lung function. *J. Pediatr.* 2010; 157: 802–803.
19. Santis G, Osborne L, Knight RA, Hodson ME. Independent genetic determinants of pancreatic and pulmonary status in cystic fibrosis. *Lancet* (London, England) England; 1990; 336: 1081–1084.
20. Weiler CA, Drumm ML. Genetic influences on cystic fibrosis lung disease severity. *Front. Pharmacol.* 2013; 4: 40.
21. Veit G, Avramescu RG, Chiang AN, Houck SA, Cai Z, Peters KW, Hong JS, Pollard HB, Guggino WB, Balch WE, Skach WR, Cutting GR, Frizzell RA, Sheppard DN, Cyr DM, Sorscher EJ, Brodsky JL, Lukacs GL. From CFTR biology toward combinatorial pharmacotherapy: expanded classification of cystic fibrosis mutations. *Mol. Biol. Cell* 2016; 27: 424–433.
22. McKone EF, Emerson SS, Edwards KL, Aitken ML. Effect of genotype on phenotype and mortality in cystic fibrosis: a retrospective cohort study. *Lancet* (London, England) England; 2003; 361: 1671–1676.
23. McKone EF, Goss CH, Aitken ML. CFTR genotype as a predictor of prognosis in cystic fibrosis. *Chest United States*; 2006; 130: 1441–1447.
24. US CF Foundation, Johns Hopkins University TH for SC. The Clinical and Functional TRanslation of CFTR (CFTR2) [Internet]. 2011. Available from: <http://cftr2.org>.
25. De Boeck K, Zolin A. Year to year change in FEV(1) in patients with cystic fibrosis and different mutation classes. *J. Cyst. Fibros. Off. J. Eur. Cyst. Fibros. Soc. Netherlands*; 2017; 16: 239–245.
26. Caley L, Smith L, White H, Peckham DG. Average rate of lung function decline in adults with cystic fibrosis in the United Kingdom: Data from the UK CF registry. *J. Cyst. Fibros. Off. J. Eur. Cyst. Fibros. Soc. Netherlands*; 2020; .
27. Davis PB, Schluchter MD, Konstan MW. Relation of sweat chloride concentration to severity of lung disease in cystic fibrosis. *Pediatr. Pulmonol.* United States; 2004; 38: 204–209.
28. Berkers G, van Mourik P, Vonk AM, Kruisselbrink E, Dekkers JF, de Winter-de Groot KM, Arends HGM, Marck-van der Wilt REP, Dijkema JS, Vanderschuren MM, Houwen RHJ, Heijerman HGM, van de Graaf EA, Elias SG, Majoor CJ, Koppelman GH, Roukema J, Bakker M, Janssens HM, van der Meer R, Vries RGJ, Clevers HC, de Jonge HR, Beekman JM, van der Ent CK. Rectal Organoids Enable Personalized Treatment of Cystic Fibrosis. *Cell Rep.* United States; 2019; 26: 1701-1708.e3.
29. Graeber SY, van Mourik P, Vonk AM, Kruisselbrink E, Hirtz S, van der Ent CK, Mall MA, Beekman JM. Comparison of Organoid Swelling and In Vivo Biomarkers of CFTR Function to Determine Effects of Lumacaftor-Ivacaftor in Patients with Cystic Fibrosis Homozygous for the F508del Mutation. *Am. J. Respir. Crit. Care Med.* United States; 2020. p. 1589–1592.

Association of Forskolin-induced Organoid Swelling with Long-term CF Disease Progression

30. Berkers G, van der Meer R, Heijerman H, Beekman JM, Boj SF, Vries RGJ, van Mourik P, Doyle JR, Audhya P, Yuan ZJ, Kinnman N, van der Ent CK. Lumacaftor/ivacaftor in people with cystic fibrosis with an A455E-CFTR mutation. *J. Cyst. Fibros. Off. J. Eur. Cyst. Fibros. Soc. Netherlands*; 2021; 20: 761–767.
31. Kerem E, Cohen-Cymberknob M, Tsabari R, Wilschanski M, Reiter J, Shoseyov D, Gileles-Hillel A, Pugatsch T, Davies JC, Short C, Saunders C, DeSouza C, Sullivan JC, Doyle JR, Chandarana K, Kinnman N. Ivacaftor in People with Cystic Fibrosis and a 3849+10kb C-T or D1152H Residual Function Mutation. *Ann. Am. Thorac. Soc.* 2021; 18: 433–441.

SUPPLEMENTARY INFORMATION

SUPPLEMENTARY TABLES

variant cDNA name	variant protein name	variant legacy name	classification [REF]	CFTR2 mutation type	CFTR1 reference to original report	Rationale for classification
c.948delT	p.Phe316LeufsX12	1078delT	I	Ins/del	This variant causes CF when combined with another CF-causing variant. This variant causes pancreatic insufficiency when combined with another variant that causes pancreatic insufficiency.	[1]
c.1006_1007insG	p.Ile336SerfsX28	1138insG	I	Ins/del	This variant causes CF when combined with another CF-causing variant. This variant causes pancreatic insufficiency when combined with another variant that causes pancreatic insufficiency.	CFTR1 reference [3]: Schwarz M, Malone G, Super M. 1992-03-16 (reference not found on PubMed).
c.1210_1delG	No protein name	1342_1delG	I	Splice	Not described in CFTR2.	CFTR1 reference [3]: Huang Q, Yuan XW, Zielenki J. 2008-07-11 (reference not found on PubMed).
c.1211delG	p.Gly404AspfsX38	1343delG	I	Ins/del	This variant causes CF when combined with another CF-causing variant. This variant causes pancreatic insufficiency when combined with another variant that causes pancreatic insufficiency.	Not described in CFTR1 [3].
						CFTR1 reference [3]: Schwarz M, Malone G, Super M. 1992-03-16 (reference not found on PubMed).
						CFTR1 reference [3]: Huang Q, Yuan XW, Zielenki J. 2008-07-11 (reference not found on PubMed).
						CFTR1 reference [3]: Schwarz M, Malone G, Super M. 1992-03-16 (reference not found on PubMed).

variant cDNA name	variant protein name	variant legacy name	Classification [REF]	muta-tion type	CFTR2	CFTR1 reference to original report	Rationale for classification
c.1545_154_6delTA	p.Tyr515X	1677deltaT	I	Ins/del	This variant causes CF when combined with another CF-causing variant. This variant causes pancreatic insufficiency when combined with another variant that causes pancreatic insufficiency.	[5]	Class I CFTR protein synthesis defect based on sequence analysis (frameshift leading to downstream PTC) that affects a critical part of the protein and is associated with Pi-CF [2].
c.1585+1G>A	No protein name	1717-1G->A	I	Splice	This variant causes CF when combined with another CF-causing variant. This variant causes pancreatic insufficiency when combined with another variant that causes pancreatic insufficiency.	[6]	Class I CFTR protein synthesis defect based on sequence analysis (frameshift leading to downstream PTC) that affects a critical part of the protein and is associated with Pi-CF [2].
c.1679+1G>C	No protein name	1811+1G->C	I	Splice	This variant causes CF when combined with another CF-causing variant. This variant causes pancreatic insufficiency when combined with another variant that causes pancreatic insufficiency.	[7]	Class I CFTR protein synthesis defect based on sequence analysis (a splice site mutation that affects an invariant splice site sequence, leading to improper splicing of the intron-exon boundary) associated with Pi-CF [6].
c.1680+1G>A	No protein name	1812-1G->A	I	Splice	This variant causes CF when combined with another CF-causing variant. This variant causes pancreatic insufficiency when combined with another variant that causes pancreatic insufficiency.	[8]	Class I CFTR protein synthesis defect based on sequence analysis (a splice site mutation that affects an invariant splice site sequence, leading to improper splicing of the intron-exon boundary) associated with Pi-CF [2].
c.1681_1682insC	p.Val562SerfsX6	1813insC	I	Ins/del	Not described in CFTR2.	CFTR1 reference [3]; Scheffer H, Wu Y, Hofstra R, Looman M, Buys C 1996-10-23 (reference not found on PubMed).	Class I CFTR protein synthesis defect based on sequence analysis (frameshift leading to downstream PTC) that affects a critical part of the protein.

variant cDNA name	variant protein name	variant legacy name	Classification [REF]	muta-tion type	CFTR2	CFTR1 reference to original report	Rationale for classification
c.1766+5G>T	No protein name	1898+5G->T	V	Splice	This variant causes CF when combined with another CF-causing variant. 67% (N=4) of patients in CFTR2 who have this variant are pancreatic insufficient.	[9]	Class V Splice mutation associated with reduced wild type CFTR function based on sequence analysis (intronic variant outside invariant splice site) and associated with some PS-CF [9].
c.1911de IG	p.Gln637 HisfsX26	2043delG	I	Ins/del	This variant causes CF when combined with another CF-causing variant. This variant causes pancreatic insufficiency when combined with another variant that causes pancreatic insufficiency.	[10]	Class I CFTR protein synthesis defect based on sequence analysis (frameshift leading to downstream PTC) that affects a critical part of the protein and is associated with PI-CF in CFTR2.
c.2051-2052de IAIAsnfsG	p.Lys684 SerfsX38	2183AA>G	I	ins/del	This variant causes CF when combined with another CF-causing variant. This variant causes pancreatic insufficiency when combined with another variant that causes pancreatic insufficiency.	CFTR1 reference [3]; Leoni GB, Rosatelli MC, Cao A 1994-01-13 (reference not found on PubMed).	Class I CFTR protein synthesis defect based on sequence analysis (frameshift leading to downstream PTC) that affects a critical part of the protein and is associated with PI-CF [2, 11].
c.2052delA	p.Lys684 AsnfsX38	2184delA	I	Ins/del	This variant causes CF when combined with another CF-causing variant. This variant causes pancreatic insufficiency when combined with another variant that causes pancreatic insufficiency.	[12]	Class I CFTR protein synthesis defect based on sequence analysis (frameshift leading to downstream PTC) that affects a critical part of the protein and is associated with PI-CF [2, 13].
c.2052 2053insA	p.Gln685ThrfsX4	2184insA	I	Ins/del	This variant causes CF when combined with another CF-causing variant. This variant causes pancreatic insufficiency when combined with another variant that causes pancreatic insufficiency.	CFTR1 reference [3]; Kalin N, Dork T, Tummier B 1992-01-02 (reference not found on PubMed).	Class I CFTR protein synthesis defect based on sequence analysis (frameshift leading to downstream PTC) that affects a critical part of the protein and is associated with PI-CF [2, 13].
c.2657+5G>A	No protein name	2789+5G->A	V	Splice	This variant causes CF when combined with another CF-causing variant. Patients with CF who have this variant are likely to be pancreatic sufficient.	[14]	Class V Splice mutation associated with reduced wild type CFTR function based on sequence analysis (intronic variant outside invariant splice site) and associated with PS-CF [2, 14].

variant cDNA name	variant protein name	variant legacy name	Classi-fication [REF]	muta-tion type	CFTR2	CFTR1 reference to original report	Rationale for classification
c.2988+1G>A	No protein name	3120+1G->A	I	Splice	This variant causes CF when combined with another CF-causing variant. This variant causes pancreatic insufficiency when combined with another variant that causes pancreatic insufficiency.	[15]	Class I CFTR protein synthesis defect based on sequence analysis (a splice site mutation that affects an invariant splice site sequence, leading to improper splicing of the intron-exon boundary) associated with PI-CF [2].
c.3140-26A>G	No protein name	3272-26A->G	V	Splice	This variant causes CF when combined with another CF-causing variant. Patients with CF who have this variant are likely to be pancreatic sufficient.	[10]	Class V splice mutation associated with reduced wild type CFTR function based on sequence analysis (intronic variant outside invariant splice site) and associated with PS-CF [2].
c.233_234insT	p.Trp79LeufsX32	365-366insT	I	Ins/del	This variant causes CF when combined with another CF-causing variant. This variant causes pancreatic insufficiency when combined with another variant that causes pancreatic insufficiency.	CFTR1 reference [3]; claudsters M, Altieri JP, Guitard C 2004-09-23 (reference not found on PubMed).	Class I CFTR protein synthesis defect based on sequence analysis (frameshift leading to downstream PTC) that affects a critical part of the protein and is associated with PI-CF in CFTR2.
c.3528d elC	p.Lys1177SerfsX15	3659delC	I	Ins/del	This variant causes CF when combined with another CF-causing variant. This variant causes pancreatic insufficiency when combined with another variant that causes pancreatic insufficiency.	[6]	Class I CFTR protein synthesis defect based on sequence analysis (frameshift leading to downstream PTC) that affects a critical part of the protein and is associated with PI-CF [2].
c.3717+1219C>T	No protein name	3849+10kbC>T	V	Splice	This variant causes CF when combined with another CF-causing variant. Patients with CF who have this variant are likely to be pancreatic sufficient.	[16]	Class V splice mutation associated with reduced wild type CFTR function based on sequence analysis (intronic variant outside invariant splice site) and associated with PS-CF [2].

variant cDNA name	variant protein name	variant legacy name	Classification [REF]	mutation type	CFTR1 reference to original report	Rationale for classification
c.3717+5G>T	No protein name	3849+5G->T	Unclassified	Splice	Not described in CFTR2.	Not described in CFTR1 [3].
						Splice mutation that is difficult to classify due to lack of data on residual CFTR function. This variant is outside the invariant splice site and likely associated with limited wild type CFTR function (class V), but this cannot be verified as the variant cDNA name, protein name and legacy name show no hits in Pubmed in the context of CF. The mutation is also not described in CFTR1 or CFTR2.
c.3773_3774insT	p.Leu1258PhefsX7	3905insT	I	Ins/del	CFTR1 reference [3]; Malik N, Hofmann S, Bosch-AlJaddoo N, Rutishauser M, Buhler E 1991-07-30 (reference not found on PubMed).	Class I CFTR protein synthesis defect based on sequence analysis (frameshift leading to downstream PTC) that affects a critical part of the protein and is associated with PI-CF [2].
c.262_263delTT	p.Leu881lefsX22	394delTT	I	Ins/del	This variant causes CF when combined with another CF-causing variant. This variant causes pancreatic insufficiency when combined with another variant that causes pancreatic insufficiency. [17]	Class I CFTR protein synthesis defect based on sequence analysis (frameshift leading to downstream PTC) that affects a critical part of the protein and is associated with PI-CF [2].
c.3884_3885insT	p.Ser1297PhefsX5	4016insT	I	Ins/del	This variant causes CF when combined with another CF-causing variant. This variant causes pancreatic insufficiency when combined with another variant that causes pancreatic insufficiency. [18]	Class I CFTR protein synthesis defect based on sequence analysis (frameshift leading to downstream PTC) that affects a critical part of the protein and is associated with PI-CF [2].

variant cDNA name	variant protein name	variant legacy name	Classi-fication [REF]	muta-tion type	CFTR2	CFTR1 reference to original report	Rationale for classification
C.4242 +2>C	No protein name	4374+2 ->C	I	Splice	Not described in CFTR2.	CFTR1 Reports 2 patients with suspected CF [3], unpublished.	Class I CFTR protein synthesis defect based on sequence analysis (a splice site mutation that affects an invariant splice site sequence (+1,+2,-1,-2), leading to improper splicing of the intron-exon boundary). Although no disease classification is present in CFTR2, we classify invariant splice site sequence variations as class I defects due to the critical impact of invariant splice mutations on splicing. The variant cDNA name, protein name and legacy name show no hits in PubMed in the context of CF.
c.4251delA	p.Glu1418A>fsX14	4382delA	V	Ins/del	This variant causes CF when combined with another CF-causing variant. Patients with CF who have this variant are likely to be pancreatic sufficient.	[19]	Class V mutation caused by a premature stop in the late C-terminus of the CFTR protein that is associated with residual CFTR function as evident by PS-CF status [2].
c.1210-33_1210-6GT[13]T[4]	No protein name	5T;TG13	V	Splice	This variant has varying consequences. Some patients with this variant have CF, when combined with another CF-causing variant. Other patients with this variant do not have CF when combined with another CF-causing variant. Patients with CF who have this variant are likely to be pancreatic sufficient.	Not described in CFTR1 [3].	class V Splice mutation based on sequence analysis (outside of the invariant splice sequence domain (+1,+2,-1,-2)) that affects expression level of wild type CFTR [20]. Associated with high residual CFTR function in intestinal organoids [21]. Varying clinical consequences are described in CFTR2 and following studies [22-24].
c.579+1G>T	No protein name	711+1G>T	I	Splice	This variant causes CF when combined with another CF-causing variant. This variant causes pancreatic insufficiency when combined with another variant that causes pancreatic insufficiency.	[25]	Class I CFTR protein synthesis defect based on sequence analysis (a splice site mutation that affects an invariant splice site sequence, leading to improper splicing of the intron-exon boundary) and associated with PI-CF [2].

variant cDNA name	variant protein name	variant legacy name	Classification [REF]	muta-tion type	CFTR1	reference to original report	Rationale for classification
c.1364C>A	p.Ala455Glu	A455E		Mis-sense	This variant causes CF when combined with another CF-causing variant. Patients with CF who have this variant are likely to be pancreatic sufficient.	[6]	Class I trafficking defect associated with normal B band and low C band, but classification is complex based on multiple observations. A455E shows comparable single channel characteristics as wild type CFTR [26] but strongly reduced C-band upon expression in heterologous expression systems and in primary epithelial CF cells, yet more C band when compared to F508del [2, 27, 28]. A455E is also responsive to VX809 or other correctors, and to potentiators [28, 29]. Based on these data, we classified the primary defect as a class II processing defect.
c.137C>A	p.Ala46Asp	A46D		Mis-sense	This variant causes CF when combined with another CF-causing variant. Insufficient data on pancreatic status.	[30]	Class II trafficking defect based on low C band in FRT cells and no response to ivacaftor [28].
c.(1584+1_1585-1)_ (1679+1_1680-1)del	No protein name	CFTRdelle ₁₁		Ins/del	This variant causes CF when combined with another CF-causing variant. This variant causes pancreatic insufficiency when combined with another variant that causes pancreatic insufficiency.	[31]	Class I CFTR protein synthesis defect based on DNA sequence analysis (large genetic deletion) associated with Pi-CF in CFTR2.
c.(2988+1_2989-1)_ (3367+1_3368-1)del	No protein name	CFTRdelle _{17a,17b}		Ins/del	This variant causes CF when combined with another CF-causing variant. This variant causes pancreatic insufficiency when combined with another variant that causes pancreatic insufficiency.	Not described in CFTR1 [3].	Class I CFTR protein synthesis defect based on DNA sequence analysis (large genetic deletion) associated with Pi-CF [2, 32].
No cDNA name	No protein name	CFTRdelle _{19,20}		Ins/del	Not described in CFTR2.	Not described in CFTR1 [3].	Class I CFTR protein synthesis defect based on DNA sequence analysis (large genetic deletion) associated with Pi-CF [33].

variant cDNA name	variant protein name	variant legacy name	Classi-fication [REF]	muta-tion type	CFTR2	CFTR1 reference to original report	Rationale for classification
c.54-5940_273+10250 del21kb	p.Ser18ArgfsX16	CFTRdele 2,3	I	Ins/del	This variant causes CF when combined with another CF-causing variant. This variant causes pancreatic insufficiency when combined with another variant that causes pancreatic insufficiency.	[34]	Class I CFTR protein synthesis defect based on DNA sequence analysis (large genetic deletion and downstream in frame PTC) associated with PI-CF [2].
c.3454G>C	p.Asp1152His	D1152H	IV	Mis-sense	This variant has varying consequences. Some patients with this variant have CF, when combined with another CF-causing variant. Other patients with this variant do not have CF when combined with another CF-causing variant. Patients with CF who have this variant are likely to be pancreatic sufficient.	[35]	Class IV mutation associated with altered pore function. D1152H is associated with a selective bicarbonate defective (CFTRBD) conductance [2, 36].
c.178G>T	p.Glu60X	E60X	I	Non-sense	This variant causes CF when combined with another CF-causing variant. This variant causes pancreatic insufficiency when combined with another variant that causes pancreatic insufficiency.	CFTR1 reference [3]; Malone G, Schwarz M, Super M 1991-11-22 (reference not available for full access).	Class I CFTR protein synthesis defect based on sequence analysis (introduced PTC) that affects a critical part of the protein and is associated with PI-CF [2].
c.2188G>T	p.Glu730X	E730X	I	Non-sense	Not described in CFTR2.	[37]	Class I CFTR protein synthesis defect based on sequence analysis (introduced PTC) that affects a critical part of the protein.
c.274G>A	p.Glu92Lys	E92K	II	Mis-sense	This variant causes CF when combined with another CF-causing variant. 44% (N=17) of patients in CFTR2 who have this variant are pancreatic insufficient.	[38]	Class II trafficking defect associated with strongly reduced CFTR maturation (Cband) in heterologous cells systems [39, 40], and no response to ivacaftor [28]. Strong rescue by VX809 [2, 41].

variant cDNA name	variant protein name	variant legacy name	Classifi-cation [REF]	muta-tion type	CFTR1 reference to original report	Rationale for classification
c.1521_1523del CTT	p.Phe508del	F508del		Ins/del	This variant causes CF when combined with another CF-causing variant. This variant causes pancreatic insufficiency when combined with another variant that causes pancreatic insufficiency.	[42–44]
c.3745G>A	p.Gly1249Arg	G1249R	Unclassi-fied	Miss-sense	This variant causes CF when combined with another CF-causing variant. 57% (N=4) of patients in CFTR2 who have this variant are pancreatic insufficient.	[46]
c.532G>A	p.Gly178Arg	G178R		Miss-sense	This variant causes CF when combined with another CF-causing variant. 75% (N=57) of patients in CFTR2 who have this variant are pancreatic insufficient.	[25]
c.1381G>A	p.Gly461Arg	G461R	Unclassi-fied	Miss-sense	Not described in CFTR2.	Not described in CFTR1 [3].
						lvacaftor responsive gating mutation associated with normal C band expression in heterologous expression models [47] and associated with PI-CF [2].
						F508del/G461R shows response to ivacaftor therapy both in vitro (organoids) and in vivo [48], however no papers have been published that experimentally characterize CFTR-protein. We therefore categorized this mutation as unclassified.

variant cDNA name	variant protein name	variant legacy name	Classi-fication [REF]	muta-tion type	CFTR1 reference to original report	Rationale for classification	
c.1624G>T	p.Gly542X	G542X	I	Non-sense	This variant causes CF when combined with another CF-causing variant. This variant causes pancreatic insufficiency when combined with another variant that causes pancreatic insufficiency.	[6]	Class I CFTR protein synthesis defect based on sequence analysis (introduced PTC) that affects a critical part of the protein and is associated with PI-CF [2].
c.1648G>T	p.Gly550X	G550X	I	Non-sense	This variant causes CF when combined with another CF-causing variant. This variant causes pancreatic insufficiency when combined with another variant that causes pancreatic insufficiency.	CFTR1 reference [3]; Deiman C, Deelan W, Halley D 1992-02-25 (reference not found on PubMed)	Class I CFTR protein synthesis defect based on sequence analysis (introduced PTC) that affects a critical part of the protein and is associated with PI-CF.
c.1882G>A	p.Gly628Arg	G628R	II	Mis-sense	This variant causes CF when combined with another CF-causing variant. Patients with CF who have this variant are likely to be pancreatic sufficient.	[10]	Class II trafficking defect associated with strongly reduced C band expression in heterologous expression model and rescue by the corrector miglustat [49]. Based on these results we have classified this mutation as class II.
c.254G>A	p.Gly85Glu	G85E	II	Mis-sense	This variant causes CF when combined with another CF-causing variant. This variant causes pancreatic insufficiency when combined with another variant that causes pancreatic insufficiency.	[25]	Class II trafficking defect associated with strongly reduced C band expression in heterologous expression model and no response to ivacaftor [2, 28].
c.2908G>C	p.Gly970Arg	G970R	I	Splice	This variant causes CF when combined with another CF-causing variant. This variant causes pancreatic insufficiency when combined with another variant that causes pancreatic insufficiency.	[37]	Fidler et al showed that the G>C change in the last position of the canonical 5' splice donor site of exon 17 weakens the likelihood that this position will be recognized as a splice donor site and showed evidence that the G970R mutation must be reclassified primarily as a splice mutation [50], in contrast with previous work suggesting a gating defect [51].

variant cDNA name	variant protein name	variant legacy name	Classifi-cation [REF]	muta-tion type	CFTR1 reference to original report	Rationale for classification
c.3080T>C	p.Ile1027Thr	I1027T	Unclassi-fied	Mis-sense	This variant does not cause CF when combined with another CF-causing variant. There may patients in the CFTR2 database with this variant who have CF, but this variant is not the cause of their CF.	Non-CF causing polymorphism that was present here in cis with F508del which designated the complex allele as class II [2].
c.1007T>A	p.Ile336Lys	I336K	II	Mis-sense	This variant causes CF when combined with another CF-causing variant. Patients with CF who have this variant are likely to be pancreatic sufficient.	[37]
c.1519_1521del-ATC	p.Ile507del	I507del	II	Ins/del	This variant causes CF when combined with another CF-causing variant. This variant causes pancreatic insufficiency when combined with another variant that causes pancreatic insufficiency.	[52]
No cDNA name	No protein name	IVS11-1G->C	I	Splice	Not described in CFTR2.	Not described in CFTR1 [3].
No cDNA name	p.Leu1034Pro	L1034P	Unclassi-fied	Mis-sense	Not described in CFTR2.	Not described in CFTR1 [3].
c.4004T>C	p.Leu1335Pro	L1335P	Unclassi-fied	Mis-sense	This variant causes CF when combined with another CF-causing variant. 61% (N=11) of patients in CFTR2 who have this variant are pancreatic insufficient.	CFTR1 reference [3]; Zelenski J, Tzountouris J, Tsui L-C 1997-08-12 (reference not found on PubMed)
						Unclassified. Variant cDNA name, protein name and legacy name show no hits in PubMed in the context of CF. The mutation is also not described in CFTR1 or CFTR2.
						Unclassified. Mutation is listed as responsive to Symdeko or trikafta (www.symdeko.com or www.trikafat.com).

variant cDNA name	variant protein name	variant legacy name	Classifi-cation [REF]	muta-tion type	CFTR2	CFTR1 reference to original report	Rationale for classification
c.617T>G	p.Leu206Trp	L206W		Mis-sense	This variant causes CF when combined with another CF-causing variant. Patients with CF who have this variant are likely to be pancreatic sufficient.	[19]	Class II trafficking defect associated with strongly reduced C band expression in heterologous expression model and no response to ivacaftor [2, 28].
c.2195T>G	p.Leu732X	L732X		Non-sense	This variant causes CF when combined with another CF-causing variant. This variant causes pancreatic insufficiency when combined with another variant that causes pancreatic insufficiency.	CFTR1 reference [3]; Malone G, Haworth A, Schwartz M 1994:10-05 (reference not available for full access)	CFTR protein synthesis defect based on sequence analysis (introduced PTC) that affects a critical part of the protein and is associated with PI-CF [2].
c.2780T>C	p.Leu927Pro	L927P	Unclassified	Mis-sense	This variant causes CF when combined with another CF-causing variant. This variant causes pancreatic insufficiency when combined with another variant that causes pancreatic insufficiency.	[54]	Unclassified. L927P may cause cystic fibrosis by interfering with conformational changes necessary for channel opening [55]. The surface expression level of the L927P mutant is 43% that of the wild-type protein, but its channel activity is only 0.1% [28]. Others reported a normal protein expression [2].
c.3909<G	p.Asn1303Lys	N1303K		Mis-sense	This variant causes CF when combined with another CF-causing variant. This variant causes pancreatic insufficiency when combined with another variant that causes pancreatic insufficiency.	[56]	Class II trafficking defect associated with strongly reduced C band expression in both heterologous and primary CF cells [29, 57]. It does not or hardly responds to ivacaftor or lumacaftor alone or in combination, but responds to VX-445 [2, 58].
c.4046delG	p.Gly1349AlafsX5	No legacy name	Unclassified	Ins/del	Not described in CFTR2.	Not described in CFTR1 [3].	CFTR protein synthesis defect, but due to the late position of the stop codon it is unclear whether the resulting protein has some associated function.

variant cDNA name	variant protein name	variant legacy name	Classification [REF]	mutation type	CFTR1 reference to original report	Rationale for classification
C.4243-3T>A	No protein name	No legacy name	Unclassified	Splice	Not described in CFTR2.	Variant cDNA name, protein name and legacy name show no hits in PubMed in the context of CF. The mutation is also not described in CFTR2. It is unclear whether the splice defect can be classified as class I or V.
No cDNA name	p.Gln1012Pro	Q1012P	Unclassified	Miss-sense	Not described in CFTR2.	Unclassified. Variant cDNA name, protein name and legacy name show no hits in PubMed in the context of CF. The mutation is also not described in CFTR1 or CFTR2.
c.1477C>T	p.Gln493X	Q493X	I	Non-sense	This variant causes CF when combined with another CF-causing variant. This variant causes pancreatic insufficiency when combined with another variant that causes pancreatic insufficiency.	[6]
c.3196C>T	p.Arg1066Cys	R1066C	II	Miss-sense	This variant causes CF when combined with another CF-causing variant. This variant causes pancreatic insufficiency when combined with another variant that causes pancreatic insufficiency.	[10]
c.3197G>A	p.Arg1066His	R1066H	II	Miss-sense	This variant causes CF when combined with another CF-causing variant. This variant causes pancreatic insufficiency when combined with another variant that causes pancreatic insufficiency.	[60]
c.3484C>T	p.Arg1162X	R1162X	I	Non-sense	This variant causes CF when combined with another CF-causing variant. This variant causes pancreatic insufficiency when combined with another variant that causes pancreatic insufficiency.	[61]

variant cDNA name	variant protein name	variant legacy name	Classification [REF]	muta-tion type	CFTR1 reference to original report	Rationale for classification
c.350G>A	p.Arg117His	R117H	N	Mis-sense	[62]	R117H is associated with altered conductance properties and was originally classified as class IV [63]. It is a complex allele associated with a intronic polyT tract (5T, 7T or 9T) that affects splicing efficiency which associates with disease severity (class V). Others have also reported trafficking defects [64] or gating defects [65]. C-band expression in heterologous systems is mostly reflective of wt CFTR. R117H shows acute responsiveness to ivacaftor in heterologous systems and primary cells but only limited response to correctors [21]. For this study, we retain the original classification of R117H as class IV mutation [2].
c.4074A>T	p.Arg1358Ser	R1358S	Unclassified	Mis-sense	Not described in CFTR2.	CFTR1 reference [3]: Férec C 1999-01-01 (reference not found on PubMed).
c.1000C>T	p.Arg334Trp	R334W	N	Mis-sense	[66]	Normal CFTR protein expression in heterologous system but altered single channel conductance characteristic of class IV [63]. Some response to ivacaftor but not lumacaftor in primary CF cells [2, 21].

variant cDNA name	variant protein name	variant legacy name	Classifi-cation [REF]	muta-tion type	CFTR2	CFTR1 reference to original report	Rationale for classification
c.1040G>C	p.Arg347Pro	R347P		Mis-sense	This variant causes CF when combined with another CF-causing variant. 64% (N=302) of patients in CFTR2 who have this variant are pancreatic insufficient.	[62]	Class I trafficking defect associated with reduced C band expression in heterologous cell expression systems. R347P was originally found to have altered channel conductance properties, but also matures very inefficiently (C-band ~15% of wild-type) and is not associated with function despite some expression [28]. Moreover, (F508del/R347P) shows no clear detectable response to ivacaftor in primary CF cells [21]. Others also found processing defects [39]. This supports a primary defect in processing (class I). The limited product that reaches the surface has likely altered channel properties [2].
c.1657C>T	p.Arg553X	R553X		Non-sense	This variant causes CF when combined with another CF-causing variant. This variant causes pancreatic insufficiency when combined with another variant that causes pancreatic insufficiency.	[67]	Class I CFTR protein synthesis defect based on sequence analysis (introduced PTC) that affects a critical part of the protein and is associated with PI-CF [2].
c.221G>C	p.Arg74Pro	R74P	Unclassi-fied	Mis-sense	Not described in CFTR2.	Not described in CFTR1.	Unclassified. Variant cDNA name, protein name and legacy name show no hits in PubMed in the context of CF. The mutation is also not described in CFTR1 or CFTR2.
c.2290C>T	p.Arg764X	R764X		Non-sense	This variant causes CF when combined with another CF-causing variant. This variant causes pancreatic insufficiency when combined with another variant that causes pancreatic insufficiency.	[15]	Class I CFTR protein synthesis defect based on sequence analysis (introduced PTC) that affects a critical part of the protein and is associated with PI-CF [2].

variant cDNA name	variant protein name	variant legacy name	Classi-fication [I REF]	muta-tion type	CFTR2	CFTR1 reference to original report	Rationale for classification
c.2353C>T p.Arg785X	R785X	I	Non-sense	This variant causes CF when combined with another CF-causing variant. This variant causes pancreatic insufficiency when combined with another variant that causes pancreatic insufficiency.	[68]	Class I CFTR protein synthesis defect based on sequence analysis (introduced PTC) that affects a critical part of the protein and is associated with PI-CF in CFTR2.	
c.3752G>A p.Ser1251Asn	S1251N	III	Mis-sense	This variant causes CF when combined with another CF-causing variant. 72% (N=84) of patients in CFTR2 who have this variant are pancreatic insufficient.	[69]	Classified as ivacaftor responsive class III gating mutation with normal C-band expression [2, 47].	
c.53G>T p.Ser18Ile	S18I	Unclassified	Mis-sense	Not described in CFTR2.	Not described in CFTR1 [3].	Unclassified. Variant cDNA name, protein name and legacy name show no hits in PubMed in the context of CF. The mutation is also not described in CFTR1 or CFTR2.	
c.1466C>A p.Ser489X	S489X	I	Non-sense	This variant causes CF when combined with another CF-causing variant. This variant causes pancreatic insufficiency when combined with another variant that causes pancreatic insufficiency.	CFTR1 reference [3]: Macdonald K, Haworth, A, Malone G, Schwarz M 1994-08-15 (reference not found on PubMed)	Class I CFTR protein synthesis defect based on sequence analysis (introduced PTC) that affects a critical part of the protein and is associated with PI-CF [2, 70].	
c.4186A>C p.Thr1396Pro	T1396P	Unclassified	Mis-sense	Not described in CFTR2.	Not described in CFTR1 [3].	Class I CFTR protein synthesis defect based on sequence analysis (introduced PTC) that affects a critical part of the protein and is associated with PI-CF [2, 71].	
c.3477delT p.Val1160X	V1160X	I	Non-sense	Not described in CFTR2.	[72]	Class I CFTR protein synthesis defect based on sequence analysis (introduced PTC) that affects a critical part of the protein and is associated with PI-CF [2].	
c.3846G>A p.Trp1282X	W1282X	I	Non-sense	This variant causes CF when combined with another CF-causing variant. This variant causes pancreatic insufficiency when combined with another variant that causes pancreatic insufficiency.	[73]	Class I CFTR protein synthesis defect based on sequence analysis (introduced PTC) that affects a critical part of the protein and is associated with PI-CF [2].	

variant cDNA name	variant protein name	variant legacy name	Classifi-cation [REF]	muta-tion type	CFTR1 reference to original report	Rationale for classification
c.2036G>A p.Trp679X	W679X		Non-sense	Not described in CFTR2.	CFTR1 Reference [3]; Walker C, Tsui L-C, Zielienski I 1999-09-27 (reference not found on PubMed).	Class I CFTR protein synthesis defect based on sequence analysis (introduced PTC) that affects a critical part of the protein.
c.2537G>A p.Trp846X	W846X		Non-sense	This variant causes CF when combined with another CF-causing variant. This variant causes pancreatic insufficiency when combined with another variant that causes pancreatic insufficiency.	[74]	Class I CFTR protein synthesis defect based on sequence analysis (introduced PTC) that affects a critical part of the protein and is associated with PI-CF [2].
c.3276G>A p.Tyr1092X	Y1092X		Non-sense	This variant causes CF when combined with another CF-causing variant. This variant causes pancreatic insufficiency when combined with another variant that causes pancreatic insufficiency.	[75]	Class I CFTR protein synthesis defect based on sequence analysis (introduced PTC) that affects a critical part of the protein and is associated with PI-CF [2].
c.325T>G p.Tyr109Asp	Y109D	Unclassified	Mis-sense	Not described in CFTR2.	Not described in CFTR1 [3].	Unclassified. One report [76] described mutation as CF-causing, elevated sweat chloride levels and pancreatic insufficiency. No characterization of protein function has been published.
c.2547C>A p.Tyr849X	Y849X		Non-sense	This variant causes CF when combined with another CF-causing variant. This variant causes pancreatic insufficiency when combined with another variant that causes pancreatic insufficiency.	[77]	Class I CFTR protein synthesis defect based on sequence analysis (introduced PTC) that affects a critical part of the protein and is associated with PI-CF in CFTR2.

Supplementary table 1. Classification of mutations.

Overview of the individual mutations in cDNA, protein and legacy name (according to the human genome variation society (HGVS) nomenclature) and corresponding CFTR classification including the rationale behind classification. The rationale is based on available literature and the clinical consequence of the mutation found in the CFTR2 database. In addition to the rationale, the original report describing the mutation for the first time was added to the table, derived from the table, derived from the CFTR1 database.

Association of Forskolin-induced Organoid Swelling with Long-term CF Disease Progression

2
2

ID	Genotype (legacy name)	Genotype classification	Mutation group
1	G542X/CFTRdele2.3	Class I	ins/del-nonsense
2	1811+1G>C/1811+1G>C	Class I	splice-splice
3	1717-1G>A/2183AA>G	Class I	ins/del-splice
4	W1282X/W1282X	Class I	nonsense-nonsense
5	G542X/W679X	Class I	nonsense-nonsense
6	1811+1G>C/1811+1G>C	Class I	splice-splice
7	R785X/R785X	Class I	nonsense-nonsense
8	1717-1G>A/3905insT	Class I	ins/del-splice
9	R1162X/3659delC	Class I	ins/del-nonsense
10	1811+1G>C/1811+1G>C	Class I	splice-splice
11	711+1G>T/CFTRdele11	Class I	ins/del-splice
12	1677delTA/3120+1G>A	Class I	ins/del-splice
13	L732X/L732X	Class I	nonsense-nonsense
14	1811+1G>C/1811+1G>C	Class I	splice-splice
15	711+1G>T/711+1G>T	Class I	splice-splice
16	F508del/L206W	Class II	ins/del-missense
17	F508del/G628R	Class II	ins/del-missense
18	F508del/I336K	Class II	ins/del-missense
19	A455E/3659delC	Class II	ins/del-missense
20	A455E/1343delG	Class II	ins/del-missense
21	R1066H/CFTRdele2.3	Class II	ins/del-missense
22	F508del/G628R	Class II	ins/del-missense
23	A455E/E60X	Class II	missense-nonsense
24	F508del/G628R	Class II	ins/del-missense
25	F508del/F508del	Class II	ins/del-ins/del
26	G542X/R1066C	Class II	missense-nonsense
27	F508del/2184delA	Class II	ins/del-ins/del
28	F508del/R347P	Class II	ins/del-missense
29	F508del/Y1092X	Class II	ins/del-nonsense
30	F508del/365-366insT(W79fs)	Class II	ins/del-ins/del
31	F508del/R1066C	Class II	ins/del-missense
32	F508del/1342-1delG	Class II	ins/del-splice
33	F508del/W846X	Class II	ins/del-nonsense
34	F508del/1717-1G>A	Class II	ins/del-splice
35	F508del/CFTRdele17a.17b	Class II	ins/del-ins/del
36	F508del/F508del	Class II	ins/del-ins/del
37	R1066C/R1066H	Class II	missense-missense

CHAPTER 2

ID	Genotype (legacy name)	Genotype classification	Mutation group
38	V1160X/E92K	Class II	missense-nonsense
39	F508del/1078delT	Class II	ins/del-ins/del
40	F508del/W1282X	Class II	ins/del-nonsense
41	F508del/R347P	Class II	ins/del-missense
42	F508del/1078delT	Class II	ins/del-ins/del
43	F508del/F508del	Class II	ins/del-ins/del
44	F508del/F508del	Class II	ins/del-ins/del
45	N1303K/G550X	Class II	missense-nonsense
46	F508del/CFTRdele19.20	Class II	ins/del-ins/del
47	F508del/F508del	Class II	ins/del-ins/del
48	F508del/R347P	Class II	ins/del-missense
49	F508del/I336K	Class II	ins/del-ins/del
50	A46D/A46D	Class II	missense-missense
51	F508del/3659delC	Class II	ins/del-ins/del
52	F508del/CFTRdele17a.17b	Class II	ins/del-ins/del
53	F508del/E730X	Class II	ins/del-nonsense
54	F508del/2183AA>G	Class II	ins/del-ins/del
55	F508del/Y1092X	Class II	ins/del-nonsense
56	F508del/1813insC	Class II	ins/del-ins/del
57	F508del/E60X	Class II	ins/del-nonsense
58	F508del/711+1G>T	Class II	ins/del-splice
59	F508del/Y1092X	Class II	ins/del-nonsense
60	F508del/G85E	Class II	ins/del-missense
61	F508del/I507del	Class II	ins/del-ins/del
62	F508del/1717-1G>A	Class II	ins/del-splice
63	F508del/W1282X	Class II	ins/del-nonsense
64	F508del/3659delC	Class II	ins/del-ins/del
65	F508del/711+1G>T	Class II	ins/del-splice
66	F508del/1717-1G>A	Class II	ins/del-splice
67	F508del/CFTRdele17a.17b	Class II	ins/del-ins/del
68	F508del/Y849X	Class II	ins/del-nonsense
69	F508del/1717-1G>A	Class II	ins/del-splice
70	N1303K/G85E	Class II	missense-missense
71	F508del CFTRdele2.3	Class II	ins/del-ins/del
72	F508del/CFTRdele17a.17b	Class II	ins/del-ins/del
73	A46D/A46D	Class II	missense-missense
74	F508del/Y849X	Class II	ins/del-nonsense
75	F508del/G85E	Class II	ins/del-missense

ID	Genotype (legacy name)	Genotype classification	Mutation group
76	F508del/S489X	Class II	ins/del-nonsense
77	F508del/2184delA	Class II	ins/del-ins/del
78	G542X/R1066C	Class II	missense-nonsense
79	F508del/711+1G>T	Class II	ins/del-splice
80	F508del/F508del	Class II	ins/del-ins/del
81	F508del/W1282X	Class II	ins/del-nonsense
82	F508del/Y1092X	Class II	ins/del-nonsense
83	F508del/N1303K	Class II	ins/del-missense
84	F508del/711+1G>T	Class II	ins/del-splice
85	I507del/4374+2T->C	Class II	ins/del-splice
86	F508del/711+1G>T	Class II	ins/del-splice
87	F508del/R1162X	Class II	ins/del-nonsense
88	F508del/G550X	Class II	ins/del-nonsense
89	F508del/G550X	Class II	ins/del-nonsense
90	F508del/F508del	Class II	ins/del-ins/del
91	F508del/F508del	Class II	ins/del-ins/del
92	F508del/Q493X	Class II	ins/del-nonsense
93	F508del/4016insT	Class II	ins/del-ins/del
94	F508del/394delTT	Class II	ins/del-ins/del
95	F508del/IVS11-1G>C	Class II	ins/del-splice
96	F508del/G550X	Class II	ins/del-nonsense
97	F508del/R1162X	Class II	ins/del-nonsense
98	F508del/R1162X	Class II	ins/del-nonsense
99	F508del/Y1092X	Class II	ins/del-nonsense
100	F508del/N1303K	Class II	ins/del-missense
101	F508del/W1282X	Class II	ins/del-nonsense
102	F508del/2184insA	Class II	ins/del-ins/del
103	F508del/F508del	Class II	ins/del-ins/del
104	F508del/R1162X	Class II	ins/del-nonsense
105	F508del/E60X	Class II	ins/del-nonsense
106	F508del/R1162X	Class II	ins/del-nonsense
107	F508del/S1251N	Class III	ins/del-missense
108	F508del/S1251N	Class III	ins/del-missense
109	F508del/S1251N	Class III	ins/del-missense
110	F508del/S1251N	Class III	ins/del-missense
111	F508del/S1251N	Class III	ins/del-missense
112	F508del/S1251N	Class III	ins/del-missense
113	F508del/S1251N	Class III	ins/del-missense

CHAPTER 2

ID	Genotype (legacy name)	Genotype classification	Mutation group
114	F508del/S1251N	Class III	ins/del-missense
115	S1251N/1717-1G>A	Class III	missense-splice
116	F508del/S1251N	Class III	ins/del-missense
117	F508del/G178R	Class III	ins/del-missense
118	3905insT/D1152H	Class IV	ins/del-missense
119	F508del/D1152H	Class IV	ins/del-missense
120	W1282X/R117H;7T	Class IV	missense-nonsense
121	F508del/R117H;7T/9T	Class IV	ins/del-missense
122	R1162X/D1152H	Class IV	missense-nonsense
123	R117H;7T/R553X	Class IV	missense-nonsense
124	R334W/N1303K	Class IV	missense-missense
125	R334W/R334W	Class IV	missense-missense
126	D1152H/R1162X	Class IV	missense-nonsense
127	R334W/R764X	Class IV	missense-nonsense
128	F508del/5T;TG13	Class V	ins/del-splice
129	F508del/5T;TG13	Class V	ins/del-splice
130	G542X/3849+10kbC>T	Class V	nonsense-splice
131	F508del/5T;TG13	Class V	ins/del-splice
132	A455E/5T;TG13	Class V	missense-splice
133	F508del/3849+10kbC>T	Class V	ins/del-splice
134	F508del/3849+10kbC>T	Class V	ins/del-splice
135	F508del/3849+10kbC>T	Class V	ins/del-splice
136	3272-26A>G/3272-26A>G	Class V	splice-splice
137	F508del/3849+10kbC>T	Class V	ins/del-splice
138	3272-26A>G/G970R	Class V	splice-splice
139	F508del/3272-26A>G	Class V	ins/del-splice
140	F508del/3272-26A>G	Class V	ins/del-splice
141	F508del/3272-26A>G	Class V	ins/del-splice
142	3272-26A>G/1898+5G>T	Class V	splice-splice
143	F508del/3272-26A>G	Class V	ins/del-splice
144	4382delA/2043delG	Class V	ins/del-ins/del
145	F508del/4382delA	Class V	ins/del-ins/del
146	F508del/2789+5G>A	Class V	ins/del-splice
147	F508del/4382delA	Class V	ins/del-ins/del
148	Y849X/2789+5G>A	Class V	nonsense-splice
149	1078delT/3272-26A>G	Class V	ins/del-splice
150	3849+10kbC>T/1717-1G>A	Class V	splice-splice

ID	Genotype (legacy name)	Genotype classification	Mutation group
151	F508del/c.4243-3T>A	Unclassified	ins/del-splice
152	F508del/R1358S	Unclassified	ins/del-missense
153	F508del;I1027T/UNK	Unclassified	ins/del-unknown
154	UNK/UNK	Unclassified	unknown-unknown
155	R553X/c.4243-3T>A	Unclassified	nonsense-splice
156	F508del/T1396P	Unclassified	ins/del-missense
157	F508del/G461R	Unclassified	ins/del-missense
158	N1303K/Q1012P	Unclassified	missense-missense
159	F508del/UNK	Unclassified	ins/del-unknown
160	R117H;7T/UNK	Unclassified	missense-unknown
161	F508del/G1249R	Unclassified	ins/del-missense
162	UNK/UNK	Unclassified	unknown-unknown
163	F508del/G1249R	Unclassified	ins/del-missense
164	F508del/UNK	Unclassified	ins/del- unknown
165	F508del/3849+5G>T	Unclassified	ins/del-splice
166	L1335P/L1335P	Unclassified	missense-missense
167	F508del/R74P	Unclassified	ins/del-missense
168	F508del/L1034P	Unclassified	ins/del-missense
169	F508del/S18I	Unclassified	ins/del-missense
170	F508del/Y109D	Unclassified	ins/del-missense
171	W1282X/L927P	Unclassified	missense-nonsense
172	F508del/UNK	Unclassified	ins/del-unknown
173	F508del/c.4046delG	Unclassified	ins/del-ins/del

Supplementary table 2. Individual genotypes of study participants.

Overview of individual genotypes with corresponding CFTR mutation classification according to the rationale described in **supplementary table 1**. Genotypes are provided in legacy name, unless stated otherwise (c. = cDNA code). Study participants were categorized into one mutation class based on the mildest of both mutation classes, or to unclassified when one of the mutation classes was unknown or uncertain. Mutation group was defined by the combination of mutation types of both alleles.

CHAPTER 2

N=107, obs=644	Coefficient (95% CI)	P-value
Age	-1.57 (-2.03 – -1.10)	<0.001*
FIS	-3.01 (-11.07 – 5.04)	0.462
FIS*age	0.49 (0.03 – 0.96)	0.039*
Treatment		
- none	Reference category	
- ivacaftor	9.63 (4.93 – 14.33)	<0.001*
- lumacaftor/ivacaftor	-4.32 (-10.70 – 2.06)	0.184
Sex		
- male	Reference category	
- female	0.16 (-6.38 – 6.71)	0.961
Genotype class		
- unclassified	Reference category	
- class I	0.93 (-14.29 – 16.16)	0.904
- class II	6.21 (-6.30 – 18.72)	0.330
- class III	7.86 (-6.99 – 22.71)	0.299
- class IV	21.37 (1.52 – 41.22)	0.349
- class V	-1.58 (-20.64 – 17.47)	0.870
SCC	-0.09 (-0.25 – 0.07)	0.264

Supplementary table 3. Association of FIS with FEV1pp decline in subgroup analysis 4-25 years.

Regression coefficients of linear mixed effects model for FEV1pp within a subgroup including participants between 4-25 years of age. FEV1pp: Forced expiratory volume in 1 second, percent predicted. Age in years. FIS: Forskolin-induced swelling, defined as the relative size increase of intestinal organoids (AUC) after 1h stimulation with 0.8 µM/L forskolin, coefficient scaled 1:1000 AUC. SCC: Sweat chloride concentration in mmol/L. FIS*age indicates the difference in annual FEV1pp decline per 1000 AUC change in FIS level. Genotype class: CFTR protein function class of the mildest of both CFTR mutations. * Significance level P < 0.05.

	N=138, obs=970		Subgroup: N=100, obs=601	
	Coefficient (95% CI)	P-value	Coefficient (95% CI)	P-value
Age	-1.25 (-1.54 – -0.96)	<0.001*	-1.68 (-2.15 – -1.21)	<0.001*
FIS	-2.93 (-8.42 – 2.56)	0.295	-5.22 (-12.15 – 1.71)	0.140
FIS*age	0.36 (0.12 – 0.61)	0.004*	0.69 (0.17 – 1.20)	0.009*
Treatment				
- none	Reference category		Reference category	
- ivacaftor	8.43 (4.79 – 12.06)	<0.001*	10.03 (4.88 – 15.17)	<0.001*
- lumacaftor/ivacaftor	-3.44 (-7.89 – 1.00)	0.129	-4.30 (-10.66 – 2.06)	0.185
Sex				
- male	Reference category		Reference category	
- female	-0.07 (-6.21 – 6.07)	0.982	0.82 (-5.72 – 7.36)	0.805
Genotype group				
- Ins/del – missense	Reference category		Reference category	
- Ins/del – nonsense	-0.24 (-9.98 – 9.51)	0.962	2.05 (-7.94 – 12.05)	0.687
- Ins/del – splice	-2.91 (-12.08 – 6.25)	0.533	-2.29 (-11.89 – 7.31)	0.640
- Ins/del – ins/del	-0.45 (-10.05 – 9.14)	0.927	1.56 (-8.72 – 11.84)	0.766
- Missense – nonsense	7.85 (-6.51 – 22.21)	0.284	8.40 (-8.39 – 25.19)	0.326
- Missense – missense	8.77 (-5.46 – 23.00)	0.227	13.84 (-1.12 – 28.79)	0.070
- Splice – splice	-6.30 (-21.46 – 8.87)	0.415	1.74 (-15.01 – 18.50)	0.838
SCC	-0.09 (-0.24 – 0.07)	0.289	-0.12 (-0.29 – 0.05)	0.176

Supplementary table 4. Association of FIS with FEV1pp decline in sensitivity analysis including genotype group.

Regression coefficients of linear mixed effects model for FEV1pp with genotype group and subgroup only including participants between 4 – 25 years of age. FEV1pp: Forced expiratory volume in 1 second, percent predicted. Age in years. FIS: Forskolin-induced swelling, defined as the relative size increase of intestinal organoids (AUC) after 1h stimulation with 0.8 µM/L forskolin, coefficient scaled 1:1000 AUC. FIS*age indicates the difference in annual FEV1pp decline per 1000 AUC change in FIS level. SCC: Sweat chloride concentration in mmol/L. Genotype group: combination of CFTR mutation types on both alleles. * Significance level P < 0.05.

CHAPTER 2

N=149, obs=1054	Coefficient (95% CI)	P-value
Age	--0.26 (-1.12 – 0.61)	0.563
FIS	1.78 (-4.05 – 7.62)	0.549
SCC	0.004 (-0.19 – 0.20)	0.971
SCC*age	-0.01 (-0.02 – 0.002)	0.121
Treatment		
- none	Reference category	
- ivacaftor	8.04 (4.61 – 11.47)	<0.001*
- lumacaftor/ivacaftor	-3.98 (-8.44 – 0.49)	0.081
Sex		
- male	Reference category	
- female	-0.75 (-6.83 – 5.32)	0.807
Genotype class		
- unclassified	Reference category	
- class I	0.73 (-13.51 – 14.97)	0.920
- class II	5.37 (-5.62 – 16.36)	0.338
- class III	10.66 (-3.45 – 24.76)	0.138
- class IV	12.11 (-4.46 – 28.69)	0.152
- class V	0.23 (-14.60 – 15.06)	0.976

Supplementary table 5. Association of SCC with FEV1pp decline

FEV1pp: Forced expiratory volume in 1 second, percent predicted. Age in years. FIS: Forskolin-induced swelling, defined as the relative size increase of intestinal organoids (AUC) after 1h stimulation with 0.8 µM/L forskolin, coefficient scaled 1:1000 AUC. SCC: Sweat chloride concentration in mmol/L. FIS*age indicates the difference in annual FEV1pp decline per 1000 AUC change in FIS level. Genotype class: CFTR protein function class of the mildest of both CFTR mutations.

* Significance level P < 0.05.

Association of Forskolin-induced Organoid Swelling with Long-term CF Disease Progression

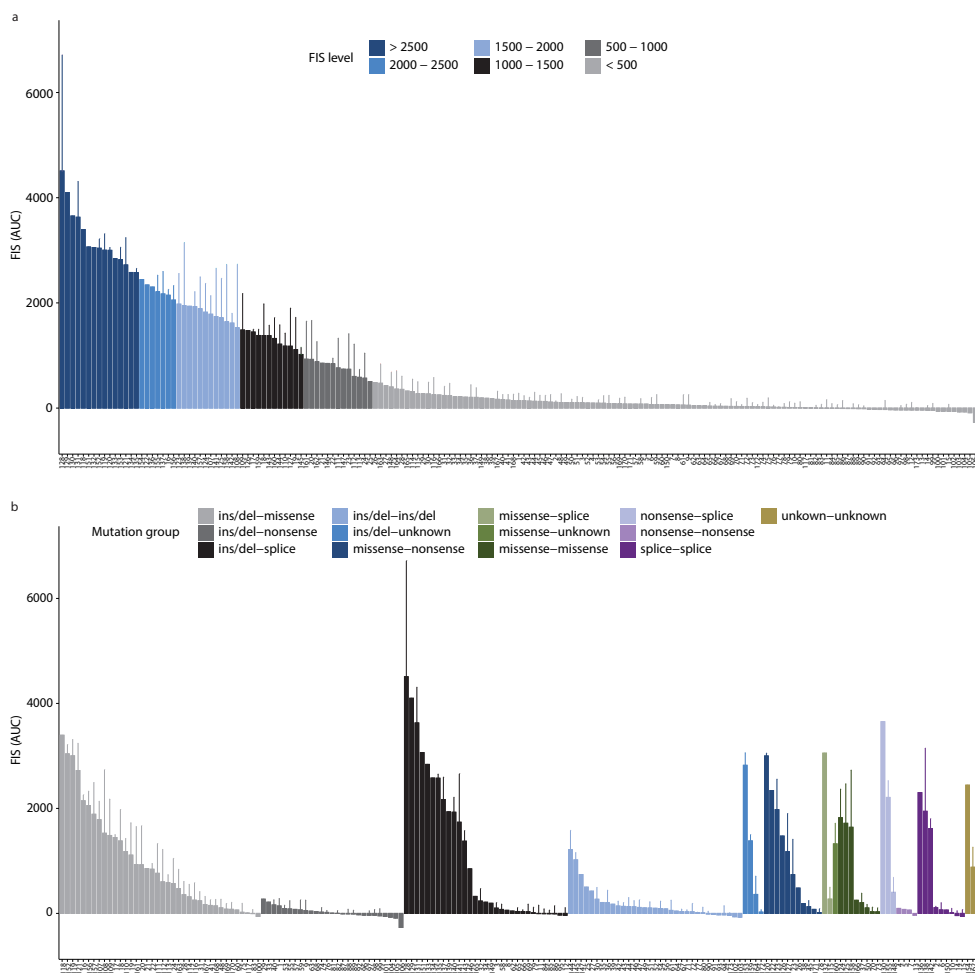
2
2

N=149, obs=1054	Coefficient (95% CI)	P-value
Age	-1.16 (-2.36 – 0.03)	0.056
FIS	-2.42 (-9.15 – 4.30)	0.480
FIS*age	0.33 (0.05 – 0.60)	0.020*
SCC	-0.09 (-0.31 – 0.12)	0.392
SCC*age	0.00 (-0.01 – 0.01)	0.995
Treatment		
- none	Reference category	
- ivacaftor	8.02 (4.61 – 11.43)	<0.001*
- lumacaftor/ivacaftor	-3.75 (-8.20 – 0.70)	0.098
Sex		
- male	Reference category	
- female	-0.99 (-7.06 – 5.07)	0.748
Genotype class		
- unclassified	Reference category	
- class I	0.51 (-13.65 – 14.67)	0.944
- class II	5.34 (-5.60 – 16.27)	0.339
- class III	10.25 (-3.82 – 24.32)	0.153
- class IV	11.09 (-5.44 – 27.63)	0.188
- class V	-2.45 (-17.33 – 12.43)	0.747

Supplementary table 6. Comparison of the association between FEV1pp decline and FIS versus SCC

FEV1pp: Forced expiratory volume in 1 second, percent predicted. Age in years. FIS: Forskolin-induced swelling, defined as the relative size increase of intestinal organoids (AUC) after 1 h stimulation with 0.8 µM/L forskolin, coefficient scaled 1:1000 AUC. SCC: Sweat chloride concentration in mmol/L. FIS*age indicates the difference in annual FEV1pp decline per 1000 AUC change in FIS level. SCC*age indicates the difference in annual FEV1pp decline per 1-unit change in SCC level. Genotype class: CFTR protein function class of the mildest of both CFTR mutations. * Significance level P < 0.05.

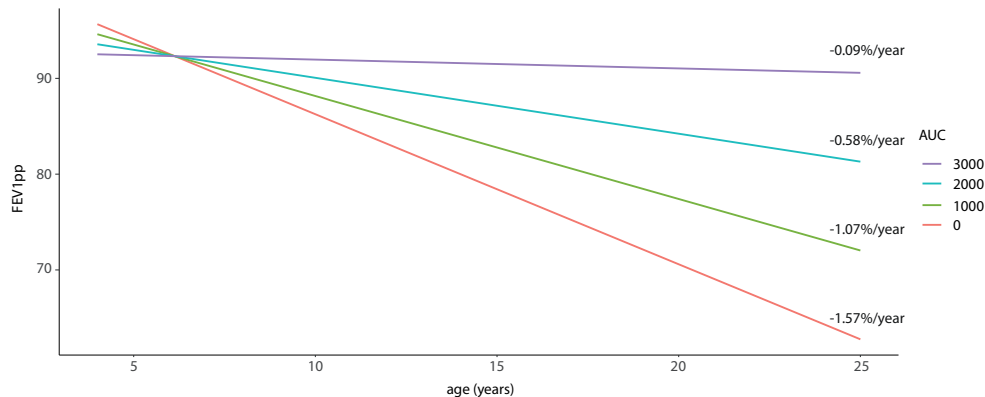
SUPPLEMENTARY FIGURES



Supplementary figure 1. Individual FIS responses

a) waterfall plot of FIS responses stimulated with 0.8 µM forskolin for 1 hour of all study participants. **b**) waterfall plot of FIS responses at 0.8 µM forskolin per mutation group. Groups were defined by the combination of the mutation type of both mutations. Bars represent mean+SD of replicates, ranging from n=2 to n=7. The numbers on the x-axes represent the participant number and correspond to the numbers in **figure 1b-c**. Genotypes are specified in **supplementary table 2**.

Association of Forskolin-induced Organoid Swelling with Long-term CF Disease Progression



Supplementary figure 2. Association of FIS with long-term FEV1pp decline in subgroup 4-25 years

Predicted FEV1pp decline based on model coefficients in **supplementary table 3**, illustrating the association between different levels of residual CFTR function and long-term FEV1pp decline in the subgroup analysis. The analysis was performed with FIS as continuous variable, yet for illustrative purposes predicted FEV1pp decline is plotted by steps of 1000 AUC from 4 to 25 years, reflecting the age range of the subgroup. Average predicted annual FEV1pp decline per AUC level is specified on the right.

REFERENCES

- Claustres M, Gerrard B, White MB, Desgeorges M, Kjellberg P, Rollin B, Dean M. A new mutation (1078delT) in exon 7 of the CFTR gene in a southern French adult with cystic fibrosis. *Genomics* 1992; 13: 907–908.
- Sosnay PR, Siklosi KR, Van Goor F, Kaniecki K, Yu H, Sharma N, Ramalho AS, Amaral MD, Dorfman R, Zielenski J, Masica DL, Karchin R, Millen L, Thomas PJ, Patrinos GP, Corey M, Lewis MH, Rommens JM, Castellani C, Penland CM, Cutting GR. Defining the disease liability of variants in the cystic fibrosis transmembrane conductance regulator gene. *Nat. Genet.* [Internet] Nature Publishing Group; 2013; 45: 1160–1167 Available from: <http://dx.doi.org/10.1038/ng.2745>.
- CFTR1 database [Internet]. Available from: <http://www.genet.sickkids.on.ca/>.
- Salinas DB, Sosnay PR, Azen C, Young S, Raraigh KS, Keens TG, Kharrazi M. Benign and deleterious cystic fibrosis transmembrane conductance regulator mutations identified by sequencing in positive cystic fibrosis newborn screen children from California. *PLoS One* 2016; 11: 1–14.
- Baranov VS, Gorbunova VN, Ivaschenko TE, Shwed NY, Osinovskaya NS, Kascheeva TK, Lebedev VM, Mikhailov A V, Vakharlovsky VG, Kuznetzova T V. Five years' experience of prenatal diagnosis of cystic fibrosis in the former U.S.S.R. *Prenat. Diagn.* 1992;
- Kerem BS, Zielenski J, Markiewicz D, Bozon D, Gazit E, Yahav J, Kennedy D, Riordan JR, Collins FS, Kommens JM, Tsui LC. Identification of mutations in regions corresponding to the two putative nucleotide (ATP)-binding folds of the cystic fibrosis gene. *Proc. Natl. Acad. Sci. U. S. A.* 1990; 87: 8447–8451.
- Petreska L, Koceva S, Efremov GD. A donor splice site mutation (1811 + 1G->C) in intron 11 of the CFTR gene identified in a patient of Macedonian origin. *Hum. Mutat.* 1996; 7: 375.
- Chillón M, Casals T, Giménez J, Nunes V, Estivill X. Analysis of the CFTR gene in the Spanish population: SSCP-screening for 60 known mutations and identification of four new mutations (Q30X, A120T, 1812-1 G->A, and 3667del4). *Hum. Mutat.* 1994; 3: 223–230.
- Zielenski J, Markiewicz D, Lin S-P, Huang F-Y, Yang-Feng TL, Tsui L-C. Skipping of exon 12 as a consequence of a point mutation (1898 + 5G → T) in the cystic fibrosis transmembrane conductance regulator gene found in a consanguineous Chinese family. *Clin. Genet.* [Internet] 1995; 47: 125–132 Available from: <https://doi.org/10.1111/j.1399-0004.1995.tb03944.x>.
- Fanen P, Ghanem N, Vidaud M, Besmond C, Martin J, Costes B, Plassa F, Goossens M. Molecular characterization of cystic fibrosis: 16 Novel mutations identified by analysis of the whole cystic fibrosis conductance transmembrane regulator (CFTR) coding regions and splice site junctions. *Genomics* 1992; 13: 770–776.
- Kilinc MO, Ninis VN, Tolun A, Estivill X, Casals T, Savov A, Dagli E, Karakoc F, Demirkol M, Huner G, Ozkinay F, Demir E, Seculi JL, Pena J, Bousono C, Ferrer-Calvete J, Calvo C, Glover G, Kremenski I. Genotype-phenotype correlation in three homozygotes and nine compound heterozygotes for the cystic fibrosis mutation 2183AA→G shows a severe phenotype. *J. Med. Genet.* 2000; 37: 307–309.
- Chevalier-Porst F, Bonardot AM, Gilly R, Chazalette JP, Mathieu M, Bozon D. Mutation analysis in 600 French cystic fibrosis patients. *J. Med. Genet.* 1994; 31: 541–544.
- Prontera P, Isidori I, Mencarini V, Pennoni G, Mencarelli A, Stangoni G, Di Cara G, Verrotti A. A Clinical and Molecular Survey of 62 Cystic Fibrosis Patients from Umbria (Central Italy) Disclosing a High Frequency (2.4%) of the 2184insA Allele: Implications for Screening. *Public Health Genomics* 2017; 19: 336–341.
- Hightsmith WE, Burch LH, Zhou Z, Olsen JC, Strong T V, Smith T, Friedman KJ, Silverman LM, Boucher RC, Collins FS, Knowles MR. Identification of a splice site mutation (2789 + 5 G > A) associated with small amounts of normal CFTR mRNA and mild cystic fibrosis. *Hum. Mutat.* 1997; 9: 332–338.
- Macek M, Mackova A, Hamosh A, Hilman BC, Selden RF, Lucotte G, Friedman KJ, Knowles MR, Rosenstein BJ, Cutting GR. Identification of common cystic fibrosis mutations in African-Americans with cystic fibrosis increases the detection rate to 75%. *Am. J. Hum. Genet.* 1997; 60: 1122–1127.

Association of Forskolin-induced Organoid Swelling with Long-term CF Disease Progression

2

16. Highsmith WE, Burch LH, Zhou Z, Olsen JC, Boat TE, Spock A, Gorvoy JD, Quittel L, Friedman KJ, Silverman LM. A novel mutation in the cystic fibrosis gene in patients with pulmonary disease but normal sweat chloride concentrations. *N. Engl. J. Med.* 1994; 331: 974–980.
17. Schwartz M, Amvret M, Claustres M, Eiken HG, Eiklid K, Schaadel C, Stolpe L, Tranebjaerg L. 394delTT: a Nordic cystic fibrosis mutation. *Hum. Genet.* 1994; 93: 157–161.
18. Cheadle JP, Al-Jader LN, Meredith AL. Two novel frame-shift mutations: 977 insA in exon 6B, and 4016 insT in exon 21, of the cystic fibrosis transmembrane conductance regulator (CFTR) gene. *Hum. Mol. Genet.* [Internet] 1993; 2: 317–319 Available from: <https://doi.org/10.1093/hmg/2.3.317>.
19. Claustres M, Laussel M, Desgeorges M, Giansily M, Culard J-F, Razakatsara G, Demaille J. Analysis of the 27 exons and flanking regions of the cystic fibrosis gene: 40 different mutations account for 91.2% of the mutant alleles in Southern France. *Hum. Mol. Genet.* [Internet] 1993; 2: 1209–1213 Available from: <https://doi.org/10.1093/hmg/2.8.1209>.
20. Nissim-Rafinia M, Chiba-Falek O, Sharon G, Boss A, Kerem B. Cellular and viral splicing factors can modify the splicing pattern of CFTR transcripts carrying splicing mutations. *Hum. Mol. Genet.* 2000; 9: 1771–1778.
21. Dekkers JF, Berkers G, Kruisselbrink E, Vonk A, De Jonge HR, Janssens HM, Bronsveld I, Van De Graaf EA, Nieuwenhuis EES, Houwen RHJ, Vleggaar FP, Escher JC, De Rijke YB, Majoor CJ, Heijerman HGM, De Winter – De Groot KM, Clevers H, Van Der Ent CK, Beekman JM. Characterizing responses to CFTR-modulating drugs using rectal organoids derived from subjects with cystic fibrosis. *Sci. Transl. Med* 2016; 8: 344–384.
22. Kerem E, Rave-Harel N, Augarten A, Madgar I, Nissim-Rafinia M, Yahav Y, Goshen R, Bentur L, Rivlin J, Aviram M, Genem A, Chiba-Falek O, Kraemer MR, Simon A, Branski D, Kerem B. A cystic fibrosis transmembrane conductance regulator splice variant with partial penetrance associated with variable cystic fibrosis presentations. *Am. J. Respir. Crit. Care Med.* 1997; 155: 1914–1920.
23. Hefferon TW, Groman JD, Yurk CE, Cutting GR. A variable dinucleotide repeat in the CFTR gene contributes to phenotype diversity by forming RNA secondary structures that alter splicing. *Proc. Natl. Acad. Sci. U. S. A.* 2004; 101: 3504–3509.
24. Groman JD, Hefferon TW, Casals T, Bassas L, Estivill X, Des Georges M, Guittard C, Koudova M, Fallin MD, Nemeth K, Fekete G, Kadasi L, Friedman K, Schwarz M, Bombieri C, Pignatti PF, Kanavakis E, Tzetis M, Schwartz M, Novelli G, D'Apice MR, Sobczynska-Tomaszewska A, Bal J, Stuhrmann M, Macek M, Claustres M, Cutting GR. Variation in a Repeat Sequence Determines Whether a Common Variant of the Cystic Fibrosis Transmembrane Conductance Regulator Gene Is Pathogenic or Benign. *Am. J. Hum. Genet.* 2004; 74: 176–179.
25. Zielinski J, Bozon D, Kerem, Markiewicz BD, Durie P, Rommens JM, Tsui LC. Identification of mutations in exons 1 through 8 of the cystic fibrosis transmembrane conductance regulator (CFTR) gene [Internet]. *Genomics* 1991. Available from: [https://doi.org/10.1016/0888-7543\(91\)90504-8](https://doi.org/10.1016/0888-7543(91)90504-8).
26. Sheppard DN, Ostegda LS, Winter MC, Welsh MJ. Mechanism of dysfunction of two nucleotide binding domain mutations in cystic fibrosis transmembrane conductance regulator that are associated with pancreatic sufficiency. *EMBO J.* 1995; 14: 876–883.
27. Cebotaru L, Rapino D, Cebotaru V, Guggino WB. Correcting the cystic fibrosis disease mutant, A455E CFTR. *PLoS One* 2014; 9: 3–8.
28. Van Goor F, Yu H, Burton B, Hoffman BJ. Effect of ivacaftor on CFTR forms with missense mutations associated with defects in protein processing or function. *J. Cyst. Fibros.* [Internet] European Cystic Fibrosis Society.; 2014; 13: 29–36 Available from: <http://dx.doi.org/10.1016/j.jcf.2013.06.008>.
29. Dekkers JF, Gondra RAG, Kruisselbrink E, Vonk AM, Janssens HM, De Winter-De Groot KM, Van Der Ent CK, Beekman JM. Optimal correction of distinct CFTR folding mutants in rectal cystic fibrosis organoids. *Eur. Respir. J.* [Internet] 2016; 48: 451–458 Available from: <http://dx.doi.org/10.1183/13993003.01192-2015>.
30. Tzetis M, Kanavakis E, Antoniadi T, Traeger-Synodinos J, Doudounakis S, Adam G, Kattamis C. Identification of two novel mutations (296 + 1G - C and A46D) in exon 2 of the CFTR gene in Greek cystic fibrosis patients. *Mol. Cell. Probes* 1995; 9: 283–285.

CHAPTER 2

31. Audrézet M-P, Chen J-M, Raguénès O, Chuzhanova N, Giteau K, Maréchal C Le, Quéré I, Cooper DN, Férec C. Genomic rearrangements in the CFTR gene: extensive allelic heterogeneity and diverse mutational mechanisms. *Hum. Mutat.* 2004; 23: 343–357.
32. Niel F, Martin J, Dastot-Le Moal F, Costes B, Boissier B, Delattre V, Goossens M, Girodon E. Rapid detection of CFTR gene rearrangements impacts on genetic counselling in cystic fibrosis. *J. Med. Genet.* 2004; 41: 1–7.
33. Costes B, Girodon E, Vidaud D, Flori E, Ardalán A, Conteille P, Fanen P, Niel F, Vidaud M, Goossens M. Prenatal detection by real-time quantitative PCR and characterization of a new CFTR deletion, 3600+15kbdel5.3kb (or CFTRdele19). *Clin. Chem.* 2000; 46: 1417–1420.
34. Dörk T, Macek M, Mekus F, Tümmeler B, Tzountzouris J, Casals T, Krebsová A, Koudová M, Sakmaryová I, Vávrová V, Zemková D, Ginter E, Petrova N V., Ivaschenko T, Baranov V, Witt M, Pogorzelski A, Bal J, Zékanowsky C, Wagner K, Stuhrmann M, Bauer I, Seydewitz HH, Neumann T, Jakubiczka S, Kraus C, Thamm B, Nechiporenko M, Livshits L, Mosse N, et al. Characterization of a novel 21-kb deletion, CFTRdele2,3(21 kb), in the CFTR gene: A cystic fibrosis mutation of Slavic origin common in Central and East Europe. *Hum. Genet.* 2000; 106: 259–268.
35. Jr WEH, Friedman KJ, Burch LH, Spock A, Silverman LM, Boucher RC, Knowles MR. A CFTR mutation (D1152H) in a family with mild lung disease and normal sweat chlorides. *Hum. Genet.* 2005; 68: 88–90.
36. LaRusch J, Jung J, General IJ, Lewis MD, Park HW, Brand RE, Gelrud A, Anderson MA, Banks PA, Conwell D, Lawrence C, Romagnuolo J, Baillie J, Alkaade S, Cote G, Gardner TB, Amann ST, Slivka A, Sandhu B, Aloe A, Kienholz ML, Yadav D, Barmada MM, Bahar I, Lee MG, Whitcomb DC. Mechanisms of CFTR Functional Variants That Impair Regulated Bicarbonate Permeation and Increase Risk for Pancreatitis but Not for Cystic Fibrosis. *PLoS Genet.* 2014; 10.
37. Cuppens H, Marynen P, De Boeck C, Cassiman JJ. Detection of 98.5% of the mutations in 200 Belgian cystic fibrosis alleles by reverse dot-blot and sequencing of the complete coding region and exon/intron junctions of the CFTR gene. *Genomics* 1993; 18: 693–697.
38. Nunes V, Chillón M, Dörk T, Tümmeler B, Casals T, Estivill X. A new missense mutation (E92K) in the first transmembrane domain of the CFTR gene causes a benign cystic fibrosis phenotypeTitle. *Hum. Mol. Genet.* [Internet] 1993; 2: 79–80Available from: <https://doi.org/10.1093/hmg/2.1.79>.
39. Veit G, Avramescu RG, Chiang AN, Houck SA, Cai Z, Peters KW, Hong JS, Pollard HB, Guggino WB, Balch WE, Skach WR, Cutting GR, Frizzell RA, Sheppard DN, Cyr DM, Sorscher EJ, Brodsky JL, Lukacs GL. From CFTR biology toward combinatorial pharmacotherapy: Expanded classification of cystic fibrosis mutations. *Mol. Biol. Cell* 2016; 27: 424–433.
40. Ensink M, De Keersmaecker L, Heylen L, Ramalho AS, Gijsbers R, Farré R, De Boeck K, Christ F, Debysen Z, Carlon MS. Phenotyping of Rare CFTR Mutations Reveals Distinct Trafficking and Functional Defects. *Cells* 2020; 9: 1–14.
41. Ren HY, Grove DE, De La Rosa O, Houck SA, Sophia P, Van Goor F, Hoffman BJ, Cyr DM. VX-809 corrects folding defects in cystic fibrosis transmembrane conductance regulator protein through action on membrane-spanning domain 1. *Mol. Biol. Cell* 2013; 24: 3016–3024.
42. Rommens J, Iannuzzi M, Kerem B, Drumm M, Melmer G, Dean M, Rozmahel R, Cole J, Kennedy D, Hidaka N, ZSIGA M, BUCHWALD M, TSUI L-C, RIORDAN JR, COLLINS FS. Identification of the Cystic Fibrosis Gene: Chromosome Walking and Jumping. *Science* (80-.). 1989; 245: 1059–1065.
43. Riordan JR, Rommens JM, Kerem B-S, Alon N, Rozmahel R, Grzelczak Z, Zielinski J, Lok S, Plavsic N, Chou J-L, Drumm ML, Iannuzzi MC, Collins FS, Tsui L-C. Identification of the Cystic Fibrosis Gene: Cloning and Characterization of Complementary DNA. *Science* (80-.). 1989; 245: 1066–1073.
44. Kerem B-S, Rommens JM, Buchanan JA, Markiewicz D, Cox TK, Chakravarti A, Buchwald M, Tsui L-C. Identification of the Cystic Fibrosis Gene: Genetic Analysis. *Science* (80-.). 1989; 245: 1073–1080.
45. Cheng SH, Gregory RJ, Marshall J, Paul S, Souza DW, White GA, O'Riordan CR, Smith AE. Defective intracellular transport and processing of CFTR is the molecular basis of most cystic fibrosis. *Cell* 1990; 63: 827–834.

Association of Forskolin-induced Organoid Swelling with Long-term CF Disease Progression

2

46. Dijkstra, Dirk-Jan W. Scheffer H, Buys CHCM. A novel mutation (G1249R) in exon 20 of the CFTR gene. *Hum. Mutat.* 1994; 4: 161–162.
47. Yu H, Burton B, Huang CJ, Worley J, Cao D, Johnson JP, Urrutia A, Joubran J, Seepersaud S, Sussky K, Hoffman BJ, Van Goor F. Ivacaftor potentiation of multiple CFTR channels with gating mutations. *J. Cyst. Fibros.* 2012; 11: 237–245.
48. Berkers G, van Mourik P, Vonk AM, Kruisselbrink E, Dekkers JF, de Winter-de Groot KM, Arends HGM, Marck-van der Wilt REP, Dijkema JS, Vanderschuren MM, Houwen RHJ, Heijerman HGM, van de Graaf EA, Elias SG, Majoor CJ, Koppelman GH, Roukema J, Bakker M, Janssens HM, van der Meer R, Vries RGJ, Clevers HC, de Jonge HR, Beekman JM, van der Ent CK. Rectal Organoids Enable Personalized Treatment of Cystic Fibrosis. *Cell Rep.* [Internet] Elsevier Company.; 2019; 26: 1701–1708.e3 Available from: <https://doi.org/10.1016/j.celrep.2019.01.068>.
49. Billet A, Melin P, Jollivet M, Mornon JP, Callebaut I, Becq F. C terminus of nucleotide binding domain 1 contains critical features for cystic fibrosis transmembrane conductance regulator trafficking and activation. *J. Biol. Chem.* 2010; 285: 22132–22140.
50. Fidler MC, Buckley A, Sullivan JC, Stacia M, Boj SF, Vries RGJ, Munck A, Higgins M, Moretto Zita M, Negulescu P, van Goor F, De Boeck K. G970R-CFTR Mutation (c.2908G>C) Results Predominantly in a Splicing Defect. *Clin. Transl. Sci.* 2021; 14: 656–663.
51. Seibert FS, Linsdell P, Loo TW, Hanrahan JW, Riordan JR, Clarke DM. Cytoplasmic loop three of cystic fibrosis transmembrane conductance regulator contributes to regulation of chloride channel activity. *J. Biol. Chem.* [Internet] © 1996 ASBMB. Currently published by Elsevier Inc; originally published by American Society for Biochemistry and Molecular Biology.; 1996; 271: 27493–27499 Available from: <http://dx.doi.org/10.1074/jbc.271.44.27493>.
52. Schwarz M, Summers C, Heptinstall L, Newton C, Markham A, Super M. A deletion mutation of the cystic fibrosis transmembrane conductance regulator (CFTR) locus: Delta I507. *1991; 290:* 393–398.
53. Lopes-Pacheco M, Sabirzhanova I, Rapinoa D, Morales MM, Guggino WB, Cebotaru L. Correctors Rescue CFTR Mutations in Nucleotide-Binding Domain 1 (NBD1) by Modulating Proteostasis. *chembiochem* 2016; 17: 493–505.
54. Hermans CJ, Veeze HJ, Drexhage VR, Halley DJJ, van den Ouweleen AMW. Identification of the L927P and ΔL1260 mutations in the CFTR gene. *Hum. Mol. Genet.* [Internet] 1994; 3: 1199–1200 Available from: <https://doi.org/10.1093/hmg/3.7.1199>.
55. Zhang Z, Liu F, Chen J. Molecular structure of the ATP-bound, phosphorylated human CFTR. *Proc. Natl. Acad. Sci. U. S. A.* 2018; 115: 12757–12762.
56. Osborne L, Santis G, Schwarz M, Klinger K, Dörk T, McIntosh I, Schwartz M, Nunes V, Jr MM, Reiss J. Incidence and expression of the N1303K mutation of the cystic fibrosis (CFTR) gene. *Hum. Genet.* 1992; 89: 653–658.
57. Gregory RJ, Rich DP, Cheng SH, Souza DW, Paul S, Manavalan P, Anderson MP, Welsh MJ, Smith AE. Maturation and function of cystic fibrosis transmembrane conductance regulator variants bearing mutations in putative nucleotide-binding domains 1 and 2. *Mol. Cell. Biol.* 1991; 11: 3886–3893.
58. Veit G, Roldan A, Hancock MA, da Fonte DF, Xu H, Hussein M, Frenkel S, Matouk E, Velkov T, Lukacs GL. Allosteric folding correction of F508del and rare CFTR mutants by elexacaftor-tezacaftor-ivacaftor (Trikafta) combination. *JCI Insight* 2020; 5: 1–14.
59. Fanen P, Labarthe R, Garnier F, Benharouga M, Goossens M, Edelman A. Cystic fibrosis phenotype associated with pancreatic insufficiency does not always reflect the cAMP-dependent chloride conductive pathway defect. Analysis of C225R-CFTR and R1066C-CFTR. *J. Biol. Chem.* 1997; 272: 30563–30566.
60. Ferec C, Audrezet MP, Mercier B, Guillermit H, Moullier P, Quere I, Verlingue C. Detection of over 98% cystic fibrosis mutations in a Celtic population. 1992; 1: 188–191.

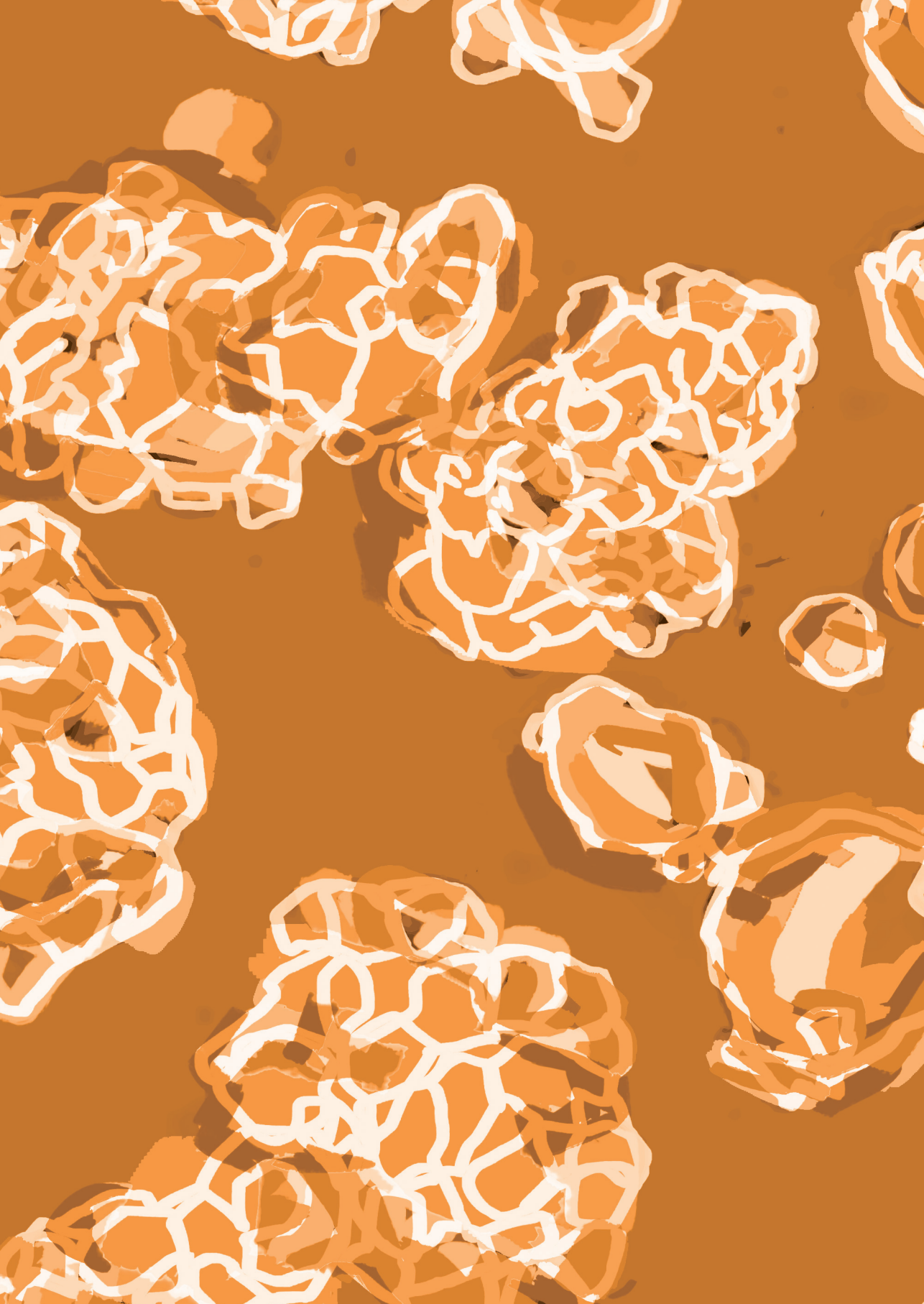
CHAPTER 2

61. Nunes V, Gasparini P, Novelli G, Gaona A, Bonizzato A, Sangiuolo F, Balassopoulou A, Giménez FJ, Dognini M, Ravnik-Glavac M. Analysis of 14 cystic fibrosis mutations in five south European populations. *Hum. Genet.* 1991; 87: 737–738.
62. Dean M, White MB, Amos J, Gerrard B, Stewart C, Khaw KT, Leppert M. Multiple mutations in highly conserved residues are found in mildly affected cystic fibrosis patients. *Cell* 1990; 61: 863–870.
63. DN S, DP R, LS O, RJ G, AE S, MJ W. Mutations in CFTR associated with mild-disease-form Cl- channels with altered pore properties. *Nature* [Internet] 1993; 362: 160–164 Available from: <http://queens.ezp1.qub.ac.uk/login?url=http://ovidsp.ovid.com/ovidweb.cgi?T=JS&CSC=Y&NEWS=N&PAGE=full-text&D=med3&AN=7680769%0Ahttp://resolver.ebscohost.com/openurl?sid=OVID:medline&id=pubmed:7680769&id=doi:&issn=0028-0836&isbn=&volume=362&issue=6416&spage=1>.
64. Gentzsch M, Ren HY, Houck SA, Quinney NL, Cholon DM, Sophia P, Chaudhry IG, Das J, Dokholyan N V., Randell SH, Cyr DM. Restoration of R117H CFTR folding and function in human airway cells through combination treatment with VX-809 and VX-770. *Am J Physiol Lung Cell Mol Physiol.* 2016; 311: L550–L559.
65. Yu YC, Sohma Y, Hwang TC. On the mechanism of gating defects caused by the R117H mutation in cystic fibrosis transmembrane conductance regulator. *J. Physiol.* 2016; 594: 3227–3244.
66. Estivill X, Ortigosa L, Pérez-Frias J, J Dapena JF, Peña L, Peña L, Llevadot R, Giménez J, Nunes V. Clinical characteristics of 16 cystic fibrosis patients with the missense mutation R334W, a pancreatic insufficiency mutation with variable age of onset and interfamilial clinical differences. *Hum. Genet.* 1995; 95: 331–336.
67. Cutting GR, Kasch LM, Rosensteint BJ, Zielenskit J, Tsuit L, Antonarakis SE. A cluster of cystic fibrosis mutations in the first nucleotide-binding fold of the cystic fibrosis conductance regulator. *1990; 346: 366–369.*
68. Hughes D, Wallace A, Taylor J, Tassabehji M, McMahon R, Hill A, Nevin N, Graham C. Fluorescent multiplex microsatellites used to define haplotypes associated with 75 CFTR mutations from the UK on 437 CF chromosomes. *Hum. Mutat.* 1996; 8: 229–235.
69. Kälin N, Dörk T, Tümmeler B. A cystic fibrosis allele encoding missense mutations in both nucleotide binding folds of the cystic fibrosis transmembrane conductance regulator. *Hum. Mutat.* 1992; 1: 204–210.
70. De Bie I, Agatep R, Scott P, Ruchon A. Report on the p.Ser489X (p.Ser489) CFTR mutation, a variant with severe associated phenotype and high prevalence in a Quebec French-Canadian cystic fibrosis patient population. *Genet. Med.* 2012; 14: 883–886.
71. Prach L, Koepke R, Kharrazi M, Keiles S, Salinas DB, Reyes MC, Pian M, Opsimos H, Otsuka KN, Hardy KA, Milla CE, Zirbes JM, Chipps B, O'Bra S, Saeed MM, Sudhakar R, Lehto S, Nielson D, Shay GF, Seastrand M, Jhawar S, Nickerson B, Landon C, Thompson A, Nussbaum E, Chin T, Wojtczak H. Novel CFTR variants identified during the first 3 years of cystic fibrosis newborn screening in California. *J. Mol. Diagnostics* [Internet] American Society for Investigative Pathology; 2013; 15: 710–722 Available from: <http://dx.doi.org/10.1016/j.jmoldx.2013.05.006>.
72. Dayangaç-Erden D, Atalay M, Emirlioğlu N, Hızal M, Polat S, Özçelik U, Yalçın E, Doğru D, Yılmaz E, Kiper N. Mutations of the CFTR gene and novel variants in Turkish patients with cystic fibrosis: 24-years experience. *Clin. Chim. Acta* 2020; 510: 252–259.
73. Vidaud M, Fanen P, Martin J, Ghanem N, Nicolas S, Goossens M. Three point mutations in the CFTR gene in French cystic fibrosis patients: identification by denaturing gradient gel electrophoresis. *Hum. Genet.* 1990; 85: 446–449.
74. Cheadle JP, Al-Jader LN, Meredith AL. A novel nonsense mutation, W846X (amber termination), in exon 14a of the cystic fibrosis transmembrane conductance regulator (CFTR) gene. *Hum. Mol. Genet.* [Internet] 1993; 2: 1067–1068 Available from: <https://doi.org/10.1093/hmg/2.7.1067>.
75. Bozon D, Zielenski J, Rininsland F, Lap-Chee Tsui. Identification of four new mutations in the cystic fibrosis transmembrane conductance regulator gene: I148T, L1077P, Y1092X, 2183AA>G. *Hum. Mutat.* [Internet] 1994; 3: 330–332 Available from: <https://doi.org/10.1002/humu.1380030329>.

Association of Forskolin-induced Organoid Swelling with Long-term CF Disease Progression

76. Liu K, Xu W, Xiao M, Zhao X, Bian C, Zhang Q, Song J, Chen K, Tian X, Liu Y, Xu KF, Zhang X. Characterization of clinical and genetic spectrum of Chinese patients with cystic fibrosis. *Orphanet J. Rare Dis.* Orphanet Journal of Rare Diseases; 2020; 15: 1-10.
77. Castaldo G, Fuccio A, Cazeneuve C, Picci L, Salvatore D, Scarpa M, Goossens M, Salvatore F. A novel nonsense mutation (Y849X) in the CFTR gene of a CF patient from southern Italy. *Hum. Mutat.* 1999; 14: 272.







CFTR RESCUE IN INTESTINAL ORGANOIDS WITH GLPG/ABBV-2737, ABBV/ GLPG-2222 AND ABBV/GLPG-2451 TRIPLE THERAPY

Published as Brief Research Report

Eyleen de Poel, Sacha Spelier, Ricardo Korporaal, Ka Wai Lai, Sylvia F. Boj, Katja Conrath,
Cornelis K. van der Ent and Jeffrey M. Beekman

Frontiers in Molecular Biosciences 8: 698358 (2021)

ABSTRACT

Cystic fibrosis transmembrane conductance regulator (CFTR) modulators have transformed the treatment of cystic fibrosis (CF) by targeting the basis of the disease. In particular, treatment regimen consisting of multiple compounds with complementary mechanisms of action have been shown to result in optimal efficacy. Here, we assessed the efficacy of combinations of the CFTR modulators ABBV/GLPG-2222, GLPG/ABBV-2737 and ABBV/GLPG-2451, and compared it to VX-770/VX-809 in 28 organoid lines heterozygous for F508del allele and a class I mutation and seven homozygous F508del organoid lines. The combination ABBV/GLPG-2222/ABBV-2737/ABBV/GLPG-2451 showed increased efficacy over VX-770/VX-809 for most organoids, despite considerable variation in efficacy between the different organoid cultures. These differences in CFTR restoration between organoids with comparable genotypes underline the relevance of continuing to optimize the ABBV/GLPG-Triple therapy, as well as the in vitro characterization of efficacy in clinically relevant models.

INTRODUCTION

Cystic fibrosis (CF) is a monogenetic, autosomal, recessive disease caused by mutations in the cystic fibrosis transmembrane conductance regulator (CFTR) gene¹. Various mutations in CFTR have been characterized that result in dysfunction or complete absence of CFTR, which is followed by ion misbalance and subsequent aberrant fluid secretion in multiple organ systems such as the intestine, airways and pancreas¹. For patients with common mutations, like F508del and G5551D multiple CFTR modulating compounds have been developed that rescue the mutation specific defects. These first generation CFTR modulating drugs however do not restore CFTR function in CF patients with 1 F508del mutation sufficiently². In line with these clinical observations, in vitro experiments still detect the presence of immature (B-band) CFTR after treatment with CFTR corrector VX-809 treated F508del cells³, providing the rationale for combining two correctors with a complementary mode of action that collectively further restore the trafficking defect. The recent discovery of the triple combination of VX-445/VX-661/VX-770 clearly shows that indeed a combination of two correctors with a potentiator is required to obtain high efficacy CFTR modulation⁴. However, recent clinical studies showed great variation in triple treatment efficacy, highlighting the need for expanding the pool of treatment options⁵. One such new triple therapy that showed effective rescue of CFTR in human bronchial epithelial cells is developed by Abbvie and consists of the Abbvie/GLPG correctors ABBV/GLPG-2222⁶ and GLPG/ABBV-2737⁷ and potentiator ABBV/GLPG-2451⁸. ABBV/GLPG-2222 and ABBV/GLPG-2451 exhibit similarities in biological activity with respectively VX-809 and VX-770, but rescue F508del-CFTR more potently⁹. In an effort to further increase the efficacy of the combination of ABBV/GLPG-2222/ABBV/GLPG-2451, another corrector with a complementary mode of action, termed GLPG/ABBV-2737 was developed that exerted functional synergy with ABBV/GLPG-2222 and VX-809⁷. Combining these modulators into a triple therapy resulted in a two-fold increase in Cl- current in F508del/F508del HBE cells compared to VX770/VX809 treatment⁶.

In this report we compare the efficacy of single, dual or triple combinations of ABBV/GLPG-2222, GLPG/ABBV-2737 and ABBV/GLPG-2451 to VX-809/VX-770 using intestinal organoids and the forskolin (FSK) induced swelling (FIS) assay¹⁰. In vitro FIS response of patient-derived intestinal organoids upon modulator therapy has been shown to predict in vivo response to therapy^{11,12}, making this model a relevant model in the context of preclinical drug discovery and lead selection. To assess efficacy and between-patient variability of the ABBV/GLPG-compounds on rescuing F508del-CFTR, we measured FIS in 35 intestinal organoid cultures, 7 expressing F508del/F508del-CFTR and 28 expressing F508del/minimal function CFTR. All organoids cultures did not exhibit swelling when exposed to solely forskolin, indicating the absence of residual CFTR function for all organoid cultures. Ultimately, the aim of this report is to assess the preclinical efficacy of a newly developed triple therapy and to identify people with CF likely to benefit from modulator therapy.

MATERIAL AND METHODS

Collection of material of primary epithelial cells

All experimentation using human tissues described herein was approved by the medical ethical committee at University Medical Center Utrecht (UMCU; TcBio#14-008) and performed following the guidelines of the European Network of Research Ethics Committees (EUREC) following European, national, and local law. Informed consent for tissue collection, generation, storage, and use of the organoids was obtained from all study participants. Biobanked intestinal organoids are stored and catalogued at the foundation Hubrecht Organoid Technology (HUB, <http://hub4organoids.eu>).

Organoid culture and FIS assay

Crypts were isolated from rectal biopsies of subjects with cystic fibrosis as previously described¹⁵. In brief, biopsies were washed with cold DMEM/F12 and incubated with 10 mM EDTA for 30 minutes. After harvesting the crypts containing supernatant, EDTA was washed away and crypts were seeded in 50% Matrigel in 24-well plates (~10 to 30 crypts in three 10-ml Matrigel droplets per well). Growth medium¹³ was further supplemented with Primocin (1:500; Invivogen). Organoids were incubated in a humidified chamber with 5% CO₂ at 37°C. Medium was refreshed every 2–3 days, and organoids were passaged 1:4 every 7 days. Prior to conducting FIS assays, organoids were cultured at least 3 weeks after thawing or crypt isolation. To quantify the organoid size increase over time, organoids are stained with calcein green (10 µM) which is added 30 minutes prior to the addition of forskolin and CFTR potentiators ABBV/GLPG-2451 and VX-770. All CFTR correctors (ABBV/GLPG-2222 and GLPG/ABBV-2737 were added during plating of the organoids, 24h prior to the FIS-assay. Forskolin was used at a 5 µM concentration, except in the FIS assay on F508del/F508del donors in which forskolin was used at 0.8 µM. All CFTR modulators were used at a 3 µM, with the exception of the FIS assay on F508del/F508del donors in which all ABBV/GLPG2451 and GLPLG/ABBV2737 were used at 1 µM and ABBV/GLPG-2222 at 0.15 µM. Organoid swelling was measured using a confocal microscope, followed by quantification of total organoid surface area per well based on calcein staining. To correct for well to well differences in total organoid area, increase of organoid surface area over time was normalized to the organoid surface area of the first time point for each well as described by¹⁵. All experiments with GLPG/ABBV compounds were conducted with 2-3 technical replicates. Orkambi stimulated FIS served as a positive control, while FIS with only forskolin served as negative control.

RESULTS

Rescue of minimal-function and residual-function CFTR mutations with ABBV/GLPG-2222, GLPG/ABBV-2737 and ABBV/GLPG-2451

We first compared the efficacy of single, dual and triple compound combinations in 3 organoid cultures harboring distinct F508del/minimal function genotypes and 1 negative control organoid culture homozygous for a consensus splice mutation (**figure 1**). Whereas single compounds did not result in increased levels of organoid swelling in F508del/R1162X and

CFTR rescue in intestinal organoids with GLPG/ABBV-2737, ABBV/GLPG-2222
and ABBV/GLPG-2451 triple therapy

F508del/711+1G>T, it resulted in a mild increase in swelling (+/- 1000 AUC) for the F508del/W1282x organoid culture. The two dual combinations of one corrector (ABBV/GLPG-2222 or GLPG/ABBV-2737) and the potentiator ABBV/GLPG-2451, resulted in substantial swelling. For two organoid cultures, expressing F508del/R1162X and F508del/711+1G>T CFTR, the combination of all three ABBV/GLPG compounds resulted in a further increased AUC. Interestingly, the combination of one corrector and ABBV/GLPG-2451 resulted in similar swelling levels as the ABBV/GLPG-Triple in the W1282X organoid culture.

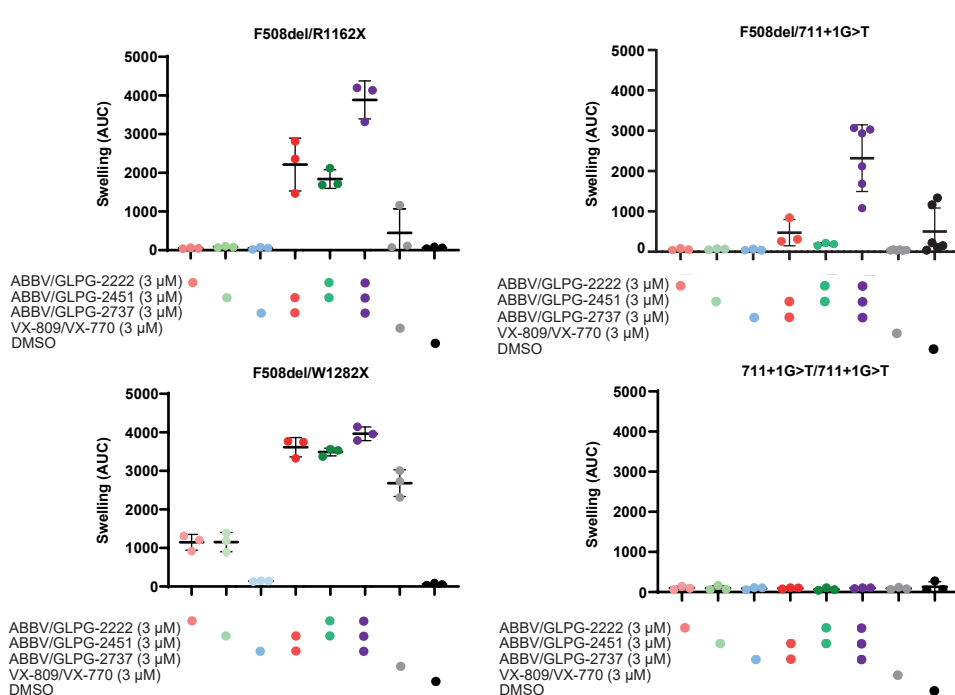


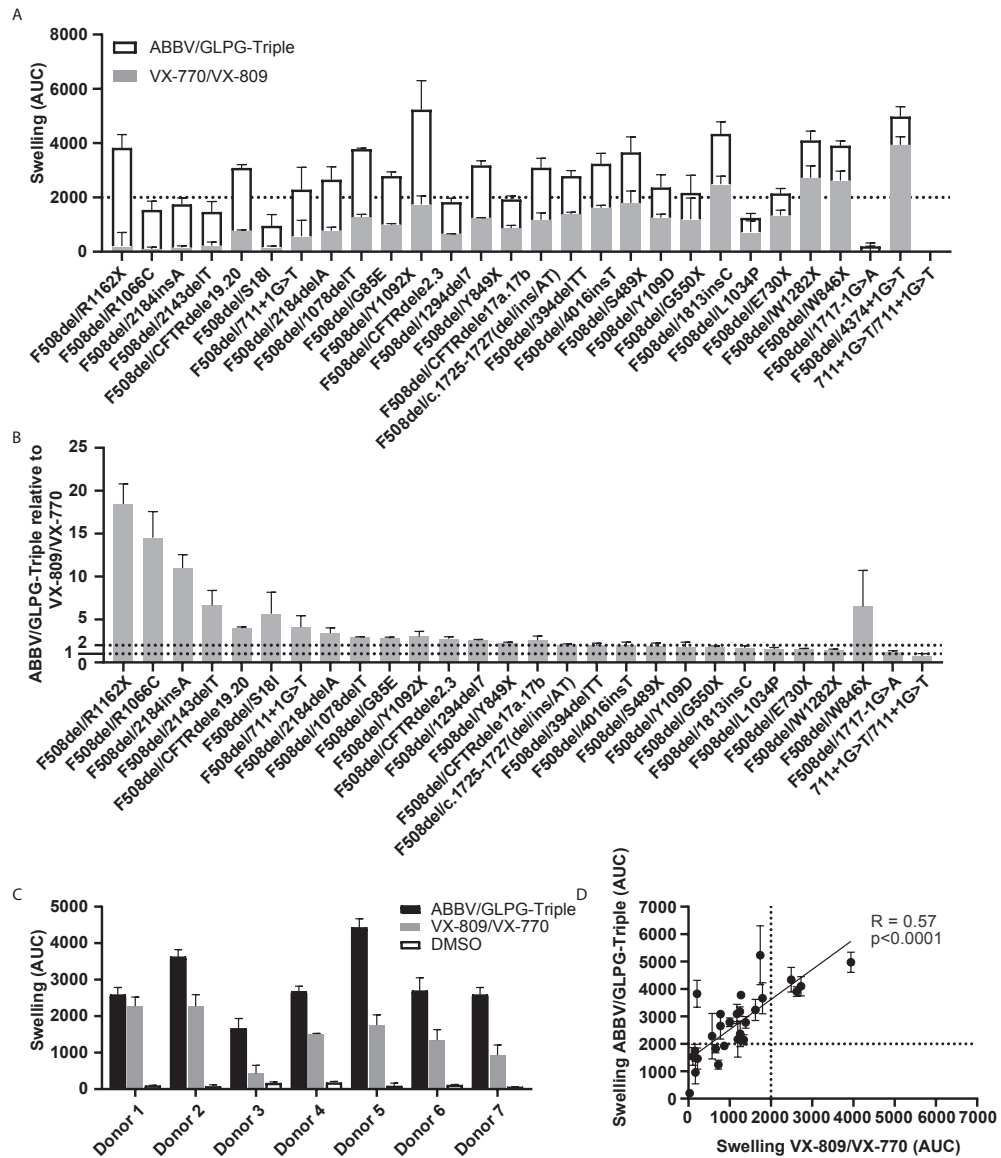
Figure 1: CFTR function rescue with single, dual and triple ABBV/GLPG modulator therapy in intestinal organoids.

FIS responses of three organoid cultures expressing F508del/minimal function genotypes and one organoid culture homozygous for 711+1G>T, stimulated with 5.0 μM forskolin for 1 hour. FIS responses were measured upon treatment with ABVV/GLPG compounds, VX-809/VX-770 and DMSO. n=3 or n=6, each bar represents mean +/- SD.

Next, the ABBV/GLPG-Triple as well as VX-809/VX-770 were tested on 28 organoid cultures harboring F508del/minimal function genotypes (**figure 2A**). Upon exposure to the ABBV/GLPG-Triple substantial AUC values were observed (AUC >2000 for 19/28 lines). Although the efficacy of the triple therapy greatly varied between the different organoid cultures, organoid swelling increased on average by 297% with the ABBV/GLPG-Triple compared to VX-809/VX-770 (**figure 2B**). Not only did we observe large variation in CFTR function rescue between organoids expressing distinct F508del/minimal function genotypes, we also observed variation in treatment response between organoids carrying F508del/F508del-CFTR (**figure 2C**).

CHAPTER 3

More-over, we compared Orkambi response and ABBV/GLPG-Triple response in the panel of 28 organoid lines and observed a linear positive correlation ($R=0.57$) indicating that organoid cultures that respond to Orkambi are likely to regain CFTR when treated with the ABBV/GLPG-Triple (figure 2D).



CFTR rescue in intestinal organoids with GLPG/ABBV-2737, ABBV/GLPG-2222 and ABBV/GLPG-2451 triple therapy

Figure 2: FIS response of F508del/minimal function organoid cultures upon ABBV/GLPG-Triple therapy.

- A.** FIS response upon VX-770/VX-809 (3 μ M, gray bars) and Abbvie-Triple (ABBV/GLPG-2222 3 μ M + GLPG/ABBV-2737 3 μ M + ABBV/GLPG-2451 3 μ M, white bars, stacked) treatment, corrected for the DMSO condition. n=3, each bar represents mean+SD. CFTR correctors were added 24h prior to FIS measurements, CFTR potentiators were simultaneously added with 5 μ M FSK.
- B.** FIS response upon the ABBV/GLPG-Triple (3 μ M) relative to VX-770/VX-809 (3 μ M) treatment, both corrected for the DMSO condition. n=3, each bar represents mean+SD. Similar raw data was used in **figure A and B**, yet differentially illustrated.
- C.** FIS response of seven F508del/F508del organoid cultures upon treatment with ABBV/GLPG-Triple (ABBV/GLPG-2222 1 μ M + GLPG/ABBV-2737 1 μ M + ABBV/GLPG-2451 1 μ M) or VX-809/VX-770 (1 μ M) and 0.8 μ M FSK. n=3, bars represent mean+SD.
- D.** Correlation of FIS responses upon the ABBV/GLPG-Triple (3 μ M) and VX-770/VX-809 (3 μ M) treatment, n=3, each datapoint represents mean+/-SD.

DISCUSSION

The objective of this study was to assess efficacy of CFTR-F508del restoration by the single ABBV/GLPG modulators (ABBV/GLPG-2222/GLPG/ABBV-2737/ABBV/GLPG-2451) and all combinations thereof in comparison to VX-809/VX-770 by measuring FIS in organoids carrying at least one single F508del allele. We observed highest CFTR-restoring efficacy with the ABBV/GLPG-Triple, which is consistent with previous studies showing the additive effect on CFTR function rescue with three compounds with complementing working mechanisms⁴. In 19 organoid cultures, AUC values of over 2000 were observed with the ABBV/GLPG-Triple. Comparable AUC values are obtained with VX-809/VX-770 and F508del/F508del organoids (around 2500 AUC¹¹), indicating that clinical efficacy of the ABBV/GLPG-Triple for pwCF compound heterozygous for F508del might be similar to the clinical effect of VX-809/VX-770 for pwCF homozygous for F508del-CFTR.

Interestingly, despite this general high efficacy, we observed great variation in response between both F508del/minimal function as well as between the F508del/F508del organoid cultures. The latter observation might indicate the presence of other cis-mutations in the CFTR gene or other genetic modifiers affecting CFTR-mediated fluid transport, two processes summarized in an excellent recent review¹³. Another possible explanation for the variation in drug efficacy between the F508del/minimal function organoids might be partial rescue of the minimal function allele with the ABBV/GLPG-modulators. We observed for example in the F508del/W1282X organoid culture some swelling response when pretreated with only 1 corrector, and hardly a difference between the dual ABBV/GLPG combinations and the triple ABBV/GLPG combination. This could be explained by the fact that the premature termination codon (PTC) mutation occurs late in the CFTR gene, resulting in only a minor truncation of the W1282X CFTR variant allowing further rescue by CFTR modulators, such as VX-770 as earlier described by¹². This illustrates the potential contribution of the compound heterozygous mutations to the observed differences. In order to assess whether the variation in drug efficacy among pwCF is the result of rescue of the minimal function allele, future drug efficacy studies should also include allele specific biochemical analysis. Additional to the observed variation, two F508del/minimal function organoid cultures (expressing F508del/W846X and F508del/4374+1G>T CFTR) hardly responded to either VX-770/VX-809 or ABBV/GLPG-Triple, which corresponds to the results obtained with the VX-659/VX-661/VX-770 study, also showing two study participants not improving in mean change in FEV1 upon VX-659/VX-661/VX-770 therapy⁵. Despite the overall variation, response to VX-770/VX-809 correlated in a linear positive manner with response to the ABBV/GLPG-Triple. This especially underlines the benefit of ABBV/GLPG-Triple therapy for patients that are mildly responsive to VX-770/VX-809.

CHAPTER 3

Whether the ABBV/GLPG-Triple therapy is specifically effective for pwCF currently not benefitting from VX-445/VX-661/VX-770 therapy remains unclear, as the clinical trial reports did not share genotypes¹⁴. Future research should therefore investigate efficacy of the VX-445/VX-661/VX-770 in a large panel of F508del/minimal function organoids. In addition, it would be interesting to compare these results to the results obtained with the ABBV/GLPG-Triple. In future studies, it could be interesting to assess the efficacy of the GLPG/ABBV compounds in nasal/bronchial epithelial cells to confirm that rescue of CFTR is also achievable in airway-derived primary cells. Intestinal organoids are however superior over nasal or bronchial epithelial organoids when assessing function of CFTR by means of organoid swelling, as swelling of intestinal organoids is completely CFTR dependent whilst additional ion channels present in airway organoids also influence swelling. The effect of CFTR-mediated airway organoid swelling could therefore be underestimated. Finally, it should be noted that the absolute swelling values obtained in this manuscript cannot be directly compared to other published drug-induced FIS data, as experiments were performed with 5 µM or 0.8 µM forskolin instead of 0.128 µM forskolin^{12,15}.

In summary, we confirm that combining compounds with complementary working mechanisms is a valuable approach for restoring CFTR function. We also show that characterizing compound efficacy in a personalized manner is required, as we observe great variation in drug efficacy between organoid cultures with comparable and even identical genotypes. Identifying individuals with a high modulator-responsive genotype ultimately will help in better understanding which genetic or cellular processes influence response to therapy and in defining personalized treatment regimes.

ACKNOWLEDGEMENTS

This study is powered by Health~Holland, Top Sector Life Sciences & Health. Health-Holland (40-41200-98-9296). Organoid experiments performed at HUB were funded by Galapagos.

AUTHOR CONTRIBUTIONS

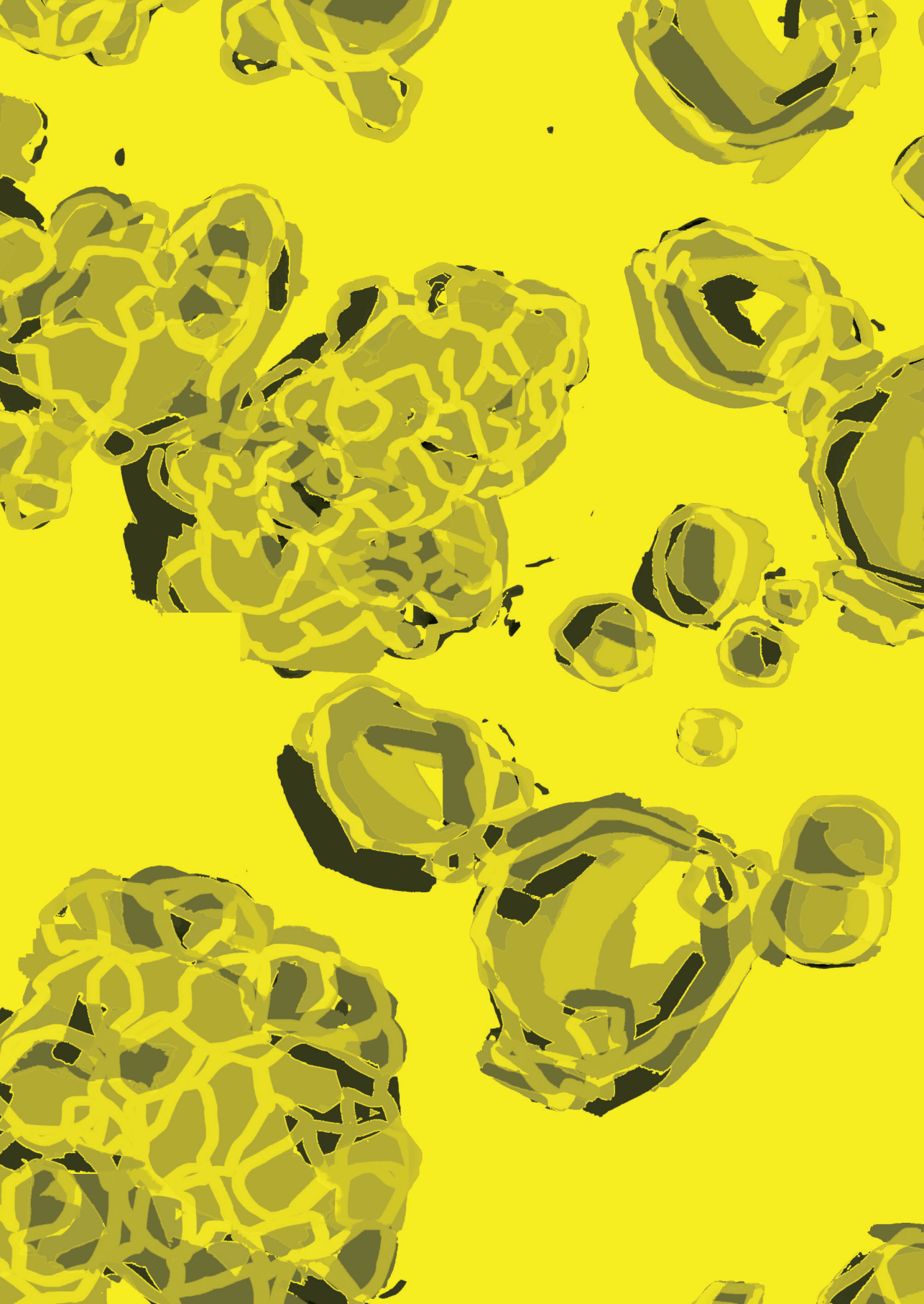
EDP Conceptualization, Formal analysis, Visualization, Writing - original draft, Writing - review & editing; SS Conceptualization, Formal analysis, Visualization, Writing - original draft, Writing - review & editing; RK Data collection, Data analysis; KWL Data collection, Data analysis; SB Conceptualization, Data curation, Formal analysis, Investigation, Methodology, Project administration; Resources; KC Conceptualization, Methodology, Supervision; CKE Funding acquisition; JB Conceptualization, Funding acquisition, Methodology, Supervision

DECLARATION OF INTEREST

HUB is a foundation which holds the exclusive rights to Organoid Technology patents. JMB and CKE are inventors on patent(s) related to the FIS-assay and received financial royalties from 2017 onward. JMB AND CKE report receiving research grant(s) and consultancy fees from various industries, including Vertex Pharmaceuticals, Proteostasis Therapeutics, Eloxx Pharmaceuticals, Teva Pharmaceutical Industries and Galapagos outside the submitted work.

REFERENCES

1. Sosnay PR, Siklosi KR, Van Goor F, Kanicki K, Yu H, Sharma N, et al. Defining the disease liability of variants in the cystic fibrosis transmembrane conductance regulator gene. *Nat Genet* [Internet]. 2013;45(10):1160–7. Available from: <http://dx.doi.org/10.1038/ng.2745>
2. Rowe SM, McColley SA, Rietschel E, Li X, Bell SC, Konstan MW, et al. Lumacaftor/ivacaftor treatment of patients with cystic fibrosis heterozygous for F508del-CFTR. *Ann Am Thorac Soc*. 2017;14(2):213–9.
3. Van Goor F, Hadida S, Grootenhuis PDJ, Burton B, Stack JH, Straley KS, et al. Correction of the F508del-CFTR protein processing defect in vitro by the investigational drug VX-809. *Proc Natl Acad Sci U S A*. 2011;108(46):18843–8.
4. Veit G, Roldan A, Hancock MA, da Fonte DF, Xu H, Hussein M, et al. Allosteric folding correction of F508del and rare CFTR mutants by elexacaftor-tezacaftor-ivacaftor (Trikafta) combination. *JCI Insight*. 2020;5(18):1–14.
5. Davies JC, Moskowitz SM, Brown C, Horsley A, Mall MA, McKone EF, et al. VX-659-Tezacaftor-Ivacaftor in Patients with Cystic Fibrosis and One or Two Phe508del Alleles. *N Engl J Med*. 2018 Oct;379(17):1599–611.
6. Wang X, Liu B, Searle X, Yeung C, Bogdan A, Greszler S, et al. Discovery of 4-[(2 R, 4 R)-4-((1-(2, 2-Difluoro-1, 3-benzodioxol-5-yl) cyclopropyl) carbonyl) amino)-7-(difluoromethoxy)-3, 4-dihydro-2 H-chromen-2-yl] benzoic Acid (ABBV/GLPG-2222), a potent cystic fibrosis transmembrane conductance regulator (CFTR) corrector. *J Med Chem*. 2018;61:1436–49.
7. de Wilde G, Gees M, Musch S, Verdonck K, Jans M, Wesse A-S, et al. Identification of GLPG/ABBV-2737, a novel class of corrector, which exerts functional synergy with other CFTR modulators. *Front Pharmacol*. 2019;10:514.
8. Van der Plas SE, Kelgtermans H, Mammoliti O, Menet C, Tricarico G, De Blieck A, et al. Discovery of GLPG2451, a Novel Once Daily Potentiator for the Treatment of Cystic Fibrosis. *J Med Chem*.
9. Singh AK, Alani S, Balut C, Fan Y, Gao W, Greszler S, et al. Discovery and characterization of ABBV/ GLPG-2222, a novel first generation CFTR corrector. *Pediatr Pulmonol* [Internet]. 2016;51:264–5. Available from: <http://www.embase.com/search/results?subaction=viewrecord&from=export&id=L612358876%5Cnhttp://dx.doi.org/10.1002/ppul.23576%5Cnhttp://sfx.library.uu.nl/utrecht?sid=EMBASE&issn=10990496&id=doi:10.1002%2Fppul.23576&atitle=Discovery+and+characterization+of+ABBV%2F>
10. Boj SF, Vonk AM, Stacia M, Su J, Vries RRG, Beekman JM, et al. Forskolin-induced Swelling in Intestinal Organoids: An In Vitro Assay for Assessing Drug Response in Cystic Fibrosis Patients. *J Vis Exp*. 2017;(120):1–12.
11. Dekkers JF, Berkers G, Kruisselbrink E, Vonk A, De Jonge HR, Janssens HM, et al. Characterizing responses to CFTR-modulating drugs using rectal organoids derived from subjects with cystic fibrosis. *Sci Transl Med*. 2016;8(344):344–84.
12. Berkers G, van Mourik P, Vonk AM, Kruisselbrink E, Dekkers JF, de Winter-de Groot KM, et al. Rectal Organoids Enable Personalized Treatment of Cystic Fibrosis. *Cell Rep* [Internet]. 2019;26(7):1701–1708. e3. Available from: <https://doi.org/10.1016/j.celrep.2019.01.068>
13. Paranjape A, Ruffin M, Harris A, Corvol H. Genetic variation in CFTR and modifier loci may modulate cystic fibrosis disease severity. *J Cyst Fibros*. 2020;19:S10–4.
14. Middleton PG, Mall MA, Dřevínek P, Lands LC, McKone EF, Polineni D, et al. Elexacaftor–Tezacaftor–Ivacaftor for Cystic Fibrosis with a Single Phe508del Allele. *N Engl J Med*. 2019;381(19):1809–19.
15. Dekkers JF, Wiegerinck CL, De Jonge HR, Bronsveld I, Janssens HM, De Winter-De Groot KM, et al. A functional CFTR assay using primary cystic fibrosis intestinal organoids. *Nat Med* [Internet]. 2013;19(7):939–45. Available from: <http://dx.doi.org/10.1038/nm.3201>





PRE-CLINICAL EFFICACY TESTING OF FDA-APPROVED DRUGS FOR NON- HOMOZYGOUS F508DEL-CFTR GENOTYPES

Manuscript in preparation

E. de Poel, S. Spelier, M.C. Hagemeijer, P. van Mourik, S.W.F. Suen, A.M. Vonk, J.E. BrunsVELD,
E. Kruisselbrink, H. Oppelaar, G. Berkers, K.M. de Winter-de Groot, S. Heida-Michel,
S.R. Jans, H. van Panhuis , M.M. van der Eerden, R. van der Meer, J. Roukema, E. Dompeling,
E.J.M. Weersink, G.H. Koppelman, R. Vries, C.K. van der Ent and J.M. Beekman

ABSTRACT

Background: CFTR function measurements in patient-derived intestinal organoids (PDIO's) associate with clinical features of cystic fibrosis and may enable drug repurposing in a personalized setting. Cystic fibrosis is a rare hereditary disease caused by mutations in both alleles of the CFTR gene. Recent therapies enable effective restoration of CFTR function of the most prevalent F508del CFTR mutation, and shift the clinical unmet need largely towards people with rare CFTR mutations. Medium-to-high throughput assays with PDIO models can help to identify drugs that modulate CFTR function and may help to select responding individuals to such drugs.

Objective: To identify CFTR function enhancing drugs from FDA-approved drugs by a PDIO-based personalized drug screening approach.

Methods: Development of a medium-to-high throughput 384-wells CFTR function assay based on forskolin-induced swelling and identification of CFTR function enhancing drugs from 1443 FDA-approved drugs using 230 PDIO's covering 167 different non-homozygous F508del-CFTR genotypes.

Results: The 384-wells FIS-assay showed to be reproducible, has a large wide dynamic range and comparable responses were obtained as with the conventional 96-well based setup. Out of 1443 FDA, 43 drugs were excluded based on toxicity, and 1400 drugs were tested on 76 PDIO. Results identified existing CFTR modulators in the FDA-drug library as most effective inducers of organoid fluid secretion. Besides CFTR modulators, drugs that target cAMP were found as second most interesting category of fluid secretion inducers.

Conclusion: This study exemplifies the feasibility of large-scale compound screening using PDIOs, and found CFTR modulators as most effective drugs of organoid fluid secretion in non-homozygous F508del PDIOs. We furthermore show the potential of repurposing drugs for people with CF carrying non-F508del homozygous organoid cultures and may provide an alternative treatment option for people that are devoid of current CFTR modulator therapies.

TAKE HOME MESSAGE

It is feasible to implement the miniaturized PDIO-based FIS-assay performed in 384-well format for a large-scale compound screening. Moreover, people with CF carrying non-homozygous F508del-CFTR genotypes will likely benefit from FDA-approved drug-therapies such as CFTR modulators or PDE4 inhibitors.

INTRODUCTION

Drug repurposing is a strategy to identify new indications for approved or investigational drugs that are outside the scope of the original medical indication^{1,2}. It is particularly relevant for individuals with rare diseases for whom limited treatments are available due to the economic and technical complexities of drug development for small populations.

Cystic fibrosis (CF) is a rare, monogenic disease caused by mutations in the CFTR gene of which more than 1700 distinct mutations have been estimated to be disease-causing³. New treatments for CF (so called CFTR modulators)^{4,5} that restore CFTR function are increasingly effective for the most prevalent F508del mutation and additional responsive mutations. However, access to these expensive treatments remains limited and the identification and development of other therapies remains needed for treatment of all people with CF⁶. Drug repurposing efforts could therefore potentially yield new therapeutic options for individuals with CF.

Patient-derived intestinal organoids (PDIO) can provide a platform for drug repurposing in CF. PDIO are multicellular 3D structures that phenotypically copy features of the originating tissue from which they grow, and especially intestinal organoids have been widely used because of their in vitro long term growth properties. We developed the first PDIO-based disease model based on forskolin-induced swelling of organoids grown from rectal biopsies of individuals with CF. Forskolin (fsk) induces fluid secretion into the organoid lumen which causes the whole organoid structure to rapidly swell in a (near-to) complete CFTR-dependent manner, which can be easily quantified with automated live-cell-microscopy⁷⁻⁹. As found by us and others, CFTR function measurements in PDIO associate with disease severity indicators of CF and therapeutic response, and enable drug discovery efforts¹⁰⁻¹² as well as the matching of patients and drugs in the laboratory. The PDIO-based screening platform is therefore well suited for finding drugs that directly or indirectly influence CFTR function.

PDIO offer several advantages for drug repurposing in comparison with more conventional airway primary cell models. In contrast with CFTR function measurements in highly differentiated airway cells grown on air-liquid interfaces, CFTR in intestinal organoids is expressed under culture conditions associated with cell expansion and not terminal differentiation¹³. This enables the rapid propagation of CFTR expressing patient-derived cells for large scale experimentation. Another advantage is that many PDIO have been biobanked and are readily accessible for research purposes. Also, the forskolin-induced swelling (FIS) assay is a phenotypic assay based on low-resolution microscopy and is performed in standard 96 wells plates that enable a relatively high assay using confocal setups with automated stages that are available at many research institutes. These combinations enable the screening of relatively high numbers of drugs and PDIO.

Here, we further miniaturize the 96-wells FIS assay towards a 384-wells assay that enables drug screening at higher throughput. We use this assay to screen 1443 FDA-approved drugs on 76 PDIO and validate the prioritized hits in 230 PDIO that are non-homozygous for F508del-CFTR mutations. Clear efficacy across many PDIO was observed for the FDA

approved CFTR modulators. Additional hits were identified of which the potentiators of endogenous cAMP (e.g. roflumilast) appeared most promising for repurposing in the context of residual CFTR function. In conclusion, we demonstrated that drug screening is feasible on a great collection of PDIO using a novel 384-well FIS assay, and we found that people with CF carrying non-homozygous F508del-CFTR genotypes can benefit from already existing and approved drugs.

MATERIALS AND METHODS

Collection of primary epithelial cells of CF patients (pwCF)

All experimentation using human tissues described herein was approved by the medical ethical committee at University Medical Center Utrecht (UMCU; TcBio#14-008 and TcBio#16-586]. Informed consent for intestinal tissue collection, generation, storage, and use of the organoids was obtained from all participating patients. Biobanked intestinal organoids are stored and catalogued (<https://huborganoids.nl/>) at the foundation Hubrecht Organoid Technology (<http://hub4organoids.eu>) and can be requested at info@hub4organoids.eu

Human intestinal organoid culture

Human intestinal organoid culture was executed as described by Vonk et al⁸.

384-well FIS assay validation

To determine 384-well forskolin induced swelling (FIS)-assay a quality replicate experiment was conducted. Three 384-wells plates were seeded with F508del/F508del organoids and three with F508del/S1251N organoids. 384-wells plates were seeded after three different organoid culture periods up to twelve weeks. The F508del/S1251N organoids were submerged in 8 µL complete culture medium, the F508del/F508del organoids in 8 µL complete culture medium supplemented with 3 µM VX-809. The next day, FIS measurements were assessed in the presence of VX-770 (3 µM) and low and high forskolin (fsk) concentrations. No swelling is induced with the low concentration (= min signal; 0.008 µM), maximum level of swelling after 1 hour is induced with the high concentration (= max signal; 5 µM). Organoid swelling was monitored for 60 minutes using a Zeiss LSM 710 confocal microscope. Total organoid surface area per well was quantified based on calcein green staining using Zen Blue Software and area under the curve over time was calculated as described by Vonk et al⁸. The minimum and maximum swelling signals were included to enable Z'-factor calculation of each 384-well plate according to the following formula: $Z'\text{-factor} = 1 - (3(\sigma_p - \sigma_n)/(\mu_p - \mu_n))$, where σ_p is the standard deviation of the max signal wells ($n=128$ per plate, + CFTR modulator(s) and 5 µM fsk), σ_n is the standard deviation of the min signal wells ($n=128$ per plate, + CFTR modulator(s) and 0.008 µM fsk), μ_p is the mean of the max signal wells, μ_n is the mean of the min signal wells. The location of min and max signal wells were deliberately placed in different columns per plate to investigate spatial uniformity and edge effects.

Comparing 384 well format with conventional 96-well format FIS assay

FIS of F508del/F508del and F508del/S1251N organoids w/w/o CFTR modulator(s) and increasing concentration of fsk performed in 96-wells plates was compared to FIS under similar conditions performed in 384-wells plates. F508del/F508del organoids were treated with VX-809 (3 μ M) for 24h prior to FIS assays. VX-770 (3 μ M) was added simultaneously with fsk for 1h. Z'-factors were calculated based on the minimal swelling signals induced with 0.008 or 0.02 μ M fsk + CFTR modulators and the maximum swelling signals induced with 5 μ M fsk + CFTR modulators.

Toxicity screen using 384-well plates

Organoids were plated into 384-wells plates and were incubated for 24h with 8 μ L complete culture medium supplemented with a single FDA compound per well (1400 compounds in total, divided over five 384-wells plates, in triplicate (twice with F508del/S1251N organoids, once with F508del/F508del organoids). Bright field images were taken per well and organoid morphology was scored by three independent investigators. A live dead assay was also performed to confirm cellular toxicity. Organoids were first stimulated with calcein green (7 μ M) for 30 minutes and propidium iodide (0.1 mg/mL) for 10 minutes prior to confocal imaging. Total organoid area per well was determined based on total calcein green staining (Zeiss, excitation at 488 nm) and amount of dead cells per well was determined by total area of PI staining (Zeiss, excitation at 564 nm) using Zen Image analysis software module (Zeiss). The ratio of total area calcein green and total area PI (=T-score) was calculated to correct for varying number of organoids between wells. To further correct for the varying organoid sizes among plates the Z-score was calculated between the compound-treated organoids and control DMSO-treated organoids per plate. The Z-score was determined according to the following formula: $z\text{-score} = (x - \mu)/\sigma$, where x is the calcein/PI ratio of each single FDA compound, μ is the mean calcein/PI ratio of 16 control wells on each plate, and σ is the standard deviation of the calcein/PI ratio of the same 16 control wells on each plate. Z-scores of the single FDA compounds were compared to Z-scores of wells treated ($n=71$) with a toxic concentration of puromycin (24h, 3 mg/ml). Z-scores that were below Q1-(3xIQR) of all the DMSO treated wells (Z-score=-2.5) or Z-score that were above Q3+(3xIQR) of all puromycin treated wells (Z-score=14.8) were excluded. Based on both the morphological screening and live-dead assay, 43 compounds were removed from the screen (listed in **supplementary table 3**).

FDA-screen testing 1400 compounds on 76 organoid cultures using 384-well FIS assay

The generation of intestinal organoids from biopsies and subsequent fluid secretion assays (FIS-assays) were performed according to previously described protocols^{8,9}, with slight adaptations for the 384-well setting of the screen. Organoids of 76 different donors were seeded in 25% matrigel on two 384-wells plates/donor using Viaflo pipet (7 μ L/well). Organoids were subsequently submerged in 8 μ L complete culture media supplemented with two FDA compounds/well (3 μ M) O/N. The bottom 8 wells of the last column of each plate were not supplemented with FDA-compounds and served as negative control as well as min signal for Z'-factor calculations. The top 8 wells of the last column of each plate contained F508del/

S1251N organoids that were treated with VX-770 (3 μM) and fsk (5 μM), serving as a positive control and max signal for Z'-factor calculations. The next day, 30 minutes prior to confocal imaging, organoids were fluorescently labeled with 5 μL calcein green (7 μM), added with the Vialo II 125 μl . 50 μL DMEM-F12 supplemented with Glutamax, Hepes, pen/strep, fsk and VX-770 (only for the top 8 wells of the last column) was added. The concentration of fsk used was donor dependent and was assessed in 24-wells plates prior to the FIS-assay. 0.02, 0.128, 0.8 and 5.0 μM fsk was added to the 24-well tissue culture plate. After 1h forskolin addition, organoid swelling was checked with a light-microscope. The fsk concentration that did not result in residual swelling was chosen for 384-well screening. Swelling of organoids in the 384-wells plates was monitored and total organoid surface area per well was quantified as described by Berkers et al. 2019³⁷. Besides fluorescent confocal images, also brightfield images were taken of each well. These brightfield images were used to screen every well by eye on induction of swelling. Of all plates the Z'-factor was determined similar to the formula described in 384-well FIS assay validation, where σ_p is the standard deviation of the 8 positive control wells/plate (F508del/S1251N organoids treated with VX-770 and 5 μM fsk), σ_n is the standard deviation of the negative control wells/plate (one of the 76 organoid cultures treated with fsk concentration as all other wells in the plate, without presence of an FDA compound), μ_p is the mean of the positive control, μ_n is the mean of the negative control. AUC values above 5963 (=Q3+(3xIQR) of all positive control wells of all plates with a Z'-factor > 5) were excluded. AUC values below -452 (=Q1-(3xIQR) of all negative control wells of all plates with a Z'-factor > 5) were also excluded. Subsequently only plates with an outlier percentage below 2% were included for hit selection. Next hits were selected if the organoid surface area of the well of interest was above mean+3xSD of the 8 negative control wells (DMSO treated) on each individual plate. Several compound combinations were identified as hit in limited number of patients based on AUC value, but increase in swelling was not observed when this was checked by eye. We therefore proceeded with only the top 5% hits, which are 37 hits that increased AUC above the threshold in most patients. The total number of hits we proceeded with in secondary screen was 34 as three of the identified hits were the positive controls (VX-770, VX-809 and VX-770/VX-809 (all 3 μM)). Since in the primary screen two compounds per well were combined, the secondary screen consisted of in total 68 individual compounds.

Secondary screen

Organoids derived from 3 distinct donors, expressing R334W/R334W, F508del/4382delA and A46D/A46D CFTR, were seeded into 96-wells plates within 50% matrigel. Organoids were submerged in complete culture medium supplemented with one of the 68 FDA compounds (3 μM), except for three wells (only DMSO). The mean swelling level of these three DMSO wells was used as reference value for calculating the Z-score of the FDA-compound-stimulated wells. Besides the negative controls, each plate contained two positive control wells with F508del/S1251N organoids that were treated with VX-770 and 5 μM fsk. For each donor suboptimal fsk concentration, a fsk concentration not yet resulting in residual swelling, was used: R334W/R334W and F508del/4382delA were stimulated with 0.128 μM fsk and A46D/A46D was stimulated with 0.8 μM fsk. Of all 64 individual compounds, 8 compounds induced swelling to such extend the Z-score reached 2 or higher. This analysis found 8 out of 68

compounds as validated hits. Three of these, roflumilast, VX-809 and VX-770 are available in the Netherlands in an oral form, usage is not associated with severe side-effects and are already used for the treatment of another pulmonary disease, and therefore proceeded with these three compounds in subsequent screens.

Identifying roflumilast responding genotypes

Hit confirmation with the secondary screen was only conducted with organoids derived from 3 donors. To investigate whether more CFTR genotypes would respond to roflumilast, FIS with roflumilast of in total 107 different organoid cultures was assessed. Not only did we test roflumilast as single agent (incubated for 24h, 3 µM), we also investigated whether it would enhance VX-770/VX-809 stimulated swelling (VX-809 (3 µM) added for 24h, VX-770 (3 µM) added simultaneously with fsk) in all 107 organoid cultures. Organoid culturing and FIS-assays were performed according to previously described protocols^{8,9} and total organoid surface area per well was quantified as described by Berkers et al. 2019³⁷. Again for all 107 donors a donor-dependent suboptimal single fsk concentration (either 0.128, 0.8 or 5.0 µM) was used for the FIS-assay. For 6 organoid cultures FIS experiments were repeated (N=3) with roflumilast alone (24h, 3 µM), roflumilast in combination with VX-809 (24h, 3 µM) + VX-770 (0h, 3 µM), VX-770 + VX-809 and Formoterol hemifumarate (3 µM, 24h). These FIS experiments were performed with 7 fsk concentrations (0.02, 0.05, 0.128, 0.32, 0.8, 2.0, 5.0 µM).

FIS with 230 organoid cultures treated with VX-770, VX-809 and VX-770/VX-809

While roflumilast exemplifies the potential of repurposing a drug developed for another disease than CF, the CFTR modulators VX-770/VX-809 increased swelling with a substantial higher degree and in a larger number of donors, indicating a higher potential for drug repurposing using the tested CFTR modulators. We therefore tested the CFTR modulators VX-770 (3 µM, simultaneously added with fsk), VX-809 (3 µM, 24h) and VX-770/VX-809 on an additional 230 cultures, covering 167 different genotypes of which 66 did not express the F508del mutation (**supplementary table 2**), using 0.128 µM fsk for all genotypes. The concentration of fsk was set to 0.128 µM as the in vitro drug effect expressed by FIS measured with this fsk concentration has previously been shown to correlate with the in vivo drug effect at group level. Consistent with those findings, we found a significant correlation (**figure 5A+B**) ($R^2=0.7$, $p<0.0001$) between the level of CFTR-modulator induced swelling of the organoids and the treatment effect expressed in absolute change in FEV1pp of reported clinical studies, listed in **table 1**. CFTR modulator induced swelling, corrected for DMSO response, of the following organoid cultures was correlated to change in FEV1 of reported clinical data: F508del/RF_Splice (n=12); F508del/2789+5G>A (n=3); F508del/3272-26A>G (n=4); F508del/3849+10kbC>T (n=5); F508del/MF (n=40); F508del/W1282X (n=5); F508del/R1066C (n=2); F508del/Y1092X (n=5); F508del/N1303K (n=5); F508del/G85E (n=2); F508del/1078deIT (n=1); F508del/1717-1G>A (n=4); F508del/2184delA (n=2); F508del/I507del (n=1); F508del/R553X (n=1); F508del/1078deIT (n=1); F508del/2143delT (n=2); F508del/2183AA>G (n=1); F508del/3659delC (n=2); F508del/3905insT (n=1); F508del/394delTT (n=1); F508del/CFTRdele2.3 (n=3); F508del/G542X (n=1); F508del/RF_missense (n=9); F508del/G551D

CHAPTER 4

(n=2); F508del/D1152H (n=1); F508del/L206W (n=1); F508del/S945L (n=1); F508del/A455E (n=4), R117H/other (n=10); R117H/F508del (n=6); R117H-7T/R1162X (n=1); R117H-7T/R553X (n=1); R117H-7T/T1857delT (n=1); R117H-7T/W1282X (n=1), S1251N/other (n=16); S1251N/F508del (n=15); S1251N/1717-1G>A (n=1). Based on the association between swelling and clinical effect we derived a heat map (**figure 5A, 5C and 5D**) to indicate the clinical potential of the in vitro FIS levels (AUC) associated with CFTR modulator use.

RESULTS

384-wells FIS-assay is spatial uniform, reproducible and has a wide dynamic range

To demonstrate the reproducibility and quality of the 384 wells plate assay, we performed replicate experiments at three different culture time points with F508del/F508del and with F508del/S1251N organoids (**figure 1A-D**). FIS measurements were assessed in the presence of VX-770 for F508del/S1251N or VX-770/VX-809 for F508del/F508del organoids. Minimal (min) and maximal (max) signal of swelling was induced with 0.008 and 5 µM fsk, respectively. The mean and spread of the min and max signals were comparable between the plates and CFTR genotypes (**figure 1A-D**). Distribution of the two fsk concentrations across and between the plates therefore did not impact on the mean or variability of the min and max signals (**figure 1A-D**). In addition, no edge effects or drift was observed (**supplementary figure 1A-C**), indicating that technical and culture-induced variation across and between plates is uniformly distributed.

We next compared the 384-wells FIS-assay performance to the conventional 96-wells assay by comparing FIS of F508del/F508del and F508del/S1251N organoids with or without CFTR modulator(s) and an increasing concentration of fsk (**figure 1E**). A similar fsk-dose dependency was observed for the 96 and 384-wells set-ups, with a slightly higher variation in 384-wells plate responses (**supplementary figure 2**). To compare the signal-over-background in relation to variation, Z'-factors were calculated from min and max swelling signals of the data shown in **figure 1A, C and E**. The mean Z'-factors from the 96-well format experiments were somewhat higher compared to the 384-well format experiments (**figure 1F**), which was caused by the observed larger standard deviations between replicates obtained with 384-wells plate measurements (**supplementary figure 2**). These data indicate that the 384-wells assay showed sufficient robustness for drug screening purposes, especially when multiple patient samples are tested for identical compounds.

Pre-clinical efficacy testing of FDA-approved drugs for non-homozygous F508del-CFTR genotypes

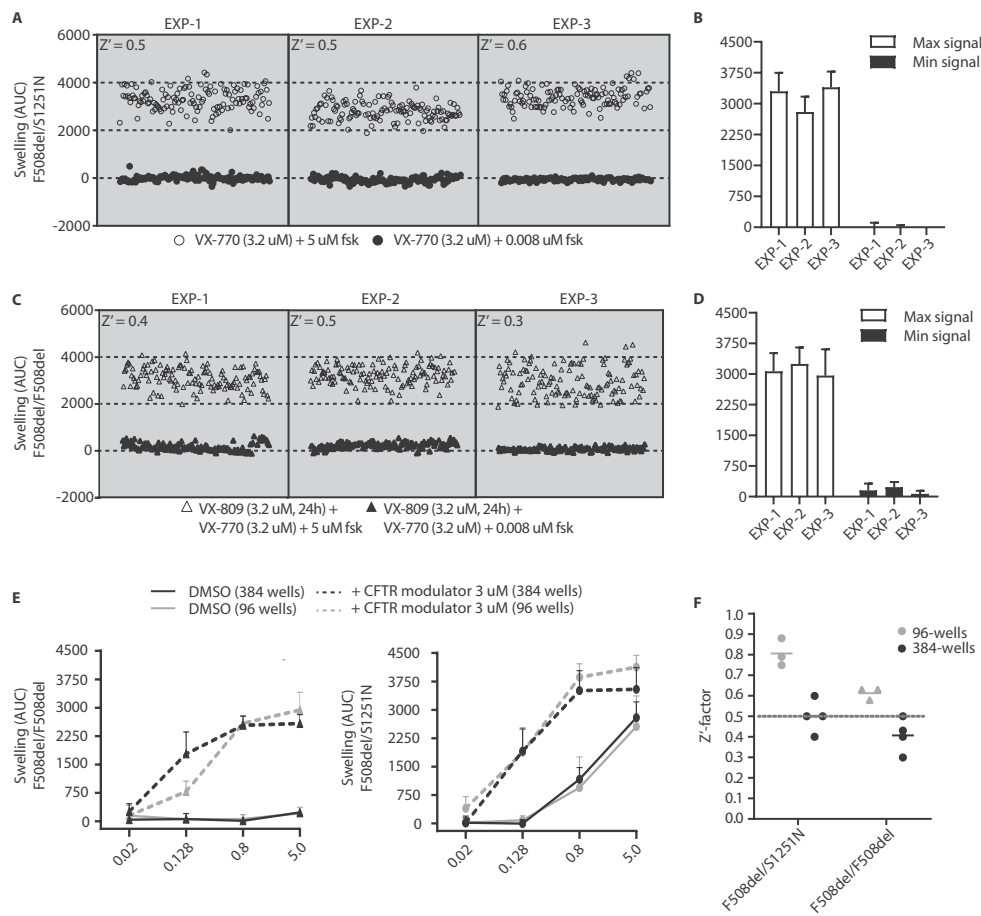


Figure 1: Reproducibility and dynamic range of 384-wells FIS assay.

Replicate experiment of three 384-wells plates with F508del/S1251N (**A**) and F508del/F508del (**B**) organoids performed on three different culturing days, up until 12 weeks. Organoids were plated and VX-809 was added to F508del/F508del organoids, 24h prior to the FIS assay. The next day, VX-770 (3.2 μ M) and a low concentration fsk (0.008 μ M) was added to 128 wells of each 384-well plate to induce minimal swelling (=min signal wells). Maximum swelling was achieved by the addition of 5 μ M fsk and VX-770 (3.2 μ M) to another 128 wells (=max signal wells). The mean+SD swelling of all min and max signal wells of each plate depicted in **A** and **C** are summarized in **figure B** and **D**, respectively. (**E**) Swelling of F508del/F508del organoids treated W/W/O VX-770/VX-809 and F508del/S1251N organoids treated W/W/O VX-770 and in presence of an increasing concentration of fsk, measured in 96-wells plates and 384-wells plates (datapoints represent mean+SD, n=3 for the 96-wells experiments, n=1 for the 384-wells experiments). (**F**) Z'-factors calculated of each replicate experiment plate in **A**, **C** and **E** according to the following formula: $Z'\text{-factor} = 1 - (3 \times (\sigma_{\text{op}} - \sigma_{\text{m}})) / (\mu_{\text{op}} - \mu_{\text{m}})$, where σ_{op} is the standard deviation of the max signal wells (+ CFTR modulator(s) and 5 μ M fsk), σ_{m} is the standard deviation of the min signal wells (+ CFTR modulator(s) and 0.008 μ M fsk), μ_{op} is the mean of the max signal wells, μ_{m} is the mean of the min signal wells.

Organoid viability affected by 43 FDA-approved compounds

Before we explored the effect of the 1443 FDA compounds on CFTR-mediated fluid secretion, we first investigated toxicity of each individual compound. The organoid viability was determined both by examining organoid morphology by three independent researchers based on bright field images as well as via a dual live-cell staining approach. First calcein green was added to stain living organoids and subsequently propidium iodide was added to visualize the dead cells (**figure 2A**). Total organoid area per well was determined based on calcein green staining and level of organoid viability per well was determined by total area of propidium iodide staining (**figure 2B**). The ratio of total area calcein green and total area PI (=T-score) was calculated to correct for varying number of organoids between wells. To further correct for varying organoid sizes among plates, the Z-score was calculated between the compound-treated organoids and control DMSO-treated organoids. Compounds that were scored as toxic generated z-scores above 2, comparable to the wells treated with a toxic concentration of puromycin (**figure 2C**). Yet, some compounds generated a z-score above 2, while organoid death in these wells was not confirmed by the organoid morphology screening (**supplementary figure 3**). Ultimately, based on both the morphological screening and a live-dead Z-score>2, 43 compounds (**figure 2C**) were excluded for further screening. The majority of the toxic compounds (84%), listed in **supplementary table 1**, are described as anti-cancer drugs, designed to inhibit cellular growth and to induce cell death. Particular antibiotics - including puromycin which we used as the toxic control in our screen -, an anti-epileptic/seizure drug, a laxative drug and drugs against pulmonary hypertension or atrial fibrillation were also identified as toxic and excluded from further screening.

Pre-clinical efficacy testing of FDA-approved drugs for non-homozygous F508del-CFTR genotypes

4

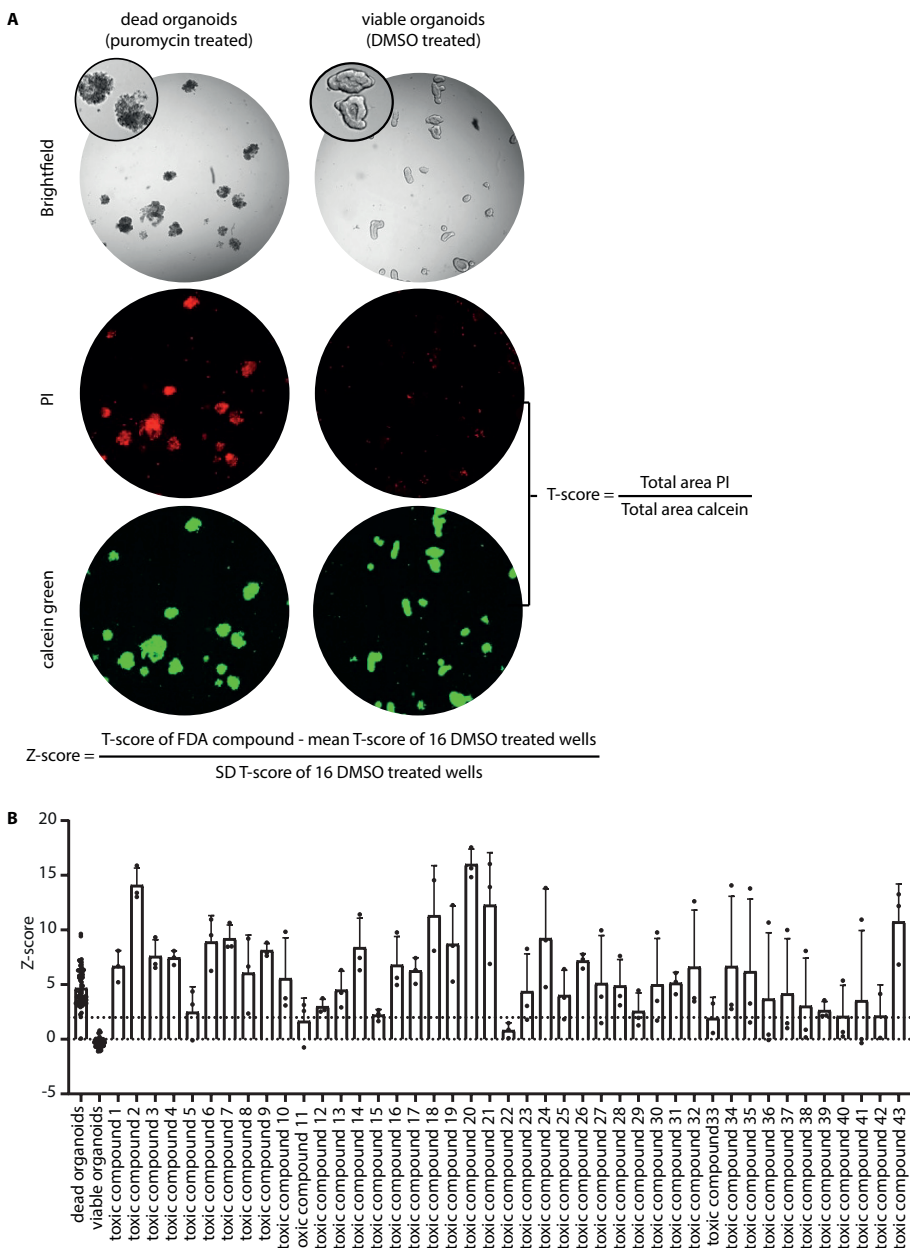


Figure 2: Organoid viability upon treatment with 1443 FDA-approved drugs

(A) Organoids were plated into 384-wells plates and were incubated for 24h with complete culture medium supplemented with a single FDA compound per well (1443 compounds in total, divided over five 384-wells plates). Bright field images were taken per well and organoid morphology was scored by three independent investigators. Total organoid area per well was determined based on calcein green staining (pre-incubated for 30 min.) and level of organoid viability per well was determined by total area of PI staining (pre-incubated for 15 min.). The ratio of total area calcein green and total area PI (=T-score) was calculated to correct for varying number of organoids between wells.

To further correct for the varying organoid sizes between plates, the Z-score was calculated between the compound-treated organoids and control (DMSO-treated) organoids. **(B)** Z-scores of the compounds labeled as toxic based on bright field image scoring, compared to Z-scores of dead organoids (treated for 24h with a toxic concentration of puromycin (3 mg/ml)) and viable organoids treated without FDA compound. Bars represent mean + SD, n=3 for toxic compounds, n=71 for dead and healthy controls.

FDA-approved drugs increase FIS in non-homozygous F508del PDIO

We next set out to study rescue of CFTR function by the selected 1400 FDA-approved compounds. Organoids of 76 different donors were used covering 58 different genotypes. All mutation classes and mutation types (e.g. frameshift, splice etc.) were represented. 62% of the included organoid cultures were compound heterozygous for the F508del allele. The majority of the remaining mutations are uncharacterized mutations. A list of all PDIO and genotypes included in this study is provided in **supplementary table 2**. To compensate for variability in baseline swelling due to residual CFTR function between PDIO, we adjusted the concentration of fsk as agonist, so that baseline swelling was not or hardly detected after 1 hour fsk stimulation (0.128 μ M fsk was used for PDIO with high residual CFTR function, 0.8 μ M in case of moderate residual function and 5.0 μ M in case of no residual function). The performance of the 384 wells assay (average Z' factor and outlier percentages) during the screening of the 76 PDIO is detailed in **supplementary figure 4**.

To screen the 1400 FDA-approved drugs, we initially pooled two compounds per well so that two 384 wells plates were sufficient per donor. A well was selected as positive when FIS was above the mean+3xSD of the 8 negative control wells (DMSO treated) within the identical plate and are indicated by the green dots in **figure 3B** (columns are compounds, rows represent PDIO). We analyzed the data in a binary (**figure 3B**) and continuous manner. Based on a binary definition of hits for each PDIO, the top 5% of hits representing 37 wells are indicated in **supplementary table 3**. Among these hits were the FDA approved CFTR modulator VX-770, VX-809 and VX-770+VX-809 included as positive controls which confirm the validity of the screening approach.

Based on the mean AUC values of the negative control wells (**supplementary figure 4E**), which were treated with the donor-specific fsk concentration, a uniform and limited level of swelling with fsk alone was confirmed. Plates where the negative control wells were measured with 0.128 μ M fsk showed to exhibit a mean Z'-factor of 0.45, while plates measured with 0.8 μ M or 5 μ M fsk exhibit a mean Z'-factor of 0.5 (**supplementary figure 4C**). Despite the lower mean Z'-factor with 0.128 μ M fsk, the spread of the Z'-factor among plates for each fsk concentration was comparable. Furthermore, the spread of the mean AUCs of the negative control wells was significantly lower than the spread of the mean AUCs of the positive control wells (S1252N organoids treated with VX-770 and 5 μ M fsk), indicating that the variation in the Z'-factors is caused by variation in the positive control wells. Despite the varying mean AUCs of the positive and negative control among plates measured on different days, a significant and strong correlation was observed between the two plates per donor measured on the same day (**supplementary figure 4E**), indicating that the observed variation is associated with organoid culturing.

AUC values above Q3+(3xIQR) (=5963) of all positive control wells or below Q1-(3xIQR) (=−452) of all negative control wells were excluded (**supplementary figure 4B**). 13 out of the 152 plates were excluded for hit selection. Eight were excluded due to imaging-related technical errors, two because positive and negative controls were missing and three due to bad organoid quality. All plates used for hit selection displayed an outlier percentage below 2% (**supplementary figure 4C**).

Since each well of the primary screen contained two compounds (**supplementary table 3**), we next set out to determine which of the in total 68 individual compounds increased CFTR-mediated fluid secretion. Organoids of three donors (R334W/R334W and F508del/4382delA, stimulated with 0.128 μ M fsk and A46D/A46D stimulated with 0.8 μ M fsk) were treated with the individual 68 FDA compounds from the 34 selected wells. To compensate for differences in fsk usage between the PDIO, positive responses were defined by an average Z-scores > 2 of the three donors. This analysis found 8 out of 68 compounds as validated hits (**figure 3C**). Four out of the 8 compounds are phosphodiesterase inhibitors. The four remaining compounds act via other targets, including CFTR, the GABA receptor, PI3K and calcium channel. Altogether, above data shows our 384-well plates based screen can enable the selection of hits that induce fluid secretion in multiple PDIO, and identified multiple FDA-approved compounds with similar mode of action as activators of intestinal fluid secretion.

CHAPTER 4

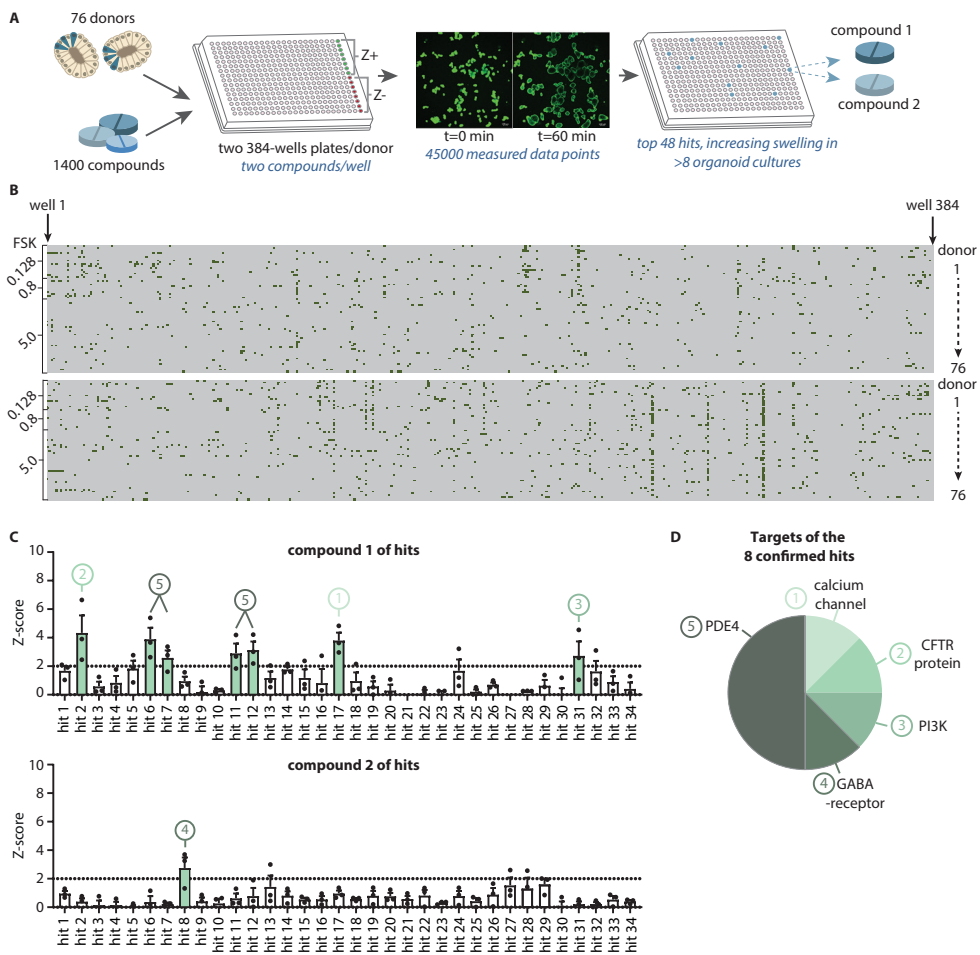


Figure 3: Hit-lead selection from a FDA-approved drug library on 70 different organoid cultures.

(A) Organoids of 76 different donors were seeded on two 384-wells plates and were submerged in complete culture media (CCM) supplemented with two FDA compounds/well (3 μ M, O/N). The last column of each plate was reserved for the positive controls (green wells) and negative controls (red wells) which were subsequently used for Z'-factor calculations. Organoid swelling was measured for 1h with a donor-specific suboptimal fsk concentration, determined prior to the 384-well plate based-FIS-assay. **(B)** Binary outcome (hit or no hit) of all wells (from left to right) and donors (from top to bottom) divided over the two 384-well plates. A well was selected as hit when $AUC > \text{mean} + 3\text{SD}$ of the 8 negative control wells (DMSO treated) per 384-wells plate and are highlighted in green. **(C)** We proceeded with 34 hits of which the in total 68 individual compounds were tested for their swelling-increasing efficacy using three organoid cultures (R334W/R334W, A46D/A46D and F508del/4382delA) and donor-dependent suboptimal fsk concentrations. The mean swelling level of three control (DMSO treated) wells was used as reference value for calculating the Z-score of the FDA-compound-stimulated wells, which are shown in **(C)** (bars represent mean + SEM, n=3). Of all 68 individual compounds, 8 compounds induced swelling to such extend the Z-score reached 2 or higher (green bars). Targets of these hit compounds are shown in **(D)**. Numbers next to the target in **figure D** correspond to those in **figure C**.

Pre-clinical efficacy testing of FDA-approved drugs for non-homozygous F508del-CFTR genotypes

4

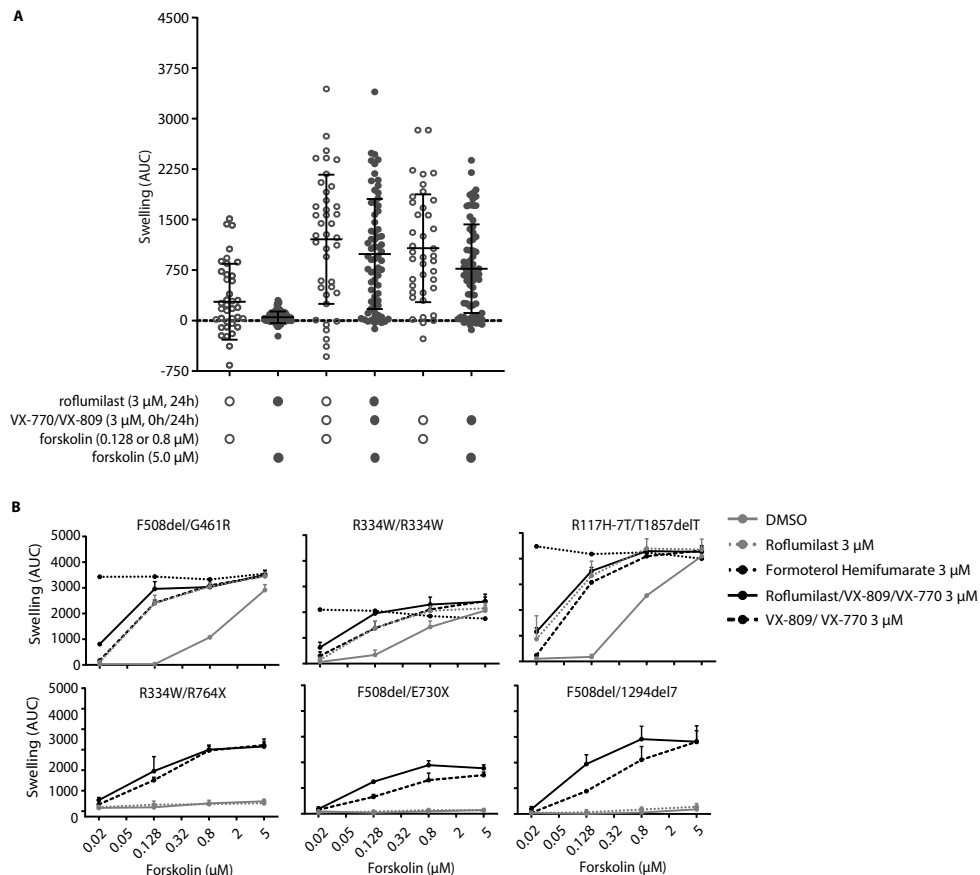


Figure 4: Repurposing of hit compounds and CFTR modulators for non-homozygous F508del-CFTR variants.
(A) FIS of in total 107 different organoid cultures treated with roflumilast as single agent (incubated for 24h, 3 μ M) and in combination with VX-770/VX-809 (VX-770: 0h, 3 μ M; VX-809:24h, 3 μ M). Swelling was normalized to the swelling of the DMSO-treated control wells to correct for varying levels of residual swelling of the distinct organoid cultures. DMSO-corrected response upon roflumilast, roflumilast/VX-770/VX-809 or VX-770/VX-809 treatment are divided based on the concentration of fsk that was added prior to the FIS assay (organoid responses measured with 0.128 + 0.8 μ M combined [open datapoints] versus organoid cultures measured with 5.0 μ M fsk [filled datapoints]). **(B)** Swelling of three organoid cultures highly responsive to roflumilast as single agent and three cultures responsive to roflumilast once CFTR function was been restored with VX-770/VX-809 (datapoints represent mean+SD, n=3) in the presence of an increasing concentration of fsk. The roflumilast response was compared to formoterol hemifumarate (both incubated for 24h, 3 μ M) and VX-809/VX-770 response.

As roflumilast and the CFTR modulators VX-770, VX-809 and VX-770/VX-809 were the most promising regarding efficacy and safety, we validated their impact on FIS using additional PDIO in 96-wells plates that allow for a better quantification of effect. Roflumilast was tested on an additional 107 different organoid cultures, covering 78 genotypes of which 34 did not express the F508del mutation (**supplementary table 2**), in combination with genotype-specific fsk concentrations. The CFTR modulators VX-770, VX-809 and VX-770/VX-809 were tested on an additional 230 cultures, covering 167 different genotypes of which 66 did not express the F508del mutation (**supplementary table 2**), using 0.128 µM fsk for all genotypes. We also investigated whether VX-770/VX-809-stimulated swelling could be further enhanced (**figure 4A**) with roflumilast. Roflumilast showed to increase swelling (AUC>500) in 12-out-of-107 PDIO (**figure 4A-B**). These PDIO responding to roflumilast as single agent, also significantly swell with the addition of high fsk (**figure 4B**), indicating presence of residual CFTR function. Interestingly, the roflumilast-mediated increase was similar to the VX-770/VX-809-mediated swelling increase. PDIO showing no response to high fsk did not respond to roflumilast. In 18 PDIO the VX-770+VX-809 rescued organoid responses were boosted by additional stimulation with roflumilast (**figure 4A**). In contrast to formoterol hemifumarate, roflumilast-stimulated swelling is absent with lower fsk concentrations (until 0.128 µM) (**figure 4B**).

While roflumilast exemplifies the potential of repurposing a drug developed for another disease than CF, the CFTR modulators VX-770/VX-809 increased swelling with a substantial higher degree and in a larger number of donors, indicating a higher potential for drug repurposing using the tested CFTR modulators. **Figure 5** shows FIS data of organoids treated with 0.128 µM fsk, as the in vitro drug effect expressed by FIS measured with this fsk concentration has previously been shown to correlate with the in vivo drug effect at group level. Consistent with those findings, we found a significant correlation (**figure 5A and 5B**) ($R^2=0.51$, $p<0.0001$) between the level of CFTR-modulator induced swelling of the organoids and the treatment effect expressed in absolute change in FEV1pp of reported clinical studies, listed in **table 1**. Based on this association we derived a heat map (**figure 5A, 5C and 5D**) to indicate the clinical potential of the in vitro FIS levels (AUC) associated with CFTR modulator use.

Treatment	Genotype	Absolute change in FEV1pp versus placebo
1. VX-770	F508del/F508del	1.72 (NS) ¹⁴
2. VX-770/VX-809	F508del/MF	0.6 (NS) ¹⁵
3. VX-770	F508del/RF_splice	5.4 (NA) ¹⁶
4. VX-770	F508del/RF_missense	3.6 (NA) ¹⁶
5. VX-770/VX-809	F508del/F508del	2.8 ($p<0.001$) ⁴
6. VX-770	R117H/other	5 ($p=0.01$) ¹⁷
7. VX-770	S1251N/other	9 (NA) ¹⁸

Table 1: Data overview of clinical trials with CFTR-correcting treatments in subjects expressing different CFTR mutations.

For the R117H trial, only data from CF subjects aged >18 were used, because subjects aged 6 to 18 had a different mean baseline FEV1 compared to those in the other trials. The numbers correlate with the numbers in **figure 5B**. Swelling of corresponding organoid cultures are shown in **figure 5A**. NS: not significant, NA: statistical analysis not performed due to small numbers for individual mutations, RF: residual function, MF: minimal function.

Pre-clinical efficacy testing of FDA-approved drugs for non-homozygous F508del-CFTR genotypes

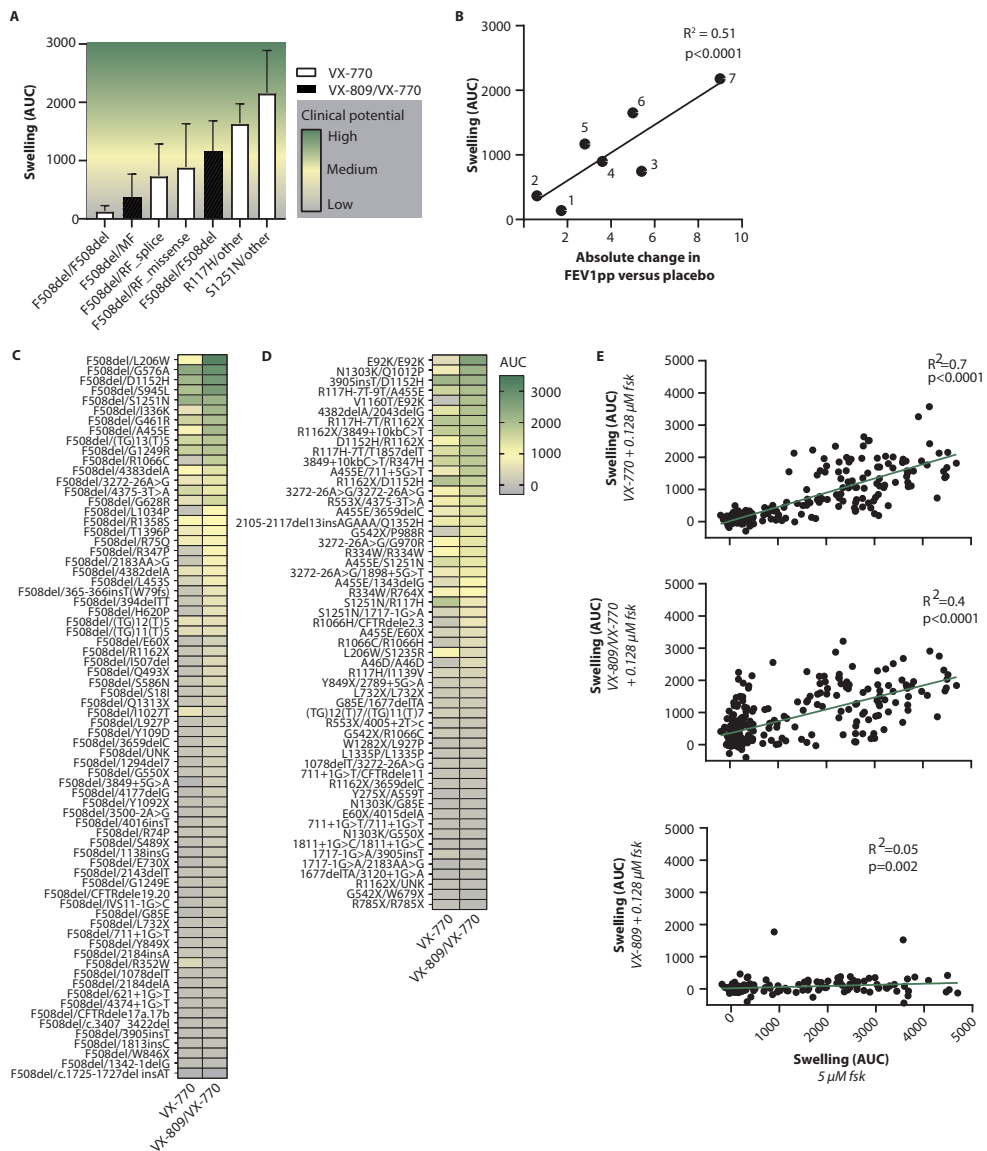


Figure 5: response of 230 PDIO cultures to VX-770, VX-809 or VX-770/VX-809.

(A) CFTR modulator-corrected swelling at 0.128 μ M fsk (AUC at $t = 60$ min) corrected for the DMSO condition presented per CFTR genotype group (bars represent mean+SEM). The genotype groups include genotypes and treatments [VX-770 (white bars) or VX-809/VX-770 (black bars)] that have been clinically assessed. The color profile was based on the clinical effectiveness of studies presented in **Table 1**. **F508del/RF_Splice (n=12):** F508del/2789+5G>A (n=3); F508del/3272-26A>G (n=4); F508del/3849+10kbC>T (n=5). **F508del/MF (n=40):** F508del/W1282X (n=5); F508del/R1066C (n=2); F508del/Y1092X (n=5); F508del/N1303K (n=5); F508del/G85E (n=2); F508del/1078delt (n=1); F508del/1717-1G>A (n=4); F508del/2184delA (n=2); F508del/I507del (n=1); F508del/R553X (n=1); F508del/1078delt (n=1); F508del/2143delT (n=2); F508del/2183AA>G (n=1); F508del/3659delC (n=2); F508del/3905inst (n=1); F508del/394delTT (n=1); F508del/CFTRdete.2.3 (n=3); F508del/G542X (n=1). **F508del/RF_missense (n=9):** F508del/G551D (n=2); F508del/D1152H (n=1); F508del/I507del (n=1); F508del/W846Q (n=1); F508del/I813insC (n=1); F508del/1342+1delG (n=1); F508del/c.1725-1727delinsAT (n=1).

CHAPTER 4

(n=1); F508del/L206W (n=1); F508del/S945L (n=1); F508del/A455E (n=4), **R117H/other (n=10):** R117H/F508del (n=6); R117H-7T/R1162X (n=1); R117H-7T/R553X (n=1); R117H-7T/T1857delT (n=1); R117H-7T/W1282X (n=1), **S1251N/other (n=16):** S1251N/F508del (n=15); S1251N/1717-1G>A (n=1). **(B)** Pearson correlation of drug-corrected rectal organoid swelling [results from (A)] versus lung function increase [results in **Table 1**] (**C-D**) The VX-770 or VX-809/VX-770-DMSO corrected swelling of rectal organoids measured with 0.128 μM fsk (AUC at t = 60 min) expressing an F508del mutation on one allele and a rare CFTR mutation on the other allele (**C**) or expressing two rare CFTR mutations (**D**). Color coding correspond with the coding in **(A)**. **(D)** Pearson correlation of DMSO-corrected PDIO swelling upon modulator therapy (VX-770, VX-809 or VX-809/VX770) and 0.128 μM fsk [results from (A, C and D)] versus DMSO-treated PDIO swelling upon 1hr stimulation with 5 μM fsk. MF = minimal function, RF = residual function, fsk = forskolin.

These data indicate that 31 genotypes had VX-770-responses beyond that of VX-770 treated F508del/splice PDIO and that 37 genotypes had VX-770/VX-809 responses beyond that of VX-770/VX-809-treated F508del/F508del PDIO, showing that many more pwCF will likely clinically benefit from modulator therapy (**figure 5C-D**). We observed a strong correlation between the baseline swelling (DMSO) at 5 μM fsk and the swelling increase with VX-770 and 0.128 μM fsk (**figure 5E**). A similar relation between residual CFTR function and VX-770/VX-809-mediated increase in swelling was observed, however with a lower R². Only two organoid cultures (E92K/E92K and A455E/(TG)13(T)5) showed an increase in CFTR function with treatment of solely VX-809, and correlation between VX-809 induced swelling response and DMSO-induced swelling response was absent (**figure 5C**).

DISCUSSION

We here show the implementation of the FIS-assay with PDIOs carrying non-homozygous F508del-CFTR genotypes for a large scale drug repurposing effort using FDA approved drugs including the CFTR modulators VX-770 and VX-809. A miniaturized version of the 96-wells assay was developed that showed a robust Z'-factor in real-life screening conditions with no experimental plates lost due to high outlier percentages. Overall, and apart from the known CFTR modulators and cAMP-modulating compounds that may hold potential in people with baseline residual CFTR function, it did not appear that drugs could be repurposed as stimulators of CFTR function. For CFTR modulators, we observed that approximately 43 out of non-F508del homozygous genotypes were associated with identical or higher modulator-induced responses as the original indications, indicating that drug repurposing of existing CFTR modulators using PDIO can be a promising treatment strategy for pwCF.

The Z'-factor is a measure for assay quality and integrates both amplitude of positive over negative control and variation within these controls. Overall, assay performance of the 384 wells plate-based screen was very acceptable (on average Z' of 0.5) but signal variation in the positive control conditions was higher than compared for 96 wells assays. This was more prominent in the context of F508del/F508del organoids upon treatment with VX809/VX770 than S1251N/F508del organoids and VX-770 treatment. This is probably caused by the use of multiple compounds that are added at consecutive days, which could introduce additional technical variability. Technical variation between plates measured on similar days was lower than between days, showing that also culture variation reduces assay reproducibility.

Additional automation such as organoid dispensers, drug printers and centrifugal washers might further reduce variation and optimize signal over background.

The PDE4-inhibitor roflumilast increased swelling in multiple organoid cultures in a fsk and CFTR genotype-dependent manner. The drug is approved in many countries in an oral form for chronic obstructive pulmonary disease and has been found safe to use in humans¹⁹. It acts to suppress the release of inflammatory mediators by several leukocyte cell types and mitigates COPD-associated malfunctions of vascular smooth muscle cells through enhancing cellular cAMP levels through inhibition of PDE4 that breaks down cAMP. An interesting observation we found was that roflumilast particularly increased swelling in organoids with baseline responses to high fsk, suggesting that roflumilast acts by enhancing cAMP that in turn then stimulates endogenously expressed and functional CFTR protein. In line with this observation, CFTR activity could also be stimulated with roflumilast in more severe mutational backgrounds when combined with VX-770+VX-809. This was also found by others using other *in vitro* models or using PDE4 inhibitors other than roflumilast²⁰⁻²⁴. CFTR-dependent stimulation of chloride and fluid transport with roflumilast has been described before, however only in the context of treating chronic bronchitis²⁵ or smoke-induced mucociliary dysfunction^{26,27}. It is also tempting to speculate that the dependency of roflumilast on endogenous stimuli of cAMP might lower the occurrence of systemic side effects that could associate with direct cAMP agonists such as $\beta 2$ agonists. The above findings support the hypothesis that roflumilast may have therapeutic potential for pwCF that have functional CFTR proteins through potentiation of cAMP concentration thereby increasing the opening of the available pool of functional CFTR proteins. In addition, PDE4 inhibitors also have beneficial anti-inflammatory and bronchodilator effects, which would provide additional benefits to pwCF²². Clinical studies should be designed to test the effects of roflumilast in pwCF and intestinal or airway *in vitro* cell models might help select responders in such studies.

The highest CFTR function rescue was achieved with the CFTR modulators VX-770 and VX-809. Consistent with the study published in 2016, we found a significant correlation between the level of the DMSO-corrected drug-induced swelling of the organoids with 0.128 μ M fsk and the treatment effect expressed in absolute change in FEV1pp of available clinical trial data of mutations present in our study. Based on this association ~23% of the genotypes included in our dataset will likely have a medium to high clinical benefit of VX-770 therapy, of which the mutations, F508del/G461R, F508del/(TG)13(T)5 , F508del/4383delA, F508del/c.4243-3T>A, F508del/R1385S, 4382delA/2043delG and R334W/R334W are particularly interesting as these mutations are currently not approved for Kalydeco (VX-770) therapy. An additional 29% of the included genotypes responded to VX-809 and VX-770 combination therapy to such extend that clinical potential is estimated to be medium or high (AUC>1000 with 0.128 μ M fsk), while none of these genotypes are currently on the VX-809/VX-770 drug label. From the genotypes without the F508del mutation (38%), which do not have access to the newest available Trikafta treatment in the near future, 19,5% did respond to VX-770 or VX-770/VX-809 therapy. These results underline the relevance of continuing to screen non-homozygous F508del-CFTR genotypes and show that repurposing of CFTR-targeted drugs is more effective than repurposing drugs that have been developed for diseases outside the CF indication.

We observed a strong correlation between the level of residual CFTR function expressed as swelling with 5 µM fsk and the level of CFTR function increase with VX-770 and 0.128 µM fsk. This indicates, similar to roflumilast and in line with previous studies^{28,29}, that VX770-mediated improvement relies on the presence of functional CFTR protein at the plasma membrane. A similar relation between residual CFTR function and VX-770/VX-809-mediated increase in swelling was observed, however less strong, as more genotypes were rescued with VX-809/VX-770, including genotypes not showing residual CFTR function. While we did not find a correlation between the VX-809 effect and the level of residual CFTR function, we identified two organoid cultures highly responding to VX-809 therapy. This observation indicates that folding of the CFTR protein is different for distinct CFTR mutations, however also indicates that there is great overlap in folding defects among many of the CFTR mutations. This observation also highlights the importance to screen drugs in a mutation specific setting as different mutations can respond differently to varying drugs.

Future research should continue to explore the hits compounds we identified in addition to the CFTR modulators and roflumilast, as they may reveal new targets and pathways acting on CFTR that can be further exploited. These hit compounds seem to act on targets or pathways involving the CFTR protein because the hit compounds did not affect swelling in organoid cultures homozygously expressing nonsense mutations. For example Voxtalisib, a PI3K and mTOR inhibitor increased organoid swelling. Other inhibitors of the PI3K/Akt/mTOR pathway have been shown to improve F508del-CFTR stability and function by stimulating autophagy in CFBE cells³⁰. Whether Voxtalisib acts with a similar MoA remains unclear for now. Another potentially interesting target we identified are GABA-activated chloride channels. Potentiation of the effects of the inhibitory neurotransmitter GABA with chlormezanone, also a compound among our hits, stimulates chloride influx through GABA-activated chloride channels³¹. Although it is believed that the GABA receptor is predominantly expressed in the nervous system, some studies describe expression in intestinal epithelial cells and furthermore show involvement in intestinal fluid secretion³²⁻³⁴, but its expression in intestinal organoids requires further validation. Swelling was also induced by one calcium channel blocker which likely stimulated CL- currents via Ca²⁺-activated Cl⁻ channels (CaCCs). Treating pwCF with above mentioned drugs is hampered due to the many reported associated serious adverse events during therapy³⁵, yet including these drugs in our screen have potentially identified several alternative pathways and modulators thereof which can be further exploited.

A limitation of the current FIS-assay is that incubation with strong cAMP-increasing drugs like β2-agonists induce swelling prior to the addition of fsk. As a result, FIS values can underestimate highly efficacious treatments that lead to significant preswelling, towards the level of healthy control organoids. This was observed for direct cAMP-increasing drugs in our screen such as β2-agonists, which previously were found to increase CFTR function in pwCF, yet with associated severe side effects³⁶. To ensure that drugs that could directly act on CFTR and thus strongly increase function were not missed, we visually checked all wells of the entire screen with the 76 individual PDIO. This confirmed that there were no drugs associated with strong preswelling, apart from β2-agonists. New assays with significant throughput that are based on automatic image analysis of steady-state phenotypes need to

be developed to complement the current assays that rely on relative changes in organoid phenotypes such as FIS.

The screening approach which was implemented combined two compounds per well to enable screening of 1400 compounds on many different organoid cultures. The rationale behind this design was to find a small selection of very potent compounds for a small selection of the mutations. We choose to validate the hit compounds in three PDIO to keep it practical and screenable. A limitation of this approach however is that we did not fully recapitulate the mutation variation of the initial screen which potentially has resulted in a loss of interesting hit compounds during the validation step. As all three organoid cultures in our validation step exhibited residual CFTR function we probably have selected for hit compounds acting on residual CFTR mutations. To fully recapitulate mutation-related variation and to identify interesting hit compounds acting on different types of mutations, future studies should therefore use an alternative approach which uses a smaller but more varying organoid panel and which tests single compounds per well.

In conclusion, a medium-high-throughput 384-wells assay was developed and implemented to match PDIO with drugs that might enhance CFTR function. From a repurposing perspective, drugs that increase the CFTR activity in cells as a potentiator of endogenous cAMP (e.g. roflumilast) appeared most promising, but overall efficacy of these hits was low and could not compete with the known CFTR modulators such as VX-809 and VX-770. The organoid-based assay has significant value to enable validation of hits from (ultra)-high throughput screening assays or to select the most promising responders for clinical trial design.

ACKNOWLEDGEMENTS

We would like to thank the people with CF who gave informed consent for generating and testing their individual organoids; all members of the research teams of the Dutch CF clinics that contributed to this work; and all colleagues of the HUB Organoid Technology for their help with generating intestinal organoids and performing FIS experiments.

FUNDING

This work was funded by grants of the Dutch Cystic Fibrosis Foundation (NCFS) as part of the HIT-CF Program and by ZonMW grant number: 91214103.

AUTHOR CONTRIBUTIONS

E.d.P. and S.S. contributed to the design of the study, the acquisition, verification, analysis and interpretation of the data and have drafted the manuscript. P.V.M., S.W.F.S., A.M.V., J.E.B., E.K., H.O., M.C.H., G.B., K.M.d.W-d.G., S.H.-M., S.R.J., H.v.P., M.M.v.d.E., R.v.d.M., J.R., E.D., E.J.M.W., G.H.K. and R.V. contributed to the acquisition of study data and revised the manuscript. C.K.v.d.E and J.M.B. have made substantial contributions to the conception and design of the study, interpretation of data and revised the manuscript.

DECLARATION OF INTERESTS

J.M.B. reports personal fees from Vertex Pharmaceuticals, Proteostasis Therapeutics, Eloxx Pharmaceuticals, Teva Pharmaceutical Industries and Galapagos, outside the submitted work; In addition, J.M.B. has a patent patent(s) related to the FIS-assay with royalties paid. C.K.v.d.E. reports grants from GSK, grants from Nutricia, TEVA, Gilead, Vertex, ProQR, Proteostasis, Galapagos NV and Eloxx outside the submitted work; In addition, C.K.v.d.E. has a patent 10006904 with royalties paid. G.H.K. reports grants from Lung Foundation of the Netherlands, Vertex Pharmaceuticals, UBBO EMMIUS foundation, GSK, TEVA the Netherlands, TETRI Foundation, European Union (H2020), outside the submitted work; and he has participated in advisory boards meetings to GSK and PURE-IMS outside the submitted work (Money to institution). All other authors have nothing to disclose.

REFERENCES

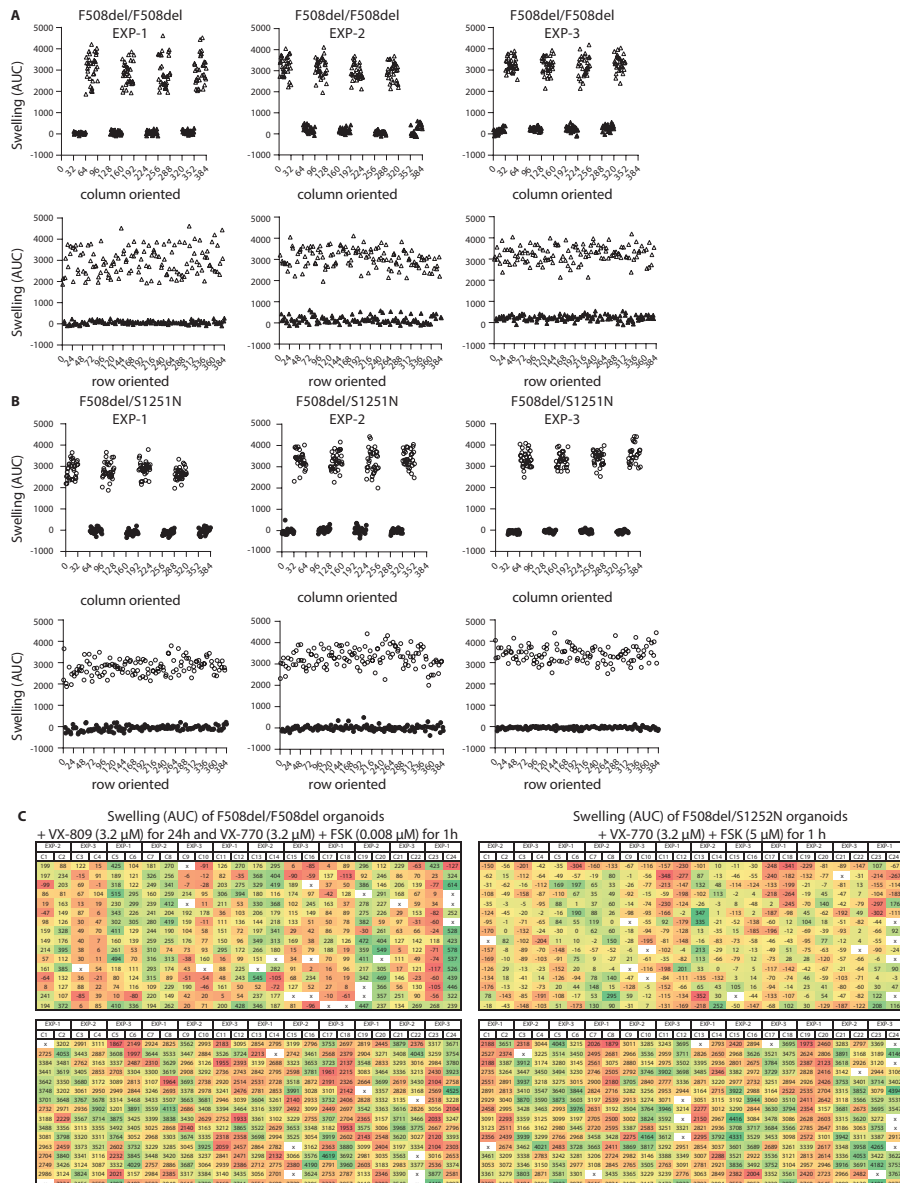
1. Pushpakom, S. et al. Drug repurposing: Progress, challenges and recommendations. *Nat. Rev. Drug Discov.* 18, 41–58 (2018).
2. Ashburn, T. T. & Thor, K. B. Drug repositioning: Identifying and developing new uses for existing drugs. *Nat. Rev. Drug Discov.* 3, 673–683 (2004).
3. Sosnay, P. R. et al. Defining the disease liability of variants in the cystic fibrosis transmembrane conductance regulator gene. *Nat. Genet.* 45, 1160–1167 (2013).
4. Wainwright, C. E. et al. Lumacaftor–Ivacaftor in Patients with Cystic Fibrosis Homozygous for Phe508del CFTR. *N. Engl. J. Med.* 373, 220–231 (2015).
5. Ramsey, B. W. et al. A CFTR Potentiator in Patients with Cystic Fibrosis and the G551D Mutation. *N. Engl. J. Med.* 365, 1663–1672 (2011).
6. Dutch cystic fibrosis society - approved mutations for CFTR modulator usage in the Netherlands - 2021. <https://ncfs.nl/over-taaislijmziekte/behandeling/status-cftr-modulatoren/>.
7. Boj, S. F. et al. Forskolin-induced Swelling in Intestinal Organoids: An In Vitro Assay for Assessing Drug Response in Cystic Fibrosis Patients. *J. Vis. Exp.* 1–12 (2017) doi:10.3791/55159.
8. Vonk, A. M. et al. Protocol for Application, Standardization and Validation of the Forskolin-Induced Swelling Assay in Cystic Fibrosis Human Colon Organoids. *STAR Protoc.* 1, 100019 (2020).
9. Dekkers, J. F. et al. A functional CFTR assay using primary cystic fibrosis intestinal organoids. *Nat. Med.* 19, 939–945 (2013).
10. Geurts, M. H. et al. Evaluating CRISPR-based Prime Editing for cancer modeling and CFTR repair in intestinal organoids. *bioRxiv* 1–14 (2020).
11. Geurts, M. H. et al. CRISPR-Based Adenine Editors Correct Nonsense Mutations in a Cystic Fibrosis Organoid Biobank. *Cell Stem Cell* 26, 503–510.e7 (2020).
12. Okiyoneda, T. et al. Mechanism-based corrector combination restores ΔF508-CFTR folding and function. *Nat. Chem. Biol.* 9, 444–454 (2013).
13. Zomer-van Ommen, D. D. et al. Comparison of ex vivo and in vitro intestinal cystic fibrosis models to measure CFTR-dependent ion channel activity. *J. Cyst. Fibros.* 17, (2018).
14. Flume, P. A. et al. Ivacaftor in subjects with cystic fibrosis who are homozygous for the F508del-CFTR mutation. *Chest* 142, 718–724 (2012).
15. Rowe, S. M. et al. Lumacaftor/ivacaftor treatment of patients with cystic fibrosis heterozygous for F508del-CFTR. *Ann. Am. Thorac. Soc.* 14, 213–219 (2017).
16. Rowe, S. M. et al. Tezacaftor–Ivacaftor in Residual-Function Heterozygotes with Cystic Fibrosis. *N. Engl. J. Med.* 377, 2024–2035 (2017).
17. Moss, R. B. et al. Efficacy and safety of ivacaftor in patients with cystic fibrosis who have an Arg117His-CFTR mutation: A double-blind, randomised controlled trial. *Lancet Respir. Med.* 3, 524–533 (2015).
18. K., D. B. et al. Efficacy and safety of ivacaftor in patients with cystic fibrosis and a non-G551D gating mutation. *J. Cyst. Fibros.* 13, 674–680 (2014).
19. Garnock-Jones, K. P. Roflumilast: A Review in COPD. *Drugs* 75, 1645–1656 (2015).
20. Turner, M. J., Luo, Y., Thomas, D. Y. & Hanrahan, J. W. The dual phosphodiesterase 3/4 inhibitor RPL554 stimulates rare class III and IV CFTR mutants. *Am. J. Physiol. - Lung Cell. Mol. Physiol.* 318, L908–L920 (2020).
21. Turner, M. J., Abbott-Banner, K., Thomas, D. Y. & Hanrahan, J. W. Cyclic nucleotide phosphodiesterase inhibitors as therapeutic interventions for cystic fibrosis. *Pharmacol. Ther.* 224, 107826 (2021).

CHAPTER 4

22. Turner, M. J., Dauletbaev, N., Lands, L. C. & Hanrahan, J. W. The phosphodiesterase inhibitor ensifentri ne reduces production of proinflammatory mediators in well differentiated bronchial epithelial cells by inhibiting PDE4. *J. Pharmacol. Exp. Ther.* 375, 414–429 (2020).
23. Turner, M. J. et al. The dual phosphodiesterase 3 and 4 inhibitor RPL554 stimulates CFTR and ciliary beating in primary cultures of bronchial epithelia. *Am. J. Physiol. - Lung Cell. Mol. Physiol.* 310, L59–L70 (2016).
24. Blanchard, E. et al. Anchored PDE4 regulates chloride conductance in wild-type and F508del-CFTR human airway epithelia. *Faseb J.* 28, 791–801 (2014).
25. Lambert, J. A. et al. Cystic fibrosis transmembrane conductance regulator activation by roflumilast contributes to therapeutic benefit in chronic bronchitis. *Am. J. Respir. Cell Mol. Biol.* 50, 549–558 (2014).
26. Schmid, A. et al. Roflumilast partially reverses smoke-induced mucociliary dysfunction. *Respir. Res.* 16, 1–11 (2015).
27. Raju, S. V. et al. Roflumilast reverses CFTR-mediated ion transport dysfunction in cigarette smoke-exposed mice. *Respir. Res.* 18, 1–8 (2017).
28. Han, S. T. et al. Residual function of cystic fibrosis mutants predicts response to small molecule CFTR modulators. *JCI insight* 3, 1–21 (2018).
29. Van Goor, F., Yu, H., Burton, B. & Hoffman, B. J. Effect of ivacaftor on CFTR forms with missense mutations associated with defects in protein processing or function. *J. Cyst. Fibros.* 13, 29–36 (2014).
30. Reilly, R. et al. Targeting the PI3K/Akt/mTOR signalling pathway in Cystic Fibrosis. *Sci. Rep.* 7, 1–13 (2017).
31. Verkman, A. S. & Galietta, L. J. Chloride channels as drug targets. *Nat Rev Drug Discov.* 8, 153–171 (2009).
32. Ma, X. et al. Activation of GABA_A receptors in colon epithelium exacerbates acute colitis. *Front. Immunol.* 9, 1–18 (2018).
33. Li, Y., Xiang, Y. Y., Lu, W. Y., Liu, C. & Li, J. A novel role of intestine epithelial GABAergic signaling in regulating intestinal fluid secretion. *Am. J. Physiol. - Gastrointest. Liver Physiol.* 303, 453–460 (2012).
34. Hyland, N. P. & Cryan, J. F. A gut feeling about GABA: Focus on GABAB receptors. *Front. Pharmacol. OCT*, 1–9 (2010).
35. Brown, J. R. et al. Vixalisib (XL765) in patients with relapsed or refractory non-Hodgkin lymphoma or chronic lymphocytic leukaemia: an open-label, phase 2 trial. *Lancet Haematol.* 5, e170–e180 (2018).
36. Vijftigschild, L. A. W. et al. 2-Adrenergic receptor agonists activate CFTR in intestinal organoids and subjects with cystic fibrosis. *European Respiratory Journal* vol. 48 768–779 (2016).
37. Berkers, G. et al. Rectal Organoids Enable Personalized Treatment of Cystic Fibrosis. *Cell Rep.* 26, 1701–1708.e3 (2019).

SUPPLEMENTARY INFORMATION

SUPPLEMENTARY FIGURES

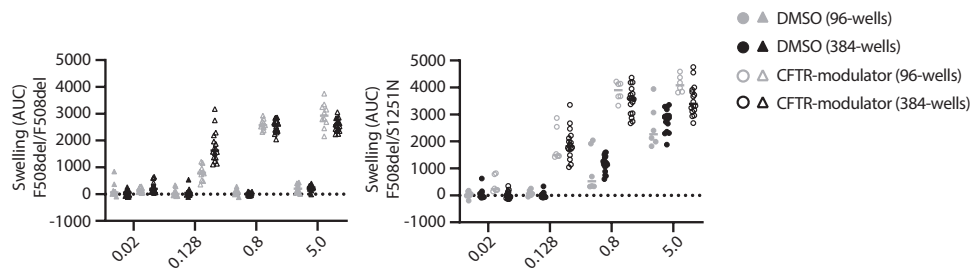


Supplementary figure 1: Spatial uniformity of 384-wells FIS assay.

Replicate experiment of three 384-wells plates with F508del/F508del (**A**) and F508del/S1251N (**B**) organoids performed on multiple culturing days, up until 12 weeks. Organoids were plated and VX-809 was added to F508del/F508del organoids, 24h prior to the FIS assay. The next day, 128 wells were treated with VX-770 (3.2 μ M) + 0.008 μ M (=min signal) fsk and another 128 wells were treated with VX-770 + 5 μ M (=max signal). Data is shown for both donors.

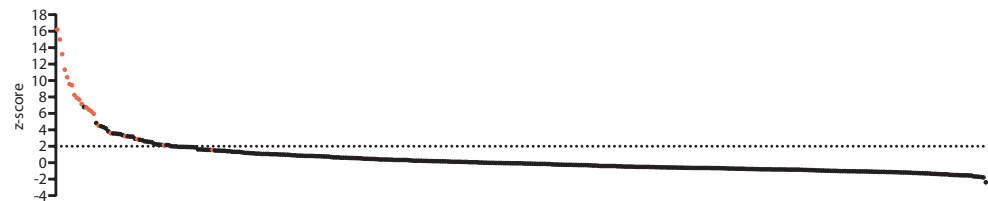
CHAPTER 4

separately in a row-oriented and column oriented fashion, to explore horizontal or vertical drift. (C) Swelling of F508del/F508del (left) and F508del/S1251N organoids (right) with 0.008 µM fsk (top plates) or 5 µM fsk (bottom plates) of the three individual experiments combined. The location of the min and max signals on the combined plates in C correspond with the location on the individual plates, meaning that the location of the max and min signal wells varied among the three individual plates per donor. Color coding is applied to assess edge effect. x = defined as outlier (see methods section for detailed definition of an outlier).



Supplementary figure 2: Organoid swelling measured in 96 or 384-wells plates.

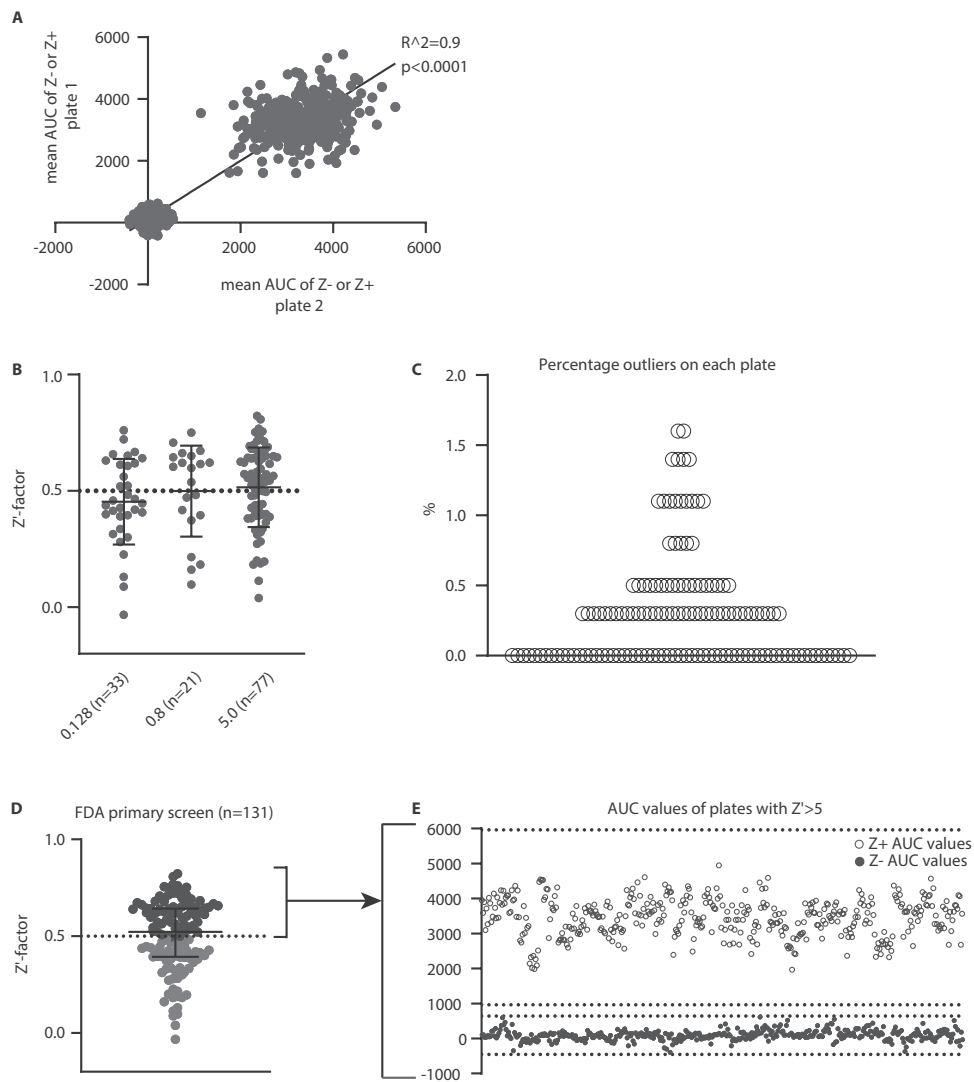
Swelling of F508del/F508del (left) organoids treated W/W/O VX-770/VX-809 and F508del/S1251N (right) organoids treated W/W/O VX-770 and in presence of an increasing concentration of fsk, measured in three independent 96-well plates (two technical replicates per plate, gray datapoints) and one 384-well plate (16 technical replicates, black datapoints).



Supplementary figure 3: Waterfall plot of mean Z-scores of 1 toxicity screen plate.

Mean Z-scores of F508del/F508del and F508del/S1251N organoids of 1 out of the 5 toxicity screen 384-wells plates. Red datapoints represent Z-scores of compounds of which organoid toxicity was confirmed based on visual screening of the bright field images (independently scored by three investigators) and were excluded from further screens.

Pre-clinical efficacy testing of FDA-approved drugs for non-homozygous F508del-CFTR genotypes



Supplementary figure 4: Quality check of the FDA-approved drug screen.

(A) Correlation between the mean AUC of the Z+ and Z- values of the two 384-well plates of all donor (dots represent mean, n=8). (B) Z'-factors of FIS experiments, plotted per fsk concentration. $Z' \text{-factor} = 1 - \frac{3(\sigma_p - \sigma_n)}{(\mu_p - \mu_n)}$, where σ_p is the standard deviation of the 8 positive control wells (F508del/S1251N organoids treated with VX-770 and 5 μM fsk), σ_n is the standard deviation of the negative control wells (individual 76 organoid cultures treated with suboptimal fsk concentration, without presence of an FDA compound), μ_p is the mean of the 8 positive control wells, μ_n is the mean of the 8 negative control wells. (C) Outlier percentage of all plates. (D) The mean Z'-factor of all plates. (E) AUC values above $>Q3 + 3xIQR$ ($=5963$) of all positive control wells (Z+ values, white open dots) or below $Q1 - 3xIQR$ ($=-452$) of all negative control wells (Z-values, black filled dots) of the plates with a $Z' \text{-factor} > 5$, were defined as outlier.

SUPPLEMENTARY TABLES

Compound number	Compound name	In vivo application
1	ABT-263 (Navitoclax)	Anti-cancer drug
2	YM155 (Sepantronium Bromide)	Anti-cancer drug
3	Bortezomib (PS-341)	Anti-cancer drug
4	Panobinostat (LBH589)	Anti-cancer drug
5	CEP-18770 (Delanzomib)	Anti-cancer drug
6	17-AAG (Tanespimycin)	Anti-cancer drug
7	Ganetespib (STA-9090)	Anti-cancer drug
8	Saracatinib (AZD0530)	Anti-cancer drug
9	Onalespib (AT13387)	Anti-cancer drug
10	Dasatinib (BMS-354825)	Anti-cancer drug
11	Docetaxel (RP56976)	Anti-cancer drug
12	Ispinesib (SB-715992)	Anti-cancer drug
13	Paclitaxel (NSC 125973)	Anti-cancer drug
14	Rigosertib (ON-01910)	Anti-cancer drug
15	Epothilone B (EPO906, Patupilone)	Anti-cancer drug
16	Flavopiridol (Alvocidib)	Anti-cancer drug
17	Topotecan (NSC609699) HCl	Anti-cancer drug
18	Epirubicin (IMI 28) HCl	Anti-cancer drug
19	Tamoxifen (ICI 46474)	Anti-cancer drug
20	Vincristine (NSC-67574)	Anti-cancer drug
21	Rufinamide	Anti-epileptic/seizure drugs
22	Volasertib (BI 6727)	Anti-cancer drug
23	Neratinib (HKI-272)	Anti-cancer drug / Inhibits Xenograph growth
24	Ixazomib (MLN2238)	Anti-cancer drug
25	Crystal Violet	triaryl methane dye
26	Ompalisib (GSK2126458, GSK458)	Anti-cancer drug
27	Carfilzomib (PR-171)	Anti-cancer drug
28	Daunorubicin (RP 13057) HCl	Anti-cancer drug
29	Cabazitaxel (XRP6258)	Anti-cancer drug
30	Bisacodyl	Laxative drug
31	Dinaciclib (SCH727965)	Anti-cancer drug
32	Vinorelbine Tartrate	Anti-cancer drug
33	Digoxin	Atrial fibrillation and heart failure drug

Pre-clinical efficacy testing of FDA-approved drugs for non-homozygous F508del-CFTR genotypes

Compound number	Compound name	In vivo application
34	Puromycin (CL13900) 2HCl	Aminonucleoside antibiotic
35	Vinblastine (NSC-49842) sulfate	Anti-cancer drug
36	Birinapant (TL32711)	Anti-cancer drug
37	Dasatinib Monohydrate	Anti-cancer drug
38	Docetaxel Trihydrate	Anti-cancer drug
39	Riociguat (BAY 63-2521)	Pulmonary hypertension drug
40	Mebendazole	Anti-cancer drug
41	Gemcitabine (LY-188011) HCl	Anti-cancer drug
42	Vancomycin HCl	Antibacterial agent
43	Fosbretabulin (Combretastatin A4 Phosphate (CA4P)) Disodium	Anti-cancer drug

Supplementary table 1: list of toxic compounds excluded from further screening.

CF code	cDNA name allele 1	protein name allele 1	Legacy name allele 1	cDNA name allele 1	protein name allele 1	Legacy name allele 1	donors included for primary screen (n=76)	donors included for roflumilast screen (n=107)	donors included for VX-770 and VX- 770/VX-809 screen (n=251, including F508del/F508del organoid cultures)
CF0075	c.1679+1G>C	no protein name	1811+1G>C	c.1679+1G>C	no protein name	1811+1G>C	x	x	x
CF0168	c.1679+1G>C	no protein name	1811+1G>C	c.1679+1G>C	no protein name	1811+1G>C	x	x	x
CF0188	c.1679+1G>C	no protein name	1811+1G>C	c.1679+1G>C	no protein name	1811+1G>C	x	x	x
CF0224	c.579+1G>T	no protein name	711+1G>T	c.579+1G>T	no protein name	711+1G>T	x	x	x
CF0236	c.579+1G>T	no protein name	711+1G>T	c.(1584+1_158 5-1).(1679+1_1680-1)del	no protein name	CFTRdel11	x	x	x
CF0271	c.1679+1G>C	no protein name	1811+1G>C	c.1679+1G>C	no protein name	1811+1G>C	x	x	x
CF0570	no cDNA name	no protein name	(TG)12(T)7	no cDNA name	no protein name	(TG)11(T)7			x
CF0576	c.3140-26A>G	no protein name	3272-26A>G	c.1766+5G>T	no protein name	1898+5G>T			x
CF0612	c.3140-26A>G	no protein name	3272-26A>G	c.3140-26A>G	no protein name	3272-26A>G			x
CF0323	c.2657+5G>T	no protein name	2789+5G>T	c.579+1G>T	no protein name	711+1G>T	x		
CF0829	c.1364C>A	p.Ala455Glu	A455E	c.579+5G>T	no protein name	711+5G>T			x
CF0645	c.3484C>T	p.Arg1162X	R1162X	c.3717+ 12191C>T	no protein name	3849+ 10kbC>T			x
CF0198	c.1657>T	p.Arg553X	R553X	c.4243-3T>A	no protein name	4375-3T>A	x	x	x

CF code	cDNA name allele 1	protein name allele 1	Legacy name allele 1	cDNA name allele 1	protein name allele 1	Legacy name allele 1	donors included for primary screen (n=76)	donors included for roflumilast screen (n=107)	donors included for VX-770 and VX- 770/VX-809 screen (n=251, including F508del/F508del organoid cultures)
CF0191	c.1519_1521delATC	p.Ile507del	I507del	c.4242+2T>G	no protein name	4374+2T>G	x	x	x
CF0414	c.948delT	p.Phe316LeufsX12	1078delT	c.3140-26A>G	no protein name	3272-26A>G	x	x	x
CF0068	c.1521_1523delCTT	p.Phe508del	F508del	c.3368-2A>G	no protein name	3500-2A>G	x	x	x
CF0134	c.1521_1523delCTT	p.Phe508del	F508del	c.579+1G>T	no protein name	711+1G>T	x	x	x
CF0228	c.1521_1523delCTT	p.Phe508del	F508del	c.3140-26A>G	no protein name	3272-26A>G	x	x	x
CF0248	c.1521_1523delCTT	p.Phe508del	F508del	c.(2988+1_2989-1)_3367 +1_3368-1)del	no protein name	CFTRdel e17a,e17b	x	x	x
CF0291	c.1521_1523delCTT	p.Phe508del	F508del	c.579+1G>T	no protein name	711+1G>T	x	x	x
CF0304	c.1521_1523delCTT	p.Phe508del	F508del	c.579+1G>T	no protein name	711+1G>T	x	x	x
CF0317	c.1521_1523delCTT	p.Phe508del	F508del	c.(3468+1_3469-1)_3963+1_3 964-1)del	no protein name	CFTRdel e19 -21	x	x	x
CF0384	c.1521_1523delCTT	p.Phe508del	F508del	c.(2988+1_2989-1)_3367+1 -3368-1)del	no protein name	CFTRdel e17a ,17b	x	x	x
CF0025	c.1521_1523delCTT	p.Phe508del	F508del	c.1210-33_1210-6GT[13]T[4]	no protein name	(TG)13T5	x	x	x

CF code	cDNA name allele 1	protein name allele 1	Legacy name allele 1	cDNA name allele 1	protein name allele 1	Legacy name allele 1	donors included for primary screen (n=76)	donors included for roflumilast screen (n=107)	donors included for VX-770 and VX- 770/NX-809 screen (n=251, including F508del/F508del organoid cultures)
CF0135	c.1521_1 523delCTT	p.Phe508del	F508del	C.579+1G>T	no protein name	711+ 1G>T		x	x
CF0308	c.1521_1 523delCTT	p.Phe508del	F508del	C.489+1G>T	no protein name	621+ 1G>T	x	x	x
CF0404	c.1521_1 523delCTT	p.Phe508del	F508del	C.3717+ 1219(C>T	no protein name	3849+ 10kbC>T	x	x	x
CF0021	c.1521_ 1523delCTT	p.Phe508del	F508del	C.1210- 33_1210- 6GT[13]T[4]	no protein name	(TG)13(T)5	x	x	x
CF0024	c.1521_1 523delCTT	p.Phe508del	F508del	C.1210- 33_1210- 6GT[13]T[4]	no protein name	(TG)13(T)5	x	x	x
CF0035	c.1521_1 523delCTT	p.Phe508del	F508del	C.1210- 33_1210- 6GT[13]T[4]	no protein name	(TG)13(T)5		x	x
CF0138	c.1521_ 1523delCTT	p.Phe508del	F508del	C.1210- 33_1210- 6GT[12]T[4]	no protein name	(TG)12(T)5		x	x
CF0173	c.1521_ 1523delCTT	p.Phe508del	F508del	C.2657+5G>A	no protein name	2789+ 5G>A		x	x
CF0220	c.1521_ 1523delCTT	p.Phe508del	F508del	C.2657+5G>A	no protein name	2789+ 5G>A		x	x
CF0229	c.1521_1 523delCTT	p.Phe508del	F508del	C.1585-1G>A	no protein name	1717- 1G>A		x	x
CF0231	c.1521_ 1523delCTT	p.Phe508del	F508del	C.3140-26A>G	no protein name	3272- 26A>G		x	x
CF0307	c.1521_1 523delCTT	p.Phe508del	F508del	C.3717+5G>T	no protein name	3849+5G>T		x	x

CF code	cDNA name allele 1	protein name allele 1	Legacy name allele 1	cDNA name allele 1	protein name allele 1	Legacy name allele 1	donors included for primary screen (n=76)	donors included for roflumilast screen (n=107)	donors included for VX-770 and VX- 770/VX-809 screen (n=251, including F508del/F508del organoid cultures)
CF0358	c.1521_- 1523delCTT	p.Phe508del	F508del	c.1725-1727del insA/I	no protein name	no legacy name			x
CF0433	c.1521_1 523delCTT	p.Phe508del	F508del	c.(2988+1_298 9-1)_3367+1_3 368-1)del	no protein name	CFTRdel17a, 17b			x
CF0437	c.1521_- 1523delCTT	p.Phe508del	F508del	no cDNA name	no protein name	IVS11-1G>C			x
CF0517	c.1521_1 523delCTT	p.Phe508del	F508del	c.579+1G>T	no protein name	711+1G>T			x
CF0540	c.1521_- 1523delCTT	p.Phe508del	F508del	c.1585-1G>A	no protein name	1717-1G>A			x
CF0542	c.1521_1 523delCTT	p.Phe508del	F508del	c.377+12 191C>T	no protein name	3849+ 10kbC>T			x
CF0551	c.1521_15 23delCTT	p.Phe508del	F508del	c.1210-1delG	no protein name	1342-1delG			x
CF0556	c.1521_- 1523delCTT	p.Phe508del	F508del	c.4243-3T>A	no protein name	4375-3T>A			x
CF0565	c.1521_1 523delCTT	p.Phe508del	F508del	c.3717+1 2191C>T	no protein name	3849+ 10kbC>T			x
CF0575	c.1521_1 523delCTT	p.Phe508del	F508del	c.3717+1 2191C>T	no protein name	3849+ 10kbC>T			x
CF0587	c.1521_1 523delCTT	p.Phe508del	F508del	c.1585-1G>A	no protein name	1717-1G>A			x
CF0592	c.1521_1523 delCTT	p.Phe508del	F508del	c.(2988+1_298 9-1)_3367+1_3 368-1)del	no protein name	CFTRdel 17a,17b			x

CF code	cDNA name allele 1	protein name allele 1	Legacy name allele 1	cDNA name allele 1	protein name allele 1	Legacy name allele 1	donors included for primary screen (n=76)	donors included for roflumilast screen (n=107)	donors included for VX-770 and VX- 770/VX-809 screen (n=251, including F508del/F508del organoid cultures)
CF0594	c.1521_152 3delCTT	p.Phe508del	F508del	c.579+1G>T	no protein name	711+1G>T			x
CF0606	c.1521_1 523delCTT	p.Phe508del	F508del	c.3140-26A>G	no protein name	3272-26A>G			x
CF0607	c.1521_1 1523delCTT	p.Phe508del	F508del	c.3140-26A>G	no protein name	3272-26A>G			x
CF0609	c.1521_1 523delCTT	p.Phe508del	F508del	c.1210- 33_1210- 6G[T]13[T]4]	no protein name	(TG)13(T)5			x
CF0620	c.1521_1 523delCTT	p.Phe508del	F508del	c.2657+5G>A	no protein name	2789+5G>A			x
CF0621	c.1521_1 1523delCTT	p.Phe508del	F508del	c.(2988+1_298 9-1)[3367+1_ 3368-1]del	no protein name	CFTRdel17a, 17b			x
CF0706	c.1521_1 523delCTT	p.Phe508del	F508del	c.1210- 33_1210- 6G[T]13[T]4]	no protein name	(TG)11(T)5			x
CF0844	c.1521_1 523delCTT	p.Phe508del	F508del	c.3407_3422del	no protein name	no legacy name			x
CF0497	c.1521_15 23delCTT	p.Phe508del	F508del	c.3717+12191 C>T	no protein name	3849+ 10kbC>T			x
CF0710	c.3752G>A	p.Ser1251A sn	S1251N	c.1585-1G>A	no protein name	1717-1G>A			x
CF0139	c.1545_154 6delTA	p.Tyr515X	1677delTA	c.2988+1G>A	no protein name	IVS16+1G>A (3120+1G>A)			x
CF0396	c.2547C>A	p.Tyr849X	Y849X	c.2657+5G>A	no protein name	2789+5G>A			x

Pre-clinical efficacy testing of FDA-approved drugs for non-homozygous F508del-CFTR genotypes

CF code	cDNA name allele 1	protein name allele 1	Legacy name allele 1	cDNA name allele 1	protein name allele 1	Legacy name allele 1	donors included for primary screen (n=76)	donors included for roflumilast screen (n=107)	donors included for VX-770 and VX- 770/VX-809 screen (n=251, including F508del/F508del organoid cultures)
CF0031	c.350G>A;12 10-12T[7] ;12 0-12T[9]	p.Arg117His ;7;9T	R117H-7T-9T	c.1364C>A	p.Ala455Glu	A455E			x
CF0007	c.1521_15 23delCTT	p.Phe508del	F508del	c.1364C>A	p.Ala455Glu	A455E	x		
CF0011	c.1521_1 523delCTT	p.Phe508del	F508del	c.1364C>A	p.Ala455Glu	A455E	x		
CF0046	c.1521_1 523delCTT	p.Phe508del	F508del	c.1364C>A	p.Ala455Glu	A455E	x		
CF0060	c.1521_1 523delCTT	p.Phe508del	F508del	c.1364C>A	p.Ala455Glu	A455E	x		
CF0088	c.375G>A	p.Ser125 1Asn	S125T/N	c.1364C>A	p.Ala455Glu	A455E	x		
CF0360	c.137C>A	p.Ala46Asp	A46D	c.137C>A	p.Ala46Asp	A46D	x	x	x
CF0361	c.137C>A	p.Ala46Asp	A46D	c.137C>A	p.Ala46Asp	A46D	x	x	x
CF0412	c.825C>G	p.Tyr275X	Y275X	c.1675G>A	p.Ala559Thr	A559T	x	x	x
CF0391	c.1624G>T	p.Gly542X	G542X	c.3196C>T	p.Arg106 6Cys	R1066C	x	x	x
CF0822	c.1624G>T	p.Gly542X	G542X	c.3196C>T	p.Arg1066 Cys	R1066C			x
CF0403	c.1521 -1523delCTT	p.Phe508del	F508del	c.3196C>T	p.Arg1066C ys	R1066C	x	x	x
CF0432	c.1521_1 523delCTT	p.Phe508del	F508del	c.3196C>T	p.Arg1066 Cys	R1066C	x		

CF code	cDNA name allele 1	protein name allele 1	Legacy name allele 1	cDNA name allele 1	protein name allele 1	Legacy name allele 1	donors included for primary screen (n=76)	donors included for roflumilast screen (n=107)	donors included for VX-770 and VX- 770/VX-809 screen (n=251, including F508del/F508del organoid cultures)
CF0400	c.3196C>T	p.Arg10 66Cys		R1066C	C.3197G>A	p.Arg10 66His	R1066H	x	x
CF044	c.350G>A; 1210-12T[7]	p.Arg117 His;7T		R117H-7T	C.3484C>T	p.Arg1162X	R1162X	x	
CF0597	c.3454G>C	p.Asp115 2His		D1152H	C.3484C>T	p.Arg1162X	R1162X	x	
CF0140	c.3752G>A	p.Ser1251 Asn		S1251N	C.350G>A	p.Arg117His	R117H	x	
CF0017	c.350G>A ,1210-12T[7]	p.Arg117Hi s;7T		R117H-7T	C.350G>A ,1210-12T[7]	p.Arg117H is;7T	R117H-7T	x	
CF0026	c.1521_1 523delCTT	p.Phe508del		F508del	C.350G>A ,1210-12T[7]	p.Arg117H is;7T	R117H-7T	x	
CF0027	c.1521_ 1523delCTT	p.Phe508del		F508del	C.350G >A,1210-12T[7]	p.Arg	R117H-7T	x	
CF0032	c.1521_ 1523delCTT	p.Phe508del		F508del	C.350G>A; 1210-12T[7]	p.Arg117 His;7T	R117H-7T	x	
CF0036	c.1521 _1523delCTT	p.Phe508del		F508del	C.350G>A;121 0,12T[7]	p.Arg117H is;7T	R117H-7T	x	
CF0562	c.3846G>A	p.Trp1282X		W1282X	C.350G>A;1 210-12T[7]	p.Arg11 7His;7T	R117H-7T	x	
CF0030	c.152 _1523delCTT	p.Phe508del		F508del	C.350G>A; 1210-12T[7]; 1210-12T[9]	p.Arg117Hi s;7T;9T	R117H-7T-9T	x	

CF code	cDNA name allele 1	protein name allele 1	Legacy name allele 1	cDNA name allele 1	protein name allele 1	Legacy name allele 1	donors included for primary screen (n=76)	donors included for roflumilast screen (n=107)	donors included for VX-770 and VX- 770/VX-809 screen (n=251, including F508del/F508del organoid cultures)
CF0038	c.1521_1 523delCTT	p.Phe508del	F508del	c.350G>A[12 10-12T[7] ,1210-12T[9]	p.Arg1 17His;7T;9T	R117H;7T;9T			x
CF0610	c.1521_15 23delCTT	p.Phe508del	F508del	c.4074A>T	p.Arg1 356Ser	R1358S			x
CF0256	c.1000C>T	p.Arg334Trp	R334W	c.1000C>T	p.Arg334Trp	R334W	x	x	x
CF0401	c.3717+1 2191C>T	no protein name	3849+ 10kbc>T	c.1040G>A	p.Arg347His	R347H	x	x	x
CF0176	c.1521_ 1523delCTT	p.Phe508del	F508del	c.1040G>C	p.Arg347Pro	R347P	x	x	x
CF0219	c.1521_1 523delCTT	p.Phe508del	F508del	c.1040G>C	p.Arg347Pro	R347P	x	x	x
CF0238	c.1521_1 523delCTT	p.Phe508del	F508del	c.1040G>C	p.Arg347Pro	R347P	x	x	x
CF0841	c.1521 -1523delCTT	p.Phe508del	F508del	c.1054C>T	p.Arg352Trp	R352W			x
CF0696	c.3873+2T>C	no protein name	4005+2T>C	c.1657C>T	p.Arg553X	R553X			x
CF0042	c.350G> A;1210-12T[7]	p.Arg117H is;7T	R117H-7T	c.1657C>T	p.Arg553X	R553X			x
CF0613	c.1521_15 23delCTT	p.Phe508del	F508del	c.1657C>T	p.Arg553X	R553X			x
CF0348	c.1521_1 523delCTT	p.Phe508del	F508del	c.224G>C	p.Arg74Pro	R74P	x	x	x

CF code	cDNA name allele 1	protein name allele 1	Legacy name allele 1	cDNA name allele 1	protein name allele 1	Legacy name allele 1	donors included for primary screen (n=76)	donors included for roflumilast screen (n=107)	donors included for VX-770 and VX- 770/VX-809 screen (n=251, including F508del/F508del organoid cultures)
CF0480	c.1521_15 23delCTT	p.Phe508del	F508del	c.224G>A	p.Arg75Gln	R75Q	x	x	x
CF0092	c.1000C>T	p.Arg334Trp	R334W	c.2290C>T	p.Arg764X	R764X	x	x	x
CF0608	c.2353C>T	p.Arg785X	R785X	c.2353C>T	p.Arg785X	R785X			x
CF0043	c.1521_1 1523delCTT	p.Phe508del	F508del	c.3909C>G	p.Asn130 3Lys	N1303K			x
CF0047	c.15 21_1523delCTT	p.Phe508del	F508del	c.3909C>G	p.Asn130 3Lys	N1303K	x		x
CF0195	c.1521_1 523delCTT	p.Phe508del	F508del	c.3909C>G	p.Asn130 3Lys	N1303K	x		x
CF0230	c.1521_1 1523delCTT	p.Phe508del	F508del	c.3909C>G	p.Asn130 3Lys	N1303K	x		x
CF0279	c.1521_1 523delCTT	p.Phe508del	F508del	c.3909C>G	p.Asn130 3Lys	N1303K	x		x
CF0572	c.3484C>T	p.Arg1162X	R1162X	c.3454G>C	p.Asp1152H is	D1152H			x
CF0478	c.3773 _3774insT	p.Leu1 258PhefsX7	3905insT	c.3454G>C	p.Asp115 2Hs	D1152H	x	x	x
CF0262	c.1521_1 523delCTT	p.Phe508del	F508del	c.3454G>C	p.Asp115 2Hs	D1152H			x
CF0563	c.3909C>G	p.Asn130 3Lys	N1303K	c.3035A>C	p.Gln1012 Pro	Q1012P	x		x
CF0253	c.1521_15 23delCTT	p.Phe508del	F508del	c.3937C>T	p.Gln1313X	Q1313X	x		x

CF code	cDNA name allele 1	protein name allele 1	Legacy name allele 1	cDNA name allele 1	protein name allele 1	Legacy name allele 1	donors included for primary screen (n=76)	donors included for roflumilast screen (n=107)	donors included for VX-770 and VX- 770/VX-809 screen (n=251, including F508del/F508del organoid cultures)
CF0174	c.1973_19 85del13ins AGAAA elCTT	p.Arg658L ysfsX4	2105_ 211>del13 insAGAAA	c.4056G>C or c.4056G>T	p.Gln1352H is	Q1352H	x	x	x
CF0488	c.1521_1523d elCTT	p.Phe508del	F508del	c.1477C>T	p.Gln493X	Q493X	x	x	x
CF0715	c.4251delA	p.Glu1418A rgfsX14	4382delA	c.1911delG	p.Gln637 HisfsX26	2043delG	x	x	x
CF0328	c.1521_15 23delCTT	p.Phe508del	F508del	c.2052_2053i nsA	p.Gln685 ThrfsX4	2184insA	x	x	x
CF0349	c.1521_152 3delCTT	p.Phe508del	F508del	c.4251delA	p.Glu141 8AgtfsX14.	4382delA	x	x	x
CF0406	c.1521_15 23delCTT	p.Phe508del	F508del	no cDNA name	p.Glu1418A rgfsX14	4383delA	x	x	x
CF0160	c.1364C>A	p.Ala455Glu	A455E	c.178G>T	p.Glu60X	E60X	x	x	x
CF0050	c.1521_1 523delCTT	p.Phe508del	F508del	c.178G>T	p.Glu60X	E60X	x	x	x
CF0351	c.1521_1 523delCTT	p.Phe508del	F508del	c.178G>T	p.Glu60X	E60X	x	x	x
CF0543	c.1521_ 1523delCTT	p.Phe508del	F508del	c.178G>T	p.Glu60X	E60X	x	x	x
CF0217	c.1521_152 3delCTT	p.Phe508del	F508del	c.2188G>T	p.Glu730Ter	E730X	x	x	x
CF0272	c.274G>A	p.Glu92Lys	E92K	c.274G>A	p.Glu92Lys	E92K	x	x	x
CF0744	c.3477delT	p.Val1160X	V1160X	c.274G>A	p.Glu92Lys	E92K	x	x	x

CF code	cDNA name allele 1	protein name allele 1	Legacy name allele 1	cDNA name allele 1	protein name allele 1	Legacy name allele 1	donors included for primary screen (n=76)	donors included for roflumilast screen (n=107)	donors included for VX-770 and VX- 770/VX-809 screen (n=251, including F508del/F508del organoid cultures)
CF0073	c.1521_152 3delCTT	p.Phe508del	F508del	c.3745G>A	p.Gly1249 Arg	G1249R	x	x	x
CF0161	c.1521_152 3delCTT	p.Phe508del	F508del	c.3745G>A	p.Gly12 49Arg	G1249R	x	x	x
CF0712	c.1521_1523 delCTT	p.Phe508del	F508del	c.3746G>A	p.Gly1249 Glu	G1249E	x	x	x
CF0171	c.1521_152 3delCTT	p.Phe508del	F508del	c.4046delG	p.Gly134 9AlafsTer5	4177delG	x	x	x
CF0625	c.1521_15 23delCTT	p.Phe508del	F508del	c.532G>A	p.Gly178Arg	G178R	x	x	x
CF0419	c.1364C>A	p.Ala455Glu	A455E	c.1211delG	p.Gly404 AspfsTer38	1343delG	x	x	x
CF0169	c.1521_1523 delCTT	p.Phe508del	F508del	c.1381G>A	p.Gly461Arg	G461R	x	x	x
CF0170	c.1521_1523d elCTT	p.Phe508del	F508del	c.1381G>A	p.Gly461Arg	G461R	x	x	x
CF0055	c.1521_1523de ICTT	p.Phe508del	F508del	c.1381G>A	p.Gly461Arg	G461R	x	x	x
CF0282	c.1624G>T	p.Gly542X	G542X	c.1624G>T	p.Gly542X	G542X	x	x	x
CF0006	c.1521_1 523delCTT	p.Phe508del	F508del	c.1624G>T	p.Gly542X	G542X	x	x	x
CF0296	c.3909C>G 03Lys	p.Asn13	N1303K	c.1648G>T	p.Gly550X	G550X	x	x	x
CF0276	c.1521_1 523delCTT	p.Phe508del	F508del	c.1648G>T	p.Gly550X	G550X	x	x	x

CF code	cDNA name allele 1	protein name allele 1	Legacy name allele 1	cDNA name allele 1	protein name allele 1	Legacy name allele 1	donors included for primary screen (n=76)	donors included for roflumilast screen (n=107)	donors included for VX-770 and VX- 770/VX-809 screen (n=251, including F508del/F508del organoid cultures)
CF0388	c.1521_1523del ICTT	p.Phe508del	F508del	c.1648G>T	p.Gly550X	G550X	x	x	x
CF0444	c.1521_1523d elCTT	p.Phe508del	F508del	c.1648G>T	p.Gly550X	G550X	x	x	x
CF0129	c.1521_1523del CTT	p.Phe508del	F508del	c.1652G>A	p.Gly551Asp	G551D	x		
CF0582	c.1521_15 23delCTT	p.Phe508del	F508del	c.1652G>A	p.Gly551Asp	G551D	x		
CF0574	c.1521_1523 delCTT	p.Phe508del	F508del	c.1727G>C	p.Gly576Ala	G576A	x		
CF0215	c.1521_1523del ICTT	p.Phe508del	F508del	c.1882G>? (C or A)	p.Gly628Arg	G628R	x	x	x
CF0422	c.1521_1523d elCTT	p.Phe508del	F508del	c.1882G>C or c.1882G>A	p.Gly628Arg	G628R(G>A) of (G>C)	x		
CF0458	c.1521_15 23delCTT	p.Phe508del	F508del	c.1882G>C	p.Gly628Arg	G628R	x		
CF0579	c.3909C>G	p.Asn1303 Lys	N1303K	c.254G>A	p.Gly85Glu	G85E	x		
CF0269	c.1521_15 23delCTT	p.Phe508del	F508del	c.254G>A	p.Gly85Glu	G85E	x	x	x
CF0519	c.1521_1 523delCTT	p.Phe508del	F508del	c.254G>A	p.Gly85Glu	G85E	x		
CF0227	c.3140_26A>G	no protein name	3272_26A>G	c.2908G>C	p.Gly970Arg	G970R	x	x	x
CF0671	c.1521_1523 delCTT	p.Phe508del	F508del	c.1859A>C	p.His620Pro	H620P	x		

CF code	cDNA name allele 1	protein name allele 1	Legacy name allele 1	cDNA name allele 1	protein name allele 1	Legacy name allele 1	donors included for primary screen (n=76)	donors included for roflumilast screen (n=107)	donors included for VX-770 and VX- 770/VX-809 screen (n=251, including F508del/F508del organoid cultures)
CF0122	c.350G>A	p.Arg117His	R117H	c.3415A>G	p.Ile1139Val	I1139V			x
CF0534	c.1521_1523d elCTT	p.Phe508del	F508del	c.3080T>C	p.Ile1027Thr	I1027T	x	x	x
CF0012	c.178G>T	p.Glu60X	E60X	c.3883delA	p.Ile1295P	4015delA	x	x	x
CF0665	c.1521_15 23delCTT	p.Phe508del	F508del	c.1007T>A	p.Ile336Lys	I336K			x
CF0754	c.1521 -1523delCTT	p.Phe508del	F508del	c.100 6_1007insG	p.Ile336Ser	1138insG			x
CF0596	c.1521_1523d elCTT	p.Phe508del	F508del	c.1519_ 1521delATC	p.Ile507del	I507del	x		x
CF0225	c.1521_152 3delCTT	p.Phe508del	F508del	c.3101T>C	p.Leu1034 Pro	L1034P	x	x	x
CF0398	c.1585-1G>A name	no protein	1717-1G>A	c.3773 -3774insT	p.Leu1	3905insT	x		x
CF0378	c.1521_1523d elCTT	p.Phe508del	F508del	c.3773_ 3774insT	p.Leu1 258PhefsX7	3905insT	x	x	x
CF0669	c.4004T>C Pro	p.Leu1335 Pro	L1335P	c.4004T>C	p.Leu13 35Pro	L1335P			x
CF0487	c.1521_1523 delCTT	p.Phe508del	F508del	c.617T>G	p.Leu20 67Trp	L206W		x	x
CF0699	c.1521_1 523delCTT	p.Phe508del	F508del	c.1358T>C	p.Leu45 35Ser	L453S		x	x
CF0342	c.1521_152 3delCTT	p.Phe508del	F508del	c.2012delT	p.Leu671X	2143delT	x	x	x

CF code	cDNA name allele 1	protein name allele 1	Legacy name allele 1	cDNA name allele 1	protein name allele 1	Legacy name allele 1	donors included for primary screen (n=76)	donors included for roflumilast screen (n=107)	donors included for VX-770 and VX- 770/VX-809 screen (n=251, including F508del/F508del organoid cultures)
CF0375	c.1521_152 3delCTT	p.Phe508del	F508del	c.2012delT	p.Leu671X	2143delT	x	x	x
CF0588	c.2195T>G	p.Leu732X	L732X	c.2195T>G	p.Leu732X	L732X			x
CF0460	c.1521_1 523delCTT	p.Phe508del	F508del	c.2195T>G	p.Leu732X	L732X	x	x	
CF0359	c.1521_1 523delCTT	p.Phe508del	F508del	c.262_263delTT	p.Leu8 8IlefsX22	394delTT	x	x	x
CF0008	c.1521_15 23delCTT	p.Phe508del	F508del	c.2780T>C	p.Leu9 27Pro	L927P	x	x	x
CF0239	c.1521_ 1523delCTT	p.Phe508del	F508del	c.2780T>C	p.Leu927 Pro	L927P	x	x	x
CF0354	c.1521_ 1523delCTT	p.Phe508del	F508del	c.2780T>C	p.Leu92 7Pro	L927P	x	x	x
CF0355	c.1521 _1523delCTT	p.Phe508del	F508del	c.2780T>C	p.Leu 927Pro	L927P	x	x	x
CF0392	c.3846G>A	p.Trp1282X	W1282X	c.2780T>C	p.Leu9 27Pro	L927P	x	x	x
CF0303	c.1364C>A	p.Ala455Glu	A455E	c.3528delC	p.Lys1177S erfsX15	3659delC	x	x	x
CF0289	c.3484C>T	p.Arg1162X	R1162X	c.3528delC	p.Lys117 7SerfsX15	3659delC	x	x	x
CF0457	c.1521 _1523delCTT	p.Phe508del	F508del	c.3528delC	p.Lys1	3659delC 177SerfsX15	x	x	x
CF0477	c.1521_ 1523delCTT	p.Phe508del	F508del	c.3528delC	p.Lys1	3659delC 177SerfsX15	x	x	x

CF code	cDNA name allele 1	protein name allele 1	Legacy name allele 1	cDNA name allele 1	protein name allele 1	Legacy name allele 1	donors included for primary screen (n=76)	donors included for roflumilast screen (n=107)	donors included for VX-770 and VX- 770/VX-809 screen (n=251, including F508del/F508del organoid cultures)
CF0431	c.1521 _1523delCTT	p.Phe508del	F508del	c.3528delC	p.Lys1 177SerfsX15	3659delC	x	x	
CF0270	c.1521 _1523delCTT	p.Phe508del	F508del	c.2052delA	p.Lys684As nfsTer38	2184delA	x	x	x
CF0820	c.1521 _1523delCTT	p.Phe508del	F508del	c.2052delA	p.Lys68 4AsnfsX38	2184delA	x	x	
CF0181	c.1585_1G>A	no protein name	1717_1G>A	c.2051_ 2052delAAinsG	p.Lys6 84SerfsX38	2183AA>G	x	x	x
CF0049	c.1521 _1523delCTT	p.Phe508del	F508del	c.2051_ 2052delAAinsG	p.Lys6 84SerfsX38	2183AA>G	x	x	x
CF0335	c.152	p.Phe508del	F508del	c.948delT	p.Phe31 6LeufsX12	1078delT	x	x	x
CF0593	c.152 _1_1523delCTT	p.Phe508del	F508del	c.948delT	p.Phe31 6LeufsX12	1078delT	x	x	
CF0015	c.152 _1_1523delCTT	p.Phe508del	F508del	c.1521_ 1523delCTT	p.Phe508del F508del		x	x	
CF0016	c.1521 _1523delCTT	p.Phe508del	F508del	c.1521_ 1523delCTT	p.Phe508del F508del		x	x	
CF0018	c.1521 _1523delCTT	p.Phe508del	F508del	c.1521_1 523delCTT	p.Phe508del F508del		x	x	
CF0020	c.152 _1_1523delCTT	p.Phe508del	F508del	c.1521_ 1523delCTT	p.Phe508del F508del		x	x	
CF0022	c.1521_1 523delCTT	p.Phe508del	F508del	c.152 _1523delCTT	p.Phe508del F508del		x	x	

CF code	cDNA name allele 1	protein name allele 1	Legacy name allele 1	cDNA name allele 1	protein name allele 1	Legacy name allele 1	donors included for primary screen (n=76)	donors included for roflumilast screen (n=107)	donors included for VX-770 and VX- 770/VX-809 screen (n=251, including F508del/F508del organoid cultures)
CF0023	c.1521_1523delCTT	p.Phe508del	F508del	c.1521_1523delCTT	p.Phe508del	F508del	x	x	x
CF0045	c.1521_1523delCTT	p.Phe508del	F508del	c.1521_1523delCTT	p.Phe508del	F508del	x	x	x
CF0059	c.1521_1523delCTT	p.Phe508del	F508del	c.1521_1523delCTT	p.Phe508del	F508del	x	x	x
CF0062	c.1521_1523delCTT	p.Phe508del	F508del	c.1521_1523delCTT	p.Phe508del	F508del	x	x	x
CF0070	c.1521_1523delCTT	p.Phe508del	F508del	c.1521_1523delCTT	p.Phe508del	F508del	x	x	x
CF0071	c.1521_1523delCTT	p.Phe508del	F508del	c.1521_1523delCTT	p.Phe508del	F508del	x	x	x
CF0080	c.1521_1523delCTT	p.Phe508del	F508del	c.1521_1523delCTT	p.Phe508del	F508del	x	x	x
CF0083	c.1521_1523delCTT	p.Phe508del	F508del	c.1521_1523delCTT	p.Phe508del	F508del	x	x	x
CF0087	c.1521_1523delCTT	p.Phe508del	F508del	c.1521_1523delCTT	p.Phe508del	F508del	x	x	x
CF0123	c.1521_1523delCTT	p.Phe508del	F508del	c.1521_1523delCTT	p.Phe508del	F508del	x	x	x
CF0130	c.1521_1523delCTT	p.Phe508del	F508del	c.1521_1523delCTT	p.Phe508del	F508del	x	x	x
CF0205	c.1521_1523delCTT	p.Phe508del	F508del	c.1521_1523delCTT	p.Phe508del	F508del	x	x	x

CF code	cDNA name allele 1	protein name allele 1	Legacy name allele 1	cDNA name allele 1	protein name allele 1	Legacy name allele 1	donors included for primary screen (n=76)	donors included for roflumilast screen (n=107)	donors included for VX-770 and VX- 770/VX-809 screen (n=251, including F508del/F508del organoid cultures)
CF0214	c.1521_1523delCTT	p.Phe508del	F508del	c.1521_1523delCTT	p.Phe508del	F508del	x	x	x
CF0232	c.1521_1523delCTT	p.Phe508del	F508del	c.1521_1523delCTT	p.Phe508del	F508del	x	x	x
CF0247	c.1521_1523delCTT	p.Phe508del	F508del	c.1521_1523delCTT	p.Phe508del	F508del	x	x	x
CF0732	c.1521_1523delCTT	p.Phe508del	F508del	c.1521_1523delCTT	p.Phe508del	F508del	x	x	x
CF0063	c.350G>A ;1210-121[T]	p.Arg117 His;7T	R117H-TT	c.1725del	p.Phe575 LeufsX4	1857delT	x	x	x
CF0823	c.1624G>T	p.Gly542X	G542X	c.2963C>G	p.Pro988Arg	P988R	x	x	x
CF0733	c.617T>G	p.Leu206Trp	L206W	c.3705T>G	p.Ser1235R 35Arg	S1235R	x	x	x
CF0216	c.1585-1G>A	no protein name	1717-1G>A	c.3752G>A	p.Ser125 1Asn	S1251N	x	x	x
CF0053	c.1521_1523delCTT	p.Phe508del	F508del	c.3752G>A	p.Ser125 1Asn	S1251N	x	x	x
CF0061	c.1521_1523delCTT	p.Phe508del	F508del	c.3752G>A	p.Ser1251A sn	S1251N	x	x	x
CF0067	c.1521_1523delCTT	p.Phe508del	F508del	c.3752G>A	p.Ser1251N 51Asn	S1251N	x	x	x
CF0099	c.1521_1523delCTT	p.Phe508del	F508del	c.3752G>A	p.Ser125 1Asn	S1251N	x	x	x
CF0106	c.1521_1523delCTT	p.Phe508del	F508del	c.3752G>A	p.Ser1251N 51Asn	S1251N	x	x	x

CF code	cDNA name allele 1	protein name allele 1	Legacy name allele 1	cDNA name allele 1	protein name allele 1	Legacy name allele 1	donors included for primary screen (n=76)	donors included for roflumilast screen (n=107)	donors included for VX-770 and VX- 770/VX-809 screen (n=251, including F508del/F508del organoid cultures)
CF0109	c.1521_1 523delCTT	p.Phe508del	F508del	c.3752G>A	p.Ser1251N 51Asn	S1251N		x	
CF0112	c.1521_1 523delCTT	p.Phe508del	F508del	c.3752G>A	p.Ser1251N Asn	S1251N		x	
CF0114	c.1521_1 523delCTT	p.Phe508del	F508del	c.3752G>A	p.Ser1251N 51Asn	S1251N		x	
CF0124	c.1521_1 523delCTT	p.Phe508del	F508del	c.3752G>A	p.Ser1251N Asn	S1251N		x	
CF0126	c.1521_1 523delCTT	p.Phe508del	F508del	c.3752G>A	p.Ser1251N Asn	S1251N		x	
CF0141	c.1521_152 3delCTT	p.Phe508del	F508del	c.3752G>A	p.Ser125 1Asn	S1251N		x	
CF0154	c.1521_152 3delCTT	p.Phe508del	F508del	c.3752G>A	p.Ser1251N Asn	S1251N		x	
CF0167	c.1521_15 23delCTT	p.Phe508del	F508del	c.3752G>A	p.Ser1251N Asn	S1251N		x	
CF0190	c.1521_1523 delCTT	p.Phe508del	F508del	c.3752G>A	p.Ser1251N Asn	S1251N		x	
CF0442	c.1521_152 3delCTT	p.Phe508del	F508del	c.3889dupT	p.Ser1297P hefsTer5	4016instT		x	
CF0334	c.3197G>A	p.Arg1066His	R1066H	c.54_5940_273+ 10250del121kb	p.Ser18Arg fsX16	CFTRdel2,3		x	
CF0386	c.1624G>T	p.Gly542X	G542X	c.54_5940_273+ +10250del121kb	p.Ser18Arg fsX16	CFTRdel2,3	x	x	

CF code	cDNA name allele 1	protein name allele 1	Legacy name allele 1	cDNA name allele 1	protein name allele 1	Legacy name allele 1	donors included for primary screen (n=76)	donors included for roflumilast screen (n=107)	donors included for VX-770 and VX- 770/VX-809 screen (n=251, including F508del/F508del organoid cultures)
CF0399	c.1521_152 3delCTT	p.Phe508del	F508del	c.54-5940_2 73+10250de 121kb	p.Ser18Arg fsX16	CFTRdel2,3	x	x	x
CF0338	c.1521_152 3delCTT	p.Phe508del	F508del	c.54-5940_27 3+10250de 121kb	p.Ser18Arg fsX16	CFTRdel2,3	x	x	x
CF0057	c.1521_15 23delCTT	p.Phe508del	F508del	c.54-5940_273 +10250del21kb	p.Ser18Arg fsX16	CFTRdel2,3	x	x	x
CF0523	c.1521_1523 delCTT	p.Phe508del	F508del	c.53G>T	p.Ser18Ile	S18I	x	x	x
CF0326	c.1521_152 3delCTT	p.Phe508del	F508del	c.53G>T	p.Ser18Ile	S18I	x	x	x
CF0623	c.1521_1 523delCTT	p.Phe508del	F508del	c.53G>T	p.Ser18Ile	S18I	x	x	x
CF0341	c.1521_15 23delCTT	p.Phe508del	F508del	c.1466G>A	p.Ser489X	S489X	x	x	x
CF0667	c.1521_152 3delCTT	p.Phe508del	F508del	c.1766G>A	p.Ser58 9Asn	S589N	x	x	x
CF0226	c.1521_15 23delCTT	p.Phe508del	F508del	c.2834C>T	p.Ser94 5Leu	S945L	x	x	x
CF0705	c.1521_ 1523delCTT	p.Phe508del	F508del	c.4186A>C	p.Thr13 96Pro	T1396P	x	x	x
CF0297	c.1521_1 523delCTT	p.Phe508del	F508del	c.1162_-11 68del/ACGACTA GlnfsX3	p.Thr388 GlnfsX3	1294del7	x	x	x

CF code	cDNA name allele 1	protein name allele 1	Legacy name allele 1	cDNA name allele 1	protein name allele 1	Legacy name allele 1	donors included for primary screen (n=76)	donors included for roflumilast screen (n=107)	donors included for VX-770 and VX- 770/VX-809 screen (n=251, including F508del/F508del organoid cultures)
CF0515	c.1521_1 523delCTT	p.Phe508del	F508del	c.3846G>A	p.Trp1282X	W1282X	x	x	x
CF0496	c.1521_ 1523delCTT	p.Phe508del	F508del	c.3846G>A	p.Trp1282X	W1282X	x	x	x
CF0069	c.1521_1 523delCTT	p.Phe508del	F508del	c.3846G>A	p.Trp1282X	W1282X	x	x	x
CF0550	c.1521_1 523delCTT	p.Phe508del	F508del	c.3846G>A	p.Trp1282X	W1282X	x	x	x
CF0428	c.3846G>A	p.Trp1282X	W1282X	c.3846G>A	p.Trp1282X	W1282X	x	x	x
CF0206	c.1521_ 1523delCTT	p.Phe508del	F508del	c.3846G>A	p.Trp1282X	W1282X	x	x	x
CF0489	c.1624G>T	p.Gly542X	G542X	c.2036G>A	p.Trp679X	W679X	x	x	x
CF0175	c.1521_ 1523delCTT	p.Phe508del	F508del	c.233_234insT	p.Trp79L eufsX32	365_366 inst(W79S)	x	x	x
CF0278	c.1521_ 1523delCTT	p.Phe508del	F508del	c.2537G>A	p.Trp846X	W846X	x	x	x
CF0250	c.1521_ 1523delCTT	p.Phe508del	F508del	c.3276C>A or c.3276C>G	p.Tyr10 92Ter	Y1092X	x	x	x
CF0315	c.1521_ 1523delCTT	p.Phe508del	F508del	c.3276C>A or c.3276C>G	p.Tyr1092 Ter	Y1092X	x	x	x
CF0314	c.1521_1 523delCTT	p.Phe508del	F508del	c.3276C>A or c.3276C>G	p.Tyr1092 Ter	Y1092X	x	x	x
CF0394	c.1521_ 1523delCTT	p.Phe508del	F508del	c.3276C>A or c.3276C>G	p.Tyr109 2Ter	Y1092X	x	x	x

CF code	cDNA name allele 1	protein name allele 1	Legacy name allele 1	cDNA name allele 1	protein name allele 1	Legacy name allele 1	donors included for primary screen (n=76)	donors included for roflumilast screen (n=107)	donors included for VX-770 and VX- 770/VX-809 screen (n=251, including F508del/F508del organoid cultures)
CF0033	c.1521_1 523delCTT	p.Phe508del	F508del	c.3276C>A or c.3276C>G	p.Tyr1092X	Y1092X	x	x	x
CF0340	c.1521_1 523delCTT	p.Phe508del	F508del	c.325T>G	p.Tyr109Asp	Y109D	x	x	x
CF0641	c.254G>A	p.Gly85Glu	G85E	c.1545_ 1546delTA	p.Tyr515X	1677delTA	x	x	x
CF0373	c.1521_1 523delCTT	p.Phe508del	F508del	c.2547C>A	p.Tyr849X	Y849X	x	x	x
CF0520	c.1521_15 23delCTT	p.Phe508del	F508del	c.2547C>A	p.Tyr849X	Y849X	x	x	x
CF0346	c.1521_ 1523delCTT	p.Phe508del	F508del	c.1681_1 682insC	p.Val56	1813insC	x	x	x
CF0583	c.1521_1 523delCTT	p.Phe508del	F508del	c.1681_1 682insC	p.Val56	1813insC	x	x	x
CF0305	c.2657+5G>A	no protein name	2789+5G>A	UNK	UNK	UNK	UNK	x	x
CF0470	c.1364C>A	p.Ala455Glu	A455E	UNK	UNK	UNK	UNK	x	x
CF0357	c.3484C>T	p.Arg1162X	R1162X	UNK	UNK	UNK	UNK	x	x
CF0284	c.350G>A ,1210-12[T]	p.Arg117H is:7T	R117H-7T	UNK	UNK	UNK	UNK	x	x
CF0187	c.1521_1 523delCTT	p.Phe508del	F508del	UNK	UNK	UNK	UNK	x	x
CF0366	c.1521_1 523delCTT	p.Phe508del	F508del	UNK	UNK	UNK	UNK	x	x

CF code	cDNA name allele 1	protein name allele 1	Legacy name allele 1	cDNA name allele 1	protein name allele 1	Legacy name allele 1	donors included for primary screen (n=76)	donors included for roflumilast screen (n=107)	donors included for VX-770 and VX- 770/VX-809 screen (n=251, including F508del/F508del organoid cultures)
CF0377	c.1521_1 523delCTT	p.Phe508del	F508del	UNK	UNK	UNK			x
CF0468	c.1521_1 523delCTT	p.Phe508del	F508del	UNK	UNK	UNK			x
CF0333	UNK	UNK	UNK	UNK	UNK	UNK			x

Supplementary table 2: list of PDIOs and genotypes included in this study. On the right is specified for which screen each PDIO is used.

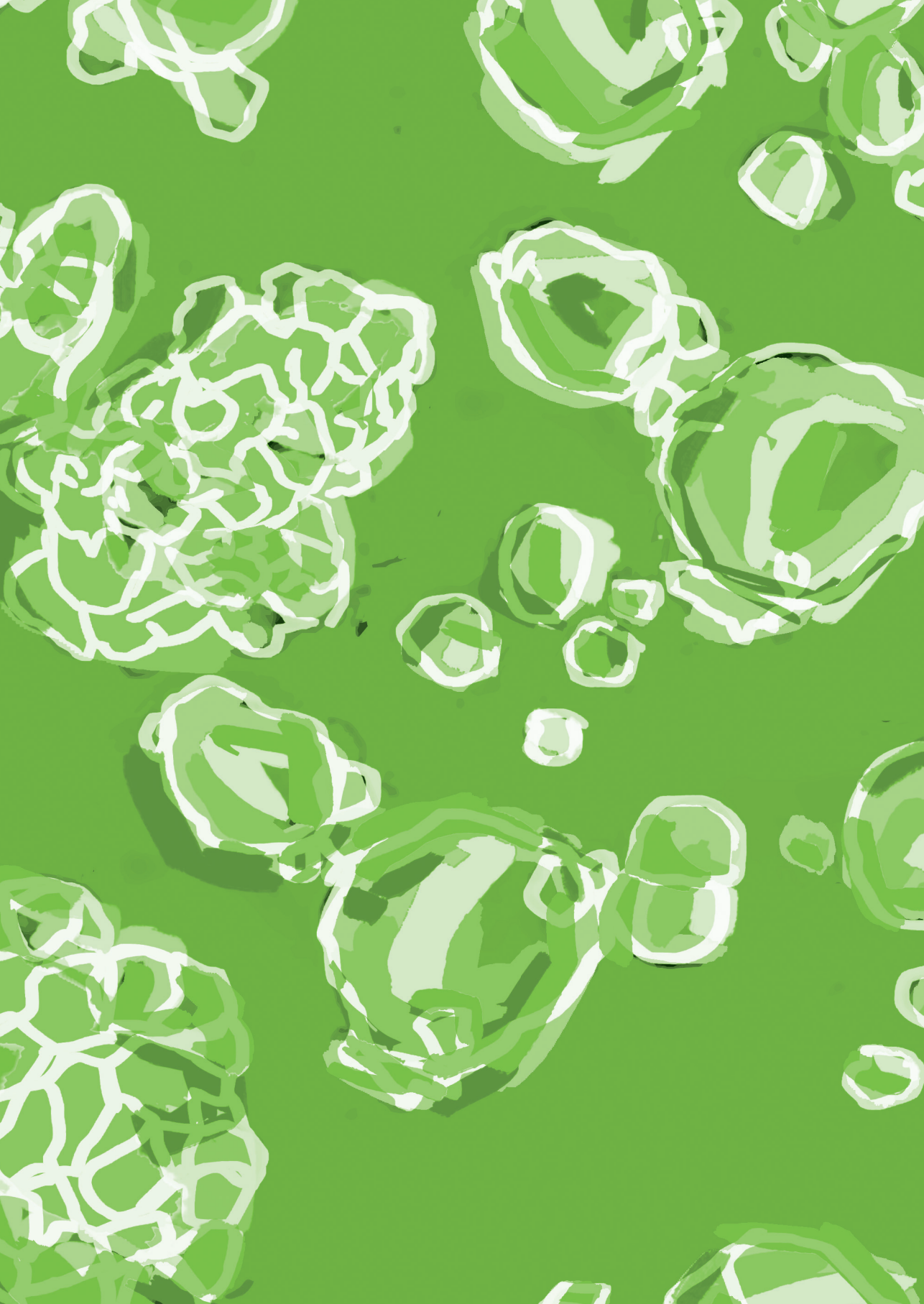
CHAPTER 4

Compound number corresponding to numbers in figure 3C	compound 1	compound 2	number of organoid cultures above threshold of AUC>3SD+mean of 8 negative control wells
NA	control - orkambi	NA	50
NA	control - VX770	NA	28
NA	control - VX809	NA	26
2	Ivacaftror (VX-770)	Doxazosin Mesylate	21
12	Roflumilast	Phenytoin sodium	20
24	Afatinib (BIBW2992) Dimaleate	Taurine	20
8	Atracurium Besylate	Chlormezanone	19
19	Benzethonium Chloride	Mupirocin	19
16	Ibrutinib (PCI-32765)	Sulfamerazine	18
32	Poziotinib (HM781-36B)	Pamidronate Disodium	18
10	LY2157299	Ceftiofur HCl	17
31	Voxalisib (XL765, SAR245409)	L-Glutamine	17
17	Azelnidipine	Probenecid	16
4	Erlotinib HCl (OSI-744)	Tamoxifen	15
13	NA	Phenytoin	15
33	Erlotinib	Procarbazine HCl	15
3	Barasertib (AZD1152-HQPA)	Edaravone	14
15	Trametinib (GSK1120212)	Biotin (Vitamin B7)	14
11	S- (+)-Ropivacaine	Naphazoline HCl	13
14	Dacomitinib (PF299804, PF299)	Methylthiouracil	13
18	BYL719	Ampicillin sodium	13
27	Uprosertib (GSK2141795)	Biapenem	13
34	Hexamethonium Bromide	Minocycline HCl	13
1	Afatinib (BIBW2992)	Raloxifene HCl	12
9	Betaxolol hydrochloride (Betoptic)	Sulindac	12
23	LEE011	Heparin sodium	12
26	AZD9291	Pemetrexed	12
20	Benzydamine HCl	Anisotropine Methylbromide	11
28	Lomitapide	Palbociclib (PD0332991) Isethionate	11

Pre-clinical efficacy testing of FDA-approved drugs for non-homozygous F508del-CFTR genotypes

Compound number corresponding to numbers in figure 3C	compound 1	compound 2	number of organoid cultures above threshold of AUC>3SD+mean of 8 negative control wells
30	Afuresertib (GSK2110183)	Dorzolamide HCl	11
5	OSI-906 (Linsitinib)	Budesonide	10
6	Cilomilast	Alprostadil	10
25	Ozanimod (RPC1063)	Tobramycin	10
7	Rolipram	Orlistat	9
21	Doxofylline	(R)-(+)-Atenolol	9
22	CO-1686 (AVL-301)	Palbociclib (PD-0332991) HCl	9
29	Pilaralisib (XL147)	Cytarabine	9

Supplementary table 3: ranking of the top 5% hit compounds in primary screen, identified as hit in most organoid cultures.





FUNCTIONAL RESTORATION OF CFTR NONSENSE MUTATIONS IN INTESTINAL ORGANOIDS

Published as Original Research Article

E. de Poel, S. Spelier, S.W.F. Suen, E. Kruisselbrink, S. Y. Graeber, M.A. Mall, E.J.M. Weersink,
M.M. van der Eerden, G.H. Koppelman, C.K. van der Ent and J.M. Beekman

Journal of Cystic Fibrosis 21: S1569-S1993 (2021)

ABSTRACT

Background: Pharmacotherapies for people with cystic fibrosis (pwCF) who have premature termination codons (PTCs) in the cystic fibrosis transmembrane conductance regulator (CFTR) gene are under development. Thus far, clinical studies focused on compounds that induce translational readthrough (RT) at the mRNA PTC location. Recent studies using primary airway cells showed that PTC functional restoration can be achieved through combining compounds with multiple mode-of-actions. Here, we assessed induction of CFTR function in PTC-containing intestinal organoids using compounds targeting RT, non-sense mRNA mediated decay (NMD) and CFTR protein modulation.

Methods: Rescue of PTC CFTR protein was assessed by the forskolin-induced swelling of 12 intestinal organoid cultures carrying distinct PTC mutations. Effects of compounds on mRNA CFTR level was assessed by RT-qPCRs.

Results: Whilst response varied between donors, significant rescue of CFTR function was achieved for most donors with the quintuple combination of a commercially available pharmacological equivalent of the RT compound (ELX-02-disulfate or ELX-02ds), NMD inhibitor SMG1i, correctors VX-445 and VX-661 and potentiator VX-770. The quintuple combination of pharmacotherapies reached swelling quantities higher than the mean swelling of three VX-809/VX-770-rescued F508del/F508del organoid cultures, indicating level of rescue is of clinical relevance as VX-770/VX-809-mediated F508del/F508del rescue in organoids correlate with substantial improvement of clinical outcome.

Conclusions: Whilst variation in efficacy was observed between genotypes as well as within genotypes, the data suggests that strong pharmacological rescue of PTC requires a combination of drugs that target RT, NMD and protein function.

TAKE HOME MESSAGES

- Pharmacological repair of CFTR function beyond F508del/F508del-VX809/VX770 in intestinal organoids with homozygous PTC mutations
- The read-through agent ELXds-02, the NMD-inhibitor SMG1i and the CFTR modulators therapy VX-661/VX-445/VX-770 were required for maximal efficacy.
- W1282X-CFTR function is partially rescued with the NMD-inhibitor SMG1i combined with the CFTR-modulators VX-661/VX-445/VX770.

INTRODUCTION

Cystic fibrosis (CF) is a monogenic, autosomal-recessive disease caused by mutations in the CFTR gene¹. Highly efficacious pharmacotherapy of the most prevalent F508del mutation shifts the unmet clinical need towards approximately 15% of people with CF (pwCF) who carry non- or low-responder CFTR mutations. The spectrum of mutations that are poorly responsive to clinically approved pharmacotherapies include the class I mutations that do not lead to full length protein (e.g. by non-sense mutations, frameshifts, consensus splice mutations, or larger rearrangements).

Approximately 10% of the worldwide CF population carry mutations that result in premature termination codons (PTC) resulting in production of truncated CFTR protein. Early work demonstrates that aminoglycoside antibiotics including gentamicin and G418 enable rescue of CFTR PTC in cell lines². These compounds reduce the fidelity of translation by affecting the pairing of cognate and near-cognate tRNAs with the mRNA, resulting in incorporation of non-cognate amino acids at the PTC site. This readthrough (RT) process facilitates continuation of translation, albeit at low efficacy². Subsequent efforts identified the PTC124 (Ataluren) as selective inducer of PTC-readthrough³. However, efficacy in many preclinical models was not reproduced^{4,5} and clinical trials with Ataluren failed to reach their primary endpoints⁶. A recently chemically-engineered aminoglycosides derivative termed ELX-02 (NB124; Eloxx Pharmaceuticals) is currently in early clinical development⁷ and showed to be effective as single treatment in intestinal organoids⁸.

Whilst readthrough agents hold potential for increasing full length protein production, their efficacy is inhibited by a control system called nonsense-mediated mRNA decay (NMD) that leads to degradation of PTC-containing mRNA molecules^{9,10}. By pharmacological inhibition of critical effectors of NMD such as SMG1 kinase (through SMG1i) or SMG7 (through NMDI-14), increased efficacy of readthrough agents has been observed in various preclinical models and laboratories¹⁰⁻¹⁴. A potential alternative to NMD-inhibition may be a recently identified CFTR amplifier (PTI-428 or nesolicafitor¹⁵) that increases CFTR mRNA quantity independent of PTC-mutations.

The reduced translational fidelity by readthrough agents induces a pool of proteins with different amino acids at the PTC site¹⁶, underlining the potential of combining CFTR protein modulators with readthrough agents to further enhance CFTR restoration^{8,10,17}. CFTR (co-)potentiators such as VX-770, APS-11¹⁸ and to some extend VX-445¹⁹, may increase the channel open probability of the readthrough-induced CFTR protein pool, whereas CFTR correctors may enhance trafficking of readthrough-CFTR protein towards the apical surface. Their combination will likely be most effective in restoring CFTR function upon readthrough.

To study the impact and repair of PTCs, we use intestinal organoids and the forskolin-induced swelling (FIS) assay as CFTR-dependent phenotypic readout that allows to quantitate individual CFTR function in response to CFTR function modulators^{20,21}. CFTR function measurements in this assay model correlate with clinical disease indicators^{22,23} and CFTR modulator responses^{21,24}. Our previous work on readthrough demonstrated no efficacy

CHAPTER 5

of PTC124 in intestinal organoids⁴, consistent with clinical trial data by others⁶, supporting the use of this assay for preclinical drug development. The purpose of this study was to investigate the capacity of commercially-available compounds with different modes-of-action to increase ELX-02ds-induced CFTR function rescue in organoids with multiple PTCs.

MATERIALS AND METHODS

Collection of primary epithelial cells of CF patients (pwCF)

Informed consent for tissue collection, generation, storage, and use of the organoids was obtained from all participating patients. Biobanked intestinal organoids are stored and catalogued (<https://huborganoids.nl/>) at the foundation Hubrecht Organoid Technology (<http://hub4organoids.eu>). Collection of patient tissue and data was performed following the guidelines of the European Network of Research Ethics Committees (EUREC) following European, national, and local law, and the study was approved by the local the medical ethical committee at UMC Utrecht biobank (TcBio document 14-008), at Charite, Berlin and at The Hebrew University, Jerusalem.

Human intestinal organoid culture

Crypts were isolated from biopsies of subjects with cystic fibrosis as previously described²¹. Organoids were incubated in a humidified chamber with 5% CO₂ at 37°C. Medium was refreshed every 2–3 days, and organoids were passaged 1:4 every 7–8 days. Prior to forskolin induced swelling assay measurements, organoids were grown at least 3 weeks after crypt isolation or thawing.

Functional assessment of CFTR function

Functional assessment of CFTR function was assessed with the forskolin-induced swelling assay, performed as described by Vonk et al²⁵. But instead of using recombinant Human R-Spondin 3 Protein, we used R-Spondin condition medium²¹. Details about the compound concentrations and incubation times can be found in **table 1**. Organoid swelling was monitored during 60–180 minutes using a Zeiss LSM 710 confocal microscope. Total organoid surface area per well was quantified based on calcein green staining as described by Vonk et al²⁵.

Compound	hours added prior to FIS assay or organoid collection for PCR	Final concentration (μ M)	Manufacturer	Mode of action
ELX-02 disulfate	48	80	MedChemExpress	Readthrough-agent
SMG1i	24	0.3	Cystic fibrosis foundation	NMD-inhibitor
PTI-428	24	0-20	MedChemExpress	CFTR amplifier
VX-770	0, added together with forskolin	3	selleck biochemicals	CFTR potentiator
VX-661, VX-445	24	3	selleck biochemicals	CFTR corrector
ASP-11	0, added together with forskolin	0-20	Kindly provided by UCSF	CFTR co-potentiator
NMDI-14	24 and 48	0-20	MedChemExpress	NMD-inhibitor
Vidaza	24	0-20	SelleckChem	NMD-inhibitor

Table 1: Final assay conditions of pharmacotherapies included in this manuscript.

5
5

Quantitative real time PCR

Organoids were cultured in tissue culture plates, either in regular culture medium or culture medium supplemented with compounds described in **table 1**. Organoids were collected from tissue culture plates, washed once with advanced DMEM/F12 and RNA was extracted using RNeasy Mini Kit (Qiagen, catalog no. 74104), following manufacturers protocol. cDNA was synthesized of 100 ng RNA with IscriptTM according to the supplied protocol (Biorad, catalog no. 1708891). qPCR reactions were executed in 96-well format with IQ SYBR green (Bio-Rad, catalog no. 1708880) and following primer sets: CFTR reverse: CCCAGGTAAGGGATGTATTGTG, CFTR forward: CAACATCTAGTGAGCAGTCAGG ;YHWAZ reverse: AAGGGACTTCCTGTAACAATGCA, YHWAZ forward: CTGGAACGGTGAAGGTGACA. Using a Biorad CFX PCR device, samples were incubated for 3 minutes at 95°C and for 39 cycles at: 10 seconds at 95°C, 30 seconds at 62°C. Relative expression levels of the treated PTC organoids were analyzed by means of $\Delta\Delta Ct$ calculations, for which YWHAZ served as housekeeping gene and mean expression level of two replicate experiments of 5 healthy control organoid samples was used as calibrator. YWHAZ expression was not affected by the different compound therapies. Melt peaks were analyzed to confirm specific primer binding.

Statistics

Data are represented as mean \pm SD or SEM (specified in figure legends). One-way ANOVA's were performed to compare mean FIS or $\Delta\Delta Ct$ values upon treatment with pharmacotherapies with DMSO at group level with Dunnett T-test as post-hoc analysis. No statistical testing was performed between the different pharmacotherapies on individual donor level. P values < 0.05 were considered statistically significant. Data analysis was performed in SPSS.

RESULTS

Overview of compound mode-of-actions and patient samples used in this study

We selected a diverse set of compounds that are commercially available (**figure 1A**) to study their capacity to enhance functional restoration upon RT of CFTR. The incorporation of an amino acid at the place of the PTC results in a pool of full-length transcripts of which function could be enhanced with CFTR modulation therapy (VX-770, VX-661, VX-445 and ASP-11). The amplifier PTI-428, or the NMD inhibitors SMG1i, NMDi-14 and Vidaza should increase the level of mRNA transcript and thereby expand the pool of PTC mRNA prone for RT. Combining these small molecules acting on different steps along the CFTR biosynthesis pathway, channel trafficking and channel gating might collectively result in CFTR function restoration of PTCs in general, to clinically relevant levels.

Currently 10% of our biobank consists of PTC mutations in which most prevalent PTC mutations are represented (**figure 1B**); yet distribution is to some extent shifted towards rare PTC variants. Also, locations of PTC mutations described in this study are well distributed across the CFTR gene (**figure 1C**) which allows us to investigate whether the location of the PTC in the CFTR gene influences drug response.

Functional restoration of CFTR nonsense mutations in intestinal organoids

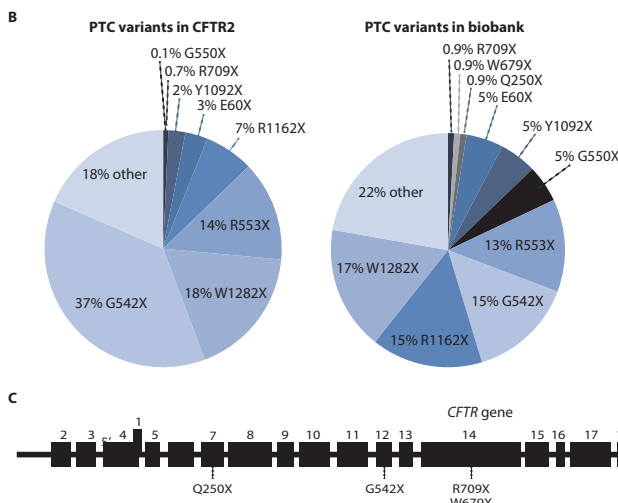
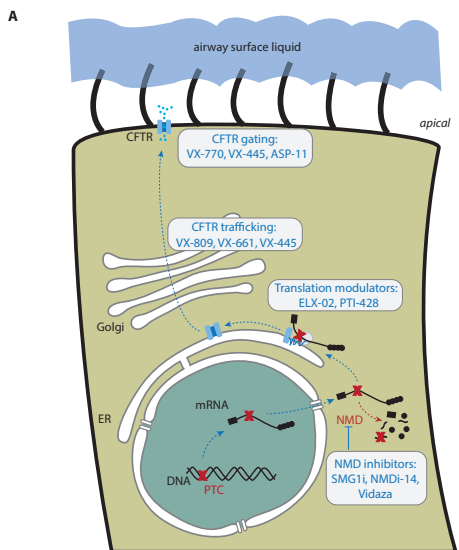


Figure 1: Schematic presentation of impact of pharmacotherapies and demographics of CFTR mutation types and PTC allele frequencies.

(A) Schematic presentation of intracellular tracking of CFTR and impact of pharmacotherapies. (B) Relative allele frequencies of specific PTC mutations in our biobank (right) compared to worldwide incidence (left). (C) Location in the *CFTR* gene of the PTC mutations included in this study.

Rescue of W1282X/W1282X function by RT, NMD-inhibition and CFTR modulation.

First, we assessed the dose-dependency and incubation times required for optimal rescue of CFTR function by RT agent ELX-02ds in 2-hours FIS measurements in a W1282X/W1282X organoid culture. ELX-02ds increased FIS dose-dependently and to a higher extend after 48h ELX-02ds pre-incubation when compared to 24h (**figure 2A-B**). We selected 80 μ M of ELX-02ds and 48h pre-incubation as condition for combination studies. Based on the dose-response of SMG1i on top of ELX-02ds and VX-661/VX-445/VX-770 (**figure 2C-D**) and reported toxicity concerns of SMG1i¹⁷, 0.3 μ M and 24h incubation were chosen for further studies. Concentrations of VX-661, VX-445 and VX-770 were set to 3 μ M based on previous work and dose-dependency was not studied in detail here. Pre-stimulation with 0.625 μ M NMDI-14 for 24 or 48h slightly increased swelling when combined with ELX-02ds (**supplementary figure 1**), but significantly less than the combination of SMG1i and ELX-02ds. NMDI-14 concentrations >2.5 μ M became toxic, shown by a decreased swelling response. We could not detect any impact of PTI-428, ASP-11 and Vidaza on rescuing W1282X/W1282X-CFTR, despite varying concentrations (0-20 μ M, 1:2 diluted) and compound backgrounds (ELX-02ds + SMG1i w/o VX-661/VX-445/VX-770) (**supplementary figure 1**). For these reasons, NMDI-14, PTI-428, ASP-11 and Vidaza were excluded from further experiments.

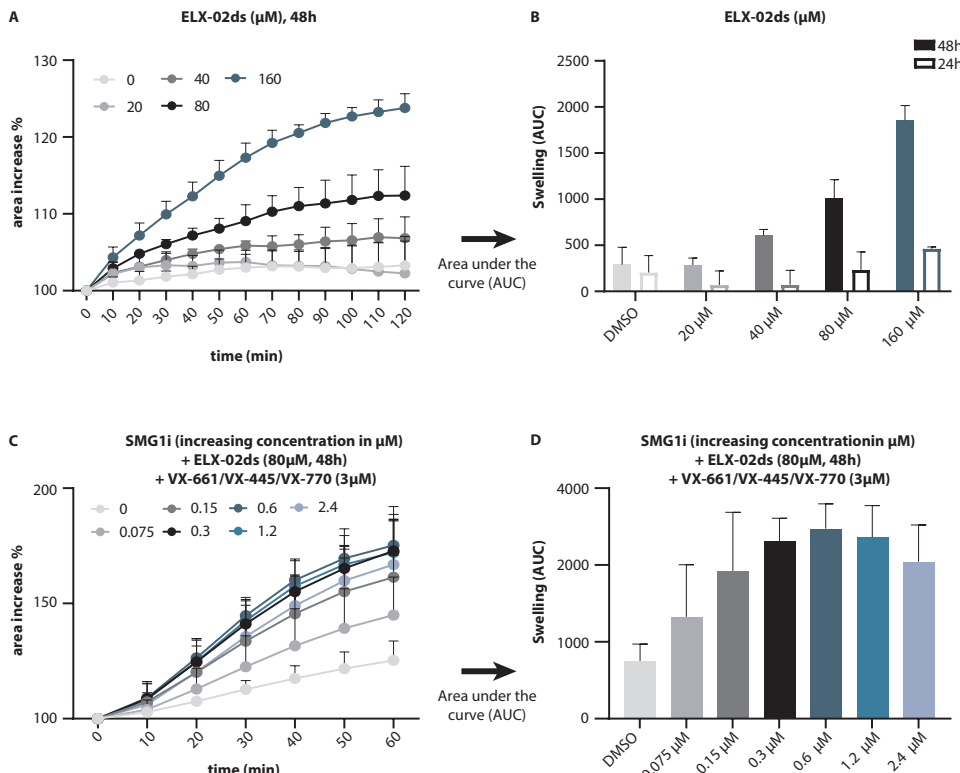


Figure 2: Dose-response assays on a W1282X/W1282X organoid culture to define optimal pharmacotherapy conditions.

(A) Area increase in time (in total for 120 min) of W1282X/W1282X organoids upon addition of increasing concentration of ELX-02ds for 24h or 48h prior to the FIS-assay. Organoid area increase was measured with the addition of 5 μ M forskolin. Datapoints represent mean+SD, n=3.

(B) FIS, measured as area under the curve of each condition shown in (A).

(C) Area increase in time (in total for 60 min) of W1282X/W1282X organoids upon addition of increasing concentration of SMG1i for 24h or 48h and ELX-02ds (80 μ M) for 48h + VX-661/VX-445 (3 μ M) for 24h prior to the FIS-assay. Organoid area increase was measured with the addition of 0.128 μ M forskolin + 3 μ M VX-770. Datapoints represent mean+SD, n=3.

(D) FIS, measured as area under the curve of each condition shown in (C).

PTC rescue with combinations of ELX-02ds, SMG1i and VX-661/VX-445/VX-770.

We next set out to study rescue of CFTR function by combined use of ELX-02ds, SMG1i and VX-661/VX-445/VX-770, and compared efficacy to VX809/VX770 or VX661/VX445/VX770 treatment of F508del/F508del organoids. Cells were stimulated with different fsk concentrations for 1h to define a fsk concentration that can quantitate PTC rescue in the dynamic range of the assay, and enable comparison with previous work. Fsk titrations demonstrated a dose-dependent relation with swelling (**figure 3A-B**). Maximal swelling was observed from 0.128 μ M fsk and higher, and fsk dose dependency and efficacy of EST in W1282X/W1282X organoids (n=3 donors) conditions was comparable to VX770/VX809 in F508del/F508del (n = 3 donors). We selected fsk 0.128 μ M for 1h for comparison of RT compound efficacies between the various organoid conditions.

We next assessed the CFTR restoring capacity of ELX-02ds, SMG1i and VX-661/VX-445/VX-770 as stand-alone compounds and combinations thereof in 8 organoid cultures homozygous for distinct PTC mutations (**figure 3C-F**) and 3 organoid cultures compound heterozygous for PTC mutations (**supplementary figure 2A**). Two organoid cultures homozygous for consensus splice mutations showed no response to compound treatment indicating PTC-dependent rescue (**supplementary figure 2B**). No single compound restored CFTR function to such extend it could be detected with 1h 0.128 μ M fsk stimulation. Swelling levels significantly increased when organoids were treated with ELX-02ds and either SMG1i (ES in **figure 3**) or VX-661/VX-445/VX-770 (ET in **figure 3**), nearly reaching AUC levels similar to VX-809/VX-770-rescued F508del/F508del organoids (**figure 3C-D**), yet the magnitude of swelling increase was donor dependent and within-genotype (W1282X/W1282X) variation was observed (**figure 3E-F**). As recent literature described that differences in mRNA sequence surrounding the PTC might influence RT, all four homozygous W1282X organoid cultures were sequenced. However, no SNPs were observed in the region 600 nucleotides before and 400 nucleotides after the PTC (data not shown). Whilst the combination SMG1i and VX-661/VX-445/VX-770 (ST in **supplementary figure 2C**) moderately rescued W1282X-CFTR, although again with within-genotype variation, functional rescue of the PTCs R1162X, G542X or W679X require the addition of the RT-agent, ELX-02ds (**supplementary figure 2C**). The most effective pharmacotherapy showed to consist of the combination of ELX-02, SMG1i and VX-661/VX-445/VX-770 (EST in **figure 3**) and resulted in tripling of the mean AUC

value compared to the dual compound therapies (**figure 3C-D**). Interestingly, in three of the W1282X/W1282X (**figure 3E**) and two homozygous PTC donors (**figure 3F**) rescue of CFTR function reached AUC levels that were in between reference AUC values of F508del/F508del organoids treated with VX-809/VX-770 (mean AUC 940 +/- 32, n=9) and VX-661/VX-445/VX-770 (mean AUC of 3327 +/- 383, n=9). As can be observed in **supplementary figure 2A**, level of swelling was halved in organoid cultures expressing one PTC mutation, yet still comparable to VX-809/VX-770-rescued F508del/F508del-CFTR. These data show that combining RT agents with NMD inhibitors and CFTR modulators represents a potential therapeutic option for treating PTC mutations.

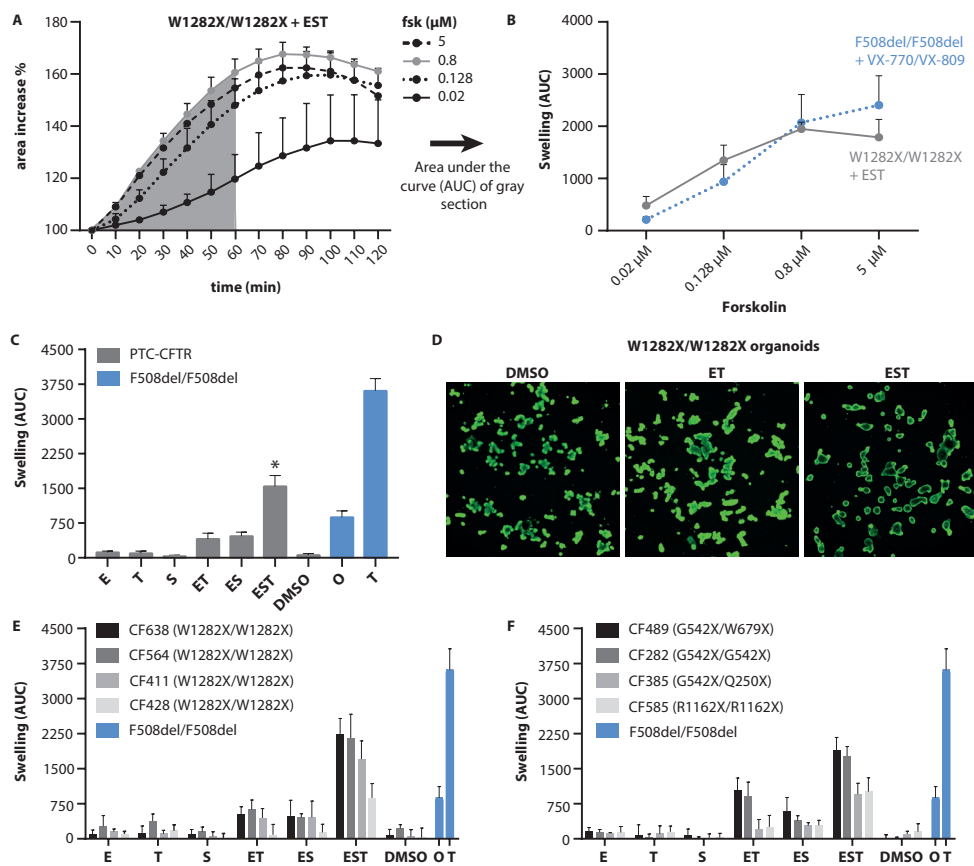


Figure 3. EIC of various homozygous PTC expressing organoid cultures upon treatment with different concentrations of forskolin (fsk) and other treatments (collectively estimated).

Figure 3: FIS of various homozygous PTC expressing organoid cultures upon treatment with pharmacotherapies that (collectively) stimulate read-through, inhibit NMD and/or modulate CFTR protein tracking or gating.

(A) Area increase in time (min) of W1282X/W1282X organoids upon addition of increasing concentration of fsk. Organoids were pre-stimulated with EST (bars represent mean+SD, n=3).

(B) Swelling (area under the curve of t=0 to t=60 minutes, gray area in **A**) of W1282XX/W1282X organoids pre-stimulated with EST (datapoints represent mean+SD, n=3) and mean swelling of three F508del/F508del organoid cultures pre-stimulated with VX-809 (3 μ M, 24h) + VX-770 (3 μ M, 0h) (datapoints represent mean+SD, n=9) upon stimulation with increasing concentration of fsk. To determine the therapeutic value of EST with 0.128 μ M fsk, the swelling levels were compared to the mean swelling levels of three organoid cultures expressing F508del/F508del-CFTR upon rescue with VX-770 (3 μ M, added with fsk) + VX-809 (3 μ M, 24h), datapoints represent mean+SD, n=9). Similar F508del/F508del data is shown in C-F and **supplementary figure 2**.

(C) Mean FIS of all homozygous PTC organoid cultures, measured for 1h in presence of 0.128 μ M fsk. Organoid cultures were pre-stimulated with E, S or T and all combinations thereof. Bars represent mean+SEM, n=8. *p-value<0.05, compared to DMSO.

(D) Microscopic images of W1282X/W1282X organoids after 60 minutes stimulation with 0.128 μ M fsk, untreated or pre-stimulated with ET or EST.

(E and F) FIS (1h, 0.128 μ M FSK) responses of four individual organoid cultures, carrying two copies of the W1282X mutation (**E**) or two PTC mutations other than W1282X (**F**) upon pharmacotherapy treatment.

Abbreviations: fsk = forskolin; E = ELX-02ds (80 μ M, 48h); S = SMG1i (0.3 μ M, 24h); T = VX-661 (3 μ M, 24h) + VX-445 (3 μ M, 24h) + VX-770 (3 μ M, added simultaneously with fsk); O = VX-809 (3 μ M, 24h) + VX-770 (3 μ M, added simultaneously with fsk).

CFTR mRNA rescue of panel of various PTC harboring organoid lines in response to combinations of ELX-02ds, SMG1i and VX-661/VX-445/VX-770.

Additionally, the expression of CFTR mRNA in response to all compounds by qRT-PCR was characterized. In general, the expression level of CFTR mRNA is lower in organoid cultures having two PTC mutations compared to WT organoids, as the expression levels of the different donors in the DMSO condition shown in **figure 4A and B** are being below 50% of WT expression (average of two replicate experiments of 5 WT/WT organoid cultures). Whilst not significant, ELX-02 shows a minor increase in CFTR mRNA. Yet, all conditions including SMG1i resulted in a significant increase in mRNA similar to or higher than 100% of WT expression in all organoid cultures. Moreover, the level of mRNA expression increase correlates with the level of CFTR function rescue by EST (R^2 of 0.74, **figure 4C**). This indicates that treatment with NMD-inhibitors is required for a high quantity of functional protein following RT, which can be further enhanced with CFTR modulation.

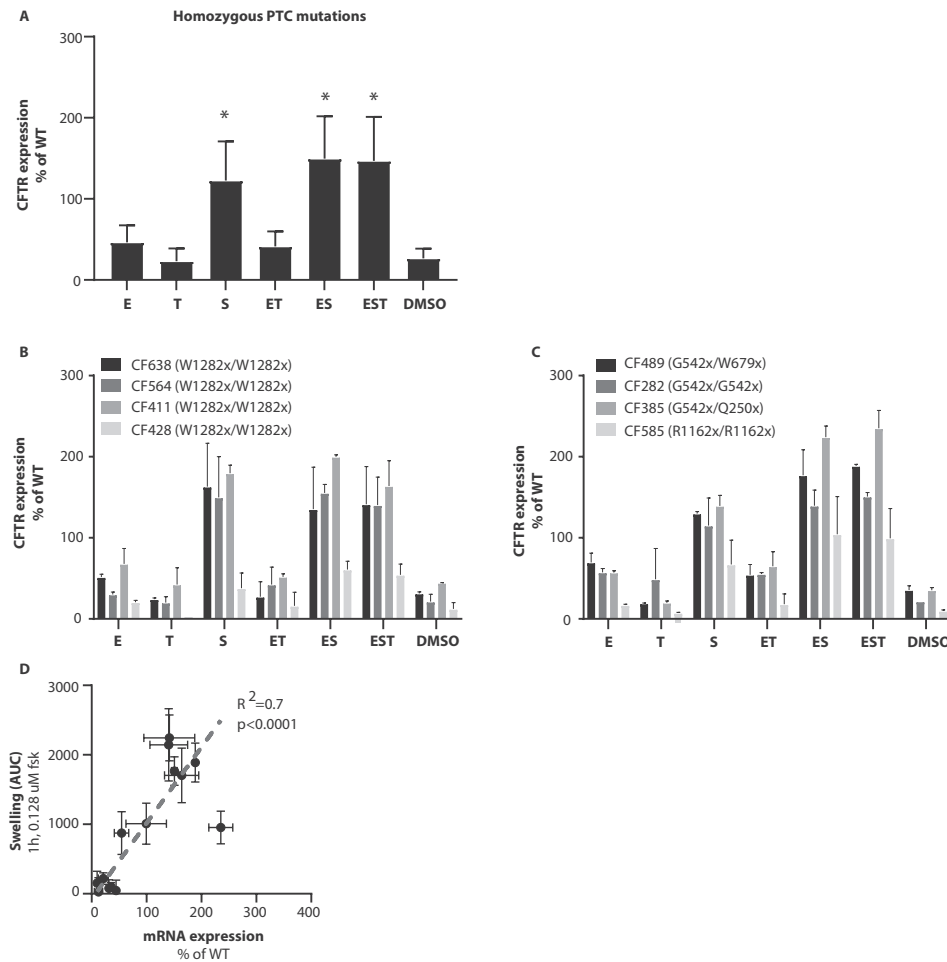


Figure 4: CFTR mRNA expression of organoid cultures homozygous for PTC mutations upon pharmacotherapy.

(A) mean mRNA expression level of CFTR, normalized to the reference genes YWHAZ and expressed in % of mean of 5 WT/WT organoid cultures (bars represent mean+SD, n=2). * $p < 0.05$, compared to DMSO.

(B and C) mRNA expression level of CFTR of individual organoid cultures. The organoid cultures and pre-treatments in A and B correspond to those in figure 3 E and F, respectively.

(D) Correlation between level of swelling (1h, 0.128 μM) and mRNA expression level of untreated (DMSO) or organoid cultures or prestimulated with EST.

Abbreviations: WT = wildtype; E = ELX-02ds (80 μM, 48h); S = SMG1i (0.3 μM, 24h); T = VX-661 (3 μM, 24h) + VX-445 (3 μM, 24h) + VX-770 (3 μM, added simultaneously with forskolin)

DISCUSSION

In this paper, we hypothesized that CFTR function of CF patient-derived organoids harboring PTC mutations, can be rescued by a combination of pharmacotherapies and investigated the contributions of PTC rescue by molecules that a) amplify CFTR transcription (PTI-428), b) enhance PTC-RT (ELX-02ds), c) inhibit NMD (SMG1i, NMDi-14 and Vidaza), d) stimulate correct CFTR protein trafficking (VX-661 and VX-445) and e) enhance gating activity of CFTR at the cell membrane (VX-770 and ASP-11). We found that a combination of ELX-02ds, SMG1i and VX-661/VX-445/VX-770 resulted in robust CFTR rescue, higher than observed with VX-809/VX-770-treated F508del/F508del organoids. We characterized compound efficacy for a panel of 12 organoid lines harboring various PTC mutations, including the most common W1282X and G542X alleles as well as less prevalent PTC alleles. We observed differences in efficacy between genotypes as well as differences within one genotype.

As the presence of a PTC mutation results in a truncated variant of the protein, efficacy of the RT-agent ELX-02ds was first characterized. In contrast to a recent study⁸, ELX-02ds as single agent did not result in AUC values that are comparable to VX-809/VX-770-treated F508del/F508del organoids. Moreover, CFTR mRNA was increased by ELX-02-mediated NMD-inhibition in the recent study, a mode of action we could not fully confirm with our qPCR data. This difference might be contributed to the commercially available ELX-02ds used in this study, versus the ELX-02 from Eloxx Pharmaceuticals itself. Despite this difference, the commercially available version has RT activity that can be strongly enhanced by NMD inhibition and clinically available CFTR protein modulators. Whilst RT is essential for restoring full-length CFTR, the pool of mRNA susceptible for RT is diminished by NMD. Multiple compounds that inhibit different components of the NMD machinery have been described, but especially SMG1 inhibition has yielded success in various preclinical models^{10,14}. We indeed found that SMG1 inhibition resulted in a concentration-dependent elevation of functional CFTR levels. A challenge concerning NMD inhibition however remains that NMD influences multiple cellular pathways. As a result, a high concentration of SMG1i has been associated with in vitro cellular toxicity¹⁷ and caution must be taken with using NMD-inhibitors as a therapeutic compound, which is likely to be the reason only a single NMD-inhibitor has reached the clinic at present-day. The NMD-inhibitor Vidaza (5-Azacytidine) has been approved for the treatment of myelodysplastic syndrome and myeloid leukemia²⁶⁻²⁸, however Vidaza therapy is associated with severe side-effects, and showed to be ineffective in our study, which was confirmed by others¹⁰. Compared to Vidaza or NMDi-14, SMG1i was the least toxic and effectively increased CFTR mRNA expression at a relatively low concentration. SMG1i is therefore an interesting target for further drug development, aiming to develop a safer, yet still effective NMD inhibitor. A strategy to develop more specific NMD inhibitors is to target a different effector protein involved in the NMD machinery. According to our results, targeting SMG7 with NMDi14 or MYC, an endogenous NMD-inhibitor, with Vidaza had no effect on CFTR function rescue. Nevertheless, many other effector proteins remain to be investigated and could potentially be targeted for more selective NMD inhibition.

Theoretically, RT and NMD together could result in normal amounts of full-length CFTR, yet we did not observe high rescue of CFTR function in our FIS assay with this dual pharmacotherapy. This can be contributed to the fact that amino acid incorporation upon RT varies per type of PTC and even per single transcript¹⁶ and may thus not fully recapitulate WT protein function or stability. Previous studies have shown that function of such W1282X variants can indeed be enhanced by combining RT agents with conventional CFTR correctors or potentiators¹⁶. In line with this study, swelling of PTC organoids upon treatment with ELX-02ds/SMG1i and VX-770/VX-661/VX-445 indeed reached AUC levels higher than that of VX-770/VX-809 treated F508del/F508del organoids. The optimal conditions for PTC restoration did not reach efficacies associated with VX-445/VX-661/VX-770 on F508del/F508del organoids. Whilst the results obtained with the ELX-02ds/SMG1i/ VX-770/VX-661/VX-445 combination are promising, pharmacokinetic and drug-drug interaction studies will have to further elucidate the feasibility of combining these 5 different pharmacotherapies *in vivo*. On this note, in this study the effect of VX-445/VX-661/VX-770 was only tested in combination. Future research should investigate whether this is indeed necessary, or whether the combination with ELX-02ds/SMG1i and a single CFTR modulator could result in sufficient functional CFTR rescue.

This report focusses on the use of intestinal organoids as preclinical test model for restoration of PTCs. Organoid FIS is completely CFTR dependent and the relation between *in vitro* swelling response and *in vivo* drug response and disease severity has been well characterized. Earlier work also found that G418 can induce CFTR function in PTC-containing organoids, but CFTR restoration by PTC-124 was not detected consistent with lack of efficacy in clinical trials with this drug^{4,6}. Biobanks of organoids have been established and such infrastructures enable not only large-scale preclinical testing in patient cells but also the recruitment of preclinical responders for clinical trials. Whereas the simple phenotypic swell readout represents one of the strengths of this model, it also represents a limitation as swelling is limited by organoid stretch that limits the dynamic range of the assay at high CFTR function. The data could be further strengthened by protein analysis to demonstrate that ELX-02ds and the various combinations induced full length mature CFTR protein, as recently showed by Crawford et al.⁸ in PTC-containing organoids rescued by ELX-02. Contradictory to this study however, Laselva et al did not observe an effect of G418 on CFTR protein level in human nasal cells (ref 10). Potentially low CFTR levels, below the detection limit of certain assays such as western blot, are sufficient to detect effects on a functional level. This is likely dependent on the exploited phenotypic assay, its sensitivity and the studied cell model. Evidently, comparison of results in different models is valuable. As recently shown by Laselva et al for example, inhibition of NMD by SMG1i and CFTR correction and potentiation by protein modulators resulted in functional rescue of W1282X in primary nasal cultures that was not enhanced with the addition of RT-agent G418. Whether this difference with the results of our study is a consequence of the use of a different model and cell type, the differences between G418 and ELX-02ds, G418 induced toxicity or even patient to patient variation remains an open question. Future research could be conducted to assess whether functional rescue of PTC's in nasal or bronchial epithelial cells is achievable with the compounds discussed in this study and whether its efficacy is comparable to the results achieved in intestinal organoids.

Overall, we observed CFTR function rescue in all organoid cultures, yet in between-genotype and within-genotype variation in the level of CFTR function rescue was also observed. RT efficacy has been described to be dependent on the identity of the PTC, from least to most susceptible: UAA<UAG<UGA, yet a donor carrying a UGA mutation on both alleles (R1162X/R1162X-CFTR), showed to be one of the lowest responding donors, indicating the between-genotype variation cannot only be explained by PTC-dependency of RT. While RT-efficacy is also moderated by the local and distant sequence surrounding the PTC^{29,30}, we did not find additional SNPs in our four W1282X/W1282X organoid cultures which could not explain the observed within-genotype variation. Nevertheless, even the low responding organoid cultures almost reached swelling levels comparable to F508del/F508del-CFTR rescued with VX-770/VX-809, indicating that independent of the PTC mutation, the level of CFTR function rescue has clinical potential.

In conclusion, this proof of concept study shows that truncated, defective CFTR protein harboring PTC mutations can be effectively repaired with a combination of pharmacotherapies. Whilst further (clinical) studies are necessary to translate these studies to the clinic, we provide a potential mechanism to resolve the unmet need for a therapeutic approach for people carrying PTC mutations.

ACKNOWLEDGEMENTS

This work was supported by grants of the Dutch Cystic Fibrosis Foundation (NCF), the Dutch Muco & Friends Foundation, the American organization Emily's Entourage and the German Federal Ministry for Education and Research (82DZL0098B1 to M.A.M.). S.Y.G is participant of the BIH-Charité Clinician Scientist Program funded by the Charité – Universitätsmedizin Berlin and the BIH. S.Y.G. is supported by a financial grant from the Christiane Herzog Stiftung, Stuttgart, Germany and the Mukoviszidose Institut gGmbH, Bonn, the research and development arm of the German Cystic Fibrosis Association Mukoviszidose e.V. Furthermore, we would like to thank the UCSF Medical Center for kindly providing ASP-11 and Michael Wilschanski and Prof. Batsheva Kerem from The Hebrew University Jerusalem for kindly providing intestinal organoids.

AUTHOR CONTRIBUTIONS

E.d.P. and S.S contributed to the design of the study, the acquisition, verification, analysis and interpretation of the data and have drafted the manuscript. S.W.F.S., E.K., K.B., S.Y.G., M.A.M., E.J.M.W., M.M.vd.E. and G.H.K. contributed to the acquisition of study data, provided resources and revised the manuscript. C.K.v.d.E and J.M.B. have made substantial contributions to the conception and design of the study, interpretation of data and revised the manuscript.

DECLARATION OF INTERESTS

J.M.B. and C.K.v.d.E. are inventors on patent(s) related to the FIS-assay and received financial royalties from 2017 onward. J.M.B report receiving research grant(s) and consultancy fees from various industries, including Vertex Pharmaceuticals, Proteostasis Therapeutics, Eloxx Pharmaceuticals, Teva Pharmaceutical Industries and Galapagos outside the submitted work. C.K.v.d.E report receiving research grant(s) grant(s) from Vertex Pharmaceuticals (money to institution) outside the submitted work. G.H.K. reports research grants from Vertex Pharmaceuticals, GSK, TEVA, Ubbo Emmius Foundation, European Union, Lung Foundation Netherlands (Money to institution), outside the submitted work. M.A.M. reports research grants and patient recruitment fees for clinical trials from Vertex, for which his institution Charité-Universitätsmedizine Berlin received payment; fees for consulting and advisory board participation from Antabio, Arrowhead, Boehringer Ingelheim, Enterprise Therapeutics, Kither Biotech, Sathera, Sterna Biologicals, and Vertex outside the submitted work. S.Y.G. reports fees for advisory board participation from Chiesi outside the submitted work. All other authors have nothing to disclose.

REFERENCES

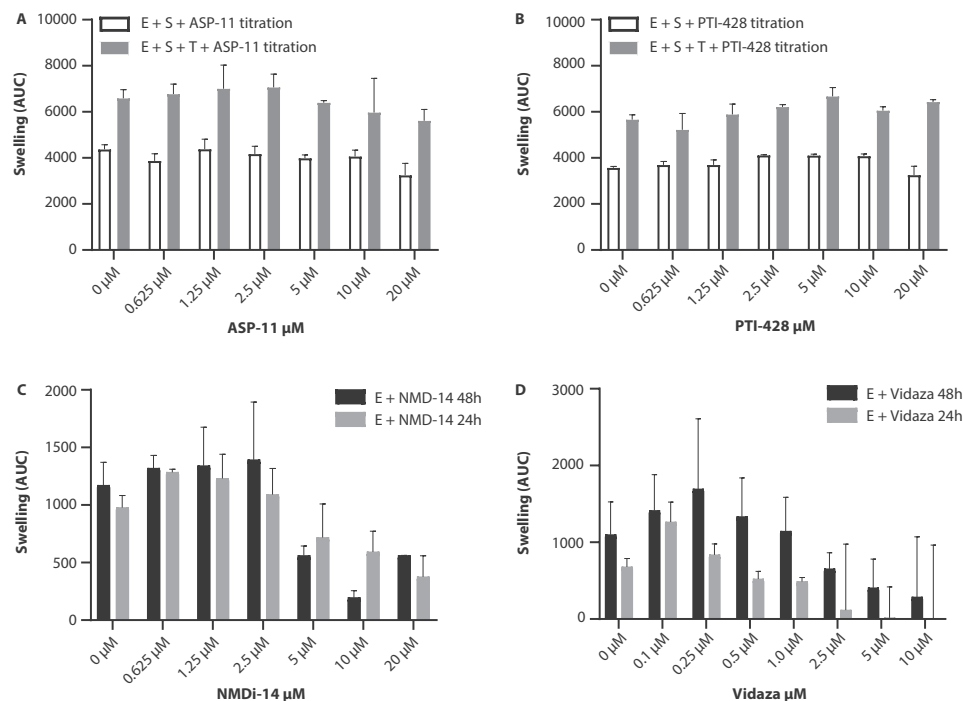
1. Mall, M. A., Mayer-Hamblett, N. & Rowe, S. M. Cystic fibrosis: Emergence of highly effective targeted therapeutics and potential clinical implications. *Am. J. Respir. Crit. Care Med.* 201, 1193–1208 (2020).
2. Howard, M., Frizzell, R. A. & Bedwell, D. M. Aminoglycoside antibiotics restore CFTR function by overcoming premature stop mutations. *Nat. Med.* 2, 467–469 (1996).
3. Welch, E. M. et al. PTC124 targets genetic disorders caused by nonsense mutations. *Nature* 447, 87–91 (2007).
4. Zomer-van Ommen, D. D. et al. Limited premature termination codon suppression by read-through agents in cystic fibrosis intestinal organoids. *J. Cyst. Fibros.* 15, 158–162 (2016).
5. McElroy, S. P. et al. A Lack of Premature Termination Codon Read-Through Efficacy of PTC124 (Ataluren) in a Diverse Array of Reporter Assays. *PLoS Biol.* 11, (2013).
6. Kerem, E. et al. Ataluren for the treatment of nonsense-mutation cystic fibrosis: A randomised, double-blind, placebo-controlled phase 3 trial. *Lancet Respir. Med.* 2, 539–547 (2014).
7. Leubitz, A. et al. A Randomized, Double-Blind, Placebo-Controlled, Multiple Dose Escalation Study to Evaluate the Safety and Pharmacokinetics of ELX-02 in Healthy Subjects. *Clin. Pharmacol. Drug Dev.* 02451, (2021).
8. Crawford, D. K. et al. Targeting G542X CFTR nonsense alleles with ELX-02 restores CFTR function in human-derived intestinal organoids. *J. Cyst. Fibros.* 1–7 (2021) doi:10.1016/j.jcf.2021.01.009.
9. Sharma, N. et al. Capitalizing on the heterogeneous effects of CFTR nonsense and frameshift variants to inform therapeutic strategy for cystic fibrosis. *PLoS Genetics* vol. 14 (2018).
10. Laselva, O. et al. Functional rescue of c.3846G>A (W1282X) in patient-derived nasal cultures achieved by inhibition of nonsense mediated decay and protein modulators with complementary mechanisms of action. *J. Cyst. Fibros.* 19, 717–727 (2020).
11. Keenan, M. M. et al. Nonsense-mediated RNA decay pathway inhibition restores expression and function of W1282X CFTR. *Am. J. Respir. Cell Mol. Biol.* 61, 290–300 (2019).
12. Yeh, J. T. & Hwang, T. C. Positional effects of premature termination codons on the biochemical and biophysical properties of CFTR. *J. Physiol.* 598, 517–541 (2020).
13. Aksit, M. A. et al. Decreased mRNA and protein stability of W1282X limits response to modulator therapy. *J. Cyst. Fibros.* 18, 606–613 (2019).
14. Valley, H. C. et al. Isogenic cell models of cystic fibrosis-causing variants in natively expressing pulmonary epithelial cells. *J. Cyst. Fibros.* 18, 476–483 (2019).
15. Giuliano, K. A. et al. Use of a High-Throughput Phenotypic Screening Strategy to Identify Amplifiers, a Novel Pharmacological Class of Small Molecules That Exhibit Functional Synergy with Potentiators and Correctors. *SLAS Discov.* 23, 111–121 (2018).
16. Xue, X. et al. Identification of the amino acids inserted during suppression of CFTR nonsense mutations and determination of their functional consequences. *Hum. Mol. Genet.* 26, 3116–3129 (2017).
17. McHugh, D. R., Cotton, C. U. & Hodges, C. A. Synergy between readthrough and nonsense mediated decay inhibition in a murine model of cystic fibrosis nonsense mutations. *Int. J. Mol. Sci.* 22, 1–20 (2021).
18. Phuan, P. W. et al. Combination potentiator ('co-potentiator') therapy for CF caused by CFTR mutants, including N1303K, that are poorly responsive to single potentiators. *J. Cyst. Fibros.* 17, 595–606 (2018).
19. Laselva, O. et al. Rescue of multiple class II CFTR mutations by elexacaftor+ tezacaftor+ivacaftor mediated in part by the dual activities of Elexacaftor as both corrector and potentiator. *Eur. Respir. J.* 2002774 (2020) doi:10.1183/13993003.02774-2020.
20. Dekkers, J. F. et al. A functional CFTR assay using primary cystic fibrosis intestinal organoids. *Nat. Med.* 19, 939–945 (2013).

CHAPTER 5

21. Berkers, G. et al. Rectal Organoids Enable Personalized Treatment of Cystic Fibrosis. *Cell Rep.* 26, 1701–1708.e3 (2019).
22. de Winter-De Groot, K. M. et al. Stratifying infants with cystic fibrosis for disease severity using intestinal organoid swelling as a biomarker of CFTR function. *Eur. Respir. J.* 52, (2018).
23. de Winter – de Groot, K. M. et al. Forskolin-induced swelling of intestinal organoids correlates with disease severity in adults with cystic fibrosis and homozygous F508del mutations. *J. Cyst. Fibros.* 19, 614–619 (2020).
24. Dekkers, J. F. et al. Supplementary Materials for Characterizing responses to CFTR-modulating drugs using rectal organoids derived from subjects with cystic fibrosis. *Sci. Transl. Med* 8, 344–84 (2016).
25. Vonk, A. M. et al. Protocol for Application, Standardization and Validation of the Forskolin-Induced Swelling Assay in Cystic Fibrosis Human Colon Organoids. *STAR Protoc.* 1, 100019 (2020).
26. Silverman, L. R. et al. Further analysis of trials with azacitidine in patients with myelodysplastic syndrome: Studies 8421, 8921, and 9221 by the Cancer and Leukemia Group B. *J. Clin. Oncol.* 24, 3895–3903 (2006).
27. Fenaux, P. et al. Azacitidine prolongs overall survival compared with conventional care regimens in elderly patients with low bone marrow blast count acute myeloid leukemia. *J. Clin. Oncol.* 28, 562–569 (2010).
28. Bhuvanagiri, M. et al. 5'-azacytidine inhibits nonsense-mediated decay in a MYC-dependent fashion. 6, 1593–1609 (2014).
29. Pranke, I. et al. Factors influencing readthrough therapy for frequent cystic fibrosis premature termination codons. *ERJ Open Res.* 4, 00080–02017 (2018).
30. Cridge, A. G., Crowe-Mcauliffe, C., Mathew, S. F. & Tate, W. P. Eukaryotic translational termination efficiency is influenced by the 3' nucleotides within the ribosomal mRNA channel. *Nucleic Acids Res.* 46, 1927–1944 (2018).

SUPPLEMENTARY INFORMATION

SUPPLEMENTARY FIGURES



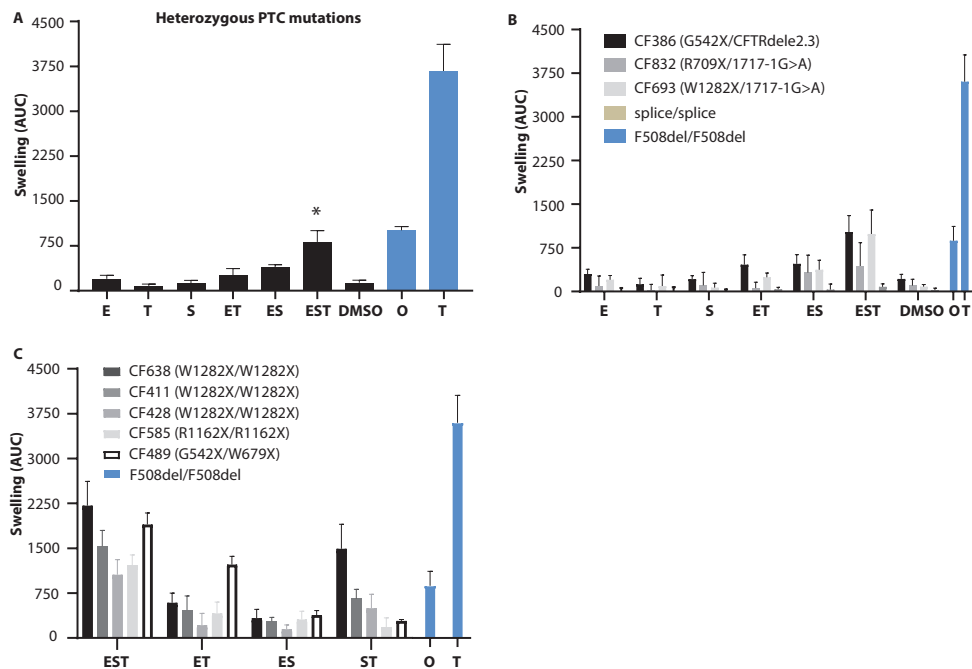
Supplementary figure 1: Dose-response assays on a W1282X/W1282X organoid culture to define proper pharmacotherapy conditions.

(A) FIS, measured for 2h in presence of 5 μM forskolin in presence of increasing concentration of ASP-11. The organoids were pre-stimulated with either E+S (white bars) or E+S+T (gray bars).

(B) FIS, measured for 2h in presence of 5 μM forskolin in presence of increasing concentration of PTI-428, added 24h prior to FIS-assay. The organoids were pre-stimulated with either E+S (white bars) or E+S+T (gray bars).

(C) FIS, measured for 2h in presence of 5 μM forskolin of organoids pre-stimulated for 48h with ELX-02 and an increasing concentration of NMDi-14 for 24h (black bars) or 48h (gray bars). Bars represent mean+SD, n=3.

(D) FIS, measured for 2h in presence of 5 μM forskolin of organoids pre-stimulated for 48h with ELX-02 and an increasing concentration of Vidaza for 24h (black bars) or 48h (gray bars). Bars represent mean+SD, n=3.



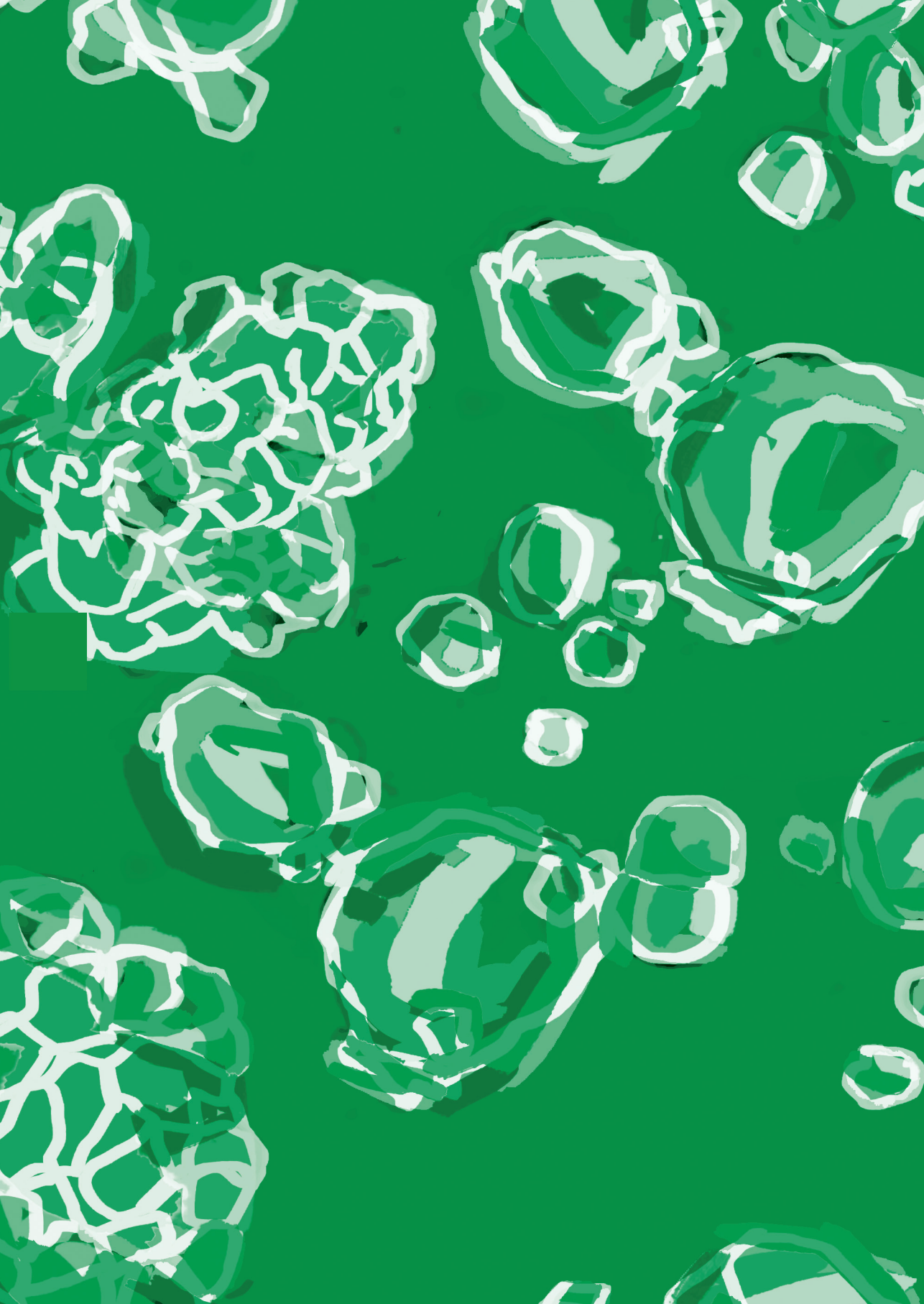
Supplementary figure 2. Response of compound heterozygous organoid cultures to pharmacotherapies and SMG1i+VX-445/VX-661/VX-770 rescued FIS of homozygous PTC organoid cultures.

(A) FIS (mean+SEM) of 3 organoid cultures compound heterozygous for a PTC mutation, measured for 1h in presence of 0.128 μ M forskolin upon pharmacotherapy treatment. Organoid cultures were pre-stimulated with E, S and/or T. To determine the therapeutic value of the investigational pharmacotherapies, the swelling levels were compared to the mean swelling levels of three organoid cultures expressing F508del/F508del-CFTR upon rescue with CFTR modulator cocktails (blue bars, mean+SD, n=9) of which clinical value is known. *p<0.05, compared to DMSO.

(B) FIS of each individual compound heterozygous organoid culture upon pharmacotherapy. Three organoid cultures homozygous for consensus splice mutations (1811+1G>C or 1717-1G>A) were included to assess whether pharmacotherapy specially rescue PTC-CFTR. Bars represent mean+SD.

(C) FIS of homozygous PTC organoid cultures pre-stimulated with S+T(ST), measured for 1 hour with 0.128 μ M forskolin. The ST pharmacotherapy was compared to the other investigational pharmacotherapies discussed in the study. Bars represent mean+SD.

Abbreviations: E = ELX-02ds (80 μ M, 48h); S = SMG1i (0.3 μ M, 24h); T = VX-661 (3 μ M, 24h) + VX-445 (3 μ M, 24h) + VX-770 (3 μ M, added simultaneously with forskolin); O = VX-809 (3 μ M, 24h) + VX-770 (3 μ M, added simultaneously with forskolin).





CRISPR-BASED ADENINE EDITORS CORRECT NONSENSE MUTATIONS IN A CYSTIC FIBROSIS ORGANOID BIOBANK

Published as Clinical and Translational Report

Eyleen de Poel, Maarten H. Geurts, Gimano D. Amatngalim, Rurika Oka, Fleur M. Meijers, Evelien Kruisselbrink, Peter van Mourik, Gitte Berkers, Karin M. de Winter-de Groot, Sabine Michel, Danya Muilwijk, Bente L. Aalbers, Jasper Mullenders, Sylvia F. Boj, Sylvia W.F. Suen, Jesse E. Brunsveld, Hettie M. Janssens, Marcus A. Mall, Simon Y. Graeber, Ruben van Boxtel, Cornelis K. van der Ent, Jeffrey M. Beekman and Hans Clevers

Cell Stem Cell 26: p503-510.e7 (2020)

ABSTRACT

Adenine base editing (ABE) enables enzymatic conversion from A-T into G-C base pairs. ABE holds promise for clinical application, as it does not depend on the introduction of double-strand breaks, contrary to conventional CRISPR/Cas9-mediated genome engineering. Here we describe a cystic fibrosis (CF) intestinal organoid biobank, representing 664 patients, of which ~20% can theoretically be repaired by ABE. We apply the SpCas9-ABE (PAM recognition sequence: NGG) and the xCas9-ABE (PAM recognition sequence: NGN) on four selected CF organoid samples. Genetic and functional repair was obtained in all four cases, while whole genome sequencing (WGS) of corrected lines of two patients did not detect off-target mutations. These observations exemplify the value of large, patient-derived organoid biobanks representing hereditary disease, and indicate that ABE may be safely applied in human cells.

INTRODUCTION

Cystic fibrosis (CF) is a life-shortening disease, caused by a wide variety of mutations in the cystic fibrosis transmembrane conductance regulator (CFTR) gene¹. Recently developed pharmacotherapies (“CFTR modulators”) restore CFTR protein function with impressive efficacy, acting on the most common mutant CFTR protein (CFTR-F508del) and potentially on other mutant CFTR proteins that share conformational defects with F508del^{2,3}. These treatments require lifelong administration and are not effective in most people with rare CFTR mutations. Therefore, permanent restoration of endogenous CFTR function using gene editing techniques remains a favorable option. In a previous study, we have shown that ‘classic’ CRISPR/Cas9-mediated homology-dependent repair (HDR) can be used to restore the CFTR-F508del mutation in intestinal organoids^{4,5}. Functional repair of CFTR was assessed using a forskolin-induced swelling (FIS) assay which is impaired in CF organoids and correlates with clinical disease severity⁶ and *in vivo* CFTR modulator response⁷⁻⁹. This assay facilitated the rapid selection of genetically-repaired, clonal organoids by phenotypic screening upon addition of forskolin. However, CRISPR/Cas9-mediated HDR is inefficient and may introduce deleterious off-target double-stranded breaks, hampering potential clinical applications¹⁰⁻¹³. Recently developed Cas9-fusion proteins, so-called base editors, circumvent these issues. Fusion of a cytidine deaminase to a partially inactive nickase Cas9 protein allows for efficient C-G to T-A base changes (C-T Base Editing, or CBE), while a fusion with an evolved TadA heterodimer performs the opposite reaction, from A-T to G-C (A-G Base Editing, or ABE)¹⁴⁻¹⁷. These DNA modulator proteins fused to Cas9 act on single-stranded DNA. Therefore, base editors act only within a small window of the single stranded R-loop that is generated upon Cas9 binding to the target sequence and in which the DNA modification enzymes (APOBEC or TadA) can show activity. This limited editing window, roughly base 4-8 within the protospacer, is defined by the specific localization of Cas9 proteins¹⁸. Cas9 genomic localization is restricted by the protospacer adjacent motif (PAM)-specificity of the protein, NGG for SpCas9^{19,20}. Recent developments have led to the generation of Cas9 alternatives such as xCas9 which shows activity on the non-canonical PAM NGN, increasing the target range of base editing²¹. Moreover, xCas9 has a higher fidelity than SpCas9 (and other Cas9 variants with less restrictive PAM requirements such as SpCas9-NG), making it a promising tool for genome engineering in a clinical setting^{22,23}.

MATERIALS AND METHODS

Experimental model and subject details

No sample-size estimate was calculated before the study was executed. The experiments were not randomized. The investigators were not blinded to allocation during experiments and outcome assessment.

Biobank establishment and governance

All experimentation using human tissues described herein was approved by the medical ethical committee at University Medical Center Utrecht (UMCU; TcBio#14-008 and TcBio#16-586) and at Charite, Berlin. Informed consent for tissue collection (nasal and intestinal), generation,

storage, and use of the organoids was obtained from all participating patients. Biobanked intestinal organoids (**supplementary table 1**) are stored and catalogued (<https://huborganoids.nl/>) at the foundation Hubrecht Organoid Technology (<http://hub4organoids.eu>) and can be requested at info@hub4organoids.eu. Distribution of organoids to third parties (academic or commercial) requires completion of a material transfer agreement and will have to be authorized through a release protocol by the medical ethical committee at UMCU. These requests will be made by HUB in order to ensure compliance with the Dutch medical research involving human subjects' act. Use of organoids is subjected to patient consent; upon consent withdrawal, distributed organoid lines and any derived material will have to be promptly disposed of. Intestinal organoids from patients that did not give broad informed consent for the HUB organoid technology (**supplementary table 2**) were generated from intestinal biopsies which were obtained for (i) standard care, (ii) voluntary participation in scientific studies, or (iii) CF diagnostic questions in accordance with local ethical guidelines. In some cases, biopsies were directly sent from external hospitals to generate organoids without intestinal current measurements. The organoids are stored in the UMCU biobank and governed by Dr. J.M. Beekman in collaboration with the principle investigator that shipped the biopsy to UMCU. The use of these organoids for research is restricted to non-commercial research, and requires approval of the associated principal investigator who shipped the sample.

Intestinal organoid culture

Intestinal organoids stored in liquid nitrogen were thawed and passaged at least 4 times prior to electroporation. Furthermore, the mutations of the organoid lines used for the CRISPR/Cas9-ABE-experiments were first confirmed by Sanger sequencing. The culturing of the organoids was performed according to previously described protocols^{4,9} except that the wnt-conditioned medium in the complete culture medium (CCM) was replaced by advanced DMEM-F12 supplemented with 1% HEPES, 1% Glutamax, 1% Pen/Strep (F12GHP), wnt-surrogate-Fc fusion protein (4 nM) and Y-27632 (10 µM) (CCM+). CCM+ was used as the standard culture medium in all intestinal organoid experiments unless stated otherwise.

Airway organoid culture

Nasal epithelial cells from a CF patient (F508del/R1162X) were collected from brushings of the inferior nasal turbinates using a cytological brush. Basal progenitor cells were isolated according to the dual SMAD inhibition method, previously described²⁴. In brief, brushed nasal cells were seeded in collagen type IV pre-coated tissue culture plates (Greiner) in BEPiCM culture medium, supplemented with 1x BEpiCGS, Penicillin/Streptomycin (100 µg/ml), Primocin (50 µg/ml), Gentamicin (50 µg/ml), Vancomycin (100 µg/ml), Y-27632 (5 µM), DMH-1 (1 µM) and A83-01 (1 µM). After isolation and passaging for at least three times, the basal progenitor cells were electroporated (described in Method Details). Subsequent expansion of electroporated cells into organoids was performed in airway organoid medium (AO medium), adapted from Sachs et al²⁵, consisting of F12^{GHP}, Primocin (50 µg/ml), N-Acetylcysteine (1.25 mM), Nicotinamide (5 mM), 1x B27 supplement, P38 MAPK inhibitor (500 nM), Y-27632 (5 µM), A83-01 (1 µM), CHIR99021 (5 µM), 20% R-Spondin 1 conditioned medium (v/v), 20% Noggin conditioned medium (v/v), FGF7 (25 ng/ml), FGF10 (100 ng/ml).

Plasmid construction

Human codon optimized base editing constructs were a kind gift from David Liu; pCMV_ABEmax_P2A_GFP (Addgene plasmid#112101), pCMV_AncBE4max_P2A_GFP (Addgene plasmid#112100)¹⁵. Codon optimized xCas9 was a kind gift from Lukas Dow (pLenti-xFNLS-P2A-Puro, Addgene plasmid#110872)¹⁷. Q5 high fidelity polymerase was used to amplify the codon optimized xCas9 sequence and was cloned into the pCMV_ABEmax_P2A_GFP, using NEBbuilder HiFi assembly mastermix according to manufacturer protocols. Site-directed mutagenesis was performed to generate a D10A xCas9 nickase using T4 ligase and Dpn1 to religate the plasmid and to generate xCas9-ABE (pMHG120_xABEmax_P2A_GFP). The empty sgRNA plasmid backbone was a kind gift from Keith Joung (BPK1520, Addgene plasmid #65777). Spacer sequences targeting the different CFTR mutations were cloned in the sgRNA plasmid backbone using inverse PCR together with the same recombination techniques as described above. All transformations in this study were performed using OneShot Mach1T1 cells and plasmid identity was checked by Sanger sequencing (Macrogen).

Intestinal organoid electroporation

The organoid electroporation protocol was adapted from Fujii et al²⁶. Organoids were maintained in CCM+ up until two days before electroporation. Two days in advance the Rspordin-conditioned medium in the CCM+ was replaced by F12^{GHP}. One day in advance 1.25% (v/v) DMSO was added to the organoids. On the day of electroporation the organoids were dissociated into single cells using accutase supplemented with Y-27632 (10 µM) for 20 minutes and TrypLE™ supplemented with Y-27632 (10 µM) for 2 minutes, both at 37°C. In experiments based on FIS selection, the cell pellet (consisting of 10⁶ cells) was resuspended in 90 µl BTXpress and combined with 10 µl plasmid solution (sgRNA-plasmid, 2.5 µg/µl, and pCMV_xABEmax_P2A_GFP-plasmid or pCMV_ABEmax_P2A_GFP-plasmid, 7.5 µg/µl). In experiments based on Hygromycin B-gold selection, the cell pellet was resuspended in 80 µl BTXpress and combined with 20 µl plasmid solution containing 2.5µg sgRNA-plasmid and 7,5µg pCMV_xABEmax_P2A_GFP-plasmid or pCMV_ABEmax_P2A_GFP-plasmid together with 10 µg PiggyBac transposon system (2.8 µg transposase + 7.2 µg hygromycin resistance containing transposon))²⁷. Electroporation was performed using NEPA21 with settings described before²⁶. After electroporation the cells were resuspended in 600ul matrigel (50% matrigel, 50% CCM+) and plated out in 20 µl droplet/well of a pre-warmed 48-wells tissue culture plates (Greiner). After polymerization, the matrigel droplets were immersed in 300 µL of CCM+ and the organoids were maintained at 37°C and 5% CO₂.

Clonal expansion of intestinal organoids

After an expansion period of at least 10 days the single cells grew out into organoids. Selection of genetically corrected organoids was based on CFTR function restoration and was assessed by adding forskolin (5 µM) to the CCM+. Pictures were made (1.25x with EVOSTM FL Auto Imaging System) prior to and 60 minutes after forskolin addition. Organoids that showed swelling after 60 minutes (indicating genetic restoration of CFTR) were individually picked with a p200 pipette and a bend p200 pipette tip. Each individual genetically corrected organoid was dissociated into single cells using accutase supplemented with Y-27632 (10 µM)

for 5 minutes at 37°C. The cells were plated out in 20 µL matrigel droplets/picked organoid (50% matrigel, 50% CCM+) in pre-warm 48-well tissue culture plates (Greiner) and maintained at 37°C and 5% CO₂. The single cells were grown towards clearly separated, single organoid structures and corrected organoids were picked and passaged after visual screening of FIS until a clonal organoid culture was established. This was confirmed by Sanger sequencing and the absence of FIS-assay unresponsive organoids after repeated passaging.

Quantification of editing efficiency

Two days after electroporation of the intestinal organoids harboring the R785X mutation, we first selected the transfected cells by FACS sorting based on GFP, expressed by the pCMV_xABEmax_P2A_GFP-plasmid or pCMV_ABEmax_P2A_GFP-plasmid on a Moflo Astrios (Beckman Coulter). The GFP+ cells were plated out (500 cells/20 µl matrigel ((50% matrigel, 50% CCM+) droplet) in pre-warm 48-wells plates and expanded for 7-9 days. To determine the editing efficiency in the pool of transfected R785X/R785X organoids, the total number of organoids was quantified using Cellprofiler 3.1.5. Next, the number of corrected organoids were identified by counting the FIS-assay responsive organoids. For the organoid lines harboring W1282X/W1282X and R553X/F508del mutations, two days post transfection, we took 20% of the electroporated cells and determined the transfection efficiency by FACS analysis on a Moflo Astrios (Beckman Coulter) as described above. The remainder of transfected non-sorted organoids were then diluted and plated (250 organoids/20 µl matrigel ((50% matrigel, 50% CCM+) droplet) pre-warm 48-wells plates and expanded for 7-9 days. We then quantified the total amount of cultured organoids by using cell-profiler 3.1.5. Editing efficiencies were determined by dividing the total amount of organoids by the transfection efficiency and the amount of FIS-assay responsive organoids.

Electroporation of basal progenitor cells

After expansion (at least passage three) of the basal progenitor cells (2D-monolayer) in collagen type IV pre-coated tissue culture plates they were dissociated with TrypLE™ for 10 minutes at 37°C @. The single basal progenitor cells were electroporated according to the protocol described in the section ‘intestinal organoid electroporation’. Next, cells were seeded in a density of 9x10⁴ cells per 30 µl matrigel (75% matrigel, 25% AO medium) droplets in a pre-warmed 24 wells suspension plates (Greiner). After solidification, droplets were overlaid with 500 µL airway AO medium and the organoids were maintained at 37°C and 5% CO₂.

Clonal selection of airway organoids

The electroporated cells grew out into organoids and after three days hygromycin (1:1000) was added to the AO culture medium to select for transfected organoids. After 4-7 days the organoids were passaged and hygromycin treatment was continued until all control organoids (not electroporated with PiggyBac-plasmids) were killed. The hygromycin resistant clones were individually picked and passaged using the same protocol as for the corrected intestinal organoids. The organoid-derived single cells were plated out in 30 µl matrigel/well

of a 24-well suspension plate (75% matrigel, 25% AO medium) and were overlaid with 500 µl AO medium and maintained at 37°C and 5% CO₂. DNA of each individual organoid clone was harvested and gene correction was assessed with Sanger sequencing.

Genotyping of clonal lines

Intestinal and airway organoid DNA was harvested from 10-20µL Matrigel/organoid suspension and DNA was extracted using the Quick-DNA microprep kit. Target regions were amplified from the genome using Q5 high fidelity polymerase primers for target region amplification can be found in **Methods S1**. Sequencing was performed using the M13F tail as all forward amplification primers for targeted sequencing contained a tail with this sequence. Base editing induced genomic alterations were confirmed by Sanger sequencing (Macrogen).

FIS-assay

To quantify the CFTR function restoration in the genetically corrected intestinal clones the FIS-assay was conducted in duplicate at three independent culture time points (n=3) according to previous published protocols⁹. In short, intestinal organoids were seeded in 96-well culture plates (Nunc) in 4 µl of 50% matrigel (+50% CCM+) containing 20 to 40 organoids and immersed in 50 µl CCM+. The day after, organoids were incubated for 30 min with 3 µM calcein green (Invitrogen) to fluorescently label the organoids and stimulated with 5 µM forskolin. Every ten minutes the total calcein green labeled area per well was monitored by a Zeiss LSM800 confocal microscope, for 60 minutes while the environment was maintained at 37°C and 5% CO₂. A Zen Image analysis software module (Zeiss) was used to quantify the organoid response (area under the curve measurements of relative size increase of organoids after 60 minutes forskolin stimulation, t = 0 min baseline of 100%).

RNA extraction

RNA was isolated with the RNeasy Mini kit (Qiagen) with a DNase digestion step (RNase-Free DNase Set, Qiagen) according to manufacturer's instructions. In short, the intestinal organoids were harvested at three independent culture time points (n=3) in F12^{GHP} and mechanically disrupted according to previous described protocol^{4,7,9}. After spinning down, the supernatant was removed and the pellet was resuspended in 350 mL RLT buffer (RNeasy Mini kit Qiagen) + β-mercaptoethanol (1%) by a 1 minute vortex. The lysates were immediately used or stored at -80 °C. The amount and purity of the RNA samples was determined with the Nanodrop ND-1000 spectrophotometer (Thermo Scientific). cDNA ranging from 500 ng to 1 µg RNA was obtained with the iScriptTM cDNA Synthesis Kit (BIO-RAD) using the supplier's protocol.

Quantitative Real Time PCR

10 µL qRT-PCR reactions were performed using BIO-RAD I-Cycler 96 wells-plates, iQTM SYBR Green Supermix (BIO-RAD), 0.4 µM forward primer and 0.4 µM reverse primer. The samples, harvested at three different culture time points (n=3), were analyzed in triplicate using a two-step real time quantitative PCR (BIO-RAD). For each primer the annealing temperature

resulting in 95-105% amplifying efficiency was determined with a gradient PCR. The amount of mRNA per sample was determined using the Livak method, (CT values were normalized with mean mRNA expression of the housekeeping genes YWAZ and β-ACTIN). Primers used for qPCR are listed in **Methods S1**.

Western blotting

First intestinal organoids were harvested in F12^{GHP}, washed with PBS and mechanically disrupted at three different culture time points (n=3). After spinning down the pellets were lysed with Laemmli buffer (4% SDS, 20% glycerol, 12% 1M Tris (pH 6.8) in MQ) supplemented with a complete protease inhibitor tablet (1 tablet/50 ml) and stored at -80°C. After thawing, the lysate suspension was homogenized and protein concentration was determined in duplicate with the BCA protein assay according to manufacturer's protocol. 50 mg protein was loaded per 50ul slots in a 6% agarose gel. The proteins were separated with SDS-page and transferred to Immobilon-FL Polyvinylidene difluoride (PVDF)-membrane using wet tank transfer O/N at 4°C. The membranes were blocked for 1 hour with Tris-buffered Saline Tween (TBST) containing 5% milk protein (ELK Campina). The membranes were incubated with TBST containing 0.5% milk protein and a pool of anti-CFTR mouse antibodies (Cystic Fibrosis Folding Consortium 450, 570 and 596; diluted 1:15000) and anti-HSP90 (diluted 1:50.000) rabbit antibodies for 3 hours at 4°C. The membranes were cut at 100 KDa and incubated with goat-anti-mouse (diluted 1:5000) or goat-anti-rabbit (diluted 1:2000) horseradish peroxidase-conjugated secondary antibody in TBST containing 0.5% milk protein. Three 15-minute wash steps with TBST and one 10-minute wash step with PBS were conducted. The PVDF membranes (one membrane per harvesting time point, n=3) were incubated for 5 minutes with SuperSignal™ West Dura Extended Duration Substrate and were developed with the ChemiDoc Touch Imaging System (BIO-RAD).

In silico target selection

To select potential CBE and ABE targets from the CFTR2 database we adapted the target calling script from Hu et al²⁸. Ensembl BioMart (Ensembl Release 97) was used to extract flanking sequences of all CFTR2 described SNPs. The used pipeline can be found on: <https://github.com/MHgeurts/CRISPR-based-adenine-editors-correct-nonsense-mutations-in-a-cystic-fibrosis-organoid-biobank>.

Whole genome sequencing and mapping

Genomic DNA was isolated from 100 µl of Matrigel/organoid suspension using DNeasy Blood & Tissue Kit, according to protocol. Standard Illumina protocols were applied to generate DNA libraries for Illumina sequencing from 20-50ng of genomic DNA. All samples (three genetically corrected clones and one non-corrected control sample of the R785X/R785X and R553X/F508del donor) were sequenced (2x150bp) by using Illumina NovaSeq to 30x base coverage. Reads were mapped against human reference genome hg19 using Burrows-Wheeler Aligner v0.5.9²⁹, with settings 'bwa mem -c 100 -M'. Duplicate sequence reads were marked using Sambamba v0.4.7.32 and realigned per donor using Genome Analysis

Toolkit (GATK) IndelRealigner v2.7.2 and quality scores were recalibrated using the GATK BaseRecalibrator v2.7.2. More details on the pipeline can be found on <https://github.com/UMCUGenetics/IAP>.

Mutation calling and filtering

Raw variants were multisample-called by using the GATK HaplotypeCaller v3.4-46³⁰ and GATK-Queue v3.4-46 with default settings and additional option ‘EMIT_ALL_CONFIDENT_SITES’. The quality of variant and reference positions was evaluated by using GATK VariantFiltration v3.4-46 with options ‘-snpFilterName LowQualityDepth -snpFilterExpression “QD < 2.0” -snpFilterName MappingQuality -snpFilterExpression “MQ < 40.0” -snpFilterName StrandBias -snpFilterExpression “FS > 60.0” -snpFilterName HaplotypeScoreHigh -snpFilterExpression “HaplotypeScore > 13.0” -snpFilterName MQRankSumLow -snpFilterExpression “MQRankSum < -12.5” -snpFilterName ReadPosRankSumLow -snpFilterExpression “ReadPosRankSum < -8.0” -cluster 3 -window 35’. To obtain high-quality somatic mutation catalogs, we applied post processing filters as described³¹. Briefly, we considered variants at autosomal chromosomes without any evidence from a paired control sample (MSCs isolated from the same bone marrow); passed by VariantFiltration with a GATK phred-scaled quality score ≥ 250 ; a base coverage of at least 20X in the clonal and paired control sample; no overlap with single nucleotide polymorphisms (SNPs) in the Single Nucleotide Polymorphism Database v137. b3730; and absence of the variant in a panel of unmatched normal human genomes (BED-file available upon request). We additionally filtered base substitutions with a GATK genotype score (GQ) lower than 99 or 10 in the clonal or paired control sample, respectively. For indels, we filtered variants with a GQ score lower than 99 in both the clonal and paired control sample and filtered indels that were present within 100 bp of a called variant in the control sample. In addition, for both SNVs and INDELs, we only considered variants with a mapping quality (MQ) score of 60 and with a variant allele frequency of 0.3 or higher in the clones to exclude in vitro accumulated mutations^{31,32}. The scripts used are available on GitHub (<https://github.com/ToolsVanBox/SNVFI>, <https://github.com/ToolsVanBox/INDELFI>). The distribution of variants was visualized using an in house developed R package (MutationalPatterns)³³.

In silico off target prediction

Potential sgRNA specific off-target events were predicted using the Cas-OFFinder open recourse tool³⁴. All potential off-targets up to 4 mismatches were taken into account. For CFTR-R785X an NGG PAM and for CFTR-R553X an NGN PAM was selected.

Mutational signature analysis

We extracted mutational signatures and estimated their contribution to the overall mutational profile as described³⁵ using an in house developed R package (MutationalPatterns)³³. **(Methods S2)**. In this analysis, we included small intestine data (previously analyzed) to explicitly extract in vivo and in vitro accumulated signatures³¹. To determine the transcriptional strand contribution and bias, we selected all point mutations that fall within gene bodies and checked whether the mutated base was located on the transcribed or

non-transcribed strand. We used a in house developed R package (MutationalPatterns) to determine transcriptional strand bias as described³³.

Quantification and statistical analysis

Statistical parameters are reported in the figure legends and the 'Method Details' section. The mean forskolin-induced swelling (AUC) and Δ CT of non-corrected control clone was compared to the mean forskolin-induced swelling and Δ CT of genetically corrected organoid clones. First the Levene's test was conducted and a QQ-plot of the residuals of the AUC and Δ CT values was made, which proved homogeneity of variances and normal distribution of the residuals. Subsequently, the One-way ANOVA was used to assess whether the differences in mean swelling and mean Δ CT between the groups were statistically significant ($\alpha>0,05$). To assess whether the AUC and Δ CT of the individual clones were significantly different from the non-corrected controls the Dunnet's test was conducted. To assess whether the difference in mean editing efficiencies between the SpCas9-ABE and HDR-treated organoids is statistically significant ($\alpha>0,05$) a paired T-test was performed after homogeneity of variances (Levene's test) and normality of the error distribution (QQ-plot of the residuals) was confirmed.

RESULTS AND DISCUSSION

Generation of CF patient-derived intestinal organoid biobank

To facilitate CF research, we generated and characterized an intestinal organoid biobank representing 664 CF patients, nearly half of the Dutch CF population (**figure 1A**). Experimental controls within this biobank consist of 29 WT and 7 CF carrier samples (**supplementary tables 1A and 1B**). This biobank covers the heterogeneity of CF mutations present in the Dutch CF population and the top 17 most prevalent mutations coincide with those in the Dutch CF registry (**figure 1B; supplementary table 1C**) (<https://www.ncfs.nl/over-cystic-fibrosis/cf-registry-2017>). Of note, as this biobanking effort has focused on infrequent CF alleles, F508del/F508del homozygous organoids are underrepresented while rare mutations are overrepresented. Indeed, we identified 61 rare mutations that are not present in the CFTR2 database (<http://cftr2.org>), currently the most comprehensive list of pathogenic mutations in CF. To our knowledge, 34 of these mutations have never been reported previously in CF patients (**supplementary tables 1D and 1E**) (<http://genet.sickkids.on.ca>).

We analyzed the number of mutations that are potentially targetable by base-editing in the CFTR2 database (<http://cftr2.org>). Of all listed mutations in the CFTR2 database, 48 (11.7%) result from TA>CG conversions and can theoretically be repaired by CBEs. Of these mutations, 30 (62.5%) have a suitable PAM (10 for spCas9-CBE and an additional 20 for xCas9-CBE). In addition, 131 (31.8%) of the disease-causing mutations are caused by CG>TA conversions and can theoretically be rescued by ABEs, of which 90 (68.7%) have a suitable PAM (23 for spCas9-ABE, and an additional 67 for xCas9-ABE) (**figure 1C**).

CRISPR-based adenine editors correct nonsense mutations in a cystic fibrosis organoid biobank

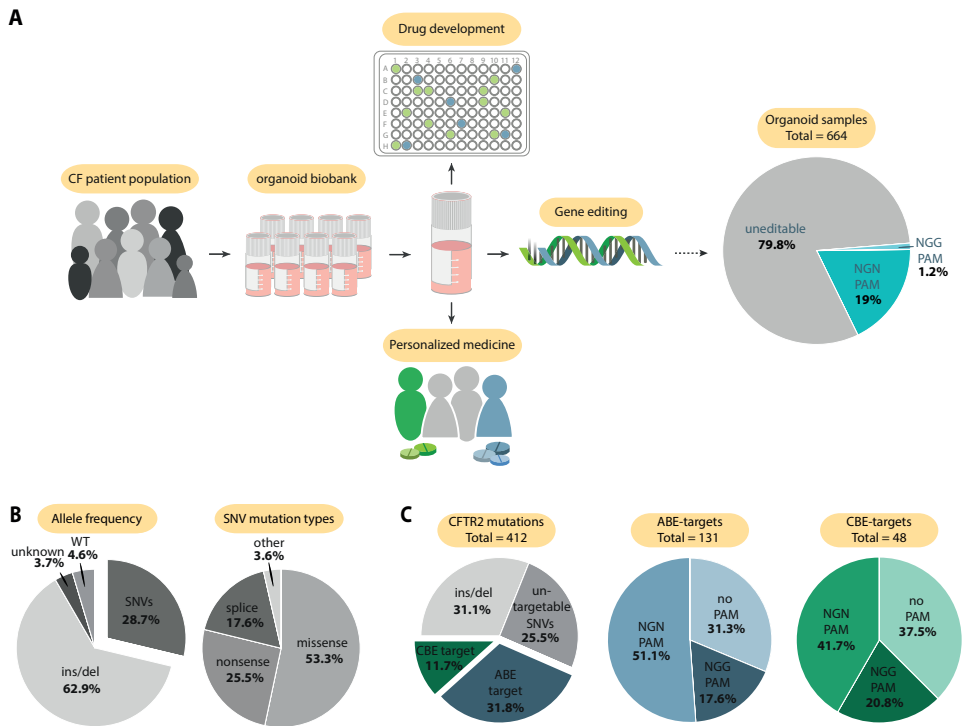


Figure 1: A CF patient-derived intestinal organoid biobank.

(a) Establishment and application of the CF patient-derived intestinal organoid biobank for drug development, personalized medicine and gene-editing. 20% of the organoid samples present in our biobank are eligible for base editing as these samples carry an editable mutation on at least one allele. **(b)** Distribution of CFTR alleles and SNVs in our biobank. **(c)** Frequency (%) of CFTR2 alleles targetable with single-base editing, where the blue fraction is ABE targetable and green fraction is CBE targetable, including a distribution of the CFTR2 alleles based on the presence of NGG and NGN PAMs.

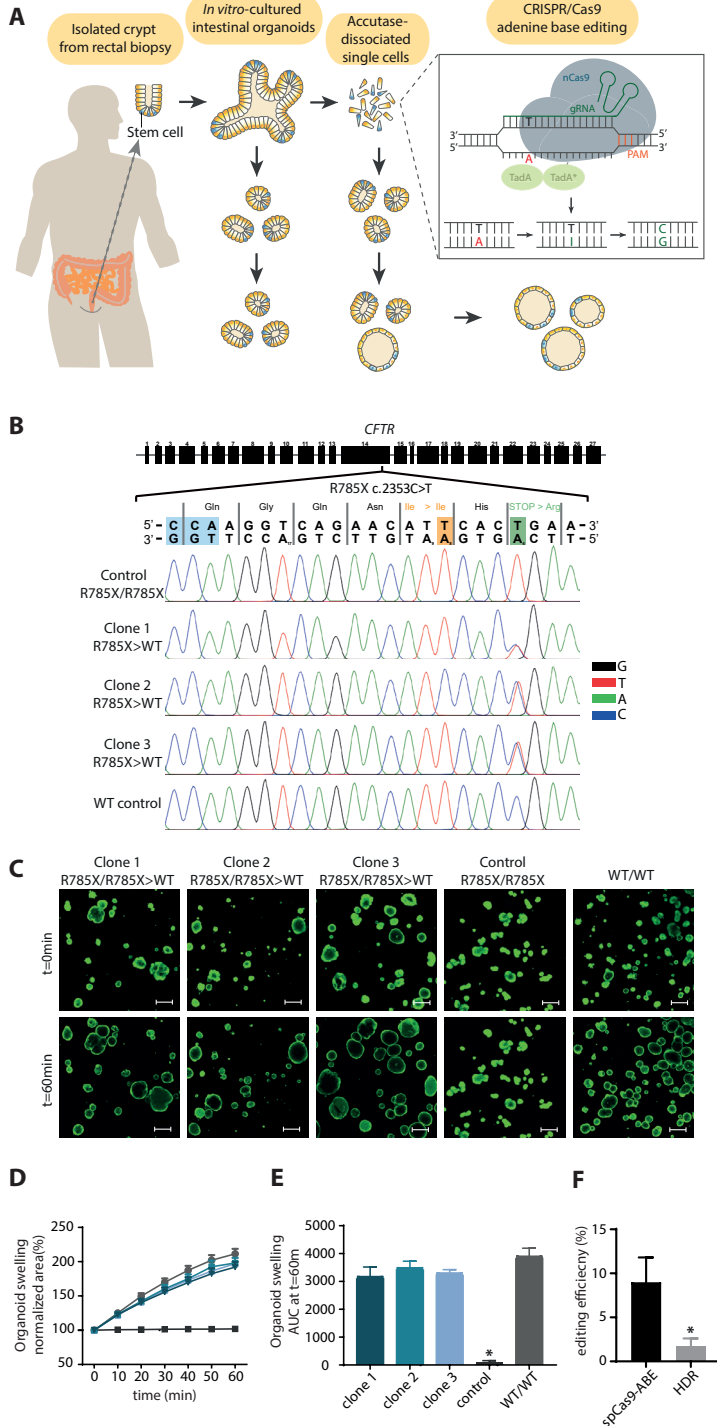


Figure 2: Adenine base editing-mediated functional repair of CFTR on Canonical PAM (NGG)

(a) Experimental design of ABE-mediated repair of CFTR in intestinal organoids **(b)** Sanger validation of R785X-CFTR repair using SpCas9-ABE in three clonal organoid cultures. The targeted base is highlighted in green, the off-target base is highlighted in orange and the PAM is highlighted in blue. **(c)** Confocal images of calcein-green-stained patient-derived intestinal organoids before and after 60 min. stimulation with forskolin. **(d)** Per well the total organoid area (xy plane in μm^2) increase relative to $t = 0$ (set to 100%) of forskolin treatment was quantified ($n=3$). **(e)** FIS as the absolute area under the curve (AUC) ($t = 60$ min; baseline, 100%), mean \pm SD; $n=3$, * $p = <0.001$, compared to the corrected organoid clones and the WT organoid sample. **(f)** Editing efficiency quantified as fraction of FIS-assay responsive organoids in the transfected pool. Bars represent mean \pm SD; $n=5$ and 3, * $p = <0.05$.

Functional repair of CFTR using adenine base editors on canonical and non-canonical PAMs

Next, we investigated base editing by SpCas9-ABE, which can theoretically correct 8 of the organoid samples in our biobank (1.2%) (**figure 1A**). Four organoid samples harbored a mutation that do not have additional adenines in the editing window or base-editing of these residues would result in a synonymous base change. We chose to correct the CFTR-R785X mutation, which is represented once as a homozygous mutation in our biobank. This mutation can be repaired by changing the adenine residue on position 5 of the spacer sequence (**figures 2A and 2B**). Editing of the single other adenine residue within the editing window would result in a synonymous mutation of the isoleucine residue on position 783 (I783I) (**figure 2B**). We electroporated an estimated 1.5×10^6 single cells of this organoid line with pCMV_ABEmax_P2A_GFP-plasmid and sgRNA-plasmid. We observed hundreds of organoids that responded to forskolin as assessed by FIS, indicating the presence of corrected cells within each of these organoid lines (**supplementary figures 1A and 1D**). Out of these FIS-assay responsive organoids, three were randomly picked and clonal lines were established by additional selection cycles, in which single cells were grown into single organoid structures that could be individually picked after visual screening for FIS (**supplementary figures 1A, 1D and 1E**). Next, Sanger sequencing was performed on the three generated clones to confirm clonal correction (**figure 2B**). The repaired clonal organoid lines exhibited FIS at WT levels upon forskolin addition, whereas unrepairs clones did not display FIS (**figures 2C-E**). The SpCas9-ABE-mediated correction of CFTR was further confirmed by CFTR protein and mRNA analysis (**supplementary figure 2**). We did observe editing of the 8th residue within the editing window in clone 2 (**figure 2B**). As expected, this synonymous mutation did not result in altered FIS when compared to clones that did not carry this silent editing event (**figures 2C-E**). Furthermore, editing efficiency of SpCas9-ABE (8.88%, $n=3$) on this target mutation was 5-fold higher compared to conventional CRISPR/Cas9-mediated HDR with the use of ssODN's (1.78%, $n=3$) (**figures 2F and supplementary figure 3**).

We next investigated base editing by xCas9-ABE which has a more promiscuous PAM as compared to SpCas9-ABE. xCas9-ABE can theoretically correct 126 of the intestinal organoid samples in our biobank (19%), of which 50 lines do not have additional adenines in the editing window (**supplementary tables 2A and 2B**). We first applied the technique on an organoid line homozygous for the most frequent nonsense mutation in our biobank, W1282X. This mutation can be repaired by converting the adenine on position 6 in the window (**figure 3A**). Of note, editing on position 7 would result in a de novo R1283G mutation, never documented

CHAPTER 6

in CF patients and therefore possibly silent (<http://genet.sickkids.on.ca/>). Upon electroporation with the self-constructed pCMV_xABEmax_P2A_GFP-plasmid and sgRNA-plasmid, editing was observed only on the desired adenine at position 6 in the window, resulting in functional CFTR repair as shown by Sanger sequencing and FIS (**figures 3A, 3C, 3D and 3F; supplementary figures 1B and 1D**). To investigate potential heterozygous ABE-mediated repair, we focused on the R553X mutation, the third most prevalent nonsense mutation as present in the CFTR2 database (<http://cftr2.org>). This mutation can be repaired by an A>G conversion at position 6 within the editing window, while no other adenines are present (**figure 3B**). The selected organoid sample harbored a F508del mutation on the second allele. Again, genetic and functional repair of CFTR was observed upon electroporation with the self-constructed pCMV_xABEmax_P2A_GFP -plasmid and sgRNA-plasmid, as shown by Sanger sequencing and FIS (**figures 3B, 3C, 3D and 3F; supplementary figures 1B and 1D**). The editing efficiencies of xCas9-ABE on the homozygous W1282X mutation (1.43% n=3) and the heterozygous R553X mutation were comparable (1.43%, n=3) (**figure 3E; supplementary figure 3**). Thus, we have shown that it is feasible to genetically correct both homozygous and heterozygous mutations in organoids using xCas9-ABE.

We confirmed the potential of xCas9-ABE in CF airway cells by growing nasal brush derived airway organoids from one patient, compound heterozygous for F508del and the nonsense mutation R1162X. As airway organoid fluid secretion is not strictly CFTR dependent, FIS could not be utilized to detect functional repair²⁵. We therefore electroporated the pCMV_xABEmax_P2A_GFP-plasmid and the pertinent sgRNA-plasmid together with a hygromycin piggyBac system to allow for selection of transfected organoids (**figure 3G**). Sanger sequencing of 100 individually picked hygromycin-resistant clones revealed correct repair of the R1162X mutation in 8% of the organoids (**figure 3H**).

CRISPR-based adenine editors correct nonsense mutations in a cystic fibrosis organoid biobank

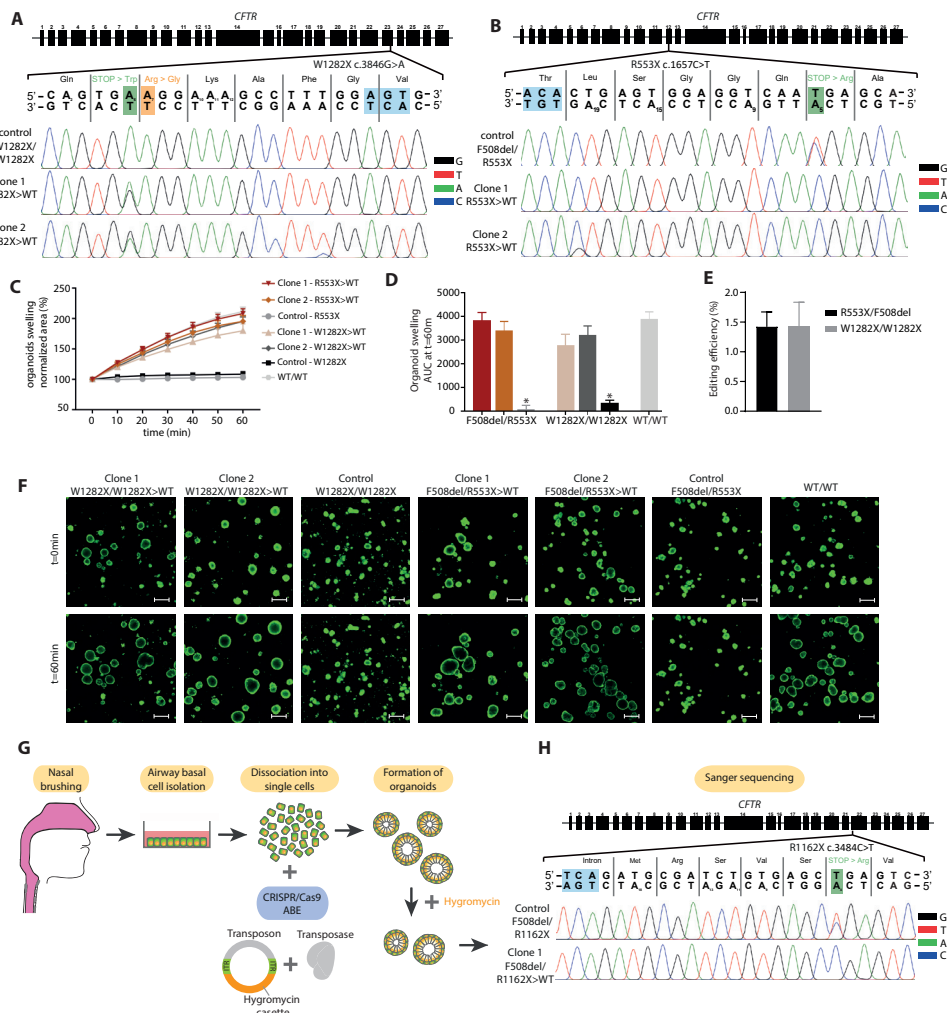


Figure 3: Adenine base editing-mediated functional repair of CFTR on non-canonical PAMs (NGN).

(a) Sanger validation of R553X-CFTR repair in two corrected clonal lines. (b) Sanger validation of W1282X-CFTR repair in two corrected clonal lines. The targeted base in **a** and **b** is highlighted in green, the off-target base is highlighted in orange and the PAM is highlighted in blue. (c) Per well, the total organoid area (μm^2) increase relative to $t = 0$ (set to 100%) of forskolin treatment was quantified. (d) FIS as the absolute area under the curve (AUC) ($t = 60$ min; baseline, 100%), mean \pm SD; $n=3$ per CFTR mutation, $*p = <0.001$, compared to the corrected organoid clones and the WT organoid sample. (e) Editing efficiency quantified as fraction of FIS-assay responsive organoids in the transfected pool. (f) Confocal images of calcein-green-stained patient-derived intestinal organoids before and after 60 min. stimulation with forskolin. (g) Experimental design of xCas9-ABE-mediated repair of R1162X-CFTR in airway organoids and Sanger tracing of repaired and non-repaired airway organoids heterozygous for R1162X-CFTR (h).

No detectable off-target effects of adenine base editors

To study potential off-target effects induced by each of the ABEs in homozygous and heterozygous repair, we performed WGS analysis on three SpCas9-ABE (R785X/R785X) and three xCas9-ABE-repaired clones (R553X/F508del) and their respective unrepairs controls. Two recent studies in mouse and rice have shown that CBEs generate a high number of off-targets while these are undetectable in ABE-treated samples^{36,37}. To date, no genome wide off-target studies have been performed in human cells to interrogate the fidelity of ABE. Analysis of in silico predicted off-target sequences (up to 4 mismatches) did not reveal any off-target hits in the predicted off-target protospacer sequence or in the 100 flanking bases up- and downstream for both R785X (**supplementary table 3A**) and R553X (**supplementary table 3B**), in all repaired clones. Furthermore, no mutational hot-spots (resulting from off-target sgRNA-dependent ABE-binding) were observed in either of the samples on a genome-wide scale, as the rainfall plot (**figure 4A**) does not present a region of hypermutation, shown by a cluster of dots at lower genomic distances. As the sample size in our study is small and differences in organoids culturing and propagation of individual clones are difficult to control for, we used a mutational signature analysis³⁵ to study base changes that could have been caused independent of cognate sgRNA binding. Signatures of repaired clones closely resembled those of the controls (Cosine similarity of 0.92) and did not show an increase in T>C SNPs (the potential result of inadvertent, off-target ABE) (**figure 4B; supplementary figure 4**). We did not observe an increased number of mutations in highly transcribed regions, implying that the TadA fusion proteins did not cause mutations in single-stranded DNA segments, as may be present during transcription (**figure 4C**). The main contributors to the total number of mutations in the corrected organoid lines were signature 1 and 18, previously described to be caused by in vivo generated cell division-related mutations and in vitro generated oxidative stress-related mutations, respectively³⁵. The mutational landscape of our SpCas9- and xCas9-ABE-repaired clones resulted from a combination of these two phenomena, as shown by a comparison to both in vivo (blood vs propagated clone) and in vitro (propagated clone vs subclone) WGS samples of the small and large intestine (**figure 4D**). Finally, we confirmed the absence of known oncogenic mutation by comparison to a list of tumor suppressors and oncogenes extracted from COSMIC³⁸, further supporting the safety of ABE (**supplementary tables 4A and 4B**).

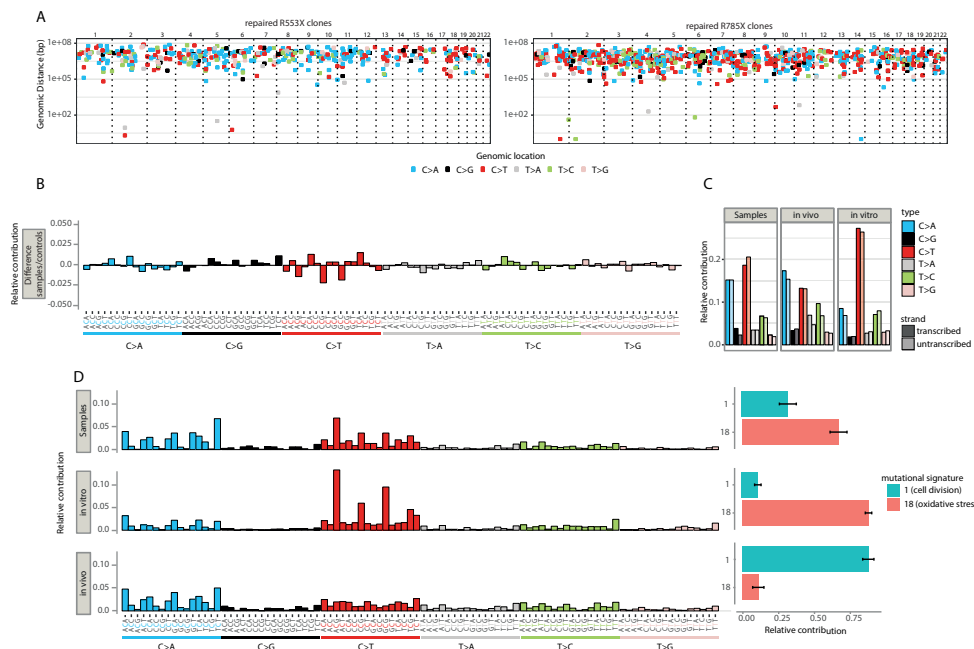


Figure 4: Off-target analysis of adenine base editors.

(a) Rainfall plots of repaired R553X and R785X clonal organoid lines. Every identified mutation is indicated with a dot (color according to mutation-type) and are ordered on the x axis from chromosome 1 to chromosome 22. The Y-axes shows the distance between each mutation and the one prior to it (the genomic distance) and is plotted on a log scale. (b) The mutational signature analysis, showed by the difference of the relative contribution of context-dependent mutation types between the repaired organoid lines ($n=6$) and their respective unrepaired controls. The X-axis shows all 96 context-dependent mutation types, a combination of the base substitution and its neighboring bases. The Y-axis shows the relative contribution of each context-dependent mutation type. (c) Relative contribution of mutations in our samples occurring on transcribed or un-transcribed regions in the genome compared to in vitro and in vivo acquired WGS datasets. The dark colored bars refer to the transcribed regions while the light colored bars refer to the untranscribed regions. Mutational signature analysis of repaired organoid lines ($n=6$) compared to an *in vitro* ($n=6$) and *in vivo* ($n=6$) dataset, and the relative contribution of the observed mutational signatures (1 and 18) in each dataset (d).

The current study demonstrates the feasibility of selective on-target base editing using ABE in human adult stem cells derived from patients with an inherited disease. A large biobank capturing the broad diversity of CF mutations in the Dutch population was critical to this exploration. The biobank has been established for diagnostic purposes of rare CF cases and therefore -to some extent- overrepresents infrequent CFTR alleles. We have investigated the feasibility of performing ABE with two different versions of this technology. Our study demonstrates that xCas9-ABE (with a 'relaxed' PAM sequence) can be applied effectively in human adult stem cells, emphasizing its clinical potential and applicability in the genetic repair of other inherited diseases. Functional repair of CFTR was obtained in rectal- and airway-derived organoids, while no genome-wide off-target effects could be detected, important for further development of ABEs. We have seen that editing efficiencies vary, depending on Cas9 and sgRNA usage, with a maximum of 9,3%.

CHAPTER 6

As it has been shown that 10% of residual CFTR function is associated with mild disease, this is within clinically relevant levels^{39,40}. Furthermore, as we did not detect any genome-wide off-targets using either SpCas9-ABE or xCas9-ABE, multiple consecutive ABE treatments could be used to increase editing efficiencies of xCas9-ABE without any adverse off-target effects. It should be noted, though that to date, efficient *in vivo* delivery of the Cas9 genome editing apparatus in humans has been challenging. Taken together, our analyses extend observations on the fidelity of ABEs in rice³⁶ and mouse³⁷ to the correction of disease-causing mutations in human stem cells.

ACKNOWLEDGEMENTS

This work was supported by the NWO building blocks of life project: Cell dynamics within lung and intestinal organoids (737.016.009), CRUK Specificancer (C6307/A29058) and grants of the Dutch Cystic Fibrosis Foundation (NCFS) as part of the HIT-CF Program and the Dutch Health Organization ZonMw, the Netherlands. Furthermore, we would like to thank the FACS facility of the Princes Maxima Centre, Utrecht, The Netherlands, for allowing us to perform sorting and analysis experiments. S.Y. Graeber is participant in the BIH-Charité Clinician Scientist Program funded by the Charité – Universitätsmedizin Berlin and the Berlin institute of Health.

AUTHOR CONTRIBUTIONS

Conceptualization, M.H.G., E.d.P., J.M.B. and H.C.; Base-editing experiments, M.H.G. and E.d.P.; Writing – original draft, M.H.G., E.d.P.; Writing – Review & Editing, M.H.G., E.d.P., J.M., H.M.J., K.M.d.W-d.G., J.M.B. and H.C.; Supervision, J.M.B. and H.C.; Fluid secretion- & biochemical assays, M.H.G., E.d.P., F.M.M.; Whole genome sequencing experiments and analysis; M.H.G., E.d.P., R.O. and R.v.B.; Tissue harvesting and biobanking, P.v.M., G. B., K.M.d.W-d.G, S.M, D.M., B.L.A, J.M., S.F.B., H.M.J., M.A.M., S.G., and C.K.v.d.E.; Tissue culturing, M.H.G., E.d.P., E.K., S.W.F.S., J.E.B.; Funding acquisition, J.M.B. and H.C.

DECLARATION OF INTERESTS

J.M.B. is an inventor on patent(s) related to the FIS-assay and received financial royalties from 2017 onward. J.M.B report receiving research grant(s) and consultancy fees from various industries, including Vertex Pharmaceuticals, Proteostasis Therapeutics, Eloxx Pharmaceuticals, Teva Pharmaceutical Industries and Galapagos outside the submitted work. H.C.holds several patents on organoid technology. Their application numbers, followed by their publication numbers (if applicable), are as follows: PCT/NL2008/050543, WO2009/022907; PCT/NL2010/000017, WO2010/090513; PCT/IB2011/002167, WO2012/014076; PCT/IB2012/052950, WO2012/168930; PCT/EP2015/060815, WO2015/173425; PCT/EP2015/077990, WO2016/083613; PCT/EP2015/077988, WO2016/083612; PCT/EP2017/054797, WO2017/149025; PCT/EP2017/065101, WO2017/220586; PCT/EP2018/086716, n/a; and GB1819224.5, n/a.

DATA AND CODE AVAILABILITY

All software tools can be found online (see Key Resources Table). The whole genome sequencing datasets generated during this study are available at European Genome-Phenome Archive, EGAS00001003951.

LEAD CONTACT AND MATERIALS AVAILABILITY

Further information and requests for reagents may be directed to, and will be fulfilled by the corresponding author H. Clevers (h.clevers@hubrecht.eu).

Genetically modified organoid lines generated in this study have been deposited to the UMCU biobank and are governed by Dr. J.M. Beekman in collaboration with the principle investigator that shipped the biopsy to UMCU.

REFERENCES

1. Sosnay, P. R. et al. Defining the disease liability of variants in the cystic fibrosis transmembrane conductance regulator gene. *Nat. Genet.* 45, 1160–1167 (2013).
2. Keating, D. et al. VX-445–Tezacaftor–Ivacaftor in Patients with Cystic Fibrosis and One or Two Phe508del Alleles. *N. Engl. J. Med.* 379, 1612–1620 (2018).
3. Ramsey, B. W. et al. A CFTR Potentiator in Patients with Cystic Fibrosis and the G551D Mutation. *N. Engl. J. Med.* 365, 1663–1672 (2011).
4. Sato, T. et al. Long-term Expansion of Epithelial Organoids From Human Colon, Adenoma, Adenocarcinoma, and Barrett's Epithelium. *Gastroenterology* 141, 1762–1772 (2011).
5. Schwank, G. et al. Functional repair of CFTR by CRISPR/Cas9 in intestinal stem cell organoids of cystic fibrosis patients. *Cell Stem Cell* 13, 653–658 (2013).
6. de Winter-De Groot, K. M. et al. Stratifying infants with cystic fibrosis for disease severity using intestinal organoid swelling as a biomarker of CFTR function. *Eur. Respir. J.* 52, (2018).
7. Berkers, G. et al. Rectal Organoids Enable Personalized Treatment of Cystic Fibrosis. *Cell Rep.* 26, 1701–1708.e3 (2019).
8. Dekkers, J. F. et al. A functional CFTR assay using primary cystic fibrosis intestinal organoids. *Nat. Med.* 19, 939–945 (2013).
9. Dekkers, J. F. et al. Characterizing responses to CFTR-modulating drugs using rectal organoids derived from subjects with cystic fibrosis. *Sci. Transl. Med* 8, 344–84 (2016).
10. Cho, S. W. et al. Analysis of off-target effects of CRISPR/Cas-derived RNA-guided endonucleases and nickases. *Genome Res.* 24, 132–141 (2014).
11. Fu, Y. et al. High-frequency off-target mutagenesis induced by CRISPR-Cas nucleases in human cells. *Nat. Biotechnol.* 31, 822–826 (2013).
12. Kosicki, M., Tomberg, K. & Bradley, A. Repair of double-strand breaks induced by CRISPR–Cas9 leads to large deletions and complex rearrangements. *Nat. Biotechnol.* 36, (2018).
13. Pattanayak, V. et al. High-throughput profiling of off-target DNA cleavage reveals RNA-programmed Cas9 nuclease specificity. *Nat. Biotechnol.* 31, 839–843 (2013).
14. Gaudelli, N. M. et al. Programmable base editing of T to G C in genomic DNA without DNA cleavage. *Nature* 551, 464–471 (2017).
15. Koblan, L. W. et al. Improving cytidine and adenine base editors by expression optimization and ancestral reconstruction. *Nat. Biotechnol.* 36, 843–848 (2018).
16. Komor, A. C., Kim, Y. B., Packer, M. S., Zuris, J. A. & Liu, D. R. Programmable editing of a target base in genomic DNA without double-stranded DNA cleavage. *Nature* 533, 420–424 (2016).
17. Zafra, M. P. et al. Optimized base editors enable efficient editing in cells, organoids and mice. *Nat. Biotechnol.* 36, 888–896 (2018).
18. Rees, H. A. & Liu, D. R. Base editing: precision chemistry on the genome and transcriptome of living cells. *nat rev Genet.* 19, 770–788 (2018).
19. Jinek, M. et al. A Programmable Dual-RNA–Guided DNA endonuclease in adaptive bacterial immunity. *Science* (80-.). 337, 816–822 (2012).
20. Mali, P. et al. RNA-Guided Human Genome Engineering via Cas9. *Science* (80-.). 823–827 (2013).
21. Hu, J. H. et al. Evolved Cas9 variants with broad PAM compatibility and high DNA specificity. *Nature* 556, 57–63 (2018).
22. Noda, T. et al. Engineered CRISPR-Cas9 nuclease with expanded targeting space. *Science* (80-.). 361, 1259–1262 (2018).

23. Chen, K. G., Zhong, P., Zheng, W. & Beekman, J. M. Pharmacological analysis of CFTR variants of cystic fibrosis using stem cell-derived organoids. *Drug Discov. Today* 00, (2019).
24. Mou, H. et al. Dual SMAD signaling inhibition enables long-term expansion of diverse epithelial basal cells. 19, 217–231 (2016).
25. Sachs, N. et al. Long-term expanding human airway organoids for disease modeling. *EMBO J.* 38, e100300 (2019).
26. Fujii, M., Matano, M., Nanki, K. & Sato, T. Efficient genetic engineering of human intestinal organoids using electroporation. *Nat. Protoc.* 10, 1474–1485 (2015).
27. Andersson-Rolf, A. et al. One-step generation of conditional and reversible gene knockouts. *Nat. Methods* 14, 287–289 (2017).
28. Hu, H. et al. Long-Term Expansion of Functional Mouse and Human Hepatocytes as 3D Organoids. *Cell* 175, 1591–1606.e19 (2018).
29. Li, H. & Durbin, R. Fast and accurate long-read alignment with Burrows-Wheeler transform. *Bioinformatics* 26, 589–595 (2010).
30. Depristo, M. A. et al. A framework for variation discovery and genotyping using next-generation DNA sequencing data. *Nat. Genet.* 43, 491–501 (2011).
31. Blokzijl, F. et al. Tissue-specific mutation accumulation in human adult stem cells during life. *Nature* 538, 260–264 (2016).
32. Jager, M. et al. Measuring mutation accumulation in single human adult stem cells by whole-genome sequencing of organoid cultures. *Nat. Protoc.* 13, 59–78 (2018).
33. Blokzijl, F., Janssen, R., van Boxtel, R. & Cuppen, E. MutationalPatterns: Comprehensive genome-wide analysis of mutational processes. *Genome Med.* 10, 1–11 (2018).
34. Bae, S., Park, J. & Kim, J. S. Cas-OFFinder: A fast and versatile algorithm that searches for potential off-target sites of Cas9 RNA-guided endonucleases. *Bioinformatics* 30, 1473–1475 (2014).
35. Alexandrov, L. B. et al. Signatures of mutational processes in human cancer. *Nature* 500, 415–21 (2013).
36. Jin, S. et al. Cytosine, but not adenine, base editors induce genome-wide off-target mutations in rice. *Science* (80-.). 364, 292–295 (2019).
37. Zuo, E. et al. Cytosine base editor generates substantial off-target single-nucleotide variants in mouse embryos. *Science* (80-.). 292, eaav9973 (2019).
38. Forbes, S. A. et al. COSMIC: Somatic cancer genetics at high-resolution. *Nucleic Acids Res.* 45, D777–D783 (2017).
39. Ferec, C. & Cutting, G. R. Assessing the disease-liability of mutations in CFTR. *Cold Spring Harb. Perspect. Med.* 2, 1–13 (2012).
40. Green, D. M. et al. Mutations that permit residual CFTR function delay acquisition of multiple respiratory pathogens in CF patients. *Respir. Res.* 11, 140 (2010).

SUPPLEMENTARY INFORMATION

SUPPLEMENTARY TABLES

Patient code	Allele 1 - Protein name	Allele 1 - Mutation type	Allele 1 - cDNA name	Allele 1 - SNP reference	Allele 2 - Protein name	Allele 2 - Mutation type	Allele 2 - cDNA name	Allele 2 - SNP reference
HUB-02-D2-001	F508del	ins/del	c.1521_1523delCTT	rs113993960	A455E	missense	c.1364C>A	rs74551128
HUB-02-D2-002	F508del	ins/del	c.1521_1523delCTT	rs113993960	F508del	ins/del	c.1521_1523delCTT	rs113993960
HUB-02-D2-003	F508del	ins/del	c.1521_1523delCTT	rs113993960	711+1G>T	splice	c.579+1G>T	rs77188391
HUB-02-D2-004	F508del	ins/del	c.1521_1523delCTT	rs113993960	R117H>T	missense	c.[350G>A;1210?12[7]]	rs78655421 (-7)
HUB-02-D2-005	1677delta	ins/del	c.1545_1546delTA	rs121908776	IVS16+1G>A >A(3120+1G>A)	splice	c.2988+1G>A	rs75096551
HUB-02-D2-006	F508del	ins/del	c.1521_1523delCTT	rs113993960	F508del	ins/del	c.1521_1523delCTT	rs113993960
HUB-02-D2-007	F508del	ins/del	c.1521_1523delCTT	rs113993960	F508del	ins/del	c.1521_1523delCTT	rs113993960
HUB-02-D2-008	F508del	ins/del	c.1521_1523delCTT	rs113993960	A455E	missense	c.1364C>A	rs74551128
HUB-02-D2-009	F508del	ins/del	c.1521_1523delCTT	rs113993960	A455E	missense	c.1364C>A	rs74551128
HUB-02-D2-010	F508del	ins/del	c.1521_1523delCTT	rs113993960	F508del	ins/del	c.1521_1523delCTT	rs113993960
HUB-02-D2-012	F508del	ins/del	c.1521_1523delCTT	rs113993960	S1251N	missense	c.3752G>A	rs74503330
HUB-02-D2-013	A455E	missense	c.1364C>A	rs74551128	E60X	nonsense	c.178G>T	rs77284892
HUB-02-D2-014	F508del	ins/del	c.1521_1523delCTT	rs113993960	G1249R	missense	c.3745G>A	rs397508602

Patient code	Allele 1 - Protein name	Allele 1 - Mutation type	Allele 1 - cDNA name	Allele 1 - SNP reference	Allele 1 - Protein name	Allele 2 - Mutation type	Allele 2 - cDNA name	Allele 2 - SNP reference
HUB-02-D2-015	F508del	ins/del	c.1521_1523delCTT	rs113993960	A455E	missense	c.1364C>A	rs74551128
HUB-02-D2-016	F508del	ins/del	c.1521_1523delCTT	rs113993960	F508del	ins/del	c.1521_1523delCTT	rs113993960
HUB-02-D2-017	F508del	ins/del	c.1521_1523delCTT	rs113993960	F508del	ins/del	c.1521_1523delCTT	rs113993960
HUB-02-D2-018	F508del	ins/del	c.1521_1523delCTT	rs113993960	F508del	ins/del	c.1521_1523delCTT	rs113993960
HUB-02-D2-019	F508del	ins/del	c.1521_1523delCTT	rs113993960	F508del	ins/del	c.1521_1523delCTT	rs113993960
HUB-02-D2-020	F508del	ins/del	c.1521_1523delCTT	rs113993960	F508del	ins/del	c.1521_1523delCTT	rs113993960
HUB-02-D2-021	F508del	ins/del	c.1521_1523delCTT	rs113993960	A455E	missense	c.1364C>A	rs74551128
HUB-02-D2-022	1717-1G>A	splice	c.1585-1G>A	rs76713772	2183AA>G	ins/del	c.2051_2052delAAinsG	rs121908799
HUB-02-D2-023	F508del	ins/del	c.1521_1523delCTT	rs113993960	A455E	missense	c.1364C>A	rs74551128
HUB-02-D2-024	F508del	ins/del	c.1521_1523delCTT	rs113993960	R117H	missense	c.350G>A	rs78655421
HUB-02-D2-025	F508del	ins/del	c.1521_1523delCTT	rs113993960	F508del	ins/del	c.1521_1523delCTT	rs113993960
HUB-02-D2-027	F508del	ins/del	c.1521_1523delCTT	rs113993960	F508del	ins/del	c.1521_1523delCTT	rs113993960
HUB-02-D2-028	R334W	missense	c.1000C>T	rs121909011	R764X	nonsense	c.2290C>T	rs121908810
HUB-02-D2-029	1811+1G>C	splice	c.1679+1G>C	rs397508263	1811+1G>C	splice	c.1679+1G>C	rs397508263
HUB-02-D2-030	I507del	ins/del	c.1519_1521delATC	rs121908745	SPLICE2	splice	c.4242+2T>G	NA

Patient code	Allele 1 - Protein name	Allele 1 - Mutation type	Allele 1 - cDNA name	Allele 1 - SNP reference	Allele 1 - Protein name	Allele 2 - Mutation type	Allele 2 - cDNA name	Allele 2 - SNP reference
HUB-02-D2-031	WT	wildtype	WT	WT	WT	wildtype	WT	WT
HUB-02-D2-032	WT	wildtype	WT	WT	WT	wildtype	WT	WT
HUB-02-D2-034	F508del	ins/del	c.1521_1523delCTT	rs113993960	F508del	ins/del	c.1521_1523delCTT	rs113993960
HUB-02-D2-037	F508del	ins/del	c.1521_1523delCTT	rs113993960	Y1092X	nonsense	c.3276C>A or c.3276C>G	rs121908761
HUB-02-D2-038	F508del	ins/del	c.1521_1523delCTT	rs113993960	R1162X	nonsense	c.3484C>T	rs74767530
HUB-02-D2-039	F508del	ins/del	c.1521_1523delCTT	rs113993960	W1282X	nonsense	c.3846G>A	rs77010898
HUB-02-D2-040	F508del	ins/del	c.1521_1523delCTT	rs113993960	F508del	ins/del	c.1521_1523delCTT	rs113993960
HUB-02-D2-041	R553X	nonsense	c.1657C>T	r574597325	SPLICE3	splice	c.4375-3T>A	NA
HUB-02-D2-042	F508del	ins/del	c.1521_1523delCTT	rs113993960	A455E	missense	c.1364C>A	rs74551128
HUB-02-D2-043	F508del	ins/del	c.1521_1523delCTT	rs113993960	G551D	missense	c.1632G>A	rs75527207
HUB-02-D2-044	F508del	ins/del	c.1521_1523delCTT	rs113993960	F508del	ins/del	c.1521_1523delCTT	rs113993960
HUB-02-D2-045	F508del	ins/del	c.1521_1523delCTT	rs113993960	F508del	ins/del	c.1521_1523delCTT	rs113993960
HUB-02-D2-046	F508del	ins/del	c.1521_1523delCTT	rs113993960	W1282X/R1283M	nonsense/missense	c.3846G>A	rs77010898
HUB-02-D2-047	F508del	ins/del	c.1521_1523delCTT	rs113993960	F508del	ins/del	c.1521_1523delCTT	rs113993960
HUB-02-D2-048	F508del	ins/del	c.1521_1523delCTT	rs113993960	G461R	missense	c.1381G>A	NA

Patient code	Allele 1 - Protein name	Allele 1 - Mutation type	Allele 1 - cDNA name	Allele 1 - SNP reference	Allele 1 - Protein name	Allele 2 - Mutation type	Allele 2 - cDNA name	Allele 2 - SNP reference
HUB-02-D2-049	F508del	ins/del	c.1521_1523delCTT	rs113993960	WT	wildtype	WT	WT
HUB-02-D2-050	F508del	ins/del	c.1521_1523delCTT	rs113993960	WT	wildtype	WT	WT
HUB-02-D2-051	F508del	ins/del	c.1521_1523delCTT	rs113993960	R1162X	nonsense	c.3484C>T	rs74767530
HUB-02-D2-052	F508del	ins/del	c.1521_1523delCTT	rs113993960	R1162X	nonsense	c.3484C>T	rs74767530
HUB-02-D2-053	S1251N	missense	c.3752G>A	rs74503330	UNK	unknown	UNK	UNK
HUB-02-D2-054	F508del	ins/del	c.1521_1523delCTT	rs113993960	F508del	ins/del	c.1521_1523delCTT	rs113993960
HUB-02-D2-055	F508del	ins/del	c.1521_1523delCTT	rs113993960	G628R	missense	c.1882G>A or c.1882G>C	rs397508316
HUB-02-D2-056	F508del	ins/del	c.1521_1523delCTT	rs113993960	E730X	nonsense	c.2188G>A	rs113993960
HUB-02-D2-057_I	F508del	ins/del	c.1521_1523delCTT	rs113993960	S1251N	missense	c.3752G>A	rs74503330
HUB-02-D2-058	F508del	ins/del	c.1521_1523delCTT	rs113993960	R347P	missense	c.1040G>C	rs77932196
HUB-02-D2-059_I	F508del	ins/del	c.1521_1523delCTT	rs113993960	2789+5G>A	splice	c.2657+5G>A	rs80224560
HUB-02-D2-061_I	F508del	ins/del	c.1521_1523delCTT	rs113993960	F508del	ins/del	c.1521_1523delCTT	rs113993960
HUB-02-D2-063	711+1G>T	splice	c.579+1G>T	rs77188391	711+1G>T	splice	c.579+1G>T	rs77188391
HUB-02-D2-064	F508del	ins/del	c.1521_1523delCTT	rs113993960	F103S	missense	c.3101T>C	NA
HUB-02-D2-065	F508del	ins/del	c.1521_1523delCTT	rs113993960	3272-26A>G	splice	c.3140-26A>G	rs76151804

Patient code	Allele 1 - Protein name	Allele 1 - Mutation type	Allele 1 - cDNA name	Allele 1 - SNP reference	Allele 2 - Protein name	Allele 2 - Mutation type	Allele 2 - cDNA name	Allele 2 - SNP reference
HUB-02-D2-066	F508del	ins/del	c.1521_1523delCTT	rs113993960	1717_1G>A	splice	c.1585_1G>A	rs76713772
HUB-02-D2-067	F508del	ins/del	c.1521_1523delCTT	rs113993960	N1303K	missense	c.3909C>G	rs80034486
HUB-02-D2-068	F508del	ins/del	c.1521_1523delCTT	rs113993960	A455E	missense	c.1364C>A	rs74551128
HUB-02-D2-069	F508del	ins/del	c.1521_1523delCTT	rs113993960	A455E	missense	c.1364C>A	rs74551128
HUB-02-D2-070	F508del	ins/del	c.1521_1523delCTT	rs113993960	A455E	missense	c.1364C>A	rs74551128
HUB-02-D2-071	F508del	ins/del	c.1521_1523delCTT	rs113993960	3272_26A>G	splice	c.1364C>A	rs76151804
HUB-02-D2-072	F508del	ins/del	c.1521_1523delCTT	rs113993960	F508del	ins/del	c.1521_1523delCTT	rs113993960
HUB-02-D2-073	F508del	ins/del	c.1521_1523delCTT	rs113993960	F508del	ins/del	c.1521_1523delCTT	rs113993960
HUB-02-D2-074	F508del	ins/del	c.1521_1523delCTT	rs113993960	F508del	ins/del	c.1521_1523delCTT	rs113993960
HUB-02-D2-075	F508del	ins/del	c.1521_1523delCTT	rs113993960	F508del	ins/del	c.1521_1523delCTT	rs113993960
HUB-02-D2-077	F508del	ins/del	c.1521_1523delCTT	rs113993960	R347P	missense	c.1040G>C	rs77932196
HUB-02-D2-078	F508del	ins/del	c.1521_1523delCTT	rs113993960	I927P	missense	c.2780T>C	rs397508435
HUB-02-D2-079	F508del	ins/del	c.1521_1523delCTT	rs113993960	F508del	ins/del	c.1521_1523delCTT	rs113993960
HUB-02-D2-080	R117H	missense	c.350G>A	r578655421	UNK	unknow	UNK	UNK
HUB-02-D2-082	F508del	ins/del	c.1521_1523delCTT	rs113993960	F508del	ins/del	c.1521_1523delCTT	rs113993960

Patient code	Allele 1 - Protein name	Allele 1 - Mutation type	Allele 1 - cDNA name	Allele 1 - SNP reference	Allele 1 - Protein name	Allele 2 - Mutation type	Allele 2 - cDNA name	Allele 2 - SNP reference
HUB-02-D2-083	F508del	ins/del	c.1521_1523delCTT	rs113993960	F508del	ins/del	c.1521_1523delCTT	rs113993960
HUB-02-D2-084	F508del	ins/del	c.1521_1523delCTT	rs113993960	G550X	nonsense	c.1648G>T	rs397508247
HUB-02-D2-085	F508del	ins/del	c.1521_1523delCTT	rs113993960	F508del	ins/del	c.1521_1523delCTT	rs113993960
HUB-02-D2-086	F508del	ins/del	c.1521_1523delCTT	rs113993960	CFTRdel17a.17b	ins/del	c.(2988+1_2989-1)_ (3367+1_3368-1)de[el]	NA
HUB-02-D2-087	711+1G>T	splice	c.579+1G>T	rs77188391	S1251N	missense	c.3752G>A	rs74503330
HUB-02-D2-090	F508del	ins/del	c.1521_1523delCTT	rs113993960	F508del	ins/del	c.1521_1523delCTT	rs113993960
HUB-02-D2-092	F508del	ins/del	c.1521_1523delCTT	rs113993960	S1251N	missense	c.3752G>A	rs74503330
HUB-02-D2-093	F508del	ins/del	c.1521_1523delCTT	rs113993960	Y1092X	nonsense	c.3276C>A or c.3276C>G	rs121908761
HUB-02-D2-095	F508del	ins/del	c.1521_1523delCTT	rs113993960	S1251N	missense	c.3752G>A	rs74503330
HUB-02-D2-096	F508del	ins/del	c.1521_1523delCTT	rs113993960	S1251N	missense	c.3752G>A	rs74503330
HUB-02-D2-097	F508del	ins/del	c.1521_1523delCTT	rs113993960	F508del	ins/del	c.1521_1523delCTT	rs113993960
HUB-02-D2-099	F508del	ins/del	c.1521_1523delCTT	rs113993960	S1251N	missense	c.3752G>A	rs74503330
HUB-02-D2-100	F508del	ins/del	c.1521_1523delCTT	rs113993960	F508del	ins/del	c.1521_1523delCTT	rs113993960
HUB-02-D2-101	F508del	ins/del	c.1521_1523delCTT	rs113993960	S1251N	missense	c.3752G>A	rs74503330
HUB-02-D2-103	F508del	ins/del	c.1521_1523delCTT	rs113993960	S1251N	missense	c.3752G>A	rs74503330

Patient code	Allele 1 - Protein name	Allele 1 - Mutation type	Allele 1 - cDNA name	Allele 1 - SNP reference	Allele 1 - Protein name	Allele 2 - Mutation type	Allele 2 - cDNA name	Allele 2 - SNP reference
HUB-02-D2-104	R334W	missense	c.100C>T	rs121909011	R334W	missense	c.100C>T	rs121909011
HUB-02-D2-107	R553X	nonsense	c.1657C>T	rs74597325	D1152H	missense	c.3454G>C	rs75541969
HUB-02-D2-112	F508del	ins/del	c.1521_1523delCTT	rs113993960	G542X	nonsense	c.1624G>T	rs113993959
HUB-02-D2-113	F508del	ins/del	c.1521_1523delCTT	rs113993960	F508del	ins/del	c.1521_1523delCTT	rs113993960
HUB-02-D2-114	F508del	ins/del	c.1521_1523delCTT	rs113993960	G85E	missense	c.254G>A	rs75961395
HUB-02-D2-115	F508del	ins/del	c.1521_1523delCTT	rs113993960	2184delA	ins/del	c.2032delA	rs121908746
HUB-02-D2-116	1811+1G>C	splice	c.1679+1G>C	rs397508263	1811+1G>C	splice	c.1679+1G>C	rs397508263
HUB-02-D2-118	F508del	ins/del	c.1521_1523delCTT	rs113993960	G550X	nonsense	c.1648G>T	rs397508247
HUB-02-D2-119	F508del	ins/del	c.1521_1523delCTT	rs113993960	W846X	nonsense	c.2537G>A	rs397508393 or rs267606722
HUB-02-D2-121	G542X	nonsense	c.1624G>T	rs113993959	G542X	nonsense	c.1624G>T	rs113993959
HUB-02-D2-122	R117H>T	missense	c.[350G>A;1210?1217]	rs78655421 (-7)	UNK	unknown	UNK	UNK
HUB-02-D2-126	R1162X	nonsense	c.3484C>T	rs74767530	3659delC	ins/del	c.3528delC	rs121908747
HUB-02-D2-128	R553X	nonsense	c.1657C>T	rs74597325	UNK	unknown	UNK	UNK
HUB-02-D2-130	N1303K	missense	c.3909C>G	rs8034486	G550X	nonsense	c.1648G>T	rs397508247
HUB-02-D2-132	F508del	ins/del	c.1521_1523delCTT	rs113993960	1294del7	ins/del	c.1162_1168delACGACTA	rs397508169

Patient code	Allele 1 - Protein name	Allele 1 - Mutation type	Allele 1 - cDNA name	Allele 1 - SNP reference	Allele 1 - Protein name	Allele 2 - Mutation type	Allele 2 - cDNA name	Allele 2 - SNP reference
HUB-02-D2-134	F508del	ins/del	c.1521_1523delCTT	rs113993960	F508del	ins/del	c.1521_1523delCTT	rs113993960
HUB-02-D2-136	A455E	missense	c.1364C>A	rs74551128	1496G>A /3659delC	missense/ ins/del	c.3528delC	rs121908747
HUB-02-D2-137	F508del	ins/del	c.1521_1523delCTT	rs113993960	711+1G>T	splice	c.579+1G>T	rs77188391
HUB-02-D2-138	F508del	ins/del	c.1521_1523delCTT	rs113993960	3849+5G>T	splice	c.3717+5G>T	NA
HUB-02-D2-139	F508del	ins/del	c.1521_1523delCTT	rs113993960	F508del	ins/del	c.1521_1523delCTT	rs113993960
HUB-02-D2-140	2789+5G>A	splice	c.2657+5G>A	rs80224560	UNK	unknown	UNK	UNK
HUB-02-D2-141	F508del	ins/del	c.1521_1523delCTT	rs113993960	Y1092X	nonsense	c.3276C>A or c.3276C>G	rs121908761
HUB-02-D2-142	F508del	ins/del	c.1521_1523delCTT	rs113993960	CFTRdel19.20	ins/del	ins/del	NA
HUB-02-D2-143	F508del	ins/del	c.1521_1523delCTT	rs113993960	Y1092X	nonsense	c.3276C>A or c.3276C>G	rs121908761
HUB-02-D2-145	G542X	nonsense	c.1624G>T	rs113993959	W1282X	nonsense	c.3846G>A	rs77010898
HUB-02-D2-146	2789+5G>T	splice	NA	NA	711+1G>T	splice	c.579+1G>T	rs77188391
HUB-02-D2-147	F508del	ins/del	c.1521_1523delCTT	rs113993960	S18I	missense	c.53G>T	NA
HUB-02-D2-149	F508del	ins/del	c.1521_1523delCTT	rs113993960	2184delA	ins/del	c.2032delA	rs121908746
HUB-02-D2-150	F508del	ins/del	c.1521_1523delCTT	rs113993960	A455E	missense	c.1364C>A	rs74551128
HUB-02-D2-151	F508del	ins/del	c.1521_1523delCTT	rs113993960	2184insA	ins/del	c.2052_2053insA	rs121908786

Patient code	Allele 1 - Protein name	Allele 1 - Mutation type	Allele 1 - cDNA name	Allele 1 - SNP reference	Allele 1 - Protein name	Allele 2 - Mutation type	Allele 2 - cDNA name	Allele 2 - SNP reference
HUB-02-D2-152	UNK	unknown	UNK	UNK	UNK	unknown	UNK	UNK
HUB-02-D2-153	F508del	ins/del	c.1521_1523delCTT	rs113993960	1078delT	ins/del	c.948delT	rs121908744
HUB-02-D2-154	UNK	unknown	UNK	UNK	UNK	unknown	UNK	UNK
HUB-02-D2-155	R1066H	missense	c.3197G>A	rs121909019	CFTRdel e2.3	ins/del	c.54_5940_273+10250del21kb	NA
HUB-02-D2-156	F508del	ins/del	c.1521_1523delCTT	rs113993960	Y109D	missense	c.325T>G	NA
HUB-02-D2-157	F508del	ins/del	c.1521_1523delCTT	rs113993960	S489X	nonsense	c.1466C>A	rs397508211
HUB-02-D2-158	F508del	ins/del	c.1521_1523delCTT	rs113993960	1813insC	ins/del	c.1681_1682insC	NA
HUB-02-D2-159	F508del	ins/del	c.1521_1523delCTT	rs113993960	4382delA	ins/del	c.4251delA	rs397508706
HUB-02-D2-161	F508del	ins/del	c.1521_1523delCTT	rs113993960	R74P	missense	c.224G>C	NA
HUB-02-D2-162	WT	wildtype	WT	WT	WT	wildtype	WT	WT
HUB-02-D2-164	WT	wildtype	WT	WT	WT	wildtype	WT	WT
HUB-02-D2-165	F508del	ins/del	c.1521_1523delCTT	rs113993960	c.1725_1727del insAT	ins/del	NA	NA
HUB-02-D2-166	F508del	ins/del	c.1521_1523delCTT	rs113993960	394delTT	ins/del	c.262_263delTT	rs121908769
HUB-02-D2-167	A46D	missense	c.137C>A	rs151020603	A46D	missense	c.137C>A	rs151020603
HUB-02-D2-168	A46D	missense	c.137C>A	rs151020603	A46D	missense	c.137C>A	rs151020603

Patient code	Allele 1 - Protein name	Allele 1 - Mutation type	Allele 1 - cDNA name	Allele 1 - SNP reference	Allele 1 - Protein name	Allele 2 - Mutation type	Allele 2 - cDNA name	Allele 2 - SNP reference
HUB-02-D2-170	F508del	ins/del	c.1521_1523delCTT	rs113993960	UNK	unknown	UNK	UNK
HUB-02-D2-172	F508del	ins/del	c.1521_1523delCTT	rs113993960	Y849X	nonsense	c.2547C>A	rs397508394
HUB-02-D2-173	F508del	ins/del	c.1521_1523delCTT	rs113993960	2143delT	ins/del	c.2012delT	rs121908812
HUB-02-D2-176	F508del	ins/del	c.1521_1523delCTT	rs113993960	UNK	unknown	UNK	UNK
HUB-02-D2-178	F508del	ins/del	c.1521_1523delCTT	rs113993960	G550X	nonsense	c.1648G>T	rs397508247
HUB-02-D2-180	G542X	nonsense	c.1624G>T	rs113993959	R1066C	missense	c.3196C>T	rs78194216
HUB-02-D2-181	G542X	nonsense	c.1624G>T	rs113993959	R1066C	missense	c.3196C>T	rs78194216
HUB-02-D2-182	W1282X	nonsense	c.3846G>A	rs77010898	L927P	missense	c.2780T>C	rs397508435
HUB-02-D2-184	F508del	ins/del	c.1521_1523delCTT	rs113993960	Y1092X	nonsense	c.3276C>A or c.3276C>G	rs121908761
HUB-02-D2-186	Y849X	nonsense	c.2547C>A	rs397508394	2789+5G>A	splice	c.2657+5G>A	rs80224560
HUB-02-D2-188	1717-1G>A	splice	c.1585-1G>A	rs76713772	3905inst	ins/del	c.3773_3774insT	rs121908789
HUB-02-D2-189	R1066C	missense	c.3196C>T	rs78194216	R1066H	missense	c.3196C>T	rs78194216
HUB-02-D2-190	3849+1 0kbC>T	splice	c.3718-2477C>T	rs75039782	R347H	missense	c.1040G>A	rs77932196
HUB-02-D2-192	F508del	ins/del	c.1521_1523delCTT	rs113993960	CFTRdel2.3	ins/del	c.54_5940_273+10250del21kb	NA
HUB-02-D2-194	F508del	ins/del	c.1521_1523delCTT	rs113993960	R1066C	missense	c.3196C>T	rs78194216

Patient code	Allele 1 - Protein name	Allele 1 - Mutation type	Allele 1 - cDNA name	Allele 1 - SNP reference	Allele 1 - cDNA reference	Allele 2 - Protein name	Allele 2 - Mutation type	Allele 2 - cDNA name	Allele 2 - SNP reference
HUB-02-D2-195	F508del	ins/del	c.1521_1523delCTT	rs113993960	3849+10kbC>T	splice	c.3718-247T>T		rs75039782
HUB-02-D2-197	F508del	ins/del	c.1521_1523delCTT	rs113993960	UNK	unknown	UNK		UNK
HUB-02-D2-198	F508del	ins/del	c.1521_1523delCTT	rs113993960	A455E	missense	c.1364C>A		rs74551128
HUB-02-D2-200	F508del	ins/del	c.1521_1523delCTT	rs113993960	A455E	missense	c.1364C>A		rs74551128
HUB-02-D2-201	1078delT	ins/del	c.948delT	rs121908744	3272-26A>G	splice	c.3140-26A>G		rs76151804
HUB-02-D2-203	F508del	ins/del	c.1521_1523delCTT	rs113993960	A455E	missense	c.1364C>A		rs74551128
HUB-02-D2-204	E60X	nonsense	c.178G>T	rs77284892	A455E	missense	c.1364C>A		rs74551128
HUB-02-D2-205	WT	wildtype	WT	WT	WT	wildtype	WT		WT
HUB-02-D2-206	F508del	ins/del	c.1521_1523delCTT	rs113993960	F508del	ins/del	c.1521_1523delCTT		rs113993960
HUB-02-D2-207	W1282X	nonsense	c.3846G>A	rs77010898	W1282X	nonsense	c.3846G>A		rs77010898
HUB-02-D2-209	A455E	missense	c.1364C>A	rs74551128	1343delG	ins/del	c.1211delG		NA
HUB-02-D2-210	F508del	ins/del	c.1521_1523delCTT	rs113993960	A455E	missense	c.1364C>A		rs74551128
HUB-02-D2-211	F508del	ins/del	c.1521_1523delCTT	rs113993960	A455E	missense	c.1364C>A		rs74551128
HUB-02-D2-212	F508del	ins/del	c.1521_1523delCTT	rs113993960	G628R	missense	c.1882G>A or c.1882G>C		rs397508316
HUB-02-D2-213	F508del	ins/del	c.1521_1523delCTT	rs113993960	G550X	nonsense	c.1648G>T		rs397508247

Patient code	Allele 1 - Protein name	Allele 1 - Mutation type	Allele 1 - cDNA name	Allele 1 - SNP reference	Allele 1 - Protein name	Allele 2 - Mutation type	Allele 2 - cDNA name	Allele 2 - SNP reference
HUB-02-D2-215	F508del	ins/del	c.1521_1523delCTT	rs113993960	3659delC	ins/del	c.3528delC	rs121908747
HUB-02-D2-216	F508del	ins/del	c.1521_1523delCTT	rs113993960	R1066C	missense	c.3196C>T	rs78194216
HUB-02-D2-217	F508del	ins/del	c.1521_1523delCTT	rs113993960	CFTRdel17a.17b	ins/del	c.[2988+1_2989-1]_del (3367+1_3368-1)del	NA
HUB-02-D2-218	F508del	ins/del	c.1521_1523delCTT	rs113993960	F508del	ins/del	c.1521_1523delCTT	rs113993960
HUB-02-D2-222	F508del	ins/del	c.1521_1523delCTT	rs113993960	1717-1G>A	splice	c.1585-1G>A	rs76713772
HUB-02-D2-223	F508del	ins/del	c.1521_1523delCTT	rs113993960	4016insT	ins/del	c.3899dupT	rs397508631
HUB-02-D2-224	A455E	missense	c.1364C>A	rs74551128	(TG)13(T)5	other	c.[1210212[5];1210-34TG[13]]	NA
HUB-02-D2-225	F508del	ins/del	c.1521_1523delCTT	rs113993960	F508del	ins/del	c.1521_1523delCTT	rs113993960
HUB-02-D2-226	F508del	ins/del	c.1521_1523delCTT	rs113993960	G550X	nonsense	c.1648G>T	rs397508247
HUB-02-D2-228	F508del	ins/del	c.1521_1523delCTT	rs113993960	F508del	ins/del	c.1521_1523delCTT	rs113993960
HUB-02-D2-229_I	W1282X	nonsense	c.3846G>A	rs77010898	W1282X	nonsense	c.3846G>A	rs77010898
HUB-02-D2-232	F508del	ins/del	c.1521_1523delCTT	rs113993960	F508del	ins/del	c.1521_1523delCTT	rs113993960
HUB-02-D2-233	F508del	ins/del	c.1521_1523delCTT	rs113993960	F508del	ins/del	c.1521_1523delCTT	rs113993960
HUB-02-D2-234	F508del	ins/del	c.1521_1523delCTT	rs113993960	F508del	ins/del	c.1521_1523delCTT	rs113993960
HUB-02-D2-235	F508del	ins/del	c.1521_1523delCTT	rs113993960	F508del	ins/del	c.1521_1523delCTT	rs113993960

Patient code	Allele 1 - Protein name	Allele 1 - Mutation type	Allele 1 - cDNA name	Allele 1 - SNP reference	Allele 2 - Protein name	Allele 2 - Mutation type	Allele 2 - cDNA name	Allele 2 - SNP reference
HUB-02-D2-236	F508del	ins/del	c.1521_1523delCTT	rs113993960	A455E	missense	c.1364C>A	rs74551128
HUB-02-D2-237	F508del	ins/del	c.1521_1523delCTT	rs113993960	F508del	ins/del	c.1521_1523delCTT	rs113993960
HUB-02-D2-239	F508del	ins/del	c.1521_1523delCTT	rs113993960	F508del	ins/del	c.1521_1523delCTT	rs113993960
HUB-02-D2-240	F508del	ins/del	c.1521_1523delCTT	rs113993960	F508del	ins/del	c.1521_1523delCTT	rs113993960
HUB-02-D2-241	F508del	ins/del	c.1521_1523delCTT	rs113993960	F508del	ins/del	c.1521_1523delCTT	rs113993960
HUB-02-D2-243	F508del	ins/del	c.1521_1523delCTT	rs113993960	F508del	ins/del	c.1521_1523delCTT	rs113993960
HUB-02-D2-244.I	F508del	ins/del	c.1521_1523delCTT	rs113993960	F508del	ins/del	c.1521_1523delCTT	rs113993960
HUB-02-D2-245	F508del	ins/del	c.1521_1523delCTT	rs113993960	F508del	ins/del	c.1521_1523delCTT	rs113993960
HUB-02-D2-247	F508del	ins/del	c.1521_1523delCTT	rs113993960	F508del	ins/del	c.1521_1523delCTT	rs113993960
HUB-02-D2-248	F508del	ins/del	c.1521_1523delCTT	rs113993960	F508del	ins/del	c.1521_1523delCTT	rs113993960
HUB-02-D2-249	F508del	ins/del	c.1521_1523delCTT	rs113993960	F508del	ins/del	c.1521_1523delCTT	rs113993960
HUB-02-D2-250	F508del	ins/del	c.1521_1523delCTT	rs113993960	F508del	ins/del	c.1521_1523delCTT	rs113993960
HUB-02-D2-251	F508del	ins/del	c.1521_1523delCTT	rs113993960	F508del	ins/del	c.1521_1523delCTT	rs113993960
HUB-02-D2-252	F508del	ins/del	c.1521_1523delCTT	rs113993960	F508del	ins/del	c.1521_1523delCTT	rs113993960
HUB-02-D2-253	F508del	ins/del	c.1521_1523delCTT	rs113993960	F508del	ins/del	c.1521_1523delCTT	rs113993960

Patient code	Allele 1 - Protein name	Allele 1 - Mutation type	Allele 1 - cDNA name	Allele 1 - SNP reference	Allele 1 - Protein name	Allele 2 - Mutation type	Allele 2 - cDNA name	Allele 2 - SNP reference
HUB-02-D2-254	F508del	ins/del	c.1521_1523delCTT	rs113993960	F508del	ins/del	c.1521_1523delCTT	rs113993960
HUB-02-D2-255	F508del	ins/del	c.1521_1523delCTT	rs113993960	A455E	missense	c.1364C>A	rs74551128
HUB-02-D2-256	F508del	ins/del	c.1521_1523delCTT	rs113993960	F508del	ins/del	c.1521_1523delCTT	rs113993960
HUB-02-D2-257	F508del	ins/del	c.1521_1523delCTT	rs113993960	F508del	ins/del	c.1521_1523delCTT	rs113993960
HUB-02-D2-258	F508del	ins/del	c.1521_1523delCTT	rs113993960	F508del	ins/del	c.1521_1523delCTT	rs113993960
HUB-02-D2-259	F508del	ins/del	c.1521_1523delCTT	rs113993960	F508del	ins/del	c.1521_1523delCTT	rs113993960
HUB-02-D2-260	F508del	ins/del	c.1521_1523delCTT	rs113993960	F508del	ins/del	c.1521_1523delCTT	rs113993960
HUB-02-D2-261	F508del	ins/del	c.1521_1523delCTT	rs113993960	F508del	ins/del	c.1521_1523delCTT	rs113993960
HUB-02-D2-263	F508del	ins/del	c.1521_1523delCTT	rs113993960	A455E	missense	c.1521_1523delCTT	rs113993960
HUB-02-D2-264	F508del	ins/del	c.1521_1523delCTT	rs113993960	A455E	missense	c.1364C>A	rs74551128
HUB-02-D2-266	F508del	ins/del	c.1521_1523delCTT	rs113993960	F508del	ins/del	c.1521_1523delCTT	rs113993960
HUB-02-D2-267	F508del	ins/del	c.1521_1523delCTT	rs113993960	F508del	ins/del	c.1521_1523delCTT	rs113993960
HUB-02-D2-268	F508del	ins/del	c.1521_1523delCTT	rs113993960	F508del	ins/del	c.1521_1523delCTT	rs113993960
HUB-02-D2-269	F508del	ins/del	c.1521_1523delCTT	rs113993960	F508del	ins/del	c.1521_1523delCTT	rs113993960
HUB-02-D2-270	F508del	ins/del	c.1521_1523delCTT	rs113993960	F508del	ins/del	c.1521_1523delCTT	rs113993960

Patient code	Allele 1 - Protein name	Allele 1 - Mutation type	Allele 1 - cDNA name	Allele 1 - SNP reference	Allele 2 - Protein name	Allele 2 - Mutation type	Allele 2 - cDNA name	Allele 2 - SNP reference
HUB-02-D2-271	F508del	ins/del	c.1521_1523delCTT	rs113993960	F508del	ins/del	c.1521_1523delCTT	rs113993960
HUB-02-D2-272	F508del	ins/del	c.1521_1523delCTT	rs113993960	F508del	ins/del	c.1521_1523delCTT	rs113993960
HUB-02-D2-273	F508del	ins/del	c.1521_1523delCTT	rs113993960	F508del	ins/del	c.1521_1523delCTT	rs113993960
HUB-02-D2-274	F508del	ins/del	c.1521_1523delCTT	rs113993960	F508del	ins/del	c.1521_1523delCTT	rs113993960
HUB-02-D2-275	F508del	ins/del	c.1521_1523delCTT	rs113993960	F508del	ins/del	c.1521_1523delCTT	rs113993960
HUB-02-D2-276	F508del	ins/del	c.1521_1523delCTT	rs113993960	F508del	ins/del	c.1521_1523delCTT	rs113993960
HUB-02-D2-277	F508del	ins/del	c.1521_1523delCTT	rs113993960	F508del	ins/del	c.1521_1523delCTT	rs113993960
HUB-02-D2-280	F508del	ins/del	c.1521_1523delCTT	rs113993960	F508del	ins/del	c.1521_1523delCTT	rs113993960
HUB-02-D2-281	F508del	ins/del	c.1521_1523delCTT	rs113993960	F508del	ins/del	c.1521_1523delCTT	rs113993960
HUB-02-D2-282	F508del	ins/del	c.1521_1523delCTT	rs113993960	F508del	ins/del	c.1521_1523delCTT	rs113993960
HUB-02-D2-283	F508del	ins/del	c.1521_1523delCTT	rs113993960	F508del	ins/del	c.1521_1523delCTT	rs113993960
HUB-02-D2-284	F508del	ins/del	c.1521_1523delCTT	rs113993960	F508del	ins/del	c.1521_1523delCTT	rs113993960
HUB-02-D2-285	F508del	ins/del	c.1521_1523delCTT	rs113993960	F508del	ins/del	c.1521_1523delCTT	rs113993960
HUB-02-D2-286	F508del	ins/del	c.1521_1523delCTT	rs113993960	F508del	ins/del	c.1521_1523delCTT	rs113993960
HUB-02-D2-287	F508del	ins/del	c.1521_1523delCTT	rs113993960	F508del	ins/del	c.1521_1523delCTT	rs113993960

Patient code	Allele 1 - Protein name	Allele 1 - Mutation type	Allele 1 - cDNA name	Allele 1 - SNP reference	Allele 2 - Protein name	Allele 2 - Mutation type	Allele 2 - cDNA name	Allele 2 - SNP reference
HUB-02-D2-288	F508del	ins/del	c.1521_1523delCTT	rs113993960	F508del	ins/del	c.1521_1523delCTT	rs113993960
HUB-02-D2-289	F508del	ins/del	c.1521_1523delCTT	rs113993960	F508del	ins/del	c.1521_1523delCTT	rs113993960
HUB-02-D2-290	F508del	ins/del	c.1521_1523delCTT	rs113993960	F508del	ins/del	c.1521_1523delCTT	rs113993960
HUB-02-D2-291	F508del	ins/del	c.1521_1523delCTT	rs113993960	F508del	ins/del	c.1521_1523delCTT	rs113993960
HUB-02-D2-292	F508del	ins/del	c.1521_1523delCTT	rs113993960	F508del	ins/del	c.1521_1523delCTT	rs113993960
HUB-02-D2-293	F508del	ins/del	c.1521_1523delCTT	rs113993960	F508del	ins/del	c.1521_1523delCTT	rs113993960
HUB-02-D2-294	F508del	ins/del	c.1521_1523delCTT	rs113993960	F508del	ins/del	c.1521_1523delCTT	rs113993960
HUB-02-D2-296	F508del	ins/del	c.1521_1523delCTT	rs113993960	F508del	ins/del	c.1521_1523delCTT	rs113993960
HUB-02-D2-297	F508del	ins/del	c.1521_1523delCTT	rs113993960	F508del	ins/del	c.1521_1523delCTT	rs113993960
HUB-02-D2-299	F508del	ins/del	c.1521_1523delCTT	rs113993960	F508del	ins/del	c.1521_1523delCTT	rs113993960
HUB-02-D2-300	F508del	ins/del	c.1521_1523delCTT	rs113993960	F508del	ins/del	c.1521_1523delCTT	rs113993960
HUB-02-D2-301	F508del	ins/del	c.1521_1523delCTT	rs113993960	F508del	ins/del	c.1521_1523delCTT	rs113993960
HUB-02-D2-302	F508del	ins/del	c.1521_1523delCTT	rs113993960	F508del	ins/del	c.1521_1523delCTT	rs113993960
HUB-02-D2-304	F508del	ins/del	c.1521_1523delCTT	rs113993960	F508del	ins/del	c.1521_1523delCTT	rs113993960
HUB-02-D2-305	F508del	ins/del	c.1521_1523delCTT	rs113993960	F508del	ins/del	c.1521_1523delCTT	rs113993960

Patient code	Allele 1 - Protein name	Allele 1 - Mutation type	Allele 1 - cDNA name	Allele 1 - SNP reference	Allele 2 - Protein name	Allele 2 - Mutation type	Allele 2 - cDNA name	Allele 2 - SNP reference
HUB-02-D2-306	F508del	ins/del	c.1521_1523delCTT	rs113993960	F508del	ins/del	c.1521_1523delCTT	rs113993960
HUB-02-D2-307	F508del	ins/del	c.1521_1523delCTT	rs113993960	F508del	ins/del	c.1521_1523delCTT	rs113993960
HUB-02-D2-308	F508del	ins/del	c.1521_1523delCTT	rs113993960	F508del	ins/del	c.1521_1523delCTT	rs113993960
HUB-02-D2-309	F508del	ins/del	c.1521_1523delCTT	rs113993960	F508del	ins/del	c.1521_1523delCTT	rs113993960
HUB-02-D2-310	F508del	ins/del	c.1521_1523delCTT	rs113993960	F508del	ins/del	c.1521_1523delCTT	rs113993960
HUB-02-D2-311	F508del	ins/del	c.1521_1523delCTT	rs113993960	F508del	ins/del	c.1521_1523delCTT	rs113993960
HUB-02-D2-312	F508del	ins/del	c.1521_1523delCTT	rs113993960	F508del	ins/del	c.1521_1523delCTT	rs113993960
HUB-02-D2-313	F508del	ins/del	c.1521_1523delCTT	rs113993960	F508del	ins/del	c.1521_1523delCTT	rs113993960
HUB-02-D2-316	F508del	ins/del	c.1521_1523delCTT	rs113993960	A455E	missense	c.1364C>A	r574551128
HUB-02-D2-317	F508del	ins/del	c.1521_1523delCTT	rs113993960	F508del	ins/del	c.1521_1523delCTT	rs113993960
HUB-02-D2-318	F508del	ins/del	c.1521_1523delCTT	rs113993960	F508del	ins/del	c.1521_1523delCTT	rs113993960
HUB-02-D2-319	F508del	ins/del	c.1521_1523delCTT	rs113993960	F508del	ins/del	c.1521_1523delCTT	rs113993960
HUB-02-D2-320	F508del	ins/del	c.1521_1523delCTT	rs113993960	F508del	ins/del	c.1521_1523delCTT	rs113993960
HUB-02-D2-321	F508del	ins/del	c.1521_1523delCTT	rs113993960	F508del	ins/del	c.1521_1523delCTT	rs113993960
HUB-02-D2-322	F508del	ins/del	c.1521_1523delCTT	rs113993960	F508del	ins/del	c.1521_1523delCTT	rs113993960

Patient code	Allele 1 - Protein name	Allele 1 - Mutation type	Allele 1 - cDNA name	Allele 1 - SNP reference	Allele 2 - Protein name	Allele 2 - Mutation type	Allele 2 - cDNA name	Allele 2 - SNP reference
HUB-02-D2-323	F508del	ins/del	c.1521_1523delCTT	rs113993960	F508del	ins/del	c.1521_1523delCTT	rs113993960
HUB-02-D2-324	F508del	ins/del	c.1521_1523delCTT	rs113993960	F508del	ins/del	c.1521_1523delCTT	rs113993960
HUB-02-D2-326	F508del	ins/del	c.1521_1523delCTT	rs113993960	F508del	ins/del	c.1521_1523delCTT	rs113993960
HUB-02-D2-327	F508del	ins/del	c.1521_1523delCTT	rs113993960	F508del	ins/del	c.1521_1523delCTT	rs113993960
HUB-02-D2-329	F508del	ins/del	c.1521_1523delCTT	rs113993960	R1162X	nonsense	c.3484C>T	rs74767530
HUB-02-D2-330	F508del	ins/del	c.1521_1523delCTT	rs113993960	R1162X	nonsense	c.3484C>T	rs74767530
HUB-02-D2-331	F508del	ins/del	c.1521_1523delCTT	rs113993960	F508del	ins/del	c.1521_1523delCTT	rs113993960
HUB-02-D2-332	F508del	ins/del	c.1521_1523delCTT	rs113993960	F508del	ins/del	c.1521_1523delCTT	rs113993960
HUB-02-D2-333	F508del	ins/del	c.1521_1523delCTT	rs113993960	F508del	ins/del	c.1521_1523delCTT	rs113993960
HUB-02-D2-335	F508del	ins/del	c.1521_1523delCTT	rs113993960	F508del	ins/del	c.1521_1523delCTT	rs113993960
HUB-02-D2-336	F508del	ins/del	c.1521_1523delCTT	rs113993960	F508del	ins/del	c.1521_1523delCTT	rs113993960
HUB-02-D2-337	F508del	ins/del	c.1521_1523delCTT	rs113993960	F508del	ins/del	c.1521_1523delCTT	rs113993960
HUB-02-D2-338	F508del	ins/del	c.1521_1523delCTT	rs113993960	F508del	ins/del	c.1521_1523delCTT	rs113993960
HUB-02-D2-339	F508del	ins/del	c.1521_1523delCTT	rs113993960	F508del	ins/del	c.1521_1523delCTT	rs113993960
HUB-02-D2-340	F508del	ins/del	c.1521_1523delCTT	rs113993960	F508del	ins/del	c.1521_1523delCTT	rs113993960

Patient code	Allele 1 - Protein name	Allele 1 - Mutation type	Allele 1 - cDNA name	Allele 1 - SNP reference	Allele 2 - Protein name	Allele 2 - Mutation type	Allele 2 - cDNA name	Allele 2 - SNP reference
HUB-02-D2-341	F508del	ins/del	c.1521_1523delCTT	rs113993960	F508del	ins/del	c.1521_1523delCTT	rs113993960
HUB-02-D2-342	F508del	ins/del	c.1521_1523delCTT	rs113993960	F508del	ins/del	c.1521_1523delCTT	rs113993960
HUB-02-D2-343	F508del	ins/del	c.1521_1523delCTT	rs113993960	F508del	ins/del	c.1521_1523delCTT	rs113993960
HUB-02-D2-344	F508del	ins/del	c.1521_1523delCTT	rs113993960	E730X	nonsense	c.2188G>T	rs113993960
HUB-02-D2-345	F508del	ins/del	c.1521_1523delCTT	rs113993960	F508del	ins/del	c.1521_1523delCTT	rs113993960
HUB-02-D2-346	F508del	ins/del	c.1521_1523delCTT	rs113993960	F508del	ins/del	c.1521_1523delCTT	rs113993960
HUB-02-D2-347	F508del	ins/del	c.1521_1523delCTT	rs113993960	F508del	ins/del	c.1521_1523delCTT	rs113993960
HUB-02-D2-349	F508del	ins/del	c.1521_1523delCTT	rs113993960	F508del	ins/del	c.1521_1523delCTT	rs113993960
HUB-02-D2-350	F508del	ins/del	c.1521_1523delCTT	rs113993960	F508del	ins/del	c.1521_1523delCTT	rs113993960
HUB-02-D2-351	F508del	ins/del	c.1521_1523delCTT	rs113993960	F508del	ins/del	c.1521_1523delCTT	rs113993960
HUB-02-D2-352	F508del	ins/del	c.1521_1523delCTT	rs113993960	F508del	ins/del	c.1521_1523delCTT	rs113993960
HUB-02-D2-353	F508del	ins/del	c.1521_1523delCTT	rs113993960	F508del	ins/del	c.1521_1523delCTT	rs113993960
HUB-02-D2-354	F508del	ins/del	c.1521_1523delCTT	rs113993960	F508del	ins/del	c.1521_1523delCTT	rs113993960
HUB-02-D2-355	F508del	ins/del	c.1521_1523delCTT	rs113993960	F508del	ins/del	c.1521_1523delCTT	rs113993960
HUB-02-D2-356	F508del	ins/del	c.1521_1523delCTT	rs113993960	F508del	ins/del	c.1521_1523delCTT	rs113993960

Patient code	Allele 1 - Protein name	Allele 1 - Mutation type	Allele 1 - cDNA name	Allele 1 - SNP reference	Allele 2 - Protein name	Allele 2 - Mutation type	Allele 2 - cDNA name	Allele 2 - SNP reference
HUB-02-D2-358	F508del	ins/del	c.1521_1523delCTT	rs113993960	F508del	ins/del	c.1521_1523delCTT	rs113993960
HUB-02-D2-359	F508del	ins/del	c.1521_1523delCTT	rs113993960	F508del	ins/del	c.1521_1523delCTT	rs113993960
HUB-02-D2-360	F508del	ins/del	c.1521_1523delCTT	rs113993960	F508del	ins/del	c.1521_1523delCTT	rs113993960
HUB-02-D2-361	F508del	ins/del	c.1521_1523delCTT	rs113993960	S1251N	missense	c.3752G>A	rs74503330
HUB-02-D2-362	F508del	ins/del	c.1521_1523delCTT	rs113993960	S1251N	missense	c.3752G>A	rs74503330
HUB-02-D2-363	F508del	ins/del	c.1521_1523delCTT	rs113993960	F508del	ins/del	c.1521_1523delCTT	rs113993960
HUB-02-D2-364	F508del	ins/del	c.1521_1523delCTT	rs113993960	F508del	ins/del	c.1521_1523delCTT	rs113993960
HUB-02-D2-365	F508del	ins/del	c.1521_1523delCTT	rs113993960	F508del	ins/del	c.1521_1523delCTT	rs113993960
HUB-02-D2-366	F508del	ins/del	c.1521_1523delCTT	rs113993960	F508del	ins/del	c.1521_1523delCTT	rs113993960
HUB-02-D2-367	F508del	ins/del	c.1521_1523delCTT	rs113993960	F508del	ins/del	c.1521_1523delCTT	rs113993960
HUB-02-D2-368	F508del	ins/del	c.1521_1523delCTT	rs113993960	F508del	ins/del	c.1521_1523delCTT	rs113993960
HUB-02-D2-370	F508del	ins/del	c.1521_1523delCTT	rs113993960	F508del	ins/del	c.1521_1523delCTT	rs113993960
HUB-02-D2-371	F508del	ins/del	c.1521_1523delCTT	rs113993960	S1251N	missense	c.3752G>A	rs74503330
HUB-02-D2-374	S1251N	missense	c.3752G>A	rs74503330	A455E	missense	c.1364C>A	rs74551128
HUB-02-D2-376	F508del	ins/del	c.1521_1523delCTT	rs113993960	F508del	ins/del	c.1521_1523delCTT	rs113993960

Patient code	Allele 1 - Protein name	Allele 1 - Mutation type	Allele 1 - cDNA name	Allele 1 - SNP reference	Allele 1 - Protein name	Allele 2 - Mutation type	Allele 2 - cDNA name	Allele 2 - SNP reference
HUB-02-D2-377	F508del	ins/del	c.1521_1523delCTT	rs113993960	F508del	ins/del	c.1521_1523delCTT	rs113993960
HUB-02-D2-380	F508del	ins/del	c.1521_1523delCTT	rs113993960	S1251N	missense	c.3752G>A	rs74503330
HUB-02-D2-381	F508del	ins/del	c.1521_1523delCTT	rs113993960	F508del	ins/del	c.1521_1523delCTT	rs113993960
HUB-02-D2-382	F508del	ins/del	c.1521_1523delCTT	rs113993960	F508del	ins/del	c.1521_1523delCTT	rs113993960
HUB-02-D2-384	F508del	ins/del	c.1521_1523delCTT	rs113993960	F508del	ins/del	c.1521_1523delCTT	rs113993960
HUB-02-D2-387	F508del	ins/del	c.1521_1523delCTT	rs113993960	F508del	ins/del	c.1521_1523delCTT	rs113993960
HUB-02-D2-389	F508del	ins/del	c.1521_1523delCTT	rs113993960	F508del	ins/del	c.1521_1523delCTT	rs113993960
HUB-02-D2-390	1811+1G>C	splice	c.1679+1G>C	rs397508263	1811+1G>C	splice	c.1679+1G>C	rs397508263
HUB-02-D2-391	4832delA	ins/del	NA	NA	NA	ins/del	c.1991del6	NA
HUB-02-D2-393	3272-26A>G	splice	c.3140-26A>G	rs76151804	3272-26A>G	splice	c.3140-26A>G	rs76151804
HUB-02-D2-394	3272-26A>G	splice	c.3140-26A>G	rs76151804	1898+5G>T	splice	c.1766+5G>T	rs121908796
HUB-02-D2-395	R1162X	nonsense	c.3484C>T	rs74767530	D1152H	missense	c.3454G>C	rs75541969
HUB-02-D2-396	3905instT	ins/del	c.3773_3774instT	rs121908789	D1152H	missense	c.3454G>C	rs75541969
HUB-02-D2-397	F508del	ins/del	c.1521_1523delCTT	rs113993960	R117H-T1-9T	missense	NA	NA
HUB-02-D2-398	F508del	ins/del	c.1521_1523delCTT	rs113993960	G1249R	missense	c.3745G>A	rs397508602

Patient code	Allele 1 - Protein name	Allele 1 - Mutation type	Allele 1 - cDNA name	Allele 1 - SNP reference	Allele 1 - Protein name	Allele 2 - Mutation type	Allele 2 - cDNA name	Allele 2 - SNP reference
HUB-02-D2-399	F508del	ins/del	c.1521_1523delCTT	rs113993960	F508del	ins/del	c.1521_1523delCTT	rs113993960
HUB-02-D2-400	F508del	ins/del	c.1521_1523delCTT	rs113993960	F508del	ins/del	c.1521_1523delCTT	rs113993960
HUB-02-D2-401	F508del	ins/del	c.1521_1523delCTT	rs113993960	R117H	missense	c.350G>A	rs78655421
HUB-02-D2-403	R1162X	nonsense	c.3484C>T	rs74767530	3272-26A>G	splice	c.3140-26A>G	rs76151804
HUB-02-D2-404	1717-1G>A	splice	c.1585-1G>A	rs76713772	3677/ins4	ins/del	NA	NA
HUB-02-D2-405	F508del	ins/del	c.1521_1523delCTT	rs113993960	R553X	nonsense	c.1657C>T	rs74597325
HUB-02-D2-406	G542X	nonsense	c.1624G>T	rs113993959	3849+10kbC>T	splice	c.3718-247C>T	rs75039782
HUB-02-D2-407	F508del	ins/del	c.1521_1523delCTT	rs113993960	E60X	nonsense	c.178G>T	rs77284892
HUB-02-D2-408	I336K	missense	c.1007T>A	rs397508139	R553X	nonsense	c.1657C>T	rs74597325
HUB-02-D2-409	F508del	ins/del	c.1521_1523delCTT	rs113993960	F508del	ins/del	c.1521_1523delCTT	rs113993960
HUB-02-D2-410	4382delA	ins/del	c.4251delA	rs397508706	2043delG	ins/del	c.1911delG	NA
HUB-02-D2-411	F508del	ins/del	c.1521_1523delCTT	rs113993960	F508del	ins/del	c.1521_1523delCTT	rs113993960
HUB-02-D2-412	F508del	ins/del	c.1521_1523delCTT	rs113993960	F508del	ins/del	c.1521_1523delCTT	rs113993960
HUB-02-D2-413	F508del	ins/del	c.1521_1523delCTT	rs113993960	F508del	ins/del	c.1521_1523delCTT	rs113993960
HUB-02-D2-414	R553X	nonsense	c.1657C>T	rs74597325	I336K	missense	c.1007T>A	rs397508139

Patient code	Allele 1 - Protein name	Allele 1 - Mutation type	Allele 1 - cDNA name	Allele 1 - SNP reference	Allele 1 - Protein name	Allele 2 - Mutation type	Allele 2 - cDNA name	Allele 2 - SNP reference
HUB-02-D2-415	F508del	ins/del	c.1521_1523delCTT	rs113993960	F508del	ins/del	c.1521_1523delCTT	rs113993960
HUB-02-D2-416	F508del	ins/del	c.1521_1523delCTT	rs113993960	F508del	ins/del	c.1521_1523delCTT	rs113993960
HUB-02-D2-417	E92K	missense	c.274G>A	rs121908751	CFTRdel2	ins/del	c.(53+1_54-1)_(164+1_165-1)del	NA
HUB-02-D2-418	R334W	missense	c.100C>T	rs121909011	N1303K	missense	c.3909C>G	rs80034486
HUB-02-D2-419	G542X	nonsense	c.1624G>T	rs113993959	I148N	missense	c.443T>A	rs35516286
HUB-02-D2-420	N1303K	missense	c.3909C>G	rs80034486	Q39X	nonsense	c.115C>T	rs397508168
HUB-02-D2-421	2143delT	ins/del	c.2012deT	rs121908812	CFTRdel2.3	ins/del	c.54-5940_273+10250del21kb	NA
HUB-02-D2-448	W1282X	nonsense	c.3846G>A	rs77010898	W1282X	nonsense	c.3846G>A	rs77010898
HUB-02-D2-449	G542X	nonsense	c.1624G>T	rs113993959	CFTRdel2.3	ins/del	c.54-5940_273+10250del21kb	NA
HUB-02-D2-450	G542X	nonsense	c.1624G>T	rs113993959	W679X	nonsense	c.2036G>A	rs397508333
HUB-02-D2-452	F508del	ins/del	c.1521_1523delCTT	rs113993960	R75Q	missense	c.224G>A	rs1800076
HUB-02-D2-453	F508del	ins/del	c.1521_1523delCTT	rs113993960	IVS11-1G>C	splice	NA	NA
HUB-02-D2-454	F508del	ins/del	c.1521_1523delCTT	rs113993960	L206W	missense	c.617T>G	rs121908752
HUB-02-D2-455	F508del	ins/del	c.1521_1523delCTT	rs113993960	UNK	unknown	UNK	UNK
HUB-02-D2-456	F508del	ins/del	c.1521_1523delCTT	rs113993960	UNK	unknown	UNK	UNK



Patient code	Allele 1 - Protein name	Allele 1 - Mutation type	Allele 1 - cDNA name	Allele 1 - SNP reference	Allele 1 - Protein name	Allele 2 - Mutation type	Allele 2 - cDNA name	Allele 2 - SNP reference
HUB-02-D2-457	F508del	ins/del	c.1521_1523delCTT	rs113993960	R553X	nonsense	c.1657C>T	rs74597325
HUB-02-D2-458	F508del	ins/del	c.1521_1523delCTT	rs113993960	3849+10kbC>T	splice	c.3718-2477C>T	rs75039782
HUB-02-D2-459	F508del	ins/del	c.1521_1523delCTT	rs113993960	W1282X	nonsense	c.3846G>A	rs77010898
HUB-02-D2-460	F508del	ins/del	c.1521_1523delCTT	rs113993960	I1027T	missense	c.3080T>C	rs1800112
HUB-02-D2-461	F508del	ins/del	c.1521_1523delCTT	rs113993960	W1282X	nonsense	c.3846G>A	rs77010898
HUB-02-D2-462	F508del	ins/del	c.1521_1523delCTT	rs113993960	W1282X	nonsense	c.3846G>A	rs77010898
HUB-02-D2-463	F508del	ins/del	c.1521_1523delCTT	rs113993960	711+1G>T	splice	c.579+1G>T	rs77188391
HUB-02-D2-464	F508del	ins/del	c.1521_1523delCTT	rs113993960	G85E	missense	c.254G>A	rs75961395
HUB-02-D2-465	F508del	ins/del	c.1521_1523delCTT	rs113993960	Y849X	nonsense	c.2547C>A	rs397508394
HUB-02-D2-466	F508del	ins/del	c.1521_1523delCTT	rs113993960	3849+10kbC>T	splice	c.3718-2477C>T	rs75039782
HUB-02-D2-467	F508del	ins/del	c.1521_1523delCTT	rs113993960	G576A	missense	c.1727G>C	rs1800098
HUB-02-D2-468	F508del	ins/del	c.1521_1523delCTT	rs113993960	3849+10kbC>T	splice	c.3718-2477C>T	rs75039782
HUB-02-D2-469	S1251N	missense	c.3752G>A	rs74503330	S1178X	nonsense	c.3533C>G	NA
HUB-02-D2-470	F508del	ins/del	c.1521_1523delCTT	rs113993960	W1282X	nonsense	c.3846G>A	rs77010898
HUB-02-D2-473	F508del	ins/del	c.1521_1523delCTT	rs113993960	F508del	ins/del	c.1521_1523delCTT	rs113993960

Patient code	Allele 1 - Protein name	Allele 1 - Mutation type	Allele 1 - cDNA name	Allele 1 - SNP reference	Allele 1 - Protein name	Allele 2 - Mutation type	Allele 2 - cDNA name	Allele 2 - SNP reference
HUB-02-D2-474	F508del	ins/del	c.1521_1523delCTT	rs113993960	F508del	ins/del	c.1521_1523delCTT	rs113993960
HUB-02-D2-475	F508del	ins/del	c.1521_1523delCTT	rs113993960	2789+5G>A	splice	c.2657+5G>A	rs80224560
HUB-02-D2-476	F508del	ins/del	c.1521_1523delCTT	rs113993960	R347P	missense	c.1040G>C	rs77932196
HUB-02-D2-477	F508del	ins/del	c.1521_1523delCTT	rs113993960	F508del	ins/del	c.1521_1523delCTT	rs113993960
HUB-02-D2-478	F508del	ins/del	c.1521_1523delCTT	rs113993960	splice1	splice	c.4243-31>A	NA
HUB-02-D2-479	N1303K	missense	c.3909C>G	rs80034486	Q1012P	missense	c.3035A>C	NA
HUB-02-D2-480	W1282X	nonsense	c.3846G>A	rs77010898	R117H>T	missense	c.[350G>A;1210?12?]	rs78655421 (-T)
HUB-02-D2-481	F508del	ins/del	c.1521_1523delCTT	rs113993960	1342-1delG	ins/del	c.1210-1delG	NA
HUB-02-D2-482	F508del	ins/del	c.1521_1523delCTT	rs113993960	3849+10kbC>T	splice	c.3718-247G>T	rs75039782
HUB-02-D2-483	F508del	ins/del	c.1521_1523delCTT	rs113993960	G628R	missense	c.1882 G>C	rs397508316
HUB-02-D2-484	F508del	ins/del	c.1521_1523delCTT	rs113993960	3659delC	ins/del	c.3528delC	rs121908747
HUB-02-D2-485	F508del	ins/del	c.1521_1523delCTT	rs113993960	Gly1349fs	ins/del	c.4046delG	NA
HUB-02-D2-486	F508del	ins/del	c.1521_1523delCTT	rs113993960	711+1G>T	splice	c.579+1G>T	rs77188391
HUB-02-D2-487	F508del	ins/del	c.1521_1523delCTT	rs113993960	CFTRdel17a.17b	ins/del	c.(2988+1_2989-1)_ (3367+1_3368-1)del	NA
HUB-02-D2-488	F508del	ins/del	c.1521_1523delCTT	rs113993960	2789+5G>A	splice	c.2657+5G>A	rs80224560



Patient code	Allele 1 - Protein name	Allele 1 - Mutation type	Allele 1 - cDNA name	Allele 1 - SNP reference	Allele 1 - Protein name	Allele 2 - Mutation type	Allele 2 - cDNA name	Allele 2 - SNP reference
HUB-02-D2-489	F508del	ins/del	c.1521_1523delCTT	rs113993960	A455E	missense	c.1364C>A	rs74551128
HUB-02-D2-490	F508del	ins/del	c.1521_1523delCTT	rs113993960	R1358S	missense	c.4074A>T	NA
HUB-02-D2-491	F508del	ins/del	c.1521_1523delCTT	rs113993960	TG(13)T(5)	other	NA	NA
HUB-02-D2-492	F508del	ins/del	c.1521_1523delCTT	rs113993960	3272-26A>G	splice	c.3140-26A>G	rs76151804
HUB-02-D2-493	F508del	ins/del	c.1521_1523delCTT	rs113993960	3272-26A>G	splice	c.3140-26A>G	rs76151804
HUB-02-D2-494	F508del	ins/del	c.1521_1523delCTT	rs113993960	A455E	missense	c.1364C>A	rs74551128
HUB-02-D2-495	F508del	ins/del	c.1521_1523delCTT	rs113993960	R1158X	nonsense	c.3472C>T	rs79850223
HUB-02-D2-496	F508del	ins/del	c.1521_1523delCTT	rs113993960	711+1G>T	splice	c.579+1G>T	ins/del
HUB-02-D2-497	D1152H	missense	c.3454G>C	rs75541969	R1162X	nonsense	c.3484C>T	rs74767530
HUB-02-D2-498	F508del	ins/del	c.1521_1523delCTT	rs113993960	1078delT	ins/del	c.948delT	rs121908744
HUB-02-D2-499	F508del	ins/del	c.1521_1523delCTT	rs113993960	CFTRdel17a.17b	ins/del	c.(2988+1_2989-1)_ (3367+1_3368-1)del	NA
HUB-02-D2-500	F508del	ins/del	c.1521_1523delCTT	rs113993960	I507del	ins/del	c.1519_1521delATC	rs121908745
HUB-02-D2-501	F508del	ins/del	c.1521_1523delCTT	rs113993960	F508del	ins/del	c.1521_1523delCTT	rs113993960
HUB-02-D2-502	F508del	ins/del	c.1521_1523delCTT	rs113993960	2183AA>G	ins/del	c.2051_2052delAAinsG	NA
HUB-02-D2-503	A455E	missense	c.1364C>A	rs74551128	UNK	unknown	UNK	UNK

Patient code	Allele 1 - Protein name	Allele 1 - Mutation type	Allele 1 - cDNA name	Allele 1 - SNP reference	Allele 1 - Protein name	Allele 2 - Mutation type	Allele 2 - cDNA name	Allele 2 - SNP reference
HUB-02-D2-506	F508del	ins/del	c.1521_1523delCTT	rs113993960	S18I	missense	c.53G>T	NA
HUB-02-D2-507	F508del	ins/del	c.1521_1523delCTT	rs113993960	1717-1G>A	splice	c.155-1G>A	rs76713772
HUB-02-D2-508	L732X	nonsense	c.2195T>G	rs397508350	L732X	nonsense	c.2195T>G	rs397508350
HUB-02-D2-509	F508del	ins/del	c.1521_1523delCTT	rs113993960	N1303K	missense	c.3909C>G	rs80034486
HUB-02-D2-510	F508del	ins/del	c.1521_1523delCTT	rs113993960	N1303K	missense	c.3909C>G	rs80034486
HUB-02-D2-511	F508del	ins/del	c.1521_1523delCTT	rs113993960	UNK	unknown	UNK	UNK
HUB-02-D2-512	1811+1G>C	splice	c.1679+1G>C	rs397508263	1811+1G>C	splice	c.1679+1G>C	rs397508263
HUB-02-D2-513	F508del	ins/del	c.1521_1523delCTT	rs113993960	3659delC	ins/del	c.3528delC	rs121908747
HUB-02-D2-514	F508del	ins/del	c.1521_1523delCTT	rs113993960	711+1G>T	splice	c.579+1G>T	rs77188391
HUB-02-D2-516	F508del	ins/del	c.1521_1523delCTT	rs113993960	F508del	ins/del	c.1521_1523delCTT	rs113993960
HUB-02-D2-518	N1303K	missense	c.3909C>G	rs80034486	G85E	missense	c.254G>A	rs75961395
HUB-02-D2-519	F508del	ins/del	c.1521_1523delCTT	rs113993960	365-366insT	ins/del	c.233dupT	rs397508366
HUB-02-D2-520	F508del	ins/del	c.1521_1523delCTT	rs113993960	A455E	missense	c.1364C>A	rs74551128
HUB-02-D2-521*	UNK	unknow	UNK	UNK	UNK	unknow	UNK	UNK
HUB-02-D2-522	F508del	ins/del	c.1521_1523delCTT	rs113993960	1717-1G>A	splice	c.155-1G>A	rs76713772

Patient code	Allele 1 - Protein name	Allele 1 - Mutation type	Allele 1 - cDNA name	Allele 1 - SNP reference	Allele 1 - Protein name	Allele 2 - Mutation type	Allele 2 - cDNA name	Allele 2 - SNP reference
HUB-02-D2-523	UNK	unknown	UNK	UNK	UNK	unknown	UNK	UNK
HUB-02-D2-525	UNK	unknown	UNK	UNK	UNK	unknown	UNK	UNK
HUB-02-D2-526	UNK	unknown	UNK	UNK	UNK	unknown	UNK	UNK
HUB-02-D2-531	F508del	ins/del	c.1521_1523delCTT	rs113993960	F508del	ins/del	c.1521_1523delCTT	rs113993960
HUB-02-D2-532	F508del	ins/del	c.1521_1523delCTT	rs113993960	A455E	missense	c.1364C>A	rs74551128
HUB-02-D2-533	F508del	ins/del	c.1521_1523delCTT	rs113993960	F508del	ins/del	c.1521_1523delCTT	rs113993960
HUB-02-D2-534	L1335P	missense	c.4004T>C	rs397508658	L1335P	missense	c.4004T>C	rs397508658
HUB-02-D2-535	W1282X	nonsense	c.3846G>A	rs77010898	1717-1G>A	splice	c.1585-1G>A	rs76713772
HUB-02-D2-536	F508del	ins/del	c.1521_1523delCTT	rs113993960	N1303K	missense	c.3909C>G	rs80034486
HUB-02-D2-537	4005+2T-c	splice	c.3873+2>C	rs146795445	R553X	nonsense	c.1657C>T	rs74597325
HUB-02-D2-538	F508del	ins/del	c.1521_1523delCTT	rs113993960	F508del	ins/del	c.1521_1523delCTT	rs113993960
HUB-02-D2-539	F508del	ins/del	c.1521_1523delCTT	rs113993960	T1396P	missense	c.4187A>C	NA
HUB-02-D2-540	F508del	ins/del	c.1521_1523delCTT	rs113993960	(TG)11(T)5	other	c.[12012[5];1210-34]G[11]]	NA
HUB-02-D2-543	UNK	unknown	UNK	UNK	UNK	unknown	UNK	UNK
HUB-02-D2-546	UNK	unknown	UNK	UNK	UNK	unknown	UNK	UNK

Patient code	Allele 1 - Protein name	Allele 1 - Mutation type	Allele 1 - cDNA name	Allele 1 - SNP reference	Allele 2 - Protein name	Allele 2 - Mutation type	Allele 2 - cDNA name	Allele 2 - SNP reference
HUB-02-D2-547	UNK	unknown	UNK	rs74597325	R709X	nonsense	UNK	UNK
HUB-02-D2-559	R553X	nonsense	c.1657>T	rs397508573	S1159F	missense	NA	NA
HUB-02-D2-560	S1159F	missense	c.3476C>T	rs80034486	L346P	missense	c.3476C>T	rs397508573
HUB-02-D2-561	N1303K	missense	c.3909C>G	NA	R334W	missense	c.1037T>C	rs397508146
HUB-02-D2-562	CFTRdel le2.3	ins/del	c.54-5940_73+10250del21kb	rs77932196	R1162X	nonsense	c.1000C>T	rs121909011
HUB-02-D2-563	R347P	missense	c.1040G>C	rs397508195	R1162X	nonsense	c.3484C>T	rs74767530
HUB-02-D2-564	V456F	missense	c.1366G>T	rs113993960	F508del	ins/del	c.3484C>T	rs74767530
HUB-02-D2-565	F508del	ins/del	c.1521_1523delCTT	rs113993960	F508del	ins/del	c.1521_1523delCTT	rs113993960
HUB-02-D2-566	F508del	ins/del	c.1521_1523delCTT	rs113993960	F508del	ins/del	c.1521_1523delCTT	rs113993960
HUB-02-D2-567	F508del	ins/del	c.1521_1523delCTT	rs113993960	F508del	ins/del	c.1521_1523delCTT	rs113993960
HUB-02-D2-568	F508del	ins/del	c.1521_1523delCTT	rs113993960	F508del	ins/del	c.1521_1523delCTT	rs113993960
HUB-02-D2-569	F508del	ins/del	c.1521_1523delCTT	rs113993960	F508del	ins/del	c.1521_1523delCTT	rs113993960
HUB-02-D2-570	2659delC	ins/del	NA	NA	N1303K	missense	c.3909C>G	rs80034486
HUB-02-D2-571	2184delA	ins/del	c.2052delA	rs121908746	D110H	missense	c.328G>C	rs113993958
TBD	1717-1G>A	splice	c.1585-1G>A	rs76713772	3905inst	ins/del	c.3773_3774inst	rs121908789
TBD	1898+1G>C	splice	c.1679+1G>C	rs397508263	Q220X	nonsense	NA	NA

Patient code	Allele 1 - Protein name	Allele 1 - Mutation type	Allele 1 - cDNA name	Allele 1 - SNP reference	Allele 1 - Protein name	Allele 2 - Mutation type	Allele 2 - cDNA name	Allele 2 - SNP reference
TBD	2789+5G>A	splice	c.2657+5G>A	rs80224560	2183AA>G	ins/del	c.2051_2052delAAinsG	rs121908799
TBD	2789+5G>A	splice	c.2657+5G>A	rs80224560	2789+5G>A	splice	c.2657+5G>A	rs80224560
TBD*	2789+5G>A	splice	c.2657+5G>A	rs80224560	L732X	nonsense		
TBD	2789+5G	splice	c.2657+5G>A	rs80224560	2789+5G1>A	splice	c.2657+5G>A	rs80224560
TBD	T>A							
TBD	308insA	ins/del	NA		3695del	ins/del	NA	NA
TBD*	394delTT	ins/del	c.262_263del	rs121908769	3659delC	ins/del	c.3659delC	rs121908811
TBD	E92K	missense	c.274G>A	rs121908751	E92K	missense	c.274G>A	rs121908751
TBD	F508del	ins/del	c.1521_1523delCTT	rs113993960	F508del	ins/del	c.1521_1523delCTT	rs113993960
TBD	F508del	ins/del	c.1521_1523delCTT	rs113993960	F508del	ins/del	c.1521_1523delCTT	rs113993960
TBD	F508del	ins/del	c.1521_1523delCTT	rs113993960	F508del	ins/del	c.1521_1523delCTT	rs113993960
TBD	F508del	ins/del	c.1521_1523delCTT	rs113993960	F508del	ins/del	c.1521_1523delCTT	rs113993960
TBD	F508del	ins/del	c.1521_1523delCTT	rs113993960	G970R	missense	c.2908G>C	rs397508453
TBD	F508del	ins/del	c.1521_1523delCTT	rs113993960	G970R	missense	c.2908G>C	rs397508453
TBD	F508del	ins/del	c.1521_1523delCTT	rs113993960	G970R	missense	c.2908G>C	rs397508453
TBD	F508del	ins/del	c.1521_1523delCTT	rs113993960	S1251N	missense	c.3752G>A	rs74503330
TBD*	G542X	nonsense	c.1624G>T	rs113993959	W1282X	nonsense	c.3846G>A	rs77010898
TBD	I336K	missense	c.1007T>A	rs397508139	R347P	missense	c.1040G>C	rs77932196
TBD*	IVS 4+1G>T	splice	NA	NA	UNK	unknown	UNK	UNK
TBD	N1303K	missense	c.3909C>G	rs80034486	CFTRdele2.3	ins/del	c.54_5940_273+10250del21kb	NA
TBD	N1303K	missense	c.3909C>G	rs80034486	Q220X	nonsense	NA	NA
TBD	Q525X	nonsense	NA	NA	3732delA	ins/del	NA	NA
TBD	Q525X	nonsense	NA	NA	3732delA	ins/del	NA	NA



Patient code	Allele 1 - Protein name	Allele 1 - Mutation type	Allele 1 - cDNA name	Allele 1 - SNP reference	Allele 1 - Protein name	Allele 2 - Mutation type	Allele 2 - cDNA name	Allele 2 - SNP reference
TBD*	R1066H	missense	c.319T>A	rs121909019	CFTRdele2	ins/del	c.54_164del111	rs1562882675
TBD	R1162X	nonsense	c.3484C>T	rs74767530	3272_26A>G	splice	c.3140_26A>G	rs76151804
TBD	R1162X	nonsense	c.3484C>T	rs74767530	3539del16	ins/del	NA	NA
TBD*	R334W	missense	c.1000C>T	rs121909011	-22del 11.4kb	ins/del	NA	NA
TBD	R553X	nonsense	c.1657C>T	rs74597325	1898+3A>G	splice	c.1766+3A>G	rs397508298
TBD	R553X	nonsense	c.1657C>T	rs74597325	G542X	nonsense	c.1624G>T	rs113993959
TBD	R75X	nonsense	NA	NA	R75X	nonsense	NA	NA
TBD*	S466X	nonsense	c.1397C>A or c.1397C>G	rs121908805	R107Q	missense	c.3209G>A	rs78769542
TBD	Ser670_Leu 671insTer	ins/del	c.2012delT	rs121908812	Ser670_Leu671insTer	ins/del	c.2012delT	rs121908812
TBD	W1282X	nonsense	c.3846G>A	rs77010898	L953fs	ins/del	c.2859_2890del	
TBD	WT	wildtype	WT	WT	WT	wildtype	WT	WT
TBD	WT	wildtype	WT	WT	WT	wildtype	WT	WT
TBD	WT	wildtype	WT	WT	WT	wildtype	WT	WT
TBD	WT	wildtype	WT	WT	WT	wildtype	WT	WT
TBD	WT	wildtype	WT	WT	WT	wildtype	WT	WT
TBD	WT	wildtype	WT	WT	WT	wildtype	WT	WT
TBD*	1717-1G>A	splice	c.1585-1G>A	rs76713772	Y1092X	nonsense	c.3276C>A or c.3276C>G	rs121908761
TBD*	F508del	ins/del	c.1521_1523delCTT	rs113993960	1717-1G>A	splice	c.1585-1G>A	rs76713772
TBD*	F508del	ins/del	c.1521_1523delCTT	rs113993960	A455E	missense	c.1364C>A	rs74551128
TBD*	F508del	ins/del	c.1521_1523delCTT	rs113993960	A455E	missense	c.1364C>A	rs74551128
TBD*	F508del	ins/del	c.1521_1523delCTT	rs113993960	F508del	ins/del	c.1521_1523delCTT	rs113993960
TBD*	F508del	ins/del	c.1521_1523delCTT	rs113993960	F508del	ins/del	c.1521_1523delCTT	rs113993960

Patient code	Allele 1 - Protein name	Allele 1 - Mutation type	Allele 1 - cDNA name	Allele 1 - SNP reference	Allele 1 - Protein name	Allele 2 - Mutation type	Allele 2 - cDNA name	Allele 2 - SNP reference
TBD*	F508del	ins/del	c.1521_1523delCTT	rs113993960	F508del	ins/del	c.1521_1523delCTT	rs113993960
TBD*	F508del	ins/del	c.1521_1523delCTT	rs113993960	G1249E	missense	c.3746G>A	rs121909040
TBD*	F508del	ins/del	c.1521_1523delCTT	rs113993960	I336K	missense	c.100T>A	rs397508139
TBD*	F508del	ins/del	c.1521_1523delCTT	rs113993960	L467F	missense	c.1399C>T	NA
TBD*	F508del	ins/del	c.1521_1523delCTT	rs113993960	N1303K	missense	c.3909C>G	rs80034486
TBD*	F508del	ins/del	c.1521_1523delCTT	rs113993960	R1162X	nonsense	c.3484C>T	rs74767530
TBD*	F508del	ins/del	c.1521_1523delCTT	rs113993960	S1251N	missense	c.3751G>A	rs74503330
TBD*	F508del	ins/del	c.1521_1523delCTT	rs113993960	S1251N	missense	c.3752G>A	rs74503330
TBD*	F508del	ins/del	c.1521_1523delCTT	rs113993960	UNK	unknown	UNK	UNK
TBD*	F508del	ins/del	c.1521_1523delCTT	rs113993960	UNK	unknown	UNK	UNK
TBD*	I336K	missense	c.100T>A	rs397508139	R553X	nonsense	c.1657C>T	rs74597325
TBD*	R117H>T	missense	c.[350G>A;1210?1217]	rs78655421 (-7)	R1162X	nonsense	c.3484C>T	rs74767530
TBD*	S1251N	missense	c.3752G>A	rs74503330	1717-1G>A	splice	c.1585-1G>A	rs76713772
TBD*	WT	wildtype	WT	WT	WT	wildtype	WT	WT

Supplementary Table 1A: Hubrecht Organoid Technology-governed Intestinal organoids. TBD = to be determined, * = sample currently not available, UNK = unknown, WT = Wildtype.

Patient code	Patient Protein name	Allele 1 - Mutation type	Allele 1 - cDNA name	Allele 1 - SNP reference	Allele 1 - Protein name	Allele 2 - Mutation type	Allele 2 - cDNA name	Allele 2 - SNP reference
CF001	F508del	ins/del	c.1521_1523delCTT	rs113993960	F508del	ins/del	c.1521_1523delCTT	rs113993960
CF002	F508del	ins/del	c.1521_1523delCTT	rs113993960	CFTRdel17a.17b	ins/del	c.(2988+1_2989-1)_(3367+1_3368-1)del	NA
CF003	F508del	ins/del	c.1521_1523delCTT	rs113993960	F508del	ins/del	c.1521_1523delCTT	rs113993960
CF006	F508del	ins/del	c.1521_1523delCTT	rs113993960	G542X	nonsense	c.1624G>T	rs113993959
CF007	F508del	ins/del	c.1521_1523delCTT	rs113993960	A455E	missense	c.1364C>A	rs74551128
CF008	F508del	ins/del	c.1521_1523delCTT	rs113993960	L927P	missense	c.2780T>C	rs397508435
CF011	F508del	ins/del	c.1521_1523delCTT	rs113993960	A455E	missense	c.1364C>A	rs74551128
CF012	E60X	nonsense	c.178G>T	rs77284892	4015delATT	ins/del	NA	NA
CF015	F508del	ins/del	c.1521_1523delCTT	rs113993960	F508del	ins/del	c.1521_1523delCTT	rs113993960
CF017	R117H-7T	missense	c.[350G>A;1210?12[7]]	NA	R117H-7T	missense	c.[350G>A;1210?12[7]]	NA
CF018	F508del	ins/del	c.1521_1523delCTT	rs113993960	F508del	ins/del	c.1521_1523delCTT	rs113993960
CF019	R117H-7T-9T	missense	NA	NA	L997F	missense	c.2991G>C	rs1800111
CF021	F508del	ins/del	c.1521_1523delCTT	rs113993960	(TG)13(T5	other	c.[1210?12[5];1210-34TG[13]]	NA
CF024	F508del	ins/del	c.1521_1523delCTT	rs113993960	(TG)13(T5	other	c.[1210?12[5];1210-34TG[13]]	NA
CF025	F508del	ins/del	c.1521_1523delCTT	rs113993960	(TG)13(T5	other	c.[1210?12[5];1210-34TG[13]]	NA
CF026	F508del	ins/del	c.1521_1523delCTT	rs113993960	R117H-7T	missense	c.[350G>A;1210?12[7]]	NA
CF027	F508del	ins/del	c.1521_1523delCTT	rs113993960	R117H-7T	missense	c.[350G>A;1210?12[7]]	NA
CF028	WT	wildtype	WT	WT	WT	wildtype	WT	WT
CF029	F508del	ins/del	c.1521_1523delCTT	rs113993960	WT	wildtype	WT	WT
CF031	R117H-7T-9T	missense	NA	NA	A455E	missense	c.1364C>A	rs74551128

Patient code	Allele 1 - Protein name	Allele 1 - Mutation type	Allele 1 - cDNA name	Allele 1 - SNP reference	Allele 1 - SNP protein name	Allele 2 - Mutation type	Allele 2 - cDNA name	Allele 2 - SNP reference
CF032	F508del	ins/del	c.1521_1523delCTT	rs113993960	R117H>T	missense	c.[350G>A;1210?12[7]]	NA
CF034	WT	wildtype	WT	WT	WT	wildtype	WT	WT
CF035	F508del	ins/del	c.1521_1523delCTT	rs113993960	(TG)13T5	other	c.[1210?12[5];1210-34T[13]]	NA
CF036	F508del	ins/del	c.1521_1523delCTT	rs113993960	R117H>T	missense	c.[350G>A;1210?12[7]]	NA
CF038	F508del	ins/del	c.1521_1523delCTT	rs113993960	R117H>T>T	missense	NA	NA
CF041	WT	wildtype	WT	WT	WT	wildtype	WT	WT
CF042	R117H>T	missense	c.[350G>A;1210?12[7]]	NA	R553X	nonsense	c.1657C>T	rs74597325
CF043	F508del	ins/del	c.1521_1523delCTT	rs113993960	N1303K	missense	c.3909C>G	rs80034486
CF045	F508del	ins/del	c.1521_1523delCTT	rs113993960	F508del	ins/del	c.1521_1523delCTT	rs113993960
CF046	F508del	ins/del	c.1521_1523delCTT	rs113993960	A455E	missense	c.1364C>A	rs74551128
CF047	F508del	ins/del	c.1521_1523delCTT	rs113993960	N1303K	missense	c.3909C>G	rs80034486
CF048	F508del	ins/del	c.1521_1523delCTT	rs113993960	F508del	ins/del	c.1521_1523delCTT	rs113993960
CF050	F508del	ins/del	c.1521_1523delCTT	rs113993960	E60X	nonsense	c.178G>T	rs77284892
CF051	F508del	ins/del	c.1521_1523delCTT	rs113993960	F508del	ins/del	c.1521_1523delCTT	rs113993960
CF052	F508del	ins/del	c.1521_1523delCTT	rs113993960	WT	wildtype	WT	WT
CF053	F508del	ins/del	c.1521_1523delCTT	rs113993960	S1251N	missense	c.3752G>A	rs74503330
CF057	F508del	ins/del	c.1521_1523delCTT	rs113993960	CFTRdele2.3	ins/del	c.54-5940_273+10250del21kb	NA
CF060	F508del	ins/del	c.1521_1523delCTT	rs113993960	A455E	missense	c.1364C>A	rs74551128
CF063	R117H>T	missense	c.[350G>A;1210?12[7]]	NA	T1857delT	ins/del	NA	NA
CF064	F508del	ins/del	c.1521_1523delCTT	rs113993960	WT	wildtype	WT	WT
CF066	F508del	ins/del	c.1521_1523delCTT	rs113993960	F508del	ins/del	c.1521_1523delCTT	rs113993960
CF068	F508del	ins/del	c.1521_1523delCTT	rs113993960	3500-2A>G	splice	c.3368-2A>G	rs755416052

Patient code	Patient Protein name	Allele 1 - Mutation type	Allele 1 - cDNA name	Allele 1 - SNP reference	Allele 1 - Protein name	Allele 2 - Mutation type	Allele 2 - cDNA name	Allele 2 - SNP reference
CF072	WT	wildtype	WT	WT	WT	wildtype	WT	WT
CF080	F508del	ins/del	c.1521_1523delCTT	rs113993960	F508del	ins/del	c.1521_1523delCTT	rs113993960
CF083	F508del	ins/del	c.1521_1523delCTT	rs113993960	F508del	ins/del	c.1521_1523delCTT	rs113993960
CF087	F508del	ins/del	c.1521_1523delCTT	rs113993960	F508del	ins/del	c.1521_1523delCTT	rs113993960
CF091	F508del	ins/del	c.1521_1523delCTT	rs113993960	F508del	ins/del	c.1521_1523delCTT	rs113993960
CF097	R851Q	missense	c.2552G>A	rs397508395	WT	wildtype	WT	WT
CF099	F508del	ins/del	c.1521_1523delCTT	rs113993960	S1251N	missense	c.3752G>A	rs74503330
CF102	F508del	ins/del	c.1521_1523delCTT	rs113993960	F508del	ins/del	c.1521_1523delCTT	rs113993960
CF110	F508del	ins/del	c.1521_1523delCTT	rs113993960	WT	wildtype	WT	WT
CF111	UNK	unknown	UNK	UNK	UNK	unknown	UNK	UNK
CF116	F508del	ins/del	c.1521_1523delCTT	rs113993960	F508del	ins/del	c.1521_1523delCTT	rs113993960
CF118	F508del	ins/del	c.1521_1523delCTT	rs113993960	G542X	nonsense	c.1624G>T	rs113993959
CF122	R117H	missense	c.350G>A	rs78655421	I1139V	missense	c.1415A>G	NA
CF131	UNK	unknown	UNK	UNK	UNK	unknown	UNK	UNK
CF132	F508del	ins/del	c.1521_1523delCTT	rs113993960	F508del	ins/del	c.1521_1523delCTT	rs113993960
CF138	F508del	ins/del	c.1521_1523delCTT	rs113993960	(TG)12(T)5	other	c.[1210?12][5]:1210-34[T][12]	NA
CF140	S1251N	missense	c.3752G>A	rs74503330	R117H	missense	c.350G>A	rs78655421
CF141	F508del	ins/del	c.1521_1523delCTT	rs113993960	S1251N	missense	c.3752G>A	rs74503330
CF148	F508del	ins/del	c.1521_1523delCTT	rs113993960	F508del	ins/del	c.1521_1523delCTT	rs113993960
CF151	F508del	ins/del	c.1521_1523delCTT	rs113993960	A455E	missense	c.1364C>A	rs74551128
CF156	F508del	ins/del	c.1521_1523delCTT	rs113993960	F508del	ins/del	c.1521_1523delCTT	rs113993960
CF162	F508del	ins/del	c.1521_1523delCTT	rs113993960	UNK	unknown	UNK	UNK
CF165	F508del	ins/del	c.1521_1523delCTT	rs113993960	A455E	missense	c.1364C>A	rs74551128

Patient code	Allele 1 - Protein name	Allele 1 - Mutation type	Allele 1 - cDNA name	Allele 1 - cDNA reference	Allele 1 - SNP reference	Allele 1 - Protein name	Allele 2 - Mutation type	Allele 2 - cDNA name	Allele 2 - SNP reference
CF169	F508del	ins/del	c.1521_1523delCTT	rs113993960	G461R	missense	c.1381G>A	NA	NA
CF170	F508del	ins/del	c.1521_1523delCTT	rs113993960	G461R	missense	c.1381G>A	NA	NA
CF174	2105+21 17del13insAGAAA	ins/del	c.1973_19 85del13insAGAAA	rs121908780	Q1352H	missense	c.4056G>C or c.4056G>T	rs113857788	
CF187	F508del	ins/del	c.1521_1523delCTT	rs113993960	(TG)11(T)5	other	NA	NA	rs80034486
CF195	F508del	ins/del	c.1521_1523delCTT	rs113993960	N1303K	missense	c.3909C>G		
CF200	R31C	missense	c.91C>T	rs1800073	D1152H	missense	c.3454G>C	rs75541969	
CF203	F508del	ins/del	c.1521_1523delCTT	rs113993960	A455E	missense	c.1364C>A	rs74551128	
CF210	F508del	ins/del	c.1521_1523delCTT	rs113993960	S1251N	missense	c.3752G>A	rs74503330	
CF216	1717+1G>A	splice	c.1585+1G>A	rs76713772	S1251N	missense	c.3752G>A	rs74503330	
CF226	F508del	ins/del	c.1521_1523delCTT	rs113993960	S945L	missense	c.2834C>T	rs397508442	
CF227	3272+26A->G	splice	c.3140+26A->G	rs76151804	G970R	missense	c.2908G>C	rs397508453	
CF236	579+1G->T	splice	c.579+1G>T	rs77188391	CFTRdel11	ins/del	c.(1584+1_1585-1)_ (1679+1_1680-1)del	NA	NA
CF245	F508del	ins/del	c.1521_1523delCTT	rs113993960	CFTRdel17a.17b	ins/del	c.(2988+1_2989-1)_ (3367+1_3368-1)del	NA	
CF253	UNK	unknown	UNK	UNK	UNK	unknown	UNK	UNK	UNK
CF258	F508del	ins/del	c.1521_1523delCTT	rs113993960	F508del	ins/del	c.1521_1523delCTT	rs113993960	rs113993960
CF259	F508del	ins/del	c.1521_1523delCTT	rs113993960	3849+10kbC>T	splice	c.3718-2477C>T	rs75039782	
CF261	F508del	ins/del	c.1521_1523delCTT	rs113993960	F508del	ins/del	c.1521_1523delCTT	rs113993960	rs113993960
CF268	F508del	ins/del	c.1521_1523delCTT	rs113993960	F508del	ins/del	c.1521_1523delCTT	rs113993960	rs113993960
CF274	F508del	ins/del	c.1521_1523delCTT	rs113993960	F508del	ins/del	c.1521_1523delCTT	rs113993960	rs113993960
CF275	F508del	ins/del	c.1521_1523delCTT	rs113993960	F508del	ins/del	c.1521_1523delCTT	rs113993960	rs113993960
CF277	F508del	ins/del	c.1521_1523delCTT	rs113993960	F508del	ins/del	c.1521_1523delCTT	rs113993960	rs113993960

Patient code	Patient Protein name	Allele 1 - Mutation type	Allele 1 - cDNA name	Allele 1 - SNP reference	Allele 1 - SNP Protein name	Allele 2 - Mutation type	Allele 2 - cDNA name	Allele 2 - SNP reference
CF280	F508del	ins/del	c.1521_1523delCTT	rs113993960	F508del	ins/del	c.1521_1523delCTT	rs113993960
CF281	F508del	ins/del	c.1521_1523delCTT	rs113993960	F508del	ins/del	c.1521_1523delCTT	rs113993960
CF283	F508del	ins/del	c.1521_1523delCTT	rs113993960	F508del	ins/del	c.1521_1523delCTT	rs113993960
CF288	F508del	ins/del	c.1521_1523delCTT	rs113993960	F508del	ins/del	c.1521_1523delCTT	rs113993960
CF292	F508del	ins/del	c.1521_1523delCTT	rs113993960	F508del	ins/del	c.1521_1523delCTT	rs113993960
CF300	F508del	ins/del	c.1521_1523delCTT	rs113993960	F508del	ins/del	c.1521_1523delCTT	rs113993960
CF301	F508del	ins/del	c.1521_1523delCTT	rs113993960	F508del	ins/del	c.1521_1523delCTT	rs113993960
CF308	F508del	ins/del	c.1521_1523delCTT	rs113993960	621+1G>T	splice	c.489+1G>T	rs78756941
CF309	F508del	ins/del	c.1521_1523delCTT	rs113993960	F508del	ins/del	c.1521_1523delCTT	rs113993960
CF310	F508del	ins/del	c.1521_1523delCTT	rs113993960	R334W	missense	c.1000C>T	rs121909011
CF312	F508del	ins/del	c.1521_1523delCTT	rs113993960	A455E	missense	c.1364C>A	rs74551128
CF313	F508del	ins/del	c.1521_1523delCTT	rs113993960	F508del	ins/del	c.1521_1523delCTT	rs113993960
CF318	F508del	ins/del	c.1521_1523delCTT	rs113993960	F508del	ins/del	c.1521_1523delCTT	rs113993960
CF319	F508del	ins/del	c.1521_1523delCTT	rs113993960	F508del	ins/del	c.1521_1523delCTT	rs113993960
CF321	F508del	ins/del	c.1521_1523delCTT	rs113993960	F508del	ins/del	c.1521_1523delCTT	rs113993960
CF330	F508del	ins/del	c.1521_1523delCTT	rs113993960	F508del	ins/del	c.1521_1523delCTT	rs113993960
CF331	F508del	ins/del	c.1521_1523delCTT	rs113993960	F508del	ins/del	c.1521_1523delCTT	rs113993960
CF332	F508del	ins/del	c.1521_1523delCTT	rs113993960	F508del	ins/del	c.1521_1523delCTT	rs113993960
CF337	F508del	ins/del	c.1521_1523delCTT	rs113993960	F508del	ins/del	c.1521_1523delCTT	rs113993960
CF338	F508del	ins/del	c.1521_1523delCTT	rs113993960	CFTRdele2.3	ins/del	c.54-5940_27_3+10250del21kb	NA
CF339	F508del	ins/del	c.1521_1523delCTT	rs113993960	F508del	ins/del	c.1521_1523delCTT	rs113993960
CF342	F508del	ins/del	c.1521_1523delCTT	rs113993960	2143delT	ins/del	c.2012delT	rs121908812
CF343	F508del	ins/del	c.1521_1523delCTT	rs113993960	F508del	ins/del	c.1521_1523delCTT	rs113993960

Patient code	Patient Protein name	Allele 1 - Mutation type	Allele 1 - cDNA name	Allele 1 - cDNA reference	Allele 1 - SNP reference	Allele 1 - Protein name	Allele 2 - Mutation type	Allele 2 - cDNA name	Allele 2 - SNP reference
CF344	F508del	ins/del	c.1521_1523delCTT	rs113993960	F508del	ins/del	c.1521_1523delCTT	rs113993960	rs113993960
CF345	F508del	ins/del	c.1521_1523delCTT	rs113993960	F508del	ins/del	c.1521_1523delCTT	rs113993960	rs113993960
CF350	F508del	ins/del	c.1521_1523delCTT	rs113993960	F508del	ins/del	c.1521_1523delCTT	rs113993960	rs113993960
CF351	F508del	ins/del	c.1521_1523delCTT	rs113993960	E60X	nonsense	c.178G>T	rs77284892	
CF353	F508del	ins/del	c.1521_1523delCTT	rs113993960	F508del	ins/del	c.1521_1523delCTT	rs113993960	rs113993960
CF354	F508del	ins/del	c.1521_1523delCTT	rs113993960	L927P	missense	c.2780T>C	rs397508435	
CF355	F508del	ins/del	c.1521_1523delCTT	rs113993960	L927P	missense	c.2780T>C	rs397508435	
CF356	F508del	ins/del	c.1521_1523delCTT	rs113993960	F508del	ins/del	c.1521_1523delCTT	rs113993960	rs113993960
CF367	F508del	ins/del	c.1521_1523delCTT	rs113993960	F508del	ins/del	c.1521_1523delCTT	rs113993960	rs113993960
CF368	R75Q	missense	c.224G>A	rs1800076	c.1221delA	ins/del	c.1221delA	NA	
CF369	F508del	ins/del	c.1521_1523delCTT	rs113993960	F508del	ins/del	c.1521_1523delCTT	rs113993960	rs113993960
CF370	F508del	ins/del	c.1521_1523delCTT	rs113993960	F508del	ins/del	c.1521_1523delCTT	rs113993960	rs113993960
CF372	F508del	ins/del	c.1521_1523delCTT	rs113993960	F508del	ins/del	c.1521_1523delCTT	rs113993960	rs113993960
CF378	F508del	ins/del	c.1521_1523delCTT	rs113993960	3905inst	ins/del	c.3773_3774insT	rs121908789	
CF379	UNK	unknown	UNK	CFTRdele13.13a	CFTRdele13.13a	ins/del	NA	NA	
CF380	N1303K	missense	c.3909C>G	rs80034486	F81L	missense	c.241 T>C	NA	
CF381	F508del	ins/del	c.1521_1523delCTT	rs113993960	F508del	ins/del	c.1521_1523delCTT	rs113993960	rs113993960
CF383	F508del	ins/del	c.1521_1523delCTT	rs113993960	c.3468 + 2dupT	ins/del	NA	NA	
CF384	F508del	ins/del	c.1521_1523delCTT	rs113993960	CFTRdele17a,17b	ins/del	c.(2988+1,2989-1)_(3367+1_3368-1)del	NA	
CF385	G542X	nonsense	c.1624G>T	rs113993959	Q250X	nonsense	c.748 C>T	NA	
CF387	UNK	unknown	UNK	UNK	UNK	unknown	UNK	UNK	
CF409	F508del	ins/del	c.1521_1523delCTT	rs113993960	F508del	ins/del	c.1521_1523delCTT	rs113993960	rs113993960
CF410	3849+10kbC>T	splice	c.3718-2477>T	rs75039782	W1282X	nonsense	c.3846G>A	rs77010898	

Patient code	Patient Protein name	Allele 1 - Mutation type	Allele 1 - cDNA name	Allele 1 - SNP reference	Allele 1 - SNP Protein name	Allele 2 - Mutation type	Allele 2 - cDNA name	Allele 2 - SNP reference
CF411	W1282X	nonsense	C.3846G>A	rs77010898	W1282X	nonsense	C.3846G>A	rs77010898
CF412	Y275X	nonsense	C.825C>G	rs193922532	A559T	missense	C.1675G>A	rs75549581
CF424	NA	NA	C.2989-2593del8899	NA	NA	NA	C.2989-2593del8899	NA
CF425	F508del	ins/del	C.1521_1523delCTT	rs113993960	I1366N	missense	C.4097T>A	NA
CF426	F508del	ins/del	C.1521_1523delCTT	rs113993960	F508del	ins/del	C.1521_1523delCTT	rs113993960
CF438	F508del	ins/del	C.1521_1523delCTT	rs113993960	I556V	missense	C.1666A>G	rs75789129
CF439	F508del	ins/del	C.1521_1523delCTT	rs113993960	F508del	ins/del	C.1521_1523delCTT	rs113993960
CF447	F508del	ins/del	C.1521_1523delCTT	rs113993960	F508del	ins/del	C.1521_1523delCTT	rs113993960
CF449	F508del	ins/del	C.1521_1523delCTT	rs113993960	F508del	ins/del	C.1521_1523delCTT	rs113993960
CF460	F508del	ins/del	C.1521_1523delCTT	rs113993960	L732X	nonsense	C.2195T>G	rs397508350
CF461	F508del	ins/del	C.1521_1523delCTT	rs113993960	F508del	ins/del	C.1521_1523delCTT	rs113993960
CF465	F508del	ins/del	C.1521_1523delCTT	rs113993960	F508del	ins/del	C.1521_1523delCTT	rs113993960
CF483	F508del	ins/del	C.1521_1523delCTT	rs113993960	(TG)13T5	other	C.[1210212[5];1210-34TG[13]]	NA
CF490	F508del	ins/del	C.1521_1523delCTT	rs113993960	A455E	missense	C.1364C>A	rs74551128
CF499	N1303K	missense	C.3909C>G	rs803034486	R334W	missense	C.1000C>T	rs121909011
CF501	F508del	ins/del	C.1521_1523delCTT	rs113993960	F508del	ins/del	C.1521_1523delCTT	rs113993960
CF503	F508del	ins/del	C.1521_1523delCTT	rs113993960	R553X	nonsense	C.1657C>T	rs74597325
CF521	F508del	ins/del	C.1521_1523delCTT	rs113993960	F508del	ins/del	C.1521_1523delCTT	rs113993960
CF523	F508del	ins/del	C.1521_1523delCTT	rs113993960	S18I	missense	C.53G>T	NA
CF554	F508del	ins/del	C.1521_1523delCTT	rs113993960	F508del	ins/del	C.1521_1523delCTT	rs113993960
CF555	F508del	ins/del	C.1521_1523delCTT	rs113993960	R553X	nonsense	C.1657C>T	rs74597325
CF557	UNK	unknown	UNK	UNK	UNK	unknown	UNK	UNK
CF569	F508del	ins/del	C.1521_1523delCTT	rs113993960	F508del	ins/del	C.1521_1523delCTT	rs113993960

Patient code	Protein name	Allele 1 - Mutation type	Allele 1 - cDNA name	Allele 1 - SNP reference	Allele 1 - Protein name	Allele 2 - Mutation type	Allele 2 - cDNA name	Allele 2 - SNP reference
CF570	(TG)12(T)7	other	NA	rs113993960	(TG)11(T)7	other	other	NA
CF583	F508del	ins/del	c.1521_1523delCTT	rs113993960	1682dup	ins/del	NA	NA
CF584	F508del	ins/del	c.1521_1523delCTT	rs113993960	F508del	ins/del	c.1521_1523delCTT	rs113993960
CF585	R1162X	nonsense	c.3484C>T	rs74767530	R1162X	nonsense	c.3484C>T	rs74767530
CF586	F508del	ins/del	c.1521_1523delCTT	rs113993960	F508del	ins/del	c.1521_1523delCTT	rs113993960
CF601	F508del	ins/del	c.1521_1523delCTT	rs113993960	(TG)13(T)5	other	c.[12102125];1210-34TG[13]	NA
CF602	F508del	ins/del	c.1521_1523delCTT	rs113993960	F508del	ins/del	c.1521_1523delCTT	rs113993960
CF608	R785X	nonsense	c.2353C>T	rs374946172	R785X	nonsense	c.2353C>T	rs374946172
CF635	F508del	ins/del	c.1521_1523delCTT	rs113993960	F508del	ins/del	c.1521_1523delCTT	rs113993960
CF636	TBD	TBD	TBD	TBD	TBD	TBD	TBD	TBD
CF637	F508del	ins/del	c.1521_1523delCTT	rs113993960	F508del	ins/del	c.1521_1523delCTT	rs113993960
CF639	F508del	ins/del	c.1521_1523delCTT	rs113993960	F508del	ins/del	c.1521_1523delCTT	rs113993960
CF640	H609R	missense	c.1826A>G	rs397508310	UNK	unknown	UNK	UNK
CF641	G85E	missense	c.254G>A	rs75961395	1677delta A	ins/del	c.1545_1546delTA	rs121908776
CF642	F508del	ins/del	c.1521_1523delCTT	rs113993960	F508del	ins/del	c.1521_1523delCTT	rs113993960
CF644	F508del	ins/del	c.1521_1523delCTT	rs113993960	A455E	missense	c.1364C>A	rs74551128
CF645	R1162X	nonsense	c.3484C>T	rs74767530	3849+10kbC>T	splice	c.3718-247C>T	rs75039782
CF657	UNK	unknown	UNK	UNK	UNK	unknown	UNK	UNK
CF658	TBD	TBD	TBD	TBD	TBD	TBD	TBD	TBD
CF659	R75Q	missense	c.224G>A	rs1800076	E528E	other	c.1584G>A, p=(CFTRexon10)(CFTR-RD)	rs1800095
CF670	F508del	ins/del	c.1521_1523delCTT	rs113993960	G542X	nonsense	c.1624G>T	rs113993959
CF671	F508del	ins/del	c.1521_1523delCTT	rs113993960	H620P	missense	c.1859A>C	rs397508314

Patient code	Allele 1 - Protein name	Allele 1 - Mutation type	Allele 1 - cDNA name	Allele 1 - SNP reference	Allele 1 - SNP protein name	Allele 2 - Mutation type	Allele 2 - cDNA name	Allele 2 - SNP reference
CF672	F508del	ins/del	c.1521_1523delCTT	rs113993960	F508del	ins/del	c.1521_1523delCTT	rs113993960
CF673	F508del	ins/del	c.1521_1523delCTT	rs113993960	F508del	ins/del	c.1521_1523delCTT	rs113993960
CF675	R117H	missense	c.350G>A	rs78655421	UNK	unknown	UNK	UNK
CF676	E528E	other	c.1584G>A, p=(CFTR, exon 10)	NA	NA	UNK	UNK	UNK
CF683	TBD	TBD	TBD	TBD	TBD	TBD	TBD	TBD
CF691	F508del	ins/del	c.1521_1523delCTT	rs113993960	F508del	ins/del	c.1521_1523delCTT	rs113993960
CF699	F508del	ins/del	c.1521_1523delCTT	rs113993960	L453S	missense	c.1358T>C	NA
CF701	F508del	ins/del	c.1521_1523delCTT	rs113993960	F508del	ins/del	c.1521_1523delCTT	rs113993960
CF702	F508del	ins/del	c.1521_1523delCTT	rs113993960	F508del	ins/del	c.1521_1523delCTT	rs113993960
CF711	F508del	ins/del	c.1521_1523delCTT	rs113993960	F508del	ins/del	c.1521_1523delCTT	rs113993960
CF721	F508del	ins/del	c.1521_1523delCTT	rs113993960	F508del	ins/del	c.1521_1523delCTT	rs113993960
CF722	F508del	ins/del	c.1521_1523delCTT	rs113993960	F508del	ins/del	c.1521_1523delCTT	rs113993960
CF723	UNK	unknown	UNK	UNK	UNK	unknown	UNK	UNK
CF752	F508del	ins/del	c.1521_1523delCTT	rs113993960	F508del	ins/del	c.1521_1523delCTT	rs113993960
CF753	F508del	ins/del	c.1521_1523delCTT	rs113993960	R117H-7T	missense	NA	NA
CF761	F508del	ins/del	c.1521_1523delCTT	rs113993960	3849+10kbC>T	splice	c.3718-2477C>T	rs75039782
CF823	G542X	nonsense	c.1624G>T	rs113993959	P988R	missense	c.2963C>G	NA
CF824	F508del	ins/del	c.1521_1523delCTT	rs113993960	M470V + 2 unknown SNPs	missense	c.1408=	rs213950
HC001	WT	wildtype	WT	WT	WT	wildtype	WT	WT
HC002	WT	wildtype	WT	WT	WT	wildtype	WT	WT
HC003	WT	wildtype	WT	WT	WT	wildtype	WT	WT
HC004	WT	wildtype	WT	WT	WT	wildtype	WT	WT
HC005	WT	wildtype	WT	WT	WT	wildtype	WT	WT

Patient code	Patient Protein name	Allele 1 - Mutation type	Allele 1 - cDNA name	Allele 1 - SNP reference	Allele 1 - SNP reference	Allele 2 - Protein name	Allele 2 - Mutation type	Allele 2 - cDNA name	Allele 2 - SNP reference
HC006	WT	wildtype	WT	WT	WT	wildtype	WT	WT	WT
HC011	WT	wildtype	WT	WT	WT	wildtype	WT	WT	WT
HC012	WT	wildtype	WT	WT	WT	wildtype	WT	WT	WT
HC013	WT	wildtype	WT	WT	WT	wildtype	WT	WT	WT
HC014	WT	wildtype	WT	WT	WT	wildtype	WT	WT	WT
HC015	WT	wildtype	WT	WT	WT	wildtype	WT	WT	WT
HC018	WT	wildtype	WT	WT	WT	wildtype	WT	WT	WT
HC041	WT	wildtype	WT	WT	WT	wildtype	WT	WT	WT

Supplementary Table 1B: Beekman laboratory-governed Intestinal Organoids. TBD = to be determined, * = sample currently not available, UNK = unknown, WT = Wildtype.

CHAPTER 6

Frequency (%)	Allele	Frequency (%)	Allele
55.1	F508del	0.2	2183AA>G
4.6	WT	0.2	2184delA
3.7	UNK	0.2	4382delA
3.2	A455E	0.2	E92K
1.9	S1251N	0.2	G461R
1.5	W1282X	0.2	G628R
1.4	N1303K	0.2	R1066H
1.3	R1162X	0.2	R75Q
1.2	G542X	0.2	S18I
1.1	R553X	0.2	Y849X
0.9	1717-1G>A	0.1	(TG)11(T)5
0.9	R117H-7T	0.1	1677delTA
0.8	3849+10kbC>T	0.1	2789+5GT>A
0.7	3272-26A>G	0.1	3732delA
0.7	711+1G>T	0.1	394delTT
0.6	2789+5G>A	0.1	CFTRdel2
0.6	(TG)13(T)5	0.1	E528E
0.6	1811+1G>C	0.1	E730X
0.6	CFTRdel2.3	0.1	G1249R
0.6	R334W	0.1	Gly1349fs
0.5	CFTRdel17a,17b	0.1	H609R
0.4	E60X	0.1	H620P
0.4	G550X	0.1	I1027T
0.4	R117H	0.1	I1139V
0.4	Y1092X	0.1	I1366N
0.4	3659delC	0.1	I148N
0.4	D1152H	0.1	I507del
0.4	I336K	0.1	L1335P
0.4	L927P	0.1	Q220X
0.4	R1066C	0.1	Q525X
0.4	R117H-7T-9T	0.1	R75X
0.4	R347P	0.1	R785X
0.3	3905insT	0.1	S1159F
0.3	A46D	0.1	S466X
0.3	G85E	0.1	Ser670_Leu671insTer
0.3	G970R	0.1	(TG)11(T)7
0.3	L732X	0.1	(TG)12(T)5
0.2	1078delT	0.1	(TG)12(T)7
0.2	2143delT	0.1	1294del7

Frequency (%)	Allele	Frequency (%)	Allele
0.1	1342-1delG	0.1	G576A
0.1	1343delG	0.1	I556V
0.1	1496C>A/3659delC	0.1	IVS 4+1G>T
0.1	1682dup	0.1	IVS11-1G>C
0.1	1717-1G>T	0.1	IVS16+1G>A(3120+1G>A)
0.1	1813insC	0.1	L206W
0.1	1898+1G>C	0.1	L346P
0.1	1898+3A>G	0.1	L453S
0.1	1898+5G>T	0.1	L467F
0.1	2043delG	0.1	L953fs
0.1	2105-2117del13insAGAAA	0.1	L997F
0.1	2184insA	0.1	M470V + 2 unknown SNPs
0.1	-22del 11.4kb	0.1	P988R
0.1	2659delC	0.1	Q1012P
0.1	2789+5G>T	0.1	Q1352H
0.1	308insA	0.1	Q250X
0.1	3500-2A->G	0.1	Q39X
0.1	3539del16	0.1	R1070Q
0.1	365-366instT	0.1	R1158X
0.1	3677ins4	0.1	R1358S
0.1	3695del	0.1	R31C
0.1	3849+5G>T	0.1	R347H
0.1	4005+2T-c	0.1	R709X
0.1	4015delATT	0.1	R74P
0.1	4016instT	0.1	R764X
0.1	579+1G->T	0.1	R851Q
0.1	621+1G>T	0.1	S1178X
0.1	A559T	0.1	S945L
0.1	c.1221delA	0.1	splice1
0.1	c.1725-1727del insAT	0.1	SPLICE2
0.1	c.3468 + 2dupT	0.1	SPLICE3
0.1	CFTRdel11	0.1	T1396P
0.1	CFTRdel13,13a	0.1	T1857delT
0.1	CFTRdel19,20	0.1	V456F
0.1	D110H	0.1	R1283M
0.1	F1033S	0.1	W679X
0.1	F81L	0.1	W846X
0.1	G1249E	0.1	Y109D
0.1	G551D	0.1	Y275X

CHAPTER 6

Supplementary Table 1C: Frequency of CFTR mutations in our biobank

Patient code	Allele 1 - Protein name	Allele 1 - cDNA name	Allele 1 - SNP reference	Allele 2 - Protein name	Allele 2 - cDNA name	Allele 2 - SNP reference
CF169	F508del	c.1521_1523delCTT	rs113993960	G461R	c.1381G>A	NA
CF170	F508del	c.1521_1523delCTT	rs113993960	G461R	c.1381G>A	NA
CF174	2105-211 7del13insAGAAA	c.1973_1 985del13insAGAAA	rs121908780	Q1352H	c.4056G>C or c.4056G>T	rs113857788
CF438	F508del	c.1521_1523delCTT	rs113993960	I556V	c.1666A>G	rs75789129
CF640	H609R	c.1826A>G	rs397508310	UNK	UNK	UNK
CF671	F508del	c.1521_1523delCTT	rs113993960	H620P	c.1859A>C	rs397508314
HUB-02-D2-014	F508del	c.1521_1523delCTT	rs113993960	G1249R	c.3745G>A	rs397508602
HUB-02-D2-048	F508del	c.1521_1523delCTT	rs113993960	G461R	c.1381G>A	NA
HUB-02-D2-055	F508del	c.1521_1523delCTT	rs113993960	G628R	c.1882G>A or c.1882G>C	rs397508316
HUB-02-D2-056	F508del	c.1521_1523delCTT	rs113993960	E730X	c.2188G>T	rs113993960
HUB-02-D2-158	F508del	c.1521_1523delCTT	rs113993960	1813insC	c.1681 _1682insC	NA
HUB-02-D2-212	F508del	c.1521_1523delCTT	rs113993960	G628R	c.1882G>A or c.1882G>C	rs397508316
HUB-02-D2-344	F508del	c.1521_1523delCTT	rs113993960	E730X	c.2188G>T	rs113993960
HUB-02-D2-398	F508del	c.1521_1523delCTT	rs113993960	G1249R	c.3745G>A	rs397508602
HUB-02-D2-410	4382delA	c.4251delA	rs397508706	2043delG	c.1911delG	NA
HUB-02-D2-419	G542X	c.1624G>T	rs113993959	I148N	c.443T>A	rs35516286
HUB-02-D2-450	G542X	c.1624G>T	rs113993959	W679X	c.2036G>A	rs397508333
HUB-02-D2-478	F508del	c.1521_1523delCTT	rs113993960	splice1	c.4243-3T>A	NA
HUB-02-D2-481	F508del	c.1521_1523delCTT	rs113993960	1342-1delG	c.1210-1delG	NA
HUB-02-D2-483	F508del	c.1521_1523delCTT	rs113993960	G628R	c.1882 G>C	rs397508316
HUB-02-D2-490	F508del	c.1521_1523delCTT	rs113993960	R1358S	c.4074A>T	NA
HUB-02-D2-561	N1303K	c.3909C>G	rs80034486	L346P	c.1037T>C	rs397508146
HUB-02-D2-564	V456F	c.1366G>T	rs397508195	R1162X	c.3484C>T	rs74767530

Patient code	Allele 1 - Protein name	Allele 1 - cDNA name	Allele 1 - SNP reference	Allele 2 - Protein name	Allele 2 - cDNA name	Allele 2 - SNP reference
HUB-02-D2-571	2184delA	c.2052delA	rs121908746	D110H	c.328G>C	rs113993958
TBD	Q525X	NA	NA	3732delA	NA	NA
TBD	Q525X	NA	NA	3732delA	NA	NA
TBD*	F508del	c.1521_1523delCTT	rs113993960	G1249E	c.3746G>A	rs121909040

Supplementary Table 1D: Reported CFTR mutations which are not present in CFTR2 mutation database.

TBD = to be determined, * = sample currently not available

CHAPTER 6

Patient code	Allele 1 - Protein name	Allele 1 - cDNA name	Allele 1 - SNP reference	Allele 2 - Protein name	Allele 2 - cDNA name	Allele 2 - SNP reference
CF012	E60X	c.178G>T	rs77284892	4015delATT		NA
CF097	R851Q	c.2552G>A	2684G>A	WT	WT	rs397508395
CF187	F508del	c.1521_1523delCTT	rs113993960	1210-34TG(11)-12T(5)		NA
CF380	N1303K	c.3909C>G	rs80034486	F81L	c.241 T>C	NA
CF383	F508del	c.1521_1523delCTT	rs113993960	c.3468 + 2dupT		NA
CF385	G542X	c.1624G>T	rs113993959	Q250X	c.748 C>T	NA
CF424	NA	c.2989-2593del8899	NA	NA	c.2989-2593del8899	NA
CF425	F508del	c.1521_1523delCTT	rs113993960	I1366N	c.4097T>A	NA
CF523	F508del	c.1521_1523delCTT	rs113993960	S18I	c.53G>T	NA
CF583	F508del	c.1521_1523delCTT	rs113993960	1682dup		NA
CF676	E528E	c.1584G>A, p.= (CFTR, exon 10)	NA	NA	unknown	UNK
CF699	F508del	c.1521_1523delCTT	rs113993960	L453S	c.1358T>C	NA
CF823	G542X	c.1624G>T	rs113993959	P988R	c.2963C>G	NA
HUB-02-D2-030	I507del	c.1519_1521delATC	rs121908745	SPLICE2	c.4242+2T>G	NA
HUB-02-D2-041	R553X	c.1657C>T	rs74597325	SPLICE3	c.4375-3T>A	NA
HUB-02-D2-064	F508del	c.1521_1523delCTT	rs113993960	F1033S	c.3101T>C	NA
HUB-02-D2-132	F508del	c.1521_1523delCTT	rs113993960	1294del7	c.1162_1168delACGACTA	rs397508169
HUB-02-D2-138	F508del	c.1521_1523delCTT	rs113993960	3849+5G>T	c.3717+5G>T	NA
HUB-02-D2-142	F508del	c.1521_1523delCTT	rs113993960	CFTRdele19.20	ins/del	NA
HUB-02-D2-146	2789+5G>T	NA	NA	711+1G>T	c.579+1G>T	rs77188391
HUB-02-D2-147	F508del	c.1521_1523delCTT	rs113993960	S18I	c.53G>T	NA
HUB-02-D2-156	F508del	c.1521_1523delCTT	rs113993960	Y109D	c.325T>G	NA
HUB-02-D2-161	F508del	c.1521_1523delCTT	rs113993960	R74P	c.224G>C	NA
HUB-02-D2-165	F508del	c.1521_1523delCTT	rs113993960	c.1725-1727delinsAT	NA	NA
HUB-02-D2-391	4832delA	NA	NA	NA	c.1991del6	NA
HUB-02-D2-404	1717-1G>A	c.1585-1G>A	rs76713772	3677ins4	NA	NA

Patient code	Allele 1 - Protein name	Allele 1 - cDNA name	Allele 1 - SNP reference	Allele 2 - Protein name	Allele 2 - cDNA name	Allele 2 - SNP reference
HUB-02-D2-469	S1251N	c.3752G>A	rs74503330	S1178X	c.3533C>G	NA
HUB-02-D2-479	N1303K	c.3909C>G	rs80034486	Q1012P	c.3035A>C	NA
HUB-02-D2-485	F508del	c.1521_1523delCTT	rs113993960	Gly1349fs	c.4046delG	NA
HUB-02-D2-506	F508del	c.1521_1523delCTT	rs113993960	S18I	c.53G>T	NA
HUB-02-D2-539	F508del	c.1521_1523delCTT	rs113993960	T1396P	c.4187A>C	NA
HUB-02-D2-570	2659delC	NA	NA	N1303K	c.3909C>G	rs80034486
TBD	R1162X	c.3484C>T	rs74767530	3539del16	NA	NA
TBD	R334W	c.1000C>T	rs121909011	-22del 11.4kb	NA	NA

Supplementary Table 1E: CFTR mutations not reported before (CFTR1 or CFTR2). TBD = to be determined, * = sample currently not available, UNK = unknown, WT = Wildtype.

Patient code	Allele 1 - Protein name	Allele 1 - Mutation type	Allele 1 - cDNA name	Allele 1 - SNP reference	Allele 2 - Protein name	Allele 2 - Mutation type	Allele 2 - cDNA name	Allele 2 - SNP reference	PAM
CF042	R117H>T	missense	c.[350G>A;1210?12[7]]	NA	R553X	nonsense	c.1657C>T	rs74597325	NGN
CF259	F508del	ins/del	c.1521_1523delCTT	rs113993960	3849+10kbC>T	splice	c.3718-2477C>T	rs75039782	NGN
CF368	R75Q	missense	c.224G>A	rs1800076	c.1221delA	ins/del	c.1221delA	NA	NGN
CF410	3849+10 kbC>T	splice	c.3718-2477C>T	rs75039782	W1282X	nonsense	c.3846G>A	rs77010898	NGN
CF503	F508del	ins/del	c.1521_1523delCTT	rs113993960	R553X	nonsense	c.1657C>T	rs74597325	NGN
CF555	F508del	ins/del	c.1521_1523delCTT	rs113993960	R553X	nonsense	c.1657C>T	rs74597325	NGN
CF585	R1162X	nonsense	c.3484C>T	rs74767530	R1162X	nonsense	c.3484C>T	rs74767530	NGN
CF608	R785X	nonsense	c.2353C>T	rs374946172	R785X	nonsense	c.2353C>T	rs374946172	NGG
CF645	R1162X	nonsense	c.3484C>T	rs74767530	3849+10kbC>T	splice	c.3718-2477C>T	rs75039782	NGN
CF659	R75Q	missense	c.224G>A	rs1800076	E528E	other	c.1584G>A p=[CFTRexon10](CFTR-RD)	rs1800095	NGN
CF761	F508del	ins/del	c.1521_1523delCTT	rs113993960	3849+10kbC>T	splice	c.3718-2477C>T	rs75039782	NGN
HUB-02-D2-014	F508del	ins/del	c.1521_1523delCTT	rs113993960	G1249R	missense	c.3745G>A	rs397508602	NGN
HUB-02-D2-028	R334W	missense	c.1000C>T	rs121909011	R764X	nonsense	c.2290C>T	rs121908810	NGG
HUB-02-D2-038	F508del	ins/del	c.1521_1523delCTT	rs113993960	R1162X	nonsense	c.3484C>T	rs74767530	NGN
HUB-02-D2-041	R553X	nonsense	c.1657C>T	rs74597325	SPLICE3	splice	c.4375-3T>A	NA	NGN
HUB-02-D2-051	F508del	ins/del	c.1521_1523delCTT	rs113993960	R1162X	nonsense	c.3484C>T	rs74767530	NGN
HUB-02-D2-052	F508del	ins/del	c.1521_1523delCTT	rs113993960	R1162X	nonsense	c.3484C>T	rs74767530	NGN

Patient code	Allele 1 - Protein name	Allele 1 - Mutation type	Allele 1 - cDNA name	Allele 1 - SNP reference	Allele 2 - Protein name	Allele 2 - Mutation type	Allele 2 - cDNA name	Allele 2 - SNP reference	PAM
HUB-02-D2-107	R553X	nonsense	c.1657C>T	rs74597325	D1152H	missense	c.3454G>C	rs75541969	NGN
HUB-02-D2-126	R1162X	nonsense	c.3484C>T	rs74767530	3659delC	ins/del	c.3528delC	rs121908747	NGN
HUB-02-D2-128	R553X	nonsense	c.1657C>T	rs74597325	UNK	unknown	UNK	UNK	NGN
HUB-02-D2-155	R1066H	missense	c.3197G>A	rs121909019	CFTRdel2.3	ins/del	c.54-5940_2 73+10250del21kb	NA	NGN
HUB-02-D2-189	R1066C	missense	c.3196C>T	rs78194216	R1066H	missense	c.3196C>T	rs78194216	NGN
HUB-02-D2-190	3849+10 kbC>T	splice	c.3718_2477C>T	rs75039782	R347H	missense	c.1040G>A	rs77932196	NGG
HUB-02-D2-195	F508del	ins/del	c.1521_1523delCTT	rs113993960	3849+10kbC>T	splice	c.3718_2477C>T	rs75039782	NGN
HUB-02-D2-329	F508del	ins/del	c.1521_1523delCTT	rs113993960	R1162X	nonsense	c.3484C>T	rs74767530	NGN
HUB-02-D2-330	F508del	ins/del	c.1521_1523delCTT	rs113993960	R1162X	nonsense	c.3484C>T	rs74767530	NGN
HUB-02-D2-395	R1162X	nonsense	c.3484C>T	rs74767530	D1152H	missense	c.3454G>C	rs75541969	NGN
HUB-02-D2-398	F508del	ins/del	c.1521_1523delCTT	rs113993960	G1249R	missense	c.3745G>A	rs397508602	NGN
HUB-02-D2-403	R1162X	nonsense	c.3484C>T	rs74767530	3272_26A>G	splice	c.3140_26A>G	rs76151804	NGN
HUB-02-D2-405	F508del	ins/del	c.1521_1523delCTT	rs113993960	R553X	nonsense	c.1657C>T	rs74597325	NGN
HUB-02-D2-406	G542X	nonsense	c.1624G>T	rs113993959	3849+10kbC>T	splice	c.3718_2477C>T	rs75039782	NGN
HUB-02-D2-408	I336K	missense	c.1007T>A	rs397508139	R553X	nonsense	c.1657C>T	rs74597325	NGN

Patient code	Allele 1 - Protein name	Allele 1 - Mutation type	Allele 1 - cDNA name	Allele 1 - SNP reference	Allele 2 - Protein name	Allele 2 - Mutation type	Allele 2 - cDNA name	Allele 2 - SNP reference	PAM	
HUB-02-D2-414	R553X	nonsense	c.1657C>T	rs74597325	I336K	missense	c.1007T>A	rs397508139	NGN	
HUB-02-D2-452	F508del	ins/del	c.1521_1523delCTT	rs113993960	R75Q	missense	c.224G>A	rs1800076	NGN	
HUB-02-D2-457	F508del	ins/del	c.1521_1523delCTT	rs113993960	R553X	nonsense	c.1657C>T	rs74597325	NGN	
HUB-02-D2-458	F508del	ins/del	c.1521_1523delCTT	rs113993960	3849+10kbC>T	splice	c.3718-2477C>T	rs75039782	NGN	
HUB-02-D2-466	F508del	ins/del	c.1521_1523delCTT	rs113993960	3849+10kbC>T	splice	c.3718-2477C>T	rs75039782	NGN	
HUB-02-D2-468	F508del	ins/del	c.1521_1523delCTT	rs113993960	3849+10kbC>T	splice	c.3718-2477C>T	rs75039782	NGN	
HUB-02-D2-482	D1152H	missense	c.1521_1523delCTT	rs113993960	3849+10kbC>T	splice	c.3718-2477C>T	rs75039782	NGN	
HUB-02-D2-497	4005+2T>c	splice	c.3454G>C	rs75541969	R1162X	nonsense	c.3484C>T	rs74767530	NGN	
HUB-02-D2-537	R553X	nonsense	c.1657C>T	rs146795445	R553X	nonsense	c.1657C>T	rs74597325	NGN	
HUB-02-D2-559	R347P	missense	c.1040G>C	rs77932196	R1162X	nonsense	c.3484C>T	rs74767530	NGN	
HUB-02-D2-563	V456F	missense	c.1366G>T	rs397508195	R1162X	nonsense	c.3484C>T	rs74767530	NGN	
HUB-02-D2-564	TBD	R553X	nonsense	c.1657C>T	rs74597325	1898+3A>G	splice	c.1766+3A>G	rs397508298	NGN
TBD	R1162X	nonsense	c.3484C>T	rs74767530	3272-26A>G	splice	c.3140-26A>G	rs76151804	NGN	
TBD	R1066H	missense	c.3197G>A	rs121909019	CFTRdel2	ins/del	c.54_164del111	rs1562882675	NGN	
TBD	R553X	nonsense	c.1657C>T	rs74597325	G542X	nonsense	c.1624G>T	rs113993959	NGN	
TBD	R75X	nonsense	NA	NA	R75X	nonsense	NA	NA	NGN	

Patient code	Allele 1 - Protein name	Allele 1 - Mutation type	Allele 1 - cDNA name	Allele 1 - SNP reference	Allele 2 - SNP reference	Allele 2 - Protein name	Allele 2 - Mutation type	Allele 2 - cDNA name	Allele 2 - SNP reference	PAM
TBD	R1162X	nonsense	c.3484C>T	rs74767530	3539del16	ins/del	NA	NA	rs78769542	NGN
TBD	S466X	nonsense	c.1397C>A or c.1397C>G	rs121908805	R1070Q	missense	c.3209G>A	NA	rs78769542	NGN
TBD*	F508del	ins/del	c.1521_1523delCTT	rs113993960	R1162X	nonsense	c.3484C>T	rs74767530	NGN	
TBD*	R117H>T	missense	c.[350G>A;1210?1271]	rs78655421 (-7)	R1162X	nonsense	c.3484C>T	rs74767530	NGN	
TBD*	I336K	missense	c.1007T>A	rs397508139	R53X	nonsense	c.1657C>T	rs74597325	NGN	

Supplementary Table 2A: CF patients in the biobank carrying a base-editable mutation on at least one allele without other editable bases in the editing window.

TBD = to be determined, * = sample currently not available, UNK = unknown, WT = Wildtype.

Patient code	Allele 1 - Protein name	Allele 1 - Mutation type	Allele 1 - cDNA name	Allele 1 - SNP reference	Allele 2 - Protein name	Allele 2 - Mutation type	Allele 2 - cDNA name	Allele 2 - SNP reference	PAM
CF053	F508del	ins/del	c.1521_1523delCTT	rs113993960	S1251N	missense	c.3752G>A	rs74503330	NGN
CF099	F508del	ins/del	c.1521_1523delCTT	rs113993960	S1251N	missense	c.3752G>A	rs74503330	NGN
CF140	S1251N	missense	c.3752G>A	rs74503330	R117H	missense	c.350G>A	rs78655421	NGN
CF141	F508del	ins/del	c.1521_1523delCTT	rs113993960	S1251N	missense	c.3752G>A	rs74503330	NGN
CF169	F508del	ins/del	c.1521_1523delCTT	rs113993960	G461R	missense	c.1381G>A	NA	NGG
CF170	F508del	ins/del	c.1521_1523delCTT	rs113993960	G461R	missense	c.1381G>A	NA	NGN
CF210	F508del	ins/del	c.1521_1523delCTT	rs113993960	S1251N	missense	c.3752G>A	rs74503330	NGN
CF216	1717-1G>A	splice	c.1585-1G>A	rs76713772	S1251N	missense	c.3752G>A	rs74503330	NGN
CF226	F508del	ins/del	c.1521_1523delCTT	rs113993960	S945L	missense	c.2834C>T	rs397508442	NGN
CF310	F508del	ins/del	c.1521_1523delCTT	rs113993960	R334W	missense	c.100C>T	rs121909011	NGN
CF411	W1282X	nonsense	c.3846G>A	rs77010838	W1282X	nonsense	c.3846G>A	rs77010898	NGN
CF499	N1303K	missense	c.3909C>G	rs80034486	R334W	missense	c.100C>T	rs121909011	NGN
CF641	G85E	missense	c.254G>A	rs75961395	I677delTA	ins/del	c.1545_1546delTA	rs121908776	NGN
HUB-02-D2-005	1677delTA	ins/del	c.1545_1546delTA	rs121908776	IVS16+1 G>A(3120+1G>A)	splice	c.2988+1G>A	rs75096551	NGN
HUB-02-D2-012	F508del	ins/del	c.1521_1523delCTT	rs113993960	S1251N	missense	c.3752G>A	rs74503330	NGN
HUB-02-D2-022	1717-1G>A	splice	c.1585-1G>A	rs76713772	2183AA>G	ins/del	c.2051_- 2052delAAinsG	rs121908799	NGN
HUB-02-D2-039	F508del	ins/del	c.1521_1523delCTT	rs113993960	W1282X	nonsense	c.3846G>A	rs77010898	NGN
HUB-02-D2-046	F508del	ins/del	c.1521_1523delCTT	rs113993960	W1282X/R1283M	nonsense/ missense	c.3846G>A	rs77010898	NGN
HUB-02-D2-048	F508del	ins/del	c.1521_1523delCTT	rs113993960	G461R	missense	c.1381G>A	NA	NGN

Patient code	Allele 1 - Protein name	Allele 1 - Mutation type	Allele 1 - name	Allele 1 - cDNA - SNP reference	Allele 1 - Protein name	Allele 2 - Mutation type	Allele 2 - name	Allele 2 - cDNA - SNP reference	PAM
HUB-02-D2-053	S1251N	missense	c.3752G>A	rs74503330	UNK	unknown	UNK	UNK	NGN
HUB-02-D2-057_I	F508del	ins/del	c.1521_1523delCTT	rs113993960	S1251N	missense	c.3752G>A	rs74503330	NGN
HUB-02-D2-059_I	F508del	ins/del	c.1521_1523delCTT	rs113993960	2789+5G>A	splice	c.2657+5G>A	rs80224560	NGN
HUB-02-D2-066	F508del	ins/del	c.1521_1523delCTT	rs113993960	1717-1G>A	splice	c.1585-1G>A	rs76713772	NGN
HUB-02-D2-087	711+1G>T	splice	c.579+1G>T	rs77188391	S1251N	missense	c.3752G>A	rs74503330	NGN
HUB-02-D2-092	F508del	ins/del	c.1521_1523delCTT	rs113993960	S1251N	missense	c.3752G>A	rs74503330	NGN
HUB-02-D2-095	F508del	ins/del	c.1521_1523delCTT	rs113993960	S1251N	missense	c.3752G>A	rs74503330	NGN
HUB-02-D2-096	F508del	ins/del	c.1521_1523delCTT	rs113993960	S1251N	missense	c.3752G>A	rs74503330	NGN
HUB-02-D2-099	F508del	ins/del	c.1521_1523delCTT	rs113993960	S1251N	missense	c.3752G>A	rs74503330	NGN
HUB-02-D2-101	F508del	ins/del	c.1521_1523delCTT	rs113993960	S1251N	missense	c.3752G>A	rs74503330	NGN
HUB-02-D2-103	R334W	missense	c.1000C>T	rs121909011	R334W	missense	c.3752G>A	rs74503330	NGN
HUB-02-D2-104	F508del	ins/del	c.1521_1523delCTT	rs113993960	G85E	missense	c.1000C>T	rs121909011	NGN
HUB-02-D2-114	2789+5G>A	splice	c.2657+5G>A	rs80224560	UNK	unknown	UNK	UNK	NGG
HUB-02-D2-140	G542X	nonsense	c.1624G>T	rs113993959	W1282X	nonsense	c.3846G>A	rs77010898	NGN
HUB-02-D2-145									

Patient code	Allele 1 - Protein name	Allele 1 - Mutation type	Allele 1 - cDNA name	Allele 1 - SNP reference	Allele 2 - Protein name	Allele 2 - Mutation type	Allele 2 - cDNA name	Allele 2 - SNP reference	PAM
HUB-02-D2-182	W1282X	nonsense	c.3846G>A	rs77010898	L927P	missense	c.2780T>C	rs397508435	NGN
HUB-02-D2-186	Y849X	nonsense	c.2547C>A	rs397508394	2789+5G>A	splice	c.2657+5G>A	rs80224560	NGN
HUB-02-D2-188	1717-1G>A	splice	c.1585-1G>A	rs76713772	3905instT	ins/del	c.3773_3774instT	rs121908789	NGN
HUB-02-D2-207	W1282X	nonsense	c.3846G>A	rs77010898	W1282X	nonsense	c.3846G>A	rs77010898	NGN
HUB-02-D2-222	F508del	ins/del	c.1521_1523delCTT	rs13993960	1717-1G>A	splice	c.1585-1G>A	rs76713772	NGN
HUB-02-D2-229,I	W1282X	nonsense	c.3846G>A	rs77010898	W1282X	nonsense	c.3846G>A	rs77010898	NGN
HUB-02-D2-361	F508del	ins/del	c.1521_1523delCTT	rs13993960	S1251N	missense	c.3752G>A	rs74503330	NGN
HUB-02-D2-362	F508del	ins/del	c.1521_1523delCTT	rs13993960	S1251N	missense	c.3752G>A	rs74503330	NGN
HUB-02-D2-371	S1251N	missense	c.1521_1523delCTT	rs13993960	S1251N	missense	c.3752G>A	rs74503330	NGN
HUB-02-D2-374	S1251N	missense	c.3752G>A	rs74503330	A455E	missense	c.1364C>A	rs7451128	NGN
HUB-02-D2-380	F508del	ins/del	c.1521_1523delCTT	rs13993960	S1251N	missense	c.3752G>A	rs74503330	NGN
HUB-02-D2-404	1717-1G>A	splice	c.1585-1G>A	rs76713772	3677ins4	ins/del	NA	NA	NGN
HUB-02-D2-417	E92K	missense	c.274G>A	rs121908751	CFTRdel2	ins/del	c.(53+1_54-1)_(164+1_165-1)del	NA	NGN
HUB-02-D2-418	R334W	missense	c.1000G>T	rs121909011	N1303K	missense	c.3909C>G	rs80034486	NGN
HUB-02-D2-448	W1282X	nonsense	c.3846G>A	rs77010898	W1282X	nonsense	c.3846G>A	rs77010898	NGN



Patient code	Allele 1 - Protein name	Allele 1 - Mutation type	Allele 1 - name	Allele 1 - cDNA - SNP reference	Allele 1 - Protein name	Allele 2 - Mutation type	Allele 2 - name	Allele 2 - cDNA - SNP reference	PAM
HUB-02-D2-459	F508del	ins/del	c.1521_1523delCTT	rs113993960	W1282X	nonsense	c.3846G>A	rs77010898	NGN
HUB-02-D2-461	F508del	ins/del	c.1521_1523delCTT	rs113993960	W1282X	nonsense	c.3846G>A	rs77010898	NGN
HUB-02-D2-462	F508del	ins/del	c.1521_1523delCTT	rs113993960	W1282X	nonsense	c.3846G>A	rs77010898	NGN
HUB-02-D2-464	F508del	ins/del	c.1521_1523delCTT	rs113993960	G85E	missense	c.254G>A	rs75961395	NGG
HUB-02-D2-469	S1251N	missense	c.3752G>A	rs74503330	S1178X	nonsense	c.3533C>G	NA	NGN
HUB-02-D2-470	F508del	ins/del	c.1521_1523delCTT	rs113993960	W1282X	nonsense	c.3846G>A	rs77010898	NGN
HUB-02-D2-475	F508del	ins/del	c.1521_1523delCTT	rs113993960	2789+5G>A	splice	c.2657+5G>A	rs80224560	NGN
HUB-02-D2-480	W1282X	nonsense	c.3846G>A	rs77010898	R117H>T	missense	c.[350G>A ;1210?12[7]]	rs78655421 (-T)	NGN
HUB-02-D2-488	F508del	ins/del	c.1521_1523delCTT	rs113993960	2789+5G>A	splice	c.2657+5G>A	rs80224560	NGN
HUB-02-D2-507	F508del	ins/del	c.1521_1523delCTT	rs113993960	1717-1G>A	splice	c.1585-1G>A	rs76713772	NGN
HUB-02-D2-518	N1303K	missense	c.3909G>G	rs80034486	G85E	missense	c.254G>A	rs75961395	NGG
HUB-02-D2-535	W1282X	nonsense	c.3846G>A	rs77010898	1717-1G>A	splice	c.1585-1G>A	rs76713772	NGN
HUB-02-D2-562	CFTRdel2.3	ins/del	c.54-5940_73+10250del21kb	NA	R334W	missense	c.1000C>T	rs121909011	NGN
TBD	2789+5G>A	splice	c.2657+5G>A	rs80224560	2183AA>G	ins/del	c.2051_20	rs121908799	NGN
TBD*	R334W	missense	c.1000C>T	rs121909011	-22del 11.4kb	ins/del	NA	NA	NGN

Patient code	Allele 1 - Protein name	Allele 1 - Mutation type	Allele 1 - cDNA name	Allele 1 - SNP reference	Allele 2 - Protein name	Allele 2 - Mutation type	Allele 2 - cDNA name	Allele 2 - SNP reference	PAM
TBD	2789+5G>A	splice	c.2657+5G>A	rs80224560	2789+5G>A	splice	c.2657+5G>A	rs80224560	NGN
TBD	Q525X	nonsense	NA	NA	3722delA	ins/del	NA	NA	NGN
TBD	Q525X	nonsense	NA	NA	3722delA	ins/del	NA	NA	NGN
TBD	1717-1G>A	splice	c.1585-1G>A	rs76713772	3905instT	ins/del	c.3773_3774instT	rs121908789	NGN
TBD	E92K	missense	c.274G>A	rs121908751	E92K	missense	c.274G>A	rs121908751	NGN
TBD	2789+5G>A	splice	c.2657+5G>A	rs80224560	L732X	nonsense			NGN
TBD	W1282X	nonsense	c.3846G>A	rs77010898	L953fs	ins/del	c.2859_2890del		NGN
TBD	1898+1G>C	splice	c.1679+1G>C	rs397508263	Q220X	nonsense	NA	NA	NGN
TBD	N1303K	missense	c.3909C>G	rs80034486	Q220X	nonsense	NA	NA	NGN
TBD	F508del	ins/del	c.1521_1523delCTT	rs11399360	S1251N	missense	c.3752G>A	rs74503330	NGN
TBD	G542X	nonsense	c.1624G>T	rs11399359	W1282X	nonsense	c.3846G>A	rs77010898	NGN
TBD*	F508del	ins/del	c.1521_1523delCTT	rs11399360	1717-1G>A	splice	c.1585-1G>A	rs76713772	NGN
TBD*	S1251N	missense	c.3752G>A	rs74503330	1717-1G>A	splice	c.1585-1G>A	rs76713772	NGN
TBD*	F508del	ins/del	c.1521_1523delCTT	rs11399360	S1251N	missense	c.3752G>A	rs74503330	NGN
TBD*	F508del	ins/del	c.1521_1523delCTT	rs11399360	S1251N	missense	c.3752G>A	rs74503330	NGN
TBD*	1717-1G>A	splice	c.1585-1G>A	rs76713772	Y1092X	nonsense	c.3276C>A or c.3276C>G	rs121908761	NGN

Supplementary Table 2B: CF patients in the biobank carrying a base-editable mutation on at least one allele but with other editable bases in the editing window. TBD = to be determined, * = sample currently not available, UNK = unknown, WT = Wildtype.

Chromosome	start	stop	strand	sequence	Mis-matches	Off-target in Spacer	Off-targets in flanks
chr7	117592500	117592522	-	TTCAGTGAATGTTCTGACCTGG	0	NA	NA
chr8	19362913	19362935	-	cTAGTGAATGTTaaGACCTAGG	3	0	0
chr8	59628566	59628588	-	TTAGTGAATGTTCTGtCCAGG	3	0	0
chr5	8612807	8612829	+	TacAGTGAatGTTCTGtCCTAGG	3	0	0
chr5	128465356	128465378	-	aTAGTGAATGtaCTGAgCTCGG	3	0	0
chr1	23085345	23085367	+	TTCAGTaaATGTTCTGAgCTGG	3	0	0
chr1	78888563	78888585	+	TccAGTGAATGtCCTGAgCTGG	3	0	0
chr2	127194619	127194641	-	TTgAGTGAATGTTCTGatCTGG	3	0	0
chr22	25577784	25577806	+	TgcAGTGAATGTTCTACatAGG	3	0	0
chr14	61252504	61252526	-	cTAGTGAatGtGCTCTGACCTGG	3	0	0
chr20	3281291	32811313	+	TgAGTGAgtGTTCTGAcCTGG	3	0	0
chr9	101967756	101967778	-	TTCAGTGAATGtCTGtCCTGG	3	0	0
chrX	18506504	18506526	-	TTctGTGAATAatGACCTGG	3	0	0
chr8	11883076	11863098	-	TTAGTCAATCTCCACCTGG	4	0	0
chr8	35676319	35676341	+	TTCttTGATGTTCTGAActTGG	4	0	0
chr8	88086567	88086589	+	TTtAGTGAATAttGAGCTGG	4	0	0
chr8	106997302	106997324	-	TTtACtGAAgTTtGACCCAGG	4	0	0
chr8	107834663	107834685	-	aTAGTGAATGTTCTGtCCTGG	4	0	0
chr8	110856086	110856108	-	TTCAAAtTAATctCTGACTTGG	4	0	0
chr8	133071277	133071299	-	TTAGTGAATGCTGtGCTGG	4	0	0
chr12	45753400	45753422	+	TTCAAGTTagTTTgGACCTGG	4	0	0
chr12	45713092	45713114	-	TTCAAGTAATGTTtGcCaTGG	4	0	0
chr12	59847944	59847966	-	TgAGTAAATGTTCTGatTGG	4	0	0
chr12	77179799	77179821	-	TgtGtGTGacAGtCTGACCTAGG	4	0	0
chr12	79448490	79448512	-	aTAGTGAAGaaGTtCTGgCaTGG	4	0	0
chr12	85180719	85180741	+	TTCAAtGAATGtAtGAACTGG	4	0	0

chromosome	start	stop	strand	sequence	Mis-matches	Off-target in Spacer	Off-targets in flanks
chr12	114083508	114083530	-	gTCAGTGAATGtaaaGACCTGG	4	0	0
chr12	116602621	116602643	-	TgCAGTGAATTTCTGACCTGG	4	0	0
chr12	118853621	118853643	+	TgCAGTGAATttATCTGacCTGG	4	0	0
chr12	119194485	119194507	+	gTCAGTttATGatCTGACCTAGG	4	0	0
chr3	5020276	5020298	-	TTAtAGAAATGTTCTGgcCTTG	4	0	0
chr3	23219052	23219074	+	TTAGTtAAIttCTGACTGG	4	0	0
chr3	33181243	33181265	-	TTCAGTGAATGtgaaGgcCTAGG	4	0	0
chr3	70633373	70693395	-	aTCAGTGAATGTTCTAagTCGG	4	0	0
chr3	8369004	83690026	-	gTAtGAATGtCTGACCAtGG	4	0	0
chr3	96706042	96706064	+	TACAGTGAAGctCTGAatCTGG	4	0	0
chr3	97422338	97422360	-	TTgAGTGAATttCTtACCTAGG	4	0	0
chr3	104774277	104774299	-	TTCAAGaGACTtCTtAtCTAGG	4	0	0
chr3	133077469	133077491	+	TTCAAGTGAgttgTCTGACCCAGG	4	0	0
chr3	133768036	133768058	+	TTCAAGTGAAGGTTgtGCCCCtGG	4	0	0
chr3	138857421	138857443	+	TTCAAGaGAATGttCTGaaaAGG	4	0	0
chr7	21144282	21144304	+	TTCAAGTGAAttttttACCGGG	4	0	0
chr7	29897267	29897289	+	TTGAGTGAATGctCTGAAatCG	4	0	0
chr7	80487203	80487225	-	TTCAAGTAGtgAtCTGACCTGG	4	0	0
chr7	89263167	89263189	+	TTCAAGTAATAttCctACCTCGG	4	0	0
chr7	111718265	111718287	+	TgCAGTGAATGgggtGAATCTGG	4	0	0
chr7	115588360	115588382	-	TTCCGTGAATgtCTGAcCTTGG	4	0	0
chr7	11527330	11527352	-	TTCAAGTGAAttccAGACCTGG	4	0	0
chr7	126685551	126685573	+	gTCAGTGAATGctCTGAcCTGG	4	0	0
chr7	134187449	134187471	-	TTCAAGTGAATGttGAcCTTGG	4	0	0
chr7	159141095	159141117	-	TcAGTGAAGttCTGAGtTAGG	4	0	0
chr4	37598207	37598229	+	TTccTGAATGttCTGttCTGG	4	0	0

Chromosome	start	stop	strand	sequence	Mis-matches	Off-target in Spacer	Off-targets in flanks
chr4	52384415	52384437	-	TTCAggGicTGTCTGCCTGG	4	0	0
chr4	78255681	78265703	+	aTgAGTGAATGTTCTGctTGG	4	0	0
chr4	105541250	105541272	-	TtgGTGAGtGTTgtGACCTGG	4	0	0
chr4	116301451	116301473	-	TcatGTGAATGTTCTGaaCTGG	4	0	0
chr4	137000820	137000842	+	TTGAGTGctGCTCTGatCTGG	4	0	0
chr4	148402251	148402273	+	TTCAgTAatTattCTGaaCTAGG	4	0	0
chr4	159412819	159412841	+	TTCAiTGAATGTTgTaAtCTAGG	4	0	0
chr4	164937631	164937653	-	TTgAGaGAATTcTGTGACCTAGG	4	0	0
chr4	178794181	178794203	-	TTCAgTAAATTTtaACCTAGG	4	0	0
chr5	4133104	4133126	+	TgCAGTGGaggTTCTGccCTAGG	4	0	0
chr5	6529451	6529473	-	aTCAggGAATGtaCTGAGCTTGG	4	0	0
chr5	37988256	37988278	+	TcCAGTGTaccCTTGACCTTGG	4	0	0
chr5	38969556	38969578	-	gTgAGTGAATGTTaaGACCTAGG	4	0	0
chr5	78043636	78043658	-	TTCACTGTATGTCgtGACCAtGG	4	0	0
chr5	117651893	117651915	+	TTaAaTCAATGctCTGACCTAGG	4	0	0
chr5	150041779	150041801	+	TTCAAGaAGaaGactCTGACCTCGG	4	0	0
chr5	163829547	163829569	+	cTtAGTGGATGTTgtGACCTTGG	4	0	0
chr5	168897568	168897590	+	TTCAgAGATGCTCTGACTtGGG	4	0	0
chr16	24002053	24002075	+	TTggGTGATCTCTGACCTGG	4	0	0
chr16	49633637	49633659	-	cTCAggGAATGTTtGgCCTGG	4	0	0
chr1	53555466	53595488	-	TggAGTGTGATGTTtGACCTTGG	4	0	0
chr1	60180825	60180847	+	TTCAgAtAAATGTTCTGatTTGG	4	0	0
chr1	63639646	63639668	+	TtAaGTAATGtGACCTTGG	4	0	0
chr1	68966615	68966637	+	aTCAiTGAAGATGTTGACCAggG	4	0	0
chr1	79161364	79161386	-	TaAGTGGATGCTGTGACCTGG	4	0	0
chr1	82586392	82586414	+	TTCAgTAAATGTTCTaAACaaGG	4	0	0

chromosome	start	stop	strand	sequence	Mis-matches	Off-target in Spacer	Off-targets in flanks
chr1	99141974	99141996	+	cTgAGTGAATGTTaaGACCTAGG	4	0	0
chr1	99139868	99139890	-	TggAGTGAATGTTaaGACCTAGG	4	0	0
chr1	155013104	155013126	-	TTGgaTaAATGTTCTGgcCTTGG	4	0	0
chr1	17951364	179751386	-	TTCAAGgaAAATGctCTGccCTTGG	4	0	0
chr1	181697048	181697070	+	TTGAGGggCTTCTGACCTGG	4	0	0
chr1	188179828	188179850	+	gTCAGTGAATAttCTGAatTTGG	4	0	0
chr1	198923277	198923299	-	TTAGTaaATGTactTGAgCTGG	4	0	0
chr1	202961143	202961165	+	TTACTGAAGGTTCTGacCCGGG	4	0	0
chr1	218300886	218300908	+	TTaAGTGAAGGTTCTGAatCCGGG	4	0	0
chr13	37569354	37569376	+	TTCAaTGAATtTgtTGACCTGG	4	0	0
chr13	38897340	38897362	-	agaCAatGAATGTTCTGACTTGG	4	0	0
chr13	40988251	40988273	-	TTCAgTGAATaTgtTgcCTTAGG	4	0	0
chr13	43689324	43689346	-	TTCAgTGAATCTCTtaACatTTGG	4	0	0
chr13	80358054	80358076	-	TTgAGTCAATGTTcaGACCTGG	4	0	0
chr13	84703547	84703569	-	TTCAggGgATGTTgcaGACCTGG	4	0	0
chr13	85290375	85290397	+	aTCAGTGAATGgtCTGAatTTGG	4	0	0
chr13	96885314	96885336	-	TTCACTGTAATGTTCTGACCTGG	4	0	0
chr2	9052859	9052881	+	TTCCCTGAAAATTCTACCTGGG	4	0	0
chr2	36240898	36240920	-	cTCAAGataATGTTCTGAtCTGGG	4	0	0
chr2	46147428	46147450	-	TaaAGTGAATGTTCTGtcTTGGG	4	0	0
chr2	76079145	76079167	+	TTCAgTgtATGTAatGACCCAGG	4	0	0
chr2	107385585	107385607	+	TgCAGTGAAGGTTCTGAGcAGG	4	0	0
chr2	132287515	132287537	+	TTCAgTGAAGGTTGAGCTGG	4	0	0
chr2	157320678	157320700	+	TTCAgTGAATGtaAcACCTAGG	4	0	0
chr2	162098292	162098314	-	TTCAgTGAActaCTGAgCTAGG	4	0	0
chr2	170432971	170432993	+	TaaAGTGAATGtaATGtCTAGG	4	0	0

Chromosome	start	stop	strand	sequence	Mis-matches	Off-target in Spacer	Off-targets in flanks
chr2	219496263	219496285	+	cTCCCTGAATGTTCTGACCAgGG	4	0	0
chr2	225018394	225018416	-	TcAACTGAATGTTCTGcCTAGG	4	0	0
chr2	234550534	234550556	-	TTcgGaGAATGTTCTGArcGGG	4	0	0
chr22	25771736	25771758	-	TTCAGTGAGTTCTGAaccTGG	4	0	0
chr19	11914262	11914284	-	TggAGTGAATGggTGA CCTCGG	4	0	0
chr21	34395863	34395885	-	TTCAGTCACTGgCTGAtCTAGG	4	0	0
chr21	43912965	43912987	+	TTCAGTGAAATGtgTttCCTCGG	4	0	0
chr15	61968013	61968035	-	TTtAGTGAGGTTAGCcCTGG	4	0	0
chr15	99736460	99736482	+	aTcAGaGAATGTTCTaccCTGGG	4	0	0
chrY	11903519	11903541	+	aTcGTGAATCTCTGAACCAgG	4	0	0
chr10	36600169	36600191	+	TTcAGTGgcTGTCTGcCTAGG	4	0	0
chr10	55557812	55557834	-	gtCAGTGAATCTTACCTCGG	4	0	0
chr10	71449698	71449720	+	TTcGTGAATGtgCTtCCTGGG	4	0	0
chr10	72375159	72375181	-	cTGAItAAcTCTTGACCTAGG	4	0	0
chr10	85752345	85752367	-	TaCAGgaAAATGTTGACCTGG	4	0	0
chr10	103204756	103204778	-	TgcAGTaaAAATGtgCTGAcTAGG	4	0	0
chr10	109977405	109977427	-	TTgactGAATGTTCTTatTTGG	4	0	0
chr6	37871251	37871273	+	TccAGTGAAATGTTCTTatTTGG	4	0	0
chr6	42801434	42801456	+	TTtAGTGAAATGTTGAcTgTGG	4	0	0
chr6	54885628	54865650	+	TTcAGTcAAAattCTGAcTTGG	4	0	0
chr6	68155795	68155817	+	TTcAGTGgcTGTCTGAcCTGG	4	0	0
chr6	72296386	72296408	+	cTTAGTGAAATGTTCTGgCCCTGG	4	0	0
chr6	83978567	83978589	+	TTcAGTtAATGTTCTGAcCAGG	4	0	0
chr6	85677371	85677393	-	aTcAGTGAAATTTGTCCTGG	4	0	0
chr6	118750800	118750822	-	TTcAAatGAgTGTCTGAAcAtTGG	4	0	0
chr6	130989127	130989149	-	TTcAAatGAAATGttCTGAtATGG	4	0	0

chromosome	start	stop	strand	sequence	Mis-matches	Off-target in Spacer	Off-targets in flanks
chr6	134309005	134309027	+	TTggGTGAATGCCCTGACCTAGG	4	0	0
chr14	54291950	54291972	-	gTCAAGAGACTTCTGACCTGGG	4	0	0
chr14	61385324	61385346	+	TcAGTGAAAGCtATGACCTGGG	4	0	0
chr14	96462036	96462058	-	cTCAGTGAGTGTtCTAGCTGGG	4	0	0
chr20	4688318	4688340	+	TgCAGTCAATTtggGACCTTGG	4	0	0
chr20	11903523	11903545	+	TTCTGTGAATTTCTGaggTTGG	4	0	0
chr20	18704370	18704392	+	TTCAgTGIAATGtgCTACATGGG	4	0	0
chr20	33991992	33992014	+	TTGAGTGCATTCTGAGCCTGG	4	0	0
chr20	34855579	34855601	+	TTTCAGTGcATGcCTGAcAAGGG	4	0	0
chr20	45460273	45460295	+	TTaaCTGAAGGTTCTACCTAGG	4	0	0
chr9	2964856	2964878	-	TTCAgTGAAATGTTtTAatTTGGG	4	0	0
chr9	76572795	76572817	+	TTCCtTGACTGtCTGACTTGGG	4	0	0
chr9	106296359	106296381	-	TTCCctTGACTGTTtACCTGGG	4	0	0
chr9	112948992	112949014	+	TTCAatTGAAAATGTTCTGtCTGGG	4	0	0
chr9	119777363	119777385	-	TTTCAGTCAATGTTCTGgttTGGG	4	0	0
chr9	137099805	137099827	+	TTCAgTGAGTggTtTGGcCTGGG	4	0	0
chrX	27288157	27288179	-	TTCAgTGAAATGtgCTGgCaGGG	4	0	0
chrX	28187830	28187852	-	aTaAtGAATGTTCTaACCTGG	4	0	0
chrX	30250773	30250795	-	cTCAGTGgATGTTGgCCTGGG	4	0	0
chrX	34559442	34559464	-	TTCAgTGCTATGtgTgACCTGGG	4	0	0
chrX	50902095	50902117	+	aggAGTGAATCTCTAACCTAGG	4	0	0
chrX	104089485	104089507	-	aTCAAGAGAATGtgTgACCTGGG	4	0	0
chrX	126958918	126958940	-	TTCAageGAATCTCTGACCTGGG	4	0	0
chrX	139207314	139207336	-	TTGAATGAATGtgCTGagCTAGG	4	0	0
chr18	1461907	1461929	-	gaAGTGAATACTCTAACCTGG	4	0	0
chr18	39019372	39019394	+	TTggGTAAaGTTCTGACCTAGG	4	0	0

Chromosome	start	stop	strand	sequence	Mis-matches	Off-target in Spacer	Off-targets in flanks
chr18	52226171	52226193	+	TTCAGTctATGTTCTAtCTGGG	4	0	0
chr18	56105258	56105280	+	cTcGTACTGTTCTGACCTGG	4	0	0
chr18	66103464	66103486	+	TtaActtAAATGTTCTGACCTGG	4	0	0
chr18	65767009	65767031	-	TTCAcTGAAaGtaaTGgcCTGG	4	0	0
chr11	10740451	10740473	+	TTCAaTGrATGcTCTGccCTAGG	4	0	0
chr11	12586616	12586638	-	TTCAggGAATGTTcctCCCTGG	4	0	0
chr11	24820918	24820940	+	aTCAgTGgATGtaTGTGAGCTTGG	4	0	0
chr11	47577339	47577361	-	TTGAGTGAATGTTCTagttTAGG	4	0	0
chr11	57560931	57560953	+	TTaaGTGAATttCTGACTgtGG	4	0	0
chr11	70901166	70901188	-	TTGAGTGAATGttGTGACTTGG	4	0	0
chr11	82113630	82113652	+	TTAGTGAATttCTGAAcCTTGG	4	0	0
chr11	111367991	111368013	-	TTGAGTGAATGcTCTGccaggGG	4	0	0
chr11	113554207	113554229	+	TTCAatTGAcTGtttTGAGCTAGG	4	0	0
chr11	117310327	117310349	+	TTagGTGAATGTTCTGAgCTTGG	4	0	0

Supplementary Table 3A: Presence of predicted in silico protospacer and flanking off-targets (R785X, N=3).

chromosome	start	stop	strand	sequence	Mis-matches	off-target in spacer	Off-targets in flanks
chr7	117587693	117587915	-	GCTCAATTGACCTCCACTCAAGTG	0	NA	NA
chr6	35371698	35371920	+	GCTCAATTGACCTCCACTCTGG	2	0	0
chr8	137437465	137437687	+	aaTCATTGACCTCCACTCAAAG	3	0	0
chr12	29024691	29024913	-	tCTCAATTGACCTCACTGAGTG	3	0	0
chr7	81460368	81460590	-	ccACATTGACCTCCACTCTGG	3	0	0
chr7	102806746	102806968	-	GCTCAGTtcCTCCACTCAAGGG	3	0	0
chr7	157687044	157687266	-	cCTCATgcACCTCCACTCAAGGG	3	0	0
chr4	11832981	11833203	-	GCTCttTGGCCCTCaACTCAGTG	3	0	0
chr5	121764648	121764870	+	GaTCATtGgGCtTaACTCAGAG	3	0	0
chr5	133047534	133047756	+	GCTCAGtGgGCtgcACTCAGCG	3	0	0
chr5	174553420	174553642	+	GCTCttTGGccTTCACTCAAGGG	3	0	0
chr16	114145	114367	+	GCTCAGtGACtTgCACTCATGG	3	0	0
chr1	7610726	7610948	-	GCTtattGACCTCCACTCtGTG	3	0	0
chr2	65227777	65227999	-	GCTCAAaTGACCAcccAcAGAG	3	0	0
chr22	50457337	50457559	+	GCCTtTTGtCTCCACTCAAGGG	3	0	0
chr15	48301631	48301853	-	GCTCAGggGACatCCACTCAAGG	3	0	0
chr15	86587211	86587433	+	GCTCctTGGccCTCCtCTCAGAG	3	0	0
chr17	42070759	42070981	-	GCTCATTGACggCCcCTCAAGGG	3	0	0
chr14	24942398	24942620	-	GCaCACTGACtTCCACTCAAGTG	3	0	0
chr14	103387702	103387924	+	GaTCATTGAtCTCACTCAGAG	3	0	0
chr20	51029240	51029462	+	GCTCAATTccCTCtCACTCAGAG	3	0	0
chr9	79299822	79300044	+	tCTCAATTGccCTCtCACTCAGAG	3	0	0
chr9	137997093	137997315	+	GCTCATTGtactCCACTCTGG	3	0	0
chrX	57924360	57924582	+	GCaCATtGgGCtCCACTCTGTG	3	0	0
chr11	25442530	25442752	-	GCTCATTaAcAtCCATCAAGGG	3	0	0
chr8	11481372	1181594	-	ccCTCAATTgAGCTCCACtTAGAG	4	0	0

Chromosome	Start	stop	strand	sequence	Mis-matches	off-target in Spacer	Off-targets in flanks
chr8	7431731	7431953	-	GCTGATTGAGCTCCACTCTtGG	4	0	0
chr8	7879598	7879820	+	GCTGATTGAGCTCCACTCTtGG	4	0	0
chr8	9875000	9875222	-	cCTCATaGACCTCCACtCTtAG	4	0	0
chr8	11483612	11483834	+	GCTtACTGACCTCCAGggAGGG	4	0	0
chr8	18387417	18387639	+	GCTCATTcACCTCCACtGtTG	4	0	0
chr8	22047129	22047351	-	GCTCttaGtCTCCACCCAGAG	4	0	0
chr8	23329540	23329762	+	GCTCATTcAactCCACAgAGGG	4	0	0
chr8	25300529	25300751	+	GCTCAaaTaACCTCCAagCAGtG	4	0	0
chr8	27548002	27548224	-	GCTtaATTGACAgcACttaAGtG	4	0	0
chr8	28360071	28360293	+	GCTCATTatCTgCACTCaAAAG	4	0	0
chr8	33323381	33323603	+	GCTgATTGACCTtCACTttGTG	4	0	0
chr8	35110250	35110472	+	tGtCATTGACCTacAtTCAGtG	4	0	0
chr8	37550985	37551207	-	GCTCttaGACCTgCaATCAGCG	4	0	0
chr8	39227093	39227315	+	GgttATTtACCTCCAATCAGtG	4	0	0
chr8	53024106	53024328	-	GCaaAgTGACttaACtCTAGAG	4	0	0
chr8	56612900	56613122	+	tCTCAttGAGtCCACTCACAG	4	0	0
chr8	74746010	74746232	-	tCTCAttGAGtCCACTCACAG	4	0	0
chr8	79897005	79897227	-	cCTCAagGAGtCCACTCACAG	4	0	0
chr8	94138378	94138600	-	GCTCcAtACCTCAactCAGGG	4	0	0
chr8	101783612	101783834	-	GCTCATTGggCCCCCACTgtACTG	4	0	0
chr8	118709786	118710008	-	atCTATTGAGtCAACTtAGCG	4	0	0
chr8	118934921	118935143	+	GgtCATtGACCTtCtCaCAGAG	4	0	0
chr8	138540375	138540597	+	GcgCATtGACttaCATtCTGGG	4	0	0
chr8	139645720	139645942	+	GCTCtcTGGCTCCACCCAGAG	4	0	0
chr8	141239802	141240024	-	GgtCATtGccCTCCACTCCctG	4	0	0
chr12	13849438	13849660	+	tCTttaTGAACtCCAttCAGAG	4	0	0

chromosome	start	stop	strand	sequence	Mis-matches	off-target in spacer	Off-targets in flanks
chr12	15007203	15007425	-	GCTctTTGACTTCCACatAGAG	4	0	0
chr12	20136134	20136356	-	GgtCCatTGACCcccACTCAGTG	4	0	0
chr12	20226432	20226654	+	GCTCATTAACCTCCtCTtcATG	4	0	0
chr12	28894893	28695115	-	GCTgATTGtCCTCCAAaaAGTG	4	0	0
chr12	31947948	31948170	-	GtTCATaGACCCTCCCCAGGG	4	0	0
chr12	43325004	43325226	+	GgaCATGACAtCCAAtCAGAG	4	0	0
chr12	51371703	51371925	-	GCTCtTGACCTCCACTCcAGG	4	0	0
chr12	57584429	57584651	-	tCTCtgTGA CCTtACTCAGTG	4	0	0
chr12	82802162	82802384	-	GCTCAgCggCCTgCACtCAGAG	4	0	0
chr12	94057764	94057986	+	GgtCATgGACgtTCCCCTCAGGG	4	0	0
chr12	98197429	98197651	+	tgTCATTGACTtACTCAGTG	4	0	0
chr12	100963631	100963853	-	GCTCCTTAACTCtCtCAGTG	4	0	0
chr12	103687719	103687941	+	GCTCtgTGA CCCCCACTtAGCG	4	0	0
chr12	124569798	124570020	-	GCTCATgGACgtTACTCAGAG	4	0	0
chr12	130634379	130634601	-	GCTCAaaGACCCCCAGtCAGAG	4	0	0
chr12	131244516	131244738	+	GCTCaggGACtCCAGcCAGGG	4	0	0
chr12	131414558	131414580	-	GCTCAGggGACtCCAGcCAGGG	4	0	0
chr12	132308146	132308368	+	GCTCAGtGAAaTCCACTtCtGGG	4	0	0
chr3	4289093	4289315	-	GCTCttTCACTCCAGtCtGAG	4	0	0
chr3	10762329	10762551	-	GCCCATTGgCCTCtCTCAGGG	4	0	0
chr3	23641881	23642103	-	GCCCATtGACTtCtACTCtGTG	4	0	0
chr3	26482689	26482911	-	GCTCATTGAtCatCtCTCAGGG	4	0	0
chr3	50786344	5078566	-	tCTCCtTGGcCTCCACTAAGAG	4	0	0
chr3	69974589	69974811	-	GgtCATtGACTtCtCTCtGAG	4	0	0
chr3	71117773	71117995	-	taTCATTGACtCCACTtCtGTG	4	0	0
chr3	71672996	71673218	+	GCTtgtTGA CCCCCACTAGTG	4	0	0

Chromosome	Start	Stop	strand	sequence	Mis-matches	off-target in Spacer	Off-targets in flanks
chr3	127268237	127268459	+	GCTctTTGAAactCCATtAGGG	4	0	0
chr3	127259960	127260182	-	GCTCATtGtCCTCCCCCTCaGG	4	0	0
chr3	131074576	131074798	+	GCTgtTTGAGtCCACcAGGG	4	0	0
chr3	134000228	134000450	-	cCTCAgTGACCTCCtCTCGTG	4	0	0
chr3	134324319	134324541	+	GCTatcTGACCTCCgCTCAGAG	4	0	0
chr3	134750294	134750516	-	GCTCAGTtgCtCCACTCAGAG	4	0	0
chr3	137609116	137609338	+	tCTCCCTGACCTCCACTCaTG	4	0	0
chr3	138077126	138077348	-	GCTCAGtGttCTCCACTCaTG	4	0	0
chr3	140319770	140319992	+	aCTCAGtCACCTCCCTCAGAG	4	0	0
chr3	143969239	143969461	+	GCaCATTAACCTtACtTAGAG	4	0	0
chr3	166955317	166955339	+	GrTCATtGgCCTCCAGcCAGGG	4	0	0
chr3	173044137	173044359	-	GCTCAGtGACtTgtCTCAGGG	4	0	0
chr3	176685649	176685871	-	GCCCATtGgCCTCCACTtaAG	4	0	0
chr3	184619574	184619796	-	GCTCATTTAgTCCCcaCaGTG	4	0	0
chr3	187801751	187801973	-	GCTCCTTGACTTCCtCTtGAG	4	0	0
chr3	192269239	192269461	+	GCITttTaACCTtgCACTCAGTG	4	0	0
chr7	5396798	5397020	+	GCTCACTGACCCgCCTCCAGGG	4	0	0
chr7	27512965	27513187	-	GCTgAaTGAatTCCACTCAGAG	4	0	0
chr7	33268613	33268835	-	actCtgTGACCTCCACTtAGGG	4	0	0
chr7	45364672	45364894	-	actGttTGACCTCCACTCaAG	4	0	0
chr7	46701544	46701766	+	GCaCATTTGCTCCCTtGTG	4	0	0
chr7	47563573	47563795	-	GCTCAGtGgCCTCaAccCAGGG	4	0	0
chr7	55143230	55143452	+	cCTCAATTGccCTCaAcAGtG	4	0	0
chr7	68892412	68892634	+	GaTctTTGtCCtCTtCAGtG	4	0	0
chr7	71777922	71778144	+	GrTCATtGtCtCatCtCAGtG	4	0	0
chr7	85205998	85206220	-	GCaATTtCACtCaACTCAGtG	4	0	0

chromosome	start	stop	strand	sequence	Mis-matches	off-target in spacer	Off-targets in flanks
chr7	117223946	117224168	-	TCTaggTGACCTCCAACTCAAGGG	4	0	0
chr7	132603362	132603584	+	atTCATTGACCTCCCTTAAGAG	4	0	0
chr7	140061232	140061454	-	GCTgACTGACCTCCggCTCTGTG	4	0	0
chr7	141729381	141729603	-	GCTAcTTGATCTCCAgTCAGAG	4	0	0
chr7	159198440	159198662	-	GCTTCACTGgCCTCCACTCTGTG	4	0	0
chr4	3676080	3676302	+	GCTtAgTGACTTCACtCAGGG	4	0	0
chr4	6072525	6072747	-	GCaCAGTgCCTgCACTCAAGG	4	0	0
chr4	16546738	16546960	+	GCTtATTGgCCTCCCTCCAGGG	4	0	0
chr4	24233446	24233668	+	ccCTCAATTAACTTgCACTTAAGAG	4	0	0
chr4	33561929	33562151	-	GCTTCACTACCTCCATTCaaAG	4	0	0
chr4	52061482	52061704	-	GCTCAGTgATCTCCAgCAGGG	4	0	0
chr4	81122278	8112500	+	GtTCttTAatCTCACTTCAGTG	4	0	0
chr4	84447151	84447373	-	GCTCAGTgACgtCtACTCAAGAG	4	0	0
chr4	90374576	90374798	+	GacaATTGACCTCCCTCAGGG	4	0	0
chr4	92371319	92371541	-	GagCATTGACTTCACtCAAG	4	0	0
chr4	97192841	97193063	-	tCaATTGACTTCAGtCAGTG	4	0	0
chr4	108880533	108880755	-	aCTCAATTGACCAataACTCAAGG	4	0	0
chr4	127661492	127661714	+	GCTTCacacATCTCCACTCAAGG	4	0	0
chr4	137562791	137563013	+	cCTCAATTACCTCttCTCAGTG	4	0	0
chr4	161382702	161382924	+	GCTCAaaTgACCTCCCCaaATCG	4	0	0
chr4	169849616	169849838	-	GCTTgcCTGtCCTCCACTCAAGGG	4	0	0
chr4	172833253	172833475	-	GCTCTTGGGatTCCAACTCAAG	4	0	0
chr4	175731415	175731637	+	GCTCAGtGtCCtCtCaCAGtG	4	0	0
chr4	178924653	178924875	+	GCaagATaGACTTCACtCAAGAG	4	0	0
chr4	181137141	181137363	+	atTCAGtGAActCCACTCAAG	4	0	0
chr4	182805643	182805865	-	ccCTACCCGACCTCCACtGAAGG	4	0	0

Chromosome	Start	Stop	strand	sequence	Mis-matches	off-target in Spacer	Off-targets in flanks
chr4	186173904	186174126	+	GCTCttTTAgatCCACTCAGGG	4	0	0
chr4	188932779	188933001	-	taTCATAgACCTgCACTCAGAG	4	0	0
chr5	1856837	1857059	+	GCTCAGggGACCCCCACCCAGAG	4	0	0
chr5	3281726	3281948	+	GCTCttTTGtcCTCtgCTCAGCG	4	0	0
chr5	3629638	3629860	+	GCTCACTGcgATTCACCCAGCG	4	0	0
chr5	3886462	3886684	-	GaTCACTGgCCCCACTCAGAG	4	0	0
chr5	14917328	14917550	+	GCTtaATGataCCACTCAGTG	4	0	0
chr5	50528962	50529184	-	catCATTTGAGgtTCCACCCAGGG	4	0	0
chr5	53914605	53914827	-	GCTCATTTcAGtTCCATCAGTG	4	0	0
chr5	81015657	81015879	-	atTCAATTGACCAAACCTCAGAG	4	0	0
chr5	107284096	107284318	+	ctgCATTTGACCTtaACTCAGAG	4	0	0
chr5	107797825	107798047	+	ccTCAATGACCTcaACTAaAGAG	4	0	0
chr5	111434559	111434781	-	taTCATTGACCTCtACTCtGTG	4	0	0
chr5	118452482	118452704	+	aCTCATTtACCACCACTCATGG	4	0	0
chr5	121842203	121842425	-	GCaAGggGACCTtCACTCAGAG	4	0	0
chr5	127416771	127416993	-	GCTaAgtGACCTCCcaTCAGAG	4	0	0
chr5	134465287	134465509	-	TCCTCTTGACTCCACTCAGAG	4	0	0
chr5	1419494126	1419494348	-	GCTCAatTggCCCCctCTCAGAG	4	0	0
chr5	151851400	151851622	-	GCTCATTGtCatTCCTCTCATGG	4	0	0
chr5	157203270	157203492	+	GCTaATTAAGtCCACTtgAGGG	4	0	0
chr5	170507490	170507712	+	ccCTCACTGACCTCACTCCTGTG	4	0	0
chr5	170643873	170644095	+	GgTCACtGAactCCCTCTAGGG	4	0	0
chr5	173599312	173599534	-	GCTCACTGtgcggCCACTCAGGG	4	0	0
chr5	176076172	176076394	-	GCTCAGtGACagCCACGAGAG	4	0	0
chr5	177761751	177761973	+	GCTCAGtGACagCCACGAGAG	4	0	0
chr5	178021796	178022018	-	GCTCAGtGACagCCACGAGAG	4	0	0

chromosome	start	stop	strand	sequence	Mis-matches	off-target in spacer	Off-targets in flanks
chr16	486776	486998	+	GCTgATTcttCCCTCAGAG	4	0	0
chr16	14331954	14332176	+	aCTCATggAAactCTACTCAGGG	4	0	0
chr16	19320096	19320318	-	cCTgATTGttCTCCggCTCAGTG	4	0	0
chr16	20211344	20211566	-	tCCCAATTGgcCTtCACTCAGTG	4	0	0
chr16	33803119	33803341	-	GCaCAatGACCTCCCCTCACTG	4	0	0
chr16	35543780	35544002	-	GCTCttTGACCTtgcCCCAGAG	4	0	0
chr16	47051356	47051578	-	cCTCgaTGACCTCCACCCAGAG	4	0	0
chr16	52333450	52333672	-	GCTCAGtgAGctgCACCCAGTG	4	0	0
chr16	56560258	56560480	-	GCTCACTGccAtaACTCTAGTG	4	0	0
chr16	61972747	61972969	+	GCatAaTGAtCTCCACTCAAG	4	0	0
chr16	69361387	69361609	-	tCTCCttGAtCTCCCCTCAGAG	4	0	0
chr16	86539137	86539359	+	tCtCCtTGtCtCtCACTtGAGAG	4	0	0
chr16	87522030	87522252	+	GCTtATtGAAaGactACTCAGTG	4	0	0
chr16	88285632	88285854	-	cCTCACTGCCcaCCACTCAGAG	4	0	0
chr16	88468441	88468663	-	GCTCCtTGAcAtTCCAtTCAGGG	4	0	0
chr16	89294761	89294983	+	GCTCccTGccCTCCAcACAGTG	4	0	0
chr1	2360426	2360648	-	GCTCAATTtCCtCaACTtGAGGG	4	0	0
chr1	3419683	3419905	+	GgtCACTGACCCCCACTtGAG	4	0	0
chr1	6437645	6437867	-	cccCATGACCTCCACTCACTG	4	0	0
chr1	7851556	7851778	-	GCTCACTGtCCCTCAaaTCAaGG	4	0	0
chr1	18602826	18603048	+	GCTCATgGagaccCACTCAGAG	4	0	0
chr1	18784361	18784583	+	cCTCAATTGccAttCACTCAGGG	4	0	0
chr1	26732618	26732840	+	cCTCAAatGACCTCCAGtaAGGG	4	0	0
chr1	31296455	31296677	-	GCTCATtttCCCTCCCTCAGAG	4	0	0
chr1	31548794	31549016	+	GtCAATTGttCTCCAtTCAGGG	4	0	0
chr1	32375450	32375672	+	GCTtCTTGACaaACTCAGAG	4	0	0

Chromosome	Start	Stop	strand	sequence	Mis-matches	off-target in Spacer	Off-targets in flanks
chr1	39498839	39499061	-	GCTCAgTgtCCggCACTCAGAG	4	0	0
chr1	44567650	44567872	-	GCTCcATGAGCTCCAGtCAGAG	4	0	0
chr1	47839397	47839619	+	cCTCATgGtCTCCACCCAGAG	4	0	0
chr1	53509480	53509702	+	GCTCACTGgcCTCtCTCAGGG	4	0	0
chr1	59420058	59420280	-	GtTCATTtATTCCACTCAGGG	4	0	0
chr1	64775537	64775759	-	GCTctTTccCTCCACTCACAG	4	0	0
chr1	69587260	69587482	-	GaTCAGtGAGgtCCACTCAGGG	4	0	0
chr1	88878770	88878992	-	GCTCCttGACCTCCcgCaCATGG	4	0	0
chr1	9722609	97922831	+	GCaCATTTGcCCTCCACTtgGAG	4	0	0
chr1	143656850	143657072	+	GtTCATAgACCTCCCCAGGG	4	0	0
chr1	179919120	179919342	+	GCTtATTGcCTCCAgTCGGG	4	0	0
chr1	18348136	186348358	-	GtTCATAgACCTCCCCAGGG	4	0	0
chr1	18701060	187001282	+	GCTCATTTGACAatGcAgTaAGTG	4	0	0
chr1	190024677	190024899	+	GCTCATTatCTCCACTCAAAG	4	0	0
chr1	191308240	191308462	+	GCTtACTGACCTCaaACTCATG	4	0	0
chr1	20192237	201992459	+	GtTtcTTGACCTtACTCAGGG	4	0	0
chr1	205586481	205586703	+	GCTCAGaaGCTCCAgTCAGTG	4	0	0
chr1	208051310	208051532	+	aCTCAATTGACCTCCcgacAGGG	4	0	0
chr1	246788280	246788502	-	GtTCATTGACCTGtCtCAGAG	4	0	0
chr1	247332392	247332614	-	GCCCCgtGACCCCCACTCAGGG	4	0	0
chr13	23066960	23067182	+	ctTCATTGACCTCCAgTCATG	4	0	0
chr13	29364651	29364873	-	GCTCtgAGAGtCCACTCAGTG	4	0	0
chr13	52902487	52902709	-	GCTCCagGccCTCCACTCAGGG	4	0	0
chr13	95177914	95178136	+	GCTtctTGccCTCCACTCAGCG	4	0	0
chr13	103857211	103857433	+	GCTCCatTccCTCCACTCAGGG	4	0	0
chr13	107947718	107947940	-	GCTCATTTGACtttCtCtG	4	0	0

chromosome	start	stop	strand	sequence	Mis-matches	off-target in spacer	Off-targets in flanks
chr13	110135266	110135488	+	GCTCACTtgCCCTgCACTCAGGG	4	0	0
chr2	4200749	4200971	-	GCTCATTGAACTCaaACTCgtGG	4	0	0
chr2	82288344	82288566	+	GCTCttTTGCCttACTCAGGG	4	0	0
chr2	15305809	15306031	+	GtTCAAtTGACatTCCACTTAGAG	4	0	0
chr2	23619952	23620174	-	GCTCAGtgCCTCCCTCAGAG	4	0	0
chr2	24814308	24814530	-	GCTCATTTGAtTCACtGttTG	4	0	0
chr2	30308934	30309156	-	GtCATTTccCTCCACCCAGAG	4	0	0
chr2	59690992	59691214	+	GCTCgtTTGACCTCCTtTHATG	4	0	0
chr2	71364114	71364336	-	tCTCCttTGAatCCtCTCAGGG	4	0	0
chr2	71874132	71874354	+	cCTCttTGTctTCACtCAGAG	4	0	0
chr2	75446991	75447213	+	cCTCATTTGACCTCttCaAGGG	4	0	0
chr2	77642572	77642794	-	TgaCATTTGACCTCCACTgtAGTG	4	0	0
chr2	87655593	87655815	+	cCTCATTTGACCTtCtCTCAaGG	4	0	0
chr2	88409008	88409230	+	GaTCAATTGACCTCtcccAAGGG	4	0	0
chr2	88408920	88409142	+	GaTCAATTGACCTCtcccAAGGG	4	0	0
chr2	101493244	101493466	+	GCTCtaTGAgtTCCACTCTAGTG	4	0	0
chr2	108299061	108299283	-	GtTCAGtgGACCTtgCTCAGGG	4	0	0
chr2	110023018	110023240	+	cCTCACTGAcTTCCACTCTGGG	4	0	0
chr2	110348150	110348372	-	cCTCACTGAcTTCCACTCTGGG	4	0	0
chr2	110851846	110852068	-	GCTCtcTGCCTgCACTCAGGG	4	0	0
chr2	111295119	111295341	-	cCTCATTTGACCTtCTCAaGG	4	0	0
chr2	114843714	114843936	-	GCTgATTaAtCTaACTCAGTG	4	0	0
chr2	116006792	116007014	-	GCCCAgTgATCCTCCACTCAG	4	0	0
chr2	127945927	127946149	+	cCTCCttTAACCTCCACTAAGTG	4	0	0
chr2	128193528	128193750	-	GCTCtgGCCtCFACTCAGGG	4	0	0
chr2	147808537	147808759	+	GCTCAaaTccccCTCCATCAGAG	4	0	0

Chromosome	Start	Stop	strand	sequence	Mis-matches	off-target in Spacer	Off-targets in flanks
chr2	156874341	156874563	+	aCTCATGGCCCTCACTgAGAG	4	0	0
chr2	169652468	169652690	+	GgtCATTTGtCCTCCACccTGGG	4	0	0
chr2	173578687	173578909	-	tATCCTTGACTCTCCtCTCAGGG	4	0	0
chr2	174930385	174930607	-	tCTCAATTGACCACCCCTgAGTG	4	0	0
chr2	187010814	187011036	+	GCTCATTcAgCCCCACTCgGTG	4	0	0
chr2	198566996	198567218	-	GagCATGACCTCCACTtAAG	4	0	0
chr2	227016633	227016855	+	GCTggTTGAGCTaCACTCAGTG	4	0	0
chr2	232920267	232920489	-	GCTCAGtaACCCCACCTCAaGG	4	0	0
chr2	236616000	236616222	+	GCTCAGtGACCTCCACCAACCG	4	0	0
chr2	237624528	237624750	+	GCTCATgGACTTCCACgCAGGG	4	0	0
chr2	240375397	240375619	+	ctTCAGtGACTtCACTCAGAG	4	0	0
chr22	21709000	21709222	+	GgaCATGACCAccCtCTAGTG	4	0	0
chr22	22838489	22838711	+	GCTCAGtGgCCTCCTtGAGCG	4	0	0
chr22	24103428	24103650	+	GCTCAGtGACTCTCCCTAG	4	0	0
chr22	24993371	24993593	-	GCTGaaTGA CtttAAGtCAGAG	4	0	0
chr22	38311463	38311685	+	GCCCTTGA CCTCCAGtCAGTG	4	0	0
chr22	40810914	40811136	-	atTAATTGACTCCACCCAGAG	4	0	0
chr22	47007038	47007260	+	tCaCATTTGACCTCCAGCCAGG	4	0	0
chr22	47388842	47389064	+	GCTCAaggGACCCCCACTgAGGG	4	0	0
chr22	49284143	49284365	+	GCTCAGtGtCAGG	4	0	0
chr22	50235401	50235623	-	GCTCATTTGactCTCCACAGGG	4	0	0
chr19	3603323	3603545	+	GatCgTTGccCTCCACTCCGGG	4	0	0
chr19	6402011	6402233	-	GCTCCtcatCTCCACTCAGGG	4	0	0
chr19	24092107	24092329	-	GCCCACTGactCTCCACTCAGGG	4	0	0
chr19	29366275	29366497	+	GgtCATTTtCCACTgAGTG	4	0	0
chr19	30107118	30107340	+	GCTgAGtGgcCTCAG	4	0	0

chromosome	start	stop	strand	sequence	Mis-matches	off-target in spacer	Off-targets in flanks
chr19	34505465	34505687	+	GCCCATTTGtCCTaACCCAGCG	4	0	0
chr19	35129063	35129285	-	GtTCActTGAAgTCCACTCAGTG	4	0	0
chr19	35361062	35361284	-	tCTCATggCcCACTCAGGG	4	0	0
chr19	38905567	38905789	+	GacCAggGACTTCCACTCAGGG	4	0	0
chr21	5082661	5082883	+	GCTCCTtgCCTCCACTCAGGG	4	0	0
chr21	31275426	31275648	+	GCaCaCTGACCTCCTtCtCAG	4	0	0
chr21	31799190	31799412	-	GCTaATTaaACCTgACTCAGAG	4	0	0
chr21	33461928	33462150	-	GtTCATTAACCttaACTCAGAG	4	0	0
chr21	42151139	42151361	+	cCTCATTGACCTCCCCCTCttTG	4	0	0
chr21	43187889	43188111	+	GCaCATTAACAcAtaCAGCAGG	4	0	0
chr21	44048175	44048397	+	GCTCtgTgtCCTgACTCAGGG	4	0	0
chr21	44179087	44179309	-	GCTCctTtgCCTCACTCAGGG	4	0	0
chr21	44549850	44550072	-	GCTCAGggGAGtTCCACTCAGGG	4	0	0
chr15	22235156	22235378	-	GCTtATTGAAactACTCAGTG	4	0	0
chr15	23895568	23895790	+	GCTCATTTGAAactCCAGgcCtGG	4	0	0
chr15	31204542	31204764	-	GCTCcTTctCgtTCCACTCAGAG	4	0	0
chr15	34848904	34849126	+	GaaCATGAtTCCACTCAGTG	4	0	0
chr15	4555392	45355614	+	tCCCAATTGccCTcaACTCAGAG	4	0	0
chr15	64119972	64120194	-	GCCtATTGttCTCCACTCAGGG	4	0	0
chr15	74292992	74293214	-	tCTCccTGAcatCCACTCAGTG	4	0	0
chr15	81134481	81134703	+	tCTCActTGACCTCAGTCCGAG	4	0	0
chrY	19554811	19555033	-	GCtttTTGccCTCtCTCAGGG	4	0	0
chr17	220762	220984	+	GCTCgggGACTTCCACTCAGTG	4	0	0
chr17	40410349	40410571	-	tttCAAatTGACTTCCACTCAGGG	4	0	0
chr17	44961994	44962216	-	GCTgAgAGAAcTCCACTCAGTG	4	0	0
chr17	45409436	45409658	-	GCTCAgTcACCTCCAGtgAGGG	4	0	0

chromosome	start	stop	strand	sequence	mis-matches	off-target in spacer	Off-targets in flanks
chr17	603887888	60388110	-	GgtCAGTGATCTCCACTaaAGTG	4	0	0
chr17	66441526	66441748	-	aggCAATTGACTCCACTaAGAG	4	0	0
chr17	67438097	67438319	+	GCACATAgGACTCTtAgTCAGTG	4	0	0
chr17	72581066	72581288	-	tCTCAATTGACCTgACaAGAG	4	0	0
chr17	78222517	78322739	+	GCTCCttGACCTCCATCaAGG	4	0	0
chr10	3926896	3927118	-	GCTtgTTGACatgCACTCAGGG	4	0	0
chr10	5987831	5988053	-	GCTtgtGAAaCTCCAaCTCAGGG	4	0	0
chr10	6525624	6525846	+	cCTCCttTGAaCTCCACaCAGAG	4	0	0
chr10	13001374	13001596	+	GCTCAGggGgGCTCACAaCAGAG	4	0	0
chr10	17049200	17049422	+	aCTCATTGACCCaaCACAGAG	4	0	0
chr10	17368532	17368754	-	GCTCAAaTACCAACCCTCTCAGTG	4	0	0
chr10	21979169	21979391	-	GCTtcTTGAGgtgCACTCAGAG	4	0	0
chr10	34051233	34051455	+	GCTCctTggCTCCACTCAGAG	4	0	0
chr10	35814893	35815115	-	GCTCAGagAACCCACaCAGGG	4	0	0
chr10	36764956	36765178	-	GCTCATTGcaatTactCTCAGTG	4	0	0
chr10	46993470	46993692	-	GCTtATTGAgatTCCACTCAAGG	4	0	0
chr10	49997484	49997706	-	GCTCctTAgATCTCAACTCAGGG	4	0	0
chr10	52148566	52148788	-	GCTCATgGactCTCCACTaAGGG	4	0	0
chr10	54690764	54690986	-	GCTCATTGACCTtCAatTgAtGG	4	0	0
chr10	70911932	70912154	-	accCAATTGccCTCCCCCTCAGAG	4	0	0
chr10	73765840	73766062	-	tCTCAATTccCTCCACTCTACTG	4	0	0
chr10	78046552	78046774	+	cCTCAATTACCTGtACTGgAGG	4	0	0
chr10	79045007	79045229	-	GCTCCaggGccCTCCACTCAGTG	4	0	0
chr10	85443636	85443858	+	cCTCAAtGccCTCACTCAGTG	4	0	0
chr10	96431357	96431579	-	GCTCtgTGAACCTCACTCAGG	4	0	0
chr10	117136710	117136932	-	GCCCCtTGccCTCCACaCAGTG	4	0	0

chromosome	start	stop	strand	sequence	Mis-matches	off-target in Spacer	Off-targets in flanks
chr10	117130675	117130897	-	GCTctTTGccggCCACTCAGGG	4	0	0
chr10	122078447	122078669	+	cCTCccTGACCTCCaCaAGAG	4	0	0
chr10	122217085	122217307	-	GgTCAGtGACCTaACTgAGAG	4	0	0
chr10	126094498	126094720	-	GCTCAAATGACaaCcCTCAAGGG	4	0	0
chr10	128310121	128310343	-	GCTCCTTGATCTCCCTGtGTG	4	0	0
chr6	14535964	145361186	-	GCTCATTTGATCTCACCCAAgG	4	0	0
chr6	15597460	15597682	+	cTCAATTGACATCCAatCTAGTG	4	0	0
chr6	45609456	45609678	-	GgtCTTTGACTCCACTCAGTG	4	0	0
chr6	51064869	51065091	-	GCTCATTTtCCCTCACAGAG	4	0	0
chr6	77333919	77334141	+	GCTCATTTGAGCTgCAGgCAGTG	4	0	0
chr6	121392347	121392569	-	tCTCTTTGtCCCTaACTCAGTG	4	0	0
chr6	136227851	136228073	+	GCaCATTTcAATCTCACTCAGAG	4	0	0
chr6	136182010	136182232	-	GCTtattTGACCTCCaCaAGAG	4	0	0
chr6	139082858	139083080	-	GCTCAcAtGtCTCCACTAAGTG	4	0	0
chr6	142336010	142336232	-	GCaCATTAAGCTTgCACAcAGAG	4	0	0
chr6	146037611	146037833	+	GCTCATTTGATCTCAGtCTGTG	4	0	0
chr6	161688643	161688865	-	GCCCAAGGACTTtCACTgAGTG	4	0	0
chr6	162891965	162892187	+	GaCCCCtGACCTCCACTCAGGG	4	0	0
chr14	20588338	20588560	-	GCTCAGtGACCTCTCTtGTG	4	0	0
chr14	35583502	35583724	+	GCTCAGtGAacAcCACgCAGGG	4	0	0
chr14	39385842	39386064	-	GCTCCTGtgCTCCCTCAGTG	4	0	0
chr14	64283318	64283540	-	GCTCATTTGATCTtCTtAGCG	4	0	0
chr14	66022654	66022876	-	GCTtAatTGAGCTgCACTCAGAG	4	0	0
chr14	73762868	73763090	+	GCTCtcTGgaCTCCACTCAGAG	4	0	0
chr14	75471207	75471429	+	GCTCAGtGgCattCACTCAGTG	4	0	0
chr14	89193492	89193714	-	GtTCAGtGACcaCCACTCAgG	4	0	0

Chromosome	Start	stop	strand	sequence	Mis-matches	off-target in Spacer	Off-targets in flanks
chr14	97000505	97000727	-	aCTCATgGACCTCCCTCAG	4	0	0
chr14	106359666	106359888	+	GCAAAatGACTCCCTCACTG	4	0	0
chr20	11678359	11678581	+	cCTCCITtACCTCACTAA GG	4	0	0
chr20	19026682	19026904	+	GCTCATTGtCCCCAActGTG	4	0	0
chr20	21631071	21631293	+	GCTCACTGccCTCCAGtCTGG	4	0	0
chr20	24254219	24254441	-	GgtCAGtCACCTCCACTgAGGG	4	0	0
chr20	32194765	32194987	-	GCTCAGggGACCTCCACTgtGG	4	0	0
chr20	38488337	38488359	-	atgCAGtGACCTCCACTCAGAG	4	0	0
chr20	57310085	57310307	+	GCCcATTAactCCAGcCAGAG	4	0	0
chr20	58991141	58991363	-	GCTCACccACCCTCCCTCAGGG	4	0	0
chr20	61439293	61439315	+	tCTCATgCACTgFACTCAGT G	4	0	0
chr9	1911862	1912084	-	aCTCATTTGAGtCCAGtAAGGG	4	0	0
chr9	16655995	16656217	-	GCTtcTTGACCTtCACTCAAtAG	4	0	0
chr9	36965169	36965391	-	GgtCTtgGACCTCCCTCAGGG	4	0	0
chr9	79550286	79659508	+	GCTCATTGACCTCtgATcgAG	4	0	0
chr9	84171224	84171446	-	GatCATTTGACAtTtcCTCAAGGG	4	0	0
chr9	85482345	85482567	+	cCTCAAAtGACCTtCACTgAGAG	4	0	0
chr9	86366448	86366670	-	aCTCAAGtGtCCCCACTCAGTG	4	0	0
chr9	86645730	86645952	-	GCTCAAGtttCCCTtACTCAGAG	4	0	0
chr9	88220834	88221056	-	GTtCATttCCCTCCACGtAGAG	4	0	0
chr9	93132724	93132946	-	GggCAAAtGccCTtCACTCAGAG	4	0	0
chr9	93712985	93713207	-	GCTCATAGAatTCCTtCTCAAtG	4	0	0
chr9	98314553	98314775	+	ccTCCtGACCTCCACTCAGCG	4	0	0
chr9	127835519	127835741	-	GCTCCTTCAACCCACTCAGGG	4	0	0
chr9	130303333	130303555	-	tCaCAcTGACCCCACTCAGGG	4	0	0
chr9	130619832	130620054	+	tCTCATgGACCTggCCtCAAGT G	4	0	0

chromosome	start	stop	strand	sequence	Mis-matches	off-target in spacer	Off-targets in flanks
chr9	130837758	130837980	+	GTTATTGACGCCACTCAGGG	4	0	0
chr9	135395823	135396045	+	GCTCATGGCCCCACAAAGG	4	0	0
chr9	135850796	135851018	+	GCTCATCCACGCCACTCAGTG	4	0	0
chrX	4697207	4697429	+	GCAATTACATCGACTCAGAG	4	0	0
chrX	12883839	12884061	+	GCTtATTACCTCCAatTAAGAG	4	0	0
chrX	20972916	20973138	+	GCTCAGTcAGtCCACtGAGGG	4	0	0
chrX	22661874	22662096	+	cCTCtaTGACCTCCACTCAGAG	4	0	0
chrX	48509303	48509525	+	cCTCtcTGccCTCCACTCAGAG	4	0	0
chrX	50618102	50618324	-	GCTCCttGccCTCCACTCAGAG	4	0	0
chrX	72114537	72114759	-	GCTCcCTACCTCaACTCAGGG	4	0	0
chrX	94871201	94871423	+	GCTCACTGAGctGAGtCAGTG	4	0	0
chrX	104815595	104815617	-	GgTCATtGGctTtACTCAGTG	4	0	0
chrX	106578802	106579024	-	GCTCATggAGcttCAGTCATG	4	0	0
chrX	112769134	112769356	-	GCTCATTTACCTCCAatTgACCG	4	0	0
chrX	120135506	120135728	+	tCTCATTTACCTCtgTCAGGG	4	0	0
chrX	124507268	124507490	+	tCTCCttTACCTCCACaCAGAG	4	0	0
chrX	139544960	139545182	+	GCTggTTGACaaTCCACCCAGAG	4	0	0
chrX	147601430	147601652	-	GCTtaATTGccatTCAAatCAGAG	4	0	0
chr18	1325084	1325306	-	GCCCATTGACatTcTCAGAG	4	0	0
chr18	27011269	27011491	-	GCTCAcgGccCTgCAGCTCAGGG	4	0	0
chr18	311625433	311625655	+	aATCACTGACCTCCACTaAGAG	4	0	0
chr18	45079608	45079830	+	GaTgATTcActTCCACTCAGTG	4	0	0
chr18	46363472	46363694	+	GCTggTTGAGtCCACTCAGTG	4	0	0
chr18	48391353	48391575	-	atTCatTGAactCCACTCAGAG	4	0	0
chr18	50711341	50711563	-	tCTCtgTGACCAccACTCAGAG	4	0	0
chr18	58622900	58623122	-	GCTCAGtAaAtTcACTCAGAG	4	0	0

Chromosome	Start	Stop	strand	sequence	Mis-matches	off-target in Spacer	Off-targets in flanks
chr18	73847038	73847260	+	aCTCAgTGACCCCCAACTCAGTG	4	0	0
chr11	2813229	2813451	+	cCTCATgcACCTCCATTCAGGG	4	0	0
chr11	14058247	14058469	-	GCTCAATTtccCAACTCTCGGG	4	0	0
chr11	15664857	15665079	+	GCTtagTGACCTCCACTCGGGG	4	0	0
chr11	58771884	58777106	-	GCTCATGtGCTTCCA g CCACtTG	4	0	0
chr11	65661946	65662168	+	GCTCAatGATCTCCAcatAGGG	4	0	0
chr11	66704558	66704780	+	GCTCcTTctCCACCCAGAG	4	0	0
chr11	69763619	69763841	-	GCaCATTGACgtTCCCTCAGAG	4	0	0
chr11	69797207	69797429	-	GCTCACTGACCTCatCTCGTG	4	0	0
chr11	70097695	70097917	-	GCTCAGTGAgtTCCACTgAGTG	4	0	0
chr11	81452634	81452856	+	cCTCATTTGAGtCaACTaAGTG	4	0	0
chr11	84623240	84623462	+	aCTCAATTaaACTCCACTCAAAG	4	0	0
chr11	84981408	84981630	-	GCCTaTAGACCTCCAACTAGAG	4	0	0
chr11	94999515	94999737	-	GCTCATTTACCACCAAA t TG	4	0	0
chr11	113349487	113349709	-	GCTCAaaGtCCTCCACTtAGAG	4	0	0
chr11	117640628	117640850	+	cCTCACTGACCTCCACaCACAG	4	0	0
chr11	119364599	119364821	-	GCaCATTGACCTCCAC a gACTG	4	0	0

Supplementary Table 3B: Presence of predicted *in silico* protospacer and flanking off-targets (R553X, N=3).

#CHROM	POS	REF>ALT	ID	Mutation_type	Gene	aa_change	pathogenicity
1	17914722	G>A	rs35497285;COSM3997092	missense	ARHGEF10L	p.Asp9Asn	not in clinvar
1	186316488	C>T	rs373565;COSM3750701	missense	TPR	p.Ser960Asn	not in clinvar
3	14220023	G>C	rs1870134;COSM4415545	missense	XPC	p.Leu16Val	benign
4	55972946	A>G	rs34231037;COSM5020657	missense	KDR	p.Cys482Arg	likely benign
4	126370647	G>A	rs12508222;COSM5009595	missense	FAT4	p.Asp282Asn	benign
8	17838238	G>T	COSM4166988	missense	PCM1	p.Cys1361Phe	not in clinvar
10	43610119	G>A	rs1799939;COSM1666596	missense	RET	p.Gly691Ser	benign/likely benign/ uncertain
12	472260	C>T	COSM1211763	missense	KDM5A	p.Val181Met	not in clinvar
12	133220526	T>C	rs5744934;COSM3753066	missense	POLE	p.Asn1396Ser	benign
17	37856534	C>T	rs193171026;COSM5414789	missense	ERBB2	p.Leu15Phe	in clinvar but unknown
19	54611471	C>T	rs202010949;COSM1396201	missense	TFPT	p.Arg156His	not in clinvar

Supplementary Table 4A: Mutations induced by ABE-mediated repair and in vitro expansion of R785X mutated organoids



#CHROM	POS	REF>ALT	ID		Mutation_type	Gene	aa_change	pathogenicity
1	2160390	C>G	rs28384811;COSM4143328	missense	SKI		p.Ala62Gly	benign
1	11308007	C>T	rs35903812;COSM5227567	missense	MTOR		p.Ala329Thr	likely benign
1	186316488	C>T	rs3753565;COSM3750701	missense	TPR		p.Ser960Asn	not in clinvar
2	141459344	C>T	rs147767913;COSM245482	missense	LRP1B		p.Gly2125Ser	not in clinvar
3	13672274	G>A	rs201224373;COSM1038940	missense	FBLN2		p.Arg1015His	not in clinvar
7	148516722	T>C	rs151023145;COSM53031	missense	EZH2		p.Asn322Ser	uncertain significance
7	148525904	C>G	rs2302427;COSM3762469	missense	EZH2		p.Asp185His	benign
8	71039118	C>G	rs22228591;COSM3982580	missense	NCOA2		p.Met1282Ile	not in clinvar
11	3723781	G>C	rs35404087;COSM3736041	missense	NUP98		p.Gln1142Glu	not in clinvar
11	108143456	C>G	rs1800057;COSM21827	missense	ATM		p.Pro1054Arg	benign
12	27844740	G>A	COSM1746913	missense	PPFBP1		p.Gly921Asp	not in clinvar
12	121416864	C>T	rs1800574;COSM5020679	missense	HNF1A		p.Ala98Val	benign/likely benign
14	35231108	A>T	rs1044140;COSM5002357	missense	BAZ1A		p.Asn1366Lys	not in clinvar
16	15818842	A>G	rs16967510;COSM5019307	missense	MYH11		p.Val1296Ala	benign/likely benign
16	72821625	C>T	rs201772357;COSM4988958	missense	ZFHX3		p.Gly3517Asp	not in clinvar
17	29496957	T>A	rs112306990;COSM24498	missense	NF1		p.Asp176Glu	benign/likely benign/uncertain
18	50832036	G>A	rs200099519;COSM4072542	missense	DCC		p.Arg667His	uncertain significance
19	18876258	G>A	rs36070283;COSM5020029	missense	CRTC1		p.Va327Ile	not in clinvar
19	45856059	C>G	COSM1681129	missense	ERCC2		p.Arg616Pro	not in clinvar

Supplementary Table 4B: Mutations induced by ABE-mediated repair and in vitro expansion of R553X mutated organoids.

CHAPTER 6

Primer name	Primer sequence	Temperature (°C)
APC_Q1403_X_sgRNA	TTGACACAAAGACTGGCTACGGGTGTTCGTCCTTCCAC	
P53_W53X_sgRNA	GACGATATTGAACAATGGTCGGTGTTCGTCCTTCCAAG	
PIK3CA_E545K_sgRNA	CTCTCTGAAATCACTGAGCACGGTGTTCGTCCTTCCAAG	
CFTR_X785R_sgRNA	AGGTCAGAACATTCACTGAGCACGGTGTTCGTCCTTCCAAG	
CFTR_X553R_sgRNA	CTGAGTGGAGGTCAATGAGCGGTGTTCGTCCTTCCAAG	
CFTR_X1162R_sgRNA	GATGCGATCTGAGCTGAGCGGTGTTCGTCCTTCCAAG	
CFTR_X1282R_sgRNA	CCAAAGGCTTCCTCACTGCGGTGTTCGTCCTTCCAAG	
Scrambled_sgRNA	TGAGTTAGCTCTGGTAGTGCAGGTGTTCGTCCTTCCAAG	
sgRNA_universal	/5Phos/GTTTAGAGCTAGAAATAGCAAGTAAATAAGGC	
ABEmax_gib_BB_FW	TCTGGCGGCTAAAAAGAACCGC	
ABEmax_gib_BB_Rev	TGATCCTCTGAAGATCCCCGCTGCTTCAGGTGTTG	
xCas9_gib_ins_FW	GGATCTCAGGAGGATCAGACAAGAAGTACAGCATGGCC	
xCas9_gib_ins_Rev	TCTTTTGAGCGCCAGTCGCTCCAGCTGAGACAGGTCGATCC	
M13F_seq	GTAAAACGACGCCAGT	
APC_Q1403_FW	GTAAAACGACGCCAGTTGCTCAGACACCCAAAAGTCCA	
APC_Q1403_Rev	CTGGAAGAACCTGGACCTCTG	
P53_W53_FW	GTAAAACGACGCCAGTCACCCATCTACAGTCCCCCTG	
P53_W53_Rev	CTTGGCTGTCAGAATGCAAG	
PIK3CA_E545_FW	GTAAAACGACGCCAGTATCATCTGTGAATCCAGAGGGGA	
PIK3CA_E545_Rev	TGCATGCTGTCAAAAGGTTGAC	
CFTR_R785_FW	GTAAAACGACGCCAGTCGAAGAGGATTCTGATGAGC	
CFTR_R785_Rev	TACTGCACCTTCCCACAG	
CFTR_R553_FW	GTAAAACGACGCCAGTGTGCCTTCAAATTCAAGATTGAGCA	
CFTR_R553_Rev	GTACATTGGAGTGGCAGGGTCT	
CFTR_W1282_FW	GTAAAACGACGCCAGTGGCTCTGGGAAGAACTGGAT	
CFTR_W1282_Rev	TAACTTGGAGGTCAAGCCACTG	
CFTR_R1162_FW	GTAAAACGACGCCAGTTGTGCAGTGCTCATAG	
CFTR_R1162_Rev	ACATTGCTCAGGCTACTGG	
CFTR_Qpcr_FW	CAACATCTAGTGAGCAGTCAGG	62.5
CFTR_Qpcr_Rev	CCCAGGTAAGGGATGTATTGTG	62.5
YWHAZ_Qpcr_FW	ATGCAACCAACACATCCTATC	61
YWHAZ_Qpcr_Rev	GCATTATTAGCGTGTGCTT	61
CTNNB1_Qpcr_FW	CTGGAACGGTGAAGGTGACA	62.5
CTNNB1_Qpcr_Rev	AAGGGACTCTGTACAATGCA	62.5
CFTR_R785X_ssODN	ATCAGCGTGTACAGCACTGGCCCCACGCTTCAGGCACGAAGGAG GCAGTCTGCTCTGAACCTGATGACACACTCAGTTAatCAgGGcCA aAACATTACCGAAGACAACAGCATCCACACGAAAGTGTCACTG GCCCTCAGGCAAACCTGACTGAACCTGGATATATTCAAGAAGGTT	

Methods S1: List of primers used in this manuscript.

Clone	R553X > WT clone 1	R553X > WT clone 2	R553X > WT clone 3	R553X -> R553X control	R785X > WT clone 1	R785X > WT clone 2	R785X > WT clone 3	R785X -> R785X control
Mutation type								
A[C>A]A	9	10	6	10	6	15	13	4
A[C>A]C	2	1	0	1	6	2	0	1
A[C>A]G	0	0	0	0	1	0	0	0
A[C>A]T	5	7	4	5	8	1	7	1
C[C>A]A	4	9	7	2	9	6	5	4
C[C>A]C	1	0	3	0	1	5	0	2
C[C>A]G	0	1	0	0	1	0	1	1
C[C>A]T	5	3	7	3	10	3	7	1
G[C>A]A	10	7	6	5	13	6	12	7
G[C>A]C	3	1	2	2	0	2	0	2
G[C>A]G	0	1	1	0	0	0	1	0
G[C>A]T	2	11	8	7	8	15	11	6
T[C>A]A	4	5	1	7	9	13	12	3
T[C>A]C	6	2	6	4	4	3	4	3
T[C>A]G	0	0	1	1	1	0	0	0
T[C>A]T	20	11	10	15	28	13	19	5
A[C>G]A	0	0	1	1	1	1	1	2
A[C>G]C	1	0	0	1	2	2	1	1
A[C>G]G	0	0	0	0	0	0	0	0
A[C>G]T	0	0	1	2	2	4	2	0
C[C>G]A	0	3	2	0	3	1	3	0
C[C>G]C	1	0	1	0	2	2	0	0
C[C>G]G	0	0	0	0	0	1	0	0
C[C>G]T	2	0	0	2	2	4	2	0
G[C>G]A	0	1	2	0	3	1	2	0
G[C>G]C	1	1	0	0	0	0	1	1
G[C>G]G	0	0	0	0	0	0	0	0
G[C>G]T	0	1	1	0	3	3	1	0
T[C>G]A	1	3	1	1	2	0	2	0
T[C>G]C	0	0	0	0	1	1	1	0
T[C>G]G	0	0	0	0	0	0	0	0
T[C>G]T	3	2	3	0	1	6	2	0
A[C>T]A	4	3	1	6	12	4	8	3

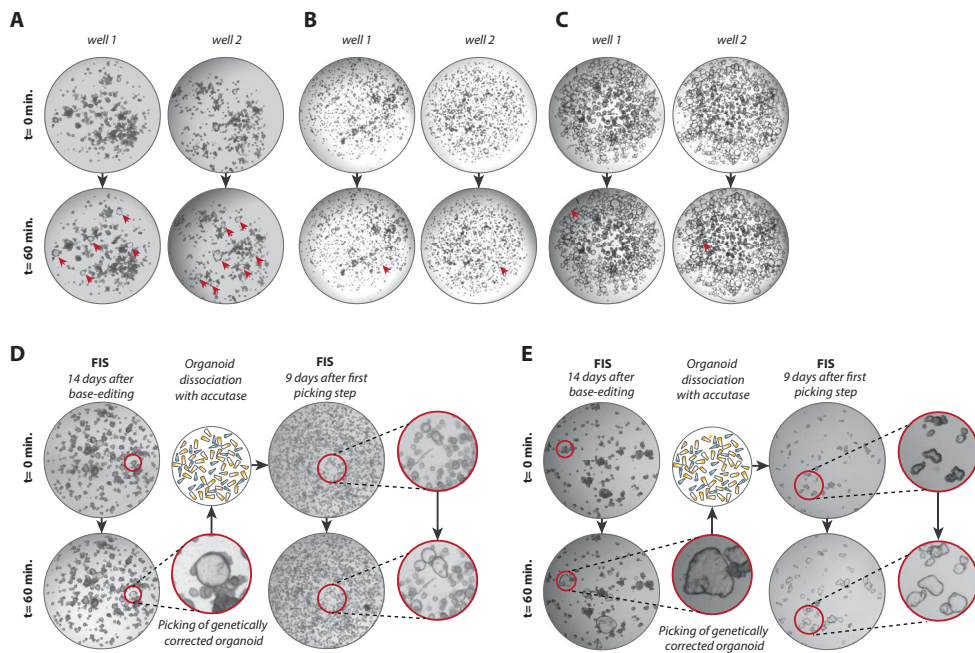
CHAPTER 6

Clone	R553X -> WT clone 1	R553X -> WT clone 2	R553X -> WT clone 3	R553X -> R553X control	R785X -> WT clone 1	R785X -> WT clone 2	R785X -> WT clone 3	R785X -> R785X control
Mutation type								
A[C>T]C	2	4	2	1	2	1	2	0
A[C>T]G	9	5	10	8	37	10	32	18
A[C>T]T	1	2	2	0	5	2	9	5
C[C>T]A	5	3	2	0	7	3	9	2
C[C>T]C	0	1	3	1	2	1	6	1
C[C>T]G	6	6	7	7	16	6	13	11
C[C>T]T	3	2	4	3	2	2	7	0
G[C>T]A	2	2	3	2	10	3	0	1
G[C>T]C	3	0	1	3	0	0	3	4
G[C>T]G	5	6	4	3	20	7	12	7
G[C>T]T	1	0	1	0	3	3	3	1
T[C>T]A	3	1	5	0	10	2	11	2
T[C>T]C	2	4	2	2	4	7	4	2
T[C>T]G	0	4	3	4	13	6	19	6
T[C>T]T	1	0	6	3	4	6	7	4
A[T>A]A	1	2	1	2	0	2	1	1
A[T>A]C	0	1	1	1	1	0	1	0
A[T>A]G	0	0	1	1	3	1	1	0
A[T>A]T	4	1	3	2	1	3	2	0
C[T>A]A	1	0	1	2	1	2	1	0
C[T>A]C	2	1	0	1	0	2	1	1
C[T>A]G	0	0	0	1	0	1	0	2
C[T>A]T	0	0	1	1	4	0	0	1
G[T>A]A	0	0	0	2	0	2	1	0
G[T>A]C	1	0	0	0	0	0	1	0
G[T>A]G	1	1	1	1	1	0	0	1
G[T>A]T	2	0	1	1	1	1	0	1
T[T>A]A	1	0	1	0	5	2	4	4
T[T>A]C	0	1	1	0	0	2	1	0
T[T>A]G	0	1	2	1	2	0	0	0
T[T>A]T	5	3	2	2	3	5	0	0
A[T>C]A	1	5	4	3	7	4	4	4
A[T>C]C	0	0	0	1	3	0	0	0

Clone	R553X > WT clone 1	R553X > WT clone 2	R553X > WT clone 3	R553X -> R553X control	R785X > WT clone 1	R785X > WT clone 2	R785X > WT clone 3	R785X -> R785X control
Mutation type								
A[T>C]G	2	2	2	2	1	3	1	0
A[T>C]T	3	2	5	0	4	6	5	2
C[T>C]A	1	2	1	0	2	4	2	1
C[T>C]C	0	1	2	0	2	3	2	1
C[T>C]G	3	1	1	1	0	1	1	2
C[T>C]T	0	1	1	2	3	0	4	0
G[T>C]A	3	1	0	0	1	3	3	1
G[T>C]C	0	1	0	2	1	1	2	1
G[T>C]G	1	0	0	0	1	0	2	2
G[T>C]T	0	1	3	0	4	5	1	3
T[T>C]A	2	3	0	1	3	4	5	3
T[T>C]C	1	1	0	1	2	2	4	1
T[T>C]G	0	1	1	2	4	1	1	1
T[T>C]T	2	2	1	1	10	2	3	3
A[T>G]A	0	0	1	0	3	3	3	0
A[T>G]C	0	0	1	1	0	0	2	0
A[T>G]G	1	2	0	0	0	0	0	0
A[T>G]T	1	0	2	2	0	2	0	0
C[T>G]A	0	1	0	0	0	0	1	0
C[T>G]C	0	1	0	0	1	0	0	0
C[T>G]G	0	2	0	0	1	3	1	0
C[T>G]T	0	1	1	1	1	0	1	2
G[T>G]A	1	0	0	0	0	1	0	0
G[T>G]C	0	1	0	0	0	1	0	0
G[T>G]G	0	0	1	0	2	0	0	0
G[T>G]T	1	0	0	0	0	1	3	0
T[T>G]A	0	0	0	0	0	1	1	1
T[T>G]C	0	0	1	0	0	0	0	0
T[T>G]G	0	0	1	2	2	3	0	1
T[T>G]T	4	3	0	2	2	0	0	0

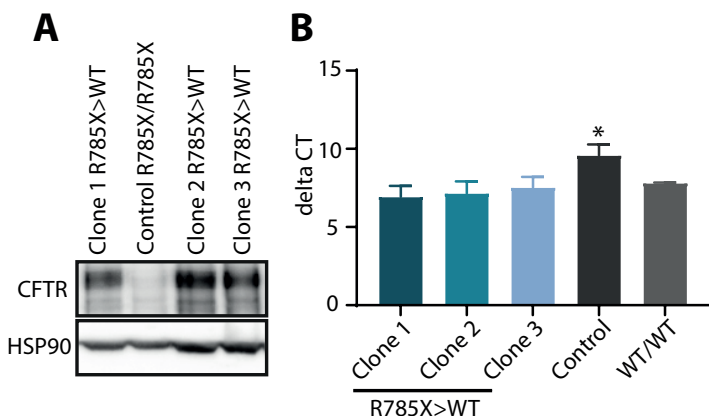
Methods S2: Absolute number of mutations in each ABE-repaired clone and their respective unrepaired controls.

SUPPLEMENTARY FIGURES



Supplementary Figure 1: Phenotypic selection and clonal expansion of ABE-repaired organoids, related to Figure 2 and 3.

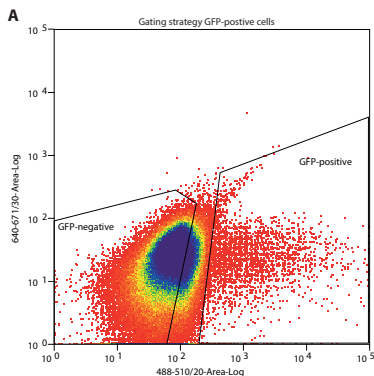
Bright field images before and after 60 min forskolin stimulation of bulk organoid cultures after electroporation, harboring R785X/R785X (**A**), F508del/R553X (**B**), and W1282X/W1282X-CFTR mutations (**C**). Organoids responding to forskolin (highlighted by the red arrowheads) were visually selected (**D**), picked and expanded until a clonal organoid culture was established. (**E**) Picking and passaging of one individual FIS-assay responsive organoid upon FACS sorting of GFP-positive cells results in a clonal organoid culture where all organoids are FIS-assay responsive. This shows that the original organoid exclusively consists of repaired cells.



Supplementary Figure 2: protein and mRNA expression of SpCas9-ABE-corrected organoids, related to Figure 2.

(A) Western-blot analysis of R785X-CFTR repair using SpCas9-ABE in three corrected clonal organoid cultures compared to non-corrected control R785X/R785X organoids. (B) qPCR deltaCTvalues of the same repaired clonal organoid cultures compared to non-corrected control organoids, bars represent mean \pm SD; N=4.

CHAPTER 6



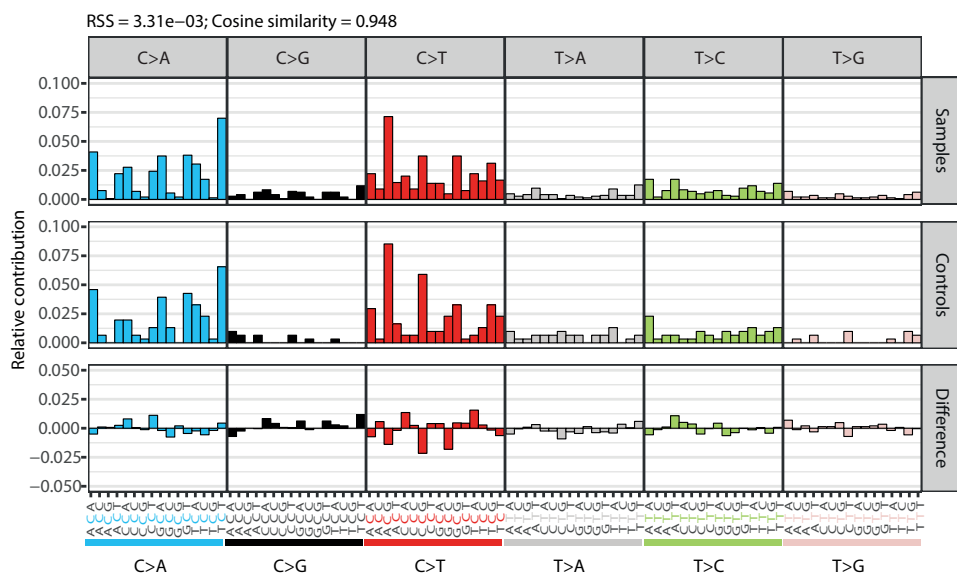
B

Sample name	# organoid outgrowth	Transfection efficiency	Amount of transfected organoids	Amount of repaired organoids	Editing efficiency	Mean editing efficiency
SpABE-785/785 n=1	*	1.71%	220	20	9.09%	8.98%
SpABE-785/785 n=2	*	0.51%	30	4	13.33%	
SpABE-785/785 n=3	*	1.55%	267	20	7.49%	
SpABE-785/785 n=4	*	1.7%	432	40	9.26%	
SpABE-785/785 n=5	*	1.99%	385	22	5.71%	
HDR-785/785 n=1	*	4.28%	689	6	0.87%	1.78%
HDR-785/785 n=2	*	3.12%	704	14	1.98%	
HDR-785/785 n=3	*	3.11%	765	19	2.48%	
xABE - 1282/1282 n=1	17689	5.9%	1044	15	1.44%	1.43%
xABE - 1282/1282 n=2	16652	4.33%	721	12	1.66%	
xABE - 1282/1282 n=3	14819	4.59%	680	8	1.18%	
xABE - 553/F508del n=1	34634	3.29%	1140	19	1.67%	1.43%
xABE - 553/F508del n=2	37407	2.25%	842	14	1.66%	
xABE - 553/F508del n=3	42221	2.19%	925	9	0.97%	

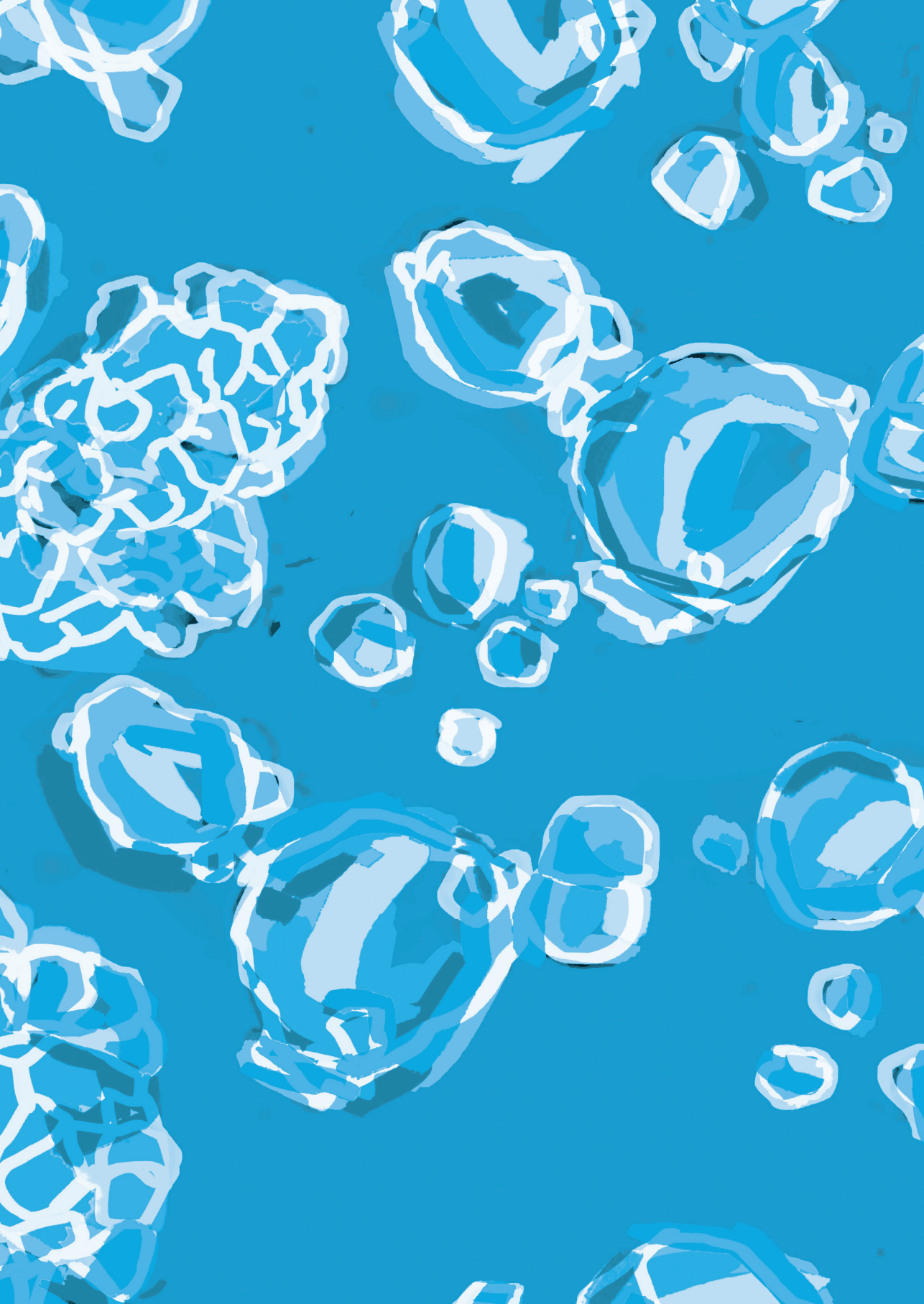
*Organoids sorted

Supplementary Figure 3: editing efficiencies in intestinal organoids, related to Figure 2 and 3.

GFP-positive cells were either sorted (* in **B**) or quantified using the gating strategy depicted in **(A)**. The editing efficiencies were calculated by dividing the total number of organoids with the transfection efficiency (only for the samples that were not sorted) and the total number of organoids that showed a swelling response upon 1h stimulation with forskolin (**B**).

**Supplementary Figure 4: mutational signature and strand bias analysis on WGS data, related to Figure 4.**

Relative contribution of mutations in three repaired R785X/R785X clonal organoid lines and three R553X/F508del clonal organoid lines. The X-axis shows all 96 context-dependent mutation types, which is a combination of the base substitution and its neighboring bases. The Y-axis shows the relative contribution of each mutation type.





EVALUATING CRISPR-BASED PRIME EDITING FOR CANCER MODELING AND CFTR REPAIR IN ORGANOID

Published as Research Article

Maarten H Geurts, Eyleen de Poel, Cayetano Pleguezuelos-Manzano, Rurika Oka , Leo Carrillo, Amanda Andersson-Rolf, Matteo Boretto, Jesse E Brunsveld, Ruben van Boxtel, Jeffrey M Beekman, Hans Clevers

Life Science Alliance (2021) 4: p1-12

ABSTRACT

Prime editing is a recently reported genome editing tool employing a nickase-cas9 fused to a reverse transcriptase that directly synthesizes the desired edit at the target site. Here, we explore the use of prime editing in human organoids. Common TP53 mutations can be correctly modeled in human adult stem cell-derived colonic organoids with efficiencies up to 25% and up to 97% in hepatocyte organoids. Next, we functionally repaired the cystic fibrosis CFTR-F508del mutation and compared prime editing to CRISPR/Cas9-mediated homology directed repair and adenine base editing on the CFTR-R785^{*} mutation. Whole genome sequencing of prime editing repaired organoids revealed no detectable off-target effects. Despite encountering varying editing efficiencies and undesired mutations at the target site, these results underline the broad applicability of prime editing for modeling oncogenic mutations and showcase the potential clinical application of this technique, pending further optimization.

TAKE HOME MESSAGE

Here, the authors use prime editing to model mutations in TP53 in hepatocyte and colon organoids after which clinical application of prime editing is evaluated by safely repairing mutations in CFTR.

INTRODUCTION

The field of genome engineering has been revolutionized by the development of the efficient genome editing tool CRISPR/Cas9. In CRISPR/Cas9-mediated genome engineering, the effector protein Cas9 is guided towards the target site in the genome by an RNA guide¹. Upon target recognition, Cas9 generates a double stranded break (DSB) that can be exploited for a variety of genome engineering strategies^{2,3}. Due to the easy reprogrammability and high efficiency of CRISPR/Cas9, the technology is widely used for gene modification and is considered to be the most promising tool for clinical gene editing. However, the repair of DSBs is often error-prone and can result in unwanted DNA damage at the target site as well as at off-target sites that closely resemble the guide RNA⁴⁻⁷. These issues have been circumvented by the development of Cas9 fusion proteins, called base editors. In base editing, a partially nuclease-inactive nickase-Cas9 (nCas9) protein is fused to either the cytidine deaminase APOBEC1A to enable C-G to T-A base pair changes or to an evolved Tada heterodimer to facilitate the opposite reaction, turning A-T base pairs into G-C base pairs^{8,9}. Base editors show high efficiency and infrequent unwanted DNA changes in a variety of model systems but are strictly limited to transition DNA substitutions¹⁰⁻¹².

To overcome these limitations, prime editing has been developed to enable both transition and transversion reactions as well as insertions and deletions of up to 80 nucleotides in length without the need to generate DSBs¹³. In prime editing, an nCas9 is fused to an engineered reverse transcriptase (RT) that is used to generate complementary DNA from an RNA template (PE2) (**figure 1**). This fusion protein is combined with a prime editing guide RNA (pegRNA) that guides the nCas9 to its target and contains the RNA template that encodes the desired edit. Upon target recognition the PAM-containing strand is nicked and the pegRNA extension binds to the nicked strand at the primer binding site (PBS). The RT-domain then uses the remainder (RT template) of the pegRNA to synthesize a 3'-DNA-flap containing the edit of interest. This DNA-flap is resolved by cellular DNA repair processes that can be further enhanced by inducing a proximal second nick in the opposing DNA strand, guided by a second (PE3) guide-RNA¹³ (**figure 1**). Prime editing holds great promise, as it can -in theory- repair 89% of all disease-causing variants¹³. Here, we apply this approach in human organoids to introduce cancer mutations and to repair mutations in the CFTR channel that cause cystic fibrosis (CF), a Mendelian disorder with high prevalence in European ancestry.

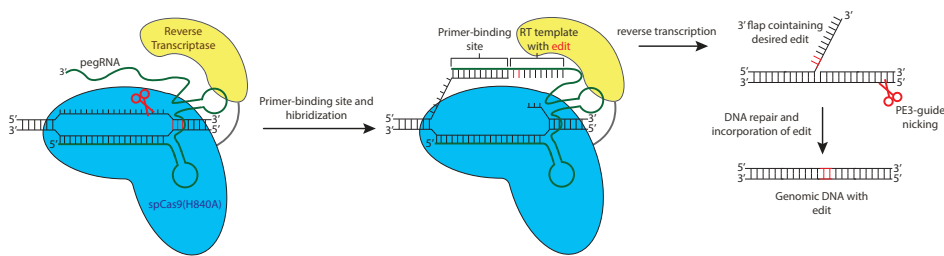


Figure 1: Principles of prime editing adapted from Anzalone et al.

Principles of prime editing. The pegRNA complexes with the nCas9(H840A)-RT prime editing fusion protein and binds to the target DNA. Upon PAM strand cleavage by nCas9 the PBS of the pegRNA extension binds the single stranded DNA upon which the RT synthesizes a 3'-DNA-flap containing the edit of interest. This 3'-flap is resolved by cellular DNA processes which can be further enhanced by introducing a proximal second nick in the opposing DNA strand, guided by a second (PE3) guide-RNA. Red scissors indicate nick site of the nCas9. RT = Reverse Transcriptase.

MATERIALS AND METHODS

Organoid culture

Intestinal organoids are cultured as previously described³⁴. In short, the wild-type human colon organoid line P26n, as previously described in³⁵ was cultured in domes of Cultrex Pathclear Reduced Growth Factor Basement Membrane Extract (BME) (3533-001, Amsbio). Domes were covered by medium containing Advanced DMEM/F12 (Gibco), 1x Glutamax, 10mmol/l HEPES, 100U/ml penicillin-streptomycin and 1x B27 (All supplied by ThermoFisher scientific), 1.25mM N-acetylcysteine, 10µM nicotinamide, 10µM p38 inhibitor SB202190 (supplied by Sigma-Aldrich). This medium was supplemented with the following growth factors: 0.4nM Wnt surrogate-Fc Fusion protein, 2% Noggin conditioned medium (U-Protein express), 20% Rspo1 conditioned medium (in-house), 50ng/ml EGF (Peprotech), 0.5 µM A83-01 and 1µM PGE2 (Tocris). Intestinal organoids derived from people with cystic fibrosis are part of a large biobank at Hub for organoids (HUB), are stored in liquid nitrogen and are passaged at least 4 times prior to electroporation experiments. Cystic fibrosis organoids are kept in Matrigel (Corning) instead of BME. Furthermore 2% Noggin conditioned medium (U-protein express) is replaced by 10% Noggin conditioned medium (in-house). Moreover, PGE2 is excluded and 30µM of P38 inhibitor SB202190 (Sigma-Aldrich) is added to expansion medium for cystic fibrosis organoids. All organoids were passaged and split once a week 1:6 and filtered through a 40 micron cell strainer (ThermoFisher scientific) to remove differentiated structures from the culture. Hepatocyte organoids were cultured as previously described³⁶.

Plasmid construction

Human codon optimized prime editing constructs were a kind gift from David Liu; pCMV_P2A_GFP (Addgene plasmid #132776), pU6-pegRNA-GG-acceptor (Addgene plasmid #132777). Human codon optimized base editing constructs were a kind gift from David Liu;

pCMV_ABEmax_P2A_GFP (Addgene plasmid # 112101). The empty sgRNA plasmid backbone was a kind gift from Keith Joung (BPK1520, Addgene plasmid #65777). The SpCas9 expressing vector was created by using Q5 high fidelity polymerase (NEB) to PCR amplify the Cas9-P2A-GFP cassette from pSpCas9 (BB)-2A-GFP (PX458), a kind gift from Feng Zhang (Addgene plasmid # 48138). This Cas9-P2A-GFP cassette was then cloned into the PE2 expression vector NEBbuilder HIFI assembly mastermix according to manufacturer protocols (NEB). pegRNA were created as previously described¹³. In brief, the pU6-pegRNA-GG-acceptor plasmid was digested overnight using Bsal-HFv2 (NEB), loaded on a gel and the 2.2kb band was extracted using the QIAquick Gel extraction kit. Oligonucleotide duplexes for the spacer, scaffold and 3'-extension with their appropriate overhangs were annealed and cloned into the digested pUF-pegRNA-GG-acceptor by golden gate assembly according to the previously described protocol¹³. PE3-guides and guides for both base editing and HDR experiments were cloned using inverse PCR together using BPK1520 as template and Q5 High fidelity polymerase. Upon PCR cleanup (Qiaquick PCR purification kit), amplicons were ligated using T4 ligase and Dpn1 (both NEB) to get rid of template DNA. All transformations in this study were performed using OneShot Mach1t1 (ThermoFisher scientific) cells and plasmid identity was checked by Sanger sequencing (Macrogen). All constructed guide-RNA sequences can be found in **supplementary table 1**.

Organoid electroporation

Organoid electroporation was performed with slight modifications to this previously described protocol^{12,37}. Wild type colon and intestinal organoids derived from cystic fibrosis patients were maintained in their respective expansion medium up until two days before electroporation. Two days in advance, the expansion medium was switched to electroporation medium which does not contain the growth-factors wnt and Rspo1. Rspindin-conditioned medium was replaced by Advanced DMEM-F12 (Gibco) supplemented by 1x Glutamax, 10mmol/l HEPES and 100U/ml penicillin-streptomycin (ThermoFisher scientific). Furthermore, the GSK-3 inhibitor CHIR99021 (Sigma-Aldrich) was added to the medium for wnt-pathway activation and rho-kinase inhibitor Y-27632 (abmole bioscience) was added to inhibit anoikis. One day prior to electroporation 1.25% (v/v) DMSO was added to the organoid medium. On the day of electroporation the organoids were dissociated into single cells using TrypLE (Gibco) supplemented with Y-27632 at 37°C for 15 minutes. During the single-cell dissociation, the organoid suspension was vigorously pipetted every 5 minutes to keep the solution homogenous. 106 cell per electroporation were resuspended in BTXpress solution and combined with 10µl plasmid solution containing 7.5 µg pCMV_PE2_P2A_GFP, pCMV_SpCas9 or pCMV_ABEmax_P2A_GFP depending on gene editing strategy and 2.5 µg per guide-RNA plasmid. In HDR experiments 2.5 µg of single stranded donor oligonucleotide, containing a WT-CFTR sequence and silent mutations to block Cas9 cleavage after repair was added to the plasmid mix. Electroporation was performed using NEPA21 with settings described before³⁷. After electroporation the cells were resuspended in 600ul Matrigel or BME (50% Matrigel/BME, 50% expansion medium) and plated out in 20 µl droplet/well of a pre-warmed 48-wells tissue culture plate (Greiner). After polymerization, the droplets were immersed in 300 µL of expansion medium and the organoids were maintained at 37°C and 5% CO2.

Phenotypic selection by forskolin induced swelling

After electroporation, organoids were expanded for 7 days and subsequently replated in 72 wells of 48-wells tissue culture plates (Greiner) to make organoids sufficiently sparse. Selection of genetically corrected organoids was based on CFTR-function restoration as assessed by adding forskolin (5 μ M) to the expansion medium. Pictures were made (1.25x on an EVOS FL Auto Imaging system) before and 60 minutes after forskolin addition. Organoids that showed swelling after 60 minutes were individually picked with a p200 pipette and a bend p200 pipette tip. Each individual genetically corrected organoid was dissociated into single cells using TrypLE supplemented with Y-27632 (10 μ M) for 10 minutes at 37°C. The cells were plated in 20 μ L matrigel droplets/picked organoid (50% matrigel, 50% CCM+) in pre-warm 48-well tissue culture plates (Greiner) and maintained at 37°C and 5% CO₂.

Phenotypic selection for oncogenic mutations

After electroporation, organoids were expanded for 5 days to offer sufficient time for recovery of the transfected cells. In prime editing experiments with the goal to mutate TP53, 10 μ M Nutlin-3 was added to the expansion medium. In prime editing experiments with the goal to mutate APC, both wnt-surrogate and Rspo1 were removed from the expansion medium. After two weeks individual organoids that survived selection were manually picked and clonally expanded as previously described.

Genotyping of clonal organoid lines

Organoid DNA was harvested from 10-20 μ L Matrigel/BME suspension and DNA was extracted using the Zymogen Quick-DNA microprep kit. Target regions were amplified from the genome using Q5 high fidelity polymerase using primers. Sequencing was performed using the M13F tail as all forward amplification primers for targeted sequencing contained a tail with this sequence. Prime editing, base editing and CRISPR/Cas9-mediated HDR induced genomic alterations were confirmed by Sanger sequencing (Macrogen). Subsequent Sanger trace deconvolution was performed with the use of the online tool ICE by Synthego.

FIS-Assay

To quantify CFTR function in the genetically corrected intestinal organoids, we conducted the Forskolin induced Swelling (FIS)-assay. This was done in duplicates at three independent culture time points (n=3) according to previously published protocols^{38,39}. In brief, intestinal organoids were seeded in 96-well culture plates in 4 μ L of 50% Matrigel. Each Matrigel dome contained roughly 20-40 organoids and was immersed in expansion medium. The day after, organoids were incubated for 30 min with 3 μ M calcein green (Invitrogen) to fluorescently label the organoids and stimulated with 5 μ M forskolin. Every ten minutes the total calcein green labeled area per well was monitored by a Zeiss LSM800 confocal microscope, for 60 minutes while the environment was maintained at 37°C and 5% CO₂. A Zen Image analysis software module (Zeiss) was used to quantify the organoid response (area under the curve measurements of relative size increase of organoids after 60 minutes forskolin stimulation, t = 0 min baseline of 100%).

Efficiency calculation of prime editing in organoids

pegRNA/PE3-guide RNA pairs were co-transfected with 10 µg PiggyBac transposon system (2.8 µg transposase + 7.2 µg hygromycin resistance containing transposon⁴⁰) as described before using the NEPA21. 5 days post transfection organoid culture medium was supplemented with 100µg/µL Hygromycin B gold (InvivoGen). 14 days after selection clonal organoids, surviving hygromycin selection were individually picked and Sanger sequencing was performed as previously described. Primer sequences can be found in **supplementary table 2**. For comparison of prime editing to conventional CRISPR/Cas9-mediated HDR and adenine base editing on the CFTR-R785* mutation we transfected pegRNA/PE3-guide pairs with pCMV_PE2_P2A_GFP, pCMV_SpCas9 with the respective sgRNA/HDR repair template combination (ssDNA oligo **supplementary table 1**) and pCMV_ABEmax_P2A_GFP with respective repair sgRNA were transfected in duplicates as previously described. 3 days post transfection, organoids were dissociated to single cells using TrypLE (Gibco) supplemented with Y-27632 at 37°C for 15 minutes. During the single-cell dissociation, the organoid suspension was vigorously pipetted every 5 minutes to keep the solution homogenous. Single cell suspensions were filtered and GFP-positive and thus transfected cells were sorted and plated at a concentration of 500 cells per 100µL using a FACS Melody (BD Biosciences). We then quantified the total amount of cultured organoids by using cell-profiler 3.1.5. Editing efficiencies were determined by dividing the total amount of organoids by the transfection efficiency and the amount of FIS-assay responsive organoids two weeks after plating.

Whole genome sequencing and mapping

Genomic DNA was isolated from 100 µl of Matrigel/organoid suspension using DNeasy Blood & Tissue Kit, according to protocol. Standard Illumina protocols were applied to generate DNA libraries for Illumina sequencing from 20-50ng of genomic DNA. All samples (five genetically corrected clones, two non-corrected control samples of the R785X/R785X donor and the clonal line prior to prime editing.) were sequenced (2x150bp) by using Illumina NovaSeq to 15x base coverage. Reads were mapped against human reference genome GRCh38 using Burrows-Wheeler Aligner v0.7.17⁴¹, with settings 'bwa mem -c 100 -M'. Duplicate sequence reads were marked using Sambamba v0.7.0 and recalibrated using the GATK BaseRecalibrator v4.1.3.0. More details on the pipeline can be found on <https://github.com/ToolsVanBox/NF-IAP>.

Mutation calling and filtering

Raw variants were multisample-called by using the GATK HaplotypeCaller v4.1.3.0⁴². The quality of variant and reference positions was evaluated by using GATK VariantFiltration v4.1.3.0 with options 'QD < 2.0' --filter-expression 'MQ < 40.0' --filter-expression 'FS > 60.0' --filter-expression 'HaplotypeScore > 13.0' --filter-expression 'MQRankSum < -12.5' --filter-expression 'ReadPosRankSum < -8.0' --filter-expression 'MQ0 >= 4 && ((MQ0 / (1.0 * DP)) > 0.1)' --filter-expression 'DP < 5' --filter-expression 'QUAL < 30' --filter-expression 'QUAL >= 30.0 && QUAL < 50.0' --filter-expression 'SOR > 4.0' --filter-name 'SNP_LowQualityDepth' --filter-name 'SNP_MappingQuality' --filter-name 'SNP_StrandBias' --filter-name 'SNP_HaplotypeScoreHigh' --filter-name 'SNP_MQRankSumLow' --filter-name 'SNP_ReadPosRankSumLow' --filter-name

'SNP_HardToValidate' --filter-name 'SNP_LowCoverage' --filter-name 'SNP_VeryLowQual' --filter-name 'SNP_LowQual' --filter-name 'SNP_SOR' -cluster 3 -window 10. To obtain high-quality somatic mutation catalogs, we applied post processing filters as described⁴³. Briefly, we considered variants at autosomal chromosomes without any evidence from a paired control sample (a clone prior to editing); passed by VariantFiltration with a GATK phred-scaled quality score ≥ 250 ; a base coverage of at least 10X in the clonal and paired control sample; no overlap with single nucleotide polymorphisms (SNPs) in the Single Nucleotide Polymorphism Database v146; and absence of the variant in a panel of unmatched normal human genomes (BED-file available upon request). We additionally filtered base substitutions with a GATK genotype score (GQ) lower than 99 or 10 in the clonal or paired control sample, respectively. For indels, we filtered variants with a GQ score lower than 99 in both the clonal and paired control sample and filtered indels that were present within 100 bp of a called variant in the control sample. In addition, for both SNVs and INDELS, we only considered variants with a mapping quality (MQ) score of 60 and with a variant allele frequency of 0.3 or higher in the clones to exclude in vitro accumulated mutations^{44,45}. The scripts used are available on GitHub (<https://github.com/ToolsVanBox/SMuRF>). The distribution of variants was visualized using an in house developed R package (MutationalPatterns)⁴⁴.

Mutational signature analysis

We extracted mutational signatures and estimated their contribution to the overall mutational profile as described using an in house developed R package (MutationalPatterns)⁴⁴ (**Methods S2**). In this analysis, we included small intestine data (previously analyzed) to explicitly extract in vivo and in vitro accumulated signatures⁴³. To determine the transcriptional strand contribution and bias, we selected all point mutations that fall within gene bodies and checked whether the mutated base was located on the transcribed or non-transcribed strand. We used a in house developed R package (MutationalPatterns) to determine transcriptional strand bias as described⁴⁴

RESULTS

Modeling common mutations in cancer in colon and hepatocyte organoids

We first characterized and optimized prime editing efficacy in adult human stem cell-derived organoids by targeting TP53, a gene that is often mutated in cancer. Previously, we have shown that TP53-mutant organoids can be selected by adding nutlin-3, a molecule that inhibits the interaction between TP53 and MDM2, to the organoid culture medium^{14,15}. By co-transfected plasmids containing genome editing components targeting TP53 with plasmids encoding a PiggyBac system conveying hygromycin resistance to transfected organoids, we can simultaneously functionally detect TP53 mutants by nutlin-3-resistance and determine editing efficiency by Sanger sequencing of hygromycin resistant clones (**figure 2A**). Using the pegFinder online software tool, we designed a single pegRNA and PE3-guide pair to introduce the R175H mutation, the most common mutation found in TP53 according to the Catalogue Of Somatic Mutations in Cancer (COSMIC)^{16,17}. The pegRNAs were designed to integrate a protospacer adjacent motif (PAM)-disrupting mutation in order to block re-binding of Cas9

after the correct editing event has occurred. We co-transfected PE2 plasmids, the pegRNA/PE3-guide pair and hygromycin resistance PiggyBac plasmids in colonic organoids by electroporation. Clonally selected organoids appeared after two weeks of nutlin-3 selection whereas control organoids, transfected with PE2 plasmids and a non-targeting scrambled sgRNA did not grow out (**figure 2B**). Manual picking of selected organoids and subsequent Sanger sequencing showed correct homozygous induction of the TP53-R175H (c.524 G>A) mutation in seven out of the eight clonally expanded colonic organoids (**figure 2C**).

To determine editing efficiency we performed Sanger sequencing on 36 hygromycin-selected colonic clones and found a single organoid harboring a heterozygous R175H mutation (**figure 2D**). Next, we performed the same experiment in hepatocytes and found a significantly increased editing efficiency clearly shown from nutlin-3 selection (**figure 2B**). Out of 36 hygromycin selected clones (**figure 2D**), 20 (55.5%) harbored a homozygous mutation, 4 (11.2%) a heterozygous mutation and two remained WT (5.5%) (**figure 2D and E**). The remaining 10 clones (27.8%) had incorporated unintended DNA changes around the target site, caused by incorrect repair of either pegRNA or PE3 guide nicking (**supplementary figure 1A**).

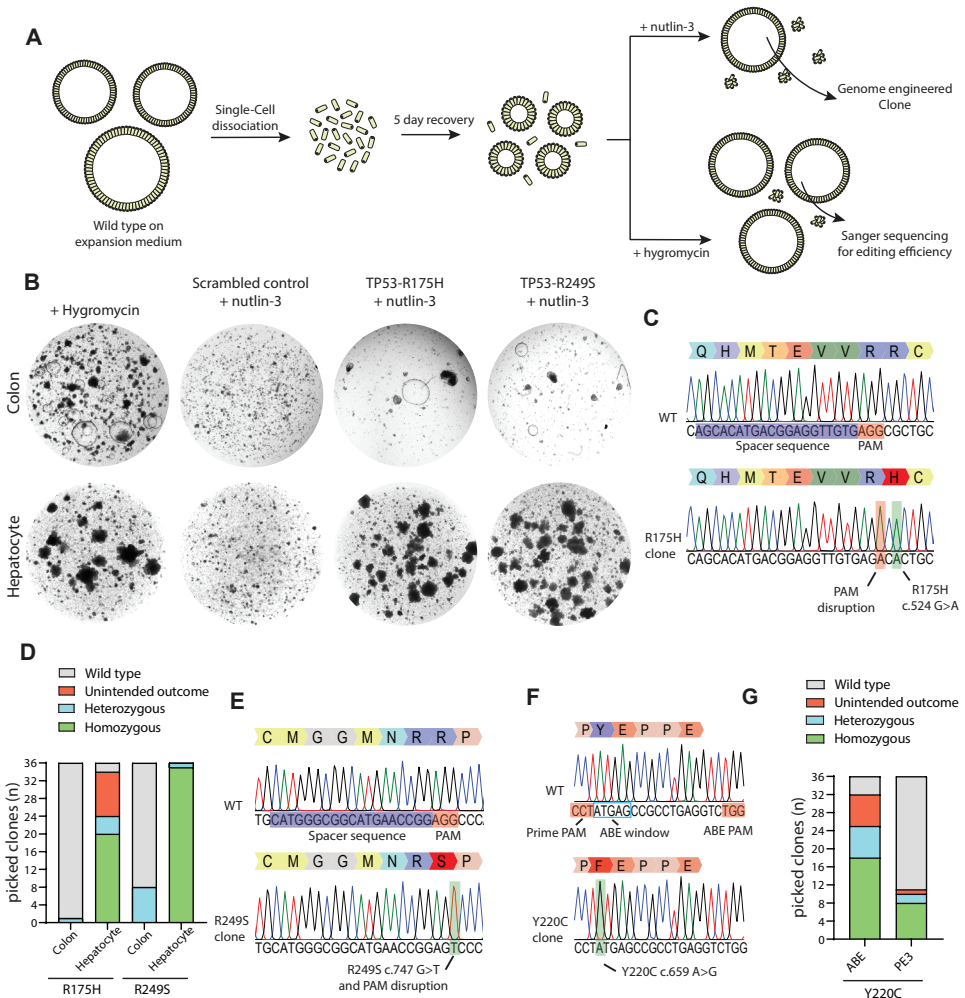
The most common mutation in TP53 in hepatocellular carcinoma is the R249S mutation most prominently caused by Aflatoxin B1. Exposure by this carcinogen that is often found in contaminated food sources results in the c.747 G>T transversion¹⁸. To generate hepatocyte and colonic organoids harboring this mutation we used the pegFinder online software tool to design a single pegRNA and PE3-guide pair to introduce the TP53-R249S mutation. No additional PAM disrupting mutation was designed as the G>T transversion itself would disrupt the PAM. We co-transfected PE2 plasmids, the pegRNA/PE3-guide pair and hygromycin resistance PiggyBac plasmids in hepatocyte and colon organoids by electroporation. Similar to the previously described experiment, clonal survival and outgrowth after two weeks of nutlin-3 selection showed an efficient mutation induction in hepatocyte organoids, while the induction of mutations was less efficient in colon organoids (**figure 2D**). Out of 36 hygromycin selected hepatocyte organoids, prime editing induced homozygous R249S mutations in 35 clones (97.2%), while a heterozygous mutation was observed in 1 clone (2.8%) (**figure 2E and F**). Editing efficiencies in colon organoids were significantly lower, 8 organoids contained heterozygous mutations (22.2%) while the other 28 remained wild type (77.8%) (**figure 2E**). Thus, prime editing induced mutations in 25% of the intestinal organoids, yet prime editing was far more efficient in hepatocytes on this target.

Next, we aimed to construct five additional mutations that are commonly found in TP53 (**supplementary figure 2A**). Only the pegRNA/PE3-guide pair designed for the induction of TP53-C176F resulted in clones capable of surviving nutlin-3 selection whereas the other pairs did not (**supplementary figure 2B**). Manual picking of these clones followed by Sanger sequencing showed correct homozygous introduction of the C176F (c.527 G>T) mutation in the TP53 gene including the designed PAM disruption mutation (**supplementary figure 2C**). Sanger sequencing of 36 hygromycin resistant clones revealed only a single clone that contained a heterozygous C176F mutation, indicating a low editing efficiency at this target site (**supplementary figure 2D**). Additionally, we designed pegRNA/PE3-guide pairs

to generate mutations in APC, the gene that is often the first to be mutated in colorectal cancer (**supplementary figure 2A**). Mutations in APC can be selected in culture by the removal of the expansion medium components WNT and R-Spondin^{14,15}. Selection for APC mutants by removal of WNT and R-Spondin after transfection of two pegRNA/PE3-guide pairs resulted in outgrowth of a single clone (**supplementary figure 2E**). Interestingly, instead of the designed APC-R1450*(c.4348 C>T) mutation, Sanger sequencing revealed a homozygous duplication of the 37 nucleotides directly upstream of the single stranded nick introduced by the SpCas9 (H840A) (**supplementary figure 2F**). These results indicated that prime editing can induce mutations in intestinal and hepatocellular adult human stem cells at varying efficiencies but may yield undesired outcomes.

Prime editing versus adenine base editing

To directly compare prime editing to base editing we focused on the TP53-Y220C (c.659 A>G) mutation. As this is an A>G transition reaction, it can be modeled by both adenine base editing and prime editing. A sgRNA for adenine base editing could be designed with the A on position 4 of the sgRNA and position 1 in the editing window, whereas a PAM on the opposite site of the intended mutation could be exploited for prime editing (**figure 2F**). We co-transfected either prime editing- or base editing-constructs with the hygromycin resistance PiggyBac system into colon organoids. To compare editing efficiency of adenine base editing versus prime editing, we Sanger-sequenced 36 hygromycin resistant colon organoid clones from both transfections. Adenine base editing resulted in correct homozygous Y220C induction in 50% of the clones and an additional 7 clones (19.6%) that harbored a correct heterozygous mutation (**figure 2G**). A further 7 clones (19.6%) had either undergone correct homozygous or heterozygous mutation induction but also harbored an additional A>G transition of the A on position 7 sgRNA (position 4 of the editing window), resulting in the unintended E221G mutation on top of Y220C (**supplementary figure 1B**). Prime editing was less efficient on this target as we observed 8 clones (22.2%) with homozygous and 2 clones (5.6%) with heterozygous mutation induction. Out of 36 clones only 1 clone (2.8%) harbored an unintended editing outcome underscoring previous observations that, compared to prime editing, base editing is more efficient but the application can be limited by additional editable residues within the editing window.

**Figure 2: Prime editing enables generation of oncogenic mutations in organoids.**

(A) Strategy to generate TP53 mutated human organoids. **(B)** Brightfield images of prime editing experiments targeting the TP53-R175H and TP53-R249S mutations compared to a negative scrambled sgRNA control and hygromycin resistance. **(C)** Sanger sequencing trace of selected clonal organoids harboring the TP53-R175H mutation compared to WT. **(D)** Prime editing efficiency on TP53-R175H and TP53-R249S as determined by Sanger sequencing on hygromycin resistant clones. **(E)** Sanger sequencing trace of selected clonal organoids harboring the TP53-R249S mutation compared to WT. **(F)** Sanger sequencing trace of selected clonal organoids harboring the TP53-Y220C mutation compared to WT. **(G)** Adenine base editing versus prime editing efficiency on the TP53-Y220C mutation as determined by Sanger sequencing of hygromycin selected clones. PAM's are shown in red and guide RNA sequences are shown in blue.

Repair of CFTR-F508del mutation using prime editing in intestinal organoids

Intestinal organoids are a suitable in vitro disease model of cystic fibrosis (CF) as fluid transport into the organoid lumen is fully dependent on the activity of the CFTR channel, stimulated by a rise in forskolin-induced intracellular cAMP levels. Wild-type organoids show a forskolin induced swelling (FIS) response whereas organoids derived from people with cystic fibrosis, expressing less functional CFTR protein, show a strongly reduced FIS response¹⁹. This in vitro assay enables the prediction of in vivo drug response and is clinically applied to tailor treatment for individuals with CF in the Netherlands²⁰. Previously we have shown that we can use this FIS-response as a direct functional readout for repair of the CFTR gene in organoids derived from CF patients, both by base editing and by classical CRISPR-mediated homology-dependent repair (HDR)^{12,21}. The most common CFTR mutation, F508del cannot be repaired by base editors. Although CRISPR/Cas9-mediated HDR has been used to repair this mutation in organoids, editing efficiency was low²¹. As such, we pursued prime editing-mediated repair of the CFTR-F508del mutation, by transfecting intestinal CF organoids carrying the homozygous CFTR- F508del mutation with pegRNA/PE3-guide pairs (**figure 3**). Forskolin treatment two weeks after electroporation showed a swelling response in a single transfected organoid (**figure 3A and 3B**). PCR amplification of the target site, followed by sub-cloning and Sanger sequencing revealed heterozygous repair of the CFTR-F508del mutation in this selected clone (**figure 3C**). We tried to further optimize prime editing by designing additional pegRNA/PE3-guide pairs with varying RT and PBS lengths and distance between the pegRNA and PE3-guide as these variables greatly impact editing efficiencies¹³(**supplementary figure 3A**). We compared editing efficiencies of 8 different combinations of pegRNA/PE3-guide pairs (PBS length=14 or 15 nucleotides, RT length= 17 or 37 nucleotides, distance to PE3 nick, 63, 21 ,41 and 82) directly to conventional CRISPR/Cas9-mediated HDR by counting forskolin-responsive organoids derived from two donors (**supplementary figure 3B**). CFTR-F508del repair by CRISPR/Cas9-mediated HDR resulted in 108 and 124 FIS responsive clones depending on the donor while prime editing never resulted in more than 4 repaired organoids, indicating low prime editing efficiencies at this target site (**figure 3D and supplementary figure 3B**). No significant differences on the number of repaired clones were observed between the two donors. Repaired clonal organoid lines generated by prime editing and CRISPR/Cas9-mediated HDR exhibited FIS at WT levels or higher, indicating complete functional repair of CFTR function in these organoids. As expected, unrepairsed clones did not respond to forskolin (**figure 3E, F and G**). Sanger sequencing followed by deconvolution of the Sanger traces of 2 additional prime edited clones and one clone repaired by CRISPR/Cas9-mediated HDR showed correct heterozygous repair of the mutation in one prime editing clone. However, the second clone as well as the clone repaired by HDR contained a small indel at the repair site in the second allele (**supplementary figure 3C**). These results indicated that, even though efficiencies are low and undesired outcomes may occur, prime editing can repair the CFTR-F508del mutation in patient-derived intestinal organoids.

Evaluating CRISPR-based prime editing for cancer modeling and CFTR repair in organoids

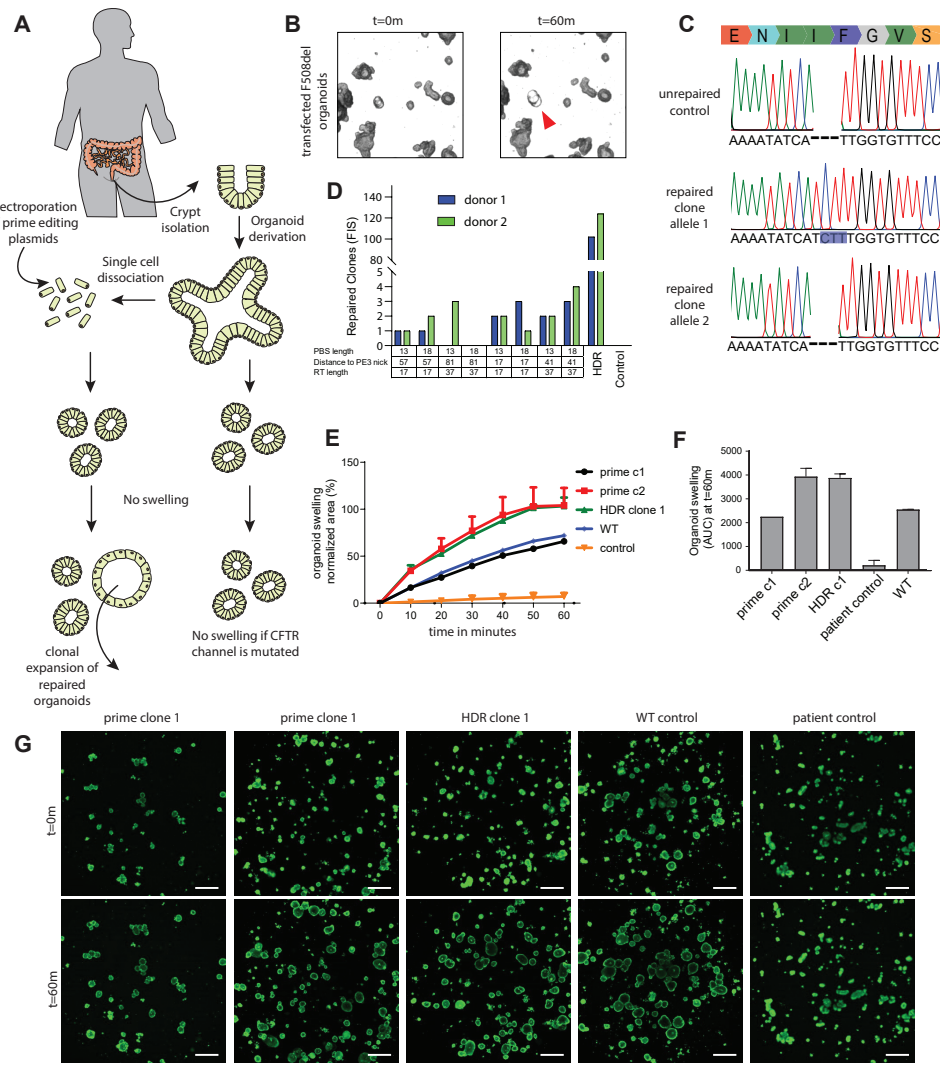


Figure 3: Functional repair of the CFTR-F508del mutation in patient derived intestinal organoids.

(A) Experimental design of prime editing-mediated repair of CFTR mutations in human intestinal organoids. **(B)** Transfected CFTR-F508del organoids before ($t=0$) and after ($t=60\text{m}$) addition of forskolin. Functionally repaired organoid indicated with red arrow. **(C)** Sanger sequencing traces of both alleles of a functionally selected CFTR-F508del organoid line compared to unrepairs control organoids. Blue box shows the prime editing induced insertion. **(D)** Prime editing efficiencies for the repair of the CFTR-F508 del mutation in two donors as measured by FIS reactive organoids compared to CRISPR/Cas9-mediated HDR and a negative scrambled sgRNA control. **(E)** Per well the total organoid area (xy plane in μm^2) increase relative to $t = 0$ (set to 100%) of forskolin treatment was quantified ($n = 3$). **(F)** FIS as the absolute area under the curve (AUC) ($t = 60\text{ min}$; baseline, 100%), mean \pm SD; $n = 3$, * $p < 0.001$, compared to the corrected organoid clones and the WT organoid sample. **(G)** Confocal images of calcein-green-stained patient-derived intestinal organoids before and after 60 min. stimulation with forskolin (scale bars, 200 μm).

Comparison of CFTR-R785* repair by prime editing versus repair by base editing

To directly compare prime editing to base editing, we focused on the repair of the CFTR-R785* mutation. Previously, we have shown that this mutation is reparable in patient-derived intestinal organoids with an editing efficiency of ~9% while HDR efficiency was below 2%¹². We designed eight pairs of pegRNA/PE3-guides with varying PBS (13 or 18), RT (27 or 30) lengths and different distances to the PE3 nick (64, 21, 43 and 82) to find optimal prime editing conditions (**supplementary figure 4A**). To assess prime editing efficiencies, we transfected CFTR-R785* organoids with a PE2-P2A-GFP plasmid together with our eight pegRNA/PE3-guide pairs in duplicates and selected transfected cells by FACS sorting (**supplementary figure 4B**). Two weeks after FACS sorting, forskolin-responsive clones were observed and counted (**figure 4A**). Most prime editing conditions resulted in FIS responsive clones, although editing efficiencies differed greatly (between 0 and 5.7% repaired clones) (**figure 4B and supplementary figure 4B**). We then compared these editing efficiencies with base editing and CRISPR/Cas9-mediated HDR, using previously established reagents¹². Forskolin treatment revealed an editing efficiency of 9.1% corrected organoids by ABE and 1.22% by CRISPR/Cas9-mediated HDR (**figure 4A and supplementary figure 4B**). Repaired clonally expanded organoid lines generated by prime editing and base editing exhibited a forskolin response similar to WT levels, indicating complete repair of CFTR function in these organoids (**figure 4C, D and E**). Sanger sequencing of three repaired organoid lines showed that two out of three clones repaired by prime editing and the ABE clone underwent correct repair of the CFTR-R785* mutation on a single allele while the second allele remained undamaged (**figure 4F and supplementary figure 4C**). The third prime edited clone as well as the HDR-repaired clone contained a small indel at the repair site on the second allele indicating DNA damage (**supplementary figure 4C**).

These results again underscore that the current version of adenine base editing is superior to prime editing in both safety and efficiency if the mutation is targetable by adenine base editing and no additional editable residues reside within the editing window¹². However, if a mutation is not reparable by base editing, prime editing may be a suitable technique. The most recent version of the CFTR2 database contains 442 mutations that have been described in cystic fibrosis patients (<http://cftr2.org>). Out of these 442 mutations, 98 have a suitable PAM (Either NGG for SpCas9 or NGN for xCas9 and SpCas9-NG for adenine base editing)^{22,23}. A further 37 can be repaired by cytidine base editing. Thus, 30.5% of the mutations in CFTR can theoretically be repaired by base editors (**figure 4G**). As prime editors are able to introduce DNA up to a size of 30bp into the genome at the target site, in principle 419 out of 442 mutations (95%) can be repaired by this technique. This makes prime editing an interesting technique for CFTR repair.

Evaluating CRISPR-based prime editing for cancer modeling and CFTR repair in organoids

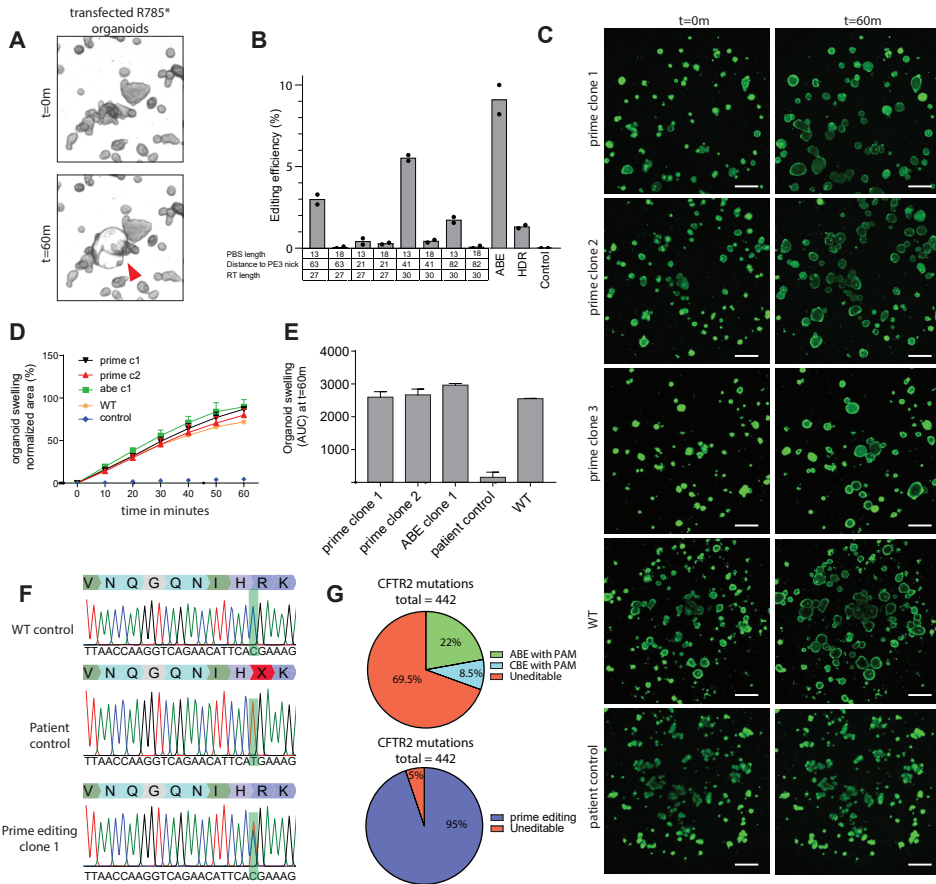


Figure 4: Functional repair of the CFTR-R785* mutation in patient derived intestinal organoids.

(A) Transfected CFTR-R785* organoids before (t=0) and after (t=60m) addition of forskolin. Functionally repaired organoid indicated with red arrow. **(B)** Prime editing efficiencies for the repair of the CFTR-R785* mutation as measured by FIS reactive organoids compared to adenine base editing, CRISPR/Cas9-mediated HDR and a negative scrambled sgRNA control. **(C)** Confocal images of calcein-green-stained patient-derived intestinal organoids before and after 60 min. stimulation with forskolin (scale bars, 200 μ m). **(D)** Per well the total organoid area (xy plane in μ m 2) increase relative to t = 0 (set to 100%) of forskolin treatment was quantified ($n = 3$). **(E)** FIS as the absolute area under the curve (AUC) (t = 60 min; baseline, 100%), mean \pm SD; $n = 3$, * $p < 0.001$, compared to the corrected organoid clones and the WT organoid sample. **(F)** Sanger sequencing traces of both alleles of a functionally selected CFTR-F508del organoid line compared to unrepairs control organoids. Blue box shows the prime editing induced insertion. **(G)** Pie chart showing mutations in CFTR that can be targeted by cytosine and adenine base editing compared to prime editing.

Prime editing does not result in genome-wide off-target effects.

To explore the safety of prime editing in the repair of CFTR we performed an off-target analysis by whole-genome sequencing (WGS). We first generated a clonal line from our bulk CFTR-R785* colon organoid line, to avoid pre-existing sequence heterogeneity in our organoid line. We transfected this clonal organoid line with pegRNA/PE3-guide pairs and the PE2 plasmids. We then picked 5 repaired organoid lines as indicated by FIS, 2 weeks after transfection. As a control, we picked two non-repaired organoids. All lines were expanded for two weeks to generate a sufficient amount for WGS (**figure 5A**). WGS revealed no significant genome wide differences in either single nucleotide variants (SNV's) (**figure 5B**) or indels (**figure 5C**). Observed SNV's were uniformly scattered across all chromosomes, without bias towards any specific genomic region (**supplementary figure 5**) As the sample size in our study was small and differences in organoids culturing and propagation of individual clones are difficult to control for, we used a mutational signature analysis²⁴ to study base changes that could have been caused independent of cognate sgRNA binding of either the pegRNA or the PE3-guide. Mutational signature analysis did not show a difference in mutational patterns supporting the safety of prime editing (Cosine similarity = 0.876) (**figure 5D**). Interestingly, even though we selected organoid for WGS by FIS responsiveness, we again observed indels around the target site in repaired organoid lines. Prime-editing resulted in correct, heterozygous repair in 3 out of 5 lines, but the other two clones carried a heterozygous 9bp insertion downstream of the R785* mutation and a heterozygous 13bp deletion directly upstream of the R785* mutation respectively (**figure 5E**). Overall, these results indicated that prime editing does not induce genome-wide off-target changes. However, performing Sanger sequencing around the target area remains key for determining correct mutational repair.

Evaluating CRISPR-based prime editing for cancer modeling and CFTR repair in organoids

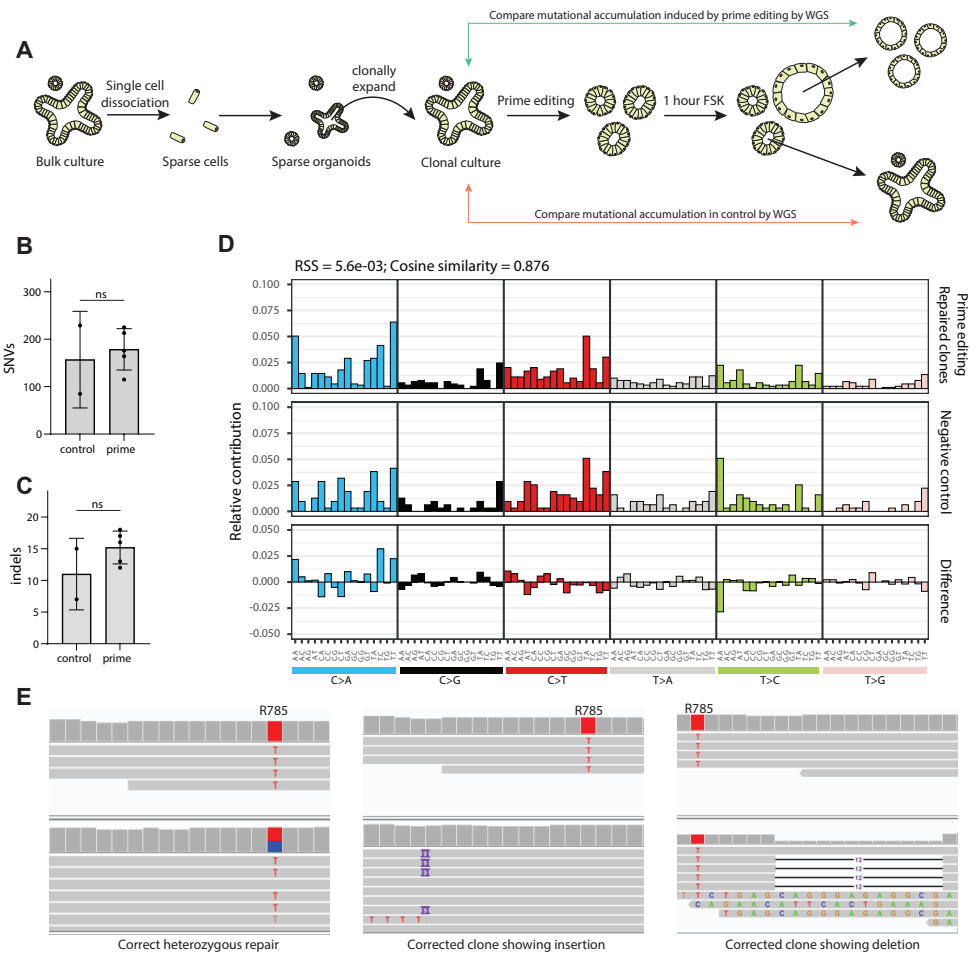


Figure 5: Genome-wide off-target analysis of prime-editing

(A) Schematic overview of the strategy to determine genome-wide off-target effects of prime editing. **(B)** Total amount of genome-wide SNVs as determined by whole genome sequencing. **(C)** Total amount of genome-wide indels as determined by whole genome sequencing. **(D)** Mutational signature analysis by relative contribution of context-dependent mutation types in two control and five prime-edited clonal organoid lines. **(E)** IGV representation of a correct heterozygous prime editing-mediated mutation repair, a clone harboring an insertion downstream of the target site and a clone with a deletion upstream of the target site.

DISCUSSION

In this study we first explore the use of prime editing for the modeling of oncogenic mutations in both hepatocyte and intestinal organoids. Our data imply that prime editing efficiencies differ greatly between organoid tissue types. Anzalone et al described similar results in the original description of prime editing where efficiencies differed greatly between cell-lines¹³. These differences between organs are important to keep in mind when designing disease modeling studies *in vitro* and *in vivo*. Moreover, we tested a total of 10 different target sequences (8 in TP53 and 2 in ACP). Out of those ten targets only 4 resulted in correct modeling of the mutation in organoids with varying efficiency. This varying efficiency of prime editing has been shown previously in organoids²⁵ and in a wide variety of targets in HEK293T cells²⁶ and is striking as SpCas9 in general exhibits robust editing over all targets harboring a suitable NGG PAM²⁷. Further development of prime editing could potentially resolve these varying editing efficiencies and might increase the robustness of the technique.

Even though correct integration of the desired edits was achieved on a variety of targets, we also uncovered undesired edits, as has been seen before in mice²⁸. Unintended indel formation around the target site was often seen on one allele, and sometimes even on both alleles. This may be explained by the need to generate a second nick on the opposing strand close to the initial nick by the PE2 machinery. The use of two sgRNAs that nick opposing strands is known to generate indels and is even often used to increase specificity of CRISPR/Cas9-mediated genome engineering²⁹. Further optimization of the prime editing fusion protein may aim to render the generation of a second nick unnecessary and might therefore decrease unintended indel formation.

Over the past years, base editing plasmids have undergone several rounds of optimization turning them into efficient genome editors^{30,31}. Recently, similar efforts are being undertaken to increase effectiveness of prime editing. NLS optimization of the PE2 fusion protein has been shown to increase editing efficiencies in adult mice *in vivo*³². Moreover, the use of two pegRNAs in trans has been shown to increase prime editing efficiency in plants³³. Utilization of these strategies might increase the effectiveness of prime editing in human cell models. Finally, as has been previously shown by Schene et al, prime editing does not introduce unwanted genome-wide off-target effects in the repair of CFTR and thus seems a safe strategy for gene repair.

In our hands, base editors are superior, both in terms of efficiency and of specificity in generating only the desired mutation¹². However, if the desired edit cannot be generated by a base editor, for instance if it regards an indel or non-transition base change, prime editing is a valuable alternative to CRISPR/Cas9-mediated HDR. Thus, prime editing is a versatile tool that can be used for disease modeling and clinical repair of most types of disease-causing mutations in human adult stem cells. Yet, it will require further improvement to allow widespread use as a technique for mutational modeling and for gene repair.

DATA AVAILABILITY

The whole genome sequencing data from this publication have been deposited to the European Genome-Phenome Archive (<https://ega-archive.org/>) and assigned the identifier: EGAS00001005358. All software tools used for sequencing data analysis can be found online at: <https://github.com/ToolsVanBox>.

ACKNOWLEDGEMENTS

This work was supported by the NOW building blocks of life project: Cell dynamics within lung and intestinal organoids (737.016.009) and CRUK Specificancer (C6307/A29058).

AUTHOR CONTRIBUTIONS

Conceptualization, M.H.G. and H.C.; Prime editing optimization in organoids, M.H.G, L.C and C.P.M.; Fluid secretion & Biochemical Assays, E.D.P.; Cloning of Prime editing plasmids, M.H.G, L.C and A.A.R.; Functional selection of oncogenic mutations in organoids, M.H.G and M.B.; Prime editing efficiency determination, M.H.G, E.D.P and J.E.B; WGS analysis, R.O and R. v. B. Writing original draft M.H.G and H.C.; Supervision, R.v.B, J.M.B and H.C.

DECLARATION OF INTERESTS

J.M.B. is an inventor on (a) patent(s) related to the FIS assay and received financial royalties from 2017 onward. J.M.B. reports receiving (a) research grant(s) and consultancy fees from various industries, including Vertex Pharmaceuticals, Proteostasis Therapeutics, Eloxx Pharmaceuticals, Teva Pharmaceutical Industries, and Galapagos outside the submitted work. H.C. holds several patents on organoid technology. Their application numbers are as follows: PCT/NL2008/050543, WO2009/022907; PCT/NL2010/000017, WO2010/090513; PCT/IB2011/002167, WO2012/014076; PCT/IB2012/052950, WO2012/168930; PCT/EP2015/060815, WO2015/173425; PCT/EP2015/077990, WO2016/083613; PCT/EP2015/077988, WO2016/083612; PCT/EP2017/054797, WO2017/149025; PCT/EP2017/065101, WO2017/220586; PCT/EP2018/086716; and GB1819224.5.

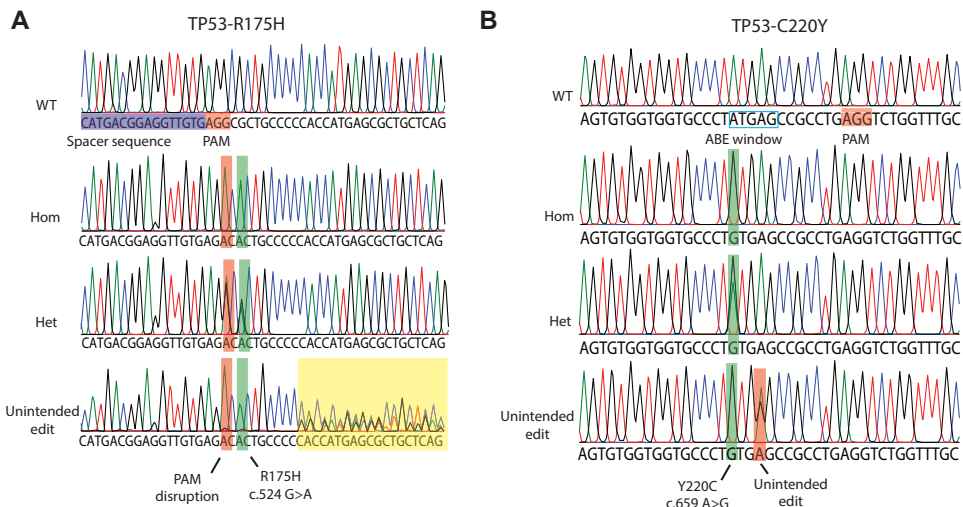
REFERENCES

1. Jinek, M. et al. A Programmable Dual-RNA–Guided DNA endonuclease in adaptive bacterial immunity. *Science* (80-). 337, 816–822 (2012).
2. Mali, P. et al. RNA-Guided Human Genome Engineering via Cas9. *Science* (80-). 328, 823–827 (2013).
3. Cong, L. et al. Multiplex genome engineering using CRISPR/Cas systems. *Science* 339, 819–23 (2013).
4. Cho, S. W. et al. Analysis of off-target effects of CRISPR/Cas-derived RNA-guided endonucleases and nickases. *Genome Res.* 24, 132–141 (2014).
5. Fu, Y. et al. High-frequency off-target mutagenesis induced by CRISPR-Cas nucleases in human cells. *Nat. Biotechnol.* 31, 822–826 (2013).
6. Kosicki, M., Tomberg, K. & Bradley, A. Repair of double-strand breaks induced by CRISPR–Cas9 leads to large deletions and complex rearrangements. *Nat. Biotechnol.* 36, (2018).
7. Pattanayak, V. et al. High-throughput profiling of off-target DNA cleavage reveals RNA-programmed Cas9 nuclease specificity. *Nat. Biotechnol.* 31, 839–843 (2013).
8. Komor, A. C., Kim, Y. B., Packer, M. S., Zuris, J. A. & Liu, D. R. Programmable editing of a target base in genomic DNA without double-stranded DNA cleavage. *Nature* 533, 420–424 (2016).
9. Gaudelli, N. M. et al. Programmable base editing of T to G C in genomic DNA without DNA cleavage. *Nature* 551, 464–471 (2017).
10. Pavlov, Y. I. et al. Cytosine, but not adenine, base editors induce genome-wide off-target mutations in rice. *Science* (80-). 368, 647–656 (2019).
11. Zuo, E. et al. Cytosine base editor generates substantial off-target single-nucleotide variants in mouse embryos. *Science* (80-). 292, eaav9973 (2019).
12. Geurts, M. H. et al. CRISPR-Based Adenine Editors Correct Nonsense Mutations in a Cystic Fibrosis Organoid Biobank. *Cell Stem Cell* 26, 503–510.e7 (2020).
13. Anzalone, A. V. et al. Search-and-replace genome editing without double-strand breaks or donor DNA. *Nature* 576, 149–157 (2019).
14. Matano, M. et al. Modeling colorectal cancer using CRISPR–Cas9–mediated engineering of human intestinal organoids. *Nat. Med.* 21, 256–262 (2015).
15. Drost, J. et al. Sequential cancer mutations in cultured human intestinal stem cells. *Nature* 521, 43–47 (2015).
16. Forbes, S. A. et al. COSMIC: Somatic cancer genetics at high-resolution. *Nucleic Acids Res.* 45, D777–D783 (2017).
17. Chow, R. D. & Chen, S. pegFinder: A pegRNA designer for CRISPR prime editing. *bioRxiv* 3825, 2020.05.06.081612 (2020).
18. Aguilar, F., Hussain, S. P. & Cerutti, P. Aflatoxin B1 induces the transversion of G->T in codon 249 of the p53 tumor suppressor gene in human hepatocytes. *Proc. Natl. Acad. Sci.* 90, 8586–8590 (1993).
19. Dekkers, J. F. et al. A functional CFTR assay using primary cystic fibrosis intestinal organoids. *Nat. Med.* 19, 939–945 (2013).
20. Berkers, G. et al. Rectal Organoids Enable Personalized Treatment of Cystic Fibrosis. *Cell Rep.* 26, 1701–1708.e3 (2019).
21. Schwank, G. et al. Functional repair of CFTR by CRISPR/Cas9 in intestinal stem cell organoids of cystic fibrosis patients. *Cell Stem Cell* 13, 653–658 (2013).
22. Noda, T. et al. Engineered CRISPR-Cas9 nuclease with expanded targeting space. *Science* (80-). 361, 1259–1262 (2018).
23. Hu, J. H. et al. Evolved Cas9 variants with broad PAM compatibility and high DNA specificity. *Nature* 556, 57–63 (2018).

24. Alexandrov, L. B. et al. Signatures of mutational processes in human cancer. *Nature* 500, 415–21 (2013).
25. Schene, I. F. et al. Prime editing for functional repair in patient-derived disease models. *Nat. Commun.* 11, 1–8 (2020).
26. Kim, H. K. et al. Predicting the efficiency of prime editing guide RNAs in human cells. *Nat. Biotechnol.* 39, 198–206 (2021).
27. Kim, H. K. et al. High-throughput analysis of the activities of xCas9, SpCas9-NG and SpCas9 at matched and mismatched target sequences in human cells. *Nat. Biomed. Eng.* 4, 111–124 (2020).
28. Aida, T. et al. Prime editing primarily induces undesired outcomes in mice. *bioRxiv* (2020).
29. Ran, F. A. et al. Double nicking by RNA-guided CRISPR Cas9 for enhanced genome editing specificity. *Cell* 154, 1380–9 (2013).
30. Koblan, L. W. et al. Improving cytidine and adenine base editors by expression optimization and ancestral reconstruction. *Nat. Biotechnol.* 36, 843–848 (2018).
31. Zafra, M. P. et al. Optimized base editors enable efficient editing in cells, organoids and mice. *Nat. Biotechnol.* 36, 888–896 (2018).
32. Liu, P. et al. Improved prime editors enable pathogenic allele correction and cancer modelling in adult mice. *Nat. Commun.* 12, (2021).
33. Lin, Q. et al. High-efficiency prime editing with optimized, paired pegRNAs in plants. *Nat. Biotechnol.* (2021) doi:10.1038/s41587-021-00868-w.
34. Sato, T. et al. Long-term Expansion of Epithelial Organoids From Human Colon, Adenoma, Adenocarcinoma, and Barrett's Epithelium. *Gastroenterology* 141, 1762–1772 (2011).
35. Van De Wetering, M. et al. Prospective derivation of a living organoid biobank of colorectal cancer patients. *Cell* 161, 933–945 (2015).
36. Hu, H. et al. Long-Term Expansion of Functional Mouse and Human Hepatocytes as 3D Organoids. *Cell* 175, 1591–1606.e19 (2018).
37. Fujii, M., Matano, M., Nanki, K. & Sato, T. Efficient genetic engineering of human intestinal organoids using electroporation. *Nat. Protoc.* 10, 1474–1485 (2015).
38. Boj, S. F. et al. Forskolin-induced Swelling in Intestinal Organoids: An In Vitro Assay for Assessing Drug Response in Cystic Fibrosis Patients. *J. Vis. Exp.* 1–12 (2017) doi:10.3791/55159.
39. Vonk, A. M. et al. Protocol for Application, Standardization and Validation of the Forskolin-Induced Swelling Assay in Cystic Fibrosis Human Colon Organoids. *STAR Protoc.* 1, 100019 (2020).
40. Andersson-Rolf, A. et al. One-step generation of conditional and reversible gene knockouts. *Nat. Methods* 14, 287–289 (2017).
41. Li, H. & Durbin, R. Fast and accurate long-read alignment with Burrows-Wheeler transform. *Bioinformatics* 26, 589–595 (2010).
42. Depristo, M. A. et al. A framework for variation discovery and genotyping using next-generation DNA sequencing data. *Nat. Genet.* 43, 491–501 (2011).
43. Blokzijl, F. et al. Tissue-specific mutation accumulation in human adult stem cells during life. *Nature* 538, 260–264 (2016).
44. Blokzijl, F., Janssen, R., van Boxtel, R. & Cuppen, E. MutationalPatterns: Comprehensive genome-wide analysis of mutational processes. *Genome Med.* 10, 1–11 (2018).
45. Jager, M. et al. Measuring mutation accumulation in single human adult stem cells by whole-genome sequencing of organoid cultures. *Nat. Protoc.* 13, 59–78 (2018).

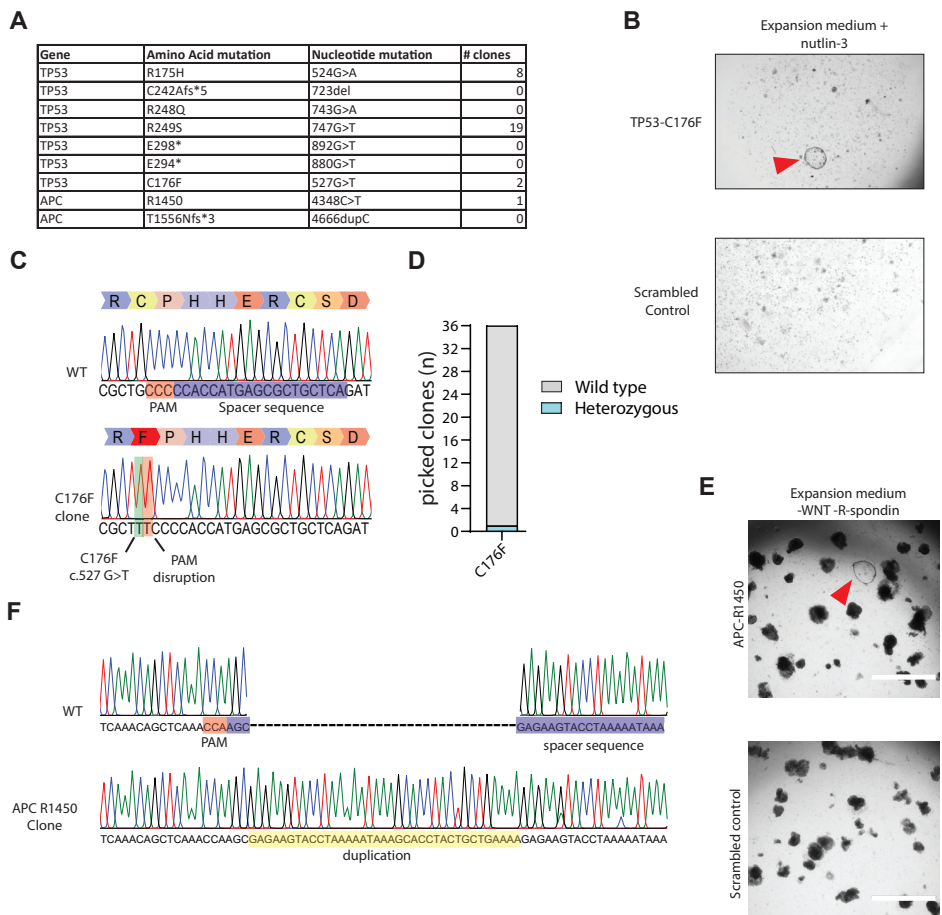
SUPPLEMENTARY INFORMATION

SUPPLEMENTARY FIGURES

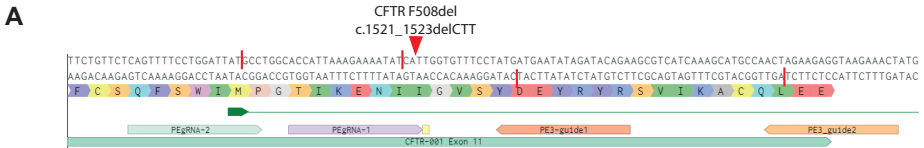


Supplementary Figure 1: Unintended editing outcomes of prime editing and adenine base editing.

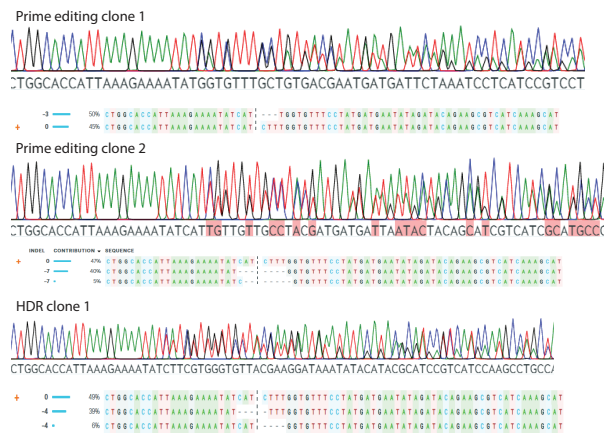
(A) Sanger traces showing editing outcome of prime editing in three prime-edited clones showing homozygous mutation induction, heterozygous mutation induction, and unintended editing outcomes. (B) Sanger traces showing editing outcome of base editing in three base-edited clones showing homozygous mutation induction, heterozygous mutation induction, and unintended editing outcomes.

**Supplementary Figure 2: Modeling of tumorigenic mutations in intestinal organoids by prime editing.**

(A) Mutations targeted for tumor modeling in organoids in TP53 and APC and the number of observed clones as observed after either selection with both the addition of nutlin-3 (TP53) or removal of wnt and Rspo1 (APC) from the culture medium. **(B)** Bright-field images of prime-editing experiments targeting the TP53-C176F compared with a negative-scrambled sgRNA control. **(C)** Sanger sequencing trace of selected clonal organoids harboring the TP53-C176F mutation compared with WT. **(D)** Prime-editing efficiency on TP53-C176F as measured by Sanger sequencing of 36 hygromycin-resistant clones. **(E)** Bright-field images of prime-editing experiments targeting the APC R1450* mutation compared with a negative-scrambled sgRNA control (Scale bar: = 2,000 μ m). **(F)** Sanger sequencing trace of selected APC R1450* clone. Insertion is shown in yellow, protospacer adjacent motif is shown in red, and spacer sequence is shown in blue.

**B**

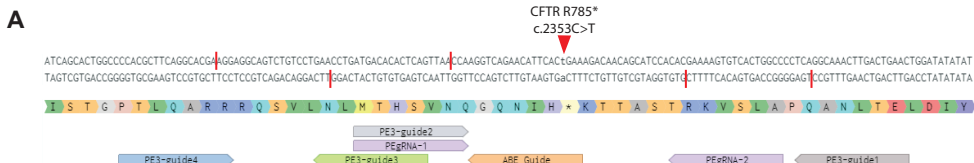
Transfection type	pegRNA	PE3-guide	PBS length	Distance PE3 nick	RT Length	# clones donor 1	# clones donor 2
PE3	pegRNA-1	PE3-guide2		13	57	17	1 1
PE3	pegRNA-1	PE3-guide2		18	57	17	1 2
PE3	pegRNA-2	PE3-guide2		13	81	37	0 3
PE3	pegRNA-2	PE3-guide2		18	81	37	0 0
PE3	pegRNA-1	PE3-guide1		13	17	17	2 2
PE3	pegRNA-1	PE3-guide1		18	17	17	3 1
PE3	pegRNA-2	PE3-guide1		13	41	37	2 2
PE3	pegRNA-2	PE3-guide1		18	41	37	3 4
Cas9-HDR	X	X	X	X	X	102	124
Negative control	X	X	X	X	X	0	0

C

Supplementary Figure 3: CFTR-F508del prime editing in intestinal organoids.

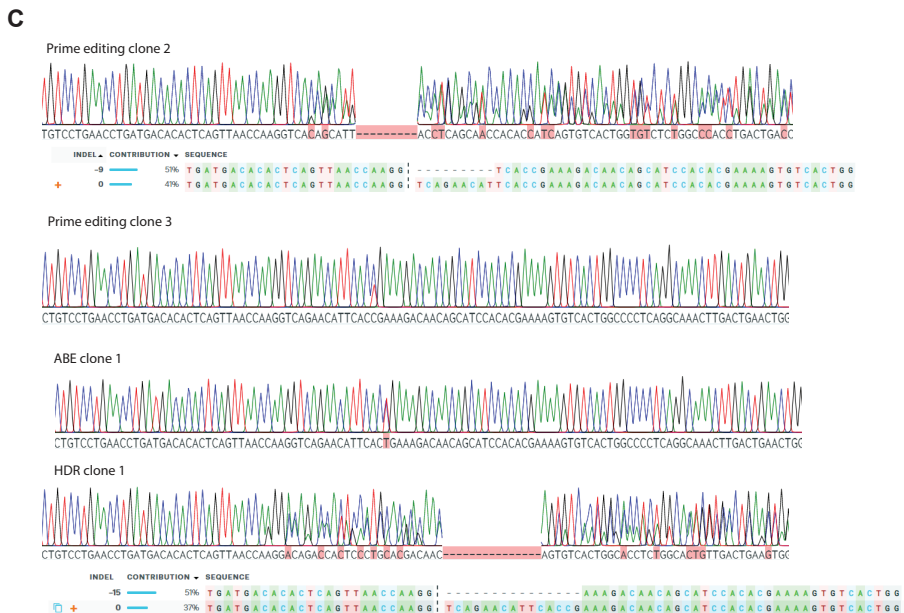
(A) Guide-RNA design for the repair of the CFTR-F508del mutation in human intestinal organoids. Red bars show the nickase sites of the guide sequences and the red arrow shows the mutation site in the DNA of organoids derived from a person with cystic fibrosis. **(B)** pegRNA/PE3-guide pairs used in transfection for the repair of the CFTR-F508del mutation compared with CRISPR/Cas9-mediated homology-dependent repair and a negative scrambled sgRNA control. Primer-binding site length, distance to PE3 nick, and reverse transcriptase lengths are shown, as well as the number of repaired clones for two organoid lines derived from individual donors. **(C)** Sanger sequencing traces and deconvoluted alleles of two additional prime-editing clones and one homology-dependent repair clone that had been selected for by forskolin-induced swelling after transfection.

Evaluating CRISPR-based prime editing for cancer modeling and CFTR repair in organoids



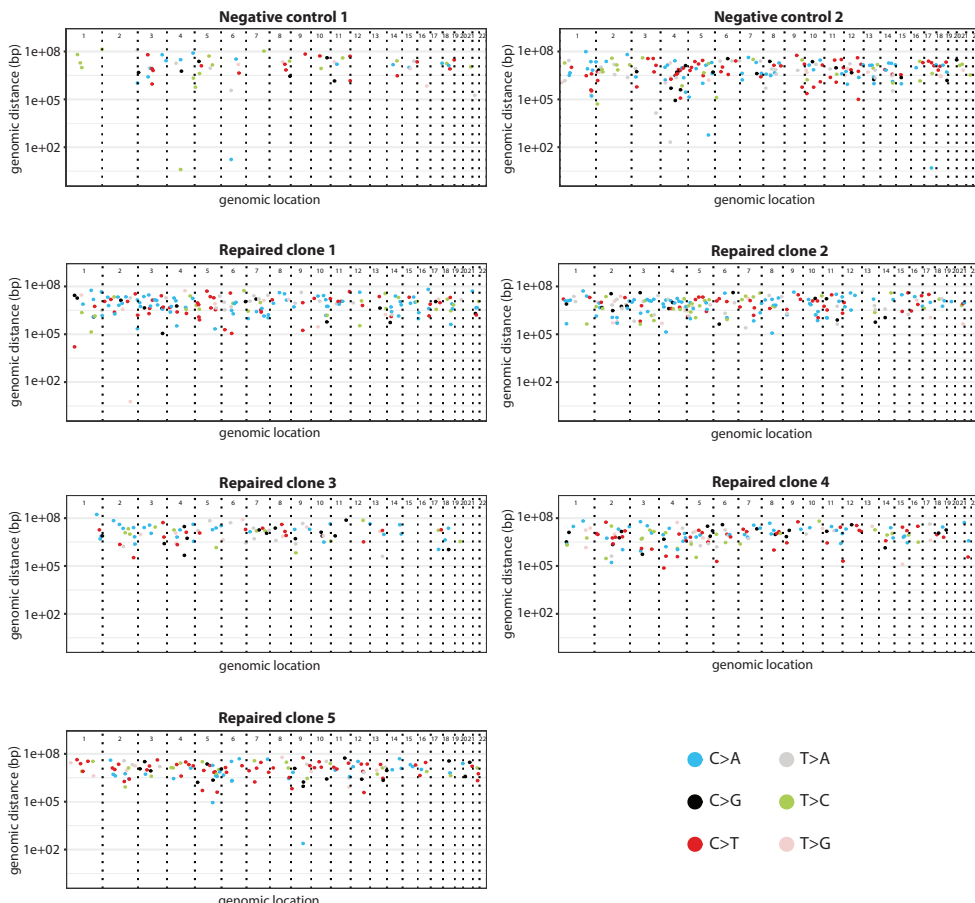
B

Transfection type	pegRNA	PE3-guide	PBS length	Distance PE3 nick	RT Length	Mean editing efficiency
PE3	pegRNA-1	PE3-guide2	13	63	27	2.90%
PE3	pegRNA-1	PE3-guide2	18	63	27	0.05%
PE3	pegRNA-1	PE3-guide2	13	21	27	0.42%
PE3	pegRNA-1	PE3-guide2	18	21	27	0.29%
PE3	pegRNA-1	PE3-guide1	13	41	30	5.53%
PE3	pegRNA-1	PE3-guide1	18	41	30	0.43%
PE3	pegRNA-2	PE3-guide1	13	82	30	1.73%
PE3	pegRNA-2	PE3-guide1	18	82	30	0.075%
ABE	X	X	X	X	X	9.1%
Cas9-HDR	X	X	X	X	X	1.23%
Negative control	X	X	X	X	X	0



Supplementary Figure 4: CFTR-R785* prime editing in intestinal organoids.

(A) Guide-RNA design for the repair of the CFTR-R785* mutation in human intestinal organoids. Red bars show the kinase sites of the guide sequences and the red arrow shows the mutation site in the DNA of organoids derived from a person with cystic fibrosis. (B) pegRNA/PE3-guide pairs used in transfection for the repair of the CFTR-R785* mutation compared with adenine base editing, CRISPR/Cas9-mediated homology-dependent repair, and a negative scrambled sgRNA control. Primer-binding site length, distance to PE3 nick, and reverse transcriptase lengths are shown, as well as the mean editing efficiency. (C) Sanger sequencing traces and deconvoluted alleles of two additional prime-editing clones, one homology-dependent repair clone, and one clone repaired by adenine base editing that had been selected for by forskolin-induced swelling after transfection.



Supplementary Figure 5: Rainfall plots of prime-edited clones and negative controls.

Rainfall plots of prime editing repaired CFTR-R785* clonal organoid lines and their respective negative controls. Every identified mutation is indicated with a dot (color according to mutation type) and is ordered on the x-axis from chromosome 1 to chromosome 22. The y-axis shows the distance between each mutation and the one before it (the genomic distance) and is plotted on a log scale.

SUPPLEMENTARY TABLES

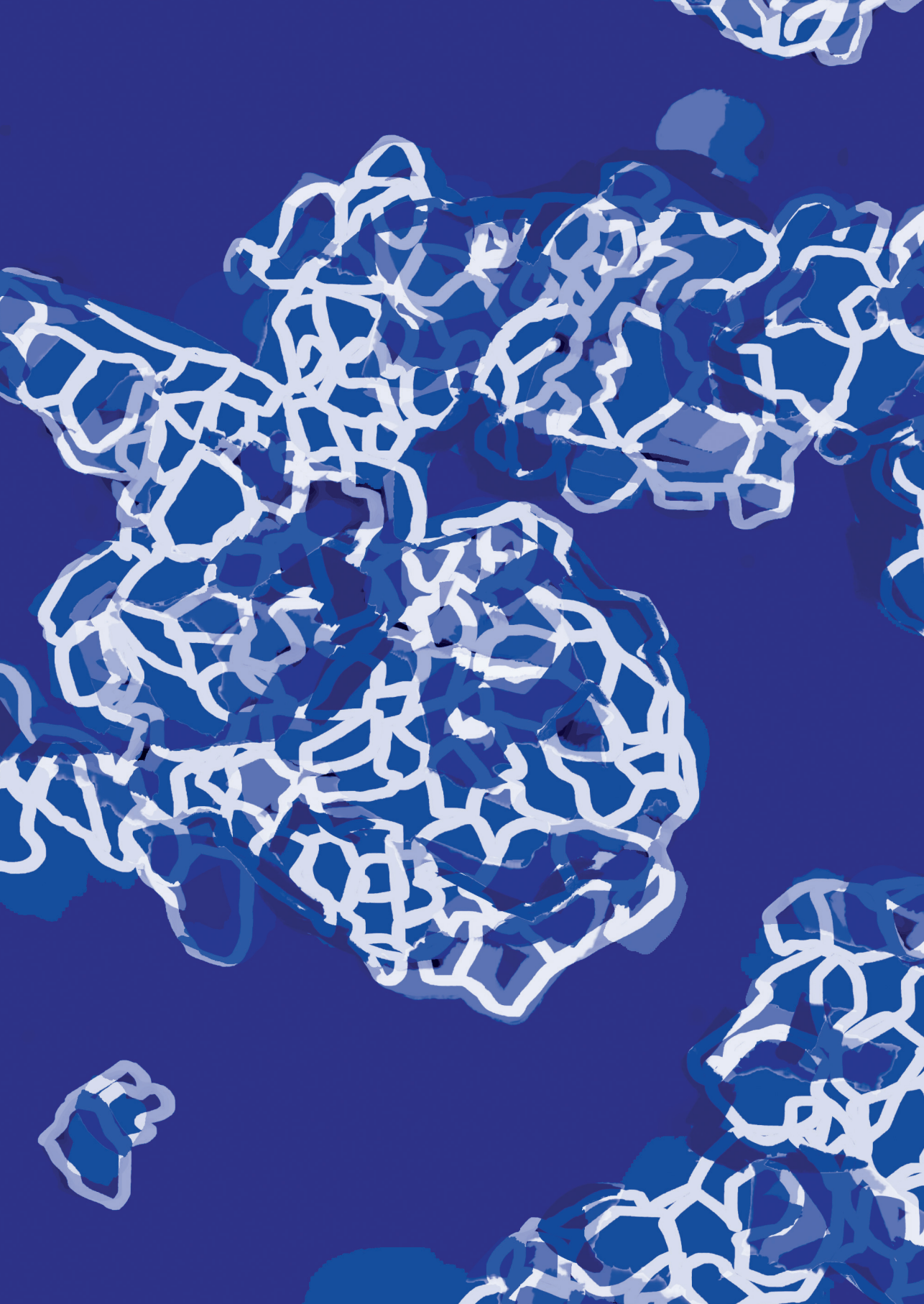
Guide type	Name	spacer	3'-extension
pegRNA	TP53-R175H	AGCACATGACGGAGTTGTG	GTCGGGGCAGGgttCAAACTTCCGTCATGT
pegRNA	TP53-C242Afs*5	CCGGTTCATGCCCATGC	GTAACAGTTCTGATGGGGGGCATGAAC
pegRNA	TP53-R248Q	CTTGCAATGGGGGATGAAC	GATGGGCTCTGGTCAATGCCCATGC
pegRNA	TP53-R249S	GCAATGGGGGATGAACGG	TGAGGATGGGactCCAGGGAGGACTAAAGCG
pegRNA	TP53-E298*	CCTCGCTTAGTCCTCG	GCTTACCACTAGCTgtCCAGGGAGGACTAAAGCG
pegRNA	TP53-E294*	AGAGAAATCTCCGAAAGAAAG	TGGTGAAGGCTaccctttTGGGAGATTG
pegRNA	TP53-C176*	CTGAGGAGCGCTATGGTGG	GtgAGGGCGCtttCCACCATGAGCGCTGCT
pegRNA	APC-R1450*	ATTTTAGGTACTTCCTGCT	AAACCAAAGtGAGAAAGTACCTAA
pegRNA	TP53-Y220C	CAGACCTCAGGGGCTATA	GGTGTTGCCCTGTGAGGCCCTGAG
pegRNA	APC-T1556Nfs*3	CATCATCTGAATCATCTAAC	GCAAGAAAAAAACTTATGATTCTGAAAAGGacatTATTAGATGATTCAAGATG
pegRNA	CFTR-F508del_1_PBS13	ACCATTAAGAAAAATATCAT	GAAAACACAAAAGGATGATACTTCTTAA
pegRNA	CFTR-F508del_1_PBS18	ACCATTAAGAAAAATATCAT	GAAAACACAAAAGGATGATACTTCTTAAATGGTG
pegRNA	CFTR-F508del_2_PBS13	CAGTTTCTGGATTATGCC	AAACACCAAAAGGATGATACTTCTTAAATGGTGCAGGCATAATCCAGGAAAC
pegRNA	CFTR-F508del_2_PBS18	CAGTTTCTGGATTATGCC	AAACACCAAAAGGATGATACTTCTTAAATGGTGCAGGCATAATCCAGGAAAC
pegRNA	CFTR-R785*-1_PBS13	ATGACACACTCAGTTAACCA	GTCCTTCGGTGAATGTTCTGACCTTGGTTAACCTGAGTGTGTCATC
pegRNA	CFTR-R785*-1_PBS18	ATGACACACTCAGTTAACCA	GTCCTTCGGTGAATGTTCTGACCTTGGTTAACCTGAGTGTGTCATC
pegRNA	CFTR-R785*-2_PBS13	GGCCAGTGTGACACTTTCGTG	ACATTACCGAAAGACAAAGACATCCACAGAAAAGTGTCACTGGCCC
pegRNA	CFTR-R785*-2_PBS18	GGCCAGTGTGACACTTTCGTG	ACATTACCGAAAGACAAAGACATCCACAGAAAAGTGTCACTGGCCC
PE3-guide	TP53-R175H-PE3	GCGGGGTGCCGGGGGGGTG	
PE3-guide	TP53-C242Afs*5-PE3	ACATGTTAAACAGTTCTGCA	
PE3-guide	TP53-R248Q-PE3	CtGGTTCATGCCCATGC	
PE3-guide	TP53-R249S-PE3	TGATGGTGAGGATGGGaCTC	
PE3-guide	TP53-E298*-PE3	CTTCACCACTAGCTgtCCC	

Guide type	Name	spacer	3'-extension
PE3-guide	TP53-E294*-PE3	GGTGAGGGCTTACCCCTTTCTTG	
PE3-guide	TP53-C176*-PE3	GCTGGTTGCCAGGGTCCCC	
PE3-guide	TP53-Y220C	AGTGGAAAGGAAATTGGCTG	
PE3-guide	APC-R1450*-PE3	ACTGCTAAAAAGAGAGAGAG	
PE3-guide	APC-T1556Nfs*3-PE3	CCAGTTAGGGAAAATGACAA	
PE3-guide	CFTR-F508del-PE3_1	TCTGTATCTATAATTCATCAT	
PE3-guide	CFTR-F508del-PE3_2	AGTTTCTTACCTCTTCTAGT	
PE3-guide	CFTR-R785*-PE3_1	GTTCAGTCAGTTGCCTGA	
PE3-guide	CFTR-R785*-PE3_2	ATGACACACTCAGTTAACCA	
PE3-guide	CFTR-R785*-PE3_3	CTGAGTGTGTCACTAGGGTC	
PE3-guide	CFTR-R785*-PE3_4	CCACGCTTCAGGGCACGAGG	
HDR-guide	CFTR-F508del_HDR	ACCATTAAGAAAAATATCAT	
HDR-guide	CFTR-R785*_HDR	TTCAgTGAATGTTCTGACCT	
ABE-guide	TP53-Y220C	CCTATGGGCCGCTGAGGTC	
ABE-guide	CFTR-R785*_ABE	TTCAgTGAATGTTCTGACCT	
CFTR-R785* HDR repair ssDNA template	ATCAGCGTGAATCAGGACTGGCCCCACGCTTACGGCACGAAGGGGAGTCGTGCTGAACCTGATGACACACTCAGTT AtCAGGCCCCCTACGGAAACTTCAACGATCCACACGAAAGTGTCACTGGCCCTCAGGAAACTTGAACCTGGATATAATTCAAAGAAGGTT		

Supplementary table 1: Constructed guide-RNA sequences.

Target	fw PCR primer	reverse PCR primer	primer for sequencing
TP53-R175H	CTGAGGTGTAGACGCCAACT	GACAACCCCTTAACCCCTC	CAGTACTCCCCCTGCCCTAAC
TP53-C176F	CTGAGGTGTAGACGCCAACT	GACAACCCCTTAACCCCTC	CAGTACTCCCCCTGCCCTAAC
TP53-R249S	TGGGACCTCTTAACCTGTGGCTT	TTCCTCTTGGCTGGGGAGGG	CCAGAAAGGACAAGGGGGTTTG
CFTR-F508del	TGGAGGCAAGTGAATCCCTGAGCGT	TCTGCTGGAGATAATGTCA	TGGAGGCAAAGTGAATCCTGAGCGT
CFTR-R785*	CGAAGAGGATTCTGATGAGC	TACTGCACCTCTTCCCACAG	TACTGCACCTCTTCCCACAG

Supplementary table 2: Primers used for PCR amplification and sequencing.





GENERAL DISCUSSION

Eyleen de Poel, Jeffrey M. Beekman, Cornelis K. van der Ent

In this thesis, we explored the role of intestinal organoids for individualized health applications and drug development in the context of cystic fibrosis. This patient-derived primary stem cell culture proved optimally suited for connecting both these domains, which up until now relied on technically distinct approaches. The association we found between organoid forskolin induced swelling (FIS) and clinical disease is relevant for individual clinical predictions but this direct clinical translatability also strengthens the validity of this model system for CF drug development. The established FIS/in vivo relations allow for a better interpretation of potential clinical benefit of preclinical drugs. Uniquely, the organoid based-model system used in early drug development stages can also be used at later pre-clinical development stages to recruit responders for clinical trials or at stages after market introduction to expand the drug label. In this chapter, we discuss the strengths and limitations of patient-derived organoids at this new interface where organoids act as a living biomarker for individualized health applications and drug development.

I. ORGANOID AS LIVING BIOMARKER FOR CF

In this section, we focus on the use of organoids as a living biomarker for different health applications. CF disease is highly variable between subjects and difficult to categorize into mild or severe¹. Likewise, treatment response vary strongly between pwCF and are difficult to predict or measure for individuals. This leads to ineffective treatments, unwanted side effects and waste of resources. Whereas characterization of individual health and disease used to rely on on-subject or ex vivo measurements, the use of organoids reshapes the landscape completely. We can now grow cells with high efficiency of virtually everyone by adding a simple growth factor cocktail which enables the study of biological functions and interventions thereof in great detail. Biobanks of such cells can shift tests from the clinic to the laboratory for current and new questions. Here, I reflect on the lessons learned and that still need to be learned on the use of organoids as a living biomarker.

Organoid FIS in comparison to other CFTR biomarkers

Biomarkers of CFTR function have long been used to diagnose CF and to classify into milder or more severe forms of CF^{2,3}. Sweat chloride measurement (SCC) is the most commonly used biomarker of CFTR function^{3,4}. In pwCF the SCC is elevated because impaired CFTR function in the sweat glands leads to defective chloride absorption. Individuals with a SCC concentration of > 60mmol/L are typically diagnosed with CF, but a SCC between 30-60 mmol/L can also indicate presence of CFTR dysfunction⁴. Additional CFTR function assays include nasal potential difference (NPD) and intestinal current measurements (ICM). NPD measures the CFTR and ENAC-dependent potential difference between the nasal epithelium and skin upon stimulation with solutions that affect ion channel activity^{4,5}. ICM measures anion transport across the epithelium ex vivo^{4,6}. First a rectal biopsy is obtained and placed in an Ussing chamber. Ion transport via multiple ion channels, including CFTR, is subsequently stimulated with the addition of compounds. CFTR function is determined based on anion transport-mediated voltage changes.

Sweat measurements are by far the most widely implemented test and can be performed at relatively few costs. NPD and ICM requires specialized equipment and well-trained staff and are relatively expensive⁴. For NPD, the individual has to sit still for one hour which hampers implementation of NPD for diagnosis of young children⁷. ICM requires fresh biopsies that lose viability within hours and only a limited number of observations can be made⁶. SCC and NPD are on-subject measurements and as such measure the CFTR function in their native environment, whereas this is somewhat limited in ICM and even more so in organoids. The on-subject measurements and to some extent ICM have the advantage to estimate the current *in vivo* CFTR function, and outcomes are generally rapidly available for patients. However, on-subject measurements are burdensome for patients which limits the number of observations that can be made. Additionally, technical interventions to increase the robustness and sensitivity of on-subject CFTR function measurement are limited due to safety concerns. This limits the generation of large datasets with repeated measurements. Another limitation of these biomarkers is their considerable technical and non-CFTR-related biological variability between measurements, which may limit their capacity to precisely and accurately quantitate individual CFTR function and consequently may lower their capacity to predict individual long-term disease progression^{3,5,6,8}.

The intestinal organoid model and the FIS-assay offer various advantages and disadvantages over the before mentioned techniques. Like the other biomarkers, FIS needs an on-subject procedure for isolation of a rectal biopsy that can be safely and easily obtained through either forceps or rectal suction biopsy. These biopsies can be shipped over long distances and extended periods for centralized organoid generation and storage in living biobanks for future applications⁹. As such, a large bio respiratory of intestinal CF organoids consisting of >600 CF organoid samples with a large range of mutations that is accessible for researchers worldwide was generated by a collaboration between Hubrecht Organoid Technology and the University Medical Centre Utrecht (**chapter 6**). The biobank covers the heterogeneity of CF mutations present in the Dutch CF population and the top 17 most prevalent mutations coincide with those in the Dutch CF registry^{10,11}. Of note, as this biobanking effort has focused on characterization of *in vitro* CFTR function and drug efficacy of infrequent CF alleles, rare mutations are overrepresented. In total 61 rare mutations were not present in the CFTR2 database¹², currently the most comprehensive list of pathogenic mutations in CF. In addition, to our knowledge, 34 of these mutations have never been reported previously in CF patients¹³. The biobanking of organoids has also important ethical considerations and we require explicit consent of patients for this activity.

Another clear advantage of organoid FIS is the ability to manipulate this biomarker through defined interventions including drugs such as CFTR modulators^{14,15}. Ex vivo ICM biopsies can also be used to assess the effect of fast-acting CFTR modulators, but longer incubations required for long-acting modulators are difficult due to tissue viability. Additionally, ICM measurements provide information at population level but are not robust enough for predicting drug response at the individual level¹⁶. Other important advantages of organoid FIS is the high, if not full, CFTR dependency of the assay and the scalability of the assay. CFTR testing can be performed without the need for manipulation, e.g. intestinal organoids do

not require pre-incubation with inhibitors since swelling is completely CFTR dependent¹⁷. In addition, the swelling assay allows for considerable throughput since the assay can be performed in 96- and 384-well format (**chapter 4**). In this way, large datasets of patients can be generated with sufficient repeated measures so more precise and accurate individual estimations of CFTR function and clinical phenotypes can be established.

Disadvantages of FIS in comparison to on-subject or other ex vivo measurements include the long time before results are available for patients due to the long culture procedure. In addition, cultures have approximately a 95% initial success rate, so people might need to come back for a biopsy. Standardization of culture reagents is highly important and difficult for components that are produced on-site with Wnt3a being one of the most important examples, as lower Wnt3a activity leads to cell differentiation and reduced CFTR function¹⁶. The culture procedure also increases the risk of accidental swaps of patient samples.

To summarize, FIS complements current on-subject/ex vivo based biomarkers of CFTR function and has strengths in terms of high CFTR function dependency, scalability and long term use but has some limitations related to in vitro culturing.

FIS can refine the current CFTR genotype-based classification system

In **chapter 2** we showed that individual CFTR function, quantitated with organoid FIS, associated with long-term disease progression defined by rate of FEV1pp decline as well as with the development of co-morbidities such as pancreatic insufficiency (PI), CF-related liver disease (CFRLD) and CF-related diabetes (CFRD). Despite the influence of genetic modifiers and other non-CFTR dependent environmental factors on CF disease severity¹⁸⁻²¹, it was remarkable to observe that in vitro FIS on intestinal cells has such a broad predictive capacity for many non-intestinal organ systems while other biomarkers of CFTR function have not shown this so clearly²². FIS not only demonstrated a large variability in CFTR function between pwCF with different genotypes but also within genotype classes, albeit at a smaller amplitude. Currently, others are replicating our findings by performing additional FIS measurements as we do here, albeit at a more limited scale²³.

An important implication of the work described in **chapter 2** is the demonstration that CFTR function in the CF population is in principle a continuous variable, determined by individual CFTR genotype and other modifiers of CFTR function. As we see a strong founder effect of the F508del mutation within the CF population, CFTR function within the CF population is not evenly distributed but left-shifted towards the lower end on the CFTR function scale. Current CFTR-based classification systems categorically define CFTR alleles as mild and a severe CF alleles, with the most mildly affected allele being dominant over the severe allele²⁴.

In conclusion, the individual CFTR function estimated through FIS can refine the current categorization methodology and can enable a better interpretation of individual disease severity and progression. This is especially relevant for many of the rare CF mutations which have not been characterized in detail making it particularly difficult to interpret and translate these molecular genotype(s) into a clinical trajectory^{24,25}. Additional studies such as

prospective cohort studies are needed to further strengthen these observations of FIS and clinical disease beyond the Dutch patient population.

FIS for selecting responders to CFTR modulators

The high CFTR dependency and in vitro scalability offers another advantage of organoid FIS over other biomarkers of CFTR function, namely the cost-effective measurements of drug effects impacting on CFTR function in an individualized setting. Whereas SCC and NPD can measure drug effects *in vivo*, FIS enables such measurements at a preclinical stage. Our previous work found that in vitro drug effects of FIS associates with changes in SCC and ppFEV1¹⁴ and that we could identify subjects with rare CFTR mutations who could benefit from available treatments¹⁵. A small library screen containing β 2-agonists also identified pwCF with residual CFTR function responsive to β 2-agonists with associated changes in NPD after introduction of β 2-agonist²⁶. This prompted us to further develop the organoid FIS platform for selecting patients who may benefit from clinically available modulators and who may not.

Chapter 4 describes the repurposing of the CFTR modulators VX-809, VX-770 (Kalydeco) and VX-809+VX-770 (Orkambi) for pwCF who are not on the label of these drugs. Previously, Dekkers et al. showed that in vitro outcomes in representative organoids at 0.128 μ M fsk linearly correlate with outcomes of published clinical trials¹⁵. As more and more clinical data is present, we repeated this analysis with an updated list of studies and representative organoids and found a similar correlation. We can use this correlation to define thresholds for potential clinical benefit of individuals whose organoids are tested for CFTR modulators. This thresholds is then defined based on the representative organoid swelling outcomes associated with published clinical trial data (e.g. ppFEV1 outcomes). Organoid FIS values below that of representative organoids for trials that did not show clinical benefit are likely to have minimal impact of treatment, whereas individuals whose organoids show FIS beyond levels of representative organoids of trials with positive outcomes are likely to have clinical benefit. Organoid FIS between values associated with negative or positive outcomes can then be ranked as potential clinical benefit. Such a ranking would identify 71 of the 185 individuals as having potential clinical benefit of VX-770 or VX-770/VX-809 therapy (**chapter 4**). Out of these 185 individuals, currently only 8 of these have access to reimbursed CFTR modulator treatment²⁷.

The discussion on thresholds remains relevant, and requires a pragmatic approach. In the above suggested approach, representative organoids are used to mimic *in vivo* conditions. Ideally, organoid thresholds are defined by comparisons of an *in vitro* organoid drug response with an *in vivo* response of the individuals who donated the organoids. Data is collected per drug and clinical benefit would be monitored in such a way that a clear selection of clinical responders and non-responders can be established. This latter point, the definition of individual clinical responders also still remains challenging and has not been agreed upon in the field. It is clear that short term clinical response indicators do not or only poorly correlate, similarly as short and long term responses^{14,28,29}. As such, a pragmatic solution as indicated in the above paragraph where organoid thresholds are defined based on average clinical drug efficacy could provide a way forward.

The current HIT-CF study that aims to develop drugs and organoid-based selection for people with rare mutations in Europe is based on this principle³⁰. Organoid-based high responders are selected and drug efficacy is compared in a cross over trial design to placebo treatment. A parallel trial using randomly selected patients is conducted to validate the organoid-based selection. Upon positive trial results in the organoid-selected responders, drug access can then be discussed with regulatory parties so people having organoid responses comparable of that of the selected subgroup in the clinical study can have access to reimbursement.

Altogether, the data in this thesis shows that it is highly feasible to test CFTR modulators on a large scale. Currently, the need to predict and select treatments is most urgent for people with rare mutations and without access to CFTR modulators. It is anticipated that a significant proportion of people without access can benefit from CFTR modulators that are already on the market, yet the regulatory path to reimbursement requires further attention.

FIS for individualized health applications – what can be improved?

The dynamic range of the FIS assay is optimally suited to measure CFTR function within the CF range, but reaches a ceiling effect at higher CFTR function levels (probably due to tensions within the organoid structure upon swelling). This leads to the use of different forskolin concentrations for different applications, which is not optimal. We found good agreement with clinical phenotypes in **chapter 2** when swelling was measured at 0.8 or 5 µM forskolin. For a proportion of the PDO's that already have considerable swelling levels without CFTR modulator therapy, the ceiling effect prevents the detection of a CFTR modulator effect when using these relatively high forskolin dosages (e.g. ivacaftor effects in S1251N organoid are underestimated at 0.8 or 5 µM forskolin). In contrast, the currently used forskolin concentration to measure drug effects (0.128 µM forskolin) is optimal for many genotypes, but underestimates e.g. effects of ivacaftor in G551D that show high *in vitro* responsiveness (and *in vivo* effects) at higher forskolin concentrations (**chapter 4**). With the development of more efficacious CFTR modulators (e.g. the triple treatment of Vertex), the negative influence of the ceiling effect may become more prominent. Instead of using a single concentration of forskolin for particular applications, a composite score might be explored that include multiple concentrations of forskolin so that a uniform technological procedure can be used to define organoid thresholds for both disease classification and therapeutic response. The new approach should also incorporate differences in residual function affecting baseline swelling so the approach can be implemented for all CF genotypes.

Another point is that the FIS assay measures the relative size increase of organoids within wells. This implies that comparisons between wells (e.g. patient organoid vs patient organoid or treatment vs control) require identical absolute sizes of organoids between wells at the start of the experiment. This is true for most conditions, but there are two notable exceptions. First, healthy control have already large fluid filled lumens and are therefore larger than CF organoids¹⁷. This is likely caused by endogenous, cellular cAMP levels that activate some of the wild type CFTR channel, leading to fluid transport and large luminal areas under steady state culture conditions. Second, highly effective potentiator treatments also lead to forskolin-independent luminal fluid transport and organoid (lumen) swelling. As potentiators

are added acutely with forskolin, this effect is only problematic when potentiators are added for longer periods (hours) to organoids before addition of forskolin. Correctors do not show these effects as corrected CFTR molecules require relatively high forskolin concentrations for channel opening. However, elexacaftor (VX-445), part of the new triple treatment VX-445, VX-661 and VX-770, has a dual corrector and potentiator mode-of-action³¹ and preincubation with both VX-661 and VX-445 results in significant swelling of many patient organoids.

Organoids conditions that associate with fluid-filled lumens and larger sizes lead to underestimation of the true CFTR response with FIS. Therefore, the FIS assay cannot be used in classical diagnostic applications that discriminate HC from CF. Likewise, it will be difficult to use the FIS assay to determine efficacies of treatment for all CF organoids when dual acting potentiator-corrector molecules such as VX-445 are measured. Another assay was designed to overcome this limitation. This assay measures the average organoid lumen area as percentage of total organoid area under steady-state conditions and not the relative area change in time as FIS does¹⁵. It discriminates clearly between HC and CF but has not been tested in the context of VX-445. However, the main disadvantage of this assay is the cumbersome annotation of lumen areas by manual drawing. New assays with significant throughput that are based on automatic image analysis of steady-state phenotypes are therefore really important to complement the current assays that rely on relative changes in organoid phenotypes such as FIS.

The use of organoids for diagnostic classification of people into CF or non-CF also remains poorly explored. As indicated above, organoids from HC show a distinct phenotype that can be quantified to discriminate between HC and CF. But the exact thresholds for this particular use and of this steady state lumen assay is still unclear. Interestingly, data from **chapter 2** might even suggest that typical CF organoids exhibiting small lumens but that show swelling upon 0.8 µM forskolin stimulation beyond 3000 AUC have a stable non-declining ppFEV1 as well as low chance of developing other co-morbidities. This amount of CFTR function and associated clinical phenotypic expression may therefore exclude the diagnosis of classical CF. New studies could be designed to test the 3000 AUC threshold for diagnostic typing.

Towards integrating organoids into the CF healthcare system

The observations described in the before mentioned sections plead for the use of the organoid model as standardized tool for predicting disease progression or therapy response. But why is the organoid assay not being implemented as such? First, the technology remains very new, not fully validated and organoid measurements require highly specialized laboratories and trained personnel. With the start of the HIT-CF Europe project³⁰, the first crucial steps for standardizing the organoid assay procedures across multiple laboratories around the world have been taken. This recently has resulted in a very detailed protocol for application and validation of the forskolin-induced swelling assay using intestinal organoids⁹, and will help to get the organoid model approved as standard diagnostic tool. Yet, a standardized protocol for research purposes still remains short of fully certified diagnostic procedures and an associated quality control standard. Many clinical diagnostic laboratories are not suited to integrate living cell technologies and

such infrastructures need to be developed. The developments described in this thesis and other similar activities in the field of e.g. cancer and other rare diseases may provide sufficient clinical need to justify the allocation of resources that are needed to set up a certified diagnostic infrastructure around the FIS assay.

Besides assessing the technical aspects of the organoid assay, the consumer's perspective also needs to be considered³². A recent study shows that the use of organoids to guide treatment decisions in CF was acceptable to 95% CF participants and 100% of community participants. The most important advantage was that organoids may improve treatment selection, the patient's quality of life and life expectancy. The primary disadvantages of organoid testing was the lack of a clear regulatory acceptance and route to reimbursement. This outweighed other disadvantages associated with the invasive procedures to get the biopsy or the lag in time before results are available. These findings indicate there is a high acceptance by pwCF to accept organoids as a tool to predict treatment response.

For now, the immediate priority for organoid testing is to accelerate access to CFTR modulators for those who can benefit but still do not have access and reimbursement. To increase the support base among the various stakeholders, it will likely help to start with high in vitro responders so that organoid inclusions can be clearly associated to positive clinical responses. From there, organoid criteria can be relaxed to ensure that people won't get excluded from modulator therapy while they may benefit. Future uses of organoids in treatment selection may involve the selection of the most optimal individual treatment when multiple treatment options are available. Organoids could also be very important for typing natural disease progression or for the diagnosis of CF in cases when clinical disease and biomarkers are unclear.

II. ORGANOID AS PRECLINICAL PLATFORM FOR THERAPY DEVELOPMENT

Here, the presented data in this thesis will be interpreted and discussed in the context of preclinical drug development. The finding that organoids recapitulate *in vivo* disease so accurately is of high importance for the development of drugs or other interventions. It not only shows that clinically relevant disease pathways are present in the model system, but also provide a framework for interpretation of drug efficacy in relation to clinical impact. We here focus on the potential role of organoids at various preclinical stages for CF drug development, how such a role can help to tackle some of the challenges associated with drug development and how the intestinal organoid model relates to other patient-derived cell models.

Organoids at various stages of drug development

Primary cell models are classically positioned at the earlier or later stages of preclinical drug development. Before the search for (small molecule) interventions in a drug discovery pipeline, biological targets that are subject to intervention need to be defined and validated.

The strong genetic base of a monogenic disease enables identification of the affected gene and downstream cellular products thereof as primary targets for treatment, as later illustrated by the successful development of CFTR protein modulators. By incorporating the biology of patients, PDOs play an important role in target identification and validation. Much of this work is carried out by academia in the form of basic research, with or without industry partners. In this thesis, our work on stop codon readthrough in **chapter 5** would fall into this category. This work increases the validity of the NMD pathways as a target for future drug development. Our work described in **chapter 6 and 7** also validates that gene editing approaches might provide future directions for treatment of particular CFTR mutations.

Once an intracellular drug target is defined, the classic route is to develop small molecules that can have a desired outcome on the selected target. Assays are designed that allow for screening of large scale drug libraries (100K-2M) to identify chemical structures. The identified hits are clustered based on their structure and activity-relation so chemical scaffolds are defined and new structures can be developed with higher efficacy and potency. This process involves multiple cycles of design, synthesis and testing. Selected molecules from this process are now drug leads and candidates for additional validation of efficacy, potency and selectivity in other biological assays with lower throughput but higher translational value than the original screening assays such as patient-derived cells or animal models. In parallel, the leads are checked for pharmacokinetic and safety profiles, and the mode-of-action is further established. From there, the selected drug leads are prioritized as drug candidates that can progress to clinical testing upon regulatory approval of the associated experimental and manufacturing documentation.

The pre-clinical high-throughput cell model that has been used to develop CFTR modulators are FRT cells that ectopically express CFTR cDNA. Hits from these FRT cell-based screens were validated in primary human bronchial epithelial (HBE) cells differentiated at air liquid interface using Ussing chamber measurements that measure transepithelial ion transport. This drug discovery pipeline has been extremely successful, but has limitations as well. The clearest limitations related to FRT and HBE cells are the lack of full CFTR biology recapitulation in FRT and throughput and access to material for HBE. Although the FRT-model has been used to identify responsive CFTR alleles, examples are also published that show that the CFTR cDNA does not represent the correct CFTR mutation defect (e.g. G970R-CFTR)^{33,34}.

As we found in this thesis, intestinal organoids provide a medium-high throughput capability as well as providing access to sufficient patient material. The 96-well based organoid FIS assay has sufficient throughput for hit-to-lead development (e.g. as we do in **chapter 3**) but requires further development for hit-identification purposes as done in FRT cells. We found that the assay can be upscaled in throughput and enable the screening of relatively large patient samples with small drug libraries of around 1400 compounds (**chapter 4**) to enable potential repurposing.

Altogether, we show that organoid-based assays have significant complementary value to HBE for drug efficacy and potency studies. Organoids have an advantage in the context of scalability: cells can be easily expanded and manipulated in the lab. This enables large scale

screening studies, but also the study of new interventions. In addition, the access to rare patients helps to focus drug development on this population who remain in large clinical need for effective treatments.

New treatments for F508del – is this still needed?

Treatment with ivacaftor (VX-770) and the first-generation correctors lumacaftor (VX-809) or tezacaftor (VX-661) results in improved lung function in patients with two F508del alleles, albeit with modest and highly variable effects between individuals. The level of CFTR function rescue is even lower in pwCF having one F58del mutation, suggesting that correction of F508del protein folding should be improved³⁵. In line with these clinical observations, *in vitro* experiments still detect the presence of immature (B-band) CFTR in VX-809 corrected F508del cells indicating additional optimization of CFTR corrector therapy is needed. This additional optimization has resulted in the development of Elexacaftor (VX-445), a next-generation corrector, which combined with VX-770 and VX-661 has yielded impressive clinical improvements, although still with considerable patient-to-patient variability^{31,37}.

In **chapter 3** we assessed the efficacy of a new triple therapy for pwCF having one F508del and one minimal function mutation and compared this to VX-809/VX-770 rescued F508del/F508del for which clinical impact has been extensively explored. The combination of two correctors and one potentiator resulted in a two-fold increase in Cl⁻ current in F508del/F508del human bronchial epithelial (HBE) cells compared to VX-770/VX-809 treatment, yet efficacy of this triple in the context of one F508del allele was not extensively explored. Of the 28 organoid cultures, 22 showed a CFTR function response similar to Orkambi-rescued F508del/F508del, indicating moderate to high clinical benefit is achievable. This triple therapy could therefore serve as a good alternative for the treatment of pwCF having one F508del allele, accounting for 90% of the CF population, that are currently devoid from modulator therapy.

The studied Abbvie/Galapagos triple combination was not as effective as the current CFTR-modulator triple therapy (VX-445, VX-770, and VX-661) that is FDA and EMA approved. The VX-445/VX-661/VX-770 combination is highly effective but high pricing limits access to these drugs, especially in less economically developed countries. Abbvie has since continued and planned a clinical trial with a new triple therapy. Such additional CFTR modulator therapies developed by other companies might help people with more common or rare mutations who may not benefit optimally from the current triple treatment. These additional treatments on the market may also stimulate competition and the cost-effectiveness of these treatments. As shown here, the organoid biobank resource that we generated together with Hubrecht Organoid Technology provided a rapid tool to prioritize the hit-to-lead process, leading to selection of the most promising candidates for clinical trials.

Repurposing FDA-approved drugs for the treatment of CF

The high proliferation rate of the intestinal organoids and the existence of a large biorespiratory with rare CFTR variants enabled us to perform the first cystic fibrosis organoid-based medium-high throughput screen, aiming to repurpose existing FDA-approved drugs

for pwCF having rare CFTR mutations. To aid screening of an FDA-approved drug library containing 1400 compounds, **chapter 4** describes the miniaturization and validation of the FIS assay screen using 384-wells plates. Most clearly, we found CFTR modulators that were part of the library as positive hits. Also, in line with a previously conducted screen containing G-protein Coupled Receptor (GPCR) agonists²⁶, we found several beta-adrenergic agonists as activators of organoid swelling. Besides beta-adrenergic agonists, we observed a swelling increase for a subset of the organoid cultures with roflumilast, a pharmacotherapy currently applied for the treatment of COPD that also modifies cellular cAMP^{38,39}. As this drug is already used for the treatment of a lung-related disease, prescribing it for CF without clinical studies is allowed if there is a clear urgent clinical need. Moreover, roflumilast appeared to restore CFTR function to a similar extend as Orkambi in a small subset of the donors and is compared to the CFTR modulators extremely cheap. Beta-adrenergic agonists increase swelling independent of the forskolin concentration, which probably explains the systemic side effects which have been observed in clinical trials²⁶, limiting clinical implementation. Organoid swelling with roflumilast, on the other hand, was forskolin dependent, which potentially lowers the occurrence of systemic side effects and as such might be more favorable than beta-adrenergic agonists. We are currently evaluating whether patients with a positivity organoid response on roflumilast and having a genotype currently not approved for modulator therapy would consider treatment with roflumilast.

In conclusion, a medium-high-throughput assay has been proven to aid in successful selection of CFTR function-increasing compounds. From a repurposing perspective, drugs that might be used to increase the CFTR activity in cells as a potentiator of endogenous cAMP (e.g. roflumilast) appeared most promising, but overall efficacy of hits was low and could not compete with the known CFTR modulators such as VX-809 and VX-770. A limitation of the medium-high-throughput approach is that it requires experience with organoid culturing and is expensive due to the use of large quantities of growth factors and Matrigel. The HTS standard operating procedure could be further automated with organoid dispensers, drug printers and centrifugal washers to further increase the throughput and reduce the level of technical variation. The 384-wells assay format may also be used to quickly screen for hits coming from (ultra)-high throughput screening assays to select the most promising drug candidates for further development.

Pharmacological repair of premature stop codons

In addition to screening 1400-FDA approved drugs, **chapter 5** elaborates on other new pharmacotherapeutic approaches for the treatment of pwCF who carry nonsense mutations leading the production of truncated CFTR protein.

Thus far, clinical studies focused on compounds that induce translational readthrough at the mRNA premature termination codon (PTC) location by incorporation of non-cognate amino acids at the PTC site, of which ELX-02 (NB124; Eloxx Pharmaceuticals) is currently the most advanced. A previous study reported ELX-02 to be moderately effective as single treatment in intestinal organoids⁴⁰ and resulted in an increase in mRNA and mature protein expression, three observations we could not repeat. A likely explanation for the difference in drug efficacy is that the compounds were derived from two different manufacturers.

Yet, consistent with other in vitro studies, **chapter 5** also shows that efficacy of ELX-02-mediated readthrough can be enhanced by simultaneously inhibiting nonsense mediated decay with SMG1i. The reduced translational fidelity by readthrough agents induces a pool of proteins with different amino acids at the PTC site⁴¹, therefore CFTR protein modulators even further enhance CFTR restoration^{31,40,42}. Although this study has provided insight into which processes need to be addressed to regain CFTR function of proteins ablated by a PTC mutation, clinical applicability is still hampered due to the requirement of safe NMD inhibitors. In conclusion, the studies described here indicate the potential of the PDO-based FIS-assay to help to identify and validate new treatment approaches for specific types of mutations as well as for individual patients.

CFTR gene editing – proof of concept for a cure

Besides preclinical applications of gene editing for disease modeling and drug development, gene editing approaches are increasingly used for the rescue of genetic disorders. CRISPR-Cas9 is nowadays the most preferred gene editing strategy based on site-specificity, efficiency and versatility. The company that developed the CFTR modulators also used CRISPR-Cas9 gene editing of ex vivo stem cells as treatment for sickle cell anemia. Other approaches are underway, including injection of Cas9-encoding mRNA for treatment of a liver disease⁴³. This exciting field is rapidly developing and might lead to a curative treatment of CF as well.

In 2012, rescue of F508del in intestinal organoids with CRISPR-Cas9 was achieved, yet due to the dependency on HDR, editing efficiency was extremely low and the introduction of deleterious off-target double-stranded breaks was high⁴⁴. In order to increase clinical potential of CRISPR-Cas9, new Cas9 proteins including base editors and prime editors have been developed. Base- and prime-editors both enable genetic rescue of point mutations, yet prime editors can also replace larger insertions and deletions of up to 80 nucleotides in length without the need to generate double stranded breaks⁴⁵. This thesis describes the implementation of those selective on-target gene editing techniques for the rescue of the CFTR defect in patient-derived intestinal stem cells. While **Chapter 6** focusses on rescuing two common point mutations generating premature stop codons in the CFTR gene with CRISPR-Cas9 adenine base editing (ABE) without creating off-target edits, **chapter 7** shows the successful rescue of F508del using prime editing. Although prime-editing indeed can be implemented for the rescue of a deletion of three base pairs (F508del), as well as for point mutations (R758X), editing efficiency was significantly lower as with CRISPR-Cas9-ABE. Moreover, **chapter 7** uncovered the presence of undesired edits, as has been detected before in mice⁴⁶.

We therefore conclude that base editors are superior to prime editors, both in terms of efficiency and of specificity in generating only the desired mutation¹⁰. However, if the desired edit cannot be generated by a base editor, for instance if it regards an indel or non-transition base change, prime editing is a valuable alternative to CRISPR/Cas9-mediated HDR, yet will require further improvement to allow widespread use as genetic rescuing technique.

Will CRISPR-Cas9 gene therapy cure CF?

Most clinical use of CRISPR/Cas9 to date has focused on ex vivo gene editing of cells followed by their re-introduction back into the patient^{47,48}. The ex vivo editing approach is highly effective for targeted applications, e.g. to enhance immune recognition of cancers^{49,50} and sickle cell disease⁵¹, but limited to a defined tissue that can be manipulated in vitro or ex vivo.

For many diseases, in vivo restoration of gene function would be most effective. Such in vivo use of CRISPR technologies in the clinic remains associated with challenges such as off-target editing, inefficient or off-target delivery, and stimulation of counterproductive immune responses. We did not observe off-target editing with CRISPR-Cas9-ABE in intestinal organoids (**chapter 6**), yet this off-target analysis was only performed on three organoid clones, basically representing three editing events. To rescue sufficient amount of CFTR in the human body, many more editing events are required which increases the risk of off-target editing. More research on safety and off-target editing is therefore needed to assess the specificity and safety of CRISPR when applied for in vivo therapy.

In addition, effectively reaching the nucleus of the desired cells and controlling Cas9 activity are also major obstacles that need to be overcome. Viral vectors might deliver Cas9 to target cells but preferentially without DNA integration to facilitate temporal control of Cas9 activity. Non-viral delivery may facilitate this, but usually at a lower efficacy than viral delivery. Yet, CRISPR-Cas9 can be delivered as DNA, RNA, or ribonucleoprotein (RNP), offering the opportunity to explore a vast variety of delivery vehicles and methods which possibly will speed up clinical implementation of the technique.

Precise targeting to defined cell subsets also remains a challenge. In the case of rescuing a genetic defect in tissues with high cellular turnover, stem cells are the ideal target to prevent washout of the gene-edited cells with non-gene-edited cells. Gene editing in tissues with limited cellular turn-over, e.g. the lungs, is presumably easier achievable as differentiated cells on the surface which are directly accessible can be targeted. However, repeated administration, with dosing intervals being driven by the lifespan of the targeted conducting airway epithelial cells might still be required. To date, most in vivo clinical trials have focused on genetically altering target tissues with direct access, such as the cervix or eye⁴⁸. As the field expands to more diseases, the ability to target the therapy, either through controlled, tissue-specific expression of Cas9, or cell-specific targeting will become more important. Moreover, editing efficiencies need to be improved, otherwise more gene-editing rounds might be needed to rescue sufficient cells, which again increases the risk of unwanted potentially deleterious off-target editing.

Consequently, the potential for in vivo gene therapy in CF is a promising avenue, especially for those who do not benefit from current pharmacotherapies. Still, challenges with cell-type specific delivery and safety remain present at this stage. It is anticipated that the use of CRISPR-Cas9 technology will be broadly explored in the preclinical and clinical domain for CF and other conditions. The coming decade will be pivotal to demonstrate the feasibility of this approach for treatment of rare monogenetic diseases such as CF.

Are mRNA-based therapeutics an alternative solution to gene therapy?

An alternative solution to gene editing which can also target any alteration at the basis of the disease, is delivery of correct copies of CFTR-encoded mRNA into cells. Promising pre-clinical in vitro results using primary cultured HNE cells showed an almost two-fold increase in cAMP-stimulated CFTR current after transfection with mRNA. The newest mRNA-based drug is MRT5005, delivered via inhalation to the lungs and allows the lung cells to create normally functioning CFTR protein. Clinical results from the early phase 1 and 2 studies reported to date, suggest that MRT5005 delivered in multiple doses to the lungs of CF patients is generally safe and well tolerated, yet increases in ppFEV1 was not observed⁵². The lack of FEV1 increasing efficacy is yet-to-be understood and additional research is ongoing to optimize future clinical development of mRNA cystic fibrosis programs, including MRT5005 and a next-generation CF candidate. Although mRNA delivery is presumably safer compared to altering the DNA with gene editing techniques, patients will require treatment on a regular basis as the defect is not permanently restored.

mRNA-based therapeutics could offer a safer solution to gene therapy for the restoration of CFTR function independent of the CFTR mutation, yet no clinical efficacy has been observed to date and whether this is caused by issues concerning exposure, delivery, transcription, dose or degradation warrants further investigation.

Intestinal organoids in comparison to other patient-derived cell models

Next to intestinal organoids, alternative organoid models have been developed that may help to understand organ-specific manifestations in CF and to better predict organ-specific drug responses. Embryonic- and induced pluripotent stem cells (IPSCs) are widely used for the generation of organoids, because their stemness and pluripotency facilitate indefinite expansion and of their potential to differentiate into almost all cell types of the human body derived from all three vertebrate germ layers^{53,54}. This has led to the emergence of other epithelial-derived organoids, like hIPSC-derived pancreas⁵⁵ or bile duct organoids⁵⁶ and allow modelling the gastrointestinal facets of cystic fibrosis. Several groups show an approach to direct hIPSC towards pancreatic progenitor cells that form organoids composed of functional acinar- and duct-like structures under 3D culture conditions⁵⁷. CFTR-mutated pancreatic organoids faithfully mirror the patients' phenotype in a functional swelling assay and therefore display a novel disease model for individualized drug testing specifically in pancreatic tissue conditions⁵⁷. IPSCs can be differentiated into cholangiocyte-like cells (CLC) and are formed in 3D CLC organoids that display functional characteristics of biliary epithelial cells such as enzymatic activity, response to secretory stimuli and expression of CFTR functionality⁵⁷. CFTR functionality was lost in CLC organoids expressing CFTR mutations, but could be rescued with modulator therapy. Current drugs have been primarily been tested in context of rescuing the lung or sweat gland phenotype of CF while the effect on pancreatic or bile duct disorders in CF patients have not yet been explored.

Although it is currently unclear to what extent the results obtained in the CLC or pancreas organoid systems are transferable to individual patients, IPSC-derived organoid models

provide the opportunity to study organ-specific differences partially affecting CF disease⁵⁷. The opportunities provided by the pluripotent state of iPSCs however come at a cost, as these fully de-differentiated stem cells require lengthy and complex culture protocols to acquire organoids that consist of a combination of differentiated cell types. As such, these iPSC-based models are potentially more useful for basic studies and drug development than as living biomarker for individual disease and treatment thereof.

Adult stem cell-derived airway organoids are of special interest as CF mortality is mainly a result of pulmonary failure and enable the assessment of airway-specific fluid transport, mucus viscosity and patient-specific drug responses⁵⁸ in the context of airway cell environment. Culturing of airway-derived cells in matrigel results in the formation of spheroids that allow for CFTR function measurement in a comparable fashion to intestinal organoids, via FIS⁵⁹. Also the presence of non-CFTR ion channels, like Na⁺ channels and TMEM16a in nasal spheroids⁶⁰ and bronchial-derived organoids⁶¹ respectively, shows the potential of using airway organoids for the development of alternative non-CFTR targeting therapies. Data from Pranke et al., indicate that in vitro observations in nasal epithelium may also correlate with in vivo modulator response⁶², confirming the importance of employing multiple patient-derived in vitro assays to predict multi-organ clinical drug efficacy and disease manifestation. Still, the overall use of intestinal organoids appears unparalleled up until now: it enables the formation of biobanks, precise and large quantities of CFTR function measurements in both a robust and sensitive manner that show associations with individual disease on a scale not shown for other culture models yet.

CONCLUDING REMARKS

Our work with PDOs remains one of the most straightforward examples of how organoid-based technologies can help research in the preclinical and clinical domain. These organoid-based culture models allow long-term in vitro expansion of patient derived cells and enable the creation of large biobanks. We have used the organoids to help understanding the disease heterogeneity observed between patients, which may enable a better individual assessment of disease severity. Additionally, organoid testing enabled us to preclinically select patients for marketed treatments (CFTR modulators), to preclinically select drugs from a large FDA-library and to explore other interventions to assist in drug development.

With CFTR function being such a key mechanism for long term CF disease development, it appears relevant to establish organoids from every individual with CF, for both baseline measurements and upon drug interventions. Rectal biopsy isolation could easily be included within standard care that takes place within the first year of a newborn that has been diagnosed with CF. Once intestinal organoids have been generated from this biopsy the individual can profit from the before mentioned possibilities the organoid-based culture model offers for its entire life. The impact of such a procedure on the whole healthcare budget for CF is limited, and it might be a more cost-effective alternative to on-subjects test of drug efficacy. This is currently especially relevant for people with rare mutations. With the ongoing development of CFTR modulators and the potential arrival of competitor products

CHAPTER 8

on the market, it may also become highly relevant to select treatments based on individual efficacy for patient groups with more common or even (seemingly) identical mutations. However, the technology remains new and more work remains needed to further grow a support base and to define the context-of-use to enable a move away from standard on-subject measurements towards in vitro off-subject measurements with organoids.

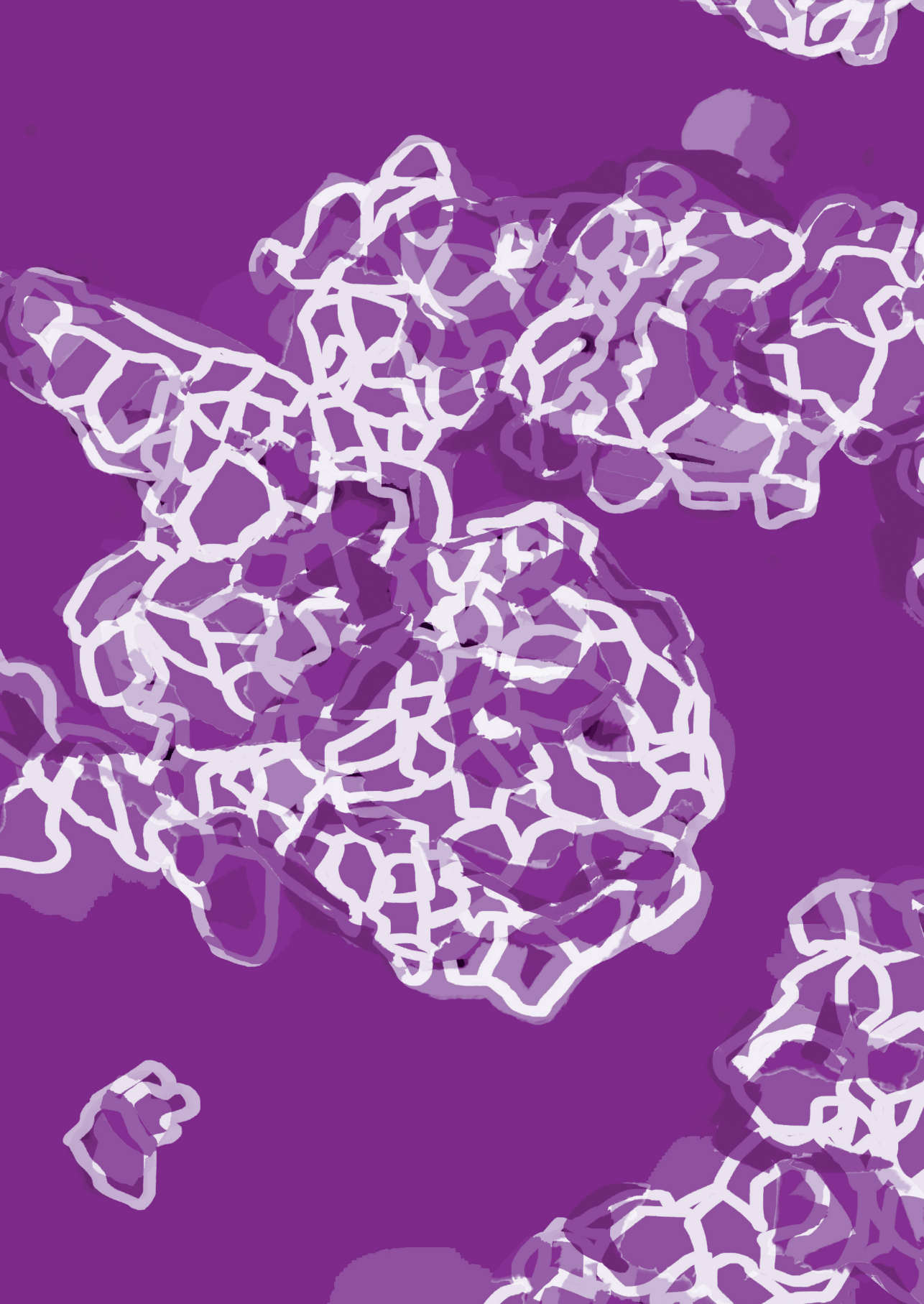
REFERENCES

1. Hinzpeter, A. et al. The importance of functional tests to assess the effect of a new CFTR variant when genotype-phenotype correlation is not possible . Clin. Case Reports 5, 658–663 (2017).
2. Beekman, J. M. et al. CFTR functional measurements in human models for diagnosis, prognosis and personalized therapy. Report on the pre-conference meeting to the 11th ECFS Basic Science Conference, Malta, 26-29 March 2014. J. Cyst. Fibros. 13, 363–372 (2014).
3. De Boeck, K. et al. CFTR biomarkers: Time for promotion to surrogate end-point? Eur. Respir. J. 41, 203–216 (2013).
4. Fernandez Elviro, C. et al. Diagnostic tools and CFTR functional assays in cystic fibrosis: utility and availability in Switzerland. Swiss Med. Wkly. 151, w20496 (2021).
5. Kyrilli, S. et al. Insights into the variability of nasal potential difference, a biomarker of CFTR activity. J. Cyst. Fibros. 19, 620–626 (2020).
6. Minso, R. et al. Intestinal current measurement and nasal potential difference to make a diagnosis of cases with inconclusive CFTR genetics and sweat test. BMJ Open Respir. Res. 7, 1–8 (2020).
7. van Mourik, P., Beekman, J. M. & van der Ent, C. K. Intestinal organoids to model Cystic Fibrosis. Eur. Respir. J. 1802379 (2019) doi:10.1183/13993003.02379-2018.
8. Collaco, J. M. et al. Sources of variation in Sweat chloride measurements in cystic fibrosis. Am. J. Respir. Crit. Care Med. 194, 1375–1382 (2016).
9. Vonk, A. M. et al. Protocol for Application, Standardization and Validation of the Forskolin-Induced Swelling Assay in Cystic Fibrosis Human Colon Organoids. STAR Protoc. 1, 100019 (2020).
10. Geurts, M. H. et al. CRISPR-Based Adenine Editors Correct Nonsense Mutations in a Cystic Fibrosis Organoid Biobank. Cell Stem Cell 26, 503–510.e7 (2020).
11. NCFS Dutch Cystic Fibrosis Registry 2019. (2020).
12. CFTR2 database. <https://cftr2.org/>.
13. CFTR1 database. <http://www.genet.sickkids.on.ca/>.
14. Berkers, G. et al. Rectal Organoids Enable Personalized Treatment of Cystic Fibrosis. Cell Rep. 26, 1701–1708.e3 (2019).
15. Dekkers, J. F. et al. Characterizing responses to CFTR-modulating drugs using rectal organoids derived from subjects with cystic fibrosis. Sci. Transl. Med 8, 344–84 (2016).
16. Zomer-van Ommen, D. D. et al. Comparison of ex vivo and in vitro intestinal cystic fibrosis models to measure CFTR-dependent ion channel activity. J. Cyst. Fibros. 17, (2018).
17. Dekkers, J. F. et al. A functional CFTR assay using primary cystic fibrosis intestinal organoids. Nat. Med. 19, 939–945 (2013).
18. Cutting, G. R. Cystic fibrosis genetics: From molecular understanding to clinical application. Nat. Rev. Genet. 16, 45–56 (2015).
19. Weiler, C. A. & Drumm, M. L. Genetic influences on cystic fibrosis lung disease severity. Front. Pharmacol. 4 APR, 1–19 (2013).
20. George, S., Lucy, O., Knight, R. A. & Hodson, M. E. Independent genetic determinants of pancreatic and pulmonary status in cystic fibrosis. Lancet 336, 1081–1084 (1990).
21. Collaco, J. M., Blackman, S. M., McGready, J., Naughton, K. M. & Cutting, G. R. Quantification of the relative contribution of environmental and genetic factors to variation in cystic fibrosis lung function. J. Pediatr. 157, 802–807.e3 (2010).
22. Beekman, J. M. Individualized medicine using intestinal responses to CFTR potentiators and correctors. Pediatr. Pulmonol. 51, S23–S34 (2016).

CHAPTER 8

23. Ramalho, A. S. et al. Correction of CFTR function in intestinal organoids to guide treatment of cystic fibrosis. *Eur. Respir. J.* 57, (2021).
24. Sosnay, P. R. et al. Defining the disease liability of variants in the cystic fibrosis transmembrane conductance regulator gene. *Nat. Genet.* 45, 1160–1167 (2013).
25. Castellani, C. et al. Consensus on the use and interpretation of cystic fibrosis mutation analysis in clinical practice. *J. Cyst. Fibros.* 7, 179–196 (2008).
26. Vijftigschild, L. A. W. et al. 2-Adrenergic receptor agonists activate CFTR in intestinal organoids and subjects with cystic fibrosis. *European Respiratory Journal* vol. 48 768–779 (2016).
27. Dutch cystic fibrosis society - approved mutations for CFTR modulator usage in the Netherlands - 2021. <https://ncfs.nl/over-taaislijmziekte/behandeling/status-cftr-modulatoren/>.
28. Graeber, S. Y. et al. Comparison of organoid swelling and in vivo biomarkers of cftr function to determine effects of lumacaftor-ivacaftor in patients with cystic fibrosis homozygous for the f508del mutation. *Am. J. Respir. Crit. Care Med.* 202, 1589–1592 (2020).
29. Fidler, M. C., Beusmans, J., Panorchan, P. & Van Goor, F. Correlation of sweat chloride and percent predicted FEV1 in cystic fibrosis patients treated with ivacaftor. *J. Cyst. Fibros.* 16, 41–44 (2017).
30. HIT-CF Europe Research Project. <https://www.hitcf.org/> (2018).
31. Laselva, O. et al. Rescue of multiple class II CFTR mutations by elexacaftor+ tezacaftor+ivacaftor mediated in part by the dual activities of Elexacaftor as both corrector and potentiator. *Eur. Respir. J.* 2002774 (2020) doi:10.1183/13993003.02774-2020.
32. Fawcett, L. K. et al. Avatar acceptability: views from the Australian Cystic Fibrosis community on the use of personalised organoid technology to guide treatment decisions. *ERJ Open Res.* 7, 00448–02020 (2021).
33. Yu, H. et al. Ivacaftor potentiation of multiple CFTR channels with gating mutations. *J. Cyst. Fibros.* 11, 237–245 (2012).
34. De Boeck, K. et al. Efficacy and safety of ivacaftor in patients with cystic fibrosis and a non-G551D gating mutation. *J. Cyst. Fibros.* 13, 674–680 (2014).
35. Wainwright, C. E. et al. Lumacaftor-Ivacaftor in Patients with Cystic Fibrosis Homozygous for Phe508del CFTR. *N. Engl. J. Med.* 373, 220–231 (2015).
36. Van Goor, F. et al. Correction of the F508del-CFTR protein processing defect in vitro by the investigational drug VX-809. *Proc. Natl. Acad. Sci. U. S. A.* 108, 18843–18848 (2011).
37. Middleton, P. G. et al. Elexacaftor–Tezacaftor–Ivacaftor for Cystic Fibrosis with a Single Phe508del Allele. *N. Engl. J. Med.* 381, 1809–1819 (2019).
38. Lambert, J. A. et al. Cystic fibrosis transmembrane conductance regulator activation by roflumilast contributes to therapeutic benefit in chronic bronchitis. *Am. J. Respir. Cell Mol. Biol.* 50, 549–558 (2014).
39. Raju, S. V. et al. Roflumilast reverses CFTR-mediated ion transport dysfunction in cigarette smoke-exposed mice. *Respir. Res.* 18, 1–8 (2017).
40. Crawford, D. K. et al. Targeting G542X CFTR nonsense alleles with ELX-02 restores CFTR function in human-derived intestinal organoids. *J. Cyst. Fibros.* 1–7 (2021) doi:10.1016/j.jcf.2021.01.009.
41. Xue, X. et al. Identification of the amino acids inserted during suppression of CFTR nonsense mutations and determination of their functional consequences. *Hum. Mol. Genet.* 26, 3116–3129 (2017).
42. McHugh, D. R., Cotton, C. U. & Hodges, C. A. Synergy between readthrough and nonsense mediated decay inhibition in a murine model of cystic fibrosis nonsense mutations. *Int. J. Mol. Sci.* 22, 1–20 (2021).
43. Gillmore, J. D. et al. CRISPR-Cas9 In Vivo Gene Editing for Transthyretin Amyloidosis. *N. Engl. J. Med.* 1–10 (2021) doi:10.1056/nejmoa2107454.
44. Schwank, G. et al. Functional repair of CFTR by CRISPR/Cas9 in intestinal stem cell organoids of cystic fibrosis patients. *Cell Stem Cell* 13, 653–658 (2013).

45. Anzalone, A. V. et al. Search-and-replace genome editing without double-strand breaks or donor DNA. *Nature* 576, 149–157 (2019).
46. Aida, T. et al. Prime editing primarily induces undesired outcomes in mice. *bioRxiv* (2020).
47. Roesch, E. A. & Drumm, M. L. Powerful tools for genetic modification: Advances in gene editing. *Pediatr. Pulmonol.* 52, S15–S20 (2017).
48. Hirakawa, M. P., Krishnakumar, R., Timlin, J. A., Carney, J. P. & Butler, K. S. Gene editing and CRISPR in the clinic: Current and future perspectives. *Biosci. Rep.* 40, (2020).
49. Lacey, S. F. & Fraietta, J. A. First Trial of CRISPR-Edited T cells in Lung Cancer. *Trends Mol. Med.* 26, 713–715 (2020).
50. Lu, Y. et al. Safety and feasibility of CRISPR-edited T cells in patients with refractory non-small-cell lung cancer. *Nat. Med.* 26, 732–740 (2020).
51. Frangoul, H. et al. CRISPR-Cas9 Gene Editing for Sickle Cell Disease and β -Thalassemia. *N. Engl. J. Med.* 384, 252–260 (2021).
52. TranslateBio. Results from Second Interim Data Analysis from Ongoing Phase 1 / 2 Clinical Trial of MRT5005 in Patients with Cystic Fibrosis (CF) was generally consistent with that previously reported for the 8 , 16 and 24 mg dose groups. <https://investors.translate.bio/node/7886/pdf> (2021).
53. James A. Thomson, Joseph Itskovitz-Eldor, Sander S. Shapiro, Michelle A. Waknitz, Jennifer J. Swiergiel, Vivienne S. Marshall, J. M. J. Embryonic Stem Cell Lines Derived from Human Blastocysts. *Science* (80-.). 282, 1145–1147 (1998).
54. Takahashi, K. et al. Induction of Pluripotent Stem Cells from Adult Human Fibroblasts by Defined Factors. *Cell* 131, 861–872 (2007).
55. Hohwieler, M. et al. Human pluripotent stem cell-derived acinar/ductal organoids generate human pancreas upon orthotopic transplantation and allow disease modelling. *Gut* 66, 473–486 (2017).
56. Mun, S. J. et al. Generation of expandable human pluripotent stem cell-derived hepatocyte-like liver organoids. *J. Hepatol.* 71, 970–985 (2019).
57. Hohwieler, M. et al. Stem cell-derived organoids to model gastrointestinal facets of cystic fibrosis. *United Eur. Gastroenterol. J.* 5, 609–624 (2017).
58. Berg, A. et al. High-Throughput Surface Liquid Absorption and Secretion Assays to Identify F508del CFTR Correctors Using Patient Primary Airway Epithelial Cultures. *SLAS Discov.* (2019) doi:10.1177/2472555219849375.
59. Brewington, J. J. et al. Detection of CFTR function and modulation in primary human nasal cell spheroids. *J. Cyst. Fibros.* 17, 26–33 (2018).
60. Pedersen, P. S., Frederiksen, O., Holstein-Rathlou, N.-H., Larsen, P. L. & Qvortrup, K. Ion transport in epithelial spheroids derived from human airway cells. *Am. J. Physiol. Cell. Mol. Physiol.* 276, L75–L80 (2017).
61. Sachs, N. et al. Long-term expanding human airway organoids for disease modeling. *EMBO J.* 38, e100300 (2019).
62. Pranke, I. et al. Might brushed nasal cells be a surrogate for CFTR modulator clinical response? *Am. J. Respir. Crit. Care Med.* 199, 123–126 (2019).





NEDERLANDSE SAMENVATTING

CYSTIC FIBROSIS ORGANOIDEN VOOR GEPERSONALISEERDE BEHANDELING EN THERAPIE ONTWIKKELING

Hoofdstuk 1: Introductie

Taaislijmziekte of cystic fibrosis (CF) is een aangeboren ziekte en wordt veroorzaakt door foutjes - ook wel mutaties genoemd - in het gen dat codeert voor het cystic fibrosis transmembrane conductance regulator (CFTR) eiwit. Iedereen met CF heeft twee mutaties in het CFTR gen, één geërfd van zijn/haar moeder en één van zijn/haar vader. Wereldwijd zijn er ongeveer 70.000 mensen met CF. In Nederland komt de ziekte bij zo'n 1.550 mensen voor en worden er jaarlijks ongeveer 25 kinderen geboren met deze ziekte. CF is dus een redelijk zeldzame aandoening.

Het CFTR-eiwit transporteert zouten zoals chloride en bicarbonaat en heeft daardoor effect op de regulatie van watertransport. Dit is met name belangrijk voor het vloeibaar, doorzichtig en dun houden van het slijm dat wordt geproduceerd in verschillende organen. Bij mensen met CF waarbij het CFTR niet goed werkt is het slijm juist erg taai en dik, vandaar de naam taaislijmziekte.

Slijm in onze luchtwegen zorgt voor het afvoeren van bacteriën en andere vervuilingen die zijn ingeademd. Bij mensen met CF is het taaie slijm niet goed in staat de afvalstoffen te vervoeren. Dit opgehopte slijm zorgt met name in de longen voor ontstekingen en leidt tot benauwdheid. Ook transporteert het slijm enzymen van de alvleesklier naar de darm. Deze enzymen zorgen ervoor dat vetten goed verteerd kunnen worden. Bij mensen met CF komen door het dikke slijm de enzymen die nodig zijn voor de vertering van deze vetten niet voldoende in de darm terecht en kunnen de darmen verstopt raken. Daarnaast hebben mensen met CF ook vaak een aangetaste alvleesklier (wat kan leiden tot diabetes) en lever.

Op dit moment zijn er naar schatting 1700 verschillende mutaties die CF kunnen veroorzaken. Deze verschillende mutaties kunnen de functie van het CFTR-eiwit verschillend beïnvloeden. De combinatie van mutaties (genotype) bepaalt dus de ernst van de uiting van ziekte. Hele ernstige mutaties leggen de productie van CFTR volledig stil met een ernstig ziektebeeld als gevolg. Bij mindere mutaties wordt nog wel een kleine hoeveelheid eiwit geproduceerd maar deze eiwitten functioneren minder goed. Deze mindere mutaties zorgen vaak voor een minder ernstig ziektebeeld.

Nieuwe ontwikkelingen in de symptoombestrijding van CF en een diagnostesting op vroegere leeftijd hebben in de afgelopen jaren tot een stijging in de levensverwachting geleid; de leeftijd van overlijden ligt gemiddeld tussen de 35 en 40 jaar. Desalniettemin is er geen behandeling beschikbaar die CF volledig geneest en blijft het een heftige ziekte waarbij mensen met CF afhankelijk van dagelijkse zorg en medicijninname.

In de afgelopen jaren heeft er ook een verschuiving plaatsgevonden in de behandeling van CF; van symptoombestrijding naar het repareren van het CFTR-eiwit met behulp van zogenoemde CFTR-modulatoren. Deze revolutionaire therapie is echter maar voor

een beperkt aantal mensen met CF met specifieke mutaties beschikbaar. Naast dat de modulatoren alleen beschikbaar zijn voor een selectie van de mensen met CF, zijn niet alle mutaties te repareren met deze modulatoren, zogenoemde klasse 1 mutaties bijvoorbeeld. Uitdagingen die er dus nog liggen voor mensen met CF en die in dit proefschrift worden behandeld zijn: 1. het vinden van nieuwe modulatoren die nog effectiever en 2. voor meer mensen met CF beschikbaar zijn en 3. het vinden en onderzoeken van nieuwe behandel methodes voor de mensen met CF met mutaties waar modulator therapie niet voor werkt.

Sinds 2013 is het mogelijk om de werkzaamheid van CFTR-eiwit op het laboratorium te meten in stamcellen van mensen met CF. Deze stamcellen worden uit de darm van mensen met CF gehaald en gebruikt om uit te groeien tot minidarmmpjes, ook wel organoiden genoemd. Organoiden bevatten dezelfde CFTR-mutaties als de persoon waarvan de organoiden zijn gemaakt. Omdat de organoiden uit stamcellen bestaat hebben ze de eigenschap oneindig te blijven groeien en kunnen ze opgeslagen worden in een biobank waarbij de organoiden voor later onderzoek weer in gebruik genomen kunnen worden. Om de CFTR-functie in deze organoiden te bepalen wordt gebruik gemaakt van de zwellingsassay. Bij gezonde organoiden wordt er via het CFTR-eiwit zouten de minidarm in gepompt. Dit trekt water aan waardoor de organoid gezwollen is, als een soort gevulde waterballon. Bij organoiden van mensen met een defect in het CFTR-eiwit is het watertransport verhinderd, met een niet of minder gezwollen organoid als gevolg. De mate van zwelling geeft dus een weerspiegeling van de CFTR-functie. Deze methode is uitermate geschikt gebleken voor het bepalen van effectiviteit van bestaande en nieuwe therapieën op het herstellen van CFTR-functie, maar ook om specifieke mensen met CF te kunnen identificeren die mogelijk baat kunnen hebben bij deze therapieën.

I. KUNNEN WE LANGE TERMIJN ZIEKTEBELOOP VOORSPellen?

Hoofdstuk 2: kan de zwelling van organoiden ziektebeloop voorspellen?

Het ziektebeloop kan erg per persoon met CF verschillen en is tot op heden lastig gebleken om te voorspellen. De verschillen in ziektebeloop zijn het resultaat van een combinatie van genetische (zoals de CFTR-mutatie) en omgevingsfactoren (bijvoorbeeld veelvuldige blootstelling aan sigarettenrook). Er bestaan al een aantal onderzoeksmethodes om CFTR-functie te bepalen, waarbij de zweetchloride meting de bekendste en meest gebruikte test is in het ziekenhuis. Helaas zijn deze methodes niet gevoelig genoeg. Daarnaast kunnen metingen binnen 1 persoon erg variëren waardoor deze testen de ziektebeloop tussen individuele mensen met CF niet goed kunnen voorspellen. Zouden de zwellingsmetingen in organoiden van mensen met CF hier verandering in kunnen brengen? Dat is de vraag die we in hoofdstuk 2 onderzoeken. Om deze vraag te kunnen beantwoorden hebben we klinische gegevens, waaronder longfunctie, alvleesklierfunctie, leverfunctie en aanwezigheid van diabetes van 176 mensen met CF gedurende 8 jaar opgevraagd. Daarnaast hebben we de CFTR-functie van deze 176 mensen met CF gemeten met de zwellingsassay. Vervolgens zijn er verschillende statistische analyses uitgevoerd om te bepalen of de CFTR-functie in de

organoiden voorspellend is voor de verschillende klinische uitkomsten per individu. Deze analyses laten zien dat er een duidelijke link is tussen de mate van CFTR-functie gemeten met de zwellingsassay en de longfunctieachteruitgang per jaar per individu. In andere woorden, mensen met CF waarvan de organoiden een lage CFTR-functie laten zien hadden een snellere daling in longfunctie dan mensen met CF waarvan de organoiden een hoge CFTR-functie laten zien. Er is niet alleen een link gevonden met longfunctieachteruitgang, er is ook een duidelijke associatie tussen de mate van zwelling en de kans op het ontwikkelen van CF gerelateerde diabetes, CF gerelateerde leverziekte en verlies in alvleesklierfunctie. Tot slot laat hoofdstuk 2 zien dat zwelling van organoiden de ernst van de ziekte beter kan voorspellen dan de zweetchloride test. Het goed kunnen voorspellen van zieke ernst is met name interessant voor mensen met CF met een zeldzame variant van de ziekte. Bij deze personen is vaak onbekend wat de genetische mutatie voor effect heeft of het uiteindelijke ziektebeloop. De zwellingsassay met organoiden van deze personen biedt hiervoor uitkomst.

II. HET PRE-KLINISCH TESTEN VAN CFTR MODULATOREN EN ANDERE BESTAANDE MEDICIJNEN

Hoofdstuk 3: zieke organoiden behandelen met een nieuwe ‘triple’ combinatie therapie

De meest voorkomende mutatie die CF veroorzaakt is de F508del mutatie. Deze mutatie heeft twee grote gevolgen op het CFTR-eiwit: 1. Er komt minder CFTR-eiwit op de buitenkant van de cel en 2. Het eiwit dat op de buitenkant van de cel terecht komt opent niet goed. De combinatie heeft als gevolg dat er minder chloride de cel uit wordt getransporteerd. Voor deze mutatie zijn er in de afgelopen jaren revolutionaire medicijnen beschikbaar gekomen, modulatoren genoemd, die in plaats van de symptomen bestrijden, specifiek het CFTR-eiwit defect kunnen repareren. Om de twee defecten te kunnen repareren zijn er twee verschillende klassen modulatoren ontwikkeld, correctoren en potentiatoren. Correctoren zorgen ervoor dat er meer eiwit op het oppervlak van de cel terecht komt en potentiatoren werken in op het eiwit dat zich op het oppervlak van de cel bevindt en zorgen ervoor dat het eiwit beter opent. Mensen met CF die twee keer de F508del mutatie hebben kunnen effectief behandeld worden met een combinatie therapie van een corrector en een potentiaator. Echter, mensen met CF die een F508del mutatie hebben in combinatie met een zeer ernstige mutatie, ook wel een klasse 1 mutatie genoemd, is bovengenoemde combinatie therapie niet effectief genoeg. Voor deze groep mensen met CF is het van belang dat er nog effectievere CFTR-modulator therapieën worden ontwikkeld zodat ook mensen met CF met een enkele F508del mutatie behandeld kunnen worden. Uit eerdere studies is gebleken dat een zogenaamde triple therapie mogelijk uitkomst kan bieden. Bij triple therapie worden twee correctoren gecombineerd met 1 potentiaator. In hoofdstuk 3 testen we de effectiviteit van zo’n nieuwe triple therapie op organoiden van mensen met CF met enkele F508del mutatie in combinatie met verschillende klasse 1 mutaties. De resultaten uit deze studie laten zien dat de nieuwe triple therapie effectiever is in het herstellen van CFTR-functie dan de al bestaande duale therapie. Daarnaast viel ons op dat er een grote variatie is CFTR-functie herstel met de triple tussen de organoiden met verschillende

klasse 1 mutaties. Dit benadrukt het belang van het testen van nieuwe medicijnen op individueel niveau aangezien gebleken is dat verschillende mutaties verschillend kunnen reageren op dezelfde therapie. Hoofdstuk 3 laat zien dat met behulp van organoiden zowel effectieve CFTR-modulator therapieën getest kunnen worden maar ook specifieke mutaties geselecteerd kunnen worden die goed zullen reageren op de therapie. De volgende stap is te onderzoeken of de mensen met CF waarvan de organoiden zijn gemeten in deze studie in dezelfde mate verbeteren na behandeling met de triple therapie.

Hoofdstuk 4: zijn er andere medicijnen die CFTR-functie kunnen herstellen?

Medicijn herpositionering is een strategie om al bestaande medicijnen te gebruiken voor de behandeling van een ziekte of variant van de ziekte waarvoor het medicijn in eerste instantie niet voor is ontwikkeld. Een voorbeeld van herpositionering tussen verschillende ziektes is het antibioticum claritromycine. Deze is ontwikkeld voor de behandeling voor de ziekte van Lyme, maar bleek later ook effectief voor de behandeling van verschillende soorten kanker. Herpositionering binnen een ziekte gebeurt ook al bij CF, zo is ivacaftor bijvoorbeeld een modulator die is ontwikkeld voor de S1251N mutatie, maar is later ook beschikbaar gekomen voor mensen met CF met andere mutaties waar Ivacaftor effectief voor bleek. Het grote voordeel van medicijn herpositionering is dat de medicijnen al geproduceerd worden en eerdere studies het gebruik veilig hebben bevonden. Dit heeft als gevolg dat het medicijn sneller en goedkoper beschikbaar zal komen voor mensen met CF dan wanneer er een volledig nieuwe therapie ontwikkeld moet worden.

Hoofdstuk 4 beschrijft zo'n grote medicijn herpositioneringsstudie waarbij 1400 verschillende medicijnen getest zijn op 76 verschillende organoiden met verschillende CFTR-mutaties. Deze 1400 medicijnen zijn of ontwikkeld voor andere aandoeningen dan CF, of voor CFTR-mutaties anders dan de mutaties beschreven in deze studie. Er is in deze studie gekozen om organoiden met twee keer de F508del mutatie uit te sluiten aangezien hier al een zeer effectieve behandeling voor bestaat en er juist behoefte is naar het vinden van effectieve behandelingen voor mensen met CF met zeldzamere varianten van CF.

Om de grote hoeveelheid medicijnen op zoveel verschillende organoiden te kunnen meten is er in deze studie voor de eerste keer gebruik gemaakt van een opgeschaalde variant van de zwellingssassay. Van de 1400 verschillende medicijnen bleken de CFTR-modulatoren het meest effectief in het grootste aantal verschillende organoiden. Er zijn een aantal andere, niet-modulator medicijnen gevonden maar deze bleken niet zo effectief de CFTR-functie te kunnen herstellen dan de CFTR-modulatoren. Desalniettemin heeft deze studie laten zien dat het 1. mogelijk is om op grote schaal medicijnen te testen voor een grote groep mensen met CF en dat 2. de al bestaande CFTR-modulatoren voor veel meer mensen met CF effectief zijn dan waarvoor ze ontwikkeld en beschikbaar zijn.

Hoofdstuk 5: het behandelen van organoiden met een zeer ernstige vorm van CF

10% van de mensen met CF hebben CF door mutaties die voor een premature stop in het DNA leiden. Bij een premature stop in het DNA wordt er een CFTR-eiwit aangemaakt wat nog maar bestaat uit een klein deel van het oorspronkelijke eiwit. Hierdoor werkt het CFTR-eiwit niet meer goed en hebben mensen met deze premature stop mutaties ernstige taaislijmziekte gerelateerde ziekteverschijnselen. Onderzoek heeft echter aangetoond dat er chemische stoffen zijn die deze premature stop als het ware kunnen maskeren. Hierdoor wordt het signaal dat ervoor zorgt dat het eiwit onvolledig wordt aangemaakt, genegeerd. Deze stoffen worden ‘read-through’-medicijnen genoemd. Het meest veelbelovende read-through medicijn van dit moment is ELX-02. Eerdere studies laten zien dat wanneer organoiden van een persoon met CF worden behandeld met ELX-02 er een deel van de CFTR eiwitten weer in volledige vorm worden aangemaakt en hierdoor de functie van het CFTR eiwit deels wordt hersteld, echter in relatief lage mate. Hoofdstuk 5 onderzoekt of ELX-02-herstelde CFTR-functie meer verhoogd kan worden door er nog twee andere stoffen aan toe te voegen. Een van die stoffen is SMG1i. In de cel bestaat er een controlesysteem die eiwitten met een PTC afbreken, dit wordt ook wel nonsense-mediated decay (NMD) genoemd. Hierdoor is er minder eiwit beschikbaar wat hersteld kan worden met ELX-02. SMG1i is een stof dat de afbraak van PTC-bevattende eiwitten remt, waardoor er meer eiwit beschikbaar is voor ELX-02 om te repareren. Ondanks dat er met de behandeling van ELX-02 meer eiwit in volledige vorm wordt aangemaakt, hebben eerdere experimenten aangetoond dat dit niet altijd tot volledig functieherstel leidt. Dit zou echter hersteld kunnen worden met CFTR-modulatoren. We hebben daarom naast SMG1i ook onderzocht of toevoeging van de meest effectieve, CFTR triple modulator therapie, Trikafta, tot een extra verhoogde CFTR-functie leidt. Hoofdstuk 5 laat inderdaad zien dat een combinatie van ELX-02, SMG1i en Trikafta tot een veelbelovend functieherstel van het CFTR-eiwit leidt waar mensen met CF in theorie baat bij zouden kunnen hebben. Wat echter behandeling van mensen met CF met deze combinatietherapie in de weg staat is dat op dit moment nog niet alle geteste medicijnen beschikbaar zijn voor klinisch gebruik. Op dit moment wordt een fase II klinische studie uitgevoerd die de effectiviteit van ELX-02 in het herstellen van de ziekteverschijnselen van mensen met een premature stop mutatie onderzoekt. Trikafta is al goedgekeurd voor de behandeling van mensen met CF. Er zijn nog geen klinische studies opgestart voor SMG1i. Om mensen met CF te laten profiteren van de veelbelovende resultaten behaald met de combinatie therapie in onze studie is er verder onderzoek nodig naar de ontwikkeling van klinisch toepasbare SMG1i-achtige medicijnen.

III. KAN GEN THERAPIE CF GENEZEN?

Hoofdstuk 6: Genetisch ziekte repareren in organoiden van mensen met een vorm van CF ongevoelig voor modulator therapie.

Hoofdstuk 6 beschrijft het bestaan van een grote biobank met organoiden die in samenwerking tussen het UMC Utrecht, verschillende CF-centra uit Europa, de Nederlandse CF stichting en Hubrecht Organoid Technology Stichting is ontwikkeld. Deze biobank maakt

het mogelijk om te onderzoeken wat er precies misgaat bij CF, om mensen met CF met bepaalde mutaties te selecteren voor specifieke therapieën en om nieuwe therapieën te onderzoeken. In hoofdstuk 6 en 7 worden de organoiden ingezet om te onderzoeken of een nieuwe gen-modulerende methode, ook wel CRISPR-Cas genoemd werkt voor het herstellen van CF in organoiden van mensen met CF.

Waar de in 2012 ontwikkelde CRISPR-Cas-techniek een fout in een gen eruit knipt en vervangt door een nieuw stukje, werkt de nieuwste CRISPR-techniek getest in hoofdstuk 6 anders. Met behulp van deze nieuwe vorm van CRISPR-Cas wordt het precieze stukje DNA wel opgespoord, maar niet weggeknipt en vervangen; het wordt ter plekke gerepareerd. Hierdoor werkt de nieuwe CRISPR-Cas techniek preciezer en worden er minder fouten gemaakt, en heeft eerder onderzoek in stamcellen uit rijst en muizen laten zien dat het een veiligere vorm is van genetische manipulatie. Hoofdstuk 6 laat zien dat deze CRISPR-techniek ook effectief en veilig werkt op menselijke cellen, namelijk op organoiden van mensen met CF.

Hoofdstuk 6 gebruikt deze techniek specifiek op organoiden van mensen met CF met zogenoemde klasse I mutaties. Deze mutaties zorgen voor een zeer ernstig ziektebeeld en tot op de dag van vandaag zijn er geen CFTR modulerende therapieën voor deze mensen met CF beschikbaar. Voor deze groep mensen met CF is gentherapie dus extra interessant. Hoofdstuk 6 laat zien dat de nieuwe CRISPR-Cas techniek de organoiden met een klasse I mutatie kunnen repareren, oftewel dat genezing van bepaalde klasse I mutaties met gentherapie in het laboratorium mogelijk is.

Hoofdstuk 7: is de meest voorkomende CFTR-mutatie te genezen met gentherapie?

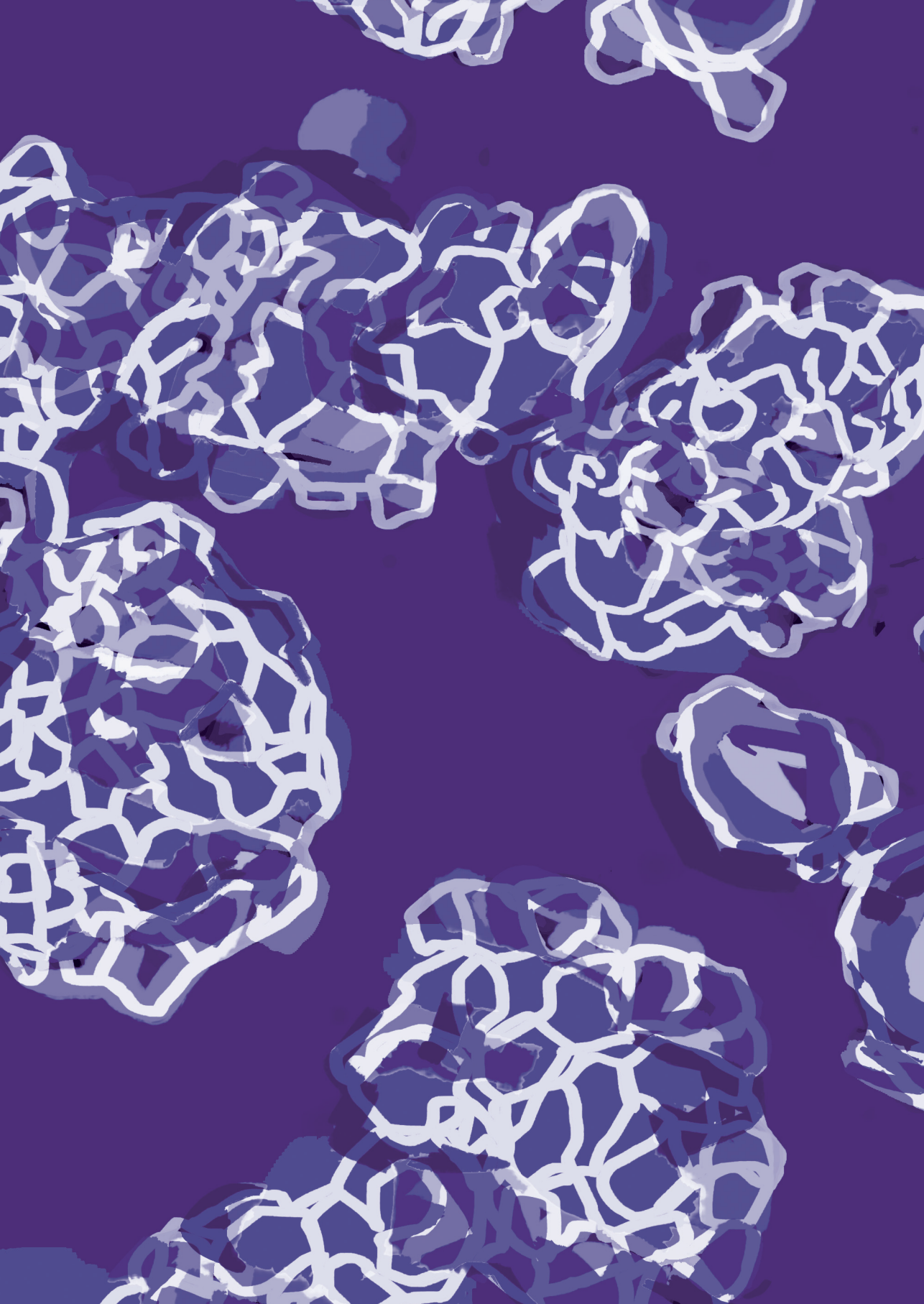
Waar hoofdstuk 6 kijkt naar de behandeling van organoiden met ernstige klasse I mutaties, beschrijft hoofdstuk 7 de genetische reparatie van de F508del mutatie, de meest voorkomende mutatie onder mensen met CF. Zoals alle genen is het CF-gen (CFTR) een stukje van een DNA-molecuul, die weer een klein onderdeel van een chromosoom is. Ieder chromosoom bestaat uit een lange reeks van vier soorten moleculen – nucleotiden - die A, T, G en C worden genoemd. Het gen dat bij CF is betrokken, bestaat uit ongeveer een kwart miljoen nucleotiden. De volgorde waarin deze nucleotiden zijn gerangschikt bevat de genetische informatie. Zij vormen een lange reeks van drie-letterige woorden die de cel de informatie geeft die hij nodig heeft om een gen goed te laten functioneren. Personen met de F508del mutatie missen precies één zo'n DNA-woord. Waar de gen techniek beschreven in hoofdstuk 6 alleen 1 nucleotide kan vervangen, kan de nieuwste CRISPR-Cas techniek, ook wel prime-editing genoemd, naast 1 letter ook een of meerdere drievertoningen vervangen. In theorie zou prime-editing de F508del mutatie dus moeten kunnen herstellen, wat in hoofdstuk 7 inderdaad bevestigd wordt in organoiden. De techniek lijkt echter wel iets meer fouten te maken dan de techniek beschreven in hoofdstuk 6, oftewel prime-editing lijkt iets minder veilig dan base-editing. Echter, prime editing is op dit moment wel een van de meest veelzijdige gen modulatie technieken waardoor deze techniek in theorie 89% van de ziektekende genetische mutaties zou kunnen repareren.

Dat de studies beschreven in hoofdstuk 6 en 7 aantonen dat de technieken werken in het laboratorium betekent niet dat mensen met CF er al van kunnen profiteren. Een grote uitdaging is het CRISPR-enzym naar de juiste plekken in het lichaam te brengen. CF is wat dat betreft ook niet de makkelijkste aandoening omdat het op zoveel verschillende lichaamsfuncties effect heeft en de CRISPR-enzymen op veel verschillende plekken terecht zouden moeten komen. Bij aandoeningen die een enkel orgaan of celtype aantasten, zoals sikkelmanemie, is de toepassing van CRISPR-Cas gemakkelijker en ook veelbelovend gebleken. Maar voordat CRISPR toegepast kan worden voor de behandeling van CF is er verder onderzoek nodig. Daarnaast kleven aan het genetisch manipuleren van cellen ook ethische aspecten. Hoofdstukken 6 en 7 focussen op het repareren van kapotte cellen. Theoretisch gezien kan deze techniek ook ingezet worden voor het veranderen van gezonde cellen, bijvoorbeeld in embryo's. Als dat mogelijk is, wil dat niet zeggen dat dat ook wenselijk is. Een maatschappelijke discussie is nodig om te bepalen hoe hier als samenleving mee om te gaan.

CONCLUSIE

Het onderzoek in dit proefschrift laat duidelijk de kracht zien van hoe de organoid technologie kan helpen in het beter begrijpen van ziekte variatie tussen mensen met CF en dat het zou kunnen helpen bij het bepalen van de ziekte ernst op individueel gebied. Daarnaast heeft het geholpen in het vinden van mogelijke nieuwe therapieën en kan de organoid technologie helpen bij het identificeren van mensen met CF die baat kunnen hebben bij bestaande en nieuwe therapieën.

Omdat CFTR-functie zo een sleutelmechanisme is voor lange termijn CF ziekte ontwikkeling, is het belangrijk dat we voor iedere individu met CF organoiden verzamelen zodat we CFTR-functie zonder en met medicatie kunnen bepalen. Daarnaast is met de continue ontwikkeling van CFTR-modulatoren en de komst van nieuwe medicijnen belangrijker geworden de passende medicatie bij de juiste mensen met CF te krijgen. Dit is met name interessant voor mensen met zeldzame vorm van CF, aangezien deze personen in de huidige medicijnontwikkelingsprogramma's worden geexcluseerd. Het isoleren van stamcellen voor de generatie van organoiden zou gemakkelijk geïntegreerd kunnen worden in standaard zorg dat plaatsvindt in het eerste jaar dat een nieuwgeborene wordt gediagnosticeerd met CF. Het grote voordeel van de organoid technologie is dat als organoiden eenmaal gemaakt zijn, de persoon waar de organoiden van afkomstig zijn voor altijd kan profiteren van de mogelijkheden die de organoiden technologie biedt. De impact van de minidarm technologie op het gehele gezondheidsbudget voor CF is minimaal en zou een kost effectievere methode kunnen zijn dan medicijntesten waarbij de patiënt iedere keer zelf aanwezig moet zijn. Desalniettemin blijft de organoid technologie een nieuwe technologie en is er meer onderzoek nodig voordat de standaard CFTR-meetmethodes, zoals de zweetchloride test, vervangen kunnen worden door de organoid meetmethode.





ADDENDA

LIST OF ABBREVIATIONS

AAV	Adeno-associated viruses
ABBV	Abbvie
ABE	adenine base editing
APC	Adenomatous polyposis coli
AUC	area under the curve
BME	Cultrex Basement Membrane Eatrix
CaCC	calcium-activated chloride channel
cAMP	cyclic adenosine monophosphate
CAS9	CRISPR-associated 9
CBE	cytosine base editing
CCM	complete culture medium
CF	cystic fibrosis
CFRD	CF related diabetes
CFRLD	CF related liver disease
CFTR	cystic fibrosis transmembrane conductance regulator
Cl-	chloride
CMV	Cytomegalovirus
COPD	chronic obstructive pulmonary disease
CRISPR	clustered regularly interspaced short palindromic repeats
DCFFPR	Dutch cystic fibrosis foundation patient registry
DIS	drug induced swelling
DMEM	Dulbecco's Modified Eagle Medium
DMSO	dimethylsulfoxide
DNA	deoxyribonucleic acid
DSB	double stranded breaks
EGF	Epidermal growth factor
ELXds	Eloxx-02-disulfate
EMA	European Medicines Agency
EPSCs	Embryonic pluripotent stem cells
EUREC	European Network of Research Ethics Committees
F/HN	Fusion protein/Hemagglutinin/Neurominidase protein
FACS	fluorescence-activated cell sorting
FDA	Food and Drug Administration
FEV1pp	forced expiratory volume in 1 second percent predicted
FIS	forskolin induced swelling
FRT	Fisher rat thyroid

FSK	forskolin
GABA	gamma-aminobutyric acid
GCPR	G-protein Coupled Receptor
GFP	green fluorescent protein
GLI	global lung function initiative
GLPG	Galapagos
HBE	human bronchial epithelial
HC	healthy control
HDR	homology directed repair
HEK	Human embryonic kidney
hIPSCs	human induced pluripotent stem cells
HNE	human nasal epithelial
HTS	high throughput screen
HUB	Hubrecht Organoid Technology
ICM	intestinal current measurement
IPSCs	induced pluripotent stem cells
LGR5+	Leucine-rich repeat-containing G-protein coupled receptor 5
MDM2	murine double minute 2
MF	minimal function
MoA	mode of action
mRNA	messenger ribonucleic acid
mTOR	mammalian target of rapamycin
nCAS9	nuclease inactive nickase-cas9
NCFS	Dutch cystic fibrosis foundation
NHEJ	non-homologous end joining
NLS	Nuclear localization sequence
NMDi	nonsense mediated decay inhibitor
NPD	nasal potential difference
NS	not significant
O/N	overnight
PAM	protospacer adjacent motif
PBS	primer binding site
PDE	phosphodiesterase
PDIO	patient-derived intestinal organoids
PDO	patient-derived organoids
pegRNA	prime editing guide ribonucleic acid
pen/strep	penicillin-streptomycin

ADDENDA

PGE2	Prostaglandin E2
PI	pancreatic insufficiency
PI	propidium iodide (only in chapter 4)
PI3K	phosphoinositide 3-kinase
PTC	premature termination codons
pwCF	people diagnosed with cystic fibrosis
qRT-PCR	Quantitative reverse transcription polymerase chain reaction
RF	residual function
RNA	ribonucleic acid
RNP	ribonucleoprotein
Rspo1	Rspordin-1
RT	read through
RT	reverse transcriptase
SCC	sweat chloride concentration
SD	standard deviation
SEM	standard error of the mean
sgRNA	single guide RNA
SLA	steady state lumen
SNV	single nucleotide variant
spCas9	Streptococcus pyogenes Cas9
TALENs	transcription activator-like effector nucleases
TP53	tumor protein p53
tRNA	transfer ribonucleic acid
UMCU	University Medical Center Utrecht
VX-445	elexacaftor
VX-661	tezacaftor
VX-661/VX-445/	
VX-770	trikafuta
VX-770	ivacaftor
VX-770/VX-809	orkambi
VX-809	lumacaftor
W/W/O	with and without
WGS	whole genome sequencing
WNT	Wingless-related integration site
WT	wildtype
xCAS9	an expanded PAM SpCas9 variant
ZNFs	zinc finger nucleases

CONTRIBUTING AUTHORS

Bente L. Aalbers

Department of Pediatric Pulmonology
University Medical Center Utrecht

Gimano D. Amatngalim

Department of Pediatric Pulmonology and Regenerative Medicine Center Utrecht
University Medical Center Utrecht

Amanda Andersson-Rolf

Hubrecht Institute
Royal Netherlands Academy of Arts and Sciences (KNAW)
University Medical Center Utrecht Oncode Institute

Jeffrey M. Beekman

Department of Pediatric Pulmonology and Regenerative Medicine Center Utrecht
University Medical Center Utrecht

Gitte Berkers

Department of Pediatric Pulmonology
University Medical Center Utrecht

Sylvia F. Boj

Hubrecht Organoid Technology (HUB)

Matteo Boretto

Hubrecht Institute
Royal Netherlands Academy of Arts and Sciences (KNAW)
University Medical Center Utrecht Oncode Institute

Ruben van Boxtel

Oncode Institute
Princess Maxima Center Utrecht

Jesse E. Brunsveld

Department of Pediatric Pulmonology and Regenerative Medicine Center Utrecht
University Medical Center Utrecht

Leo Carrillo

Hubrecht Institute
Royal Netherlands Academy of Arts and Sciences (KNAW)
University Medical Center Utrecht Oncode Institute

ADDENDA

Hans Clevers

Hubrecht Institute
Royal Netherlands Academy of Arts and Sciences (KNAW)
University Medical Center Utrecht Oncode Institute

Katja Conrath

Galapagos NV

Edward Dompeling

Maastricht University Medical Center

Marcel M. van der Eerden

Department of Pulmonology
Erasmus University Medical Center

René M.J.C. Eijkemans

Department of Data Science and Biostatistics
Julius Center for Health Sciences and Primary Care
University Medical Center Utrecht

Cornelis K. van der Ent

Department of Pediatric Pulmonology
University Medical Center Utrecht

Maarten H. Geurts

Hubrecht Institute, Royal Netherlands Academy of Arts and Sciences (KNAW)
University Medical Center Utrecht Oncode Institute

Simon Y. Graeber

Department of Pediatric Respiratory Medicine
Immunology and Critical Care Medicine
Charité-Universitätsmedizin Berlin
Berlin Institute of Health (BIH)
German Center for Lung Research (DZL)

Marne C. Hagemeijer

Department of Clinical Genetics
Erasmus University Medical Center

Sabine Heida-Michel

Department of Pediatric Pulmonology
University Medical Center Utrecht

Stephan R. Janssens

Department of Pediatric Pulmonology
University Medical Center Utrecht

Hettie M. Janssens

Department of Pediatrics
division of Respiratory Medicine and Allergology
Erasmus University Medical Center
Sophia's Children's Hospital

Gerard H. Koppelman

Department of Pediatric Pulmonology and Pediatric Allergology
Groningen Research Institute for Asthma and COPD (GRIAC)
University Medical Center Groningen

Ricardo Korporaal

Hubrecht Organoid Technology (HUB)

Evelien Kruisselbrink

Department of Pediatric Pulmonology and Regenerative Medicine Center Utrecht
University Medical Center Utrecht

Ka Wai Lai

Hubrecht Organoid Technology (HUB)

Marcus A. Mall

Department of Pediatric Respiratory Medicine
Immunology and Critical Care Medicine
Charité-Universitätsmedizin Berlin
Berlin Institute of Health (BIH)
German Center for Lung Research (DZL)

Renske van der Meer

Haga Teaching Hospital

Fleur M. Meijers

Department of Pediatric Pulmonology and Regenerative Medicine Center Utrecht
University Medical Center Utrecht

Peter van Mourik

Department of Pediatric Pulmonology
University Medical Center Utrecht

ADDENDA

Danya Muilwijk

Department of Pediatric Pulmonology
University Medical Center Utrecht

Jasper Mullenders

Hubrecht Organoid Technology (HUB)

Hugo Oppelaar

Department of Pediatric Pulmonology and Regenerative Medicine Center Utrecht
University Medical Center Utrecht

Rurika Oka

Oncode Institute
Princess Maxima Center Utrecht

Hannah van Panhuis

Department of Pediatric Pulmonology
University Medical Center Utrecht

Cayetano Pleguezuelos-Manzano

Hubrecht Institute
Royal Netherlands Academy of Arts and Sciences (KNAW)
University Medical Center Utrecht Oncode Institute

Jolt Roukema

Radboud Institute for Health Sciences
Radboud University Medical Center

Sacha Spelier

Department of Pediatric Pulmonology and Regenerative Medicine Center Utrecht
University Medical Center Utrecht

Sylvia W.F. Suen

Department of Pediatric Pulmonology and Regenerative Medicine Center Utrecht
University Medical Center Utrecht

Annelotte M. Vonk

Department of Pediatric Pulmonology and Regenerative Medicine Center Utrecht
University Medical Center Utrecht

Rob Vries

Hubrecht Organoid Technology (HUB)

Els J.M. Weersink

Amsterdam University Medical Center, location AMC

Karin M. de Winter-de Groot

Department of Pediatric Pulmonology
University Medical Center Utrecht

Domenique D. Zomer-van Ommen

Dutch Cystic Fibrosis Foundation (NCFS)

ACKNOWLEDGEMENTS - DANKWOORD

Dit proefschrift is mede tot stand gekomen dankzij het werk en de steun van velen. Alle mensen die -elk op hun eigen manier- deze periode voor mij zo onvergetelijk hebben gemaakt, wil ik hierbij dan ook enorm bedanken!

Allereerst Jeff, mijn promotor, ontzettend bedankt dat ik deel heb uit mogen maken van jouw team. Dankjewel voor je eerlijkheid, oprechtheid en ongenuanceerdheid. Wij zijn allebei niet op ons mondje gevallen met hilarische en persoonlijke gesprekken tot gevolg. Op professioneel gebied heb ik ontzettend veel van je geleerd. Je bent een enorme doorzetter en ik heb bewondering voor die eindeloze energie om door te kunnen blijven gaan, tot in de nachtelijke uurtjes als het moet. Daarnaast ben je echt een out of the box denker en een wandelende (CF) encyclopedie. Ook wil ik je enorm bedanken voor je steun bij het schrijfproces van de artikelen en dit proefschrift. Zonder jou was het nooit zo mooi en compleet geworden!

Kors, ook mijn promotor, jou wil ik bedanken voor je kritische beoordeling van mijn stukken en dit proefschrift. Ik bewonder de rust die je uitstraalt. Jij hebt er mede voor gezorgd dat ik weinig stress heb ervaren tijdens mijn PhD traject. Ik wil je ook graag bedanken voor het laten inzien waar we het onderzoek echt voor doen; de CF patiënt. Dit heeft mij altijd extra gemotiveerd om door te gaan, ook als het even tegen zat.

Het Beekman team, wat mis ik jullie zeg. Zo'n fijn team om onderdeel van te mogen zijn. Een team waarin iedereen voor elkaar klaar staat, elkaar helpt waar nodig en iedereen echt oprocht geïnteresseerd in elkaar is. Ontzettend bedankt voor de gezellige avondjes, voor de lekkere etentjes en dat jullie er voor mij waren tijdens mijn PhD traject. Zonder jullie was mijn PhD niet zo'n feestje geweest!

Evelien en Annelot, de ruggengraat van de groep. Het was heel fijn om als groentje bij jullie in het team te komen. Op bijna elke vraag had één van jullie wel een antwoord. De vele kappersavondjes bij jou Annelot, onder het genot van heerlijk eten, zal ik ook niet snel vergeten. Het is een perfect voorbeeld voor hoe hecht het team, ook buiten werk, was. Het heeft ook een aantal hilarische fotomomenten opgeleverd, en scrollen door mijn digitale fotoalbum maakt me dan ook altijd aan het lachen. Het was wel even schrikken toen jullie beiden kort na elkaar besloten het team te verlaten. Zoveel kennis en expertise dat verdween uit de groep. Gelukkig hebben jullie het enorm naar jullie zin en gun ik jullie natuurlijk al het plezier en geluk met jullie verdere carrière.

Juliet, jij brengt nuchterheid met een enorme dosis humor in de groep. Ook heb ik je altijd een rustige en stabiele factor van de groep gevonden. Heel veel succes met het afronden van je proefschrift, ik ben heel benieuwd naar het eindresultaat!

Marne, mijn lab en congresmaatje. Het duurde eventjes voordat we de gezamenlijke connectie hadden, maar toe we die eenmaal gevonden hadden waren we beste labmaatjes. Wat hebben wij VEEL werk samen verricht. We waren een geoliede machine in het uitplaten

en meten van high throughput zwellingssassays. Ik had het regenboog project nooit zonder je kunnen EN willen doen. Je gekkigheid, humor maar ook je ontevredenheid die duidelijk van je gezicht te lezen was maakte mij altijd enorm aan het lachen. We hebben ook veel congressen met elkaar mogen bezoeken waarbij we geen enkel eindfeestje hebben overgeslagen. Tot in de late uurtjes stonden we te dansen en gingen we uit ons dak, waar ik de volgende dag dan wel altijd een beetje spijt van had. Weet je nog in Albufeira...dat is denk ik wel de vervelendste maar ook grappigste herinnering die ik van een congres heb. Iemand was met het fantastische idee gekomen dolfinen te gaan spotten op open zee. De combinatie van het hebben van een kater en zeeziekte heeft mij nog nooit zo lang stil gehouden. Toen ik hoorde dat ook jij het team ging verlaten was ik wel even geschockt. Hoe kon ik nou zonder mijn labmaatje? Voor jou was het een ontzettend mooie kans om een nieuwe carrière te starten in het Erasmus, waar je nog steeds met veel plezier werkt. Ontzettend bedankt voor de mooie tijd die we samen hebben beleefd!

Lisa, Hetty en Gimano, bedankt voor de gezelligheid, de goede gesprekken en de fijne samenwerking. Hetty, ik bewonder je kracht tot verbinden. Ondanks dat jij als enige van het team een totaal ander ziektebeeld onderzoekt ben je altijd net zo'n onderdeel van het team geweest als de rest. Ik vergat vaak dat je helemaal geen CF onderzoek deed. Ik bewonder enorm hoe je je staande houdt in een team waar je weinig medeonderzoekers hebt om mee te sparren. Jij komt er wel! Gimano, bedankt voor de goede gesprekken en ik ben altijd onder de indruk geweest van je enorme parate kennis over luchtwegkweken en daarbuiten. Jij bent in mijn ogen een rasechte onderzoeker die tot in detail alles uit wil zoeken. Ik hoop dat je ooit je eigen groep mag leiden of je eigen bedrijf hebt opgestart! Lisa, ook jij bent een enorme doorzetter en een heel fijn mens om mee samen te werken. Ik wens je heel veel succes met het afronden van je PhD en je carrière in het ziekenhuis of huisartsenpraktijk. Ik weet zeker dat je een hele fijne dokter gaat worden!

Sylvia, Jesse en later ook Loes, zonder jullie enorme ondersteuning had ik nooit zoveel werk kunnen verrichten die dit proefschrift mogelijk hebben gemaakt. Jullie stonden altijd klaar om te helpen, om mee te denken en waren altijd bereid jullie werk opzij te schuiven om plaats te maken voor mij, ontzettend bedankt daarvoor.

Sacha, ik wil jou in het bijzonder bedanken voor de vele projecten die we samen aan het einde van mijn PhD traject gedaan hebben. Je bent een keiharde werker en ik bewonder je assertiviteit in het opzoeken en benaderen van nieuwe samenwerkingen. Je bent een echte verbinder, zowel op je werk als privé. Een echte sfeermaker die altijd even vraagt hoe het met je gaat. Ik ben trots op onze gezamenlijke stukken en ik weet zeker dat nog veel meer mensen blij zullen zijn met je samen te mogen werken.

Lieve collega's van de afdeling kinderlongziekten. Ondanks dat we niet in hetzelfde gebouw werkten heb ik mij altijd heel welkom bij jullie gevoeld als ik weleens het WKZ binnen wandelde. Gitte, Peter en Sabine, jullie heb ik beter kunnen leren kennen vanwege de vele congressen die we samen hebben bezocht. Wat kon ik toch altijd met jullie lachen. Het was een feestje om met jullie op congres te mogen. Gitte, jij bent altijd super gezellig en in voor een geintje. Bedankt voor de leuke tijd die we samen hebben doorgebracht. Peter, jouw humor

ADDENDA

in combinatie met je extreme rust maakt je een heel fijn persoon om bij aanwezig te zijn. Heel veel succes met jullie opleidingen in het UMCU en met jullie gezinnen. Mirjam, wat ben jij toch een lief mens. ALTIJD sta jij klaar om te helpen. Je werkt keihard om het voor iedereen zo gemakkelijk mogelijk te maken. Niet alleen op zakelijk vlak ben je een grote ondersteuning, ook privé vergeet je je collega's nooit, door verjaardagskaartjes, cadeaumanden en afscheid presentjes te regelen. Karin, bedankt voor je kritische blik op mijn onderzoek, het stellen van goede vragen en de hulp bij het regenboogproject. En net als Kors deed ook jij mij eraan herinneren dat de patiënt op nummer 1 staat. Een gegeven dat bij mij weleens naar de achtergrond verdween, maar mij weer extra motiveerde, dank daarvoor!

Eindeloos het internet afspeuren voor de classificatie en klinische consequentie van HEEL VEEL mutaties was nooit gelukt zonder de hulp van jou Danya, onzettend bedankt daarvoor! Mede dankzij jouw onzettende doorzettingsvermogen en precisie hebben we een heel gaaf artikel kunnen publiceren. En als ik het even niet meer zag zitten was jij daar om mij weer te motiveren. Je droge humor en je duidelijke manier van communiceren maken je een fantastisch mens om mee samen te werken. Wat zal jij een fijne longarts worden!

Maarten, zonder jou was dit proefschrift niet zo compleet geworden. Zonder jou had ik nooit zoveel clones kunnen prikken, zoveel elektroporaties kunnen doen of zoveel kweken kunnen doorzetten. En boven alles, nooit zoveel plezier gehad in mijn werk. Lachen om nerdgrapjes, allebei het even niet meer zien zitten maar elkaar er toch doorheen slepen met humor, 'lekkere' koffie en Milka chocoladerepen voor 0,80 eurocent zijn een greep uit de fijne herinneringen die ik heb aan onze samenwerking. Ik bewonder je intelligentie, je kennis over CRISPR-CAS onderzoek en je doorzettingsvermogen. Heel veel succes met het afronden van je proefschrift. En met die carrière van jou komt het wel goed, bedrijven zijn gek als ze zo'n expert en leuk mens als jou niet willen hebben in hun team!

Paranimfen, Sylvia en Sacha, jullie reactie op de vraag om mijn paranimf te willen zijn was onvergetelijk. Zo'n enthousiaste reactie had ik alleen maar kunnen dromen. Onzettend bedankt voor jullie hulp en steun tijdens mijn verdediging.

Beste leden van de beoordelingscommissie, hartelijk dank voor de grondige bestudering, kritische beoordeling en goedkeuring van dit proefschrift.

Beste opponenten, hartelijk dank voor jullie bereidheid dit proefschrift grondig te bestuderen en voor het stellen van kritische vragen.

Coauteurs, onzettend bedankt voor jullie waardevolle bijdrage aan dit proefschrift.

To all collaborators around the world, thanks for your support, input for this thesis and fun on the CF conferences.

Dank aan alle CF-centra in Nederland en alle anderen die zich inzetten voor mensen met CF. Ook de mensen met CF, bedankt voor jullie inzet voor de wetenschap. Zonder jullie organoiden had het onderzoek in dit proefschrift nooit tot stand kunnen komen. Nederlandse

Cystic Fibrose Stichting, bedankt voor de financiële ondersteuning van dit onderzoek en de fijne samenwerking.

Even niet aan werk denken....daar heb je lieve vriendinnetjes voor!! Milou en Irene, dankjewel voor jullie onvoorwaardelijke liefde en steun. Ik ben ontzettend dankbaar dat jullie mijn vriendinnetjes zijn. De vele etentjes en high tea's waren heerlijk en onze twerkcursus, stippencursus en escape room waren hilarisch. Anna, Frances, Michelle en Saskia, jullie heb ik leren kennen tijdens mijn bachelor stage en hebben sindsdien altijd contact gehouden. Het was heel fijn een club meiden om me heen te hebben die allemaal een soortgelijk traject hebben doorgemaakt. Lab frustraties, grapjes en roddels kunnen delen is op zijn tijd heel erg fijn. Bedankt voor jullie steun, gezelligheid en humor!

Lieve papa's, mam, zussie en Dan, bedankt voor jullie onvoorwaardelijke liefde en de gezellige weekendjes weg. Ook hebben jullie geen familiedag of rondleiding op het lab gemist, dank voor deze interesse in mijn onderzoek!

Kevin....liefje! Jou kan ik niet genoeg bedanken. Je bent ECHT mijn maatje. Wat heb ik genoten van het samen klussen in ons nieuwe huis, onze heerlijke vakanties op camping Le Brasilia en het starten van ons nieuwe gezinnetje. Tijdens deze nieuwe fase in ons leven ben je zo'n ontzettende steun voor mij geweest. En naast een fantastische partner ben je een geweldige papa voor onze kleine Abel (maar dat wist ik natuurlijk al....). Ik hou van je!!

LIST OF PUBLICATIONS

This thesis

D. Muilwijk*, **E. de Poel***, P. van Mourik, S.W.F. Suen, A.M. Vonk, J.E. Brunsveld, E. Kruisselbrink, H. Oppelaar, M.C. Hagemeijer, G. Berkers, K.M. de Winter-de Groot, S. Heida-Michel, S.R. Jans, H. van Panhuis, M.M. van der Eerden, R. van der Meer, J. Roukema, E. Dompeling, E.J.M. Weersink, G.H. Koppelman, R. Vries, D.D. Zomer-van Ommen, M.J.C. Eijkemans, C.K. van der Ent and J.M. Beekman. FORSKOLIN-INDUCED ORGANOID SWELLING IS ASSOCIATED WITH LONG-TERM CF DISEASE PROGRESSION. European Respiratory Journal. January 2022

E. de Poel, S. Spelier, R. Korporaal, K.W. Lai, S.F. Boj, K. Conrath, C.K. van der Ent and J.M. Beekman. CFTR RESCUE IN INTESTINAL ORGANOIDS WITH GLPG/ABBV-2737, ABBV/ GLPG-2222 AND ABBV/GLPG-2451 TRIPLE THERAPY. Frontiers in Molecular Biosciences. September 2021

E. de Poel, S. Spelier, S.W.F. Suen, E. Kruisselbrink, S. Y. Graeber, M.A. Mall, E.J.M. Weersink, M.M. van der Eerden, G.H. Koppelman, C.K. van der Ent and J.M. Beekman. FUNCTIONAL RESTORATION OF CFTR NONSENSE MUTATIONS IN INTESTINAL ORGANOIDS. Journal of Cystic Fibrosis. In press 2021

M.H. Geurts*, **E. de Poel***, G.D. Amatngalim, R. Oka, F.M. Meijers, E. Kruisselbrink, P. van Mourik, Gitte Berkers, K.M. de Winter-de Groot, S. Michel, D. Muilwijk, B.L. Aalbers, J. Mullenders, S.F. Boj, S.W.F. Suen, J.E. Brunsveld, H.M. Janssens, M.A. Mall, S.Y. Graeber, R. van Boxtel, C.K. van der Ent, J.M. Beekman and H. Clevers. CRISPR-BASED ADENINE EDITORS CORRECT NONSENSE MUTATIONS IN A CYSTIC FIBROSIS ORGANOID BIOBANK. Cell Stem Cell. April 2020

M.H Geurts, **E. de Poel**, C. Pleguezuelos-Manzano, R. Oka , L. Carrillo, A. Andersson-Rolf, M. Boretto, J.E Brunsveld, R. van Boxtel, J.M. Beekman, H. Clevers. EVALUATING CRISPR-BASED PRIME EDITING FOR CANCER MODELING AND CFTR REPAIR IN ORGANOIDS. Life Science Alliance. August 2021

Other publications

A. Ghigo, A. Murabito, V. Sala, A. Rita Pisano, S. Bertolini, A. Gianotti, E. Caci, A. Premchandar, F. Pirozzi^{1,6}, K. Ren, A. Della Sala, W. Richter, **E. de Poel**, M. Matthey, A. Montresor, S. Caldrer, R. A. Cardone, F. Civiletti, A. Costamagna, N.L. Quinney, C. Butnarasu, S. Visentin, D. Ramel, M. Laffargue, C.G. Tocchetti, R. Levi, M. Conti, X. Lu, P. Melotti, C. Sorio, V. De Rose, F. Facchinetti, V. Fanelli, D. Wenzel, B. Fleischmann, M.A. Mall, J.M. Beekman, C. Laudanna, M. Gentzsch, G.L. Lukacs, N. Pedemonte and E. Hirsch. AIRWAY ADMINISTRATION OF A PI3K γ MIMETIC PEPTIDE TRIGGERS CFTR GATING, BRONCHODILATION AND REDUCED INFLAMMATION IN OBSTRUCTIVE AIRWAY DISEASES. *Sci. Transl. Med.* In press

C.S. Mahon, G.C. Wildsmith, D. Haksar, **E. de Poel**, J.M. Beekman, R.J. Pieters, M.E. Webba and W. Bruce Turnbull. A 'CATCH-AND-RELEASE' RECEPTOR FOR THE CHOLERA TOXIN. *Faraday Discuss.* March 2109

D. Haksar, **E. de Poel**, L. Quarles van Ufford, S. Bhatia, R. Haag, J.M. Beekman and R.J. Pieters. STRONG INHIBITION OF CHOLERA TOXIN B SUBUNIT BY AFFORDABLE, POLYMER-BASED MULTIVALENT INHIBITORS. *Bioconjugate Chem.* January 2019

D.D. Zomer-van Ommen, **E. de Poel**, E. Kruisselbrink, H. Oppelaar, A.M. Vonk, H.M. Janssens, C.K. van der Ent, M.C. Hagemeyer and J.M. Beekman. COMPARISON OF EX VIVO AND IN VITRO INTESTINAL CYSTIC FIBROSIS MODELS TO MEASURECFTR-DEPENDENT ION CHANNEL ACTIVITY. *J. Cyst. Fibros.* February 2018

N.T. Awatade, S.Ramalhoa, I.A.L. Silva, V. Felício, H.M. Botelhoa, **E. de Poel**, A.M. Vonk, J.M. Beekman, C. M. Farinh and M.D. Amaral. R560S: A CLASS II CFTR MUTATION THAT IS NOT RESCUED BY CURRENT MODULATORS. *J. Cyst. Fibros.* July 2018

P.M.W. van Kempen, F.J. Verdam, **E. de Poel**, W.W. Braunius, R.A. de Weger, R.J.J. van Es, W. Grolman, S.M. Willems. TP53 Y220C IS A HOTSPOT MUTATION IN OROPHARYNGEAL SQUAMOUS CELL CARCINOMA. *Pathobiology.* October 2014

CURRICULUM VITAE

Eyleen de Poel was born on February 23rd 1992 in Groningen, the Netherlands. She grew up in Assen where she graduated from secondary school at Dr. Nassau College Quintus Assen in 2010. In the same year she moved to Utrecht to start her bachelor Biology, where here enthusiasm for research started. After finishing her bachelor Biology in 2013 she started with the master Biology of disease. During her master she did her first internship at the Veterinary Medicine Department Utrecht. Her enthusiasm for CF research using intestinal organoids started after visiting the stem cell congress in Utrecht where work on intestinal organoids was presented. This has encouraged her to start her second internship at the Beekman laboratory, part of the pediatric pulmonology department in the Wilhelmina's Children's hospital Utrecht. In 2016 she obtained her Master of Science in Biology of Disease and in the same year she started her PhD project, also at the Beekman laboratory. Her PhD project focused on using intestinal organoids for personalized treatment of CF patients and for the development and validation of new therapies for CF, under supervision of Prof. Dr. J.M. Beekman and Prof. Dr. C.K. van der Ent. In September 2021 she started working as a medical science liaison at Chiesi Pharmaceuticals Nederland.

Eyleen lives in Hoef en Haag, together with Kevin and their 4-months old son Abel.

A

